biomedicines

NASH and Systemic Complications

From Basic to Clinical Research

Edited by
Ronit Shiri-Sverdlov and Sabine Baumgartner

Printed Edition of the Special Issue Published in *Biomedicines*

www.mdpi.com/journal/biomedicines

MDPI

NASH and Systemic Complications: From Basic to Clinical Research

NASH and Systemic Complications: From Basic to Clinical Research

Editors

Ronit Shiri-Sverdlov
Sabine Baumgartner

MDPI • Basel • Beijing • Wuhan • Barcelona • Belgrade • Manchester • Tokyo • Cluj • Tianjin

Editors

Ronit Shiri-Sverdlov
Maastricht University
The Netherlands

Sabine Baumgartner
Maastricht University
The Netherlands

Editorial Office
MDPI
St. Alban-Anlage 66
4052 Basel, Switzerland

This is a reprint of articles from the Special Issue published online in the open access journal *Biomedicines* (ISSN 2227-9059) (available at: http://www.mdpi.com).

For citation purposes, cite each article independently as indicated on the article page online and as indicated below:

LastName, A.A.; LastName, B.B.; LastName, C.C. Article Title. *Journal Name* **Year**, *Volume Number*, Page Range.

ISBN 978-3-0365-2978-3 (Hbk)
ISBN 978-3-0365-2979-0 (PDF)

Contents

biomedicines

MDPI

Editorial

NASH and Systemic Complications: From Basic to Clinical Research

Sabine Baumgartner [1,*] and Ronit Shiri-Sverdlov [2,*]

[1] Department of Nutrition and Movement Sciences, School of Nutrition and Translational Research in Metabolism (NUTRIM), Maastricht University, Universiteitssingel 50, 6229 ER Maastricht, The Netherlands
[2] Department of Molecular Genetics, School of Nutrition and Translational Research in Metabolism (NUTRIM), Maastricht University, Universiteitssingel 50, 6229 ER Maastricht, The Netherlands
* Correspondence: sabine.baumgartner@maastrichtuniversity.nl (S.B.); r.sverdlov@maastrichtuniversity.nl (R.S.-S.)

Nonalcoholic fatty liver disease (NAFLD) is known as the hepatic manifestation of the metabolic syndrome, and while most patients develop simple steatosis, up to one-third can develop nonalcoholic steatohepatitis (NASH). NASH is a chronic inflammatory condition of the liver that can further progress to fibrosis and cirrhosis, which may eventually lead to liver failure and death. In this Special Issue, 12 scientific contributions, including nine reviews and three original research articles, address basic and clinical research on NASH and its systemic complications. Articles were divided into three subtopics: (1) mechanistic tools to investigate all disease aspects of NAFLD; (2) extrahepatic manifestations of NASH; and (3) promising biomarkers to diagnose NASH and interventions to treat NASH.

Currently, the mechanisms by which inflammation is triggered within the context of NASH are unknown. Consequently, therapeutic options are poor, non-invasive markers to detect NASH do not exist and the long-term burden to society is constantly increasing. Ultimately, there is an urgent need for a physiological "humanized" model that displays a liver phenotype identical to human disease, including all stages and systemic characteristics. In this Special Issue, Oligschläger et al. [1] provide an overview on the currently existing murine models and describe the advantages, limitations and challenges in using each model. While murine models are considered indispensable tools for studying chronic liver disease pathology, the majority of the existing models do not demonstrate all the disease stages or do not have the systemic characteristic of NASH. Therefore, selection of the model is highly dependent on the research question. Furthermore, as NASH progression greatly varies across different strains, it is often not sufficient to include only one model in each study. Considering the ethical issues related to the use of animals in research, the high costs and the low success rate of clinical trials which are based on murine models, great effort has been put to develop surrogate to the animal testing. One of the most promising recent and cost-effective alternative approaches is to employ machine learning and artificial intelligence on organ-on-a-chip technology. Such a high-throughput approach allows for the early identification of mechanisms leading to NASH and the assessment of the efficacy and toxicity of novel treatments. De Chiara et al. [2] provide a wide overview of the new implementation of organ-on-a-chip into the field of NAFLD, the current findings and limitations. They further elaborate on the multiple opportunities which will enable us to drastically limit the use of preclinical models and accelerate translational research in the field of NASH. Recently, organ-on-a-chip has also been used as a model to investigate the complex mechanisms which leads to the transition to hepatocellular carcinoma (HCC). In this Special Issue, Ramai et al. [3] review the pathogenesis of NASH leading to HCC and emerging pathological concepts. These mechanisms include the effects of cellular, genetic, immunologic, metabolic, and endocrine pathways. Combing artificial intelligence with complex organ-on-a-chip tools will allow us to investigate the interaction between these pathways in a rapid and accurate manner and aid the development of personalized

Citation: Baumgartner, S.; Shiri-Sverdlov, R. NASH and Systemic Complications: From Basic to Clinical Research. *Biomedicines* **2021**, *9*, 1913. https://doi.org/10.3390/biomedicines9121913

Received: 6 December 2021
Accepted: 8 December 2021
Published: 14 December 2021

treatment to NASH, as well as HCC patients, as organ-on-a-chip technologies need to be further developed before they will lead to the identifications of early and reliable diagnostic methods. In the meanwhile, extensive efforts are put to establishing imaging modalities for the identification of individuals at risk to develop advanced stage of NASH. Currently there are several imaging modalities for the assessment of hepatic steatosis and fibrosis. The extensive use in these imaging modalities within the context of NASH is described in the review of Grat et al. [4]. However, identification of inflammation by these tools and predication of the chance for complications based on early images remains a challenge. The 13C-aminopyrine breath test (ABT) evaluates the microsomal liver function and could be a potential candidate to allow the discrimination between simple steatosis to NASH. Using this approach, in this Special Issue, Verlinden et al. [5] aimed to evaluate a potential change in liver function in NASH patients and to assess the diagnostic power to detect NASH. They demonstrated that the microsomal liver function of patients with NASH is significantly decreased, even in the absence of fibrosis. Nevertheless, while the 13C-aminopyrine breath test show promise in diagnosis, they currently do not allow for predication of local and extrahepatic systemic complications of NASH. Within this context, extracellular vesicles (EVs) have gained increased attention due to their function as mediators of cellular communication. In their review, Højland Ipsen et al. [6] provide an update on current experimental and clinical findings of the role of EVs in NASH progression and point towards the potential of EVs as disease markers and treatment targets. Within the same context, leptin, an adipokine involved in energy homeostasis and lipid metabolism, has also been investigated as a potential biomarker and as a target of treatment in the NAFLD spectrum. Jiménez-Cortegana et al. [7] describe that the use of leptin is debatable, since it has been shown to be an independent predictor of the presence or development of NAFLD, while it has also been associated with hepatic steatosis and could promote the induction of NASH or liver fibrosis in NAFLD patients. As a therapeutic option, the use of leptin is controversial due to its proinflammatory properties but does highlight that the development of leptin analogues and leptin sensitizers is promising. Overall, these recent developments in preclinical and surrogate models as well as non-invasive tools to assess NASH are expected to drastically accelerate the speed by which new knowledge regarding NASH progression is gained as well as the identification of novel pharmaceutical target(s) and accurate timing for treatment.

NAFLD comprises a wide range of liver disorders, from simple steatosis to NASH and—if not treated—life-threatening complications such as cirrhosis and HCC. In addition to effects on hepatic-related events, evidence also points towards a link of NAFDL/NASH with extra-hepatic complications, including central nervous system (CNS) diseases. In this Special Issue, Colognesi et al. [8] summarize the main correlations observed between NAFLD/NASH and CNS dysfunctions, such as depression, cognitive impairments, dementia and Alzheimer's disease (AD), where an inflammatory state and oxidative stress both play a pivotal role. Even though there are conflicting results whether there is a causal relation between liver damage and the development of cognitive dysfunction, many signaling pathways are altered in both NAFLD/NASH and CNS dysfunction, suggesting that these diseases at least share a pathogenetic component. The pathology of NAFLD has also been linked to a lower microbial diversity and an altered gut barrier integrity, exposing the host to bacterial components and inducing immune responses and inflammation. Indeed, NASH patients have an increased intestinal permeability and a decreased bacterial overgrowth, which correlated with the severity of steatosis. In addition, several lines of evidence support increased intestinal permeability and bacterial translocation as possible causes in the development of metabolic disease, such as the metabolic syndrome and type 2 diabetes. As presented by Plaza-Díaz et al. [9] in this Special Issue, the potential role of alterations in gut microbiota in NASH as biomarker for prognosis and diagnosis is promising. Moreover, the involvement of microbiota as a potential target to treat for NAFLD and NASH by supplementation of prebiotics and probiotics and fecal microbiota transplantation is discussed.

Dietary imbalances are increasingly recognized as the root cause of NASH-related comorbidities and Simón et al. [10] describe in this Special Issue that a deficit in magnesium, a micronutrient found in most green vegetables, legumes, peas, beans and nuts, might aggravate NASH and its related diseases. The authors characterized the potential role that magnesium might play in the development of liver diseases and metabolic syndrome. They have demonstrated that magnesium supplementation is linked to reduced NASH-related mortality and future studies to investigate the potential of magnesium as a therapeutic approach are warranted. Therapeutic options to treat NAFLD and NASH are often targeted to improve glucose metabolism since dysregulations in glucose homeostasis are an important driver in the pathogenesis of NASH. Previous studies demonstrated beneficial effects of antiglycemic treatments in diabetic NASH patients, while not much is known concerning their effect in a non-diabetic setting. In this Special Issue, Hupa-Breier et al. [11] investigate the effect of long-acting GLP-1 agonist dulaglutide and sodium-glucose cotransporter 2 (SGLT-2) inhibitor empagliflozin and their combination in a non-diabetic mouse model of NASH. Even though this GLP-1 agonist and SGLT-2 inhibitor did not prevent hepatic steatosis, dulaglutide and the combination of dulaglutide with empagliflozin improved glucose homeostasis and induced anti-inflammatory and anti-fibrotic pathways, which could have important implications for the treatment of NASH. As described above, pharmacological therapy often addresses NASH-associated co-morbidities, while treatments targeting the liver itself are scarce. Mesenchymal stromal cell (MSC) transplantation has been shown to ameliorate hepatic lipid load, tissue inflammation and fibrosis in rodent animal models of NASH. However, the mechanisms of these MSCs are not known, which is crucial to improve their therapeutic potential. In this Special Issue, Hsu et al. [12] transplanted bone marrow-derived MSCs into the livers of a NASH mouse model. The diet that was used to induce NASH in this model was characterized by an impairment of the central carbon and amino acid metabolism, which was probably the trigger for mitochondrial and peroxisomal dysfunction. Transplanting MSCs in the host livers ameliorated lipid storage and associated perturbance of tissue homeostasis likely by donating healthy mitochondria to the hepatocytes, which provided oxidative capacity for lipid breakdown and thus recovery of liver tissue.

While we have increased our mechanistic knowledge regarding the pathogenesis of NASH within the last decade, treatment options are still limited and liver biopsies have remained the gold standard for diagnosis. To achieve major clinical breakthrough for NASH patients, it is not sufficient to use a single animal model since each model has specific limitations. Furthermore, we should rely more on alternative models such as organ-on-a-chip, which will enable us to explore unknown aspects of disease pathogenesis much faster and serve as clinically relevant surrogates for murine models. Another important direction to improve patient's health is to pay more attention to extrahepatic, organ specific and systemic effects, which are associated with NASH. This Special Issue describes several metabolic disturbances related to NASH which should be monitored more closely in in preclinical studies and in patient populations. As demonstrated in this issue, the technological developments in disease models along with advanced mathematical data analysis and the view of NASH as a systemic disease, already generated new opportunities for the discovery of novel drugs and diagnostic tools to monitor diseases progression.

In summary, the articles in this Special Issue include an up-to-date overview of the rapidly developing technologies, novel targets for intervention and insights in the field in NASH. Additionally, these articles describe the major challenges in the field, strategies to overcome them and suggestions for future directions. To improve patient's outcome, clinicians, as well as scientists with biomedical, nutrition, physics and mathematics backgrounds, should join forces. Although challenges remain, the future of the field seems promising as these novel technologies and developments are expected to lead to progress in NASH.

Author Contributions: Conceptualization, writing—original draft preparation and writing—review and editing, S.B. and R.S.-S. All authors have read and agreed to the published version of the manuscript.

Funding: This research received no external funding.

Conflicts of Interest: The authors declare no conflict of interest.

References

1. Oligschlaeger, Y.; Shiri-Sverdlov, R. NAFLD Preclinical Models: More than a Handful, Less of a Concern? *Biomedicines* **2020**, *8*, 28. [CrossRef] [PubMed]
2. De Chiara, F.; Ferret-Minana, A.; Ramon-Azcon, J. The Synergy between Organ-on-a-Chip and Artificial Intelligence for the Study of NAFLD: From Basic Science to Clinical Research. *Biomedicines* **2021**, *9*, 248. [CrossRef] [PubMed]
3. Ramai, D.; Tai, W.; Rivera, M.; Facciorusso, A.; Tartaglia, N.; Pacilli, M.; Ambrosi, A.; Cotsoglou, C.; Sacco, R. Natural Progression of Non-Alcoholic Steatohepatitis to Hepatocellular Carcinoma. *Biomedicines* **2021**, *9*, 184. [CrossRef] [PubMed]
4. Grat, K.; Grat, M.; Rowinski, O. Usefulness of Different Imaging Modalities in Evaluation of Patients with Non-Alcoholic Fatty Liver Disease. *Biomedicines* **2020**, *8*, 298. [CrossRef] [PubMed]
5. Verlinden, W.; Van Mieghem, E.; Depauw, L.; Vanwolleghem, T.; Vonghia, L.; Weyler, J.; Driessen, A.; Callens, D.; Roosens, L.; Dirinck, E.; et al. Non-Alcoholic Steatohepatitis Decreases Microsomal Liver Function in the Absence of Fibrosis. *Biomedicines* **2020**, *8*, 546. [CrossRef] [PubMed]
6. Ipsen, D.H.; Tveden-Nyborg, P. Extracellular Vesicles as Drivers of Non-Alcoholic Fatty Liver Disease: Small Particles with Big Impact. *Biomedicines* **2021**, *9*, 93. [CrossRef] [PubMed]
7. Jimenez-Cortegana, C.; Garcia-Galey, A.; Tami, M.; del Pino, P.; Carmona, I.; Lopez, S.; Alba, G.; Sanchez-Margalet, V. Role of Leptin in Non-Alcoholic Fatty Liver Disease. *Biomedicines* **2021**, *9*, 762. [CrossRef] [PubMed]
8. Colognesi, M.; Gabbia, D.; De Martin, S. Depression and Cognitive Impairment-Extrahepatic Manifestations of NAFLD and NASH. *Biomedicines* **2020**, *8*, 229. [CrossRef] [PubMed]
9. Plaza-Diaz, J.; Solis-Urra, P.; Aragon-Vela, J.; Rodriguez-Rodriguez, F.; Olivares-Arancibia, J.; Alvarez-Mercado, A.I. Insights into the Impact of Microbiota in the Treatment of NAFLD/NASH and Its Potential as a Biomarker for Prognosis and Diagnosis. *Biomedicines* **2021**, *9*, 145. [CrossRef] [PubMed]
10. Simon, J.; Delgado, T.C.; Martinez-Cruz, L.A.; Martinez-Chantar, M.L. Magnesium, Little Known But Possibly Relevant: A Link between NASH and Related Comorbidities. *Biomedicines* **2021**, *9*, 125. [CrossRef] [PubMed]
11. Hupa-Breier, K.L.; Dywicki, J.; Hartleben, B.; Wellhoner, F.; Heidrich, B.; Taubert, R.; Mederacke, Y.E.; Lieber, M.; Iordanidis, K.; Manns, M.P.; et al. Dulaglutide Alone and in Combination with Empagliflozin Attenuate Inflammatory Pathways and Microbiome Dysbiosis in a Non-Diabetic Mouse Model of NASH. *Biomedicines* **2021**, *9*, 353. [CrossRef] [PubMed]
12. Hsu, M.J.; Karkossa, I.; Schafer, I.; Christ, M.; Kuhne, H.; Schubert, K.; Rolle-Kampczyk, U.E.; Kalkhof, S.; Nickel, S.; Seibel, P.; et al. Mitochondrial Transfer by Human Mesenchymal Stromal Cells Ameliorates Hepatocyte Lipid Load in a Mouse Model of NASH. *Biomedicines* **2020**, *8*, 350. [CrossRef] [PubMed]

biomedicines

MDPI

Review

NAFLD Preclinical Models: More than a Handful, Less of a Concern?

Yvonne Oligschlaeger * and Ronit Shiri-Sverdlov

Department of Molecular Genetics, School of Nutrition and Translational Research in Metabolism (NUTRIM), Maastricht University, Universiteitssingel 50, 6229 ER, Maastricht, The Netherlands; r.sverdlov@maastrichtuniversity.nl

* Correspondence: yvonneoligschlaeger@ziggo.nl

Received: 14 January 2020; Accepted: 5 February 2020; Published: 8 February 2020

Abstract: Non-alcoholic fatty liver disease (NAFLD) is a spectrum of liver diseases ranging from simple steatosis to non-alcoholic steatohepatitis, fibrosis, cirrhosis, and/or hepatocellular carcinoma. Due to its increasing prevalence, NAFLD is currently a major public health concern. Although a wide variety of preclinical models have contributed to better understanding the pathophysiology of NAFLD, it is not always obvious which model is best suitable for addressing a specific research question. This review provides insights into currently existing models, mainly focusing on murine models, which is of great importance to aid in the identification of novel therapeutic options for human NAFLD.

Keywords: NAFLD; mouse models; multifactorial disease; translational value

1. Introduction

Due to excess intake of fat- and/or sugar-enriched diets and a lack of exercise, overweight and obesity are currently a major and continuously growing public health concern. Strongly associated with the increasing trend in obesity is the metabolic syndrome (MetS), in which disturbed lipid homeostasis and metabolic inflammation are taking the lead. Besides type 2 diabetes (T2D) and cardiovascular diseases, MetS increases the risk of developing non-alcoholic fatty liver disease (NAFLD), the most prevalent chronic liver disease worldwide [1]. The spectrum of NAFLD ranges from benign simple steatosis [2] to steatohepatitis (NASH) and end-stage liver diseases. If steatosis is not managed in time, resident liver cells (e.g., Kupffer and hepatic stellate cells) become activated and immune cells (mainly macrophages) infiltrate the liver, a condition defined as NASH. This progressive form of NAFLD [3] can further trigger hepatocyte damage with/without fibrosis and increase the risk of cirrhosis [4] and hepatocellular carcinoma (HCC) [5]. In contrast to alcoholic liver disease- and viral hepatitis-induced HCC, NASH-related HCC is currently the most rapid growing indication for liver transplant in HCC patients [6].

Obviously, there is an urgent need for a reliable 'humanized' model that displays a liver phenotype that is identical to human disease, with macrovesicular steatosis, lobular inflammation, hepatocellular ballooning (including Mallory-Denk bodies), and fibrosis as predominant features. Subsequently, an optimal NAFLD model should have the ability to further progress to advanced fibrosis, cirrhosis, and ultimately HCC. Moreover, it should encompass MetS-related characteristics, such as obesity, disturbed lipid, glucose and insulin metabolism, as well as systemic inflammation. So far, using a wide variety of preclinical models, considerable efforts have recently been made to better understand the pathogenesis of human NAFLD and/or related clinical questions. However, none of these models resemble the complete human NAFLD spectrum, including related metabolic features that recapitulate this chronic liver disease. For instance, several models, exposed to various dietary compositions, have broadened our knowledge with regard to NAFLD progression, in particular early-onset low-grade

inflammation. Alternative models (genetic or chemically-induced) provided insights into fibrotic features of human NAFLD, one of the most important predictors of human NASH progression [7]. Other models have been more suitable for testing therapeutic interventions in the context of NAFLD/NASH. Nevertheless, there are still significant unmet needs with regard to non-invasive diagnostic methods, therapeutic target identification, and drug development, which implies the need for robust preclinical models [8]. In the current Review, we will provide an update on existing preclinical NAFLD models. This Review focuses on rodents, mainly on mouse models, which are relatively low in costs and therefore allow for studying metabolic and genetic drivers of NAFLD/NASH within a considerable time frame. Moreover, these models serve as an important and well-controlled tool for preclinical drug testing in a multisystemic environment.

2. Insights into Available Preclinical Models for Non-alcoholic Fatty Liver Disease

A wide variety of dietary, genetic, chemically-induced, and/or other rodent models ([8–16]) have greatly advanced our understandings on NAFLD pathophysiology, as will be discussed in the following sections (see also Figure 1, Table 1).

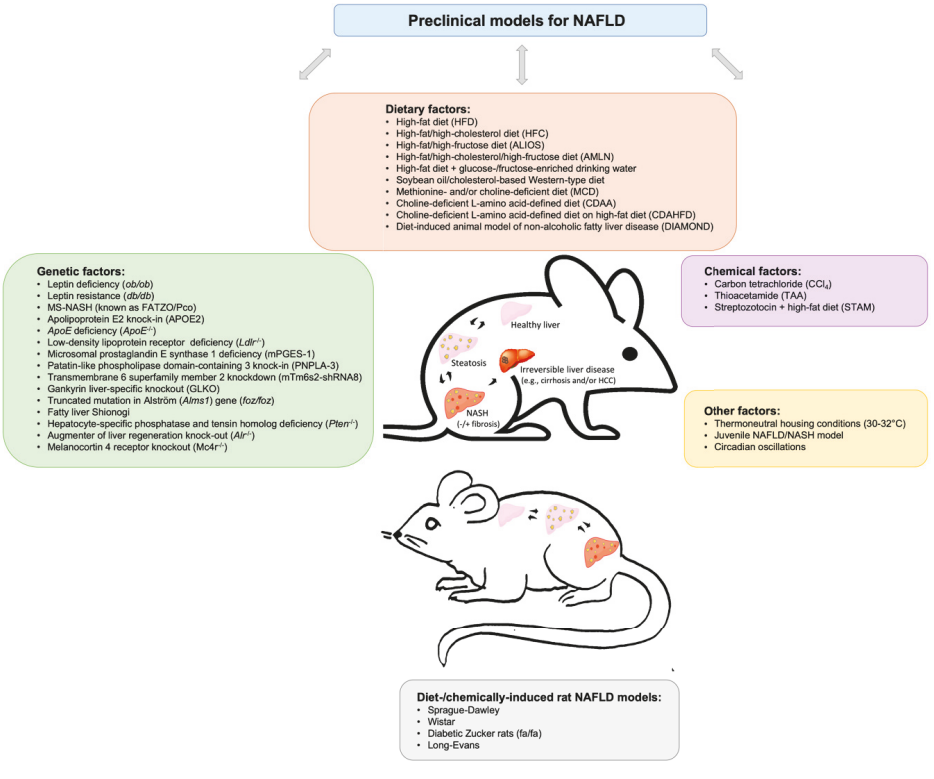

Figure 1. Brief schematic overview of existing preclinical models involving a variety of dietary, genetic, chemical, and other factors to study non-alcoholic fatty liver disease (NAFLD).

2.1. Dietary Murine Models

Diet-induced obesity is known to be the most common risk factor for NAFLD in humans [17]. The experimental NAFLD/NASH models are often based on overnutrition, a condition that can be induced by means of diets varying in macronutrient composition, amongst others.

One of the simplest ways of disturbing lipid metabolism, inducing steatosis and moderate NASH, is by the administration of a regular high-fat diet (HFD; 60% fat, 20% proteins, 20% carbohydrates) [18,19]. For instance, feeding wild-type C57BL/6 mice a HFD for 10–12 weeks resulted in phenotypic changes such as hyperlipidemia, hyperinsulinemia, and glucose intolerance [19,20]. Despite hepatic steatosis, inflammatory cell infiltration was not present until 19 weeks of HFD intake [19]. While after long-term (34–36 weeks) HFD feeding, significant increases in circulating liver enzyme levels, i.e., alanine aminotransferase (ALT) and aspartate aminotransferase (AST) were observed [19], these mice showed only minor signs of inflammation and fibrosis [21], even after prolonged administration up to 50 weeks [19]. Yet, after chronic feeding (80 weeks) of HFD, which mimics lifetime HFD consumption and enables proper design of treatment options, Velázquez et al. [17] demonstrated that mice displayed obesity and insulin resistance. In addition, these mice were shown to develop NAFLD features, including hepatic steatosis, cell injury, portal and lobular inflammation, hepatic ER stress, as well as fibrosis [17]. In line with Chen et al. [22], which showed a deterioration in NAFLD when germ-free mice were inoculated with the Firmicutes phyla, they also found increases in the Firmicutes phyla in response to prolonged HFD [17]. Though intestinal permeability was not measured in this study, these data pointed towards diet-induced gut-microbial dysbiosis [17], a well-known microbial event that has been previously observed in NAFLD patients [23]. Yet, it is unclear whether a similar but shorter dietary intervention would also provide insights into NAFLD progression [17].

In contrast to regular HFD, the atherogenic diet, composed of 1.25% cholesterol plus 0.5% cholate, resulted in increased plasma and liver lipid levels and was shown to induce NASH with hepatocellular ballooning in a time-dependent manner from 6–24 weeks [24]. Notably, the addition of a high-fat component exacerbated the histologic severity of NASH, and resulted in hepatic insulin resistance, oxidative stress, and activation of hepatic stellate cells [24]. Exposure to HFD containing 0.1–2.0% cholesterol (HFC) [25,26] for seven months in murine models, such as wild-type C57BL/6 mice, resulted in the development of obesity, hepatomegaly, hepatic steatosis, and varying degrees of steatohepatitis [27].

Due to the variability in disease onset and limited development of fibrosis, a novel so-called Amylin Liver NASH (AMLN) model was generated [28]. This model covers a high-fat/high-fructose (40%/22%) diet containing trans-fatty acids (~18%) and high-cholesterol (2%), thereby better resembling the Western-type diet and subsequent development of NASH features. Remarkably, only after 26–30 weeks of feeding an AMLN diet, wild-type C57BL/6 developed marked steatosis, moderate lobular inflammation and hepatocellular ballooning [29]. However, when obese leptin-deficient *ob/ob* mice were fed a similar AMLN diet for 12 weeks, mice displayed an accelerated and more pronounced metabolic NASH phenotype as compared to wild-type C57BL/6 [29]. Indeed, it is well-known that *ob/ob* mice, which carry a homozygous mutation in the leptin gene that protect it from binding to its receptor, are susceptible to insulin resistance and T2D, thus being predisposed to metabolic features resembling NAFLD [30]. Yet, spontaneous progression from simple steatosis to NASH and hepatic fibrosis is rather prevented in these mice [31], pointing towards the need of a second stimulus.

More recently, according to the FDA-ban on trans-fats as food additives [32], another obesogenic trans-fat-free diet substituted with saturated fat (palm oil) was explored [33]. This so-called Gubra Amylin NASH (GAN) diet has a nutrient composition and caloric density (40% high-fat, 22% high-fructose 2% high-cholesterol) similar to AMLN diet. Upon feeding *ob/ob* mice GAN diet for 16 weeks, animals displayed biopsy-confirmed liver lesions with features of fibrotic NASH. While these features were similar to AMLN-fed *ob/ob* mice, GAN-fed *ob/ob* mice showed a more pronounced weight gain and increased adiposity. In contrast, wild-type C57BL/6 mice required a prolonged feeding period (28 weeks) of GAN diet to induce consistent fibrotic NASH. However, compared to AMLN diet, GAN-fed wild-type mice had significantly greater body weight gain. Altogether, obesogenic GAN diet induces hallmarks of fibrotic NASH in both models [33], suggesting its suitability for preclinical therapeutic testing against NASH.

Administering an alternative fast-food-like nutritional regime based on high-fat/high-fructose/high-cholesterol (41%/30%/2%) was also shown to induce NASH in various genotypes [34]. These models included wild-type C57BL/6, *ob/ob* mice as well as KK-A^{y} [35] mice, the latter carrying a mutation in the Agouti gene that increases its susceptibility to human NAFLD-like metabolic alterations [36]. Relevantly, Abe et al. [34] showed that *ob/ob* mice under these conditions displayed more pronounced NAFLD activity score, fibrosis progression, obesity and hyperinsulinemia compared to the other models. Given that the metabolic, histologic, and transcriptomic features observed in *ob/ob* mice were similar to human NASH, this model may be further explored as a potential preclinical tool to discover novel drugs for NASH [34].

Relevantly, Henkel et al. [37] explored the impact of long-term exposure (20 weeks) with a high-caloric (43%) Western-type diet composed of soy-bean oil (high n-6-PUFA, 25g/100g) and 0.75% cholesterol. In contrast to cholesterol-free HFD [38], dietary cholesterol in soybean oil resulted in increased Kupffer cell activation and oxidative stress as well as hepatic steatosis, ballooning, inflammation and fibrosis in wild-type C57BL/6 [37], which closely resembles clinical NASH features. In line, when mice were fed an alternative high-caloric (45%) cholesterol-free HFD (composed of lard (21g/100g)/soy-bean oil (3g/100g)/5% fructose in drinking water), only mild steatosis and no signs of hepatic inflammation and fibrosis were observed [37]. Thus, in agreement with previous studies [25,26,38–40], these findings indicate that the supplementation of dietary cholesterol triggers experimental hepatic inflammation and fibrosis [37].

Other dietary variants were explored by Montandon et al. [41], comparing the high-fat atherogenic diet (60% fat plus 1.25% cholesterol and 0.5% cholic acid) versus the commonly used methionine/choline-deficient diet (MCD). In line with others [24,42], wild-type C57BL/6 mice fed a cholesterol/cholate-rich diet showed increases in hepatic cholesterol and free fatty acids, while MCD mice predominantly accumulated triglycerides in their livers [41]. Strikingly, MCD caused a reduction in liver weights, whereas atherogenic diet did not [41]. Moreover, MCD increased hepatic damage, lobular inflammation, lipogranulomas, tissue fibrosis, and liver enzymes compared to mice fed a cholesterol/cholate-rich diet. In addition, transcriptional analyses revealed a dysregulation in extracellular matrix remodeling and hepatic stellate cell activation in response to MCD, but not an atherogenic diet [41]. Altogether, these data pointed towards a more severe form of NASH in MCD mice [41], which was in line with previous studies showing that MCD triggered extensive hepatic inflammation in rats [43] and mice [44–46] within a very short time frame. To overcome the lack of severe hepatic fibrosis often observed in preclinical models, mice are commonly fed MCD [47] or a diet low in/deficient for choline (CD) [48]. Although CD exacerbated fatty liver [48], MCD resulted in rapid NASH development with severe liver fibrosis within 4–10 weeks, likely as a consequence of reduced VLDL synthesis and hepatic-β oxidation [20]. While liver inflammation and elevated circulating liver enzyme levels returned back to normal levels after switching the diet back to control within 16 weeks, fibrosis and CD68-positive macrophages remained present [47].

It is also interesting to note that leptin-resistant *db/db* mice (which carry a mutation in the leptin receptor gene [49] and lack the ability to spontaneously develop hepatic inflammation [35,50]) displayed marked hepatic inflammation and fibrosis in response to feeding an MCD diet for four weeks [45]. These data suggest that, similar to *ob/ob* mice [31,51], *db/db* mice need a second stimulus to induce NASH [45]. Nevertheless, it is noteworthy that all MCD models rather showed significant reductions in weight, concomitant loss in liver mass and cachexia, as well as low serum levels of insulin, fasting glucose, leptin and triglycerides, and a lack of insulin resistance [12,45,52]. Given that these preclinical observations are opposite to the effects seen in overweight and obese individuals with NAFLD, these data suggest that the use of MCD models as preclinical tools to represent human NAFLD is rather limited [53]. Further, though *ob/ob* and *db/db* models serve as useful preclinical tools that mimic insulin resistance as observed in humans, it should be kept in mind that these mice bear mutations that are not prevalent in obese humans or NASH patients.

Relevantly, compared to the MCD diet, mice on a choline-deficient L-amino acid-defined (CDAA) diet developed a more severe degree of NASH and fibrosis, while not having any signs of weight loss [54]. Yet, only after long-term feeding, i.e., 5–6 months with CDAA diet, wild-type C57BL/6 mice displayed increased plasma lipid levels and HOMA-IR, pointing towards the development of insulin resistance [55]. It is relevant to note that the combination of CDAA with HFD may be capable of catalysing the development of NASH [54], though humanized features of metabolic disturbances will be absent in this model [11,54].

The American lifestyle induced obesity syndrome (ALIOS) diet is also a frequently used diet, in which high fat is combined with fructose-containing drinking water [56]. Compared to high trans-fat diets without additional fructose, these mice showed increased body weight and reduced insulin sensitivity, whereas no alterations in the degree of steatosis or liver transaminase levels were observed [11,56]. Moreover, in response to ALIOS diet, some pro-fibrogenic genes were found to be increased, while fibrosis was not detectable [56]. However, when mice were additionally administered a low weekly dose of intraperitoneal carbon tetrachloride (CCl_4), these animals were shown to develop progressive stages of human fatty liver disease, ranging from simple steatosis to inflammation, fibrosis, and cancer [57]. Nevertheless, one important limitation of ALIOS is related to its dietary composition, as the amount of trans-fat per kilogram is greater than in commonly used fast foods [56].

Another promising model is the so-called diet-induced animal model of non-alcoholic fatty liver disease (DIAMOND). This model is based on wild-type C57BL/6 mice that were crossed with S129S1/svlmJ, a commonly used model to create mice with targeted mutations. After approximately four months of Western-type diet (42% kcal fat, 0.1% cholesterol, 3.1 g/L d-fructose, 18.9 g/L d-glucose), these mice have shown to recapitulate key physiological and metabolic features of human NASH [58]. However, a limitation of this dietary intervention is the high frequency of HCC development and suppression of cholesterol synthesis, which is substantially different from the human situation [12,58].

While in response to a chow diet, MS-NASH mice [59] (formerly known as FATZO/Pco mice, a cross between wild-type C57BL/6J and obesity-prone AKR/J mice [60]) spontaneously develop obesity [61], feeding these mice a Western-type fructose-supplemented diet resulted in progressive features of NAFLD/NASH [59,62]. Given the concomitant dysregulation in metabolic status, these data point towards a novel tool for studying NAFLD with high translational value.

In summary, the above-described models have provided better insights into NAFLD/NASH pathogenesis. Nevertheless, it is noteworthy that these models failed to consistently achieve the full spectrum of human NASH, thereby limiting its preclinical validity.

2.2. Genetic Murine Models

Genetic animal models are essential for unravelling the underlying mechanisms related to the progression of NAFLD. Besides obesogenic *db/db* [45] and *ob/ob* mice [31,51], other models frequently used to study the total spectrum of human NAFLD and associated complications are based on genetically-modified mice in which the murine *ApoE* gene is being substituted by the human apolipoprotein E2 (APOE2) gene, referred to as the APOE2ki model [63]. Whereas wild-type C57BL/6 mice only developed simple steatosis in response to HFD, APOE2ki mice also displayed early-stage hepatic inflammation [63]. Yet, it is important to note that the inflammatory response did not persist in these mice [63]. Therefore, it is very likely that APOE2 gene is not the main gene responsible for the development of hepatic inflammation [25,63].

Relevantly, a complete lack of the murine *ApoE* gene, i.e., *ApoE*$^{-/-}$ model [64], resulted in hyperlipidemia after feeding these mice a high-fat diet [64]. Yet, under these conditions, mice spontaneously developed atherosclerotic plaques, while lacking humanized lipoprotein profiles [64], which suggests that this model is less suitable for human NAFLD research.

Remarkably, existing knowledge on the low-density lipoprotein receptor (*Ldlr*), an important gene regulating the transport of non-modified lipids into macrophages, led to a major breakthrough in the field of NASH [25,63]. By a complete depletion of the *Ldlr*, mice fed a HFC diet for 3–12 weeks

were able to resemble lifestyle-induced sustained hepatic inflammation [63]. Moreover, these mice displayed high levels of circulating LDL and low levels of HDL, thus closely mimicking the human lipoprotein profile [63]. Hence, this model is considered a physiological model to investigate early onset of NASH [25,63]. While the severity of fibrosis is rather mild, these mice have been shown to develop more fibrosis compared to regular C57BL/6 mice on a similar diet [25,63].

A more recent study investigated the relation between prostaglandin E2 and the severity of NASH, both in a clinical and preclinical context [65]. In general, prostaglandin E_2, a member of the prostaglandin family, is known to play an important role during the inflammatory processes [66,67] in diseases such as rheumatoid arthritis and osteoarthritis [68]. However, its exact role in hepatic inflammation remains unknown. Henkel et al. [65] showed that a deficiency in the expression of enzymes responsible for murine prostaglandin E2 synthesis triggered a tumor necrosis factor α (TNFα)-dependent inflammatory response in the liver, thereby increasing the severity of diet-induced murine NASH. However, given that fibrosis and genotype-specific differences in macrophage infiltration were rather absent [65], it is very likely that the timing of feeding intervention (20 weeks) was not optimal to allow for advanced-stages disease development.

Another well-known model is based on a knock-in of the Patatin-like phospholipase domain-containing 3 (PNPLA3) polymorphism [20], which was found to be present in approximately one-fifth of our population [69,70]. PNPLA3 is a functional enzyme with acyltransferase and/or lipase activity towards phospholipids and/or triglycerides and retinyl esters, respectively [71]. When mice, carrying a mutation at position 148 of the *Pnpla3* gene were fed a high-sucrose diet, animals displayed increased levels of triglycerides and fatty acids, resulting in increased hepatic steatosis [72]. Nevertheless, no significant changes in hepatic inflammatory gene expression or fibrosis were observed [72]. Furthermore, in response to HFD, the development of hepatic steatosis was absent [72]. These data point towards diet as a primary trigger for PNPLA3-polymorphism-associated hepatic steatosis [72], thereby not covering the full spectrum of NAFLD.

Similarly, hepatic knockdown of transmembrane 6 superfamily member 2 (*Tm6sf2*), a gene responsible for regulating hepatic lipid metabolism and associated with increased susceptibility to human NAFLD [73], resulted in increased hepatic fat content and decreased VLDL secretion [74]. Though the specific role of *Tm6sf2* gene is not yet known, these data point towards its contribution to NAFLD development, and hence, its translational applicability. Remarkably, a recent meta-analysis showed that rs58542926 polymorphism significantly associated with chronic liver disease in the overall population [73]. These novel data pointed towards the diagnostic ability of TM6SF2-polymorphism to identify individuals at higher risk for developing NAFLD, cirrhosis, and HCC, as well as alcohol-dependent liver disease [73].

Another recent study investigated the role of Gankyrin (Gank) [75], an oncogene frequently expressed in several types of cancer [76] and a strong driver of liver proliferation. Using mice carrying a liver-specific deletion in Gank, it was shown that feeding a HFD for 6–7 months prevented fibrosis development in $Gank^{-/-}$ mice compared to HFD-fed wild-type mice [75]. While $Gank^{-/-}$ mice showed a higher degree of hepatic steatosis compared to HFD-fed wild-type mice, it has been postulated that hepatic steatosis protects the liver from fibrosis, and therefore liver proliferation could be a trigger for hepatic fibrosis [75]. Hence, the therapeutic potential of inhibiting hepatic proliferation as a strategy against NAFLD should be further investigated.

A more recent genetically-modified model that has become popular in NAFLD research is the obese *foz/foz* mouse model, which carries an 11-base pair truncating mutation in the Alström gene *Alms1* [12,14,77]. *Alms1* is widely expressed and disrupted by mutations in a human obesity syndrome, referred to as Alstroöm syndrome [78]. When feeding a HFD within a time frame of ten months, *foz/foz* mice displayed features of MetS, including obesity, hyperglycemia, hyperlipidemia, and insulin resistance [77]. In addition, these mice spontaneously developed steatosis, hepatic inflammation, and fibrosis [77]. Yet, while all *foz/foz* models have shown to develop obesity, some develop higher NAFLD activity scores and/or fibrosis than others, implying that the severity of NASH in these mice

is inconsistent [14]. Moreover, given that the exact role of *Alms1* is not yet completely understood, the translational character of this model is rather limited.

Another mouse model that spontaneously develops hepatic inflammation with rather a mild degree of fibrosis is the lean polygenetic fatty liver Shionogi (FLS) [79,80]. Remarkably, when backcrossing these mice with *ob/ob* mice, severe liver steatosis, inflammation, advanced fibrosis, and spontaneous HCC appeared to develop [81]. Nevertheless, due to its uncontrollable heterogeneity in disease onset, these models are scarcely used [82].

Other studies have used the hepatocyte-specific phosphatase and tensin homolog (PTEN)-deficient mouse model as a model for NAFLD [83,84]. PTEN, which is a phosphatase with activities towards both protein and lipids, was first discovered as a tumor suppressor protein [85]. More recently, its function as a metabolic regulator, also in the liver, has received increasing attention [85]. Indeed, PTEN-deficient mice were shown to display human-like lipid accumulation followed by liver fibrosis and HCC [83,84]. Nevertheless, these mice do not exhibit obvious human-like NASH features, such as increased circulating fatty acid levels and obesity, thereby limiting its translational potential.

In contrast, others studied the role of augmenter of liver regeneration (*Alr*) in the context of NAFLD [86]. ALR, encoded by Growth Factor ERV1 homolog of *Saccharomyces cerevisiae* (*Gfer*), is an ubiquitous and multifunctional protein [86] that plays a vital role in liver generation, via regulating Natural Killer cell function [87], as well as other liver-related functions [88], including Kupffer cell activation [89]. Though mice deficient for *Alr* were prone to develop excessive hepatic steatosis [86], hepatic lipid accumulation was reversed at 4–8 weeks. Despite reversal of steatosis, mice developed hepatic inflammation, including hepatocellular necrosis, ductal proliferation, and fibrosis, which preceded dysplasia and HCC tumor development by nearly 60% one year after birth [11,86]. Hence, this model could aid in better understanding the progression from hepatic necrosis, inflammation, and fibrosis to carcinogenesis.

Another example is the melanocortin 4 receptor knockout (*Mc4r-/-*) mouse model [90]. MC4R is a G protein-coupled receptor expressed in hypothalamic nuclei being involved in regulating food intake and body weight [90]. Whereas chow-fed *Mc4r-/-* mice were shown to develop late onset obesity, hyperphagia, and simple steatosis due to genetic mutation, feeding a HFD induced ballooning degeneration, hepatic inflammation, and pericellular fibrosis [9]. In line with these results, using MRI-based techniques, Yamada et al. [91] recently showed that *Mc4r-/-* mice fed a HFD for 20 weeks developed obesity and NASH with clear signs of moderate fibrosis. Given their ability to functionally mimic the human NASH disease state, this model holds potential for studying hepatic dysfunction during advanced stages of NASH.

Alternative genetic models to study NASH progression and (spontaneously developing) HCC are the Tsumura-Suzuki Obese Diabetes (TSOD) mice, keratin 18-, NF-κB essential modulator (NEMO)-, and methionine adenosyltransferase 1A (MAT1a)-deficient models [92]. TSOD mice spontaneously developed NAFLD-related features, including T2D, obesity, glucosuria, hyperglycemia, and hyperinsulinemia without any special treatment [93]. Keratin 18 deficiency in mice serves as a model of NASH-associated liver carcinogenesis [94]. Liver-specific deletion of *NEMO* triggered steatosis, NASH, inflammatory fibrosis and subsequently HCC [95]. *Mat1a* gene deletion in mice impaired VLDL synthesis and plasma lipid homeostasis, thereby contributing to NAFLD development [96]. Yet, these models are generally less common and therefore less well-described in literature.

2.3. Chemically-induced Murine Models

As earlier described, alternative ways to explore the progression and/or regression of liver fibrosis and subsequent development of cirrhosis is by targeting the liver with CCL_4 [57] or other chemotoxins, such as thioacetamide (TAA) [8,11,12]. For instance, biweekly administration of CCl_4 for six weeks led to increased circulating aminotransferase and alkaline phosphatase levels in Balb/C mice [97]. In addition, CCL_4 caused a dose-dependent progression of liver fibrosis [97]. However, the exact

pathophysiological mechanism underlying hepatic fibrogenesis, in particular the role of hepatic stellate cells, requires further investigation.

More recently, co-administration of TAA and western-type diet for eight weeks in wild-type C57BL/6 mice was shown to induce hepatic inflammation, severe diffuse fibrosis, and collagen deposition [98]. Nevertheless, due to significant reductions in body weight, these models do not optimally resemble humanized NASH etiology.

One prominent model developed to better understand the progression from NAFLD to HCC is the STAM model, in which neonates received a low dose of streptozotocin, followed by a HFD starting from four weeks of age [99]. At ~6 weeks, ~8–12 weeks, and ~16–20 weeks of age, these mice developed inflammation and hepatocellular ballooning, progressive fibrosis, and HCC, respectively [99]. Concomitantly, these mice had reduced body weight and insulin levels compared to HFD-fed mice [99]. These data imply that NAFLD progression is likely an artificial process that does not accurately reflect human disease pathology, thereby limiting its preclinical potential.

Similar to the clinical situation, many preclinical NAFLD studies in dietary and genetic models demonstrated increased severity in males [100,101]. However, it should be noted that sex differences may vary between models and genotypes [25,102]. For instance, we previously showed that female *Ldlr*$^{-/-}$ and APOE2ki mice fed HFD displayed a very early hepatic inflammatory response [25]. Similarly, it was demonstrated that female C57BL/6 wild-type mice fed a high-fructose diet developed greater hepatic inflammation despite having similar liver steatosis as compared to male mice [103]. Other studies showed that female juvenile NAFLD/NASH models displayed hepatic oxidative stress, whereas male animals rather developed hepatic inflammation [104]. In line with these results, it was more recently shown that high fat intake (60% kcal and 34.9% g fat, 20% kcal and 26.2% g protein, and 20% kcal and 26.3% g carbohydrate) by juvenile female mice contributed to NAFLD development, whereas similar fat intake by maternal-offspring (i.e., high-fat intake two weeks before conception and during gestation and lactation) resulted in the successful establishment of NASH [105]. These data suggest that maternal exposure, as well as the HFD component, contribute to the degree of NAFLD disease severity in juvenile female offspring [105].

2.4. Other Murine Models

Besides a role for genetic and dietary factors in preclinical NAFLD development, recent focus has also discretely shifted towards the relevance of housing conditions, thereby introducing a novel concept of thermoneutral housing (30–32 °C) [106]. Compared to standard housing conditions, mice housed under thermoneutral conditions were not only shown to induce a pro-inflammatory immune response, but also to deteriorate HFD-induced NASH progression [106]. Additionally, mice displayed increased intestinal permeability and alterations in gut microbiome, features mimicking the human situation [106]. Although these hallmarks could also partially refute the sex bias that is often observed in murine models of NAFLD, there were no signs of hepatic fibrosis, neither in male nor in female C57BL/6 wild-type mice [106]. Altogether, these data propose that a dietary stimulus is prerequisite for liver fibrosis development.

It is well-known that the liver is a central metabolic organ, whose functions are capable of adapting to rhythmical changes of environment. Indeed, it has been previously shown that circadian rhythm is driving oscillations in hepatic triglyceride levels, inflammation, oxidative stress, mitochondrial dysfunction, and hepatic insulin resistance [107,108]. Moreover, it has been recently suggested that chronic disruption of circadian rhythm may spontaneously induce the progression from NAFLD to NASH, fibrosis, and HCC [20,109], similar to the human situation, pointing towards its translational value.

Last but not least, there has also been increased awareness on the validity and reproducibility of preclinical studies on NAFLD [110–112]. For instance, it has been shown that murine liver fibrosis is affected by sampling variation [8]. More recently, Jensen et al. [2] demonstrated that feeding wild-type C57BL/6 mice a high-fat/high-fructose/high-cholesterol diet (40%/20%/2%) for 16 weeks

resulted in significant intraindividual differences in fibrosis score and several hepatic biomarkers. Nevertheless, differences in sample variation were absent in other routinely used NAFLD rodent models [2]. These data pointed towards the importance of standardizing sampling site location during preclinical liver biopsy procedures, thereby supporting the ability to compare experimental outcomes between individual murine NASH studies.

2.5. Rat NAFLD Models

In addition to the importance of murine models, preclinical studies on NAFLD pathogenesis are also frequently performed using rats. Rat models are thought to be more susceptible to HFD, and thus may display more severe and/or earlier histological features of NAFLD compared to mice [113]. A small selection of rat studies on NAFLD will be highlighted in this section.

Similar to mice, commonly used rat models refer to nutritional, genetic, and combined models (extensively reviewed elsewhere [114,115]), of which Sprague–Dawley [116,117], Wistar [118], and/or diabetic Zucker rats (fa/fa) [119] are well-known examples. For instance, Lieber et al. [120] and others [117] reported that Sprague–Dawley rats on a HFD (71% fat/11% carbohydrates/18% proteins) were able to develop insulin resistance, mild-to-marked steatosis, inflammation and/or fibrogenesis, thereby reproducing key features of human NASH. Yet, when fed a standard Lieber–DeCarli diet (35% fat, 47% carbohydrates, 18% proteins), rats displayed no signs of steatosis, inflammation, or fibrosis [120]. Diabetic Zucker rats, a well-characterized model of NAFLD, displayed similar features as its murine counterparts *ob/ob* and *db/db* mice, i.e., spontaneous development of severe obesity, steatosis, and insulin resistance [11]. Moreover, it was shown that Zucker rats are in need of an additional stimulus for onset of NASH [119]. Relevantly, when comparing 4 weeks of MCD diet between different rat models (i.e., Wistar, Long–Evans, and Sprague–Dawley rats), the Wistar strain was associated with the highest degree of hepatic fat accumulation [121], pointing either towards strain-dependency or the impact of dietary exposure time.

Altogether, rat models are useful tools for providing additional valuable insights into the complex pathogenesis of steatosis/NASH (but not HCC), even though dietary or chemical interventions in these animals do not fully resemble the human situation.

3. Therapeutic Approaches in Preclinical NAFLD Models

In addition to exploring NAFLD etiology, preclinical models are critically important for testing how potential therapeutic drugs can interfere with the progression of this chronic disease [115].

Previously, Zheng et al. [27] chronically exposed HFC-treated mice with Ezetimibe, which is known to reduce plasma LDL by selectively binding to the intestinal cholesterol transporter Niemann–Pick type C1-like 1. After four weeks of Ezetimibe, significant improvements in fatty liver were observed, which were associated with a decrease in hepatic triglycerides, cholesteryl esters, and free cholesterol [27]. Additionally, chronic treatment with Ezetimibe resulted in significant reductions in plasma ALT activity, pointing towards its ability to serve as a novel treatment for HFC-induced NAFLD [27].

Trevaskis et al. [51] treated HFD-induced wild-type C57BL/6 and *ob/ob* mice with GLP-1R agonist AC3174, an exenatide analog. AC3174 treatment significantly reduced intrahepatic lipid accumulation, plasma triglycerides, and ALT levels, likely due to its contribution in weight loss [51]. Additionally, data suggested that AC3174 modestly improved the histological severity of fibrosis, which was demonstrated by a decrease in liver collagen-1 protein. Altogether, these findings suggest that AC3174 may play a beneficial role in the treatment of key aspects of fibrotic NASH.

Domitrovic et al. [97] investigated the therapeutic effect of luteolin in the context of liver fibrosis. Luteolin is a member of the flavonoid family, which has shown to exhibit hepatoprotective activity in acute liver damage, amongst others [122]. Administration of luteolin to CCL_4-treated mice resulted in a dose-dependent reduction in hepatic fibrosis [97]. Although studies on the impact of luteolin in a more chronic model of liver fibrosis are desired, these data pointed towards therapeutic application of this drug in patients with hepatic fibrosis [97]. Similarly, in a study of Ganbold et al. [3], it was recently

shown that administration of isorhamnetin, another natural flavonoid to human-like NASH mice, resulted in improved steatosis, liver injury, and fibrosis, pointing towards its therapeutic potential in NASH.

More recently, Khurana et al. [117] studied the role of inhibiting extracellular cathepsin D, a lysosomal enzyme that plays a role in lipid-related disorders, including NAFLD [123,124]. Using HFD-fed Sprague–Dawley rats, it was shown that inhibition of extracellular cathepsin D improved hepatic steatosis and reduced plasma levels of insulin and hepatic transaminases [117]. These data suggest that modulation of extracellular cathepsins may serve as a novel therapeutic modality for NAFLD [117].

Gehrke et al. [125] recently investigated eight to ten week-old wild-type C57BL/6 male mice that were fed an obesogenic diet (fructose/glucose supplementation in drinking water). In this study, mice were either challenged with voluntary wheel running or were kept on a sedentary lifestyle intervention [125]. Similar to well-known forced exercise models [126], voluntary wheel running protected these mice from HFD-induced pro-inflammatory and pro-fibrogenic states, as shown by decreased hepatic macrophage infiltration and improved fatty acid and glucose homeostasis. These data were in line with Kawanishi et al. [126], showing that exercise training reduced macrophage infiltration and adipose tissue inflammation by attenuating neutrophil infiltration in HFD-fed C57BL/6 mice. Thus, it is very likely that physical exercise exhibits beneficial effects and compensates for shortcomings of certain therapeutic approaches [125,126].

Table 1. Overview of commonly used dietary, genetic, chemically-induced, and other murine models of non-alcoholic steatohepatitis (NASH).

Type of Mouse Model	Treatment or Intervention	Phenotypical Outcome and Relevance to Human Disease	Author(s)
Dietary Models			
High-fat diet (HFD)	HFD containing 60% fat administered to C57BL6/J	After 10-12w, induction of obesity, insulin resistance and hyperlipidemia. After long-term exposure (36w), no or only minimal signs of inflammation and fibrosis. After chronic feeding (80w), hepatic steatosis, cell injury, portal & lobular inflammation and fibrosis.	Velázquez et al. [17], Ito et al. [19], Chen et al. [20], Vonghia et al. [21]
Atherogenic diet	Diet containing 1.25% cholesterol and 0.5% cholate	Increased plasma and liver lipid levels. From 6–24 weeks, induction NASH with hepatocellular ballooning in a time-dependent manner.	Matsuzawa et al. [24]
High-fat atherogenic diet	HFD containing 1.25% cholesterol and 0.5% cholate	Exacerbated NASH features including hepatic insulin resistance, oxidative stress, activation of hepatic stellate cells.	Matsuzawa et al. [24], Montandon et al. [41], Larter et al. [42]
High-fat/high-cholesterol diet (HFC)	HFC containing 21% milk butter, 0.2% cholesterol	After short-term HFC diet, only steatosis in C57BL/6 mice. Steatosis with severe inflammation in female *Ldlr*$^{-/-}$ and APOE2ki hyperlipidemic mice. After seven days, severe hepatic inflammation but no steatosis in male hyperlipidemic mice. After seven months, development of obesity, hepatomegaly, hepatic steatosis and varying degrees of steatohepatitis in C57BL/6 mice.	Wouters et al. [25,26] Zheng et al. [27]
High-fat/high-cholesterol/ high-fructose diet (AMLN)	Diet containing 40% high-fat and 22% fructose, supplemented with ~18% trans-fat and 2% cholesterol	After 26–30w, marked steatosis, moderate lobular inflammation and hepatocellular ballooning in C57BL/6 and *ob/ob* mice.	Clapper et al. [28], Kristiansen et al. [29]

Table 1. *Cont.*

Type of Mouse Model	Treatment or Intervention	Phenotypical Outcome and Relevance to Human Disease	Author(s)
Gubra amylin diet (GAN)	High-fat (40 kcal-%, of which 0% trans-fat and 46% saturated fatty acids by weight), fructose (22%), sucrose (10%), cholesterol (2%)	After 8-16w, more pronounced weight gain and a highly similar phenotype of biopsy-confirmed fibrotic NASH in C57BL/6 and *ob/ob* mice.	Boland et al. [33]
High-fat/high-fructose/ high-cholesterol	Composed of 41% fat, 30% fructose, 2% cholesterol	Induction NASH in various models.	Abe et al. [34], Kennedy et al. [35], Suto et al. [36]
Soybean-oil-based Western-type diet	Western-type diet containing 25g/100 g n-6-PUFA-rich soybean oil +/- 0.75% cholesterol	After long-term exposure (20w), hepatic steatosis, inflammation and fibrosis, weight gain, insulin resistance, hepatic lipid peroxidation and oxidative stress in C57BL/6 mice.	Henkel et al. [37]
High-caloric cholesterol-free HFD	Composed of lard (21g/100g)/soy-bean oil (3g/100g)/5% fructose in drinking water	Only mild steatosis. No signs of hepatic inflammation and fibrosis.	Wouters et al. [25,26], Henkel et al. [37], Subramanian et al. [38], Mari et al. [39], Savard et al. [40]
Choline-deficient diet	C57BL/6 mice were fed HFD (45% of calories) for 8 weeks. During the final 4 weeks, diets were choline-deficient (or choline-supplemented)	Amplified liver fat accumulation, while improved glucose tolerance.	Raubenheimer et al. [48]
Methionine/choline-deficient diet (MCD)	Diet lacking methionine and choline, but containing high sucrose (40%) and moderate fat (10%)	After 2w, severe steatohepatitis with elevated serum AST and ALT levels. After 10w, additional Kupffer cell infiltration and irreversible fibrosis. After 1.5-4w, no signs of insulin resistance.	Santhekadur et al. [12], Montandon et al. [41], Itagaki et al. [47], Rinella et al. [52], Al Rajabi et al. [53]
Choline-deficient L-amino acid-defined diet (CDAA)	Choline-deficient L-amino acid-defined diet containing carbohydrates (68,5%), proteins (17,4%) and fats (14%)	Within a few weeks, fatty liver followed by mild features of NASH in C57BL/6J mice. After >20w, mild-to-moderate fibrosis and insulin resistance.	Van Herck et al. [11], Matsumoto et al. [54], Miura et al. [55]
Choline-deficient L-amino acid-defined diet on high-fat diet (CDAHFD)	Choline-deficient, L-amino acid-defined, HFD consisting of 60 kcal% fat and 0.1% methionine by weight	Excessive liver fat accumulation, increased circulating liver enzymes and progressive hepatic fibrosis.	Matsumoto et al. [54]
High-fat/high-fructose diet (ALIOS)	HFD with fructose-containing drinking water. Additional administration of a low weekly dose of intraperitoneal carbon tetrachloride (CCl_4)	After 16w, substantial steatosis with necro-inflammatory changes and increased ALT levels. No difference in steatosis degree or ALT levels if compared to without additional fructose. Development of progressive stages of human-like fatty liver disease.	Tetri et al. [56], Tsuchida et al. [57]
Diet-induced animal model of non-alcoholic fatty liver disease (DIAMOND)	High fat/carbohydrate diet (Western diet) with 42% kcal from fat, containing cholesterol (0.1%), with a high fructose/glucose solution (23.1 g/L d-fructose +18.9 g/L d-glucose)	After 16w, obesity, liver injury, dyslipidemia and insulin resistance, sustained up to 52w. Parent strains 129S1/SvImJ or C57BL/6 lacked insulin resistance and steatohepatitis or developed delayed insulin resistance.	Santhekadur et al. [12], Asgharpour et al. [58]

Table 1. *Cont.*

Type of Mouse Model	Treatment or Intervention	Phenotypical Outcome and Relevance to Human Disease	Author(s)
High-fat diet + glucose/ fructose-enriched drinking water	Obesogenic diet containing ((35.5% w/w) crude fat (58 kJ%), 22.8 MJ/kg = 5.45 kcal/g) and fructose (55% w/v) and glucose (45% w/v) enriched drinking water. After 8 weeks of dietary feeding, mice were randomly assigned to a voluntary wheel running group or a sedentary group.	Voluntary wheel running prevented HFD-induced pro-inflammatory / fibrogenic states in C57BL/6 mice. Hepatic steatosis was prevented by alterations in key liver metabolic processes.	Gehrke et al. [125]
Genetic Models			
Leptin deficiency (*ob/ob*)	Leptin-deficient (*ob/ob*) mice are predisposed to develop NASH and fibrosis, whereas not when maintained on regular chow diet. Treatment with high-fat/high-fructose/ high-cholesterol diet.	Lack the ability to spontaneously develop hepatic inflammation. After 12-26w, increased adiposity, total cholesterol and elevated plasma liver enzymes upon diet high in trans-fat (40%), fructose (22%) and cholesterol (2%). After treatment with high-fat/high-fructose/high-cholesterol diet, development of metabolic, histologic and transcriptomic features similar to human NASH.	Kristiansen et al. [29], Abe et al. [34], Trevaskis et al. [51]
Leptin resistance (*db/db*)	*db/db* mice are deficient in the leptin receptor, with dramatic elevations in circulating leptin concentrations. Dietary intervention with an MCD diet for 4 weeks.	Lack the ability to spontaneously develop hepatic inflammation and thus needs to be combined with a nutritional model for NASH. After 4w MCD diet, mice displayed marked hepatic inflammation and fibrosis.	Kennedy et al. [35], Sahai et al. [45], Hummel et al. [50]
MS-NASH (FATZO/Pco)	Mice spontaneous development of obesity	After 20w of fructose-supplemented diet, hepatic steatosis, lobular inflammation, ballooning and fibrosis.	Sun et al. [62]
Apolipoprotein E2 knock-in (APOE2)	Murine ApoE replaced by the human APOE2 gene	After 12w of HFC, steatosis in conjunction with early but not sustained hepatic inflammation.	Wouters et al. [25,26], Bieghs et al. [63]
ApoE deficiency (*ApoE*$^{-/-}$)	Complete deficiency in the murine ApoE gene	After 7w of Western diet, abnormal glucose tolerance, hepatomegaly, weight gain and full spectrum of NASH, while lacking humanized lipoprotein profiles.	Schierwagen et al. [64]
Low-density lipoprotein receptor deficiency (*Ldlr*$^{-/-}$)	Complete deficiency of the murine Ldl receptor, an important gene regulating the transport of non-modified lipids into macrophages	After 3-12w of HFC diet, resemblance to lifestyle-induced early-onset hepatic inflammation. High and low levels of circulating LDL and HDL, respectively, closely mimicked the human lipoprotein profile. Development of mild fibrosis.	Wouters et al. [25,26], Bieghs et al. [63]
Microsomal prostaglandin E synthase 1 (mPGES1) deficiency	Mice with global deletion of mPGES-133 were backcrossed on C57BL/6J	TNFα-dependent inflammatory response in murine liver. Increased severity of diet-induced murine NASH.	Henkel et al. [65]
Patatin-like phospholipase domain-containing 3 (PNPLA-3) knock-in	Mice carried I148M mutation in the Pnpla3 gene and were fed a high-sucrose or HFD diet for 4 weeks	Accumulation of PNPLA3 on lipid droplets. Development of hepatic steatosis.	Smagris et al. [72]
Transmembrane 6 superfamily member 2 knockdown (mTm6s2-shRNA8)	Adeno-associated virus-mediated short hairpin RNA knockdown of Tm6sf2 in liver of C57BL/6J mice	Increased hepatic fat content and decreased VLDL secretion, recapitulating the effects observed in humans carrying the TM6SF2-167Lys mutation	Kozlitina et al. [74]

Table 1. *Cont.*

Type of Mouse Model	Treatment or Intervention	Phenotypical Outcome and Relevance to Human Disease	Author(s)
Gankyrin liver-specific knockout (GLKO)	Cre-Alb mice were backcrossed with LoxP-Gank mice	Gankyrin generally drives liver proliferation. After 6-7 months of HFD, higher degree of hepatic steatosis but prevention of fibrosis development in GLKO mice compared to wild-type mice.	Cast et al. [75]
Truncated mutation in Alström (Alms1) gene (*foz/foz*)	11-base pair truncating mutation in the Alström gene ALMS1. Lack of knowledge regarding the exact role of Alms1	After 6 months of HFD, MetS features, including obesity, hyperglycemia / lipidemia and insulin resistance. Mice spontaneously develop steatosis, hepatic inflammation and fibrosis.	Santhekadur et al. [12], Jiang et al. [14], Arsov et al. [77]
Fatty liver Shionogi	Spontaneous development of hepatic inflammation with rather a mild degree of fibrosis. Uncontrollable heterogeneity in disease onset	Backcrossing with *ob/ob* mice resulted in severe liver steatosis, inflammation, advanced fibrosis and spontaneous HCC	He et al. [82]
Hepatocyte-specific phosphatase and tensin homolog deficiency ($Pten^{-/-}$)	PTEN deficiency specific in the liver	After 40w of age, steatosis, inflammation and fibrosis in the liver. After 74-78w of age, HCC was present in 83% of males and 50% of female mice.	Watanabe et al. [83], Takakura et al. [84]
Augmenter of liver regeneration knock-out ($Alr^{-/-}$)	Liver-specific deletion of augmenter of liver regeneration	4-8w after birth, steatohepatitis with hepatocellular necrosis, ductular proliferation and fibrosis. 1y after birth, HCC in nearly 60% of the mice	Van Herck et al. [11], Gandhi et al. [89]
Melanocortin 4 receptor knockout ($Mc4r^{-/-}$)	Mice with targeted disruption of melanocortin 4 receptor, which is a seven-transmembrane G protein–coupled receptor that is expressed in the hypothalamic nuclei	Development of simple steatosis. Upon feeding HFD, development of human-like NASH, including obesity, insulin resistance and dyslipidemia. After 20w HFD, obesity and NASH with clear signs of moderate fibrosis, functionally mimicking the human NASH disease state.	Itoh et al. [90], Yamada et al. [91]
Chemically-induced Models			
Carbon tetrachloride (CCL_4)	Biweekly injections of CCl_4	After 6w, increased circulating liver enzymes and dose-dependent progression of liver fibrosis in Balb/C mice	Domitrovic et al. [97]
Thioacetamide (TAA)	Three times/week IP injection thioacetamide (75mg/kg) in combination with western-type diet	After 8w, hepatic inflammation, severe diffuse fibrosis and collagen deposition in C57BL/6 mice	Hansen et al. [8] Van Herck et al. [11] Santhekadur et al. [12]
Streptozotocin + high-fat diet (STAM)	200 µg streptozotocin at 2 days after birth and feeding ad libitum with high-fat diet at 4 weeks of age	Between 6-20w of age, hepatic inflammation, hepatocellular ballooning, progressive fibrosis and HCC. Reduced body weight and insulin levels compared to HFD-fed mice	Fujii et al. [99]
Other models			
C57BL/6 background	Mice were housed in separate specific pathogen-free units maintained at either 22°C (standard) or 30-33°C (thermoneutral)	After 24w of thermoneutral housing, exacerbated HFD-driven NAFLD pathogenesis. Increased intestinal permeability and alterations in gut microbiome, mimicking the human situation.	Giles et al. [106]
C57BL/6 background	Juvenile NASH model: immediately after weaning, mice were fed HFC diet for a total of 16 weeks (4, 8, 12 and 16 weeks of diet)	Hepatic oxidative stress in female juvenile NAFLD/NASH models, whereas hepatic inflammation in males	Marin et al. [104]

Table 1. *Cont.*

Type of Mouse Model	Treatment or Intervention	Phenotypical Outcome and Relevance to Human Disease	Author(s)
C57BL/6 background	Juvenile NAFLD/NASH model: HFD were administered 2 weeks before conception and during gestation and lactation	Offspring HFC intake resulted in NAFLD, maternal-offspring fat intake contributed to NASH in juvenile female mice	Zhou et al. [105]
Models with circadian oscillations (e.g., *Per1/2*$^{-/-}$ or liver-specific *Bmal1* knockout mice)	The effects of feeding time and circadian clocks on murine liver	Circadian rhythm drives oscillations in hepatic triglyceride levels, inflammation, oxidative stress, mitochondrial dysfunction and hepatic insulin resistance. Chronic disruption of circadian rhythm may spontaneously induce the progression from NAFLD to NASH, fibrosis and HCC	Adamovich et al. [107], Jacobi et al. [108], Kettner et al. [109]
C57BL/6 background	Mice (and other rodent models) were fed a high-fat/high-fructose/ high-cholesterol for 16 weeks	Significant intraindividual differences in fibrosis score and hepatic biomarkers pointed towards the importance of standardizing sampling site location during preclinical liver biopsy procedures	Jensen et al. [2]

4. Clinical Relevance: Comparisons with Clinical Data

In general, NAFLD is considered the hepatic manifestation of MetS. Consequently, well-established therapeutic compounds against T2D and impaired lipid metabolism are thought to exert beneficial effects that mitigate the pathological features of NASH. One such example is the nuclear receptor peroxisome proliferator-activated receptor (PPAR) (extensively reviewed elsewhere [127]), due to its involvement in regulating lipid metabolism and inflammation. For instance, it was previously shown that hepatic *Pparα* inversely correlated with insulin resistance and NASH severity [128]. Remarkably, in this clinical study, histological improvements were positively associated with *Pparα* expression in patients with NASH [128], pointing towards the therapeutic potential of PPARα-agonists. Fibrates, which activate PPARα, are the most effective class of agents for lowering elevated triglyceride-rich lipoproteins [129]. While fenofibrate did not ameliorate liver histology in biopsy-proven NAFLD, a selective PPARα agonist, also known as Pemafibrate, did improve liver function in patients with dyslipidemia [130], which was previously established in diet-induced murine models of NAFLD [131].

Another isoform of PPAR, PPAR-δ, is involved in dyslipidemia and activation of PPAR-δ by means of a selective agonist, referred to as seladelpar (MBX-8025), beneficially affected plasma lipid levels and showed favorable trends in insulin resistance and waist circumference in patients with dyslipidemia [132]. More recently, these data were further supported using in-vivo studies, showing that seladelpar improved glucose metabolism, as well as plasma and hepatic lipid levels in obese *foz/foz* mice [133]. Collectively, these data pointed towards seladelpar as a potential novel therapy for NASH.

Another strategy is based on insulin-sensing drugs, known as Thiazolidinediones, which target the PPAR-γ isoform [134]. Examples of PPAR-γ agonists are lobeglitazone, pioglitazone, and rosiglitazone, of which the latter two are currently off-label and off-market, respectively [127]. When diabetic patients with NAFLD were treated with lobeglitazone, patients showed improvements in hepatic steatosis, glycemic, and lipid profiles, as well as liver enzyme levels [134]. In line, it was shown that HFD-induced obese mice treated with lobeglitazone improved glucose homeostasis as well as hepatic and plasma lipid levels [135]. Hence, these data pointed towards lobeglitazone as a potential treatment option for NAFLD.

Relevantly, the use of elafibranor (dual PPAR-α/δ agonist, clinical phase III trial) as a single drug regime is thought to be promising with regard to NASH, as shown by significant improvements of human NASH pathology without deteriorating hepatic fibrosis [136]. These data were further corroborated by findings in rodent studies of NAFLD [137]. Additionally, the development of anti-fibrotic therapies has recently received increasing attention [138]. Therefore, due to its multifactorial

character, current treatment modalities should focus on both the reversal of NASH [139] and fibrosis [138].

Strategies, which currently hold clinical potential in late-stage drug development, include specific complementary agonists, i.e., for PPAR receptor subtypes and farnesoid X receptor (FXR) [139]. Using AMLN diet-induced obese mice with biopsy-confirmed NASH, Roth et al. [139] demonstrated that combined treatment with Elafibrinor and obeticholic acid (FXR agonist) significantly ameliorated histological features of steatosis, inflammation and fibrosis. Additionally, compared to single regimens, combined treatment targeted hepatic molecular mechanisms, thereby further improving NASH and fibrogenesis [139].

To conclude, in addition to the selective—but relevant—approaches described above, additional therapeutic options for NAFLD have been studied in preclinical and/or clinical settings [16], or are currently under investigation.

5. Conclusions

Although current preclinical NAFLD models can be considered indispensable tools for studying chronic liver disease pathology, it should be noted that the majority of existing rodent models mainly focus on certain stages of the disease rather than the total spectrum. Additionally, it is noteworthy that the NAFLD disease progression greatly varies across different strains [140]. Therefore, depending on its research question, careful model selection is highly recommended. Such selection should also properly consider sex, age, and hormonal status and must be based on prior knowledge, as it will have a large impact on data interpretation and its translational potential. Thus, our common goal is to establish an ideal preclinical model that—in addition to developing hepatic inflammation and fibrosis, along with obesity, high cholesterol, and insulin resistance—also responds to promising therapeutic interventions. This implies that future studies should continue focusing on recapitulating the multifactorial character of human NAFLD in preclinical models.

Author Contributions: Conceptualization, writing—original draft preparation and writing—review and editing, figure preparation, Y.O. and R.S.-S.; funding acquisition, R.S.-S. All authors have read and agreed to the published version of the manuscript.

Funding: This research was funded by the Dutch Organization for Scientific Research (NWO; VIDI grant no. 016.126.327), ASPASIA (grant no. 015.008.043) and TKI-LSH (grant no. 40-41200-98-9306).

Conflicts of Interest: The authors declare no conflict of interest.

Abbreviations

ALIOS	American Lifestyle Induced Obesity Syndrome
ALMS1	Alström
ALR	Augmenter of liver regeneration
APOE2ki	Apolipoprotein E2 knock-in
CCl_4	Carbon tetrachloride
CD	Diet deficient for/low in choline
CDAA	Choline-deficient L-amino acid-defined diet
DIAMOND	Diet-induced animal model of non-alcoholic fatty liver disease
FLS	Fatty liver Shionogi
FXR	Farnesoid X receptor
Gank	Gankyrin
GFER	Growth Factor ERV1 homolog of *Saccharomyces cerevisiae*
HCC	Hepatocellular carcinoma
HFC	High-fat/high-cholesterol diet
HFD	High-fat diet
Ldlr	Low-density lipoprotein receptor
MAT1a	methionine adenosyltransferase 1A

MC4R	Melanocortin 4 receptor
MetS	Metabolic Syndrome
MS-NASH	Mice formerly known as FATZO/Pco
NAFLD	Non-alcoholic fatty liver disease
NASH	Non-alcoholic steatohepatitis
NEMO	NF-κB essential modulator
PNPLA3	Patatin-like phospholipase domain-containing 3
PPAR	Peroxisome proliferator-activated receptor
PTEN	Phosphatase and tensin homolog
T2D	Type 2 Diabetes
TAA	Thioacetamide
TM6SF2	Transmembrane 6 superfamily member 2
TNFα	Tumor necrosis factor α
TSOD	Tsumura-Suzuki Obese Diabetes

References

1. Younossi, Z.M.; Golabi, P.; de Avila, L.; Paik, J.M.; Srishord, M.; Fukui, N.; Qiu, Y.; Burns, L.; Afendy, A.; Nader, F. The global epidemiology of NAFLD and NASH in patients with type 2 diabetes: A systematic review and meta-analysis. *J. Hepatol.* **2019**, *71*, 793–801. [CrossRef] [PubMed]
2. Jensen, V.S.; Tveden-Nyborg, P.; Zacho-Rasmussen, C.; Quaade, M.L.; Ipsen, D.H.; Hvid, H.; Fledelius, C.; Wulff, E.M.; Lykkesfeldt, J. Variation in diagnostic NAFLD/NASH read-outs in paired liver samples from rodent models. *J. Pharmacol. Toxicol. Methods* **2019**, *101*, 106651. [CrossRef] [PubMed]
3. Ganbold, M.; Owada, Y.; Ozawa, Y.; Shimamoto, Y.; Ferdousi, F.; Tominaga, K.; Zheng, Y.W.; Ohkohchi, N.; Isoda, H. Isorhamnetin Alleviates Steatosis and Fibrosis in Mice with Nonalcoholic Steatohepatitis. *Sci. Rep.* **2019**, *9*, 16210. [CrossRef] [PubMed]
4. Li, B.; Zhang, C.; Zhan, Y.T. Nonalcoholic Fatty Liver Disease Cirrhosis: A Review of Its Epidemiology, Risk Factors, Clinical Presentation, Diagnosis, Management, and Prognosis. *Can. J. Gastroenterol. Hepatol.* **2018**, *2018*, 2784537. [CrossRef] [PubMed]
5. Anstee, Q.M.; Reeves, H.L.; Kotsiliti, E.; Govaere, O.; Heikenwalder, M. From NASH to HCC: Current concepts and future challenges. *Nat. Rev. Gastroenterol. Hepatol.* **2019**, *16*, 411–428. [CrossRef] [PubMed]
6. Wong, R.J.; Cheung, R.; Ahmed, A. Nonalcoholic steatohepatitis is the most rapidly growing indication for liver transplantation in patients with hepatocellular carcinoma in the U.S. *Hepatology* **2014**, *59*, 2188–2195. [CrossRef]
7. Younossi, Z.M.; Loomba, R.; Anstee, Q.M.; Rinella, M.E.; Bugianesi, E.; Marchesini, G.; Neuschwander-Tetri, B.A.; Serfaty, L.; Negro, F.; Caldwell, S.H.; et al. Diagnostic modalities for nonalcoholic fatty liver disease, nonalcoholic steatohepatitis, and associated fibrosis. *Hepatology* **2018**, *68*, 349–360. [CrossRef]
8. Hansen, H.H.; Feigh, M.; Veidal, S.S.; Rigbolt, K.T.; Vrang, N.; Fosgerau, K. Mouse models of nonalcoholic steatohepatitis in preclinical drug development. *Drug Discov. Today* **2017**. [CrossRef]
9. Haczeyni, F.; Yeh, M.M.; Ioannou, G.N.; Leclercq, I.A.; Goldin, R.; Dan, Y.Y.; Yu, J.; Teoh, N.C.; Farrell, G.C. Mouse models of non-alcoholic steatohepatitis: A reflection on recent literature. *J. Gastroenterol. Hepatol.* **2018**, *33*, 1312–1320. [CrossRef]
10. Lau, J.K.; Zhang, X.; Yu, J. Animal models of non-alcoholic fatty liver disease: Current perspectives and recent advances. *J. Pathol.* **2017**, *241*, 36–44. [CrossRef]
11. Van Herck, M.A.; Vonghia, L.; Francque, S.M. Animal Models of Nonalcoholic Fatty Liver Disease-A Starter's Guide. *Nutrients* **2017**, *9*, 1072. [CrossRef] [PubMed]
12. Santhekadur, P.K.; Kumar, D.P.; Sanyal, A.J. Preclinical models of non-alcoholic fatty liver disease. *J. Hepatol.* **2018**, *68*, 230–237. [CrossRef] [PubMed]
13. Jahn, D.; Kircher, S.; Hermanns, H.M.; Geier, A. Animal models of NAFLD from a hepatologist's point of view. *Biochim. Biophys. Acta Mol. Basis Dis.* **2019**, *1865*, 943–953. [CrossRef] [PubMed]
14. Jiang, M.; Wu, N.; Chen, X.; Wang, W.; Chu, Y.; Liu, H.; Li, W.; Chen, D.; Li, X.; Xu, B. Pathogenesis of and major animal models used for nonalcoholic fatty liver disease. *J. Int. Med. Res.* **2019**, *47*, 1453–1466. [CrossRef] [PubMed]

15. Palladini, G.; Di Pasqua, L.G.; Berardo, C.; Siciliano, V.; Richelmi, P.; Perlini, S.; Ferrigno, A.; Vairetti, M. Animal Models of Steatosis (NAFLD) and Steatohepatitis (NASH) Exhibit Hepatic Lobe-Specific Gelatinases Activity and Oxidative Stress. *Can. J. Gastroenterol. Hepatol.* **2019**, *2019*, 5413461. [CrossRef]
16. Zhong, F.; Zhou, X.; Xu, J.; Gao, L. Rodent Models of Nonalcoholic Fatty Liver Disease. *Digestion* **2019**, 1–14. [CrossRef]
17. Velazquez, K.T.; Enos, R.T.; Bader, J.E.; Sougiannis, A.T.; Carson, M.S.; Chatzistamou, I.; Carson, J.A.; Nagarkatti, P.S.; Nagarkatti, M.; Murphy, E.A. Prolonged high-fat-diet feeding promotes non-alcoholic fatty liver disease and alters gut microbiota in mice. *World J. Hepatol.* **2019**, *11*, 619–637. [CrossRef]
18. Jacobs, A.; Warda, A.S.; Verbeek, J.; Cassiman, D.; Spincemaille, P. An Overview of Mouse Models of Nonalcoholic Steatohepatitis: From Past to Present. *Curr. Protoc. Mouse Biol.* **2016**, *6*, 185–200. [CrossRef]
19. Ito, M.; Suzuki, J.; Tsujioka, S.; Sasaki, M.; Gomori, A.; Shirakura, T.; Hirose, H.; Ito, M.; Ishihara, A.; Iwaasa, H.; et al. Longitudinal analysis of murine steatohepatitis model induced by chronic exposure to high-fat diet. *Hepatol. Res.* **2007**, *37*, 50–57. [CrossRef]
20. Chen, K.; Ma, J.; Jia, X.; Ai, W.; Ma, Z.; Pan, Q. Advancing the understanding of NAFLD to hepatocellular carcinoma development: From experimental models to humans. *Biochim. Biophys. Acta Rev. Cancer* **2019**, *1871*, 117–125. [CrossRef]
21. Vonghia, L.; Ruyssers, N.; Schrijvers, D.; Pelckmans, P.; Michielsen, P.; De Clerck, L.; Ramon, A.; Jirillo, E.; Ebo, D.; De Winter, B.; et al. CD4+ROR gamma t++ and Tregs in a Mouse Model of Diet-Induced Nonalcoholic Steatohepatitis. *Mediators Inflamm.* **2015**, *2015*, 239623. [CrossRef] [PubMed]
22. Chen, Y.H.; Chiu, C.C.; Hung, S.W.; Huang, W.C.; Lee, Y.P.; Liu, J.Y.; Huang, Y.T.; Chen, T.H.; Chuang, H.L. Gnotobiotic mice inoculated with Firmicutes, but not Bacteroidetes, deteriorate nonalcoholic fatty liver disease severity by modulating hepatic lipid metabolism. *Nutr. Res.* **2019**, *69*, 20–29. [CrossRef] [PubMed]
23. Raman, M.; Ahmed, I.; Gillevet, P.M.; Probert, C.S.; Ratcliffe, N.M.; Smith, S.; Greenwood, R.; Sikaroodi, M.; Lam, V.; Crotty, P.; et al. Fecal microbiome and volatile organic compound metabolome in obese humans with nonalcoholic fatty liver disease. *Clin. Gastroenterol. Hepatol.* **2013**, *11*, 868–875 e861-863. [CrossRef] [PubMed]
24. Matsuzawa, N.; Takamura, T.; Kurita, S.; Misu, H.; Ota, T.; Ando, H.; Yokoyama, M.; Honda, M.; Zen, Y.; Nakanuma, Y.; et al. Lipid-induced oxidative stress causes steatohepatitis in mice fed an atherogenic diet. *Hepatology* **2007**, *46*, 1392–1403. [CrossRef] [PubMed]
25. Wouters, K.; van Gorp, P.J.; Bieghs, V.; Gijbels, M.J.; Duimel, H.; Lutjohann, D.; Kerksiek, A.; van Kruchten, R.; Maeda, N.; Staels, B.; et al. Dietary cholesterol, rather than liver steatosis, leads to hepatic inflammation in hyperlipidemic mouse models of nonalcoholic steatohepatitis. *Hepatology* **2008**, *48*, 474–486. [CrossRef] [PubMed]
26. Wouters, K.; van Bilsen, M.; van Gorp, P.J.; Bieghs, V.; Lutjohann, D.; Kerksiek, A.; Staels, B.; Hofker, M.H.; Shiri-Sverdlov, R. Intrahepatic cholesterol influences progression, inhibition and reversal of non-alcoholic steatohepatitis in hyperlipidemic mice. *FEBS Lett.* **2010**, *584*, 1001–1005. [CrossRef]
27. Zheng, S.; Hoos, L.; Cook, J.; Tetzloff, G.; Davis, H., Jr.; van Heek, M.; Hwa, J.J. Ezetimibe improves high fat and cholesterol diet-induced non-alcoholic fatty liver disease in mice. *Eur. J. Pharmacol.* **2008**, *584*, 118–124. [CrossRef]
28. Clapper, J.R.; Hendricks, M.D.; Gu, G.; Wittmer, C.; Dolman, C.S.; Herich, J.; Athanacio, J.; Villescaz, C.; Ghosh, S.S.; Heilig, J.S.; et al. Diet-induced mouse model of fatty liver disease and nonalcoholic steatohepatitis reflecting clinical disease progression and methods of assessment. *Am. J. Physiol. Gastrointest Liver Physiol.* **2013**, *305*, G483–G495. [CrossRef]
29. Kristiansen, M.N.; Veidal, S.S.; Rigbolt, K.T.; Tolbol, K.S.; Roth, J.D.; Jelsing, J.; Vrang, N.; Feigh, M. Obese diet-induced mouse models of nonalcoholic steatohepatitis-tracking disease by liver biopsy. *World J. Hepatol.* **2016**, *8*, 673–684. [CrossRef]
30. Larter, C.Z.; Yeh, M.M. Animal models of NASH: Getting both pathology and metabolic context right. *J. Gastroenterol. Hepatol.* **2008**, *23*, 1635–1648. [CrossRef]
31. Leclercq, I.A.; Farrell, G.C.; Schriemer, R.; Robertson, G.R. Leptin is essential for the hepatic fibrogenic response to chronic liver injury. *J. Hepatol.* **2002**, *37*, 206–213. [CrossRef]
32. US. Food Drug Administration. Final Determination Regarding Partially Hydrogenated Oils (Removing Trans Fat). Available online: https://www.federalregister.gov/documents/2018/05/21/2018-10714/final-determination-regarding-partially-hydrogenated-oils (accessed on 21 May 2018).

33. Boland, M.L.; Oro, D.; Tolbol, K.S.; Thrane, S.T.; Nielsen, J.C.; Cohen, T.S.; Tabor, D.E.; Fernandes, F.; Tovchigrechko, A.; Veidal, S.S.; et al. Towards a standard diet-induced and biopsy-confirmed mouse model of non-alcoholic steatohepatitis: Impact of dietary fat source. *World J. Gastroenterol.* **2019**, *25*, 4904–4920. [CrossRef] [PubMed]
34. Abe, N.; Kato, S.; Tsuchida, T.; Sugimoto, K.; Saito, R.; Verschuren, L.; Kleemann, R.; Oka, K. Longitudinal characterization of diet-induced genetic murine models of non-alcoholic steatohepatitis with metabolic, histological, and transcriptomic hallmarks of human patients. *Biol. Open* **2019**, *8*. [CrossRef] [PubMed]
35. Kennedy, A.J.; Ellacott, K.L.; King, V.L.; Hasty, A.H. Mouse models of the metabolic syndrome. *Dis. Model. Mech.* **2010**, *3*, 156–166. [CrossRef]
36. Suto, J.; Matsuura, S.; Imamura, K.; Yamanaka, H.; Sekikawa, K. Genetic analysis of non-insulin-dependent diabetes mellitus in KK and KK-Ay mice. *Eur. J. Endocrinol.* **1998**, *139*, 654–661. [CrossRef] [PubMed]
37. Henkel, J.; Coleman, C.D.; Schraplau, A.; Jhrens, K.; Weber, D.; Castro, J.P.; Hugo, M.; Schulz, T.J.; Kramer, S.; Schurmann, A.; et al. Induction of steatohepatitis (NASH) with insulin resistance in wildtype B6 mice by a western-type diet containing soybean oil and cholesterol. *Mol. Med.* **2017**, *23*, 70–82. [CrossRef]
38. Subramanian, S.; Goodspeed, L.; Wang, S.; Kim, J.; Zeng, L.; Ioannou, G.N.; Haigh, W.G.; Yeh, M.M.; Kowdley, K.V.; O'Brien, K.D.; et al. Dietary cholesterol exacerbates hepatic steatosis and inflammation in obese LDL receptor-deficient mice. *J. Lipid Res.* **2011**, *52*, 1626–1635. [CrossRef]
39. Mari, M.; Caballero, F.; Colell, A.; Morales, A.; Caballeria, J.; Fernandez, A.; Enrich, C.; Fernandez-Checa, J.C.; Garcia-Ruiz, C. Mitochondrial free cholesterol loading sensitizes to TNF- and Fas-mediated steatohepatitis. *Cell Metab.* **2006**, *4*, 185–198. [CrossRef]
40. Savard, C.; Tartaglione, E.V.; Kuver, R.; Haigh, W.G.; Farrell, G.C.; Subramanian, S.; Chait, A.; Yeh, M.M.; Quinn, L.S.; Ioannou, G.N. Synergistic interaction of dietary cholesterol and dietary fat in inducing experimental steatohepatitis. *Hepatology* **2013**, *57*, 81–92. [CrossRef]
41. Montandon, S.A.; Somm, E.; Loizides-Mangold, U.; de Vito, C.; Dibner, C.; Jornayvaz, F.R. Multi-technique comparison of atherogenic and MCD NASH models highlights changes in sphingolipid metabolism. *Sci. Rep.* **2019**, *9*, 16810. [CrossRef]
42. Larter, C.Z.; Yeh, M.M.; Haigh, W.G.; Williams, J.; Brown, S.; Bell-Anderson, K.S.; Lee, S.P.; Farrell, G.C. Hepatic free fatty acids accumulate in experimental steatohepatitis: Role of adaptive pathways. *J. Hepatol.* **2008**, *48*, 638–647. [CrossRef] [PubMed]
43. Weltman, M.D.; Farrell, G.C.; Liddle, C. Increased hepatocyte CYP2E1 expression in a rat nutritional model of hepatic steatosis with inflammation. *Gastroenterology* **1996**, *111*, 1645–1653. [CrossRef]
44. Fan, Y.; Zhang, W.; Wei, H.; Sun, R.; Tian, Z.; Chen, Y. Hepatic NK cells attenuate fibrosis progression of non-alcoholic steatohepatitis in dependent of CXCL10-mediated recruitment. *Liver Int.* **2019**. [CrossRef] [PubMed]
45. Sahai, A.; Malladi, P.; Pan, X.; Paul, R.; Melin-Aldana, H.; Green, R.M.; Whitington, P.F. Obese and diabetic db/db mice develop marked liver fibrosis in a model of nonalcoholic steatohepatitis: Role of short-form leptin receptors and osteopontin. *Am. J. Physiol. Gastrointest Liver Physiol.* **2004**, *287*, G1035–G1043. [CrossRef]
46. Sahai, A.; Malladi, P.; Melin-Aldana, H.; Green, R.M.; Whitington, P.F. Upregulation of osteopontin expression is involved in the development of nonalcoholic steatohepatitis in a dietary murine model. *Am. J. Physiol. Gastrointest Liver Physiol.* **2004**, *287*, G264–G273. [CrossRef]
47. Itagaki, H.; Shimizu, K.; Morikawa, S.; Ogawa, K.; Ezaki, T. Morphological and functional characterization of non-alcoholic fatty liver disease induced by a methionine-choline-deficient diet in C57BL/6 mice. *Int. J. Clin. Exp. Pathol.* **2013**, *6*, 2683–2696.
48. Raubenheimer, P.J.; Nyirenda, M.J.; Walker, B.R. A choline-deficient diet exacerbates fatty liver but attenuates insulin resistance and glucose intolerance in mice fed a high-fat diet. *Diabetes* **2006**, *55*, 2015–2020. [CrossRef]
49. Ikejima, K.; Okumura, K.; Lang, T.; Honda, H.; Abe, W.; Yamashina, S.; Enomoto, N.; Takei, Y.; Sato, N. The role of leptin in progression of non-alcoholic fatty liver disease. *Hepatol. Res.* **2005**, *33*, 151–154. [CrossRef]
50. Hummel, K.P.; Dickie, M.M.; Coleman, D.L. Diabetes, a new mutation in the mouse. *Science* **1966**, *153*, 1127–1128. [CrossRef]
51. Trevaskis, J.L.; Griffin, P.S.; Wittmer, C.; Neuschwander-Tetri, B.A.; Brunt, E.M.; Dolman, C.S.; Erickson, M.R.; Napora, J.; Parkes, D.G.; Roth, J.D. Glucagon-like peptide-1 receptor agonism improves metabolic, biochemical, and histopathological indices of nonalcoholic steatohepatitis in mice. *Am. J. Physiol. Gastrointest Liver Physiol.* **2012**, *302*, G762–G772. [CrossRef]

52. Rinella, M.E.; Green, R.M. The methionine-choline deficient dietary model of steatohepatitis does not exhibit insulin resistance. *J. Hepatol.* **2004**, *40*, 47–51. [CrossRef] [PubMed]
53. Al Rajabi, A.; Castro, G.S.; da Silva, R.P.; Nelson, R.C.; Thiesen, A.; Vannucchi, H.; Vine, D.F.; Proctor, S.D.; Field, C.J.; Curtis, J.M.; et al. Choline supplementation protects against liver damage by normalizing cholesterol metabolism in Pemt/Ldlr knockout mice fed a high-fat diet. *J. Nutr.* **2014**, *144*, 252–257. [CrossRef] [PubMed]
54. Matsumoto, M.; Hada, N.; Sakamaki, Y.; Uno, A.; Shiga, T.; Tanaka, C.; Ito, T.; Katsume, A.; Sudoh, M. An improved mouse model that rapidly develops fibrosis in non-alcoholic steatohepatitis. *Int. J. Exp. Pathol.* **2013**, *94*, 93–103. [CrossRef] [PubMed]
55. Miura, K.; Kodama, Y.; Inokuchi, S.; Schnabl, B.; Aoyama, T.; Ohnishi, H.; Olefsky, J.M.; Brenner, D.A.; Seki, E. Toll-like receptor 9 promotes steatohepatitis by induction of interleukin-1beta in mice. *Gastroenterology* **2010**, *139*, 323–334.e327. [CrossRef] [PubMed]
56. Tetri, L.H.; Basaranoglu, M.; Brunt, E.M.; Yerian, L.M.; Neuschwander-Tetri, B.A. Severe NAFLD with hepatic necroinflammatory changes in mice fed trans fats and a high-fructose corn syrup equivalent. *Am. J. Physiol. Gastrointest Liver Physiol.* **2008**, *295*, G987–G995. [CrossRef] [PubMed]
57. Tsuchida, T.; Lee, Y.A.; Fujiwara, N.; Ybanez, M.; Allen, B.; Martins, S.; Fiel, M.I.; Goossens, N.; Chou, H.I.; Hoshida, Y.; et al. A simple diet- and chemical-induced murine NASH model with rapid progression of steatohepatitis, fibrosis and liver cancer. *J. Hepatol.* **2018**, *69*, 385–395. [CrossRef] [PubMed]
58. Asgharpour, A.; Cazanave, S.C.; Pacana, T.; Seneshaw, M.; Vincent, R.; Banini, B.A.; Kumar, D.P.; Daita, K.; Min, H.K.; Mirshahi, F.; et al. A diet-induced animal model of non-alcoholic fatty liver disease and hepatocellular cancer. *J. Hepatol.* **2016**, *65*, 579–588. [CrossRef]
59. Neff, E.P. Farewell, FATZO: A NASH mouse update. *Lab. Anim. (NY)* **2019**, *48*, 151. [CrossRef]
60. Alexander, J.; Chang, G.Q.; Dourmashkin, J.T.; Leibowitz, S.F. Distinct phenotypes of obesity-prone AKR/J, DBA2J and C57BL/6J mice compared to control strains. *Int. J. Obes. (Lond.)* **2006**, *30*, 50–59. [CrossRef]
61. Peterson, R.G.; Jackson, C.V.; Zimmerman, K.M.; Alsina-Fernandez, J.; Michael, M.D.; Emmerson, P.J.; Coskun, T. Glucose dysregulation and response to common anti-diabetic agents in the FATZO/Pco mouse. *PLoS ONE* **2017**, *12*, e0179856. [CrossRef]
62. Sun, G.; Jackson, C.V.; Zimmerman, K.; Zhang, L.K.; Finnearty, C.M.; Sandusky, G.E.; Zhang, G.; Peterson, R.G.; Wang, Y.J. The FATZO mouse, a next generation model of type 2 diabetes, develops NAFLD and NASH when fed a Western diet supplemented with fructose. *BMC Gastroenterol.* **2019**, *19*, 41. [CrossRef] [PubMed]
63. Bieghs, V.; Van Gorp, P.J.; Wouters, K.; Hendrikx, T.; Gijbels, M.J.; van Bilsen, M.; Bakker, J.; Binder, C.J.; Lutjohann, D.; Staels, B.; et al. LDL receptor knock-out mice are a physiological model particularly vulnerable to study the onset of inflammation in non-alcoholic fatty liver disease. *PLoS ONE* **2012**, *7*, e30668. [CrossRef] [PubMed]
64. Schierwagen, R.; Maybuchen, L.; Zimmer, S.; Hittatiya, K.; Back, C.; Klein, S.; Uschner, F.E.; Reul, W.; Boor, P.; Nickenig, G.; et al. Seven weeks of Western diet in apolipoprotein-E-deficient mice induce metabolic syndrome and non-alcoholic steatohepatitis with liver fibrosis. *Sci. Rep.* **2015**, *5*, 12931. [CrossRef] [PubMed]
65. Henkel, J.; Coleman, C.D.; Schraplau, A.; Johrens, K.; Weiss, T.S.; Jonas, W.; Schurmann, A.; Puschel, G.P. Augmented liver inflammation in a microsomal prostaglandin E synthase 1 (mPGES-1)-deficient diet-induced mouse NASH model. *Sci. Rep.* **2018**, *8*, 16127. [CrossRef]
66. Horrillo, R.; Planaguma, A.; Gonzalez-Periz, A.; Ferre, N.; Titos, E.; Miquel, R.; Lopez-Parra, M.; Masferrer, J.L.; Arroyo, V.; Claria, J. Comparative protection against liver inflammation and fibrosis by a selective cyclooxygenase-2 inhibitor and a nonredox-type 5-lipoxygenase inhibitor. *J. Pharmacol. Exp. Ther.* **2007**, *323*, 778–786. [CrossRef]
67. Karck, U.; Peters, T.; Decker, K. The release of tumor necrosis factor from endotoxin-stimulated rat Kupffer cells is regulated by prostaglandin E2 and dexamethasone. *J. Hepatol.* **1988**, *7*, 352–361. [CrossRef]
68. Park, J.Y.; Pillinger, M.H.; Abramson, S.B. Prostaglandin E2 synthesis and secretion: The role of PGE2 synthases. *Clin. Immunol.* **2006**, *119*, 229–240. [CrossRef]
69. Anstee, Q.M.; Day, C.P. The Genetics of Nonalcoholic Fatty Liver Disease: Spotlight on PNPLA3 and TM6SF2. *Semin. Liver Dis.* **2015**, *35*, 270–290. [CrossRef]
70. Romeo, S.; Kozlitina, J.; Xing, C.; Pertsemlidis, A.; Cox, D.; Pennacchio, L.A.; Boerwinkle, E.; Cohen, J.C.; Hobbs, H.H. Genetic variation in PNPLA3 confers susceptibility to nonalcoholic fatty liver disease. *Nat. Genet.* **2008**, *40*, 1461–1465. [CrossRef]

71. Pingitore, P.; Romeo, S. The role of PNPLA3 in health and disease. *Biochim. Biophys. Acta Mol. Cell Biol. Lipids* **2019**, *1864*, 900–906. [CrossRef]
72. Smagris, E.; BasuRay, S.; Li, J.; Huang, Y.; Lai, K.M.; Gromada, J.; Cohen, J.C.; Hobbs, H.H. Pnpla3I148M knockin mice accumulate PNPLA3 on lipid droplets and develop hepatic steatosis. *Hepatology* **2015**, *61*, 108–118. [CrossRef] [PubMed]
73. Chen, X.; Zhou, P.; De, L.; Li, B.; Su, S. The roles of transmembrane 6 superfamily member 2 rs58542926 polymorphism in chronic liver disease: A meta-analysis of 24,147 subjects. *Mol. Genet. Genomic Med.* **2019**, *7*, e824. [CrossRef] [PubMed]
74. Kozlitina, J.; Smagris, E.; Stender, S.; Nordestgaard, B.G.; Zhou, H.H.; Tybjaerg-Hansen, A.; Vogt, T.F.; Hobbs, H.H.; Cohen, J.C. Exome-wide association study identifies a TM6SF2 variant that confers susceptibility to nonalcoholic fatty liver disease. *Nat. Genet.* **2014**, *46*, 352–356. [CrossRef] [PubMed]
75. Cast, A.; Kumbaji, M.; D'Souza, A.; Rodriguez, K.; Gupta, A.; Karns, R.; Timchenko, L.; Timchenko, N. Liver Proliferation Is an Essential Driver of Fibrosis in Mouse Models of Nonalcoholic Fatty Liver Disease. *Hepatol. Commun.* **2019**, *3*, 1036–1049. [CrossRef]
76. Qian, Y.W.; Chen, Y.; Yang, W.; Fu, J.; Cao, J.; Ren, Y.B.; Zhu, J.J.; Su, B.; Luo, T.; Zhao, X.F.; et al. p28(GANK) prevents degradation of Oct4 and promotes expansion of tumor-initiating cells in hepatocarcinogenesis. *Gastroenterology* **2012**, *142*, 1547–1558.e1514. [CrossRef]
77. Arsov, T.; Silva, D.G.; O'Bryan, M.K.; Sainsbury, A.; Lee, N.J.; Kennedy, C.; Manji, S.S.; Nelms, K.; Liu, C.; Vinuesa, C.G.; et al. Fat aussie—A new Alstrom syndrome mouse showing a critical role for ALMS1 in obesity, diabetes, and spermatogenesis. *Mol. Endocrinol.* **2006**, *20*, 1610–1622. [CrossRef]
78. Collin, G.B.; Marshall, J.D.; Ikeda, A.; So, W.V.; Russell-Eggitt, I.; Maffei, P.; Beck, S.; Boerkoel, C.F.; Sicolo, N.; Martin, M.; et al. Mutations in ALMS1 cause obesity, type 2 diabetes and neurosensory degeneration in Alstrom syndrome. *Nat. Genet.* **2002**, *31*, 74–78. [CrossRef]
79. Soga, M.; Kishimoto, Y.; kawaguchi, J.; Nakai, Y.; Kawamura, Y.; Inagaki, S.; Katoh, K.; Oohara, T.; Makino, S.; Oshima, I. The FLS mouse: A new inbred strain with spontaneous fatty liver. *Lab. Anim. Sci.* **1999**, *49*, 269–275.
80. Semba, T.; Nishimura, M.; Nishimura, S.; Ohara, O.; Ishige, T.; Ohno, S.; Nonaka, K.; Sogawa, K.; Satoh, M.; Sawai, S.; et al. The FLS (fatty liver Shionogi) mouse reveals local expressions of lipocalin-2, CXCL1 and CXCL9 in the liver with non-alcoholic steatohepatitis. *BMC Gastroenterol.* **2013**, *13*, 120. [CrossRef]
81. Sugihara, T.; Koda, M.; Kishina, M.; Kato, J.; Tokunaga, S.; Matono, T.; Ueki, M.; Murawaki, Y. Fatty liver Shionogi-ob/ob mouse: A new candidate for a non-alcoholic steatohepatitis model. *Hepatol. Res.* **2013**, *43*, 547–556. [CrossRef]
82. He, L.; Tian, D.A.; Li, P.Y.; He, X.X. Mouse models of liver cancer: Progress and recommendations. *Oncotarget* **2015**, *6*, 23306–23322. [CrossRef] [PubMed]
83. Watanabe, S.; Horie, Y.; Kataoka, E.; Sato, W.; Dohmen, T.; Ohshima, S.; Goto, T.; Suzuki, A. Non-alcoholic steatohepatitis and hepatocellular carcinoma: Lessons from hepatocyte-specific phosphatase and tensin homolog (PTEN)-deficient mice. *J. Gastroenterol. Hepatol.* **2007**, *22* (Suppl. 1), S96–S100. [CrossRef]
84. Takakura, K.; Oikawa, T.; Tomita, Y.; Mizuno, Y.; Nakano, M.; Saeki, C.; Torisu, Y.; Saruta, M. Mouse models for investigating the underlying mechanisms of nonalcoholic steatohepatitis-derived hepatocellular carcinoma. *World J. Gastroenterol.* **2018**, *24*, 1989–1994. [CrossRef] [PubMed]
85. Chen, C.Y.; Chen, J.; He, L.; Stiles, B.L. PTEN: Tumor Suppressor and Metabolic Regulator. *Front. Endocrinol. (Lausanne)* **2018**, *9*, 338. [CrossRef] [PubMed]
86. Gandhi, C.R.; Chaillet, J.R.; Nalesnik, M.A.; Kumar, S.; Dangi, A.; Demetris, A.J.; Ferrell, R.; Wu, T.; Divanovic, S.; Stankeiwicz, T.; et al. Liver-specific deletion of augmenter of liver regeneration accelerates development of steatohepatitis and hepatocellular carcinoma in mice. *Gastroenterology* **2015**, *148*, 379–391.e374. [CrossRef] [PubMed]
87. Francavilla, A.; Vujanovic, N.L.; Polimeno, L.; Azzarone, A.; Iacobellis, A.; Deleo, A.; Hagiya, M.; Whiteside, T.L.; Starzl, T.E. The in vivo effect of hepatotrophic factors augmenter of liver regeneration, hepatocyte growth factor, and insulin-like growth factor-II on liver natural killer cell functions. *Hepatology* **1997**, *25*, 411–415. [CrossRef]
88. Ibrahim, S.; Weiss, T.S. Augmenter of liver regeneration: Essential for growth and beyond. *Cytokine Growth Factor Rev.* **2019**, *45*, 65–80. [CrossRef]

89. Gandhi, C.R.; Murase, N.; Starzl, T.E. Cholera toxin-sensitive GTP-binding protein-coupled activation of augmenter of liver regeneration (ALR) receptor and its function in rat kupffer cells. *J. Cell Physiol.* **2010**, *222*, 365–373. [CrossRef]
90. Itoh, M.; Suganami, T.; Nakagawa, N.; Tanaka, M.; Yamamoto, Y.; Kamei, Y.; Terai, S.; Sakaida, I.; Ogawa, Y. Melanocortin 4 receptor-deficient mice as a novel mouse model of nonalcoholic steatohepatitis. *Am. J. Pathol.* **2011**, *179*, 2454–2463. [CrossRef]
91. Yamada, T.; Kashiwagi, Y.; Rokugawa, T.; Kato, H.; Konishi, H.; Hamada, T.; Nagai, R.; Masago, Y.; Itoh, M.; Suganami, T.; et al. Evaluation of hepatic function using dynamic contrast-enhanced magnetic resonance imaging in melanocortin 4 receptor-deficient mice as a model of nonalcoholic steatohepatitis. *Magn. Reson. Imaging* **2019**, *57*, 210–217. [CrossRef]
92. Denk, H.; Abuja, P.M.; Zatloukal, K. Animal models of NAFLD from the pathologist's point of view. *Biochim. Biophys. Acta Mol. Basis Dis.* **2019**, *1865*, 929–942. [CrossRef]
93. Nishida, T.; Tsuneyama, K.; Fujimoto, M.; Nomoto, K.; Hayashi, S.; Miwa, S.; Nakajima, T.; Nakanishi, Y.; Sasaki, Y.; Suzuki, W.; et al. Spontaneous onset of nonalcoholic steatohepatitis and hepatocellular carcinoma in a mouse model of metabolic syndrome. *Lab. Invest.* **2013**, *93*, 230–241. [CrossRef] [PubMed]
94. Bettermann, K.; Mehta, A.K.; Hofer, E.M.; Wohlrab, C.; Golob-Schwarzl, N.; Svendova, V.; Schimek, M.G.; Stumptner, C.; Thuringer, A.; Speicher, M.R.; et al. Keratin 18-deficiency results in steatohepatitis and liver tumors in old mice: A model of steatohepatitis-associated liver carcinogenesis. *Oncotarget* **2016**, *7*, 73309–73322. [CrossRef] [PubMed]
95. Luedde, T.; Beraza, N.; Kotsikoris, V.; van Loo, G.; Nenci, A.; De Vos, R.; Roskams, T.; Trautwein, C.; Pasparakis, M. Deletion of NEMO/IKKgamma in liver parenchymal cells causes steatohepatitis and hepatocellular carcinoma. *Cancer Cell* **2007**, *11*, 119–132. [CrossRef] [PubMed]
96. Cano, A.; Buque, X.; Martinez-Una, M.; Aurrekoetxea, I.; Menor, A.; Garcia-Rodriguez, J.L.; Lu, S.C.; Martinez-Chantar, M.L.; Mato, J.M.; Ochoa, B.; et al. Methionine adenosyltransferase 1A gene deletion disrupts hepatic very low-density lipoprotein assembly in mice. *Hepatology* **2011**, *54*, 1975–1986. [CrossRef]
97. Domitrovic, R.; Jakovac, H.; Tomac, J.; Sain, I. Liver fibrosis in mice induced by carbon tetrachloride and its reversion by luteolin. *Toxicol. Appl. Pharmacol.* **2009**, *241*, 311–321. [CrossRef]
98. Sharma, L.; Gupta, D.; Abdullah, S.T. Thioacetamide potentiates high cholesterol and high fat diet induced steato-hepatitic changes in livers of C57BL/6J mice: A novel eight weeks model of fibrosing NASH. *Toxicol. Lett.* **2019**, *304*, 21–29. [CrossRef]
99. Fujii, M.; Shibazaki, Y.; Wakamatsu, K.; Honda, Y.; Kawauchi, Y.; Suzuki, K.; Arumugam, S.; Watanabe, K.; Ichida, T.; Asakura, H.; et al. A murine model for non-alcoholic steatohepatitis showing evidence of association between diabetes and hepatocellular carcinoma. *Med. Mol. Morphol* **2013**, *46*, 141–152. [CrossRef]
100. Jena, P.K.; Sheng, L.; Liu, H.X.; Kalanetra, K.M.; Mirsoian, A.; Murphy, W.J.; French, S.W.; Krishnan, V.V.; Mills, D.A.; Wan, Y.Y. Western Diet-Induced Dysbiosis in Farnesoid X Receptor Knockout Mice Causes Persistent Hepatic Inflammation after Antibiotic Treatment. *Am. J. Pathol.* **2017**, *187*, 1800–1813. [CrossRef]
101. Norheim, F.; Hui, S.T.; Kulahcioglu, E.; Mehrabian, M.; Cantor, R.M.; Pan, C.; Parks, B.W.; Lusis, A.J. Genetic and hormonal control of hepatic steatosis in female and male mice. *J. Lipid Res.* **2017**, *58*, 178–187. [CrossRef]
102. Lonardo, A.; Nascimbeni, F.; Ballestri, S.; Fairweather, D.; Win, S.; Than, T.A.; Abdelmalek, M.F.; Suzuki, A. Sex Differences in Nonalcoholic Fatty Liver Disease: State of the Art and Identification of Research Gaps. *Hepatology* **2019**, *70*, 1457–1469. [CrossRef] [PubMed]
103. Spruss, A.; Henkel, J.; Kanuri, G.; Blank, D.; Puschel, G.P.; Bischoff, S.C.; Bergheim, I. Female mice are more susceptible to nonalcoholic fatty liver disease: Sex-specific regulation of the hepatic AMP-activated protein kinase-plasminogen activator inhibitor 1 cascade, but not the hepatic endotoxin response. *Mol. Med.* **2012**, *18*, 1346–1355. [CrossRef] [PubMed]
104. Marin, V.; Rosso, N.; Dal Ben, M.; Raseni, A.; Boschelle, M.; Degrassi, C.; Nemeckova, I.; Nachtigal, P.; Avellini, C.; Tiribelli, C.; et al. An Animal Model for the Juvenile Non-Alcoholic Fatty Liver Disease and Non-Alcoholic Steatohepatitis. *PLoS ONE* **2016**, *11*, e0158817. [CrossRef] [PubMed]
105. Zhou, L.; Liu, D.; Wang, Z.; Dong, H.; Xu, X.; Zhou, S. Establishment and Comparison of Juvenile Female Mouse Models of Nonalcoholic Fatty Liver Disease and Nonalcoholic Steatohepatitis. *Gastroenterol. Res. Pract.* **2018**, *2018*, 8929620. [CrossRef] [PubMed]
106. Giles, D.A.; Moreno-Fernandez, M.E.; Stankiewicz, T.E.; Graspeuntner, S.; Cappelletti, M.; Wu, D.; Mukherjee, R.; Chan, C.C.; Lawson, M.J.; Klarquist, J.; et al. Thermoneutral housing exacerbates nonalcoholic

fatty liver disease in mice and allows for sex-independent disease modeling. *Nat. Med.* **2017**, *23*, 829–838. [CrossRef] [PubMed]
107. Adamovich, Y.; Rousso-Noori, L.; Zwighaft, Z.; Neufeld-Cohen, A.; Golik, M.; Kraut-Cohen, J.; Wang, M.; Han, X.; Asher, G. Circadian clocks and feeding time regulate the oscillations and levels of hepatic triglycerides. *Cell Metab.* **2014**, *19*, 319–330. [CrossRef]
108. Jacobi, D.; Liu, S.; Burkewitz, K.; Kory, N.; Knudsen, N.H.; Alexander, R.K.; Unluturk, U.; Li, X.; Kong, X.; Hyde, A.L.; et al. Hepatic Bmal1 Regulates Rhythmic Mitochondrial Dynamics and Promotes Metabolic Fitness. *Cell Metab.* **2015**, *22*, 709–720. [CrossRef]
109. Kettner, N.M.; Voicu, H.; Finegold, M.J.; Coarfa, C.; Sreekumar, A.; Putluri, N.; Katchy, C.A.; Lee, C.; Moore, D.D.; Fu, L. Circadian Homeostasis of Liver Metabolism Suppresses Hepatocarcinogenesis. *Cancer Cell* **2016**, *30*, 909–924. [CrossRef]
110. Baker, M. 1,500 scientists lift the lid on reproducibility. *Nature* **2016**, *533*, 452–454. [CrossRef]
111. Begley, C.G.; Ellis, L.M. Drug development: Raise standards for preclinical cancer research. *Nature* **2012**, *483*, 531–533. [CrossRef]
112. Goodman, S.N.; Fanelli, D.; Ioannidis, J.P. What does research reproducibility mean? *Sci. Transl. Med.* **2016**, *8*, 341ps312. [CrossRef] [PubMed]
113. Zou, Y.; Li, J.; Lu, C.; Wang, J.; Ge, J.; Huang, Y.; Zhang, L.; Wang, Y. High-fat emulsion-induced rat model of nonalcoholic steatohepatitis. *Life Sci.* **2006**, *79*, 1100–1107. [CrossRef] [PubMed]
114. Kucera, O.; Cervinkova, Z. Experimental models of non-alcoholic fatty liver disease in rats. *World J. Gastroenterol.* **2014**, *20*, 8364–8376. [CrossRef] [PubMed]
115. Rodrigues, A.A.; Andrade, R.S.B.; Vasconcelos, D.F.P. Relationship between Experimental Diet in Rats and Nonalcoholic Hepatic Disease: Review of Literature. *Int. J. Hepatol.* **2018**, *2018*, 9023027. [CrossRef]
116. Maciejewska, D.; Lukomska, A.; Dec, K.; Skonieczna-Zydecka, K.; Gutowska, I.; Skorka-Majewicz, M.; Styburski, D.; Misiakiewicz-Has, K.; Pilutin, A.; Palma, J.; et al. Diet-Induced Rat Model of Gradual Development of Non-Alcoholic Fatty Liver Disease (NAFLD) with Lipopolysaccharides (LPS) Secretion. *Diagnostics (Basel)* **2019**, *9*, 205. [CrossRef]
117. Khurana, P.; Yadati, T.; Goyal, S.; Dolas, A.; Houben, T.; Oligschlaeger, Y.; Agarwal, A.K.; Kulkarni, A.; Shiri-Sverdlov, R. Inhibiting Extracellular Cathepsin D Reduces Hepatic Steatosis in Sprague(-)Dawley Rats (dagger). *Biomolecules* **2019**, *9*, 171. [CrossRef]
118. Maeso-Diaz, R.; Boyer-Diaz, Z.; Lozano, J.J.; Ortega-Ribera, M.; Peralta, C.; Bosch, J.; Gracia-Sancho, J. New Rat Model of Advanced NASH Mimicking Pathophysiological Features and Transcriptomic Signature of The Human Disease. *Cells* **2019**, *8*, 1062. [CrossRef]
119. Carmiel-Haggai, M.; Cederbaum, A.I.; Nieto, N. A high-fat diet leads to the progression of non-alcoholic fatty liver disease in obese rats. *FASEB J.* **2005**, *19*, 136–138. [CrossRef]
120. Lieber, C.S.; Leo, M.A.; Mak, K.M.; Xu, Y.; Cao, Q.; Ren, C.; Ponomarenko, A.; DeCarli, L.M. Model of nonalcoholic steatohepatitis. *Am. J. Clin. Nutr.* **2004**, *79*, 502–509. [CrossRef]
121. Kirsch, R.; Clarkson, V.; Shephard, E.G.; Marais, D.A.; Jaffer, M.A.; Woodburne, V.E.; Kirsch, R.E.; Hall Pde, L. Rodent nutritional model of non-alcoholic steatohepatitis: Species, strain and sex difference studies. *J. Gastroenterol. Hepatol.* **2003**, *18*, 1272–1282. [CrossRef]
122. Domitrovic, R.; Jakovac, H.; Milin, C.; Radosevic-Stasic, B. Dose- and time-dependent effects of luteolin on carbon tetrachloride-induced hepatotoxicity in mice. *Exp. Toxicol. Pathol.* **2009**, *61*, 581–589. [CrossRef]
123. Walenbergh, S.M.; Houben, T.; Rensen, S.S.; Bieghs, V.; Hendrikx, T.; van Gorp, P.J.; Oligschlaeger, Y.; Jeurissen, M.L.; Gijbels, M.J.; Buurman, W.A.; et al. Plasma cathepsin D correlates with histological classifications of fatty liver disease in adults and responds to intervention. *Sci. Rep.* **2016**, *6*, 38278. [CrossRef]
124. Houben, T.; Oligschlaeger, Y.; Hendrikx, T.; Bitorina, A.V.; Walenbergh, S.M.A.; van Gorp, P.J.; Gijbels, M.J.J.; Friedrichs, S.; Plat, J.; Schaap, F.G.; et al. Cathepsin D regulates lipid metabolism in murine steatohepatitis. *Sci. Rep.* **2017**, *7*, 3494. [CrossRef]
125. Gehrke, N.; Biedenbach, J.; Huber, Y.; Straub, B.K.; Galle, P.R.; Simon, P.; Schattenberg, J.M. Voluntary exercise in mice fed an obesogenic diet alters the hepatic immune phenotype and improves metabolic parameters—An animal model of life style intervention in NAFLD. *Sci. Rep.* **2019**, *9*, 4007. [CrossRef] [PubMed]
126. Kawanishi, N.; Niihara, H.; Mizokami, T.; Yada, K.; Suzuki, K. Exercise training attenuates neutrophil infiltration and elastase expression in adipose tissue of high-fat-diet-induced obese mice. *Physiol. Rep.* **2015**, *3*. [CrossRef] [PubMed]

127. Boeckmans, J.; Natale, A.; Rombaut, M.; Buyl, K.; Rogiers, V.; De Kock, J.; Vanhaecke, T.; R, M.R. Anti-NASH Drug Development Hitches a Lift on PPAR Agonism. *Cells* **2019**, *9*, 37. [CrossRef] [PubMed]
128. Francque, S.; Verrijken, A.; Caron, S.; Prawitt, J.; Paumelle, R.; Derudas, B.; Lefebvre, P.; Taskinen, M.R.; Van Hul, W.; Mertens, I.; et al. PPARalpha gene expression correlates with severity and histological treatment response in patients with non-alcoholic steatohepatitis. *J. Hepatol.* **2015**, *63*, 164–173. [CrossRef] [PubMed]
129. Shipman, K.E.; Strange, R.C.; Ramachandran, S. Use of fibrates in the metabolic syndrome: A review. *World J. Diabetes* **2016**, *7*, 74–88. [CrossRef] [PubMed]
130. Ishibashi, S.; Arai, H.; Yokote, K.; Araki, E.; Suganami, H.; Yamashita, S.; Group, K.S. Efficacy and safety of pemafibrate (K-877), a selective peroxisome proliferator-activated receptor alpha modulator, in patients with dyslipidemia: Results from a 24-week, randomized, double blind, active-controlled, phase 3 trial. *J. Clin. Lipidol.* **2018**, *12*, 173–184. [CrossRef]

131. Honda, Y.; Kessoku, T.; Ogawa, Y.; Tomeno, W.; Imajo, K.; Fujita, K.; Yoneda, M.; Takizawa, T.; Saito, S.; Nagashima, Y.; et al. Pemafibrate, a novel selective peroxisome proliferator-activated receptor alpha modulator, improves the pathogenesis in a rodent model of nonalcoholic steatohepatitis. *Sci. Rep.* **2017**, *7*, 42477. [CrossRef]
132. Bays, H.E.; Schwartz, S.; Littlejohn, T., 3rd; Kerzner, B.; Krauss, R.M.; Karpf, D.B.; Choi, Y.J.; Wang, X.; Naim, S.; Roberts, B.K. MBX-8025, a novel peroxisome proliferator receptor-delta agonist: Lipid and other metabolic effects in dyslipidemic overweight patients treated with and without atorvastatin. *J. Clin. Endocrinol. Metab* **2011**, *96*, 2889–2897. [CrossRef] [PubMed]
133. Haczeyni, F.; Wang, H.; Barn, V.; Mridha, A.R.; Yeh, M.M.; Haigh, W.G.; Ioannou, G.N.; Choi, Y.J.; McWherter, C.A.; Teoh, N.C.; et al. The selective peroxisome proliferator-activated receptor-delta agonist seladelpar reverses nonalcoholic steatohepatitis pathology by abrogating lipotoxicity in diabetic obese mice. *Hepatol. Commun.* **2017**, *1*, 663–674. [CrossRef] [PubMed]
134. Lee, Y.H.; Kim, J.H.; Kim, S.R.; Jin, H.Y.; Rhee, E.J.; Cho, Y.M.; Lee, B.W. Lobeglitazone, a Novel Thiazolidinedione, Improves Non-Alcoholic Fatty Liver Disease in Type 2 Diabetes: Its Efficacy and Predictive Factors Related to Responsiveness. *J. Korean Med. Sci.* **2017**, *32*, 60–69. [CrossRef] [PubMed]
135. Choung, S.; Joung, K.H.; You, B.R.; Park, S.K.; Kim, H.J.; Ku, B.J. Treatment with Lobeglitazone Attenuates Hepatic Steatosis in Diet-Induced Obese Mice. *PPAR Res.* **2018**, *2018*, 4292509. [CrossRef] [PubMed]
136. Ratziu, V.; Harrison, S.A.; Francque, S.; Bedossa, P.; Lehert, P.; Serfaty, L.; Romero-Gomez, M.; Boursier, J.; Abdelmalek, M.; Caldwell, S.; et al. Elafibranor, an Agonist of the Peroxisome Proliferator-Activated Receptor-alpha and -delta, Induces Resolution of Nonalcoholic Steatohepatitis Without Fibrosis Worsening. *Gastroenterology* **2016**, *150*, 1147–1159.e1145. [CrossRef] [PubMed]
137. Tolbol, K.S.; Kristiansen, M.N.; Hansen, H.H.; Veidal, S.S.; Rigbolt, K.T.; Gillum, M.P.; Jelsing, J.; Vrang, N.; Feigh, M. Metabolic and hepatic effects of liraglutide, obeticholic acid and elafibranor in diet-induced obese mouse models of biopsy-confirmed nonalcoholic steatohepatitis. *World J. Gastroenterol.* **2018**, *24*, 179–194. [CrossRef]
138. Alukal, J.J.; Thuluvath, P.J. Reversal of NASH fibrosis with pharmacotherapy. *Hepatol. Int.* **2019**, *13*, 534–545. [CrossRef]
139. Roth, J.D.; Veidal, S.S.; Fensholdt, L.K.D.; Rigbolt, K.T.G.; Papazyan, R.; Nielsen, J.C.; Feigh, M.; Vrang, N.; Young, M.; Jelsing, J.; et al. Combined obeticholic acid and elafibranor treatment promotes additive liver histological improvements in a diet-induced ob/ob mouse model of biopsy-confirmed NASH. *Sci. Rep.* **2019**, *9*, 9046. [CrossRef]
140. Hui, S.T.; Kurt, Z.; Tuominen, I.; Norheim, F.; R, C.D.; Pan, C.; Dirks, D.L.; Magyar, C.E.; French, S.W.; Chella Krishnan, K.; et al. The Genetic Architecture of Diet-Induced Hepatic Fibrosis in Mice. *Hepatology* **2018**, *68*, 2182–2196. [CrossRef]

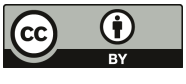

biomedicines

MDPI

Review

The Synergy between Organ-on-a-Chip and Artificial Intelligence for the Study of NAFLD: From Basic Science to Clinical Research

Francesco De Chiara [1,*], Ainhoa Ferret-Miñana [1] and Javier Ramón-Azcón [1,2]

[1] Biosensors for Bioengineering Group, Institute for Bioengineering of Catalonia (IBEC), The Barcelona Institute of Science and Technology (BIST), Baldiri I Reixac 10–12, 08028 Barcelona, Spain; aferret@ibecbarcelona.eu (A.F.-M.); jramon@ibecbarcelona.eu (J.R.-A.)

[2] ICREA-Institució Catalana de Recerca i Estudis Avançats, 08010 Barcelona, Spain

* Correspondence: fdechiara@ibecbarcelona.eu; Tel.: +34-93-40-39735

Abstract: Non-alcoholic fatty liver affects about 25% of global adult population. On the long-term, it is associated with extra-hepatic compliances, multiorgan failure, and death. Various invasive and non-invasive methods are employed for its diagnosis such as liver biopsies, CT scan, MRI, and numerous scoring systems. However, the lack of accuracy and reproducibility represents one of the biggest limitations of evaluating the effectiveness of drug candidates in clinical trials. Organ-on-chips (OOC) are emerging as a cost-effective tool to reproduce in vitro the main NAFLD's pathogenic features for drug screening purposes. Those platforms have reached a high degree of complexity that generate an unprecedented amount of both structured and unstructured data that outpaced our capacity to analyze the results. The addition of artificial intelligence (AI) layer for data analysis and interpretation enables those platforms to reach their full potential. Furthermore, the use of them do not require any ethic and legal regulation. In this review, we discuss the synergy between OOC and AI as one of the most promising ways to unveil potential therapeutic targets as well as the complex mechanism(s) underlying NAFLD.

Keywords: NAFLD; extra-hepatic outcome; organ-on-a-chip; artificial intelligence

Citation: De Chiara, F.; Ferret-Miñana, A.; Ramón-Azcón, J. The Synergy between Organ-on-a-Chip and Artificial Intelligence for the Study of NAFLD: From Basic Science to Clinical Research. *Biomedicines* **2021**, *9*, 248. https://doi.org/10.3390/biomedicines9030248

Academic Editors: Ronit Shiri-Sverdlov and Sabine Baumgartner

Received: 29 January 2021
Accepted: 25 February 2021
Published: 2 March 2021

1. Introduction

Non-alcoholic fatty liver disease (NAFLD) is defined as a continuum of abnormalities caused by lipid accumulation within the liver defined as hepatic steatosis. Fatty liver is considered as the liver manifestation of metabolic syndrome when is accompanied by simultaneously presence of three or more of the following features: high triglycerides, hypertension, visceral obesity, insulin resistance and high cholesterol, in the absence or reduced alcohol intake [1]. It ranges from non-alcoholic fatty liver (NAFL), characterized by > 5% of steatotic hepatocytes, to its more advanced and aggressive form known as non-alcoholic steatohepatitis (NASH). This latter form is characterized by extended liver inflammation and often accompanied by fibrosis which may progress to cirrhosis and hepatocellular carcinoma (HCC) (Figure 1). The strongest predictor of NAFLD/NASH is central or visceral obesity, rather than general obesity, while the presence of advanced fibrosis is the strongest predictor of mortality in those patients [2,3].

The global prevalence of NAFLD has been estimated around 25.24% with highest peak of 30.45% in South America, whereas NASH ranges from 3 to 5% globally. These numbers increase when other factors are considered, for example, the estimated prevalence of NAFLD and NASH in patients with type 2 diabetes mellitus rise up to 21.51% and 43.63%, respectively, while 51.34% and 81.83% in people affected by obesity [4]. The gold standard for the diagnosis of NAFLD/NASH is the liver biopsy although many non-invasive methods—ultrasonography, computed tomography scan and magnetic resonance imaging/spectroscopy—and various scores—NAS score, FIB-4, fatty liver index and

NAFLD fibrosis score—are considered valid alternatives [5–8]. However, this potpourri of techniques, the intra- and inter-variability of pathologists in liver biopsies evaluation [9], and the non-standardized site location of biopsies [10] interfere with the inclusion of patients in clinical trials, but most important, compromise the possibility to assess the efficacy of treatments in clinical trials.

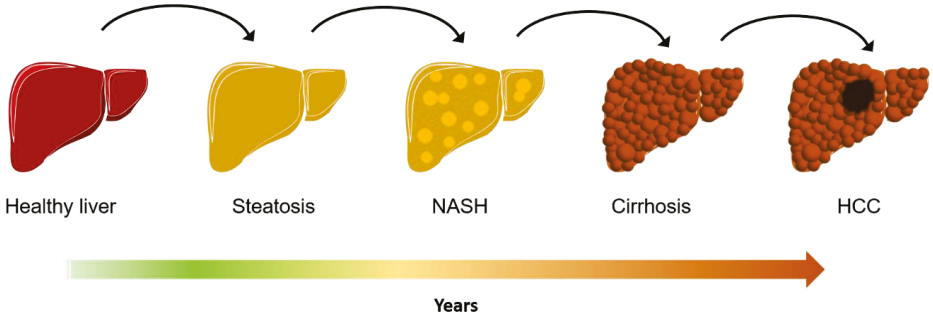

Figure 1. Representation of natural progression of Non-alcoholic fatty liver disease.

In the last 10 years, many technologies such as tissue engineering, sensing, and microfluidics are converging to build more sophisticated organ(s)-on-a-chip (OOC). The aim is to reproduce in vitro the physiological conditions for drug screening purposes in order to increase the success rate of clinical trials [11]. This system ranges from multicellular to multiorgan set-up in both healthy and diseased disposition, where the responses to perturbation/treatment can be monitored in real-time regardless from the mechanisms of action. The OOCs are changing the translational science paradigm being an extremely cost-effective surrogate to the animal testing with a far higher predictive power and shorter time of response. The impact of these tools is the ability to assess at same time the efficacy and toxicity of new treatments giving important insights about their biological activity. Those platforms are designed to deeper investigate the mechanism(s) of action of a specific disease, its early detection, as well as the effectiveness of a drug and its potential side effects. The OOCs are reaching a level of complexity comparable with real organs allowing the early identification of crucial features of NAFLD to intervene efficiently. The new OOCs 2.0 are high-throughput devices where mini-tissues in three-dimensional (3D) are subjected to a microfluidic regimen and integrated with a sensor platform capable of collecting massive amount of data in real time [12–14]. Just to give an idea, over 200 Gigabytes of data can be generated by a single time-lapse experiment of 72 h where three images of 10,000 cells (one brightfield plus two fluorescent bands) for six timepoints/hours at two Megabytes/each are taken. Another example is the over millions of datapoints that can be easily collected from a 384 wells microfluidic platform in real-time [15]. Unfortunately, at moment the data generated by these platforms have far outpaced our capacity to process and analyze them creating an important analytic bottleneck.

One of the most promising approaches is to employ machine learning and artificial intelligence to metabolize these unprecedent amount of data. Although traditional machine learning offers advanced data processing capabilities, the advent of its most important component, the deep learning, made possible to analyze massive unstructured data such as images, drug-target interactions and computational biology [16–19]. These AI-based techniques employ algorithms that learn without direct programming overcoming the limitation of human recognition boosting human knowledge in various fields.

In this review we will discuss: (i) the implication of other organs in the progression of the disease; (ii) how the recent advances in OOCs field might improve the knowledge on early onset of NAFLD; (iii) how the artificial intelligence could help in tasks such as classifying known NAFLD-associated features while identifying new ones.

2. Extra-Hepatic Outcomes: NAFLD as Multiorgan Disease

In the past years, various lines of investigation have proved that NAFLD extends beyond the liver paving the way to multiorgan failure, and eventually death (Figure 2).

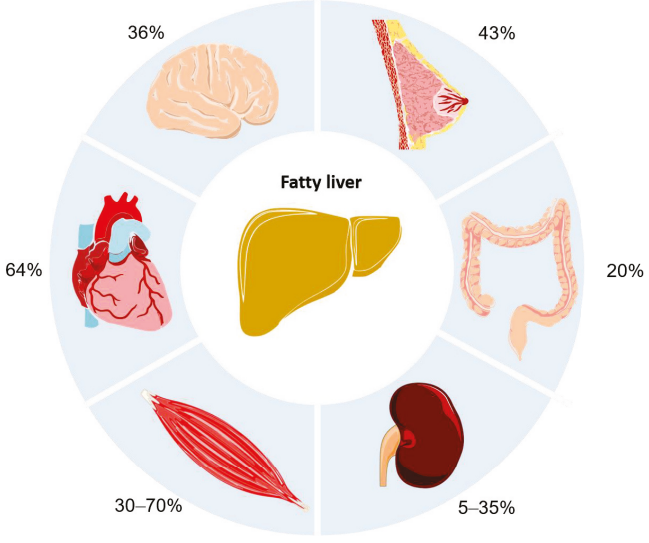

Figure 2. Incidence of extra-hepatic complication in non-alcoholic fatty liver disease.

In the meta-analysis of Targher et al. [20], 64% of patients with NAFLD are at risk of cardiovascular disease (CVD), which represents the first cause of death. The outcomes range from non-fatal to fatal CVD complications such as angina, stroke, and myocardial infarction [21]. Obesity and other metabolic disorders like insulin resistance, atherogenic dyslipidemia, increased uric acid, reduced vitamin D, and impaired fibrinolysis are common risk factors of NAFLD and CVD [22].

Following CVD, the most frequent cause of death among NAFLD patients are the extra-hepatic malignancies, where colorectal cancer in males and breast cancer in females are the most prevalent types [23]. Specifically, Mantovani et al. [24] showed that in male patients with NAFLD, the prevalence of colorectal adenomas is 20.4% as opposed to 15.8% in those without NAFLD whilst the prevalence of colorectal cancer is 2.4% for NAFLD vs 1.97% without NAFLD [25]. On the other hand, NAFLD has been concurrently found associated with breast cancer in 45.2% of the female cohort vs the 16.4% of the controls [26]. Other evidence confirmed that visceral obesity, metabolic syndrome, and insulin resistance contribute to colorectal cancer progression [27], while disturbances in insulin metabolism, hormonal imbalance and inflammation are associated to higher risk of breast cancer [28].

Sarcopenia—referred as progressive and generalized loss of skeletal muscle mass and strength—is one more extra-hepatic complication that recently has been linked to NAFLD [29]. Between 30–70% of NAFLD patients with cirrhosis suffer sarcopenia [30], which increase the risk of worse outcomes in post-hepatic transplanted patients. Those patients have higher rates of mortality compared to non-sarcopenic patients [31]. Hence, sarcopenia is listed as exclusion criteria for a liver transplant [32].

Kidneys can be also affected by NAFLD. The decreased glomerular filtration rate and proteinuria, specific for chronic kidney disease (CKD), have been found in 20–55% of patients with NAFLD in contrast to 5–35% in patients without NAFLD. Moreover, there is a strong correlation between the stage of NAFLD and the severity of CKD [32]. Last evidence links the increased release of proinflammatory and prothrombotic molecules due to NAFLD to the promotion of vascular and renal injury [33].

The brain is also non-exempted from NAFLD-induced damage. Studies have associated NAFLD and cerebrovascular events (CVE), although data are frequently inconclusive. For example, El Azeem et al. observed CVE in 36% of NAFLD patients [34]. The associated complications were the asymptomatic brain lesions, alterations in cerebral perfusion and activity, cognitive impairment, brain aging, and increased risk of both ischemic and hemorrhagic stroke [35]. NAFLD and cerebrovascular accidents share some risk factors such as type II diabetes and obesity mainly related to metabolic syndrome [36]. Furthermore, recent findings indicate that the chronic inflammatory environment and ammonia generated by NAFLD might lead to microglia activation causing micro and macrovascular damage in the brain [37–39].

Other minor complications linked to NAFLD are skin-related (such as psoriasis), obstructive sleep apnea, osteoporosis, hormonal dysregulation (as polycystic ovary), male sexual disfunction, hypothyroidism, periodontitis, urolithiasis, etc. [40].

In NAFLD, multiple pathways are concurrently dysregulated. The liver homeostasis is chronically compromised by low level of inflammation and lipid accumulation. However, how this propagates to the other organs or vice versa the failure of other organs exacerbates the liver damage is still unknown. Further work is still urgently needed to elucidate the mechanism of interorgan cross talk in order to develop the right pharmaceutical target(s) or identify the right timing for treatment.

3. Organ-on-a-Chip 2.0

The organ-on-a-chip (OOC) revolutionized the way how the drug screening process was done, mimicking and miniaturizing the physiologic environment of almost any organ. In the last five years, these platforms have become more sophisticated thanks to a multidisciplinary approach. Three are the critical components of those platforms: the 3D tissue, the microfluidic, and the integrated sensing system.

The first of them is the three-dimensional structure obtained by mixing cells with a biomaterial in a pre-specified structure. In vivo, the liver is structured in hexagonal functional units defined lobules of 1–2 mm in size. At center of each lobule there is a large vein called "central vein" that drain blood from the small vessels (capillary) (Figure 3). At six corners, the lobules are delimited by the portal triad composed of bile duct, portal vein and hepatic artery. The cells placed between these two structures are organized according to their function. They are divided in non-parenchymal cells, composed by Kupffer cells (KC), liver sinusoidal endothelial cells (LSEC), and hepatic stellate cells (HSC) and parenchymal cells, hepatocytes, that constitute roughly the 20% and 80% of the liver mass, respectively. While the functions of non-parenchymal cells span from maintaining the structural organization of the liver (HSC) to regulate exchange with blood (LSEC) and immune response (KC), the function of parenchymal (hepatocytes) is to perform most of the metabolic jobs such as decomposition and synthesis of sugars and fats, ammonia removal and synthesis of bile acids. The place where the hepatocytes are located between the portal triad and central vein is extremely important for the body and it is known as zonation [41]. The environment of the cells closer to portal triad is rich in oxygen and glucose because the cells perform the processes that are more energetically demanding, such as glycolysis, bile acid production and xenobiotic metabolism. The mid-lobule hepatocytes are specialized in modulation of insulin growth factors and iron metabolism while the cells in the proximity of central vein are dedicated to gluconeogenesis, β-oxidation and cholesterol metabolism [41].

The cellular organization of the liver represents an essential factor for the hepatocytes' optimal working condition but, at same time, the most significant challenge for the mimetic tissue engineering. In fact, when these cells are taken out from this configuration, they rapidly lose their polarization, capacity to replicate as well as some of the liver-specific functions. One of the first approach oriented towards the preservation of functionality of hepatocytes was made in the 1991 when Dunn et al. demonstrated that primary rat hepatocytes growth on collagen substrate were able to maintain polarity and release albumin, transferrin, and urea for two weeks. Once a second layer of collagen was added

on top of these hepatocytes, those functions were prolonged for six weeks [42]. A different approach to prolong the hepatocytes' phenotype, has been adopted by Suurmond et al. that cocultured hepatocytes, endothelial and Kupffer cells in 3D spheroids maintained in inter-connected honeycomb wells [43]. Interestingly, the presence of endothelial cells improves the function of hepatocytes—increase in urea albumin secretion—but not any other further improvement was induced by Kupffer cells. Conversely, the presence of the Kupffer cells determined an increase in lipid accumulation, and release of Tumor Necrosis Factor-α (TNFα) and Interleukin-6 (IL-6). These examples show that both the interaction with non-parenchymal cells and the presence of extracellular matrix are essential to recreate a useful in vitro model of NAFLD. Others crucial factors often neglected in many studies are the cell density and the contact with other cell types [44–46].

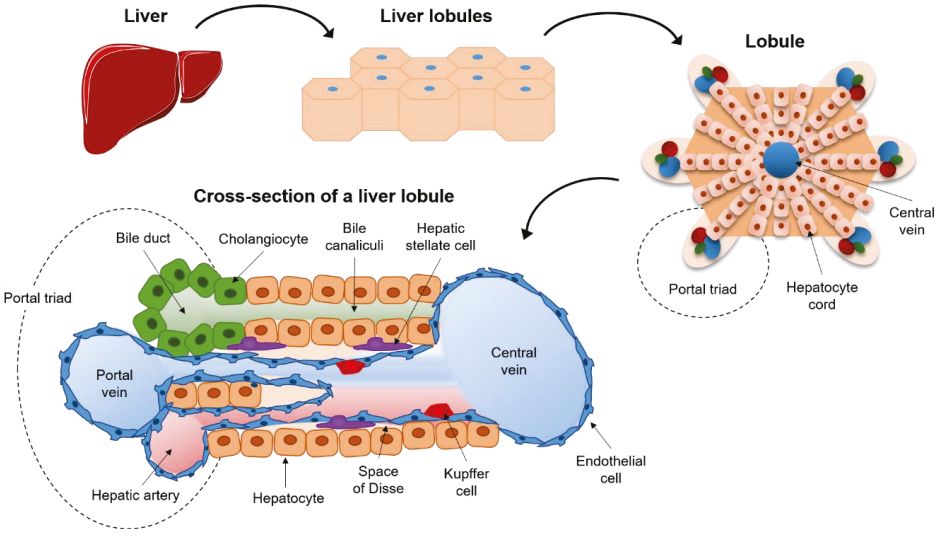

Figure 3. Schematic representation of liver lobule. The liver is composed of hexagonal functional unit known as lobule homogeneous throughout all the liver. Hepatic stellate cells give structural support to the endothelial cells which regulate the exchange with blood. Kupffer cells are the macrophage of the liver and responsible for the initial immune response in case of an insult. The hepatocytes represent the metabolic factory of the liver and organized according to their function. This anatomical configuration is the main challenge of tissue engineering.

Recently, giant steps towards the replacements of extracellular matrix with synthetic biocompatible polymers have been made. These biopolymers with controlled diffusion properties mimic natural tissue stiffness, making it possible to keep hepatocytes' phenotype and functions for a longer time. The most studied materials for tissue engineering are based on natural origins like gelatin, alginate, and cellulose [47–49] or synthetic materials such as poly L-lactic acid, poly (lactic-co-glycolic acid) and polycaprolactone [50–52]. Many variables, under the operator's control, concur in the design and fabrication of these three-dimensional biopolymers. Porosity and stiffness are the essential variables to build a functional 3D structure compatible with cell viability and functionality [47]. The optimal pore size allows the cells to attach, interact, and form aggregates [53–55]. On the other hand, the scaffold must prevent the cells from escaping as well as constitute some sort of protection against the host's immune system in case of implantation. Stiffness instead affects cell adhesion, motility, and polarization (referred to as the cell's ability to differentiate in space and function). Generally, a healthy human liver has a stiffness that ranges from 3 to 8 kPa which can increase about 30% when fibrosis and fibrosis-related processes are in place [56]. Overall, rigid materials, with a stiffness that resemble the fibrotic state,

enhance hepatocytes attachment, proliferation, mobility, and dedifferentiation [57,58]. It is biological plausible because of the intense cellular recruitment that takes place surrounding the damaged/fibrotic area where a high number of undifferentiated cells are needed to replace the dead ones. On the other hand, gene expression and the release of soluble markers of liver functionality, increase in hepatocytes encapsulated in soft substrates [48].

Microfluidic and shear stress have been shown to improve cell phenotype in vitro. An OOC is by definition a microfluidic cell culture device fabricated using microchip manufacturing techniques. These tools are provided with continuously perfused chambers where living cells are arranged to simulate tissue- and organ-level physiology. These devices produce tissue and organ functionality not possible with conventional 2D or 3D culture systems by recapitulating the body's physicochemical microenvironments and vascular perfusion. Control of fluid flow in chips has proved enormously useful. Viscous forces dominate over inertial ones at small length scales, then the flow is laminar if the 'microfluidic' channel's diameter is less than about one millimeter. Laminar flow allows the generation of physical and chemical gradients, which have been exploited for non-invasive study of directional cell migration [59–61], cardiac tissue formation [62], nerve axon outgrowth [63], and graded metabolic [64], differentiation [65], and neurotoxin [66] responses, as well as analysis of subcellular structure [59] and cell-cell junctional integrity [67]. Fluid shear stresses can be controlled independently of physical and chemical gradients by altering flow rates or channel dimensions [68,69] and separating cells from the flow path using a nano porous membrane [68] or micro-engineered posts that restrict cell passage [70]. Fluid-mechanical computational models can be applied to optimize microchannel geometry and enhance oxygen and nutrient delivery, thereby increasing cell survival and function [68].

Accurate representation of in vivo organ physiology and drug pharmacokinetics can be achieved in OOC devices through precise control of cellular microenvironments; however, quantitative information extraction is equally essential. OOC integrated with new sensing technology allows easier intra- and extracellular measurements across different tissues. Biosensors are analytical devices consisting of a biological component (enzyme, receptor, oligonucleotide, cell, antibody, etc.) in intimate contact with a physical transducer that convert the biorecognition process into a measurable signal (electrical or optical) (Figure 4).

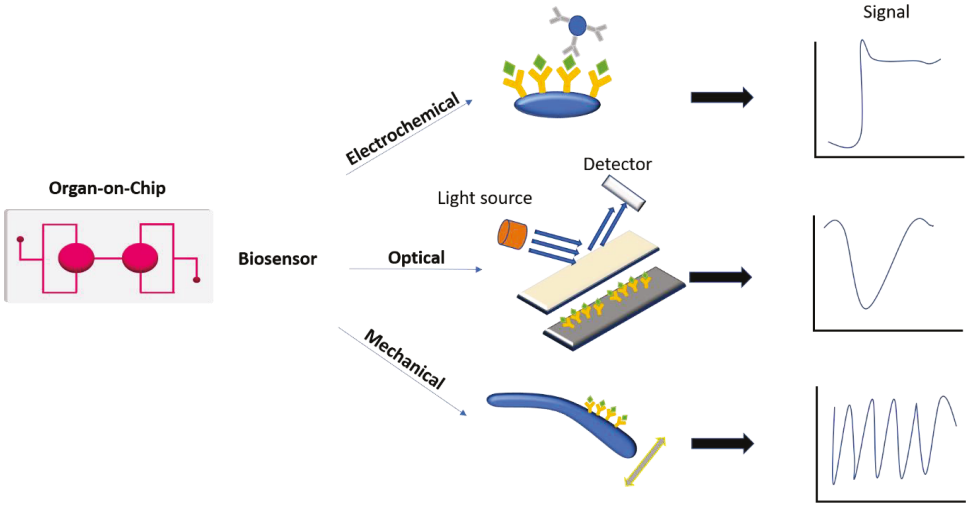

Figure 4. Examples of sensor platforms that can be integrated with organ-on-a-chip. Electrochemical biosensors measure the change of potential, current, conductance, or impedance induced by the immunoreaction. Optical biosensors determine the change in the optical properties of interaction between analyte and receptor. Mechanical biosensors assess the angular deflection due to molecular binding.

Because of its simplicity electrochemical transduction is the oldest and most common methods used in biosensors. They can determine the level of biomarkers by measuring the change of potential, current, conductance, or impedance caused by the immunoreaction. From all possible electrochemical transduction systems those based on recording amperometric signal generated after an enzymatic reaction have seen greatest development [71]. Amperometric biosensors are based on the measurement of the current generated by oxidation/reduction of redox species at the electrode surface, which is maintained at an appropriate electric potential. The current observed has a linear relationship with the concentration of the electroactive species. The electrode is usually constructed of platinum, gold, or carbon.

Optical transducers are based on various technologies involving optical phenomena, which are the result of an interaction of analyte with receptor. This group may be further subdivided according to the optical properties that have been applied in sensing (i.e., absorbance, reflectance, luminescence, fluorescence, refractive index, and surface plasmon resonance (SPR), and light scattering). The plasmon resonance is an evanescent electromagnetic field generated at the surface of a metal conductor (usually Ag or Au) when excited by the impact of light of an appropriate wavelength at a particular angle (α). Since distinct SPR prototypes (Biacore, IASys, etc.) have appeared in the market, a significant number of applications of this principle have been reported during the last years. Recently, localized surface plasmon resonance (LSPR) has been confirmed as a perfect candidate for OOC integration [72].

Microcantilever (MCL) translate molecular recognition of biomolecules into nanomechanical motion that is commonly coupled to an optical or piezo-resistive read-out detector system. Microcantilever sensors rely on their deflection to indicate sensing. Thus, molecular adsorption onto the sensing element shifts the resonance frequency and changes its surface forces (surface stress). Surface stress due to conformation change of proteins and other polymers has been a recent focus of MCL research. MCL that respond to conformational change-induced surface stress are promising transducers of chemical information and are ideal for developing microcantilever-based biosensors. (Figure 4).

OOCs can be employed to study the crosstalk between different cell populations of the same organ allowing further understanding of complex metabolic diseases. Current OOCs assays heavily rely on fluorescence microscopy and have mainly been used for specialized proof-of-concept studies, for example, in angiogenesis [73–75], in electrophysiology [76,77], and in pharmacological modulation of cell growth [76,78,79]. However, fluorescent labelling is a qualitative method and end-point assay losing all the real-time changes in metabolic behavior of the cells. There are few examples of OOCs where 3D functional tissues are integrated with an in-built sensor platform. Some lab-on-chip assays allow to measure parameters, such as oxygen concentration [80–82], pH level [83,84], and glucose consumption [85]. The use of antibodies add specificity to the sensors in detecting biomarkers, such as insulin or IL6 from complex biological media [71,86]. These biosensors are based on redox or enzymatic reactions that imply incubation and washing steps therefore limiting the value of the data acquired and not providing real-time information. Ideally, the next OOC platforms equipped with sophisticated built-in sensors would provide real-time data at cellular level.

4. Artificial Intelligence and NAFLD

Since 1970, when the potential of applying artificial intelligence technology in clinical setting was discussed, only few AI solutions were successfully employed. The main tasks performed were literature mining, automated experiments, and data collection [87–90]. For the following 20 years, there was a general loss of interest towards AI solutions in medicine known as "AI winter" that lasted until the end 90′s when "big data" became available. According to the website ClinicalTrials.gov, the ongoing clinical trials using big data and artificial intelligence are 3417 and 405, respectively.

AI is the ability of a computer-based machine to apply a pre-determined set of rules (algorithm) to solve a specific task. By definition, these machines have the capacity to accurately predict a determined outcome or even take a decision that mitigates that outcome in a timely fashion. Both capabilities are prerogative of most human beings. To succeed in their task, these machines need to process a set of initial values (input) to generate a different set of values (output) thanks to a task-tailored algorithm. AI technology is a collection of physical (e.g., intelligent prostheses for handicapped people, robot performing surgeries) and virtual (e.g., predictive models that guide the clinicians' decisions) applications. The Electronic Health Records (EHR) keep records of both practice and clinical management of patients during episodes of patient care and represents the primary reason of the tremendous upsurge of the virtual retrospective studies [91] (Figure 5).

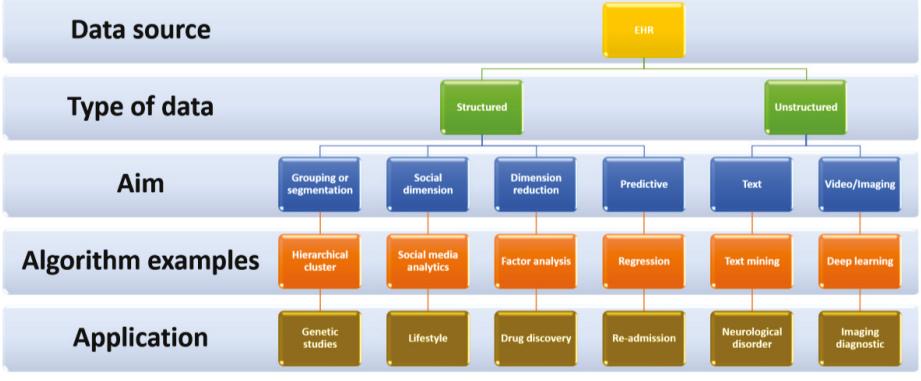

Figure 5. Electronic Health Records (EHR) workflow.

Whilst computers can be programmed to perform better and more efficient tasks compared with humans, we are years far from AI tools capable to replace the latter in the medical practice, and more specifically, in the decision-making process. Machine learning, and its most powerful component deep learning, are crucial to make a machine able to acquire, analyze and interpret data in humanly fashion. The three most common approaches used are unsupervised, supervised, and reinforced learning [92]. The difference between the first two is the presence or not of a clean and labelled dataset to train the algorithm in order "to learn". The limitation of these two approaches is the need of large dataset to train properly the algorithm, in case of supervised learning, and the low accuracy for the unsupervised. Differently, a reinforced algorithm interacts continuously with environment getting a feedback from it [93,94]. Every time it performs a task, it gets back an index, generally higher for the success and lower for the failure of the task. In that way, the algorithm modify itself to tend always to the higher index possible. However, this can lead to longer waiting time (Figure 6).

Nowadays, we are just mining massive amount of data to get insights about diseases. The next and closer step is to carry out predictive analysis to detect the early onset of the disease or at least identify its stronger risks factors. However, in medicine the main limitations are (i) the short follow-up of the patients—that reduce the predicting power of the models applied—and (ii) the inclusion during the analyses of potential hidden cofounding factors—that limit the matched-pair in clinical trial design causing a failure of the study. So far in NAFLD, only few papers have attempted to apply and implement the use of AI and machine learning mainly for its diagnosis. For example, Han Ma et al. investigated 11 machine learning (ML) techniques in a cross-sectional study of 2522 patients with NAFLD (assessed by ultrasonic examination), coming up with the conclusion that "users could focus only in five features—body weight, triglycerides, alanine aminotransferase, gamma-glutamyl transpeptidase, and levels of serum uric acid—that

contribute to the NAFLD phenotype". In this study, the Bayesian network model gave the best performance (the Bayesian network model consists in a graphical scheme where the nodes or features are connected each other according to causal relationship among them) [95]. A different approach has been used by Heinemann et al. where they attempt to automate the Kleiner score—ballooning, inflammation, steatosis, and fibrosis as main histopathological features—for the diagnosis of NASH for NAFLD/NASH models using a whole slide of liver rat and mouse stained by Masson's trichrome. Four models of convolutional neural networks for image classification have been employed. Although it seems a very interesting approach, it is very difficult to apply to human [96]. First, this approach needs years of validation performed by expert pathologists to train the algorithm properly. Second, the high variability of the human evaluation of liver biopsies already in place using standard features. Third, the human biopsy is a tiny portion of tissue which most of the time is not representative of the whole organ.

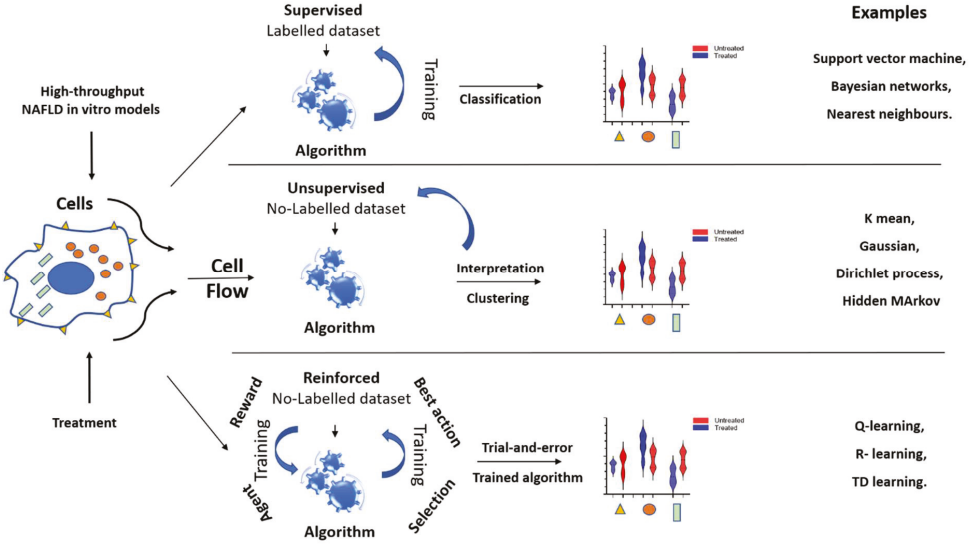

Figure 6. Supervised, Unsupervised, and reinforced learning applications for organ-on-a-chip.

Despite the advantages in applying AI for the diagnosis or treatment of patients, many challenges still exist in the quality and quantity of the collected data. First, the reduced number of samples affect the consistency and accuracy of the analysis. Second, the implementation of AI in medicine is faster than the ethical and legal regulation of the field. From this point of view, the biggest issues are data privacy, safety, and transparency [97].

5. In Vitro NAFLD Features Recognition: The Synergy between OOC and AI

The application of AI to the OOCs enables to analyze parameters that could not be considered so far for the study of NAFLD. Furthermore, their low in cost and automation propel them from engineering research into to any biomedical fields. With incredibly fast progress of OOCs in mimicking the complexity of native anatomical structures, many deep learning techniques developed for human can be applied. Deep learning is the biggest part of machine learning techniques and it is employed to recognizes pattern from the data using many levels of interpretation of unstructured data (images, text etc.). Its main limitation is the use of big training dataset that, in case of OOCs, is resolved using single cells images. For example, Guo et al. developed a high-throughput single cell lipid screening using an optofluidic time-stretch quantitative phase microscopy [98,99]. The combination of the quantitative phase imaging and machine learning allows the physical classification of cells

(shape, area etc.) with high accuracy. This system can spot rare or even unknown events without a training dataset (unsupervised learning) and applicable to various fields. For example, it could be employed to study the kinetic of di- and triglyceride accumulation in spheroids of primary human hepatocytes trough imaging [100]. The rationale would be the understanding of fat trafficking inside the cells and its timing.

In another example, Blasi et al. demonstrated that it is possible to determine the cells' DNA content, live or fixed, using brightfield and darkfield images obtained via imaging flow cytometry. Moreover, the cells' mitotic phase can be also assessed [101]. The machine learning algorithm is trained against a dataset specific for the cell type or the interested feature. An interesting application would be the assessment of the in vitro regenerative capacity of hepatocytes according to their cell cycle phase. In fact, in patients with NAFLD, liver regeneration is compromised making these patients not optimal recipient for a transplanted organ [102]. One more study conducted by Chu et al. employed a machine learning based control system for microfluidic microencapsulation [103]. This system assesses via real-time the quality of the microencapsulation using spheroids images. This technology could be very useful to spot abnormal spheroids in a 3D printing high throughput platform therefore increasing the reproducibility for drug screening purposes.

These are only three examples of new technologies built for machine and deep learning techniques that might be applicable to identify the early pathological phenotypic changes of the cells or evaluate the efficacy of drugs candidates. On the other hand, many are the algorithm generated to analyze old data or applicable to old technologies. For example, Das et al. used light microscopic image acquisition from stained slides to extract 96 features to discriminate between Plasmodium-infected and non-infected erythrocytes [104]. The ability to discriminate the healthy or diseased status according to the shape would be extremely interesting in evaluating the change in shape in hepatic stellate cells strictly in contact with hepatocytes [105].

In another example, Mirsky et al. employed interferometric phase microscopy to develop a machine learning based classification method for sperm analyses and characterization [106]. The algorithm was able to extract 89 custom-designed features. This technology could be easily applicable to measure the degree of lysosomal permeabilization in hepatocytes upon treatment with saturated and unsaturated lipids [107]. This would give important insight about cell death. Ko et al. combines the nanofluidic technology with machine learning to discriminate between patients suffering of pancreatic cancer and healthy subject [108]. Although few human samples were analyzed, this study showed the potential of combining different technologies, in this case, nanofluidic, exosome screening and machine learning to better characterize patients in order to improve the success/failure ratio of clinical trial and/or treatment effectiveness.

6. Body on a Chip: An Exponential Growth in Complexity

The liver is the shield of the body protecting it from endogenous and exogenous substances. Once it fails in its function, many other organs are subjected to a continuous pathogenic signal that inexorably will lead to their failure, on a short time (acute) or a long time (chronic), if not neutralized. However, little information is available about the actors and their kinetic in pathogenesis of NAFLD.

Very few multiple organs on a chip have been developed in the last years to unveil the crosstalk between organs during the pathology. For example, Lee and Sung built a gut-liver on a chip to study the lipid accumulation as well as a potential treatment for reducing it [109]. Although the model is based on the use HepG2 (hepatoma cell line)—phenotypically and genotypically very different from healthy hepatocytes—they showed the importance of proinflammatory cytokine Tumor Necrosis Factor-α on the gut absorption permeability of the lipids. Interestingly, TNFα per se, did not exert any effect on the lipid's accumulation in liver cells. On the same line, Ahluwalia et al. cocultured hepatic, endothelial, and different amount of adipose cells in an interconnected tissue models for the study of obesity and its lipid-related molecules and pro-inflammatory

markers [110]. They showed the increase of pro-inflammatory markers such as Interleukin-6 and Monocyte chemoattractant protein-1 in endothelial and liver cells when connected to adipose tissue demonstrating the adipose tissue as an important source of inflammatory cytokine production.

These are only two examples of multiple organs interaction under the high load lipids intake regimen. However, a far more complex platform is necessary to identify both the players and the temporal role of them during the pathogenesis and progression of NAFLD. Real-time sensing system that targets concurrently multiple proteins and soluble factors and a computer-aided system to help in the analysis and interpretation would dramatically transform these platforms in the next few years. More important than a technological transition, it is the interaction of different fields such as biology, physiology, medicine, and engineering that will allow the full comprehension of the data generated by these platforms.

7. Conclusions

NAFLD is a multifactorial disease with unknown cause(s). Machine and deep learning are mainly used to improve the performance of OOCs. At the moment, the real job of these techniques is to reduce the dimensionality of the large number of variables or measurements to allow us to extrapolate useful information. The marriage between OOCs and artificial intelligence overcome the risk to apply AI-based application directly to human and therefore no need of ethical approval. In the next 10 years, artificial intelligence will turn these devices output in a real-time source of clinically relevant information improving medical decision. It is not too far to imagine a multi-organ on a chip completely controlled by algorithm that regulates the fluidic, the injection of treatments the measurement while correlates and interprets the outcome at same time. The combination of these two technologies will allow to analyze not only standard but also new features helping the pharmaceutical companies for screening of massive number of molecules in very short period. Furthermore, it will give a more exhaustive information compared with the traditional methods so far employed such as: discovering synergy between treatments, finding more effective concentrations, unveiling, and reducing potential side effect of drugs. From the patient's point of view, the incorporation of these new OOCs could improve the stratification of recruited patients in clinical trials, saving cost and time, accelerating the development of precision medicine, and helping the clinicians in the diagnostic.

Author Contributions: Conceptualization, F.D.C. and A.F.-M.; resources, J.R.-A.; writing—original draft preparation, F.D.C., A.F.-M., and J.R.-A.; writing—review and editing, F.D.C., A.F.-M., and J.R.-A.; funding acquisition, J.R.-A. All authors have read and agreed to the published version of the manuscript.

Funding: This work has been developed in the context of BLAD project (2019 LLAV 00056) with the support of AGAUR (Generalitat de Catalunya) and the European Community under the Catalonian ERDF operational program (European Regional Development Fund) 2014–2020. This project received financial support from the European Research Council program under grants ERC-StG-DAMOC (714317), the Spanish Ministry of Economy and Competitiveness, through the "Severo Ochoa" Program for Centres of Excellence in R&D (SEV-2016–2019) and "Retos de investigación: Proyectos I+D+i" (TEC2017-83716-C2-2-R), the CERCA Programme/Generalitat de Catalunya (2014- SGR-1460) and Fundación Bancaria "la Caixa"—Obra Social "la Caixa" (project IBEC-La Caixa Healthy Ageing).

Institutional Review Board Statement: Not applicable.

Informed Consent Statement: Not applicable.

Data Availability Statement: Data sharing not applicable.

Acknowledgments: We would like to thank Alice Senni for the kind proofread of the manuscript.

Conflicts of Interest: The authors declare no conflict of interest.

References

1. Adams, L.A.; Lymp, J.F.; St. Sauver, J.; Sanderson, S.O.; Lindor, K.D.; Feldstein, A.; Angulo, P. The natural history of nonalcoholic fatty liver disease: A population-based cohort study. *Gastroenterology* **2005**. [CrossRef]
2. Pang, Q.; Zhang, J.-Y.; Song, S.-D.; Qu, K.; Xu, X.-S.; Liu, S.-S.; Liu, C. Central obesity and nonalcoholic fatty liver disease risk after adjusting for body mass index. *World J. Gastroenterol.* **2015**, *21*, 1650–1662. [CrossRef]
3. Hagström, H.; Nasr, P.; Ekstedt, M.; Hammar, U.; Stål, P.; Hultcrantz, R.; Kechagias, S. Fibrosis stage but not NASH predicts mortality and time to development of severe liver disease in biopsy-proven NAFLD. *J. Hepatol.* **2017**, *67*, 1265–1273. [CrossRef] [PubMed]
4. Younossi, Z.M.; Koenig, A.B.; Abdelatif, D.; Fazel, Y.; Henry, L.; Wymer, M. Global epidemiology of nonalcoholic fatty liver disease—Meta-analytic assessment of prevalence, incidence, and outcomes. *Hepatology* **2016**. [CrossRef] [PubMed]
5. Lonardo, A.; Leoni, S.; Alswat, K.A.; Fouad, Y. History of Nonalcoholic Fatty Liver Disease. *Int. J. Mol. Sci.* **2020**, *21*, 5888. [CrossRef]
6. Marchesini, G.; Day, C.P.; Dufour, J.F.; Canbay, A.; Nobili, V.; Ratziu, V.; Tilg, H.; Roden, M.; Gastaldelli, A.; Yki-Jarvinen, H.; et al. EASL-EASD-EASO Clinical Practice Guidelines for the management of non-alcoholic fatty liver disease. *J. Hepatol.* **2016**. [CrossRef]
7. Rinella, M.E.; Tacke, F.; Sanyal, A.J.; Anstee, Q.M. Report on the AASLD/EASL joint workshop on clinical trial endpoints in NAFLD. *J. Hepatol.* **2019**, *71*, 823–833. [CrossRef]
8. Machado, M.V.; Cortez-Pinto, H. Non-invasive diagnosis of non-alcoholic fatty liver disease. A critical appraisal. *J. Hepatol.* **2013**, *58*, 1007–1019. [CrossRef] [PubMed]
9. Davison, B.A.; Harrison, S.A.; Cotter, G.; Alkhouri, N.; Sanyal, A.; Edwards, C.; Colca, J.R.; Iwashita, J.; Koch, G.G.; Dittrich, H.C. Suboptimal reliability of liver biopsy evaluation has implications for randomized clinical trials. *J. Hepatol.* **2020**. [CrossRef]
10. Jensen, V.S.; Tveden-Nyborg, P.; Zacho-Rasmussen, C.; Quaade, M.L.; Ipsen, D.H.; Hvid, H.; Fledelius, C.; Wulff, E.M.; Lykkesfeldt, J. Variation in diagnostic NAFLD/NASH read-outs in paired liver samples from rodent models. *J. Pharm. Toxicol. Methods* **2020**, *101*, 106651. [CrossRef]
11. Fogel, D.B. Factors associated with clinical trials that fail and opportunities for improving the likelihood of success: A review. *Contemp. Clin. Trials Commun.* **2018**, *11*, 156–164. [CrossRef]
12. Freag, M.S.; Namgung, B.; Reyna Fernandez, M.E.; Gherardi, E.; Sengupta, S.; Jang, H.L. Human Nonalcoholic Steatohepatitis on a Chip. *Hepatol. Commun.* **2020**. [CrossRef]
13. Bulutoglu, B.; Rey-Bedón, C.; Kang, Y.B.A.; Mert, S.; Yarmush, M.L.; Usta, O.B. A microfluidic patterned model of non-alcoholic fatty liver disease: Applications to disease progression and zonation. *Lab Chip* **2019**, *19*, 3022–3031. [CrossRef] [PubMed]
14. Gori, M.; Simonelli, M.C.; Giannitelli, S.M.; Businaro, L.; Trombetta, M.; Rainer, A. Investigating Nonalcoholic Fatty Liver Disease in a Liver-on-a-Chip Microfluidic Device. *PLoS ONE* **2016**, *11*, e0159729. [CrossRef] [PubMed]
15. Trietsch, S.J.; Naumovska, E.; Kurek, D.; Setyawati, M.C.; Vormann, M.K.; Wilschut, K.J.; Lanz, H.L.; Nicolas, A.; Ng, C.P.; Joore, J.; et al. Membrane-free culture and real-time barrier integrity assessment of perfused intestinal epithelium tubes. *Nat. Commun.* **2017**. [CrossRef] [PubMed]
16. Jordan, N.V.; Bardia, A.; Wittner, B.S.; Benes, C.; Ligorio, M.; Zheng, Y.; Yu, M.; Sundaresan, T.K.; Licausi, J.A.; Desai, R.; et al. HER2 expression identifies dynamic functional states within circulating breast cancer cells. *Nature* **2016**, *537*, 102–106. [CrossRef]
17. McKinney, S.M.; Sieniek, M.; Godbole, V.; Godwin, J.; Antropova, N.; Ashrafian, H.; Back, T.; Chesus, M.; Corrado, G.S.; Darzi, A.; et al. International evaluation of an AI system for breast cancer screening. *Nature* **2020**, *577*, 89–94. [CrossRef] [PubMed]
18. Kobayashi, H.; Lei, C.; Wu, Y.; Huang, C.-J.; Yasumoto, A.; Jona, M.; Li, W.; Wu, Y.; Yalikun, Y.; Jiang, Y.; et al. Intelligent whole-blood imaging flow cytometry for simple, rapid, and cost-effective drug-susceptibility testing of leukemia. *Lab Chip* **2019**, *19*, 2688–2698. [CrossRef] [PubMed]
19. Isozaki, A.; Harmon, J.; Zhou, Y.; Li, S.; Nakagawa, Y.; Hayashi, M.; Mikami, H.; Lei, C.; Goda, K. AI on a chip. *Lab Chip* **2020**, *20*, 3074–3090. [CrossRef]
20. Targher, G.; Byrne, C.D.; Lonardo, A.; Zoppini, G.; Barbui, C. Non-alcoholic fatty liver disease and risk of incident cardiovascular disease: A meta-analysis. *J. Hepatol.* **2016**. [CrossRef]
21. Federico, A.; Dallio, M.; Masarone, M.; Persico, M.; Loguercio, C. The epidemiology of non-alcoholic fatty liver disease and its connection with cardiovascular disease: Role of endothelial dysfunction. *Eur. Rev. Med. Pharmacol. Sci.* **2016**, *20*, 4731–4741.
22. Lonardo, A.; Sookoian, S.; Pirola, C.J.; Targher, G. Non-alcoholic fatty liver disease and risk of cardiovascular disease. *Metabolism* **2016**, *65*, 1136–1150. [CrossRef]
23. Kim, G.A.; Lee, H.C.; Choe, J.; Kim, M.J.; Lee, M.J.; Chang, H.S.; Bae, I.Y.; Kim, H.K.; An, J.; Shim, J.H.; et al. Association between non-alcoholic fatty liver disease and cancer incidence rate. *J. Hepatol.* **2018**. [CrossRef]
24. Mantovani, A.; Dauriz, M.; Byrne, C.D.; Lonardo, A.; Zoppini, G.; Bonora, E.; Targher, G. Association between nonalcoholic fatty liver disease and colorectal tumours in asymptomatic adults undergoing screening colonoscopy: A systematic review and meta-analysis. *Metabolism* **2018**. [CrossRef]
25. Shen, H.; Lipka, S.; Kumar, A.; Mustacchia, P. Association between nonalcoholic fatty liver disease and colorectal adenoma: A systemic review and meta-analysis. *J. Gastrointest. Oncol.* **2014**. [CrossRef]
26. Nseir, W.; Abu-Rahmeh, Z.; Tsipis, A.; Mograbi, J.; Mahamid, M. Relationship between non-alcoholic fatty liver disease and breast cancer. *Isr. Med. Assoc. J.* **2017**, *19*, 242–245. [PubMed]

27. Campbell, P.T.; Deka, A.; Jacobs, E.J.; Newton, C.C.; Hildebrand, J.S.; McCullough, M.L.; Limburg, P.J.; Gapstur, S.M. Prospective study reveals associations between colorectal cancer and type 2 diabetes mellitus or insulin use in men. *Gastroenterology* **2010**. [CrossRef] [PubMed]
28. Lohmann, A.E.; Goodwin, P.J.; Chlebowski, R.T.; Pan, K.; Stambolic, V.; Dowling, R.J.O. Association of obesity-related metabolic disruptions with cancer risk and outcome. *J. Clin. Oncol.* **2016**, *34*, 4249–4255. [CrossRef] [PubMed]
29. Kim, G.; Lee, S.E.; Lee, Y.B.; Jun, J.E.; Ahn, J.; Bae, J.C.; Jin, S.M.; Hur, K.Y.; Jee, J.H.; Lee, M.K.; et al. Relationship Between Relative Skeletal Muscle Mass and Nonalcoholic Fatty Liver Disease: A 7-Year Longitudinal Study. *Hepatology* **2018**. [CrossRef]
30. Montano-Loza, A.J.; Meza-Junco, J.; Prado, C.M.M.; Lieffers, J.R.; Baracos, V.E.; Bain, V.G.; Sawyer, M.B. Muscle Wasting Is Associated With Mortality in Patients With Cirrhosis. *Clin. Gastroenterol. Hepatol.* **2012**. [CrossRef] [PubMed]
31. Tsien, C.; Garber, A.; Narayanan, A.; Shah, S.N.; Barnes, D.; Eghtesad, B.; Fung, J.; Mccullough, A.J.; Dasarathy, S. Post-liver transplantation sarcopenia in cirrhosis: A prospective evaluation. *J. Gastroenterol. Hepatol.* **2014**. [CrossRef] [PubMed]
32. Marcuccilli, M.; Chonchol, M. NAFLD and chronic kidney disease. *Int. J. Mol. Sci.* **2016**, *17*, 562. [CrossRef] [PubMed]
33. Targher, G.; Byrne, C.D. Non-alcoholic fatty liver disease: An emerging driving force in chronic kidney disease. *Nat. Rev. Nephrol.* **2017**, *13*, 297–310. [CrossRef] [PubMed]
34. El Azeem, H.A.; Khalek, E.S.A.; El-Akabawy, H.; Naeim, H.; Khalik, H.A.; Alfifi, A.A. Association between nonalcoholic fatty liver disease and the incidence of cardiovascular and renal events. *J. Saudi Hear. Assoc.* **2013**. [CrossRef] [PubMed]
35. Weinstein, G.; Zelber-Sagi, S.; Preis, S.R.; Beiser, A.S.; DeCarli, C.; Speliotes, E.K.; Satizabal, C.L.; Vasan, R.S.; Seshadri, S. Association of nonalcoholic fatty liver disease with lower brain volume in healthy middle-aged adults in the Framingham Study. *JAMA Neurol.* **2018**. [CrossRef]
36. Fargion, S.; Porzio, M.; Fracanzani, A.L. Nonalcoholic fatty liver disease and vascular disease: State-of-the-art. *World J. Gastroenterol.* **2014**, *20*, 13306. [CrossRef]
37. Lombardi, R.; Fargion, S.; Fracanzani, A.L. Brain involvement in non-alcoholic fatty liver disease (NAFLD): A systematic review. *Dig. Liver Dis.* **2019**, *51*, 1214–1222. [CrossRef]
38. Hadjihambi, A.; De Chiara, F.; Hosford, P.S.; Habtetion, A.; Karagiannis, A.; Davies, N.; Gourine, A.V.; Jalan, R. Ammonia mediates cortical hemichannel dysfunction in rodent models of chronic liver disease. *Hepatology* **2017**, 65. [CrossRef]
39. Jalan, R.; De Chiara, F.; Balasubramaniyan, V.; Andreola, F.; Khetan, V.; Malago, M.; Pinzani, M.; Mookerjee, R.P.; Rombouts, K. Ammonia produces pathological changes in human hepatic stellate cells and is a target for therapy of portal hypertension. *J. Hepatol.* **2016**, 64. [CrossRef]
40. Rosato, V.; Masarone, M.; Dallio, M.; Federico, A.; Aglitti, A.; Persico, M. NAFLD and extra-hepatic comorbidities: Current evidence on a multi-organ metabolic syndrome. *Int. J. Environ. Res. Public Health* **2019**, *16*, 3415. [CrossRef]
41. Manco, R.; Itzkovitz, S. Liver zonation. *J. Hepatol.* **2021**, *74*, 466–468. [CrossRef]
42. Dunn, J.C.Y.; Tompkins, R.G.; Yarmush, M.L. Long-Term in Vitro Function of Adult Hepatocytes in a Collagen Sandwich Configuration. *Biotechnol. Prog.* **1991**, *7*, 237–245. [CrossRef] [PubMed]
43. Suurmond, C.-A.E.; Lasli, S.; van den Dolder, F.W.; Ung, A.; Kim, H.-J.; Bandaru, P.; Lee, K.; Cho, H.-J.; Ahadian, S.; Ashammakhi, N.; et al. In Vitro Human Liver Model of Nonalcoholic Steatohepatitis by Coculturing Hepatocytes, Endothelial Cells, and Kupffer Cells. *Adv. Healthc. Mater.* **2019**, *8*, 1901379. [CrossRef]
44. Wei, G.; Wang, J.; Lv, Q.; Liu, M.; Xu, H.; Zhang, H.; Jin, L.; Yu, J.; Wang, X. Three-dimensional coculture of primary hepatocytes and stellate cells in silk scaffold improves hepatic morphology and functionality in vitro. *J. Biomed. Mater. Res. Part A* **2018**, *106*, 2171–2180. [CrossRef] [PubMed]
45. Baze, A.; Parmentier, C.; Hendriks, D.F.G.; Hurrell, T.; Heyd, B.; Bachellier, P.; Schuster, C.; Ingelman-Sundberg, M.; Richert, L. Three-Dimensional Spheroid Primary Human Hepatocytes in Monoculture and Coculture with Nonparenchymal Cells. *Tissue Eng. Part C Methods* **2018**, *24*, 534–545. [CrossRef] [PubMed]
46. Abu-Absi, S.F.; Hansen, L.K.; Hu, W.-S. Three-dimensional co-culture of hepatocytes and stellate cells. *Cytotechnology* **2004**, *45*, 125–140. [CrossRef]
47. Kim, Y.; Kang, K.; Jeong, J.; Paik, S.S.; Kim, J.S.; Park, S.A.; Kim, W.D.; Park, J.; Choi, D. Three-dimensional (3D) printing of mouse primary hepatocytes to generate 3D hepatic structure. *Ann. Surg. Treat. Res.* **2017**, *92*, 67–72. [CrossRef]
48. Lewis, P.L.; Green, R.M.; Shah, R.N. 3D-printed gelatin scaffolds of differing pore geometry modulate hepatocyte function and gene expression. *Acta Biomater.* **2018**, *69*, 63–70. [CrossRef]
49. Krüger, M.; Oosterhoff, L.A.; van Wolferen, M.E.; Schiele, S.A.; Walther, A.; Geijsen, N.; De Laporte, L.; van der Laan, L.J.W.; Kock, L.M.; Spee, B. Cellulose Nanofibril Hydrogel Promotes Hepatic Differentiation of Human Liver Organoids. *Adv. Healthc. Mater.* **2020**. [CrossRef]
50. Török, E.; Lutgehetmann, M.; Bierwolf, J.; Melbeck, S.; Düllmann, J.; Nashan, B.; Ma, P.X.; Pollok, J.M. Primary human hepatocytes on biodegradable poly(l-lactic acid) matrices: A promising model for improving transplantation efficiency with tissue engineering. *Liver Transpl.* **2011**. [CrossRef]
51. Li, J.; Li, L.; Yu, H.; Cao, H.; Gao, C.; Gong, Y. Growth and metabolism of human hepatocytes on biomodified collagen poly(lactic-co-glycolic acid) three-dimensional scaffold. *Asaio J.* **2006**. [CrossRef]
52. Xiao, Y.; Zhou, M.; Zhang, M.; Liu, W.; Zhou, Y.; Lang, M. Hepatocyte culture on 3D porous scaffolds of PCL/PMCL. *Colloids Surf. B Biointerfaces* **2019**, *173*, 185–193. [CrossRef]

53. Loh, Q.L.; Choong, C. Three-dimensional scaffolds for tissue engineering applications: Role of porosity and pore size. *Tissue Eng. Part B Rev.* **2013**, *19*, 485–502. [CrossRef]
54. Krieghoff, J.; Picke, A.-K.; Salbach-Hirsch, J.; Rother, S.; Heinemann, C.; Bernhardt, R.; Kascholke, C.; Möller, S.; Rauner, M.; Schnabelrauch, M.; et al. Increased pore size of scaffolds improves coating efficiency with sulfated hyaluronan and mineralization capacity of osteoblasts. *Biomater. Res.* **2019**, *23*, 26. [CrossRef] [PubMed]
55. Tytgat, L.; Kollert, M.R.; Van Damme, L.; Thienpont, H.; Ottevaere, H.; Duda, G.N.; Geissler, S.; Dubruel, P.; Van Vlierberghe, S.; Qazi, T.H. Evaluation of 3D Printed Gelatin-Based Scaffolds with Varying Pore Size for MSC-Based Adipose Tissue Engineering. *Macromol. Biosci.* **2020**, *20*, 1900364. [CrossRef] [PubMed]
56. Roulot, D.; Czernichow, S.; Le Clésiau, H.; Costes, J.L.; Vergnaud, A.C.; Beaugrand, M. Liver stiffness values in apparently healthy subjects: Influence of gender and metabolic syndrome. *J. Hepatol.* **2008**, *48*, 606–613. [CrossRef]
57. Ruoß, M.; Rebholz, S.; Weimer, M.; Grom-Baumgarten, C.; Athanasopulu, K.; Kemkemer, R.; Käß, H.; Ehnert, S.; Nussler, A.K. Development of Scaffolds with Adjusted Stiffness for Mimicking Disease-Related Alterations of Liver Rigidity. *J. Funct. Biomater.* **2020**, *11*, 17. [CrossRef] [PubMed]
58. Hosseini, V.; Maroufi, N.F.; Saghati, S.; Asadi, N.; Darabi, M.; Ahmad, S.N.S.; Hosseinkhani, H.; Rahbarghazi, R. Current progress in hepatic tissue regeneration by tissue engineering. *J. Transl. Med.* **2019**, *17*, 383. [CrossRef] [PubMed]
59. Takayama, S.; Ostuni, E.; LeDuc, P.; Naruse, K.; Ingber, D.E.; Whitesides, G.M. Subcellular positioning of small molecules. *Nature* **2001**. [CrossRef]
60. Li Jeon, N.; Baskaran, H.; Dertinger, S.K.W.; Whitesides, G.M.; Van De Water, L.; Toner, M. Neutrophil chemotaxis in linear and complex gradients of interleukin-8 formed in a microfabricated device. *Nat. Biotechnol.* **2002**. [CrossRef]
61. Prentice-Mott, H.V.; Chang, C.H.; Mahadevan, L.; Mitchison, T.J.; Irimia, D.; Shah, J.V. Biased migration of confined neutrophil-like cells in asymmetric hydraulic environments. *Proc. Natl. Acad. Sci. USA* **2013**. [CrossRef]
62. Radisic, M.; Deen, W.; Langer, R.; Vunjak-Novakovic, G. Mathematical model of oxygen distribution in engineered cardiac tissue with parallel channel array perfused with culture medium containing oxygen carriers. *Am. J. Physiol. Hear. Circ. Physiol.* **2005**. [CrossRef]
63. Xiao, R.R.; Zeng, W.J.; Li, Y.T.; Zou, W.; Wang, L.; Pei, X.F.; Xie, M.; Huang, W.H. Simultaneous generation of gradients with gradually changed slope in a microfluidic device for quantifying axon response. *Anal. Chem.* **2013**. [CrossRef]
64. Peng, C.C.; Liao, W.H.; Chen, Y.H.; Wu, C.Y.; Tung, Y.C. A microfluidic cell culture array with various oxygen tensions. *Lab Chip* **2013**. [CrossRef]
65. Cimetta, E.; Cannizzaro, C.; James, R.; Biechele, T.; Moon, R.T.; Elvassore, N.; Vunjak-Novakovic, G. Microfluidic device generating stable concentration gradients for long term cell culture: Application to Wnt3a regulation of β-catenin signaling. *Lab Chip* **2010**. [CrossRef] [PubMed]
66. Seidi, A.; Kaji, H.; Annabi, N.; Ostrovidov, S.; Ramalingam, M.; Khademhosseini, A. A microfluidic-based neurotoxin concentration gradient for the generation of an in vitro model of Parkinson's disease. *Biomicrofluidics* **2011**. [CrossRef] [PubMed]
67. Chen, S.; Lee, L.P. Non-invasive microfluidic gap junction assay. *Integr. Biol.* **2010**. [CrossRef]
68. Carraro, A.; Hsu, W.M.; Kulig, K.M.; Cheung, W.S.; Miller, M.L.; Weinberg, E.J.; Swart, E.F.; Kaazempur-Mofrad, M.; Borenstein, J.T.; Vacanti, J.P.; et al. In vitro analysis of a hepatic device with intrinsic microvascular-based channels. *Biomed. Microdev.* **2008**. [CrossRef]
69. Griep, L.M.; Wolbers, F.; de Wagenaar, B.; ter Braak, P.M.; Weksler, B.B.; Romero, I.A.; Couraud, P.O.; Vermes, I.; van der Meer, A.D.; van den Berg, A. BBB ON CHIP: Microfluidic platform to mechanically and biochemically modulate blood-brain barrier function. *Biomed. Microdev.* **2013**, *15*, 145–150. [CrossRef] [PubMed]
70. Lee, P.J.; Hung, P.J.; Lee, L.P. An artificial liver sinusoid with a microfluidic endothelial-like barrier for primary hepatocyte culture. *Biotechnol. Bioeng.* **2007**. [CrossRef]
71. Ortega, M.A.; Fernández-Garibay, X.; Castaño, A.G.; De Chiara, F.; Hernández-Albors, A.; Balaguer-Trias, J.; Ramón-Azcón, J. Muscle-on-a-chip with an on-site multiplexed biosensing system for: In situ monitoring of secreted IL-6 and TNF-α. *Lab Chip* **2019**, *19*. [CrossRef]
72. Lopez-Muñoz, G.A.; Ortega, M.A.; Ferret-Miñana, A.; De Chiara, F.; Ramón-Azcón, J. Direct and Label-Free Monitoring of Albumin in 2D Fatty Liver Disease Model Using Plasmonic Nanogratings. *Nanomaterials* **2020**, *10*, 2520. [CrossRef] [PubMed]
73. Corcoran, M.P.; Lamon-Fava, S.; Fielding, R.A. Skeletal muscle lipid deposition and insulin resistance: Effect of dietary fatty acids and exercise. *Am. J. Clin. Nutr.* **2007**, *85*, 662–677.
74. Osaki, T.; Sivathanu, V.; Kamm, R.D. Crosstalk between developing vasculature and optogenetically engineered skeletal muscle improves muscle contraction and angiogenesis. *Biomaterials* **2018**. [CrossRef] [PubMed]
75. Theberge, A.B.; Yu, J.; Young, E.W.K.; Ricke, W.A.; Bushman, W.; Beebe, D.J. Microfluidic Multiculture Assay to Analyze Biomolecular Signaling in Angiogenesis. *Anal. Chem.* **2015**. [CrossRef] [PubMed]
76. Uzel, S.G.M.; Platt, R.J.; Subramanian, V.; Pearl, T.M.; Rowlands, C.J.; Chan, V.; Boyer, L.A.; So, P.T.C.; Kamm, R.D. Microfluidic device for the formation of optically excitable, three-dimensional, compartmentalized motor units. *Sci. Adv.* **2016**. [CrossRef]
77. Wevers, N.R.; Van Vught, R.; Wilschut, K.J.; Nicolas, A.; Chiang, C.; Lanz, H.L.; Trietsch, S.J.; Joore, J.; Vulto, P. High-throughput compound evaluation on 3D networks of neurons and glia in a microfluidic platform. *Sci. Rep.* **2016**. [CrossRef] [PubMed]
78. Oh, S.; Ryu, H.; Tahk, D.; Ko, J.; Chung, Y.; Lee, H.K.; Lee, T.R.; Jeon, N.L. "open-top" microfluidic device for in vitro three-dimensional capillary beds. *Lab Chip* **2017**. [CrossRef]

79. Jang, K.J.; Suh, K.Y. A multi-layer microfluidic device for efficient culture and analysis of renal tubular cells. *Lab Chip* **2010**. [CrossRef]
80. Suzuki, H.; Hirakawa, T.; Watanabe, I.; Kikuchi, Y. Determination of blood pO2 using a micromachined Clark-type oxygen electrode. *Anal. Chim. Acta* **2001**. [CrossRef]
81. Wang, L.; Acosta, M.A.; Leach, J.B.; Carrier, R.L. Spatially monitoring oxygen level in 3D microfabricated cell culture systems using optical oxygen sensing beads. *Lab Chip* **2013**. [CrossRef]
82. Bellin, D.L.; Sakhtah, H.; Rosenstein, J.K.; Levine, P.M.; Thimot, J.; Emmett, K.; Dietrich, L.E.P.; Shepard, K.L. Integrated circuit-based electrochemical sensor for spatially resolved detection of redox-active metabolites in biofilms. *Nat. Commun.* **2014**. [CrossRef]
83. Eklund, S.E.; Cliffel, D.E.; Kozlov, E.; Prokop, A.; Wikswo, J.; Baudenbacher, F. Modification of the Cytosensor^{TM} microphysiometer to simultaneously measure extracellular acidification and oxygen consumption rates. *Anal. Chim. Acta* **2003**. [CrossRef]
84. Wu, M.H.; Lin, J.L.; Wang, J.; Cui, Z.; Cui, Z. Development of high throughput optical sensor array for on-line pH monitoring in micro-scale cell culture environment. *Biomed. Microdev.* **2009**. [CrossRef]
85. Obregón, R.; Ahadian, S.; Ramón-Azcón, J.; Chen, L.; Fujita, T.; Shiku, H.; Chen, M.; Matsue, T. Non-invasive measurement of glucose uptake of skeletal muscle tissue models using a glucose nanobiosensor. *Biosens. Bioelectron.* **2013**. [CrossRef]
86. Hernández-Albors, A.; Castaño, A.G.; Fernández-Garibay, X.; Ortega, M.A.; Balaguer, J.; Ramón-Azcón, J. Microphysiological sensing platform for an in-situ detection of tissue-secreted cytokines. *Biosens. Bioelectron. X* **2019**. [CrossRef]
87. Schwartz, W.B. Medicine and the Computer. *New Engl. J. Med.* **1970**, *283*, 1257–1264. [CrossRef]
88. Andrade, M.A.; Bork, P. Automated extraction of information in molecular biology. *FEBS Lett.* **2000**, *476*, 12–17. [CrossRef]
89. Ghassemi, M.; Naumann, T.; Schulam, P.; Beam, A.L.; Chen, I.Y.; Ranganath, R. Practical guidance on artificial intelligence for health-care data. *Lancet Digit. Heal.* **2019**, *1*, e157–e159. [CrossRef]
90. Stein, H.S.; Gregoire, J.M. Progress and prospects for accelerating materials science with automated and autonomous workflows. *Chem. Sci.* **2019**. [CrossRef] [PubMed]
91. Ambinder, E.P. Electronic health records. *J. Oncol. Pr.* **2005**, *1*, 57–63. [CrossRef] [PubMed]
92. Abràmoff, M.D.; Lavin, P.T.; Birch, M.; Shah, N.; Folk, J.C. Pivotal trial of an autonomous AI-based diagnostic system for detection of diabetic retinopathy in primary care offices. *NPJ Digit. Med.* **2018**. [CrossRef]
93. Raghu, A.; Komorowski, M.; Singh, S. Model-based reinforcement learning for sepsis treatment. *arXiv* **2018**, arXiv:1811.09602. Available online: https://arxiv.org/abs/1811.09602 (accessed on 23 November 2018).
94. Yom-Tov, E.; Feraru, G.; Kozdoba, M.; Mannor, S.; Tennenholtz, M.; Hochberg, I. Encouraging Physical Activity in Patients With Diabetes: Intervention Using a Reinforcement Learning System. *J. Med. Internet Res.* **2017**. [CrossRef] [PubMed]
95. Ma, H.; Xu, C.; Shen, Z.; Yu, C.; Li, Y. Application of Machine Learning Techniques for Clinical Predictive Modeling: A Cross-Sectional Study on Nonalcoholic Fatty Liver Disease in China. *Biomed. Res. Int.* **2018**, *2018*, 4304376. [CrossRef]
96. Heinemann, F.; Birk, G.; Stierstorfer, B. Deep learning enables pathologist-like scoring of NASH models. *Sci. Rep.* **2019**, *9*, 18454. [CrossRef] [PubMed]
97. Gerke, S.; Minssen, T.; Cohen, G. Ethical and legal challenges of artificial intelligence-driven healthcare. *Artif. Intell. Healthc.* **2020**, 295–336. [CrossRef]
98. Guo, B.; Lei, C.; Kobayashi, H.; Ito, T.; Yalikun, Y.; Jiang, Y.; Tanaka, Y.; Ozeki, Y.; Goda, K. High-throughput, label-free, single-cell, microalgal lipid screening by machine-learning-equipped optofluidic time-stretch quantitative phase microscopy. *Cytom. Part A* **2017**, *91*, 494–502. [CrossRef] [PubMed]
99. Chen, C.L.; Mahjoubfar, A.; Tai, L.-C.; Blaby, I.K.; Huang, A.; Niazi, K.R.; Jalali, B. Deep Learning in Label-free Cell Classification. *Sci. Rep.* **2016**, *6*, 21471. [CrossRef] [PubMed]
100. Kozyra, M.; Johansson, I.; Nordling, Å.; Ullah, S.; Lauschke, V.M.; Ingelman-Sundberg, M. Human hepatic 3D spheroids as a model for steatosis and insulin resistance. *Sci. Rep.* **2018**, *8*, 14297. [CrossRef]
101. Blasi, T.; Hennig, H.; Summers, H.D.; Theis, F.J.; Cerveira, J.; Patterson, J.O.; Davies, D.; Filby, A.; Carpenter, A.E.; Rees, P. Label-free cell cycle analysis for high-throughput imaging flow cytometry. *Nat. Commun.* **2016**, *7*, 10256. [CrossRef] [PubMed]
102. Caldez, M.J.; Bjorklund, M.; Kaldis, P. Cell cycle regulation in NAFLD: When imbalanced metabolism limits cell division. *Hepatol. Int.* **2020**, *14*, 463–474. [CrossRef] [PubMed]
103. Chu, A.; Nguyen, D.; Talathi, S.S.; Wilson, A.C.; Ye, C.; Smith, W.L.; Kaplan, A.D.; Duoss, E.B.; Stolaroff, J.K.; Giera, B. Automated detection and sorting of microencapsulation via machine learning. *Lab Chip* **2019**, *19*, 1808–1817. [CrossRef]
104. Das, D.K.; Ghosh, M.; Pal, M.; Maiti, A.K.; Chakraborty, C. Machine learning approach for automated screening of malaria parasite using light microscopic images. *Micron* **2013**, *45*, 97–106. [CrossRef] [PubMed]
105. Hetherington, A.M.; Sawyez, C.G.; Zilberman, E.; Stoianov, A.M.; Robson, D.L.; Borradaile, N.M. Differential Lipotoxic Effects of Palmitate and Oleate in Activated Human Hepatic Stellate Cells and Epithelial Hepatoma Cells. *Cell. Physiol. Biochem.* **2016**, *39*, 1648–1662. [CrossRef]
106. Mirsky, S.K.; Barnea, I.; Levi, M.; Greenspan, H.; Shaked, N.T. Automated analysis of individual sperm cells using stain-free interferometric phase microscopy and machine learning. *Cytom. Part A* **2017**. [CrossRef]
107. Feldstein, A.E.; Werneburg, N.W.; Canbay, A.; Guicciardi, M.E.; Bronk, S.F.; Rydzewski, R.; Burgart, L.J.; Gores, G.J. Free fatty acids promote hepatic lipotoxicity by stimulating TNF-α expression via a lysosomal pathway. *Hepatology* **2004**, *40*, 185–194. [CrossRef]

108. Ko, J.; Bhagwat, N.; Yee, S.S.; Ortiz, N.; Sahmoud, A.; Black, T.; Aiello, N.M.; McKenzie, L.; O'Hara, M.; Redlinger, C.; et al. Combining Machine Learning and Nanofluidic Technology to Diagnose Pancreatic Cancer Using Exosomes. *ACS Nano* **2017**. [CrossRef]
109. Lee, S.Y.; Sung, J.H. Gut–liver on a chip toward an in vitro model of hepatic steatosis. *Biotechnol. Bioeng.* **2018**, *115*, 2817–2827. [CrossRef]
110. Ahluwalia, A.; Misto, A.; Vozzi, F.; Magliaro, C.; Mattei, G.; Marescotti, M.C.; Avogaro, A.; Iori, E. Systemic and vascular inflammation in an in-vitro model of central obesity. *PLoS ONE* **2018**, *13*, e0192824. [CrossRef]

biomedicines

MDPI

Review

Natural Progression of Non-Alcoholic Steatohepatitis to Hepatocellular Carcinoma

Daryl Ramai [1], Waqqas Tai [1], Michelle Rivera [1], Antonio Facciorusso [2], Nicola Tartaglia [3], Mario Pacilli [3], Antonio Ambrosi [3], Christian Cotsoglou [4] and Rodolfo Sacco [2,*]

[1] Department of Internal Medicine, The Brooklyn Hospital Center, Brooklyn, NY 11201, USA; dramai@tbh.org (D.R.); wtai@tbh.org (W.T.); mirivera@tbh.org (M.R.)
[2] Section of Gastroenterology, Department of Medical and Surgical Sciences, University of Foggia, 71122 Foggia, Italy; antonio.facciorusso@virgilio.it
[3] General Surgery Unit, Department of Medical and Surgical Sciences, University of Foggia, 71122 Foggia, Italy; nicola.tartaglia@unifg.it (N.T.); m.pacilli2010@gmail.com (M.P.); antonio.ambrosi@unifg.it (A.A.)
[4] General Surgey Unit, Department of Surgery, ASST-Vimercate, 20871 Vimercate, Italy; christian.cotsoglou@asst-vimercate.it
* Correspondence: r.sacco@ao-pisa.toscana.it

Abstract: Non-alcoholic steatohepatitis (NASH) is a chronic and progressive form of non-alcoholic fatty liver disease (NAFLD). Its global incidence is increasing which makes NASH an epidemic and a public health threat. Due to repeated insults to the liver, patients are at risk for developing hepatocellular carcinoma (HCC). The progression of NASH to HCC was initially defined according to a two-hit model which involved the development of steatosis, followed by lipid peroxidation and inflammation. However, current research defines a "multi-hit" or "multi-parallel hit" model which synthesizes several contributing pathways involved in progressive fibrosis and oncogenesis. This perspective considers the effects of cellular, genetic, immunologic, metabolic, and endocrine pathways leading up to HCC which underscores the complexity of this condition. This article will provide an updated review of the pathogenic mechanisms leading from NASH to HCC as well as an exploration of the role of biomarkers and screening.

Keywords: non-alcoholic steatohepatitis; hepatocellular carcinoma; pathogenesis

Citation: Ramai, D.; Tai, W.; Rivera, M.; Facciorusso, A.; Tartaglia, N.; Pacilli, M.; Ambrosi, A.; Cotsoglou, C.; Sacco, R. Natural Progression of Non-Alcoholic Steatohepatitis to Hepatocellular Carcinoma. *Biomedicines* **2021**, *9*, 184. https://doi.org/10.3390/biomedicines9020184

Academic Editor: Ronit Shiri-Sverdlov

Received: 3 January 2021
Accepted: 9 February 2021
Published: 12 February 2021

1. Introduction

Non-alcoholic steatohepatitis (NASH) is a chronic and progressive disease which leads to the accumulation of fatty deposits in the liver (steatosis) and subsequent inflammation [1]. NASH is a progression of non-alcoholic fatty liver disease (NAFLD) which is an umbrella term used to describe various forms of fatty liver disease in patients without alcohol consumption [2]. The prevalence of NALFD is increasing globally and is estimated to be about 25% [3]. However, this number is likely an underrepresentation, and the true prevalence of NALFD is much higher. Moreover, the prevalence of NAFLD among patients with diabetes is 56%, while the overall prevalence of NASH in diabetics is approximately 37% [4].

Globally, NASH has an incidence rate of 5.3 per 1000 and a hepatocellular carcinoma (HCC) incidence rate among patients diagnosed with NASH of 0.44 per 1000 persons [4]. Furthermore, in the US, NASH accounts for 18% of all HCC cases (an eightfold increase from 2002 to 2017) [5]. Being that NASH is on the rise, and given its significant risk for developing HCC, it is important to fully understand the mechanisms behind this progressive disease to derive more targeted therapies [6]. This article reviews the pathogenesis of NASH leading to HCC and emerging pathological concepts.

2. NASH and Liver Fibrosis

There are multifactorial insults that combine to induce cellular damage and activate cell death which leads to progressive liver disease. Persistence of these insults ultimately leads to activation of hepatic stellate cells, collagen deposition, and hepatic fibrogenesis (scar formation) [7]. Fibrosis in adults with noncirrhotic NASH is perisinusoidal, usually seen initially in acinar zone 3 [8]. Progressive scarring can develop followed by bridging fibrosis and cirrhosis [8].

In a systematic review and meta-analysis of paired liver biopsy studies, two distinct subsets of liver fibrosis were identified: rapid progressors (progression of stage 0 to bridging fibrosis or cirrhosis) and slow progressors (progression from stage 0 to stage 1 or 2 fibrosis) [9]. From this study, 20% of patients who developed interval fibrosis progression were classified as a rapid progressor. Furthermore, in patients with NASH and baseline F0 fibrosis, the annual fibrosis progression rate was on average 7.1 years to progress to stage 1, which was about half the average time for patients with NAFLD. From this meta-analysis, 40 (34.5%) patients developed progressive fibrosis, 45 (38.8%) patients remained stable, and 31 (26.7%) patients had improvement in fibrosis [9]. Thus, patients with NASH are at high risk for developing rapid liver disease. This poses serious public health implications for liver-related morbidity and mortality, especially in the absence of disease-modifying therapy.

3. Risk Factors for Fibrosis Progression

It is well known that NAFLD is strongly associated with metabolic syndrome, which includes obesity, dyslipidemia, hypertension, and increases the risk for developing type 2 diabetes melitus (T2DM) [10]. A 2020 cross-sectional study showed that progression of fibrosis stage in NASH was more likely to occur among obese patients [11]. In patients who progressed to the next stage or advanced stage fibrosis (141 patients), 59% had obesity, 57% had either hypertension, dyslipidemia, T2DM, or cardiovascular diseases.

The progression of NASH is less predictable than other forms of chronic liver disease. Lifestyle changes including weight reduction, physical exercise, and nutrient composition is vital to slowing the progression of liver fibrosis [12]. A mouse study compared metabolic and histological effects of a diet on the basis of composition and showed that a fast-food diet (high cholesterol, high saturated fat, and high fructose) administered for 6 months led to features of metabolic syndrome and NASH with progressive fibrosis [13]. In a study where 13 individuals were subjected to high-calorie fast-food meals, elevated serum alanine aminotransferase (ALT) levels and increased steatosis were found within a period of 4 weeks [14]. Additionally, Wei et al. demonstrated that fibrotic response was driven by high dietary fat. In C57Bl/6J mice models, choline-deficient, amino acid-defined (CDAA) diets with increasing fat content (10–60% by calories) were associated with steatohepatitis with robust fibrosis and ductular proliferation that progressed to cirrhosis and HCC within 24 weeks. [15]. However, Pompili et al. showed that a high carbohydrate–low fat diet was equally as harmful as a high fat diet alone [16].

These differences in diet may account for different rates of progressive liver disease. However, the current literature appears to indicate that carbohydrates (such as fructose) act in a synergistic fashion with diets rich in fat content (i.e., Western diet) to increase liver lipid accumulation, induce inflammation, and fibrosis [17].

This effect of diet in combination with oxidative stress was further exacerbated with long-term liver X receptor (LXR) agonist stimulation/expression [18]. LXR is an oxysterol-activated nuclear receptor involved in the control of major metabolic pathways for cholesterol homeostasis and lipogenesis where its expression has been correlated with intrahepatic inflammation and fibrosis [19].

Conversely, Schuppan et al. highlighted the role of lifestyle changes, such as weight loss, physical exercise, and a healthier nutrient composition on inflammation and fibrosis in NASH [12]. It demonstrated that an intensive weight loss program in 293 patients with NASH, 261 of whom were biopsied after 52 weeks, led to resolution of NASH in 25%, and reduced fibrosis in 19%. In those patients who lost $\geq$10% of body weight,

NASH resolved in 90% and fibrosis improved in 45% [13]. Follow up studies on morbidly obese patients that underwent bariatric surgery demonstrated that the extent of weight loss can also correlate with the degree of resolution of NASH and even fibrosis regression [12]. Overall, these studies highlight the contribution of dietary composition and body weight in the development or regression of NASH and progressive fibrosis.

Of note, while NAFLD/NASH is defined by the absence of alcohol, however, a large proportion of patients consume mild to moderate amounts of alcohol. In a longitudinal study of 285 participants, Ajmera et al. reported that modest alcohol use was associated with less improvement in steatosis and level of aspartate transaminase, as well as lower odds of NASH resolution, compared with no use of alcohol [20]. However, a review of the literature has demonstrated conflicting results [21].

4. From "Double-Hit" to "Multi-Hit"

The first modern mechanism of NASH transformation to HCC was thought to have occurred via a "two-hit hypothesis" [22–24]. Initially, patients with obesity and/or T2DM develop insulin resistance [25]. Animal models have shown that high fat diets induce obesity-related insulin resistance and the release of inflammatory signals via toll-like receptor (TLR4) and nuclear factor kappa-light-chain-enhancer of activated B cells (NF-κB) pathways [26]. Chronic insulinemia impairs skeletal muscle and hepatic insulin signaling which promotes hepatic steatosis [27]. Moreover, excessive amounts of free fatty acids are produced from insulin-resistant adipose tissues via lipolysis. This creates a perpetual cycle of insulin resistance, accumulation of fatty acid metabolites, and steatosis [28].

The first hit is the development of steatosis, followed by lipid peroxidation caused by oxidation and inflammation of the liver, leading to necroinflammation and fibrosis, and ultimately HCC. Peroxidation of lipids found in cell membranes may lead to necrosis and megamitochondria [29]. The end products of this process include 4-hydroxynonenal and malondialdehyde (MDA) which activates hepatic stellate cells. Hepatic stellate cells are primarily capable of collagen production which crosslinks cytokeratins to produce Mallory bodies as well as promote chemotaxis of neutrophils [30–32]. MDA is also capable of inflammation by activating NF-κB which is a cell mediator in the expression of proinflammatory cytokines and adhesion molecules such as TNF-a, IL-8, intercellular adhesion molecule 1, and E-selectin [33,34].

However, many patients with steatosis never progress to fibrosis. This suggests that in addition to the "first hit," a "second hit" is needed for the development of necroinflammation. Potential sources for this "second hit" include increased expression of CYP2E1 which can generate free radicals [35]. This inductive process is mediated in non-alcoholics by ketones and fatty acids (i.e., high fat diet) [36]. In patients with obesity and steatosis, the progression to fibrosis is accelerated by rapid weight loss during dieting, intestinal bypass surgery, surgical stress, alcohol intake, and T2DM, all of which increases free fatty acids in the liver.

The high concentration of free fatty acids in the liver provides a source of oxidative stress by peroxisomal b-oxidation which leads to the production of hydrogen peroxide. In the presence of iron, highly reactive hydroxyl radicals are released which contributes to mitochondrial damage and the precipitation of NASH/liver fibrosis [37–40]. This source of oxidative stress is required for initiating enough lipid peroxidation to overcome normal cellular defense mechanisms and produce necroinflammation [41,42].

Furthermore, diets with unbalanced polyunsaturated fatty acids (PUFA) have been linked to NALFD. Long term consumption of a Western diet which is high in saturated fat, omega-6 fatty acids and sugar (especially fructose), while deficient in omega-3 fatty acids, contributes to the development and progression of NAFLD [43]. Lower ratios of omega-6 to omega-3 have been shown to have a direct effect on Wnt signaling, decreasing expression of pro-inflammatory genes, and exhibiting less liver injury [44].

Diets high in sugars have been implicated in liver tumorigenesis. Qiao et al. reported that glucose induced advanced glycosylation end product-specific receptor (AGER) which

was critical for liver tumorigenesis. Hyperglycemia appears to support cell proliferation, colony-formation capacity, and in vivo tumor growth while inhibiting apoptosis in HCC cells as well as other cancer types [45]. Furthermore, a follow-up study demonstrated that inadequate maintenance of blood glucose in patients with T2DM was a significant risk factor for HCC recurrence [46].

While still highly popularized, the simplicity of this hypothesis undermines the complex nature of NASH to HCC carcinogenesis. Further research has been done which has suggested a "multi-hit" or "multi-parallel hit" theory that takes into consideration several theorized models, all of which play a role in the oncogenesis of HCC [23]. There are currently four additional proposed prongs to the multi-hit theory which includes genetics, immunologic, metabolic, and endocrine pathways (Figure 1).

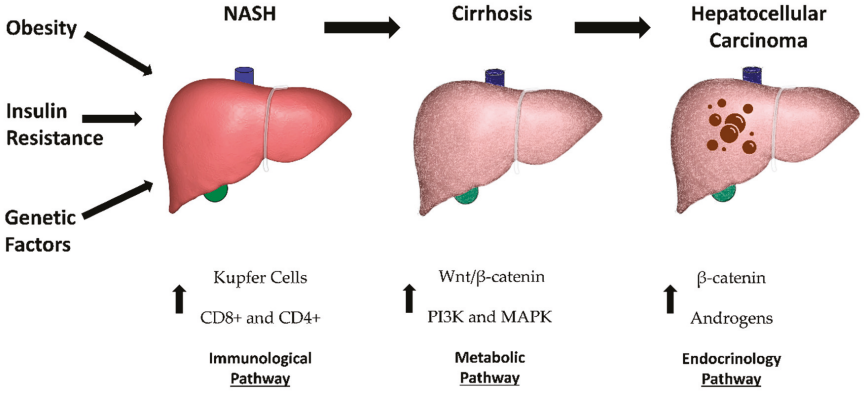

Figure 1. Risk factors and proposed mechanisms for non-alcohol steatosis (NASH) progression to hepatocellular carcinoma (HCC).

4.1. Genetic Mechanism

Genetic modifiers have been shown to play a role in the pathogenesis of liver fibrosis in NASH. Two genes have been well established with proposed mechanisms: patatin-like phospholipase domain-containing protein 3 (PNPLA3) and transmembrane 6 superfamily member 2 (TM6SF2) [47,48]. PNPLA3 is an adiponutrin that is found in intracellular membrane fractions within hepatocytes and has lipolytic activity [49]. PNLPA3 has been established as having a direct association with hepatic steatosis, steatohepatitis, elevated plasma liver enzyme levels, hepatic fibrosis, and cirrhosis [50–53]. PNLPA3 also has a role in retinol metabolism and production by hepatic cells, which likely has a role in inflammation of the liver [54]. It has been observed in mice and human models that diets high in fat and carbohydrate create an anabolic milieu thereby upregulating PNPLA3 [55–58]. Perttilä et al. showed that glucose exerts an indirect effect on PNPLA3 via carbohydrate response element-binding protein (ChREBP) in hepatocyte [59]. PNPLA3 expression is upregulated by both insulin and glucose [60].

Knockout PNPLA3 mice models on a high fat diet have reduced liver fat content despite the high fat diet. This suggests that the PNPLA3 gene plays a profound role in lipid esterification and lipogenesis in the liver [61,62]. In a 2018 study, it was shown that PNPLA3 mediates the transfer of polyunsaturated fatty acids from triglycerides to phospholipids in hepatocytes [63]. In other words, elevated PNPLA3 protein levels lead to lipogenesis thereby increasing the amount of fat content within the liver. Conversely, reducing *PNPLA3* expression levels could potentially attenuate its negative effect on hepatic lipolysis [64]. However, some studies have cited contrary evidence [65]. This suggest that previous research may have unknown confounding variables such as up or down stream regulators and compensatory mechanisms which need to be further defined.

On the other hand, TM6SF2 is believed to function as a lipid transporter which may interact with proteins involved in intestinal absorption [66]. Studies using confocal microscopy have demonstrated localization of GFP tagged TM6SF2 to the endoplasmic reticulum and Golgi compartment. Knockout TM6SF2 in-vitro experiments showed reduced secretion of triglyceride-rich lipoproteins and Apo-B [67]. As a result, there was increased lipid droplet number and size. Alternatively, overexpression of TM6SF2 showed decreased number and size of lipid droplets. In vivo studies further support this phenotypic expression of TM6SF2. Overall, these studies suggest that TM6SF2 regulated lipid influx and efflux depending on its deletion, mutation, or overexpression.

Individuals carrying the minor (T) allele of TM6SF2 rs58542926 (167K) appear prone to developing NAFLD with advanced fibrosis and so are more likely to experience liver-related disease rather than cardiovascular morbidity [68]. Alternatively, carriage of the C-allele is associated with dyslipidemia and cardiovascular disease with a lower incidence of NASH [69]. Nevertheless, further studies with associated human genetic variants will greatly inform our understanding of the pathophysiology and interrelationship between NASH and stages of fibrosis.

Dysregulation in the synthesis of fatty acids is associated with NASH. Prior studies have shown that FADS1 is a regulator of hepatic lipid composition [70]. However, Chiappini et al. showed concomitant increase in saturated and unsaturated long chain fatty acids (LCFA) with significant decrease in polyunsaturated very long chain fatty acids (VLCFA) from impaired activity of FADS1, independent of obesity [71]. Such metabolic alterations may generate broad effects since LCFA is a substrate for the synthesis of eicosanoids and phospholipids, and a precursor for the synthesis of lipid signaling pro-inflammatory molecules [72–74].

It is important to note the role of microRNA (miRNA). Prior studies have shown that miRNA is associated with NASH [75]. There has also been miRNA that have correlated with distinct pathways which leads to the oncogenesis of hepatocellular carcinoma [76]. When cross-referencing both miRNA for NASH and HCC, no distinct miRNA was found, but common pathways have been identified [77]. For example, in mice models there are distinct miRNA associated with the phosphatase and tensin homolog (PTEN) protein in the NASH and HCC pathway [78]. In mice models, those that were PTEN deficient developed steatosis, hepatomegaly, and HCC [79]. Mutual pathways leading to a disease state for both NASH and HCC further develop the idea that there is not only a link but the possibility for association or progression of one disease state to the next.

While there are specific genetic mutations that have clinically significate roles in the oncogenesis of HCC, there is another component that cannot be overlooked—DNA damage repair and response. DNA damage is a daily occurrence within the human genome from various internal and external processes that persistently lead to DNA damage. In the setting of improper repair with inadequate or overstimulated response there is potential for HCC to develop.

In various mice models for studying NASH, it has been shown that as oxidative damage increases, DNA repair enzymes decrease in direct proportions. This logically suggests that DNA repair deficiency can lead to NASH and potentially HCC. This has a more profound impact clinically as patients with inherited or acquired DNA repair enzyme dysfunction leads to susceptibility to NASH and progression to HCC [80]. For example, ataxia-telangiectasia mutated (ATM) kinase deficiency leads to a syndrome known as ataxia-telangiectasia. The ATM is known for its contribution to DNA genomic stability and role in DNA repair [81–83]. When ATM is no longer functional it has been seen in mice models that develop steatosis and fibrosis and as established is well known inciting factor for the development of HCC [84]. In study by Schults et al., the authors were able to evaluate liver biopsy specimens and determine that the specimens that expressed a high degree of inflammation, also expressed a reduction in DNA damage repair, further supporting the hypothesis that DNA repair plays a role in HCC progression [85].

Another protein being currently studied in DNA-dependent protein kinase (DNA-PK) plays a role in the repair of DNA breaks, and interestingly plays a role in lipogenesis as well [86]. DNA-PK is interesting—while in ATM there is a downregulation leading to more DNA damage, in DNA-PK there is upregulation which leads to DNA damage. DNA-PK works when both strands in the DNA molecule break DNA-PK which forces the two broken strands back together in a process called non-homologues end joining [87]. Since DNA-PK does not correct for any missing nucleotides and sequences when recombining the strands, this leads to an error prone process. DNA-PK results in upregulation of DNA repair; as DNA-PK repairs, DNA is also prone to cause DNA error leading to DNA mutations and unstable cells thereby leading to HCC [88,89]. There are studies being done that are evaluating whether patients with NASH-associated HCC with DNA-PK upregulation are found to have a worse response to localized chemoembolization therapy [90]. With this information, there are current studies being done to determine targeted therapy to downregulate DNA-PK activity in patients with HCC, with preliminary data with in vivo and in vitro studies suggesting suppression of DNA-PK as a promising therapy [91].

While we have described the major and established genetic players in NASH and HCC, other genes have been identified which require further investigation. Desterke et al. identified 25 genes that are commonly found to be dysregulated during steatosis progression to NASH and cancer [92]. Furthermore, Nwosu et al. identified 634 metabolic-related genes mostly (n = 350) downregulated and involved in physiologic hepatocyte metabolic functions (e.g., xenobiotic, fatty acid, and amino acid metabolism) and upregulated (n = 284) in glycolysis, pentose phosphate pathway, nucleotide biosynthesis, tricarboxylic acid cycle, oxidative phosphorylation, proton transport, membrane lipid, and glycan metabolism [93]. These genes are potentially relevant targets for clinical studies, however, they require additional investigation.

4.2. WNT/β-Catenin Signaling

In those patients that display insulin resistance and hyperinsulinemia, there is an increase in serum insulin and insulin-like growth factor. Insulin and insulin growth factor-1 (IGF-1) bind to respective receptors which leads to the activation of two distinct pathways, downstream PI3K and MAPK pathways [94,95]. It has been established that PI3K and MAPK pathways play a role in oncogenesis by induction of cell proliferation and inhibition of apoptosis. Furthermore, downstream of MAPK leads to activation of Wnt/β-catenin which leads to fibrosis and HCC [96].

Interestingly, mice with wild-type or mutant β-catenin are not able to develop spontaneous liver cancer [97,98]. As a result, inactivation of β-catenin alone is not sufficient to develop HCC. However, β-catenin activation may work in tandem with other oncogenic pathways including insulin/IGF-1/IRS-1/MAPK, H-RAS, MET, AKT and chemicals to promote HCC [99–101]. Other epigenetic modifications may also contribute to the activation of Wnt/β-catenin signaling, including hypermethylation of Wnt antagonists, deacetylation of histones in the AXIN2 promoter, and downregulation of microRNAs negatively regulating Wnt/β-catenin signaling.

Lastly, while not fully understood, it is important to note the tumor microenvironment and the role of autophagy. Autophagy is an evolutionary conservative intracellular mechanism involved in diverse liver physiology and pathology. Unlike other tissues or organs, autophagy in the liver leads to synthesis of adipose tissue which leads to NASH [102–104]. Activation of autophagy inhibited proliferation of HepG2 cells in blocking GOC3/Wnt/B-catenin signaling [105,106]. Furthermore, autophagy can induce Monocarboxylate transporter 1 (MCT1) expression which is involved in lactic acid transport and H+ clearance in cancer cells, by activating Wnt/β-catenin signaling. Overall, this process leads to metastasis and glycolysis in HCC cells [107]. In addition, pharmacological inhibition of v-ATPase/autophagy blocks HCC cell proliferation (Table 1).

Table 1. Pathways contributing to the development of hepatocellular carcinoma (HCC) from non-alcoholic steatohepatitis (NASH).

Pathway	Primary Mechanism
Cellular	Steatosis followed by lipid peroxidation
Genetic	Elevated PNPLA3 protein levels facilitate lipogenesis Decreased TM6SF2 levels reduce lipid efflux, increase lipid droplet number and size
Immunologic	Cytokine release recruit Kupfer cells and contribute to NASH Decreased NK cells associated with infiltration of monocyte-derived macrophages
Metabolic	Insulin and IGF-1 signaling associated with PI3K and MAPK activation of Wnt/β-catenin along with epigenetic modifications facilitate fibrosis
Endocrine	Androgens stimulate transcription of cell cycle-related kinase (CCRK) which upregulate β-catenin

Another important aspect in the Wnt pathway is the role of exosomes. Prior studies have shown an association between exosomes and Wnt signaling in the migration of gastric and colon cancer cells [108–111]. However, it is unclear whether Wnt signaling plays a critical role in the invasion and migration of liver cancer and warrants further investigation.

4.3. Immunological Pathway

The next prong that needs to be evaluated is the immune response in the setting of liver injury from reactive oxygen species (ROS). When ROS disrupt the mitochondria and lipid peroxidation, this leads to a release of inflammatory markers including tumor necrosis factor-alpha (TNF-α), interleukin-6 (IL-6), leptin, and adiponectin [91]. In patients with insulin resistance, there are reduced levels of adiponectin which directly leads to an increase in angiogenesis and decrease in apoptosis, thereby increasing the risk of NASH conversion to HCC [112,113].

The role of the adaptive immune system is still very unclear, but several mouse models have been developed. Two studies have shown that CD8+ and CD4+ T-lymphocytes are involved in liver damage and subsequent oncogenesis [114,115]. Furthermore, as more liver damage occurs from steatosis, Kupfer Cells are activated which recruit other cells thereby contributing to NASH [116,117]. On the other hand, natural killer cells are activated by ligands and cytokines (CD107a and cytokine production of IFN-γ, TGF-β and IL-10) have been associated with a protective role in liver disease [116,118].

Mice that were induced to have macrovesicular steatosis, necro-inflammation and fibrosis in the liver showed increase numbers of NK cells in the liver but decreased in the spleen [119]. In NK cell-deficient Nfil3-/- mice, similar levels of TG and macrovesicular steatosis was observed, but more inflammatory infiltration and increased collagen deposition were found in the liver. Furthermore, the depletion of NK cells caused a significant increase in the infiltration of monocyte-derived macrophages [120]. Overall, the data suggest that intrahepatic NK cells play a protective role against the fibrosis progression in NASH [121].

Sonic Hedgehog genes have been shown to play a major role in liver repair through the mobilization of hepatic precursor cells [122]. In studies where SHH signaling is impaired, improper liver repair leads to the conversion of NASH to HCC [101]. Further studies are needed to define the pathophysiological role of the adaptive immune system in the development and progression of NASH into HCC.

4.4. Endocrine Pathway

The final prong in this multi-hit model for the oncogenesis of NASH to HCC is the endocrine pathway. As previously reported above, middle-age men had the highest incidence of NASH to HCC, which derives the question of whether gender-specific hormones play a role in NASH and HCC (Figure 2). Reports have shown that patients with hypothyroidism might lead to NASH, cirrhosis and potentially liver cancer via the development of hyperlipidemia and obesity [123]. Similarly, patients with growth hormone deficiency

have a metabolic-syndrome-like phenotype that is also associated with the development of NASH [123]. Polycystic ovary syndrome is a common endocrine disorder that is often associated with insulin resistance, the metabolic syndrome, altered levels of liver enzymes and the development of NASH [123].

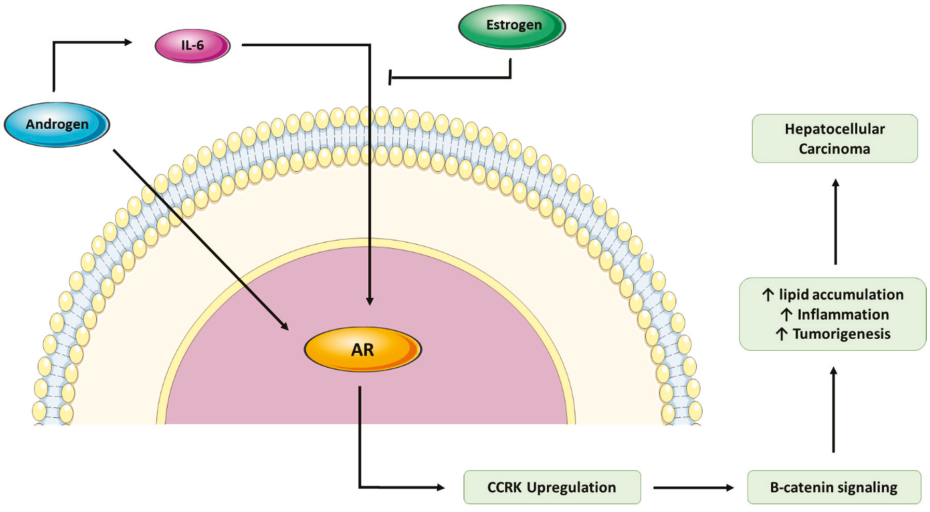

Figure 2. Role of androgens and estrogens in tumorigenesis. AR: androgen receptor, CCRK: cell cycle-related kinase.

In addition, adrenal failure is increasingly reported in patients with end-stage liver disease and in patients who have received a liver transplant, which suggests a bidirectional relationship between liver and endocrine functions [123]. Recent findings support a role of dehydroepiandrosterone sulfate deficiency in the development of advanced NASH [123]. In an early study from 1995, it was proposed that male androgens promote HCC compared to estrogen which suppresses the development of HCC [124]. In 2012 it was determined that androgens stimulate the transcription of cell cycle-related kinase (CCRK) which upregulates β-catenin [125]. Murine studies with knockout CCRK showed suppressed hepatic lipid accumulation, inflammation and tumorigenicity in NASH and HCC models. Mechanistically, obesity-induced pro-inflammatory and upregulated CCRK expression led to the activation of the mTORC1 pathway crucial for lipid/glucose homeostasis, immunosuppression, and tumorigenesis [126]. The data suggest that CCRK functions as a major signaling hub in obesity-associated hepatic oncogenesis [123].

5. GALAD Score and Role of Biomarkers

The GALAD score was originally curated by Johnson et al. with the goal of establishing a quantitative model for the development of HCC in chronic liver disease patients [127]. The score measures five variables including gender, age, α fetoprotein, AFP-L3%, and des-carboxy-prothrombin. In a validation study in 2016, the GALAD score had a sensitivity of 85.6% and a specificity of 93.3%. The GALAD score showed a superior detection rate of early-stage HCC and AFP-negative tumors [128]. In patients with NASH, the GALAD score has also been shown to detect HCC independent of cirrhosis or stage of HCC with a sensitivity of 91.2% and a specificity of 95.2% [129].

Other novel biomarkers have become potential candidates for HCC screening. In an animal model study, two potential markers—serum glycoprotein osteopontin and dickkopf-1—were determined [130]. Another potential marker is circulating tumor DNA (ctDNA) which can be used to determine if specific genetic mutations have occurred [131]. The ctDNA would be for common pathways involved in HCC oncogenesis such as p53 signaling, the Wnt–β-

catenin pathway, chromatin remodeling, responses to oxidative stress (for example, KEAP1 and NFE2L2) or telomere maintenance pathways [96]. Additionally, circulating miR-122, (a liver-specific miRNA) responsible for liver homeostasis, has emerged as a sensitive biomarker for liver injury [132]. A few genes have also been discovered that can become hypomethylated or hypermethylated and can be detected via ctDNA of these genes; there are three currently proposed in the involvement of HCC oncogenesis: GSTP1, RASSF1 and LINE [133–135] (Table 2).

Table 2. Possible biomarkers used for the detection of hepatocellular carcinoma (HCC).

Biomarker	Role in HCC Development
Osteopontin	Glycoprotein of the extracellular matrix, overly expressed in HCC
Dickkopf-1	Inhibitor of Wnt/β-catenin signaling, overly expressed in HCC
miR-122	Marker of liver injury; suppressed in HCC
GSTP1	Negatively correlated with tumor size and overall survival
RASSF1	Positively correlated with longer overall survival and better prognosis
LINE-1	Hypomethylation associated with shorter overall survival

GSTP1 has been negatively correlated with tumor size and serum alpha-fetoprotein (AFP) in HCC patients while higher GSTP1 levels have been associated with longer overall survival and better prognosis [136]. RASSF1 has been shown to be hypermethylated and can be used as a biomarker to distinguish HCC from other liver neoplasms [137]. LINE-1 hypomethylation was shown to be associated with shorter overall survival [137].

Furthermore, the emergence of machine learning-based approaches opens a new avenue for early diagnosis of NASH and HCC. Chiappini et al. demonstrated using mouse models that machine learning based on prediction analysis of microarrays was able to identify lipid signatures related to NASH (21 lipids out of 149 in the liver and 14 lipids out of 155 in the serum) [138]. Further clinical and cost-effective studies are needed to validate these potential biomarkers in the diagnosis and prognosis of this condition.

6. Screening and Cost

NAFLD is a global epidemic and is becoming the leading cause of chronic liver disease worldwide, with an estimated prevalence of approximately 20–30% in Western populations [3,139]. However, this estimate is largely underrepresented, and the true prevalence is likely higher. As the rates of T2DM and obesity increase worldwide, it is expected that NAFLD will become more common. NAFLD-related cirrhosis is currently the third most common indication, after hepatitis C and alcoholic cirrhosis, and is anticipated to become the leading indication for liver transplantation in the USA within the next one to two decades [140]. However, given the current trajectory and scale of this epidemic, NAFLD/NASH threatens the future of liver transplantations due to a lack of viable organs to meet the demand [141,142].

Additionally, long-term mortality studies in NAFLD patients during 28 years of follow-up showed a 69% (standardized mortality ratio (SMR) = 1.69; 95% confidence interval [CI], 1.24–2.25) higher risk of death compared to a matched cohort [143]. The main factor leading to early mortality and morbidity in NAFLD patients is the development of advanced fibrosis [144]. Hence, it is crucial to investigate and consider this condition during its early stages prior to fibrotic changes. Identifying patients with NASH in earlier stages of fibrosis is supported by several smaller studies and a recent meta-analysis that demonstrated a 1.41-, 9.57-, 16.69- and 42.3-fold increase in liver-related mortality, in subjects with stage 1, 2, 3 and 4 fibrosis, respectively [145].

Given the increased mortality rate associated with advanced fibrosis, a form of practical routine screening of NAFLD is necessary to improve patient outcomes. The standard for definitive diagnosis of NAFLD/NASH is performed by liver biopsy to assess for steatosis, inflammation, and fibrosis. However, the invasiveness of liver biopsy prevents its

routine use, hence, better and less invasive diagnostic modalities are needed to detect NAFLD/NASH. The use of biomarkers and non-invasive assessments of liver disease can be initially used in screening for NAFLD, NASH, and early fibrosis, as they have been shown to be reliable predictors of liver-related outcomes and overall mortality [146].

Currently, there is no standard medical therapy with proven efficacy available for treating NAFLD/NASH [147]. Most patients are advised to engaged in lifestyle and dietary modifications. Due to its wide prevalence and rising incidence, the diagnosis and treatment of NASH is costly. In the US, the annual economic burden of NAFLD is estimated to be USD 103 billion, where NASH accounted for about USD 15.4 billion [148]. Without taking into consideration the cost of treatment, the 10-year burden is estimated to surpass USD 1 trillion. Thus, the importance of consensus in screening and treatment guidelines is needed. However, no guidelines exist among professional organizations to recommend screening.

7. Summary

NASH is a growing global epidemic and public health threat. Concomitantly, the incidence of HCC is projected to increase worldwide [120]. Our review shows several pathways by which NASH progresses to HCC. It underscores the complexity of this disease and the effects of cellular, genetic, immunologic, metabolic, and endocrine pathways. However, over the last decade there has been progress in identifying pharmacological targets as well as potential biomarkers. However, the rapidity at which this disease is rising supersedes scientific momentum. As a result, further work is needed if we are to understand and develop methods for decreasing steatosis, rates of fibrosis, and HCC.

Funding: This research received no external funding.

Institutional Review Board Statement: Not applicable.

Informed Consent Statement: Not applicable.

Conflicts of Interest: The authors declare no conflict of interest.

References

1. Perumpail, B.J.; Khan, M.A.; Yoo, E.R.; Cholankeril, G.; Kim, D.; Ahmed, A. Clinical epidemiology and disease burden of nonalcoholic fatty liver disease. *World J. Gastroenterol.* **2017**, *23*, 8263–8276. [CrossRef] [PubMed]
2. Chalasani, N.; Younossi, Z.; LaVine, J.E.; Diehl, A.M.; Brunt, E.M.; Cusi, K.; Charlton, M.; Sanyal, A.J. The Diagnosis and Management of Non-alcoholic Fatty Liver Disease: Practice Guideline by the American Gastroenterological Association, American Association for the Study of Liver Diseases, and American College of Gastroenterology. *Gastroenterology* **2012**, *142*, 1592–1609. [CrossRef] [PubMed]
3. Younossi, Z.M.; Koenig, A.B.; Abdelatif, D.; Fazel, Y.; Henry, L.; Wymer, M. Global epidemiology of nonalcoholic fatty liver disease-Meta-analytic assessment of prevalence, incidence, and outcomes. *Hepatology* **2016**, *64*, 73–84. [CrossRef]
4. Younossi, Z.M.; Golabi, P.; De Avila, L.; Paik, J.M.; Srishord, M.; Fukui, N.; Qiu, Y.; Burns, L.; Afendy, A.; Nader, F. The global epidemiology of NAFLD and NASH in patients with type 2 diabetes: A systematic review and meta-analysis. *J. Hepatol.* **2019**, *71*, 793–801. [CrossRef] [PubMed]
5. Younossi, Z.; Stepanova, M.; Ong, J.P.; Jacobson, I.M.; Bugianesi, E.; Duseja, A.; Eguchi, Y.; Wong, V.W.; Negro, F.; Yilmaz, Y.; et al. Nonalcoholic Steatohepatitis Is the Fastest Growing Cause of Hepatocellular Carcinoma in Liver Transplant Candidates. *Clin. Gastroenterol. Hepatol.* **2019**, *17*, 748–755.e3. [CrossRef] [PubMed]
6. Estes, C.; Razavi, H.; Loomba, R.; Younossi, Z.; Sanyal, A.J. Modeling the epidemic of nonalcoholic fatty liver disease demonstrates an exponential increase in burden of disease. *Hepatology* **2018**, *67*, 123–133. [CrossRef] [PubMed]
7. Iredale, J.P. Models of liver fibrosis: Exploring the dynamic nature of inflammation and repair in a solid organ. *J. Clin. Investig.* **2007**, *117*, 539–548. [CrossRef]
8. Brunt, E.M.; Janney, C.G.; Di Bisceglie, A.M.; Neuschwander-Tetri, B.A.; Bacon, B.R. Nonalcoholic steatohepatitis: A proposal for grading and staging the histological lesions. *Am. J. Gastroenterol.* **1999**, *94*, 2467–2474. [CrossRef]
9. Singh, S.; Allen, A.M.; Wang, Z.; Prokop, L.J.; Murad, M.H.; Loomba, R. Fibrosis Progression in Nonalcoholic Fatty Liver vs Nonalcoholic Steatohepatitis: A Systematic Review and Meta-analysis of Paired-Biopsy Studies. *Clin. Gastroenterol. Hepatol.* **2015**, *13*, 643–654.e9. [CrossRef]
10. Younossi, Z.; Anstee, Q.M.; Marietti, M.; Hardy, T.; Henry, L.; Eslam, M.; George, J.; Bugianesi, E. Global burden of NAFLD and NASH: Trends, predictions, risk factors and prevention. *Nat. Rev. Gastroenterol. Hepatol.* **2018**, *15*, 11–20. [CrossRef] [PubMed]
11. Pedra, G.; Casas, L.R.; Dhillon, H.; Schattenberg, J.M.; Gomez, M.R. Fibrosis progression in NASH: Real-world data from the US population. *J. Hepatol.* **2020**, *73*, S518–S519. [CrossRef]

12. Schuppan, D.; Surabattula, R.; Wang, X.Y. Determinants of fibrosis progression and regression in NASH. *J. Hepatol.* **2018**, *68*, 238–250. [CrossRef] [PubMed]
13. Charlton, M.; Krishnan, A.; Viker, K.; Sanderson, S.; Cazanave, S.; McConico, A.; Masuoko, H.; Gores, G. Fast food diet mouse: Novel small animal model of NASH with ballooning, progressive fibrosis, and high physiological fidelity to the human condition. *Am. J. Physiol. Liver Physiol.* **2011**, *301*, G825–G834. [CrossRef]
14. Parikh, N.; Marrero, W.J.; Wang, J.; Steuer, J.; Tapper, E.B.; Konerman, M.A.; Singal, A.G.; Hutton, D.W.; Byon, E.; Lavieri, M.S. Projected increase in obesity and non-alcoholic-steatohepatitis-related liver transplantation waitlist additions in the United States. *Hepatology* **2018**, *70*, 487–495. [CrossRef] [PubMed]
15. Wei, G.; An, P.; Vaid, K.A.; Nasser, I.; Huang, P.; Tan, L.; Zhao, S.; Schuppan, D.; Popov, Y.V. Comparison of murine steatohepatitis models identifies a dietary intervention with robust fibrosis, ductular reaction, and rapid progression to cirrhosis and cancer. *Am. J. Physiol. Liver Physiol.* **2020**, *318*, G174–G188. [CrossRef] [PubMed]
16. Pompili, S.; Vetuschi, A.; Gaudio, E.; Tessitore, A.; Capelli, R.; Alesse, E.; Latella, G.; Sferra, R.; Onori, P. Long-term abuse of a high-carbohydrate diet is as harmful as a high-fat diet for development and progression of liver injury in a mouse model of NAFLD/NASH. *Nutrition* **2020**, *1*, 110782. [CrossRef] [PubMed]
17. Ishimoto, T.; Lanaspa, M.A.; Rivard, C.J.; Roncal-Jimenez, C.A.; Orlicky, D.J.; Cicerchi, C.; Mcmahan, R.H.; Abdelmalek, M.F.; Rosen, H.R.; Jackman, M.R.; et al. High-fat and high-sucrose (western) diet induces steatohepatitis that is dependent on fructokinase. *Hepatology* **2013**, *58*, 1632–1643. [CrossRef] [PubMed]
18. Shimizu, Y.; Tamura, T.; Kemmochi, A.; Owada, Y.; Ozawa, Y.; Hisakura, K.; Matsuzaka, T.; Shimano, H.; Nakano, N.; Sakashita, S.; et al. Oxidative stress and Liver X Receptor agonist induce hepatocellular carcinoma in Non-alcoholic steatohepatitis model. *J. Gastrolenterol. Hepatol.* 2020. [CrossRef] [PubMed]
19. Ahn, S.B.; Jang, K.; Jun, D.W.; Lee, B.H.; Shin, K.J. Expression of Liver X Receptor Correlates with Intrahepatic Inflammation and Fibrosis in Patients with Nonalcoholic Fatty Liver Disease. *Dig. Dis. Sci.* **2014**, *59*, 2975–2982. [CrossRef] [PubMed]
20. Ajmera, V.; Belt, P.; Wilson, L.A.; Gill, R.M.; Loomba, R.; Kleiner, D.E.; Neuschwander-Tetri, B.A.; Terrault, N. Among Patients With Nonalcoholic Fatty Liver Disease, Modest Alcohol Use Is Associated With Less Improvement in Histologic Steatosis and Steatohepatitis. *Clin. Gastroenterol. Hepatol.* **2018**, *16*, 1511–1520.e5. [CrossRef]
21. Weng, G.; Dunn, W. Effect of alcohol consumption on nonalcoholic fatty liver disease. *Transl. Gastroenterol. Hepatol.* **2019**, *4*, 70. [CrossRef]
22. Day, C.P.; James, O.F. Steatohepatitis: A tale of two "hits"? *Gastroenterology* **1998**, *114*, 842–845. [CrossRef]
23. Takaki, A.; Kawai, D.; Yamamoto, K. Multiple Hits, Including Oxidative Stress, as Pathogenesis and Treatment Target in Non-Alcoholic Steatohepatitis (NASH). *Int. J. Mol. Sci.* **2013**, *14*, 20704–20728. [CrossRef] [PubMed]
24. Kawano, Y.; Cohen, D.E. Mechanisms of hepatic triglyceride accumulation in non-alcoholic fatty liver disease. *J. Gastroenterol.* **2013**, *48*, 434–441. [CrossRef]
25. Sumida, Y.; Niki, E.; Naito, Y.; Yoshikawa, T. Involvement of free radicals and oxidative stress in NAFLD/NASH. *Free Radic. Res.* **2013**, *47*, 869–880. [CrossRef] [PubMed]
26. Kim, F.; Pham, M.; Luttrell, I.; Bannerman, D.D.; Tupper, J.; Thaler, J.; Hawn, T.R.; Raines, E.W.; Schwartz, M.W. Toll-Like Receptor-4 Mediates Vascular Inflammation and Insulin Resistance in Diet-Induced Obesity. *Circ. Res.* **2007**, *100*, 1589–1596. [CrossRef] [PubMed]
27. Cusi, K. Role of Insulin Resistance and Lipotoxicity in Non-Alcoholic Steatohepatitis. *Clin. Liver Dis.* **2009**, *13*, 545–563. [CrossRef] [PubMed]
28. Arner, P. The adipocyte in insulin resistance: Key molecules and the impact of the thiazolidinediones. *Trends Endocrinol. Metab.* **2003**, *14*, 137–145. [CrossRef]
29. Letteron, P.; Fromenty, B.; Benoît, T.; Degott, C.; Pessayre, D. Acute and chronic hepatic steatosis lead to in vivo lipid peroxidation in mice. *J. Hepatol.* **1996**, *24*, 200–208. [CrossRef]
30. Parola, M.; Pinzani, M.; Casini, A.; Albano, E.; Poli, G.; Gentilini, A.; Gentilini, P.; Dianzani, M.U. Stimulation of lipid peroxidation or 4-hydroxynonenal treatment increases procollagen alpha 1(I) gene expression in human live fat-storing cells. *Biochim. Biophys. Res. Commun.* **1993**, *194*, 1044–1050. [CrossRef]
31. Lee, K.S.; Buck, M.; Houglum, K.; Chojkier, M. Activation of hepatic stellate cells by TGF alpha and collagen type I is mediated by oxidative stress through c-myb expression. *J. Clin. Investig.* **1995**, *96*, 2461–2468. [CrossRef]
32. Curzio, M.; Esterbauer, H.; Dianzani, M.U. Chemotactic activity of hydroxyalkenals on rat neutrophils. *Int. J. Tissue React.* **1985**, *7*, 137–142. [PubMed]
33. Jaeschke, H.; Wang, Y.; Essani, N.A. Reactive oxygen species activate the transcription factor NF-kB in the liver by induction of lipid peroxidation (abstr). *Hepatology* **1996**, *24*, 238A.
34. Baeuerle, P.A.; Henkel, T. Function and activation of NF-kB in the immune system. *Annu. Rev. Immunol.* **1994**, *12*, 141–179. [CrossRef] [PubMed]
35. Weltman, M.D.; Farrell, G.C.; Hall, P.; Ingelman-Sundberg, M.; Liddle, C. Hepatic cytochrome P450 2E1 is increased in patients with nonalcoholic steatohepatitis. *Hepatology* **1998**, *27*, 128–133. [CrossRef] [PubMed]
36. Weltman, M.D.; Farrell, G.C.; Liddle, C. Increased hepatocyte CYP2E1 expression in a rat nutritional model of hepatic steatosis with inflammation. *Gastroenterology* **1996**, *111*, 1645–1653. [CrossRef]

37. Al-Busafi, S.A.; Bhat, M.; Wong, P.; Ghali, P.; Deschenes, M. Antioxidant Therapy in Nonalcoholic Steatohepatitis. *Hepat. Res. Treat.* **2012**, *2012*, 1–8. [CrossRef]
38. Browning, J.D.; Horton, J.D. Molecular mediators of hepatic steatosis and liver injury. *J. Clin. Investig.* **2004**, *114*, 147–152. [CrossRef]
39. Brunt, E.M.; Kleiner, D.E.; Wilson, L.A.; Belt, P.; Neuschwander-Tetri, B.A.; for the NASH Clinical Research Network (CRN). Nonalcoholic fatty liver disease (NAFLD) activity score and the histopathologic diagnosis in NAFLD: Distinct clinicopathologic meanings. *Hepatology* **2010**, *53*, 810–820. [CrossRef]
40. George, D.; Goldwurm, S.; Macdonald, G.A.; Cowley, L.L.; Walker, N.I.; Ward, P.J.; Jazwinska, E.C.; Powell, L.W. Increased hepatic iron concentration in nonalcoholic steatohepatitis is associated with increased fibrosis. *Gastroenterology* **1998**, *114*, 311–318. [CrossRef]
41. Zangar, R.C.; Novak, R.F. Effects of Fatty Acids and Ketone Bodies on Cytochromes P450 2B, 4A, and 2E1 Expression in Primary Cultured Rat Hepatocytes. *Arch. Biochem. Biophys.* **1997**, *337*, 217–224. [CrossRef]
42. Ockner, R.K.; Kaikus, R.M.; Bass, N.M. Fatty-acid metabolism and the pathogenesis of hepatocellular carcinoma: Review and hypothesis. *Hepatology* **1993**, *18*, 669–676. [CrossRef]
43. Simopoulos, A.P. Dietary Omega-3 Fatty Acid Deficiency and High Fructose Intake in the Development of Metabolic Syndrome, Brain Metabolic Abnormalities, and Non-Alcoholic Fatty Liver Disease. *Nutrients* **2013**, *5*, 2901–2923. [CrossRef]
44. Warner, D.R.; Warner, J.B.; Hardesty, J.E.; Song, Y.L.; Chen, C.; Chen, Z.; Kang, J.X.; McClain, C.J.; Kirpich, I.A. Beneficial effects of an endogenous enrichment in n3-PUFAs on Wnt signaling are associated with attenuation of alcohol-mediated liver disease in mice. *FASEB J.* **2021**, *35*, e21377. [CrossRef] [PubMed]
45. Qiao, Y.; Zhang, X.; Zhang, Y.; Wang, Y.; Xu, Y.; Liu, X.; Sun, F.; Wang, J. High glucose stimulates tumorigenesis in hepatocellular carcinoma cells through AGER-dependent O-GlcNAcylation of c-Jun. *Diabetes* **2016**, *65*, 619–632. [CrossRef] [PubMed]
46. Hosokawa, T.; Kurosaki, M.; Tsuchiya, K.; Matsuda, S.; Muraoka, M.; Suzuki, Y.; Tamaki, N.; Yasui, Y.; Nakata, T.; Nishimura, T.; et al. Hyperglycemia is a significant prognostic factor of hepatocellular carcinoma after curative therapy. *World J. Gastroenterol.* **2013**, *19*, 249–257. [CrossRef] [PubMed]
47. Romeo, S.; Kozlitina, J.; Xing, C.; Pertsemlidis, A.; Cox, D.; Pennacchio, L.A.; Boerwinkle, E.; Cohen, J.C.; Hobbs, H.H. Genetic variation in PNPLA3 confers susceptibility to nonalcoholic fatty liver disease. *Nat. Genet.* **2008**, *40*, 1461–1465. [CrossRef]
48. Kozlitina, J.; Smagris, E.; Stender, S.; Nordestgaard, B.G.; Zhou, H.H.; Tybjærg-Hansen, A.; Vogt, T.F.; Hobbs, H.H.; Cohen, J.C. Exome-wide association study identifies a TM6SF2 variant that confers susceptibility to nonalcoholic fatty liver disease. *Nat. Genet.* **2014**, *46*, 352–356. [CrossRef]
49. Kumari, M.; Schoiswohl, G.; Chitraju, C.; Paar, M.; Cornaciu, I.; Rangrez, A.Y.; Wongsiriroj, N.; Nagy, H.M.; Ivanova, P.T.; Scott, S.A.; et al. Adiponutrin Functions as a Nutritionally Regulated Lysophosphatidic Acid Acyltransferase. *Cell Metab.* **2012**, *15*, 691–702. [CrossRef] [PubMed]
50. Singal, A.G.; Manjunath, H.; Yopp, A.C.; Beg, M.S.; Marrero, J.A.; Gopal, P.; Waljee, A.K. The Effect of PNPLA3 on Fibrosis Progression and Development of Hepatocellular Carcinoma: A Meta-analysis. *Am. J. Gastroenterol.* **2014**, *109*, 325–334. [CrossRef]
51. Sookoian, S.; Pirola, C.J. Meta-analysis of the influence of I148M variant of patatin-like phospholipase domain containing 3 gene (PNPLA3) on the susceptibility and histological severity of nonalcoholic fatty liver disease. *Hepatology* **2011**, *53*, 1883–1894. [CrossRef] [PubMed]
52. Bruschi, F.; Tardelli, M.; Claudel, T.; Trauner, M. PNPLA3 expression and its impact on the liver: Current perspectives. *Hepatic Med. Evid. Res.* **2017**, *9*, 55–66. [CrossRef] [PubMed]
53. Pingitore, P.; Romeo, S. The role of PNPLA3 in health and disease. *Biochim. Biophys. Acta Mol. Cell Biol. Lipids.* **2019**, *1864*, 900–906. [CrossRef]
54. Baulande, S.; Lasnier, F.; Lucas, M.; Pairault, J. Adiponutrin, a Transmembrane Protein Corresponding to a Novel Dietary- and Obesity-linked mRNA Specifically Expressed in the Adipose Lineage. *J. Biol. Chem.* **2001**, *276*, 33336–33344. [CrossRef] [PubMed]
55. Facciorusso, A. The influence of diabetes in the pathogenesis and the clinical course of hepatocellular carcinoma: Recent findings and new perspectives. *Curr. Diabetes. Rev.* **2013**, *9*, 382–386. [CrossRef] [PubMed]
56. Moldes, M.; Beauregard, G.; Faraj, M.; Peretti, N.; Ducluzeau, P.-H.; Laville, M.; Rabasa-Lhoret, R.; Vidal, H.; Cleément, K. Adiponutrin gene is regulated by insulin and glucose in human adipose tissue. *Eur. J. Endocrinol.* **2006**, *155*, 461–468. [CrossRef] [PubMed]
57. Huang, Y.; He, S.; Li, J.Z.; Seo, Y.-K.; Osborne, T.F.; Cohen, J.C.; Hobbs, H.H. A feed-forward loop amplifies nutritional regulation of PNPLA3. *Proc. Natl. Acad. Sci. USA* **2010**, *107*, 7892–7897. [CrossRef]
58. Dubuquoy, C.; Robichon, C.; Lasnier, F.; Langlois, C.; Dugail, I.; Foufelle, F.; Girard, J.; Burnol, A.-F.; Postic, C.; Moldes, M. Distinct regulation of adiponutrin/PNPLA3 gene expression by the transcription factors ChREBP and SREBP1c in mouse and human hepatocytes. *J. Hepatol.* **2011**, *55*, 145–153. [CrossRef]
59. Perttilä, J.; Huaman-Samanez, C.; Caron, S.; Tanhuanpää, K.; Staels, B.; Yki-Järvinen, H.; Olkkonen, V.M. PNPLA3 is regulated by glucose in human hepatocytes, and its I148M mutant slows down triglyceride hydrolysis. *Am. J. Physiol. Endocrinol. Metab.* **2012**, *302*, E1063–E1069. [CrossRef]
60. Hoekstra, M.; Li, Z.; Kruijt, J.K.; Van Eck, M.; Van Berkel, T.J.; Kuiper, J. The expression level of non-alcoholic fatty liver disease-related gene PNPLA3 in hepatocytes is highly influenced by hepatic lipid status. *J. Hepatol.* **2010**, *52*, 244–251. [CrossRef] [PubMed]

61. Kumashiro, N.; Yoshimura, T.; Cantley, J.L.; Majumdar, S.K.; Guebre-Egziabher, F.; Kursawe, R.; Vatner, D.F.; Fat, I.; Kahn, M.; Erion, D.M.; et al. Role of patatin-like phospholipase domain-containing 3 on lipid-induced hepatic steatosis and insulin resistance in rats. *Hepatology* **2013**, *57*, 1763–1772. [CrossRef] [PubMed]
62. Mitsche, M.A.; Hobbs, H.H.; Cohen, J.C. Patatin-like phospholipase domain–containing protein 3 promotes transfers of essential fatty acids from triglycerides to phospholipids in hepatic lipid droplets. *J. Biol. Chem.* **2018**, *293*, 6958–6968. [CrossRef]
63. Basuray, S.; Wang, Y.; Smagris, E.; Cohen, J.C.; Hobbs, H.H. Accumulation of PNPLA3 on lipid droplets is the basis of associated hepatic steatosis. *Proc. Natl. Acad. Sci. USA* **2019**, *116*, 9521–9526. [CrossRef]
64. Carlsson, B.; Lindén, D.; Brolén, G.; Liljeblad, M.; Bjursell, M.; Romeo, S.; Loomba, R. Review article: The emerging role of genetics in precision medicine for patients with non-alcoholic steatohepatitis. *Aliment. Pharmacol. Ther.* **2020**, *51*, 1305–1320. [CrossRef] [PubMed]
65. Lindén, D.; Ahnmark, A.; Pingitore, P.; Ciociola, E.; Ahlstedt, I.; Andréasson, A.-C.; Sasidharan, K.; Madeyski-Bengtson, K.; Zurek, M.; Mancina, R.M.; et al. Pnpla3 silencing with antisense oligonucleotides ameliorates nonalcoholic steatohepatitis and fibrosis in Pnpla3 I148M knock-in mice. *Mol. Metab.* **2019**, *22*, 49–61. [CrossRef]
66. Mahdessian, H.; Taxiarchis, A.; Popov, S.; Silveira, A.; Franco-Cereceda, A.; Hamsten, A.; Eriksson, P.; Hooft, F.V. TM6SF2 is a regulator of liver fat metabolism influencing triglyceride secretion and hepatic lipid droplet content. *Proc. Natl. Acad. Sci. USA* **2014**, *111*, 8913–8918. [CrossRef]
67. Li, B.-T.; Sun, M.; Li, Y.-F.; Wang, J.-Q.; Zhou, Z.-M.; Song, B.-L.; Luo, J. Disruption of the ERLIN–TM6SF2–APOB complex destabilizes APOB and contributes to non-alcoholic fatty liver disease. *PLoS Genet.* **2020**, *16*, e1008955. [CrossRef] [PubMed]
68. Day, C.P.; Anstee, Q.M. The Genetics of Nonalcoholic Fatty Liver Disease: Spotlight on PNPLA3 and TM6SF2. *Semin. Liver Dis.* **2015**, *35*, 270–290. [CrossRef] [PubMed]
69. Goffredo, M.; Caprio, S.; Feldstein, A.E.; D'Adamo, E.; Shaw, M.M.; Pierpont, B.; Savoye, M.; Zhao, H.; Bale, A.E.; Santoro, N. Role ofTM6SF2rs58542926 in the pathogenesis of nonalcoholic pediatric fatty liver disease: A multiethnic study. *Hepatology* **2015**, *63*, 117–125. [CrossRef] [PubMed]
70. Wang, L.; Athinarayanan, S.; Jiang, G.; Chalasani, N.; Zhang, M.; Liu, W. Fatty acid desaturase 1 gene polymorphisms control human hepatic lipid composition. *Hepatology* **2014**, *61*, 119–128. [CrossRef] [PubMed]
71. Chiappini, F.; Coilly, A.; Kadar, H.; Gual, P.; Tran, A.; Desterke, C.; Samuel, D.; Duclos-Vallée, J.-C.; Touboul, D.; Bertrand-Michel, J.; et al. Metabolism dysregulation induces a specific lipid signature of nonalcoholic steatohepatitis in patients. *Sci. Rep.* **2017**, *7*, 46658. [CrossRef] [PubMed]
72. Guillou, H.; Zadravec, D.; Martin, P.G.; Jacobsson, A. The key roles of elongases and desaturases in mammalian fatty acid metabolism: Insights from transgenic mice. *Prog. Lipid Res.* **2010**, *49*, 186–199. [CrossRef] [PubMed]
73. Naudí, A.; Jové, M.; Ayala, V.; Portero-Otín, M.; Barja, G.; Pamplona, R. Membrane lipid unsaturation as physiological adaptation to animal longevity. *Front. Physiol.* **2013**, *4*, 372. [CrossRef] [PubMed]
74. Van Meer, G.; Voelker, D.R.; Feigenson, G.W. Membrane lipids: Where they are and how they behave. *Nat. Rev. Mol. Cell Biol.* **2008**, *9*, 112–124. [CrossRef] [PubMed]
75. Cheung, O.; Puri, P.; Eicken, C.; Contos, M.J.; Mirshahi, F.; Maher, J.W.; Kellum, J.M.; Min, H.; Luketic, V.A.; Sanyal, A.J. Nonalcoholic steatohepatitis is associated with altered hepatic MicroRNA expression. *Hepatology* **2008**, *48*, 1810–1820. [CrossRef]
76. Takaki, Y.; Saito, Y.; Takasugi, A.; Toshimitsu, K.; Yamada, S.; Muramatsu, T.; Kimura, M.; Sugiyama, K.; Suzuki, H.; Arai, E.; et al. Silencing of microRNA-122 is an early event during hepatocarcinogenesis from non-alcoholic steatohepatitis. *Cancer Sci.* **2014**, *105*, 1254–1260. [CrossRef] [PubMed]
77. Khalid, A.; Hussain, T.; Manzoor, S.; Saalim, M.; Khaliq, S. PTEN: A potential prognostic marker in virus-induced hepatocellular carcinoma. *Tumor Biol.* **2017**, *39*, 1010428317705754. [CrossRef] [PubMed]
78. Liu, Y.; Qi, X.; Zeng, Z.; Wang, L.; Wang, J.; Zhang, T.; Xu, Q.; Shen, C.; Zhou, G.; Yang, S.; et al. CRISPR/Cas9-mediated p53 and Pten dual mutation accelerates hepatocarcinogenesis in adult hepatitis B virus transgenic mice. *Sci. Rep.* **2017**, *7*, 2796. [CrossRef]
79. Xu, Z.; Hu, J.; Cao, H.; Pilo, M.G.; Cigliano, A.; Shao, Z.; Xu, M.; Ribback, S.; Dombrowski, F.; Calvisi, D.F.; et al. Loss of Pten synergizes with c-Met to promote hepatocellular carcinoma development via mTORC2 pathway. *Exp. Mol. Med.* **2018**, *50*, e417. [CrossRef]
80. Gao, D.; Wei, C.; Chen, L.; Huang, J.; Yang, S.; Diehl, A.M. Oxidative DNA damage and DNA repair enzyme expression are inversely related in murine models of fatty liver disease. *Am. J. Physiol. Liver Physiol.* **2004**, *287*, G1070–G1077. [CrossRef] [PubMed]
81. McKinnon, P.J. ATM and the Molecular Pathogenesis of Ataxia Telangiectasia. *Annu. Rev. Pathol. Mech. Dis.* **2012**, *7*, 303–321. [CrossRef]
82. Ditch, S.; Paull, T.T. The ATM protein kinase and cellular redox signaling: Beyond the DNA damage response. *Trends Biochem. Sci.* **2012**, *37*, 15–22. [CrossRef] [PubMed]
83. Guo, Z.; Kozlov, S.; Lavin, M.F.; Person, M.D.; Paull, T.T. ATM Activation by Oxidative Stress. *Science* **2010**, *330*, 517–521. [CrossRef] [PubMed]
84. Daugherity, E.K.; Balmus, G.; Al Saei, A.; Moore, E.S.; Abdallah, D.A.; Rogers, A.B.; Weiss, R.S.; Maurer, K.J. The DNA damage checkpoint protein ATM promotes hepatocellular apoptosis and fibrosis in a mouse model of non-alcoholic fatty liver disease. *Cell Cycle* **2012**, *11*, 1918–1928. [CrossRef] [PubMed]

85. Schults, M.A.; Nagle, P.W.; Rensen, S.S.; Godschalk, R.W.; Munnia, A.; Peluso, M.; Claessen, S.M.; Greve, J.W.; Driessen, A.; Verdam, F.J.; et al. Decreased nucleotide excision repair in steatotic livers associates with myeloperoxidase-immunoreactivity. *Mutat. Res. Mol. Mech. Mutagen.* **2012**, *736*, 75–81. [CrossRef]
86. Collis, S.J.; Deweese, T.L.; Jeggo, P.A.; Parker, A.R. The life and death of DNA-PK. *Oncogene* **2004**, *24*, 949–961. [CrossRef]
87. Evert, M.; Frau, M.; Tomasi, M.; Latte, G.; Simile, M.; Seddaiu, M.; Zimmermann, A.; Ladu, S.; Staniscia, T.; Brozzetti, S.; et al. Deregulation of DNA-dependent protein kinase catalytic subunit contributes to human hepatocarcinogenesis development and has a putative prognostic value. *Br. J. Cancer* **2013**, *109*, 2654–2664. [CrossRef]
88. Wong, R.H.; Chang, I.; Hudak, C.S.S.; Hyun, S.; Kwan, H.-Y.; Sul, H.S. A Role of DNA-PK for the Metabolic Gene Regulation in Response to Insulin. *Cell* **2009**, *136*, 1056–1072. [CrossRef]
89. Fautrel, A.; Andrieux, L.; Musso, O.; Boudjema, K.; Guillouzo, A.; Langouët, S. Overexpression of the two nucleotide excision repair genes ERCC1 and XPC in human hepatocellular carcinoma. *J. Hepatol.* **2005**, *43*, 288–293. [CrossRef]
90. Cornell, L.; Munck, J.M.; Alsinet, C.; Villanueva, A.; Ogle, L.; Willoughby, C.E.; Televantou, D.; Thomas, H.D.; Jackson, J.; Burt, A.D.; et al. DNA-PK—A Candidate Driver of Hepatocarcinogenesis and Tissue Biomarker That Predicts Response to Treatment and Survival. *Clin. Cancer Res.* **2015**, *21*, 925–933. [CrossRef] [PubMed]
91. Pascale, R.M.; Joseph, C.; Latte, G.; Evert, M.; Feo, F.; Calvisi, D.F. DNA-PKcs: A promising therapeutic target in human hepatocellular carcinoma? *DNA Repair Amst.* **2016**, *47*, 12–20. [CrossRef] [PubMed]
92. Desterke, C.; Chiappini, F. Lipid Related Genes Altered in NASH Connect Inflammation in Liver Pathogenesis Progression to HCC: A Canonical Pathway. *Int. J. Mol. Sci.* **2019**, *20*, 5594. [CrossRef]
93. Nwosu, Z.C.; Megger, D.A.; Hammad, S.; Sitek, B.; Roessler, S.; Ebert, M.P.; Meyer, C.; Dooley, S. Identification of the Consistently Altered Metabolic Targets in Human Hepatocellular Carcinoma. *Cell. Mol. Gastroenterol. Hepatol.* **2017**, *4*, 303–323.e1. [CrossRef]
94. Janku, F.; Kaseb, A.O.; Tsimberidou, A.M.; Wolff, R.A.; Kurzrock, R. Identification of novel therapeutic targets in the PI3K/AKT/mTOR pathway in hepatocellular carcinoma using targeted next generation sequencing. *Oncotarget* **2014**, *5*, 3012–3022. [CrossRef] [PubMed]
95. Yang, S.; Liu, G. Targeting the Ras/Raf/MEK/ERK pathway in hepatocellular carcinoma. *Oncol. Lett.* **2017**, *13*, 1041–1047. [CrossRef] [PubMed]
96. Chettouh, H.; Lequoy, M.; Fartoux, L.; Vigouroux, C.; Desbois-Mouthon, C. Hyperinsulinaemia and insulin signalling in the pathogenesis and the clinical course of hepatocellular carcinoma. *Liver Int.* **2015**, *35*, 2203–2217. [CrossRef] [PubMed]
97. Kim, S.; Jeong, S. Mutation hotspots in the beta-catenin gene: Lessons from the human cancer genome databases. *Mol. Cells* **2019**, *42*, 8–16. [PubMed]
98. Harada, N.; Miyoshi, H.; Murai, N.; Oshima, H.; Tamai, Y.; Oshima, M.; Taketo, M.M. Lack of tumorigenesis in the mouse liver after adenovirus-mediated expression of a dominant stable mutant of beta-catenin. *Cancer Res.* **2002**, *62*, 1971–1977.
99. Longato, L.; de la Monte, S.; Kuzushita, N.; Horimoto, M.; Rogers, A.B.; Slagle, B.L.; Wands, J.R. Overexpression of insulin receptor substrate-1 and hepatitis Bx genes causes premalignant alterations in the liver. *Hepatology* **2009**, *49*, 1935–1943. [CrossRef] [PubMed]
100. Harada, N.; Oshima, H.; Katoh, M.; Tamai, Y.; Oshima, M.; Taketo, M.M. Hepatocarcinogenesis in mice with beta-catenin and Ha-ras gene mutations. *Cancer Res.* **2004**, *64*, 48–54. [CrossRef] [PubMed]
101. Zhan, N.; Michael, A.A.; Wu, K.; Zeng, G.; Bell, A.; Tao, J.; Monga, S.P. The effect of selective c-MET inhibitor on hepatocellular carcinoma in the MET-active, beta-catenin-mutated mouse model. *Gene Expr.* **2018**, *18*, 135–147. [CrossRef] [PubMed]
102. Onal, G.; Kutlu, O.; Gozuacik, D.; Emre, S.D. Lipid Droplets in Health and Disease. *Lipids Health Dis.* **2017**, *16*, 1–15. [CrossRef] [PubMed]
103. Liu, L.; Liao, J.-Z.; He, X.-X.; Li, P.-Y. The role of autophagy in hepatocellular carcinoma: Friend or foe. *Oncotarget* **2017**, *8*, 57707–57722. [CrossRef] [PubMed]
104. Mao, Y.; Yu, F.; Wang, J.; Guo, C.; Fan, X. Autophagy: A new target for nonalcoholic fatty liver disease therapy. *Hepatic Med. Evid. Res.* **2016**, *8*, 27–37. [CrossRef]
105. Yazdani, H.O.; Huang, H.; Tsung, A. Autophagy: Dual response in the development of hepatocellular carcinoma. *Cells* **2019**, *8*, 91. [CrossRef]
106. Hu, P.; Cheng, B.; He, Y.; Wei, Z.; Wu, D.; Meng, Z. Autophagy suppresses proliferation of HepG2 cells via inhibiting glypican-3/wnt/beta-catenin signaling. *Onco. Ther.* **2018**, *11*, 193–200. [CrossRef]
107. Fan, Q.; Yang, L.; Zhang, X.; Ma, Y.; Li, Y.; Dong, L.; Zong, Z.; Hua, X.; Su, D.; Li, H.; et al. Autophagy promotes metastasis and glycolysis by upregulating MCT1 expression and Wnt/beta-catenin signaling pathway activation in hepatocellular carcinoma cells. *J. Exp. Clin. Cancer Res.* **2018**, *37*, 9. [CrossRef]
108. Shao, C.; Yang, F.; Miao, S.; Liu, W.; Wang, C.; Shu, Y.; Shen, H. Role of hypoxia-induced exosomes in tumor biology. *Mol. Cancer* **2018**, *17*, 1–8. [CrossRef]
109. Li, R.; Wang, Y.; Zhang, X.; Feng, M.; Ma, J.; Li, J.; Yang, X.; Fang, F.; Xia, Q.; Zhang, Z.; et al. Exosome-mediated secretion of LOXL4 promotes hepatocellular carcinoma cell invasion and metastasis. *Mol. Cancer* **2019**, *18*, 1–19. [CrossRef]
110. Harada, T.; Yamamoto, H.; Kishida, S.; Kishida, M.; Awada, C.; Takao, T.; Kikuchi, A. Wnt5b-associated exosomes promote cancer cell migration and proliferation. *Cancer Sci.* **2017**, *108*, 42–52. [CrossRef]

111. Mao, J.; Liang, Z.; Zhang, B.; Yang, H.; Li, X.; Fu, H.; Zhang, X.; Yan, Y.; Xu, W.; Qian, H. UBR2 enriched in p53 deficient mouse bone marrow mesenchymal stem cell-exosome promoted gastric cancer progression via Wnt/beta-catenin pathway. *Stem Cells* **2017**, *35*, 2267–2279. [CrossRef] [PubMed]
112. Park, E.J.; Lee, J.H.; Yu, G.-Y.; He, G.; Ali, S.R.; Holzer, R.G.; Österreicher, C.H.; Takahashi, H.; Karin, M. Dietary and Genetic Obesity Promote Liver Inflammation and Tumorigenesis by Enhancing IL-6 and TNF Expression. *Cell* **2010**, *140*, 197–208. [CrossRef] [PubMed]
113. Shen, J.; Yeh, C.-C.; Wang, Q.; Gurvich, I.; Siegel, A.B.; Santella, R.M. Plasma Adiponectin and Hepatocellular Carcinoma Survival Among Patients Without Liver Transplantation. *Anticancer. Res.* **2016**, *36*, 5307–5314. [CrossRef] [PubMed]
114. Carbone, F.; La Rocca, C.; Matarese, G. Immunological functions of leptin and adiponectin. *Biochimie* **2012**, *94*, 2082–2088. [CrossRef]
115. Ma, C.; Kesarwala, A.H.; Eggert, T.; Medina-Echeverz, J.; Kleiner, D.E.; Jin, P.; Stroncek, P.J.D.F.; Terabe, M.; Kapoor, V.; Elgindi, M.; et al. NAFLD causes selective CD4+ T lymphocyte loss and promotes hepatocarcinogenesis. *Nature* **2016**, *531*, 253–257. [CrossRef]
116. Wolf, M.J.; Adili, A.; Diehl, K.; Abdullah, Z.; Boege, Y.; Stemmer, K.; Ringelhan, M.; Simonavicius, N.; Egger, M.; Wohlleber, D.; et al. Metabolic Activation of Intrahepatic CD8+ T Cells and NKT Cells Causes Nonalcoholic Steatohepatitis and Liver Cancer via Cross-Talk with Hepatocytes. *Cancer Cell* **2014**, *26*, 549–564. [CrossRef] [PubMed]
117. Lanthier, N. Targeting Kupffer cells in non-alcoholic fatty liver disease/non-alcoholic steatohepatitis: Why and how? *World J. Hepatol.* **2015**, *7*, 2184–2188. [CrossRef] [PubMed]
118. Martin-Murphy, B.V.; You, Q.; Wang, H.; De La Houssaye, B.A.; Reilly, T.P.; Friedman, J.E.; Ju, C. Mice Lacking Natural Killer T Cells Are More Susceptible to Metabolic Alterations following High Fat Diet Feeding. *PLoS ONE* **2014**, *9*, e80949. [CrossRef] [PubMed]
119. Tian, Z.; Chen, Y.; Gao, B. Natural killer cells in liver disease. *Hepatology* **2013**, *57*, 1654–1662. [CrossRef]
120. Fan, Y.; Zhang, W.; Wei, H.; Sun, R.; Tian, Z.; Chen, Y. Hepatic NK cells attenuate fibrosis progression of non-alcoholic steatohepatitis in dependent of CXCL10-mediated recruitment. *Liver Int.* **2019**, *40*, 598–608. [CrossRef]
121. Zheng, X.; Zeng, W.; Gai, X.; Xu, Q.; Li, C.; Liang, Z.; Tuo, H.; Liu, Q. Role of the Hedgehog pathway in hepatocellular carcinoma (Review). *Oncol. Rep.* **2013**, *30*, 2020–2026. [CrossRef] [PubMed]
122. Della Corte, C.M.; Viscardi, G.; Papaccio, F.; Esposito, G.; Martini, G.; Ciardiello, D.; Martinelli, E.; Ciardiello, F.; Morgillo, F. Implication of the Hedgehog pathway in hepatocellular carcinoma. *World J. Gastroenterol.* **2017**, *23*, 4330. [CrossRef] [PubMed]
123. Loria, P.; Carulli, L.; Bertolotti, M.; Lonardo, A. Endocrine and liver interaction: The role of endocrine pathways in NASH. *Nat. Rev. Gastroenterol. Hepatol.* **2009**, *6*, 236–247. [CrossRef] [PubMed]
124. Nagasue, N.; Yu, L.; Yukaya, H.; Kohno, H.; Nakamura, T. Androgen and oestrogen receptors in hepatocellular carcinoma and surrounding liver parenchyma: Impact on intrahepatic recurrence after hepatic resection. *BJS* **1995**, *82*, 542–547. [CrossRef]
125. Awuah, P.K.; Monga, S.P. Cell cycle-related Kinase links androgen receptor & β-catenin signaling in HCC: Why men are at a loss? *Hepatology* **2012**, *55*, 970–973.
126. Sun, H.; Yang, W.; Tian, Y.; Zeng, X.; Zhou, J.; Mok, M.T.S.; Tang, W.; Feng, Y.; Xu, L.; Chan, A.W.H.; et al. An inflammatory-CCRK circuitry drives mTORC1-dependent metabolic and immunosuppressive reprogramming in obesity-associated hepatocellular carcinoma. *Nat. Commun.* **2018**, *9*, 1–16. [CrossRef]
127. Johnson, P.J.; Pirrie, S.J.; Cox, T.F.; Berhane, S.; Teng, M.; Palmer, D.; Morse, J.; Hull, D.; Patman, G.; Kagebayashi, C.; et al. The Detection of Hepatocellular Carcinoma Using a Prospectively Developed and Validated Model Based on Serological Biomarkers. *Cancer Epidemiol. Biomark. Prev.* **2014**, *23*, 144–153. [CrossRef]
128. Best, J.; Bechmann, L.P.; Sowa, J.-P.; Sydor, S.; Dechêne, A.; Pflanz, K.; Bedreli, S.; Schotten, C.; Geier, A.; Berg, T.; et al. GALAD Score Detects Early Hepatocellular Carcinoma in an International Cohort of Patients With Nonalcoholic Steatohepatitis. *Clin. Gastroenterol. Hepatol.* **2020**, *18*, 728–735.e4. [CrossRef]
129. Best, J.; Bilgi, H.; Heider, D.; Schotten, C.; Manka, P.; Bedreli, S.; Gorray, M.; Ertle, J.; Van Grunsven, L.A.; Dechêne, A. The GALAD scoring algorithm based on AFP, AFP-L3, and DCP significantly improves detection of BCLC early stage hepatocellular carcinoma. *Z. Gastroenterol.* **2016**, *54*, 1296–1305. [CrossRef] [PubMed]
130. Hwang, A.; Shi, C.; Zhu, E.; Naaz, F.; Zhou, P.; Rasheed, Z.; Liu, M.; Jung, L.S.; Duan, B.; Li, J.; et al. Supervised learning reveals circulating biomarker levels diagnostic of hepatocellular carcinoma in a clinically relevant model of non-alcoholic steatohepatitis; An OAD to NASH. *PLoS ONE* **2018**, *13*, e0198937. [CrossRef] [PubMed]
131. Ng, C.K.Y.; Di Costanzo, G.G.; Terracciano, L.M.; Piscuoglio, S. Circulating Cell-Free DNA in Hepatocellular Carcinoma: Current Insights and Outlook. *Front. Med.* **2018**, *5*, 78. [CrossRef]
132. Thakral, S.; Ghoshal, K. miR-122 is a unique molecule with great potential in diagnosis, prognosis of liver disease, and therapy both as miRNA mimic and antimir. *Curr. Gene Ther.* **2015**, *15*, 142–150. [CrossRef] [PubMed]
133. Zhang, Y.-J.; Wu, H.-C.; Shen, J.; Ahsan, H.; Tsai, W.Y.; Yang, H.-I.; Wang, L.-Y.; Chen, S.-Y.; Chen, C.-J.; Santella, R.M. Predicting Hepatocellular Carcinoma by Detection of Aberrant Promoter Methylation in Serum DNA. *Clin. Cancer Res.* **2007**, *13*, 2378–2384. [CrossRef] [PubMed]
134. Tangkijvanich, P.; Hourpai, N.; Rattanatanyong, P.; Wisedopas, N.; Mahachai, V.; Mutirangura, A. Serum LINE-1 hypomethylation as a potential prognostic marker for hepatocellular carcinoma. *Clin. Chim. Acta* **2007**, *379*, 127–133. [CrossRef] [PubMed]
135. Xu, R.-H.; Wei, W.; Krawczyk, M.; Wang, W.; Luo, H.; Flagg, K.; Yi, S.; Shi, W.; Quan, Q.; Li, K.; et al. Circulating tumour DNA methylation markers for diagnosis and prognosis of hepatocellular carcinoma. *Nat. Mater.* **2017**, *16*, 1155–1161. [CrossRef] [PubMed]

136. Liu, X.; Tan, N.; Liao, H.; Pan, G.; Xu, Q.; Zhu, R.; Zou, L.; He, S.; Zhu, H. High GSTP1 inhibits cell proliferation by reducing Akt phosphorylation and is associated with a better prognosis in hepatocellular carcinoma. *Oncotarget* **2017**, *9*, 8957–8971. [CrossRef] [PubMed]
137. Schagdarsurengin, U.; Wilkens, L.; Steinemann, D.; Flemming, P.; Kreipe, H.H.; Pfeifer, G.P.; Schlegelberger, B.; Dammann, R. Frequent epigenetic inactivation of the RASSF1A gene in hepatocellular carcinoma. *Oncogene* **2003**, *22*, 1866–1871. [CrossRef]
138. Chiappini, F.; Desterke, C.; Bertrand-Michel, J.; Guettier, C.; Le Naour, F. Hepatic and serum lipid signatures specific to nonalcoholic steatohepatitis in murine models. *Sci. Rep.* **2016**, *6*, 31587. [CrossRef]
139. Alexander, M.; Loomis, A.K.; Fairburn-Beech, J.; Van Der Lei, J.; Duarte-Salles, T.; Prieto-Alhambra, D.; Ansell, D.; Pasqua, A.; Lapi, F.; Rijnbeek, P.; et al. Real-world data reveal a diagnostic gap in non-alcoholic fatty liver disease. *BMC Med.* **2018**, *16*, 130. [CrossRef]
140. Zezos, P.; Renner, E.L. Liver transplantation and non-alcoholic fatty liver disease. *World J. Gastroenterol.* **2014**, *20*, 15532–15538. [CrossRef]
141. Orman, E.S.; Mayorga, M.E.; Wheeler, S.B.; Townsley, R.M.; Toro-Diaz, H.H.; Hayashi, P.H.; Iv, A.S.B. Declining liver graft quality threatens the future of liver transplantation in the United States. *Liver Transplant.* **2015**, *21*, 1040–1050. [CrossRef] [PubMed]
142. Wegermann, K.; Suzuki, A.; Mavis, A.M.; Abdelmalek, M.F.; Diehl, A.M.; Moylan, C.A. Tackling NAFLD: Three Targeted Populations. *Hepatology* **2020**. [CrossRef] [PubMed]
143. Söderberg, C.; Stål, P.; Askling, J.; Glaumann, H.; Lindberg, G.; Marmur, J.; Hultcrantz, R. Decreased survival of subjects with elevated liver function tests during a 28-year follow-up. *Hepatology* **2010**, *51*, 595–602. [CrossRef]
144. Altamirano, J.; Qi, Q.; Choudhry, S.; Abdallah, M.; Singal, A.K.; Humar, A.; Bataller, R.; Borhani, A.A.; Duarte-Rojo, A. Non-invasive diagnosis: Non-alcoholic fatty liver disease and alcoholic liver disease. *Transl. Gastroenterol. Hepatol.* **2020**, *5*, 31. [CrossRef]
145. Dulai, P.S.; Singh, S.; Patel, J.; Soni, M.; Prokop, L.J.; Younossi, Z.; Sebastiani, G.; Ekstedt, M.; Hagstrom, H.; Nasr, P.; et al. Increased risk of mortality by fibrosis stage in nonalcoholic fatty liver disease: Systematic review and meta-analysis. *Hepatology* **2017**, *65*, 1557–1565. [CrossRef]
146. Torok, N.J.; Dranoff, J.A.; Schuppan, D.; Friedman, S.L. Strategies and endpoints of antifibrotic drug trials: Summary and recommendations from the AASLD Emerging Trends Conference, Chicago, June 2014. *Hepatology* **2015**, *62*, 627–634. [CrossRef] [PubMed]
147. Younossi, Z.M.; Blissett, D.; Blissett, R.; Henry, L.; Stepanova, M.; Younossi, Y.; Racila, A.; Hunt, S.; Beckerman, R. The economic and clinical burden of nonalcoholic fatty liver disease in the United States and Europe. *Hepatology* **2016**, *64*, 1577–1586. [CrossRef] [PubMed]
148. Valery, P.C.; Laversanne, M.; Clark, P.J.; Petrick, J.L.; McGlynn, K.A.; Bray, F. Projections of primary liver cancer to 2030 in 30 countries worldwide. *Hepatology* **2018**, *67*, 600–611. [CrossRef]

biomedicines

MDPI

Review

Usefulness of Different Imaging Modalities in Evaluation of Patients with Non-Alcoholic Fatty Liver Disease

Karolina Grąt [1,*], Michał Grąt [2] and Olgierd Rowiński [1]

[1] Second Department of Clinical Radiology, Medical University of Warsaw, 02-097 Warsaw, Poland; olgierd.rowinski@wum.edu.pl

[2] Department of General, Transplant and Liver Surgery, Medical University of Warsaw, 02-097 Warsaw, Poland; michal.grat@gmail.com

* Correspondence: karolina.grat@gmail.com

Received: 16 July 2020; Accepted: 19 August 2020; Published: 21 August 2020

Abstract: Non-alcoholic fatty liver disease (NAFLD) and non-alcoholic steatohepatitis (NASH) are becoming some of the major health problems in well-developed countries, together with the increasing prevalence of obesity, metabolic syndrome, and all of their systemic complications. As the future prognoses are even more disturbing and point toward further increase in population affected with NAFLD/NASH, there is an urgent need for widely available and reliable diagnostic methods. Consensus on a non-invasive, accurate diagnostic modality for the use in ongoing clinical trials is also required, particularly considering a current lack of any registered drug for the treatment of NAFLD/NASH. The aim of this narrative review was to present current information on methods used to assess liver steatosis and fibrosis. There are several imaging modalities for the assessment of hepatic steatosis ranging from simple density analysis by computed tomography or conventional B-mode ultrasound to magnetic resonance spectroscopy (MRS), magnetic resonance imaging proton density fat fraction (MRI-PDFF) or controlled attenuation parameter (CAP). Fibrosis stage can be assessed by magnetic resonance elastography (MRE) or different ultrasound-based techniques: transient elastography (TE), shear-wave elastography (SWE) and acoustic radiation force impulse (ARFI). Although all of these methods have been validated against liver biopsy as the reference standard and provided good accuracy, the MRS and MRI-PDFF currently outperform other methods in terms of diagnosis of steatosis, and MRE in terms of evaluation of fibrosis.

Keywords: NASH; NAFLD; liver stiffness; liver steatosis; controlled attenuation parameter; transient elastography; MRI PDFF; MR spectroscopy

1. Introduction

Non-alcoholic fatty liver disease (NAFLD) is a chronic liver condition with globally increasing incidence rates. It is associated with the worldwide increasing prevalence of overweight, obesity, and metabolic syndrome, and is becoming one of the most important health system issues in the developed countries [1,2]. NAFLD, which is defined as an excessive accumulation of fat in hepatocytes, may progress to non-alcoholic steatohepatitis (NASH), and further into fibrosis, with all of its complications—the development of liver cirrhosis, portal hypertension, and hepatocellular carcinoma [3]. It has also been proven that patients with NAFLD have a higher risk for the occurrence of cardiovascular incidents [4–6] and increased risk for developing chronic kidney disease [7]. Remarkably, it is estimated that up to 35% of citizens of the United States of America (USA) are affected by NAFLD, which makes it the most prevalent liver disease in the USA [8]. Accordingly, end-stage liver disease in the course of NASH has already become one of the most common indications for liver transplantation

in the USA. Importantly, recent analyses predict a further increase in the prevalence of NASH, with more than 60% of Americans estimated to be affected by the year 2030 [9,10]. Therefore, major effects on the access to liver transplantation, pre-transplant-mortality, wait-list dynamics, and the general outcomes of liver transplant recipients are expected. As grafts with excessive fat accumulation are not suitable for transplantation, increasing prevalence of NASH influences the donor pool. Recently various techniques, such as hypothermic oxygenated machine perfusion, have been proposed to improve the quality of grafts (Figure 1).

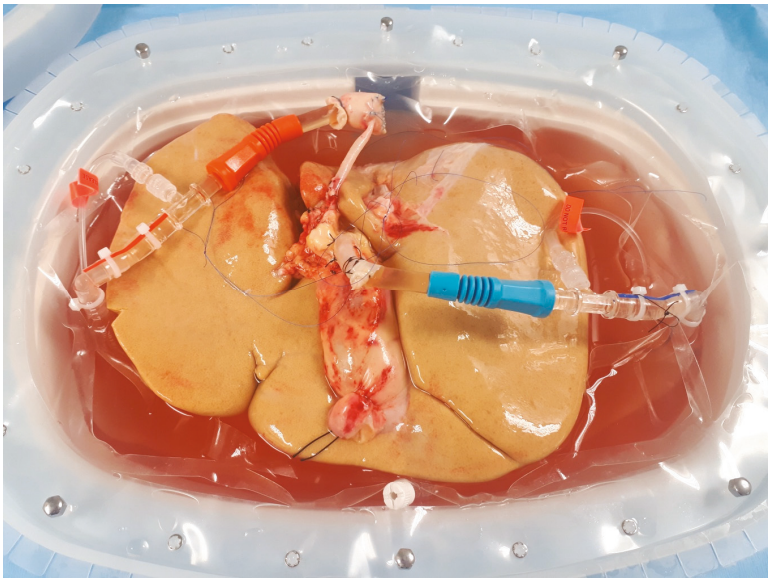

Figure 1. Liver allograft with extensive steatosis undergoing hypothermic oxygenated machine perfusion. Image from the authors' department.

Histopathological evaluation of liver biopsy still remains the gold standard for the diagnosis of NAFLD and NASH. Liver biopsy is also used as the reference standard for the assessment of other methods, despite several disadvantages. Due to the invasive character, it is associated with the risk of potentially severe complications. Further, the costs of frequent liver biopsies are relatively high [11–13]. What is more, some authors suggest that the results might be misleading, as the specimen may not be representative of the whole organ, especially in relatively benign changes. Therefore, alternative non-invasive methods of more representative assessment of liver steatosis have been proposed and validated in the recent years. Ideally, those should be non-invasive, widely available and cost-effective. As there are many ongoing clinical trials on new therapies for patients with NAFLD and NASH, new methods should be particularly characterized by the clinical utility to perform regular follow-up in order to verify treatment results. Moreover, it should also enable precise quantitative evaluation of the current status of liver parenchyma.

This is a narrative review aimed at presenting the current information on various methods used for the assessment of liver steatosis and fibrosis. Further, available data on their prognostic role in patients with NAFLD are discussed. The choice of the articles for this narrative review was made after evaluation by the authors following screening of abstracts in the PUBMED database, using the following search terms: "NASH diagnosis", "NAFLD diagnosis", "liver steatosis", "liver spectroscopy", "PDFF", "proton density fat fraction", "computed tomography liver steatosis", "liver elastography", "controlled attenuation parameter".

2. Techniques Using Computed Tomography

Computed tomography (CT) scans provide valuable information on the extent of liver steatosis, basing on the analyses of the organ density. The most basic techniques, which are simply based either on the measurement of the liver density on non-contrast enhanced scans or comparisons between the density of the liver to the density of the spleen [14], can accurately detect liver steatosis exceeding 20%, but fail to provide sufficient accuracy in patients with hepatic steatosis of lesser extent [15]. In a metanalysis performed by Bohte et al., the overall specificity of CT in the diagnosis of any liver steatosis (with biopsy used as the reference standard) was as low as 46–72%, with the lowest accuracy observed for mild forms of fat accumulation. Currently, there are no algorithms for precise and accurate quantitative assessment of fat content in the liver tissue. Therefore, the use of CT seems rather limited to general stratification of patients and it is not a suitable diagnostic modality in long term follow-up; for example, in patients undergoing treatment for NAFLD/NASH. Even extensive steatosis of more than 50% of hepatocytes can present with a density higher than the standard cut-off of 40 Hounsfield units, as shown on Figure 2.

Nevertheless, several variations of the standard scanning technique have been proposed in order to enhance the diagnostic accuracy of the CT scans. One is the use of a standardized calibration phantom, placed beneath the patients back during the CT examination. In a recent study from 2020, Guo et al. provided evidence that the utilization of this protocol enables the calculation of hepatic steatosis far more accurately, with sensitivity and specificity of 76% and 85%, respectively, for the detection of mild steatosis (involving at least 5% of hepatocytes), and 85% and 98%, respectively, for the detection of moderate steatosis (involving at least 14% of hepatocytes) [16]. The clinical usefulness of this method is especially supported by relatively high positive and negative predictive values of 78% and 83%, respectively, for mild steatosis, and 82% and 97%, respectively, for moderate steatosis. Importantly, this technique needs to be adjusted for particular type of CT scanner, as the basic liver density in Hounsfield units may differ between different manufacturers.

Computed tomography fails to detect early stages of liver fibrosis, and can only show signs of advanced stages, for example nodular shape of the liver, evidence of portal hypertension etc. Nevertheless, some authors have proposed advanced algorithms for the assessment of liver fibrosis on CT scans—for example, analysis of liver texture [17], analysis of the nodularity of the liver surface [18,19] or incorporating data from the CT into an multiparametric tool (data from the CT scans combined with laboratory tests) [20]. All of these have succeeded in providing good accuracy, especially in higher stages of fibrosis. In a study of 556 patients, Lubner et al. created a model based on a combination of four factors indicating liver texture, which provided and area under the receiver operating curve of 0.82, 0.82 and 0.86 for the diagnosis of any (≥F1), significant (≥F2), and severe (≥F3) fibrosis, respectively [17]. While liver surface nodularity analysis provided excellent areas under the curve for the detection of both mild and severe fibrosis, the findings seem limited by almost identical cut-off values of 2.8, 2.77 and 2.9 for significant (≥F2) fibrosis, severe (≥F3) fibrosis and cirrhosis (F4), respectively [19]. Although the corresponding cut-offs were more separated in another study on liver surface nodularity, the overlapping values in patients with different stages of fibrosis remained as a major limitation of its clinical utility [18]. Regarding inclusion of computed tomography features into a multiparametric model, a combination of nine factors assessed on CT with Fibrosis-4 score [21] and aspartate transaminase-to-platelets ratio index [22] was proposed. It resulted in moderate improvement in the diagnostic accuracy with respect to mild (F1), moderate (F2), and severe (F3) fibrosis in a study performed on 469 patients, yet with hepatitis C virus infection [20].

a.

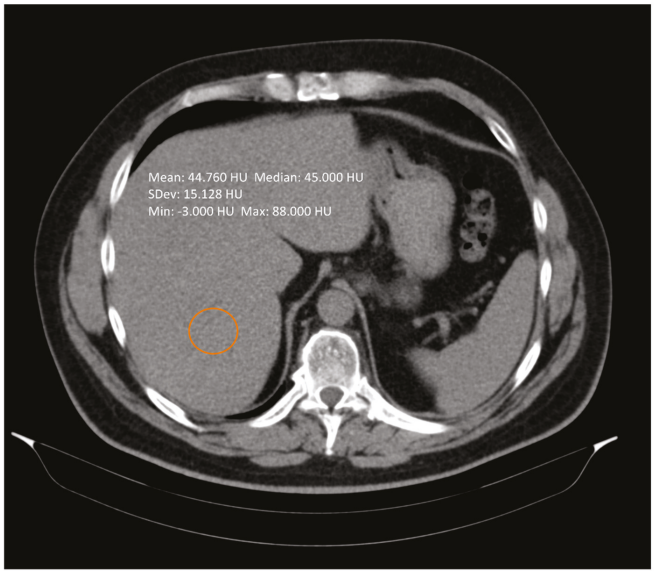

b.

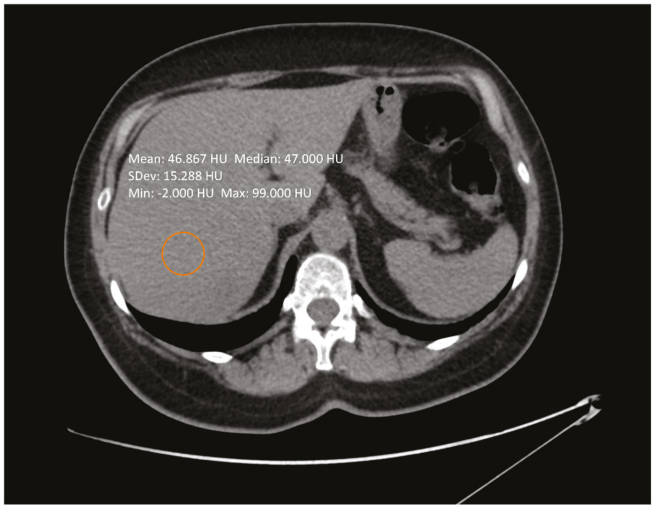

Figure 2. Non-contrast enhanced computed tomography scan of a patient with (**a**) 60% of hepatic steatosis (**b**) 80% of hepatic steatosis. In both cases simple measurement of the liver density was not suggestive on such severe changes. Images from the authors' department.

In addition to evaluation of the status of liver parenchyma, many studies have shown that computed tomography is a good diagnostic modality for the purpose of analyzing patients' body composition, in particular the amount of visceral and subcutaneous fat, and this may be especially important in patients dealing with obesity (which is the case in the vast majority of NASH/NAFLD patients), as the simple Body Mass Index (BMI) has been shown to provide insufficient accuracy [23]. For instance, in a study performed on 76 patients with liver cirrhosis, more than 20% of patients with

normal body mass index had an increased amount of adipose tissue, whereas 40% of overweight patients were found to have normal amount of adipose tissue [24]. The amount of fat tissue may be measured on a single CT scan (usually on the level of the body of the third lumbar vertebra), based on the threshold of Hounsfield units, which is a fast and easy technique. There is no consensus on the optimal cut-off points. What is more, some authors define their proposed cut-off values as simple area (not adjusted for the height), which can significantly impair wide use in different populations. Notably, even in homogeneous populations, the cut-off values differ significantly; for example, in different studies on the Korean population, authors proposed values for the visceral fat area ranging from 92.6 cm^2 to 140 cm^2 for men and from 75 to 100 cm^2 for women [25–29]. The measurement can be also propagated on the whole abdominal scans (manually or by using advanced algorithms) [30,31] to calculate the whole visceral fat tissue volume. It is, however, unclear, whether evaluation of the latter provides any benefits over single-scan assessments and this should be elucidated further, yet the arguments for the use of volume over surface analyses include: independence from bowel movement and patients' breathing, individual constitutional characteristics or bowel capacity. Previous studies have shown that excess amounts of fat tissue (both visceral and subcutaneous) play an important role in carcinogenesis, and also in hepatocellular carcinoma (HCC) [24,32]. Therefore, it seems reasonable to routinely evaluate the amount of fat tissue in patients undergoing CT scans, especially in a group of NASH patients, who can progress to liver cirrhosis and develop HCC.

Obviously, one of the biggest disadvantages of CT scans is patient exposure to radiation, which precludes its regular, repeated, and life-long use, for example during regular follow-up for the assessment of NAFLD progression. However, CT scans are much more available than the MR scans and their cost is lower. What is more important, many patients are undergoing computed tomography for other indications, and the assessment of hepatic steatosis can be performed at the same time to provide additional, valuable clinical information.

3. Magnetic Resonance Imaging Techniques

New techniques in magnetic resonance imaging (MRI) have been proven to provide good specificity and sensitivity in detecting liver steatosis and are now the reference standard to which other diagnostic imaging modalities should be compared. The most promising method with excellent results and—very importantly—standard examination technique, not requiring any additional equipment, is the chemical shift-encoded MRI proton density fat fraction (MRI-PDFF). The examination can be performed on both 1.5 T and 3.0 T scanners [33,34], which are widely available at most hospitals. The technique is usually based on acquisition of 6-echo chemical-shift-encoded gradient-echo sequences, but it has been shown that acquisition of less—for example 2 or 4 echo sequences—provides nearly identical results. However, in some cases—for instance in patients with iron deposition in the liver parenchyma—the results may be influenced in case of dual-echo or triple-echo methods, which is not the case with multi-echo [35]. MRI-PDFF method has been validated in comparison to magnetic resonance spectroscopy [34,36–38] and also provides excellent intra-examination repeatability [34] and inter-examination repeatability [39]. Importantly, the results are highly comparable among different fields and scanner manufacturers [40].

A recent meta-analysis by Gu et al., including studies with biopsy as the reference standard, has shown that MRI-PDFF provides excellent diagnostic accuracy, with a sensitivity of 93% for the detection of any grade of steatosis (defines as affecting at least 5% of hepatocytes) and a corresponding specificity of 94% [41]. Further, utilization of MRI-PDFF enables classification into different grades of hepatic steatosis with sensitivity and specificity of 74% and 87–90%, respectively, regarding the diagnosis of higher-grade steatosis. Another study performed by Middleton et al. has shown that MRI-PDFF performs well also in terms of monitoring patients during treatment, in particular in the assessment of discrete changes in liver steatosis in patients with decrease or increase in steatosis grade [42]. Importantly, the MRI-PDFF assessment was highly concordant with liver biopsy assessment regarding changes in liver histology, as 71% of patients with increasing steatosis were diagnosed as such with MRI-PDFF. Further, MRI-PDFF assessment showed an improvement in 91% of patients

with decreasing steatosis. Only minor changes in MRI-PDFF assessment were noted in patients with stable histopathological findings. Figure 3 presents an example of two MRI-PDFF examinations in one patient, showing improvement in the degree of hepatic steatosis.

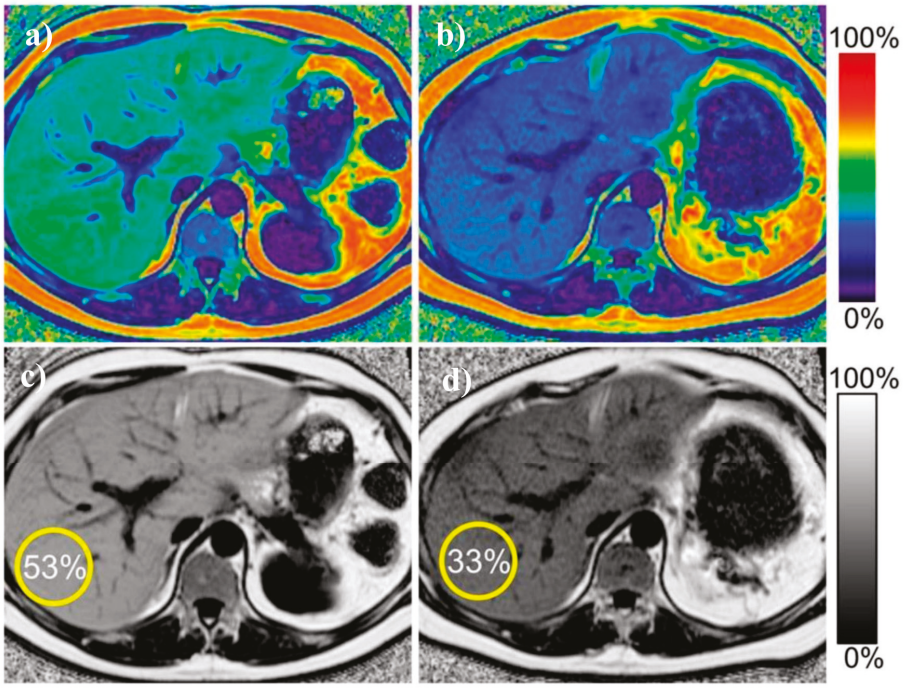

Figure 3. Example of proton density fat fraction liver maps in the same patient before and after treatment. Improvement in the liver steatosis and reduction in liver size is visible. (**a**) pre-treatment color-scale map (**b**) post-treatment color-scale map (**c**) pretreatment gray-scale map (**d**) post-treatment grey-scale map. Figure from Reeder SB, et al. Quantitative Assessment of Liver Fat with Magnetic Resonance Imaging and Spectroscopy. *J. Magn. Reson. Imaging* **2011**, *34*, 729–749 [43].

Although performing very well in terms of analyzing the amount of fat in the liver tissue, MRI-PDFF does not succeed in evaluating other variables that are clinically relevant. A study by Wildman-Tobriner et al. on patients taking part in clinical trials aimed at NAFLD/NASH has shown that the MRI-PDFF values overlap between patients with and without fibrosis, as well as between those with high and low NASH activity scores (NAS ≥ 4). Thus, MRI-PDFF does not seem to allow for discrimination between patients with mild and severe changes in histopathological examination [44]. Importantly, evaluation of steatosis using MRI-PDFF was compromised in case of concomitant fibrosis, with the correlation coefficient for the rate of hepatic steatosis and MRI-PDFF in patients with liver fibrosis of 0.60 as compared to the corresponding R of 0.86 in case of no fibrosis [45]. Therefore, MRI-PDFF should be cautiously interpreted in patients with either imaging or clinical suspicion of liver fibrosis.

Magnetic resonance spectroscopy (MRS) allows us to calculate steatosis by directly measuring chemical composition of tissue in a chosen voxel, basing on the signal strength from each component (protons from water and fat) [46,47]. It is a well-established and accurate method of non-invasive liver fat quantification that has been validated and served as the reference standard in numerous studies [48–54]. A metanalysis performed by Bohte et al. (with histology used as a reference) has shown that the specificity of MRS in terms of detection of mild steatosis is 92% and increases up to

96% for the detection of more advanced fatty accumulation (>25%, >30% or >33%, depending on the study) [15]. These results are in line with a more recent study by Chiang et al., in which the MRS findings were compared to histological examinations in living liver donors with the reported sensitivity and specificity rates of the MR spectroscopy of 95% and 98%, respectively [55]. However, MRS requires sophisticated post-processing methods (spectral analysis), which substantially limits the accessibility to this method, as not every scanner is equipped with this modality. Figure 4 presents an example of liver spectroscopy, with a voxel representing the analyzed region and a corresponding spectrum. Moreover, in contrast to MRI-PDFF, which enables mapping of the whole organ, MRS analyses involve only a small portion of the liver parenchyma. The latter is therefore susceptible for sampling errors, similar to what liver biopsy is criticized for. The MRI-PDFF method is also less dependent on patient compliance. As the acquisition time for MRI-PDFF is shorter than that in the MRS, it is easier for the patient to remain still without breathing and it is also less time consuming in general [36,56].

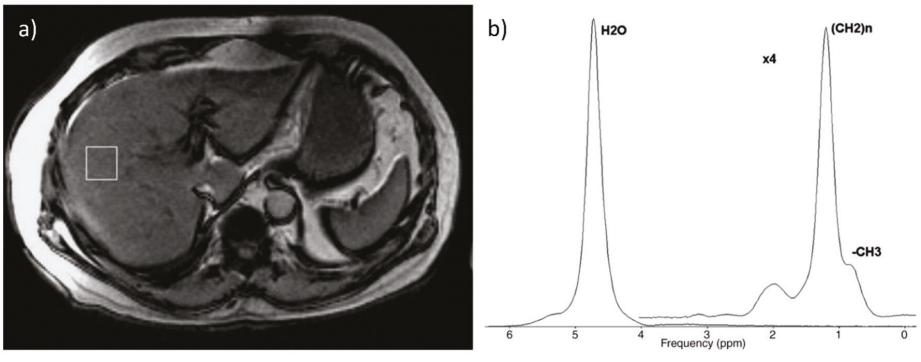

Figure 4. Example of spectroscopic examination: (**a**) voxel located in the right lobe (**b**) corresponding spectrum. Figure from Borra RJ, et al. Nonalcoholic fatty liver disease: rapid evaluation of liver fat content with in-phase and out-of-phase MR imaging. *Radiology* **2009**, *250*, 130–136 [57].

Magnetic resonance elastography (MRE) enables non-invasive assessment of hepatic fibrosis and is currently considered the most accurate non-invasive modality for its assessment, with a very good reproducibility and repeatability [58,59]. In a pooled analysis performed by Singh et al., the mean area under the receiver operating characteristics curve (with 95% confidence interval) values for diagnosing any (≥F1), significant (≥F2) or severe (≥F3) fibrosis and cirrhosis (F4) were 0.86 (0.82–0.90), 0.87 (0.82–0.93), 0.90 (0.84–0.94) and 0.91 (0.76–0.95), respectively [60]. These results were confirmed in another pooled analysis from 2020, by Liang Y. et al., in which the reported corresponding area under the receiver operating characteristics curve values were 0.89, 0.93, 0.93, and 0.95, respectively. The sensitivity rates in that study for of detection mild, significant, and severe liver fibrosis, and liver cirrhosis were 77%, 87%, 89%, and 94%, respectively, with the corresponding specificity rates of 90%, 86%, 84%, and 75%, respectively [61]. MRE also has its major disadvantages, including its high cost and insufficient availability, especially due to the fact that MR scanners are not regularly equipped with the elastography module. Nevertheless, MR elastography provides very good results and corresponds well to the fibrosis stage as assessed by the histopathological examination of liver biopsies. An example of magnetic resonance elastography is presented in Figure 5 [62].

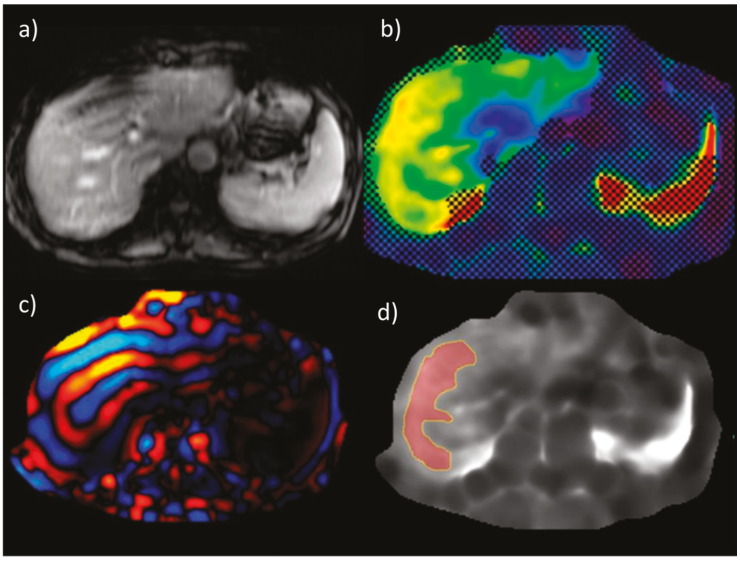

Figure 5. An example of liver stiffness measurement by magnetic resonance elastography (**a**) anatomic images (**b**) confidence map of an elastogram (**c**) wave image data (**d**) elastogram with free drawn region of interest. Figure from Chang, W., et al., Liver Fibrosis Staging with MR Elastography: Comparison of Diagnostic Performance between Patients with Chronic Hepatitis B and Those with Other Etiologic Causes. *Radiology* **2016**, *280*, 88–97 [62].

The stiffness of healthy liver parenchyma in MRE is reported to be between 2.05 to 2.12 kPa [59], and the cut-off for normal liver stiffness is proposed to be set at 2.5 kPa [63]. However, the proposed cut-off values for discriminating between particular stages of fibrosis slightly differ among various studies and authors, with some authors also suggesting that the actual cut-off values may also be dependent upon the type of underlying liver disease. Chang et al., in their study on patients with chronic liver disease and healthy living liver donors, have shown that the MR elastography findings corresponded well with the stage of fibrosis with the areas under the receiver operating characteristics curve values ranging between 0.92 and 0.97. However, the actual liver stiffness value pointing towards the presence of cirrhosis remarkably differed between patients with hepatitis B virus infection (3.67 kPa) and those with other liver diseases (4.65 kPa) [62].

Liver stiffness can also be assessed by magnetic resonance with the use of diffusion weighted imaging (DWI); however, the results are inferior to MR elastography [64–66]. A meta-analysis by Wang et al. has shown that the sensitivity of MRE is 94% in detection of significant (≥F2) and 96% in detection of severe fibrosis (≥F2), remarkably higher than the corresponding values observed for DWI of 77% and 84%, respectively [66]. Some authors try to combine the DWI MR method with serum markers to increase the diagnostic accuracy, and the results show that this may be a reasonable alternative in cases where standard MRE is not available [67]. The authors of that study combined the DWI MR with the aspartate aminotransferase–to–platelet radio index (APRI) [22] and the Fibrosis-4 score, known as the FIB-4 [21]. This increased the diagnostic performance for discrimination between fibrosis grades 0–1 and 2–4: the area under the curve for DWI only was 0.72 and increased to 0.81 and 0.78 after addition of APRI and FIB-4, respectively. The performance to discriminate severe fibrosis (grades 0–2 versus 3–4) also increased −0.79 for DWI only, 0.83 for DWI + APRI, and 0.81 for DWI + FIB-4.

Standard abdominal MR examinations also allows the calculation of the amount of visceral and subcutaneous adipose tissue; however, due to the fact that the scanned area is usually limited to the

liver and does not cover the whole abdominal cavity, it might be impossible to calculate all of the volumes (for example whole volume of visceral fat tissue).

4. Ultrasound Based Techniques

Liver steatosis can be detected on a regular B mode ultrasound; however, the diagnostic accuracy is low. Signs of liver steatosis on ultrasound typically comprise hyperechoic, bright liver (the echogenicity of the liver is usually compared to the echogenicity of the kidney), posterior attenuation or impaired visualization of intrahepatic vessels.

Studies have shown that the diagnosis of moderate or severe grades of liver steatosis by ultrasound is characterized by sensitivity and specificity rates of 80–91% and 87–98%, respectively. Nevertheless, these values drop to as low as 53% and 77%, respectively, when detecting steatosis of any grade [68–72].

Controlled attenuation parameter (CAP) is a relatively new method introduced by the Fibro-Scan. It measures liver attenuation to assess the degree of liver steatosis. The results are presented as dB/m (ranging from 100–400) and according to the manufacturers' recommendation reflect the degree of steatosis [73,74]. This method has emerged relatively recently, with the first clinical studies published in 2010 [75], but has gained widespread acceptance and has been validated in numerous studies. Particularly good diagnostic accuracy of CAP was reported in a multicenter prospective study performed on the Chinese population (CAP measurements were compared with biopsy as a reference standard), with areas under the receiver operating characteristics curve of 0.92, 0.92 and 0.88 for detection of steatosis of at least 5%, 34%, and 67%, respectively [76]. These results are in line with another prospective study performed on Korean population, which reported the corresponding values for CAP of 0.885 for the detection of mild steatosis (sensitivity 73.1%, specificity 95.2%), 0.894 for detection of moderate steatosis (sensitivity 82.4%, specificity 86.1%) and 0.800 for detection of severe steatosis (sensitivity 77.8%, specificity 84.1%) [77]. The clinical utility of using CAP as a reference for the assessment of liver steatosis is largely limited by the low positive predictive value. In a study by Ferraioloi et al., the positive predictive values for the detection of mild or moderate steatosis using CAP cut-offs of 219 dB/M and 296 dB/M, respectively, were both below 60% despite relatively large areas under the receiver operating characteristics curve of 0.76 and 0.82, respectively [78]. A meta-analysis performed by Shi KQ et al. has consistently shown that CAP has good sensitivity and specificity, however the authors of the study concluded, that it should not be widely used as a standard method of steatosis assessment due to insufficient accuracy [79]. The positive and negative predictive vales of CAP ranged between 78–80% and 78–84%, depending on the stage of steatosis aimed for detection. Another meta-analysis by Karloas et al. has shown a good accuracy for the diagnosis of any or moderate steatosis with area under the receiver operating characteristics curve for >S0 and >S1 of 0.823 and 0.865, respectively [80]. A metanalysis by Pu et al. from 2019 also provided confirmation of acceptable sensitivity and specificity of CAP in detection of moderate and severe steatosis, yet pointed towards several factors, including age and body mass index, as potentially influencing its accuracy [81].

CAP has been shown to provide inferior diagnostic accuracy in comparison to MRI-PDFF in a study comparing these two methods with a biopsy reference: area under the receiver operating characteristics curve for MRI-PDFF in detection of any steatosis was 0.99 as compared to significantly lower value of 0.85 observed for CAP [82]. These results were also confirmed by another prospective study, which showed even lower value for CAP (0.77 versus 0.99 for MRI-PDFF) [83].

One of the biggest limitations of the use of CAP measurement was the M probe depth, which was not sufficient for obese patients. The manufacturer responded to that problem by introducing the XL probe, allowing for measurement in more overweight patients. The accuracy of measurements with the M and XL probe seem similar [84–86]. Although being an easy and relatively cheap method, CAP has also serious limitations when assessing patients with ascites and obesity, which substantially limits it use in the NAFLD/NASH patients, as vast majority of them is overweight.

Fibroscan device also allows the measurement of the liver stiffness by using the transient elastography technique (TE). There are some reports suggesting that although TE provides very good

results, the accuracy in patients with NAFLD/NASH might be decreased. This is because the liver stiffness measurement can be affected by CAP values, particularly with respect to overestimation of the degree of liver fibrosis in the steatotic liver. Therefore, some authors have proposed different cut-off values for NAFLD patients when diagnosing fibrosis in TE [73,87]. In particular, high risk of false positive TE results with respect to detection of significant (F2–F4) and severe (F3–F4) liver fibrosis was noted for the liver stiffness ranges of 8.5–10.5 kPa and 10.1–12.5 kPa, respectively, in case of CAP of 300 to 339 dB/M, and 8.5–11.6 kPa and 10.1–13.6 kPa, respectively, in case of CAP exceeding 340 dB/M [73]. As both liver stiffness measurement by TE and steatosis measurement by CAP are available in the Fibroscan, the adjustment of the cut-off values can be done quickly and easily. However, the results of other studies are conflicting. In a recent study by Eddowes et al. performed on 450 patients with biopsy as reference, the accurate assessment of liver fibrosis and steatosis was reported with no negative influence of steatosis on the measurement of liver stiffness [88]. Although being a cheap, widely available, and easily performed technique, TE has inferior accuracy when comparing to magnetic resonance elastography. The area under the receiver operating characteristics curve for detection of any fibrosis (≥F1) using MRE was 0.82, which was significantly higher than that calculated for TE (0.67) [82]. Figure 6 presents an example of steatosis and fibrosis assessment (Fibroscan) with controlled attenuation parameters and transient elastography.

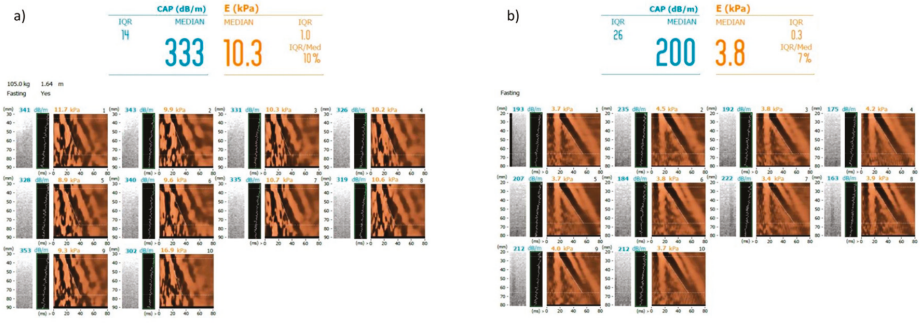

Figure 6. Examples of steatosis assessment by controlled attenuation parameter and liver stiffness assessment by transient elastography (Fibroscan) (**a**) in a patient with severe liver steatosis (grade 3) and severe fibrosis (F3) (**b**) in a patient with no liver steatosis (grade 0) and no liver fibrosis (F0). Images courtesy of Dr. Maciej Janik and Prof. Piotr Milkiewicz from the Liver and Internal Medicine Unit, Medical University of Warsaw.

Another two methods of fibrosis assessment include the shear wave elastography (SWE) and acoustic radiation force impulse (ARFI), both of which can be integrated in regular ultrasound devices. SWE and ARFI have some notable disadvantages, such as the necessity to perform the measurement with patient holding breath. The results may also be influenced by the experience of the performing physician and in case of a recent food intake [89]. All the three methods provide results which are highly correlated with the fibrosis grade and have relatively good accuracy in detecting fibrosis. In a study comparing SWE, TE and ARFI performed by Casinotto et al., all three methods showed very similar diagnostic characteristics for the detection of corresponding grades of liver fibrosis [90]. Similar results were obtained by Lee et al., who also reported the similar ability of TE, SWE and ARFI in the diagnosis of liver fibrosis in a population of Asian NAFLD patients [91]. However, in another study, SWE was shown to provide superior results to TE in the accuracy of detecting any fibrosis, as well as discriminating between different fibrosis grades with areas under the receiver operating characteristics curve for SWE and TE for different fibrosis grades as follows: 0.86 and 0.80, respectively, for any fibrosis (≥F1); 0.88 and 0.78, respectively, for significant (≥F2) fibrosis; 0.93 and 0.83, respectively, for severe (≥F3) fibrosis; and 0.98 and 0.92, respectively, for cirrhosis (F4) [92]. Another study also

showed superiority of SWE over TE and ARFI in diagnosing grade F2 or F3 of fibrosis, but without statistical difference regarding diagnosing mild fibrosis (F1) or cirrhosis (F4) [93]. Figure 7 presents an example of liver stiffness measurement by shear-wave elastography.

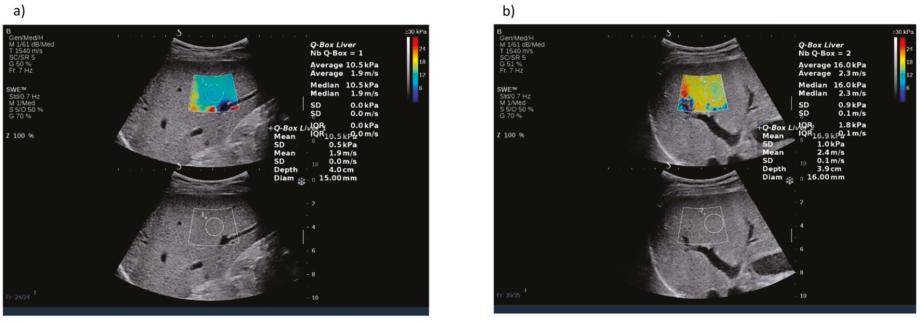

Figure 7. Examples of fibrosis assessment by shear wave elastography (**a**) in a patient with severe liver fibrosis (F3) (**b**) in a patient with cirrhosis (F4). Images courtesy of Dr. Maciej Janik and Prof. Piotr Milkiewicz from the Liver and Internal Medicine Unit, Medical University of Warsaw.

5. Dual-Energy X-ray Absorptiometry

Dual energy X-ray absorptiometry is a quick, relatively inexpensive and safe method of body composition assessment. Due to its clinical usefulness, it has gained wide acceptance and has been proposed in guidelines for the assessment of sarcopenia and obesity in the elderly population (European Working Group on Sarcopenia in Older People Consensus) [94,95]. Interestingly, some authors have proposed the implementation of special algorithms into the DXA examination to assess the liver fat amount. Bazzocchi et al. proposed placing a region of interest (ROI) in the location of the liver to calculate the amount of hepatic fat and have shown good correlation with liver steatosis assessed by biopsy (ϱ = 0.610–0.619; $p < 0.001$), with an area under the curve ranging from 0.929 to 0.551 (depending upon sex and BMI category) [96].

6. Predictive Role of Imaging Methods in Patients with NAFLD

Patients with NAFLD are at high risk of developing systemic complications of the disease. This includes, in particular, the development of cardiovascular diseases and occurrence of cardiovascular events in case of underlying pathologies. In a 2014 study based on more than two thousand middle-aged adults without any known liver or heart disease, liver attenuation on computed tomography of less than 40 Hounsfield units, indicative of hepatic steatosis, was associated with approximately 30% more frequent occurrence of coronary artery calcifications and approximately 70% more frequent occurrence of abdominal aortic calcifications [97]. However, this significant association disappeared following adjustment for the amount of visceral fat, pointing towards the pivotal role of the latter as a major contributor to the development of atherosclerosis. Attenuation of the liver under 40 Hounsfield units on computed tomography scans was also found to be associated with subclinical cardiac remodeling and dysfunction in another population-based study, yet this was also largely attributable to increased amount of visceral adipose tissue [98]. These findings were recently supported by the results of the CARDIA study, in which the association between attenuation of the liver under 40 Hounsfield units and several structural and functional heart features lost significance following adjustment for obesity [99]. The same parameter predicted the presence of coronary microvascular dysfunction, which was an independent prognostic factor for the occurrence of a composite cardiovascular event end-point [100]. Notably, hepatic steatosis and fibrosis assessed on TE and CAP were similarly related to the presence of diastolic myocardial dysfunction in a study by Lee et al. [101]. Increased liver stiffness, as indicated by the results of SWE, increased the ability to predict the presence of coronary heart disease [102].

An analysis performed on 50 overweight adolescents revealed that intrahepatic fat content assessed on magnetic resonance spectroscopy was significantly associated with dyslipidemia independently of visceral fat content, as indicated by its positive correlation with plasma triglycerides, triglyceride to high-density lipoprotein ratio, or small dense low-density lipoprotein concentration, among others [103]. Further, the results of large cross-sectional Kangbuk Samsung Health Study comprising more than 100 thousand individuals pointed towards hepatic steatosis assessed on ultrasound as a significant predictor of the presence of coronary artery calcifications [104]. Increased prevalence of coronary artery calcifications in patients with ultrasound evidence for hepatic steatosis was independent of the presence of obesity.

Multiparametric evaluation of MR enabled prediction of the occurrence of liver-related clinical events in a study of 112 patients performed by Pavlides et al. [105]. More specifically, the use of liver inflammation and fibrosis score derived from analysis of T1 and T2 sequences led to the categorization of patients into subgroups based on the risk of developing clinical complications, with score values under 2 being characterized by a 100% negative predictive value. Additional MR analysis of hepatic iron and fat content further increased the predictive capacity of the model. In more than a thousand patients with severe liver fibrosis in the course of NAFLD, the baseline liver stiffness value was strongly associated with the occurrence of both decompensation of liver function and hepatocellular carcinoma, along with liver-related mortality [106]. Subgroup analysis from the same study performed by Petta et al. additionally provided evidence for the prognostic significance of the changes in liver stiffness measurement on TE by at least 20% with respect to those clinical outcomes and, furthermore, overall patient survival. Similarly, MRE-assessed liver stiffness exceeding 6.48 kPa was found to be predictive for the occurrence of liver function decompensation, with higher liver stiffness values also observed in patients with ascites, encephalopathy, and esophageal variceal bleeding [107].

7. Conclusions

Although there are several noninvasive, accurate methods of the assessment of hepatic steatosis or fibrosis, liver biopsy is currently the only method that allows for the precise assessment of both, and moreover also the assessment of the inflammatory process. However, given that the prevalence of obesity, metabolic syndrome and NAFLD is and will be increasing in the upcoming years, alternative, widely accessible and noninvasive methods need to be introduced. Brief summary on the use of imaging techniques on detection of liver steatosis and fibrosis is shown on Figures 8 and 9, respectively. Computed tomography only enables the diagnosis of higher grades of hepatic steatosis; however, new algorithms have been proposed to improve the diagnostic ability. Magnetic resonance spectroscopy provides highly reliable results, but its use is limited due to sophisticated postprocessing.

Proton density fat fraction MRI and the controlled attenuation parameter are the most promising techniques—MRI-PDFF with its ability to reliable quantify the fat percentage and the CAP, with low-cost machines, that can easily be used in outpatient clinics for initial screening purposes. Together with noninvasive methods of liver stiffness measurement, especially the magnetic resonance elastography or TE and SWE, those methods might be of crucial significance in distinguishing patients with moderate or severe changes for further assessment with liver biopsy. Computed tomography, magnetic resonance and transient elastography should be interpreted with respect to predicting patients' clinical outcomes. Tables 1 and 2 present a summary of diagnostic parameters of different methods for steatosis and fibrosis assessment.

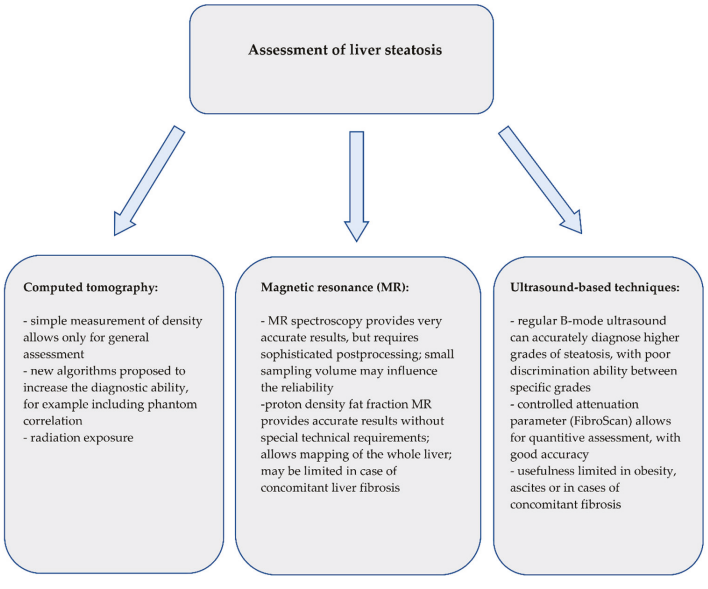

Figure 8. Summary of the imaging techniques for the assessment of liver steatosis.

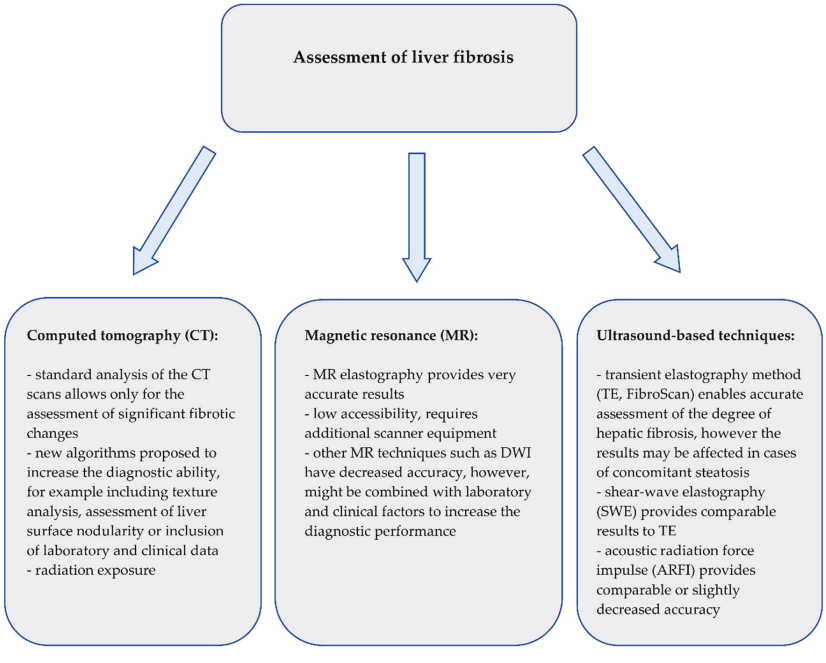

Figure 9. Summary of the imaging techniques for the assessment of liver fibrosis.

Table 1. Summary of the diagnostic parameters of different methods of steatosis assessment.

	Proposed Cut-Off	Sensitivity %	Specificity %
Computed tomography			
simple density measurement			
any steatosis (grade 1–3)	n/a	22–712 [14,15]	86–98 [14,15]
moderate steatosis (grade 2–3)	40 HU	60–82 [14,15]	88–98 [14,15]
phantom calibration [16]			
any steatosis (grade 1–3)	n/a	76% [16]	85% [16]
moderate steatosis (grade 2–3)	n/a	85% [16]	98% [16]
Magnetic resonance			
spectroscopy			
any steatosis (grade 1–3)	n/a	77–95 [15,53,55,56]	81–98 [15,53,55,56]
moderate steatosis (grade 2–3)	n/a	41–91 [15,53,56]	85–99 [15,53,56]
proton density fat fraction			
any steatosis (grade 1–3)	n/a	86–97 [35,36,41–45]	82–100 [35,36,41–45]
moderate steatosis (grade 2–3)	n/a	61–84 [35,36,41–45]	83–96 [35,36,41–45]
Ultrasound based techniques			
simple visual assessment			
any steatosis (grade 1–3)	subjective assessment	53–82 [15,68–72]	76–90 [15,68–72]
moderate steatosis (grade 2–3)		78–91 [15,68–72]	77–98 [15,68–72]
controlled attenuation parameter			
any steatosis	214–289 dB/m [76–80]	66–92 [76–81]	52–96 [76–81]
moderate steatosis	233–311 dB/m [76–80]	60–93 [76–81]	70–92 [76–81]

n/a—Not applicable; HU—Hounsfield Units.

Table 2. Summary of the diagnostic parameters of different methods of fibrosis assessment.

	Proposed Cut-Off	Sensitivity %	Specificity %
Computed tomography			
experimental algorithms			
any fibrosis (≥F1)	n/a	65–78 [18,19]	88–100 [18,19]
significant fibrosis (≥F2)	n/a	68–80 [18,19]	80–97 [18,19]
severe fibrosis (≥F3)	n/a	83–89 [18,19]	84–85 [18,19]
cirrhosis (F4)	n/a	90–98 [18,19]	80–85 [18,19]
Magnetic resonance			
elastography			
any fibrosis (≥F1)	1.77–5.02 kPa [60–62]	75–81 [60–62]	77–100 [60–62]
significant fibrosis (≥F2)	2.38–5.37 kPa [60–62,64]	79–97 [60–62,64]	81–100 [60–62,64]
severe fibrosis (≥F3)	2.43–5.97 kPa [60–62,64]	83–100 [60–62,64]	84–95 [60–62,64]
cirrhosis (F4)	2.74–6.7 kPa [60–62,64]	88–100 [60–62,64]	75–95 [60–62,64]
diffusion weighted imaging			
any fibrosis (≥F1)	n/a	75–86 [64–66]	71–94 [64–66]
significant fibrosis (≥F2)	n/a	67–92 [64–66]	61–91 [64–66]
severe fibrosis (≥F3)	n/a	48–90 [64–66]	65–100 [64–66]
cirrhosis (F4)	n/a	75–100 [64–66]	60–72 [64–66]
Ultrasound based techniques			
acoustic radiation force impulse			
any fibrosis (≥F1)	1.35 m/s [93]	61 [93]	96 [93]
significant fibrosis (≥F2)	0.95–1.38 m/s [90,91,93]	46–90 [90,91,93]	36–91 [90,91,93]
severe fibrosis (≥F3)	1.15–1.53 m/s [90,91,93]	59–90 [90,91,93]	63–90 [90,91,93]
cirrhosis (F4)	1.3–2.04 m/s [90,91,93]	44–90 [90,91,93]	67–90 [90,91,93]
transient elastography			
any fibrosis (≥F1)	6.7–8 kPa [92,93]	65–83 [92,93]	83–91 [92,93]
significant fibrosis (≥F2)	6.2–9.8 kPa [90–93]	60–90 [90–93]	45–92 [90–93]
severe fibrosis (≥F3)	8–12.5 kPa [90–93]	57–90 [90–93]	61–92 [90–93]
cirrhosis (F4)	9.5–16.1 kPa [90–93]	65–92 [90–93]	62–92 [90–93]
shear wave elastography			
any fibrosis (≥F1)	6.5–7.8 kPa [92,93]	68–84 [92,93]	91–100 [92,93]
significant fibrosis (≥F2)	6.3–8.7 kPa [90–93]	71–90 [90–93]	50–92 [90–93]
severe fibrosis (≥F3)	8.3–10.7 kPa [90–93]	71–91 [90–93]	71–90 [90–93]
cirrhosis (F4)	10.1–15.1 kPa [90–93]	58–97 [90–93]	72–93 [90–93]

n/a—Not applicable.

Author Contributions: All authors have read and agreed to the published version of the manuscript.

Funding: This research received no external funding.

Acknowledgments: The authors would like to express their gratitude for Maciej Janik and Piotr Milkiewicz from the Liver and Internal Medicine Unit, Medical University of Warsaw, for providing pictures presented in Figures 6 and 7. Michał Grąt received a stipend for outstanding young scientists from the Ministry of Science and Higher Education of the Republic of Poland (571/STYP/14/2019).

Conflicts of Interest: The authors declare no conflict of interest.

Abbreviations

NAFLD	non-alcoholic fatty liver disease
NASH	non-alcoholic steatohepatitis
MRS	magnetic resonance spectroscopy
MRI-PDFF	magnetic resonance imaging proton density fat fraction
CAP	controlled attenuation parameter
MRE	magnetic resonance imaging
TE	transient elastography
SWE	shear wave elastography
ARFI	acoustic radiation force impulse
CT	computed tomography
BMI	body mass index
HCC	hepatocellular carcinoma
NAS	NASH activity score
DWI	diffusion weighted imaging
APRI	aminotransferase-to-platelet ratio index
FIB-4	Fibrosis-4 score

References

1. Chalasani, N.; Younossi, Z.; Lavine, J.E.; Diehl, A.M.; Brunt, E.M.; Cusi, K.; Charlton, M.; Sanyal, A.J. The diagnosis and management of non-alcoholic fatty liver disease: Practice Guideline by the American Association for the Study of Liver Diseases, American College of Gastroenterology, and the American Gastroenterological Association. *Hepatology* **2012**, *55*, 2005–2023. [CrossRef] [PubMed]
2. Vernon, G.; Baranova, A.; Younossi, Z.M. Systematic review: The epidemiology and natural history of non-alcoholic fatty liver disease and non-alcoholic steatohepatitis in adults. *Aliment. Pharmacol. Ther.* **2011**, *34*, 274–285. [CrossRef] [PubMed]
3. Oda, K.; Uto, H.; Mawatari, S.; Ido, A. Clinical features of hepatocellular carcinoma associated with nonalcoholic fatty liver disease: A review of human studies. *Clin. J. Gastroenterol.* **2015**, *8*, 1–9. [CrossRef] [PubMed]
4. Arulanandan, A.; Ang, B.; Bettencourt, R.; Hooker, J.; Behling, C.; Lin, G.Y.; Valasek, M.A.; Ix, J.H.; Schnabl, B.; Sirlin, C.B.; et al. Association between quantity of liver fat and cardiovascular risk in patients with nonalcoholic fatty liver disease independent of nonalcoholic steatohepatitis. *Clin. Gastroenterol. Hepatol.* **2015**, *13*, 1513–1520.e1. [CrossRef]
5. Jennings, J.; Faselis, C.; Yao, M.D. NAFLD-NASH: An under-recognized epidemic. *Curr. Vasc. Pharmacol.* **2018**, *16*, 209–213. [CrossRef]
6. Motamed, N.; Rabiee, B.; Poustchi, H.; Dehestani, B.; Hemasi, G.R.; Khonsari, M.R.; Maadi, M.; Saeedian, F.S.; Zamani, F. Non-alcoholic fatty liver disease (NAFLD) and 10-year risk of cardiovascular diseases. *Clin. Res. Hepatol. Gastroenterol.* **2017**, *41*, 31–38. [CrossRef]
7. Athyros, V.G.; Tziomalos, K.; Katsiki, N.; Doumas, M.; Karagiannis, A.; Mikhailidis, D.P. Cardiovascular risk across the histological spectrum and the clinical manifestations of non-alcoholic fatty liver disease: An update. *World J. Gastroenterol.* **2015**, *21*, 6820–6834. [CrossRef]
8. Younossi, Z.M.; Koenig, A.B.; Abdelatif, D.; Fazel, Y.; Henry, L.; Wymer, M. Global epidemiology of nonalcoholic fatty liver disease-Meta-analytic assessment of prevalence, incidence, and outcomes. *Hepatology* **2016**, *64*, 73–84. [CrossRef]

9. Estes, C.; Razavi, H.; Loomba, R.; Younossi, Z.; Sanyal, A.J. Modeling the epidemic of nonalcoholic fatty liver disease demonstrates an exponential increase in burden of disease. *Hepatology* **2018**, *67*, 123–133. [CrossRef]
10. Agopian, V.G.; Kaldas, F.M.; Hong, J.C.; Whittaker, M.; Holt, C.; Rana, A.; Zarrinpar, A.; Petrowsky, H.; Farmer, D.; Yersiz, H.; et al. Liver transplantation for nonalcoholic steatohepatitis: The new epidemic. *Ann. Surg.* **2012**, *256*, 624–633. [CrossRef]
11. Spengler, E.K.; Loomba, R. Recommendations for diagnosis, referral for liver biopsy, and treatment of nonalcoholic fatty liver disease and nonalcoholic steatohepatitis. *Mayo Clin. Proc.* **2015**, *90*, 1233–1246. [CrossRef] [PubMed]
12. Leoni, S.; Tovoli, F.; Napoli, L.; Serio, I.; Ferri, S.; Bolondi, L. Current guidelines for the management of non-alcoholic fatty liver disease: A systematic review with comparative analysis. *World J. Gastroenterol.* **2018**, *24*, 3361–3373. [CrossRef] [PubMed]
13. Chalasani, N.; Younossi, Z.; Lavine, J.E.; Charlton, M.; Cusi, K.; Rinella, M.; Harrison, S.A.; Brunt, E.M.; Sanyal, A.J. The diagnosis and management of nonalcoholic fatty liver disease: Practice guidance from the American Association for the Study of Liver Diseases. *Hepatology* **2018**, *67*, 328–357. [CrossRef] [PubMed]
14. Piekarski, J.; Goldberg, H.I.; Royal, S.A.; Axel, L.; Moss, A.A. Difference between liver and spleen CT numbers in the normal adult: Its usefulness in predicting the presence of diffuse liver disease. *Radiology* **1980**, *137*, 727–729. [CrossRef] [PubMed]
15. Bohte, A.E.; van Werven, J.R.; Bipat, S.; Stoker, J. The diagnostic accuracy of US, CT, MRI and 1H-MRS for the evaluation of hepatic steatosis compared with liver biopsy: A meta-analysis. *Eur. Radiol.* **2011**, *21*, 87–97. [CrossRef] [PubMed]
16. Guo, Z.; Blake, G.M.; Li, K.; Liang, W.; Zhang, W.; Zhang, Y.; Xu, L.; Wang, L.; Brown, J.K.; Cheng, X.; et al. Liver fat content measurement with quantitative CT validated against MRI Proton density fat fraction: A prospective study of 400 healthy volunteers. *Radiology* **2020**, *294*, 89–97. [CrossRef] [PubMed]
17. Lubner, M.G.; Jones, D.; Kloke, J.; Said, A.; Pickhardt, P.J. CT texture analysis of the liver for assessing hepatic fibrosis in patients with hepatitis C virus. *Br. J. Radiol.* **2019**, *92*, 20180153. [CrossRef]
18. Pickhardt, P.J.; Malecki, K.; Kloke, J.; Lubner, M.G. Accuracy of liver surface nodularity quantification on MDCT as a noninvasive biomarker for staging hepatic fibrosis. *AJR Am. J. Roentgenol.* **2016**, *207*, 1194–1199. [CrossRef]
19. Lubner, M.G.; Jones, D.; Said, A.; Kloke, J.; Lee, S.; Pickhardt, P.J. Accuracy of liver surface nodularity quantification on MDCT for staging hepatic fibrosis in patients with hepatitis C virus. *Abdom. Radiol. (N. Y.)* **2018**, *43*, 2980–2986. [CrossRef]
20. Pickhardt, P.J.; Graffy, P.M.; Said, A.; Jones, D.; Welsh, B.; Zea, R.; Lubner, M.G. Multiparametric CT for noninvasive staging of hepatitis C virus-related liver fibrosis: Correlation with the histopathologic fibrosis score. *AJR Am. J. Roentgenol.* **2019**, *212*, 547–553. [CrossRef]
21. Sterling, R.K.; Lissen, E.; Clumeck, N.; Sola, R.; Correa, M.C.; Montaner, J.; Mark, S.S.; Torriani, F.J.; Dieterich, D.T.; Thomas, D.L.; et al. Development of a simple noninvasive index to predict significant fibrosis in patients with HIV/HCV coinfection. *Hepatology* **2006**, *43*, 1317–1325. [CrossRef] [PubMed]
22. Wai, C.T.; Greenson, J.K.; Fontana, R.J.; Kalbfleisch, J.D.; Marrero, J.A.; Conjeevaram, H.S.; Lok, A.S. A simple noninvasive index can predict both significant fibrosis and cirrhosis in patients with chronic hepatitis C. *Hepatology* **2003**, *38*, 518–526. [CrossRef] [PubMed]
23. Strulov Shachar, S.; Williams, G.R. The obesity paradox in cancer-moving beyond BMI. *Cancer Epidemiol. Biomark. Prev.* **2017**, *26*, 13–16. [CrossRef] [PubMed]
24. Grąt, K.; Pacho, R.; Grąt, M.; Krawczyk, M.; Zieniewicz, K.; Rowiński, O. Impact of body composition on the risk of hepatocellular carcinoma recurrence after liver transplantation. *J. Clin. Med.* **2019**, *8*, 1672. [CrossRef]
25. Kim, H.I.; Kim, J.T.; Yu, S.H.; Kwak, S.H.; Jang, H.C.; Park, K.S.; Kim, S.Y.; Lee, H.K.; Cho, Y.M. Gender differences in diagnostic values of visceral fat area and waist circumference for predicting metabolic syndrome in Koreans. *J. Korean Med. Sci.* **2011**, *26*, 906–913. [CrossRef]
26. Lim, S.; Kim, J.H.; Yoon, J.W.; Kang, S.M.; Choi, S.H.; Park, Y.J.; Kim, K.W.; Cho, N.H.; Shin, H.; Park, K.S.; et al. Optimal cut points of waist circumference (WC) and visceral fat area (VFA) predicting for metabolic syndrome (MetS) in elderly population in the Korean Longitudinal Study on Health and Aging (KLoSHA). *Arch. Gerontol. Geriatr.* **2012**, *54*, e29–e34. [CrossRef]

27. Hyun, Y.J.; Kim, O.Y.; Jang, Y.; Ha, J.W.; Chae, J.S.; Kim, J.Y.; Yeo, H.Y.; Paik, J.K.; Lee, J.H. Evaluation of metabolic syndrome risk in Korean premenopausal women: Not waist circumference but visceral fat. *Circ. J.* **2008**, *72*, 1308–1315. [CrossRef]
28. Zhou, C.J.; Cheng, Y.F.; Xie, L.Z.; Hu, W.L.; Chen, B.; Xu, L.; Huang, C.J.; Cai, M.; Shen, X.; Liu, C.B. Metabolic syndrome, as defined based on parameters including visceral fat area, predicts complications After surgery for rectal cancer. *Obes. Surg.* **2020**, *30*, 319–326. [CrossRef]
29. Seo, J.A.; Kim, B.G.; Cho, H.; Kim, H.S.; Park, J.; Baik, S.H.; Choi, D.S.; Park, M.H.; Jo, S.A.; Koh, Y.H.; et al. The cutoff values of visceral fat area and waist circumference for identifying subjects at risk for metabolic syndrome in elderly Korean: Ansan Geriatric (AGE) cohort study. *BMC Public Health* **2009**, *9*, 443. [CrossRef]
30. Weston, A.D.; Korfiatis, P.; Kline, T.L.; Philbrick, K.A.; Kostandy, P.; Sakinis, T.; Sugimoto, M.; Takahashi, N.; Erickson, B.J. Automated abdominal segmentation of CT scans for body composition analysis using deep learning. *Radiology* **2019**, *290*, 669–679. [CrossRef]
31. Lee, S.J.; Liu, J.; Yao, J.; Kanarek, A.; Summers, R.M.; Pickhardt, P.J. Fully automated segmentation and quantification of visceral and subcutaneous fat at abdominal CT: Application to a longitudinal adult screening cohort. *Br. J. Radiol.* **2018**, *91*, 20170968. [CrossRef] [PubMed]
32. Montano-Loza, A.J.; Mazurak, V.C.; Ebadi, M.; Meza-Junco, J.; Sawyer, M.B.; Baracos, V.E.; Kneteman, N. Visceral adiposity increases risk for hepatocellular carcinoma in male patients with cirrhosis and recurrence after liver transplant. *Hepatology* **2018**, *67*, 914–923. [CrossRef] [PubMed]
33. Kang, G.H.; Cruite, I.; Shiehmorteza, M.; Wolfson, T.; Gamst, A.C.; Hamilton, G.; Bydder, M.; Middleton, M.S.; Sirlin, C.B. Reproducibility of MRI-determined proton density fat fraction across two different MR scanner platforms. *J. Magn. Reson. Imaging* **2011**, *34*, 928–934. [CrossRef] [PubMed]
34. Yokoo, T.; Shiehmorteza, M.; Hamilton, G.; Wolfson, T.; Schroeder, M.E.; Middleton, M.S.; Bydder, M.; Gamst, A.C.; Kono, Y.; Kuo, A.; et al. Estimation of hepatic proton-density fat fraction by using MR imaging at 3.0 T. *Radiology* **2011**, *258*, 749–759. [CrossRef] [PubMed]
35. Kang, B.K.; Yu, E.S.; Lee, S.S.; Lee, Y.; Kim, N.; Sirlin, C.B.; Cho, E.Y.; Yeom, S.K.; Byun, J.H.; Park, S.H.; et al. Hepatic fat quantification: A prospective comparison of magnetic resonance spectroscopy and analysis methods for chemical-shift gradient echo magnetic resonance imaging with histologic assessment as the reference standard. *Invest. Radiol.* **2012**, *47*, 368–375. [CrossRef]
36. Di Martino, M.; Pacifico, L.; Bezzi, M.; Di Miscio, R.; Sacconi, B.; Chiesa, C.; Catalano, C. Comparison of magnetic resonance spectroscopy, proton density fat fraction and histological analysis in the quantification of liver steatosis in children and adolescents. *World J. Gastroenterol.* **2016**, *22*, 8812–8819. [CrossRef]
37. Noureddin, M.; Lam, J.; Peterson, M.R.; Middleton, M.; Hamilton, G.; Le, T.A.; Bettencourt, R.; Changchien, C.; Brenner, D.A.; Sirlin, C.; et al. Utility of magnetic resonance imaging versus histology for quantifying changes in liver fat in nonalcoholic fatty liver disease trials. *Hepatology* **2013**, *58*, 1930–1940. [CrossRef]
38. Hines, C.D.; Frydrychowicz, A.; Hamilton, G.; Tudorascu, D.L.; Vigen, K.K.; Yu, H.; McKenzie, C.A.; Sirlin, C.B.; Brittain, J.H.; Reeder, S.B. T(1) independent, T(2) (*) corrected chemical shift based fat-water separation with multi-peak fat spectral modeling is an accurate and precise measure of hepatic steatosis. *J. Magn. Reson. Imaging* **2011**, *33*, 873–881. [CrossRef]
39. Negrete, L.M.; Middleton, M.S.; Clark, L.; Wolfson, T.; Gamst, A.C.; Lam, J.; Changchien, C.; Deyoung-Dominguez, I.M.; Hamilton, G.; Loomba, R.; et al. Inter-examination precision of magnitude-based MRI for estimation of segmental hepatic proton density fat fraction in obese subjects. *J. Magn. Reson. Imaging* **2014**, *39*, 1265–1271. [CrossRef]
40. Yokoo, T.; Serai, S.D.; Pirasteh, A.; Bashir, M.R.; Hamilton, G.; Hernando, D.; Hu, H.H.; Hetterich, H.; Kühn, J.P.; Kukuk, G.M.; et al. Linearity, bias, and precision of hepatic proton density fat fraction measurements by using MR imaging: A meta-analysis. *Radiology* **2018**, *286*, 486–498. [CrossRef]
41. Gu, J.; Liu, S.; Du, S.; Zhang, Q.; Xiao, J.; Dong, Q.; Xin, Y. Diagnostic value of MRI-PDFF for hepatic steatosis in patients with non-alcoholic fatty liver disease: A meta-analysis. *Eur. Radiol.* **2019**, *29*, 3564–3573. [CrossRef] [PubMed]
42. Middleton, M.S.; Heba, E.R.; Hooker, C.A.; Bashir, M.R.; Fowler, K.J.; Sandrasegaran, K.; Brunt, E.M.; Kleiner, D.E.; Doo, E.; Van Natta, M.L.; et al. Agreement between magnetic resonance imaging proton density fat fraction measurements and pathologist-assigned steatosis grades of liver biopsies from adults with nonalcoholic steatohepatitis. *Gastroenterology* **2017**, *153*, 753–761. [CrossRef] [PubMed]

43. Reeder, S.B.; Cruite, I.; Hamilton, G.; Sirlin, C.B. Quantitative assessment of liver fat with magnetic resonance imaging and spectroscopy. *J. Magn. Reson. Imaging* **2011**, *34*, 729–749. [CrossRef] [PubMed]
44. Wildman-Tobriner, B.; Middleton, M.M.; Moylan, C.A.; Rossi, S.; Flores, O.; Chang, Z.A.; Abdelmalek, M.F.; Sirlin, C.B.; Bashir, M.R. Association between magnetic resonance imaging-proton density fat fraction and liver histology features in patients with nonalcoholic fatty liver disease or nonalcoholic steatohepatitis. *Gastroenterology* **2018**, *155*, 1428–1435.e2. [CrossRef]
45. Idilman, I.S.; Aniktar, H.; Idilman, R.; Kabacam, G.; Savas, B.; Elhan, A.; Celik, A.; Bahar, K.; Karcaaltincaba, M. Hepatic steatosis: Quantification by proton density fat fraction with MR imaging versus liver biopsy. *Radiology* **2013**, *267*, 767–775. [CrossRef]
46. Thomsen, C.; Becker, U.; Winkler, K.; Christoffersen, P.; Jensen, M.; Henriksen, O. Quantification of liver fat using magnetic resonance spectroscopy. *Magn. Reson. Imaging* **1994**, *12*, 487–495. [CrossRef]
47. Chang, J.S.; Taouli, B.; Salibi, N.; Hecht, E.M.; Chin, D.G.; Lee, V.S. Opposed-phase MRI for fat quantification in fat-water phantoms with 1H MR spectroscopy to resolve ambiguity of fat or water dominance. *AJR Am. J. Roentgenol.* **2006**, *187*, W103–W106. [CrossRef]
48. Wei, J.L.; Leung, J.C.; Loong, T.C.; Wong, G.L.; Yeung, D.K.; Chan, R.S.; Chan, H.L.; Chim, A.M.; Woo, J.; Chu, W.C.; et al. Prevalence and severity of nonalcoholic fatty liver disease in non-obese patients: A population study using proton-magnetic resonance spectroscopy. *Am. J. Gastroenterol.* **2015**, *110*, 1306–1314. [CrossRef]
49. Longo, R.; Pollesello, P.; Ricci, C.; Masutti, F.; Kvam, B.J.; Bercich, L.; Crocè, L.S.; Grigolato, P.; Paoletti, S.; de Bernard, B.; et al. Proton MR spectroscopy in quantitative in vivo determination of fat content in human liver steatosis. *J. Magn. Reson. Imaging* **1995**, *5*, 281–285. [CrossRef]
50. Zhang, H.J.; He, J.; Pan, L.L.; Ma, Z.M.; Han, C.K.; Chen, C.S.; Chen, Z.; Han, H.W.; Chen, S.; Sun, Q.; et al. Effects of moderate and vigorous exercise on nonalcoholic fatty liver disease: A randomized clinical trial. *JAMA Intern. Med.* **2016**, *176*, 1074–1082. [CrossRef]
51. Kramer, H.; Pickhardt, P.J.; Kliewer, M.A.; Hernando, D.; Chen, G.H.; Zagzebski, J.A.; Reeder, S.B. Accuracy of liver fat quantification with advanced CT, MRI, and ultrasound techniques: Prospective comparison with MR spectroscopy. *AJR Am. J. Roentgenol.* **2017**, *208*, 92–100. [CrossRef]
52. Heger, M.; Marsman, H.A.; Bezemer, R.; Cloos, M.A.; van Golen, R.F.; van Gulik, T.M. Non-invasive quantification of triglyceride content in steatotic rat livers by (1)H-MRS: When water meets (too much) fat. *Acad. Radiol.* **2011**, *18*, 1582–1592. [CrossRef] [PubMed]
53. Zheng, D.; Guo, Z.; Schroder, P.M.; Zheng, Z.; Lu, Y.; Gu, J.; He, X. Accuracy of MR imaging and MR spectroscopy for detection and quantification of hepatic steatosis in living liver donors: A meta-analysis. *Radiology* **2017**, *282*, 92–102. [CrossRef] [PubMed]
54. Raptis, D.A.; Fischer, M.A.; Graf, R.; Nanz, D.; Weber, A.; Moritz, W.; Tian, Y.; Oberkofler, C.E.; Clavien, P.A. MRI: The new reference standard in quantifying hepatic steatosis? *Gut* **2012**, *61*, 117–127. [CrossRef]
55. Chiang, H.J.; Chang, W.P.; Chiang, H.W.; Lazo, M.Z.; Chen, T.Y.; Ou, H.Y.; Tsang, L.L.; Huang, T.L.; Chen, C.L.; Cheng, Y.F. Magnetic resonance spectroscopy in living-donor liver transplantation. *Transplant. Proc.* **2016**, *48*, 1003–1006. [CrossRef] [PubMed]
56. Cassidy, F.H.; Yokoo, T.; Aganovic, L.; Hanna, R.F.; Bydder, M.; Middleton, M.S.; Hamilton, G.; Chavez, A.D.; Schwimmer, J.B.; Sirlin, C.B. Fatty liver disease: MR imaging techniques for the detection and quantification of liver steatosis. *Radiographics* **2009**, *29*, 231–260. [CrossRef]
57. Borra, R.J.; Salo, S.; Dean, K.; Lautamäki, R.; Nuutila, P.; Komu, M.; Parkkola, R. Nonalcoholic fatty liver disease: Rapid evaluation of liver fat content with in-phase and out-of-phase MR imaging. *Radiology* **2009**, *250*, 130–136. [CrossRef]
58. Lee, Y.; Lee, J.M.; Lee, J.E.; Lee, K.B.; Lee, E.S.; Yoon, J.H.; Yu, M.H.; Baek, J.H.; Shin, C.I.; Han, J.K.; et al. MR elastography for noninvasive assessment of hepatic fibrosis: Reproducibility of the examination and reproducibility and repeatability of the liver stiffness value measurement. *J. Magn. Reson. Imaging* **2014**, *39*, 326–331. [CrossRef]
59. Lee, D.H.; Lee, J.M.; Han, J.K.; Choi, B.I. MR elastography of healthy liver parenchyma: Normal value and reliability of the liver stiffness value measurement. *J. Magn. Reson. Imaging* **2013**, *38*, 1215–1223. [CrossRef]
60. Singh, S.; Venkatesh, S.K.; Loomba, R.; Wang, Z.; Sirlin, C.; Chen, J.; Yin, M.; Miller, F.H.; Low, R.N.; Hassanein, T.; et al. Magnetic resonance elastography for staging liver fibrosis in non-alcoholic fatty liver disease: A diagnostic accuracy systematic review and individual participant data pooled analysis. *Eur. Radiol.* **2016**, *26*, 1431–1440. [CrossRef]

61. Liang, Y.; Li, D. Magnetic resonance elastography in staging liver fibrosis in non-alcoholic fatty liver disease: A pooled analysis of the diagnostic accuracy. *BMC Gastroenterol.* **2020**, *20*, 89. [CrossRef] [PubMed]
62. Chang, W.; Lee, J.M.; Yoon, J.H.; Han, J.K.; Choi, B.I.; Yoon, J.H.; Lee, K.B.; Lee, K.W.; Yi, N.J.; Suh, K.S. Liver fibrosis staging with MR elastography: Comparison of diagnostic performance between patients with chronic hepatitis B and those with other etiologic causes. *Radiology* **2016**, *280*, 88–97. [CrossRef] [PubMed]
63. Srinivasa Babu, A.; Wells, M.L.; Teytelboym, O.M.; Mackey, J.E.; Miller, F.H.; Yeh, B.M.; Ehman, R.L.; Venkatesh, S.K. Elastography in chronic liver disease: Modalities, techniques, limitations, and future directions. *Radiographics* **2016**, *36*, 1987–2006. [CrossRef] [PubMed]
64. Hennedige, T.P.; Wang, G.; Leung, F.P.; Alsaif, H.S.; Teo, L.L.; Lim, S.G.; Wee, A.; Venkatesh, S.K. Magnetic resonance elastography and diffusion weighted imaging in the evaluation of hepatic fibrosis in chronic hepatitis B. *Gut Liver* **2017**, *11*, 401–408. [CrossRef]
65. Wang, Y.; Ganger, D.R.; Levitsky, J.; Sternick, L.A.; McCarthy, R.J.; Chen, Z.E.; Fasanati, C.W.; Bolster, B.; Shah, S.; Zuehlsdorff, S.; et al. Assessment of chronic hepatitis and fibrosis: Comparison of MR elastography and diffusion-weighted imaging. *AJR Am. J. Roentgenol.* **2011**, *196*, 553–561. [CrossRef]
66. Wang, Q.B.; Zhu, H.; Liu, H.L.; Zhang, B. Performance of magnetic resonance elastography and diffusion-weighted imaging for the staging of hepatic fibrosis: A meta-analysis. *Hepatology* **2012**, *56*, 239–247. [CrossRef]
67. Kromrey, M.L.; Le Bihan, D.; Ichikawa, S.; Motosugi, U. Diffusion-weighted MRI-based virtual elastography for the assessment of liver fibrosis. *Radiology* **2020**, *295*, 127–135. [CrossRef]
68. Palmentieri, B.; de Sio, I.; La Mura, V.; Masarone, M.; Vecchione, R.; Bruno, S.; Torella, R.; Persico, M. The role of bright liver echo pattern on ultrasound B-mode examination in the diagnosis of liver steatosis. *Dig. Liver Dis.* **2006**, *38*, 485–489. [CrossRef]
69. Van Werven, J.R.; Marsman, H.A.; Nederveen, A.J.; Smits, N.J.; ten Kate, F.J.; van Gulik, T.M.; Stoker, J. Assessment of hepatic steatosis in patients undergoing liver resection: Comparison of US, CT, T1-weighted dual-echo MR imaging, and point-resolved 1H MR spectroscopy. *Radiology* **2010**, *256*, 159–168. [CrossRef]
70. Petzold, G.; Lasser, J.; Rühl, J.; Bremer, S.C.B.; Knoop, R.F.; Ellenrieder, V.; Kunsch, S.; Neesse, A. Diagnostic accuracy of B-Mode ultrasound and Hepatorenal Index for graduation of hepatic steatosis in patients with chronic liver disease. *PLoS ONE* **2020**, *15*, e0231044. [CrossRef]
71. Hernaez, R.; Lazo, M.; Bonekamp, S.; Kamel, I.; Brancati, F.L.; Guallar, E.; Clark, J.M. Diagnostic accuracy and reliability of ultrasonography for the detection of fatty liver: A meta-analysis. *Hepatology* **2011**, *54*, 1082–1090. [CrossRef] [PubMed]
72. Lee, S.S.; Park, S.H.; Kim, H.J.; Kim, S.Y.; Kim, M.Y.; Kim, D.Y.; Suh, D.J.; Kim, K.M.; Bae, M.H.; Lee, J.Y.; et al. Non-invasive assessment of hepatic steatosis: Prospective comparison of the accuracy of imaging examinations. *J. Hepatol.* **2010**, *52*, 579–585. [CrossRef] [PubMed]
73. Petta, S.; Wong, V.W.; Cammà, C.; Hiriart, J.B.; Wong, G.L.; Marra, F.; Vergniol, J.; Chan, A.W.; Di Marco, V.; Merrouche, W.; et al. Improved noninvasive prediction of liver fibrosis by liver stiffness measurement in patients with nonalcoholic fatty liver disease accounting for controlled attenuation parameter values. *Hepatology* **2017**, *65*, 1145–1155. [CrossRef] [PubMed]
74. Sasso, M.; Miette, V.; Sandrin, L.; Beaugrand, M. The controlled attenuation parameter (CAP): A novel tool for the non-invasive evaluation of steatosis using Fibroscan. *Clin. Res. Hepatol. Gastroenterol.* **2012**, *36*, 13–20. [CrossRef] [PubMed]
75. Sasso, M.; Beaugrand, M.; de Ledinghen, V.; Douvin, C.; Marcellin, P.; Poupon, R.; Sandrin, L.; Miette, V. Controlled attenuation parameter (CAP): A novel VCTE™ guided ultrasonic attenuation measurement for the evaluation of hepatic steatosis: Preliminary study and validation in a cohort of patients with chronic liver disease from various causes. *Ultrasound Med. Biol.* **2010**, *36*, 1825–1835. [CrossRef]
76. Shen, F.; Zheng, R.D.; Mi, Y.Q.; Wang, X.Y.; Pan, Q.; Chen, G.Y.; Cao, H.X.; Chen, M.L.; Xu, L.; Chen, J.N.; et al. Controlled attenuation parameter for non-invasive assessment of hepatic steatosis in Chinese patients. *World J. Gastroenterol.* **2014**, *20*, 4702–4711. [CrossRef]
77. Chon, Y.E.; Jung, K.S.; Kim, S.U.; Park, J.Y.; Park, Y.N.; Kim, D.Y.; Ahn, S.H.; Chon, C.Y.; Lee, H.W.; Park, Y.; et al. Controlled attenuation parameter (CAP) for detection of hepatic steatosis in patients with chronic liver diseases: A prospective study of a native Korean population. *Liver Int.* **2014**, *34*, 102–109. [CrossRef]

78. Ferraioli, G.; Tinelli, C.; Lissandrin, R.; Zicchetti, M.; Dal Bello, B.; Filice, G.; Filice, C. Controlled attenuation parameter for evaluating liver steatosis in chronic viral hepatitis. *World J. Gastroenterol.* **2014**, *20*, 6626–6631. [CrossRef]
79. Shi, K.Q.; Tang, J.Z.; Zhu, X.L.; Ying, L.; Li, D.W.; Gao, J.; Fang, Y.X.; Li, G.L.; Song, Y.J.; Deng, Z.J.; et al. Controlled attenuation parameter for the detection of steatosis severity in chronic liver disease: A meta-analysis of diagnostic accuracy. *J. Gastroenterol. Hepatol.* **2014**, *29*, 1149–1158. [CrossRef]
80. Karlas, T.; Petroff, D.; Sasso, M.; Fan, J.G.; Mi, Y.Q.; de Lédinghen, V.; Kumar, M.; Lupsor-Platon, M.; Han, K.H.; Cardoso, A.C.; et al. Individual patient data meta-analysis of controlled attenuation parameter (CAP) technology for assessing steatosis. *J. Hepatol.* **2017**, *66*, 1022–1030. [CrossRef]
81. Pu, K.; Wang, Y.; Bai, S.; Wei, H.; Zhou, Y.; Fan, J.; Qiao, L. Diagnostic accuracy of controlled attenuation parameter (CAP) as a non-invasive test for steatosis in suspected non-alcoholic fatty liver disease: A systematic review and meta-analysis. *BMC Gastroenterol.* **2019**, *19*, 51. [CrossRef] [PubMed]
82. Park, C.C.; Nguyen, P.; Hernandez, C.; Bettencourt, R.; Ramirez, K.; Fortney, L.; Hooker, J.; Sy, E.; Savides, M.T.; Alquiraish, M.H.; et al. Magnetic resonance elastography vs. transient elastography in detection of fibrosis and noninvasive measurement of steatosis in patients with biopsy-proven nonalcoholic fatty liver disease. *Gastroenterology* **2017**, *152*, 598–607.e2. [CrossRef] [PubMed]
83. Runge, J.H.; Smits, L.P.; Verheij, J.; Depla, A.; Kuiken, S.D.; Baak, B.C.; Nederveen, A.J.; Beuers, U.; Stoker, J. MR Spectroscopy-derived proton density fat fraction is superior to controlled attenuation parameter for detecting and grading hepatic steatosis. *Radiology* **2018**, *286*, 547–556. [CrossRef] [PubMed]
84. Chan, W.K.; Nik Mustapha, N.R.; Wong, G.L.; Wong, V.W.; Mahadeva, S. Controlled attenuation parameter using the FibroScan® XL probe for quantification of hepatic steatosis for non-alcoholic fatty liver disease in an Asian population. *United Eur. Gastroenterol. J.* **2017**, *5*, 76–85. [CrossRef]
85. Oeda, S.; Takahashi, H.; Imajo, K.; Seko, Y.; Ogawa, Y.; Moriguchi, M.; Yoneda, M.; Anzai, K.; Aishima, S.; Kage, M.; et al. Accuracy of liver stiffness measurement and controlled attenuation parameter using FibroScan® M/XL probes to diagnose liver fibrosis and steatosis in patients with nonalcoholic fatty liver disease: A multicenter prospective study. *J. Gastroenterol.* **2020**, *55*, 428–440. [CrossRef]
86. Cardoso, A.C.; Cravo, C.; Calçado, F.L.; Rezende, G.; Campos, C.F.F.; Neto, J.M.A.; Luz, R.P.; Soares, J.A.S.; Moraes-Coelho, H.S.; Leite, N.C.; et al. The performance of M and XL probes of FibroScan for the diagnosis of steatosis and fibrosis on a Brazilian nonalcoholic fatty liver disease cohort. *Eur. J. Gastroenterol. Hepatol.* **2020**, *32*, 231–238. [CrossRef]
87. Lee, J.I.; Lee, H.W.; Lee, K.S. Value of controlled attenuation parameter in fibrosis prediction in nonalcoholic steatohepatitis. *World J. Gastroenterol.* **2019**, *25*, 4959–4969. [CrossRef]
88. Eddowes, P.J.; Sasso, M.; Allison, M.; Tsochatzis, E.; Anstee, Q.M.; Sheridan, D.; Guha, I.N.; Cobbold, J.F.; Deeks, J.J.; Paradis, V.; et al. Accuracy of fibroscan controlled attenuation parameter and liver stiffness measurement in assessing steatosis and fibrosis in patients with nonalcoholic fatty liver disease. *Gastroenterology* **2019**, *156*, 1717–1730. [CrossRef]
89. Popescu, A.; Bota, S.; Sporea, I.; Sirli, R.; Danila, M.; Racean, S.; Suseanu, D.; Gradinaru, O.; Ivascu Siegfried, C. The influence of food intake on liver stiffness values assessed by acoustic radiation force impulse elastography-preliminary results. *Ultrasound Med. Biol.* **2013**, *39*, 579–584. [CrossRef]
90. Cassinotto, C.; Boursier, J.; de Lédinghen, V.; Lebigot, J.; Lapuyade, B.; Cales, P.; Hiriart, J.B.; Michalak, S.; Bail, B.L.; Cartier, V.; et al. Liver stiffness in nonalcoholic fatty liver disease: A comparison of supersonic shear imaging, FibroScan, and ARFI with liver biopsy. *Hepatology* **2016**, *63*, 1817–1827. [CrossRef]
91. Lee, M.S.; Bae, J.M.; Joo, S.K.; Woo, H.; Lee, D.H.; Jung, Y.J.; Kim, B.G.; Lee, K.L.; Kim, W. Prospective comparison among transient elastography, supersonic shear imaging, and ARFI imaging for predicting fibrosis in nonalcoholic fatty liver disease. *PLoS ONE* **2017**, *12*, e0188321. [CrossRef] [PubMed]
92. Leung, V.Y.; Shen, J.; Wong, V.W.; Abrigo, J.; Wong, G.L.; Chim, A.M.; Chu, S.H.; Chan, A.W.; Choi, P.C.; Ahuja, A.T.; et al. Quantitative elastography of liver fibrosis and spleen stiffness in chronic hepatitis B carriers: Comparison of shear-wave elastography and transient elastography with liver biopsy correlation. *Radiology* **2013**, *269*, 910–918. [CrossRef] [PubMed]
93. Cassinotto, C.; Lapuyade, B.; Mouries, A.; Hiriart, J.B.; Vergniol, J.; Gaye, D.; Castain, C.; Le Bail, B.; Chermak, F.; Foucher, J.; et al. Non-invasive assessment of liver fibrosis with impulse elastography: Comparison of Supersonic Shear Imaging with ARFI and FibroScan®. *J. Hepatol.* **2014**, *61*, 550–557. [CrossRef] [PubMed]

94. Cruz-Jentoft, A.J.; Baeyens, J.P.; Bauer, J.M.; Boirie, Y.; Cederholm, T.; Landi, F.; Martin, F.C.; Michel, J.P.; Rolland, Y.; Schneider, S.M.; et al. Sarcopenia: European consensus on definition and diagnosis: Report of the European Working Group on Sarcopenia in Older People. *Age Ageing* **2010**, *39*, 412–423. [CrossRef]
95. Cruz-Jentoft, A.J.; Bahat, G.; Bauer, J.; Boirie, Y.; Bruyère, O.; Cederholm, T.; Cooper, C.; Landi, F.; Rolland, Y.; Sayer, A.A.; et al. Sarcopenia: Revised European consensus on definition and diagnosis. *Age Ageing* **2019**, *48*, 16–31. [CrossRef]
96. Bazzocchi, A.; Diano, D.; Albisinni, U.; Marchesini, G.; Battista, G.; Guglielmi, G. Liver in the analysis of body composition by dual-energy X-ray absorptiometry. *Br. J. Radiol.* **2014**, *87*, 20140232. [CrossRef]
97. Van Wagner, L.B.; Ning, H.; Lewis, C.E.; Shay, C.M.; Wilkins, J.; Carr, J.J.; Terry, J.G.; Lloyd-Jones, D.M.; Jacobs, D.R., Jr.; Carnethon, M.R. Associations between nonalcoholic fatty liver disease and subclinical atherosclerosis in middle-aged adults: The coronary artery risk development in young adults study. *Atherosclerosis* **2014**, *235*, 599–605. [CrossRef]
98. VanWagner, L.B.; Wilcox, J.E.; Colangelo, L.A.; Lloyd-Jones, D.M.; Carr, J.J.; Lima, J.A.; Lewis, C.E.; Rinella, M.E.; Shah, S.J. Association of nonalcoholic fatty liver disease with subclinical myocardial remodeling and dysfunction: A population-based study. *Hepatology* **2015**, *62*, 773–783. [CrossRef]
99. Van Wagner, L.B.; Wilcox, J.E.; Ning, H.; Lewis, C.E.; Carr, J.J.; Rinella, M.E.; Shah, S.J.; Lima, J.A.C.; Lloyd-Jones, D.M. Longitudinal association of non-alcoholic fatty liver disease with changes in myocardial structure and function: The CARDIA study. *J. Am. Heart Assoc.* **2020**, *9*, e014279.
100. Vita, T.; Murphy, D.J.; Osborne, M.T.; Bajaj, N.S.; Keraliya, A.; Jacob, S.; Diaz Martinez, A.J.; Nodoushani, A.; Bravo, P.; Hainer, J.; et al. Association between nonalcoholic fatty liver disease at ct and coronary microvascular dysfunction at myocardial perfusion PET/CT. *Radiology* **2019**, *291*, 330–337. [CrossRef]
101. Lee, Y.H.; Kim, K.J.; Yoo, M.E.; Kim, G.; Yoon, H.J.; Jo, K.; Youn, J.C.; Yun, M.; Park, J.Y.; Shim, C.Y.; et al. Association of non-alcoholic steatohepatitis with subclinical myocardial dysfunction in non-cirrhotic patients. *J. Hepatol.* **2018**, *68*, 764–772. [CrossRef] [PubMed]
102. Song, Y.; Dang, Y.; Wang, P.; Tian, G.; Ruan, L. CHD is associated with higher grades of NAFLD predicted by liver stiffness. *J. Clin. Gastroenterol.* **2020**, *54*, 271–277. [CrossRef] [PubMed]
103. Jin, R.; Le, N.A.; Cleeton, R.; Sun, X.; Cruz Muños, J.; Otvos, J.; Vos, M.B. Amount of hepatic fat predicts cardiovascular risk independent of insulin resistance among Hispanic-American adolescents. *Lipids Health Dis.* **2015**, *14*, 39. [CrossRef] [PubMed]
104. Chang, Y.; Ryu, S.; Sung, K.C.; Cho, Y.K.; Sung, E.; Kim, H.N.; Jung, H.S.; Yun, K.E.; Ahn, J.; Shin, H.; et al. Alcoholic and non-alcoholic fatty liver disease and associations with coronary artery calcification: Evidence from the Kangbuk Samsung Health Study. *Gut* **2019**, *68*, 1667–1675. [CrossRef] [PubMed]
105. Pavlides, M.; Banerjee, R.; Sellwood, J.; Kelly, C.J.; Robson, M.D.; Booth, J.C.; Collier, J.; Neubauer, S.; Barnes, E. Multiparametric magnetic resonance imaging predicts clinical outcomes in patients with chronic liver disease. *J. Hepatol.* **2016**, *64*, 308–315. [CrossRef] [PubMed]
106. Petta, S.; Sebastiani, G.; Viganò, M.; Ampuero, J.; Wai-Sun Wong, V.; Boursier, J.; Berzigotti, A.; Bugianesi, E.; Fracanzani, A.L.; Cammà, C.; et al. Monitoring occurrence of liver-related events and survival by transient elastography in patients with nonalcoholic fatty liver disease and compensated advanced chronic liver disease. *Clin. Gastroenterol. Hepatol.* **2020**. [CrossRef]
107. Han, M.A.T.; Vipani, A.; Noureddin, N.; Ramirez, K.; Gornbein, J.; Saouaf, R.; Baniesh, N.; Cummings-John, O.; Okubote, T.; Setiawan, V.W.; et al. MR elastography-based liver fibrosis correlates with liver events in nonalcoholic fatty liver patients: A multi-center study. *Liver Int.* **2020**. [CrossRef]

biomedicines

MDPI

Article

Non-Alcoholic Steatohepatitis Decreases Microsomal Liver Function in the Absence of Fibrosis

Wim Verlinden [1,2,*], Eugénie Van Mieghem [1], Laura Depauw [1], Thomas Vanwolleghem [1,2], Luisa Vonghia [1,2], Jonas Weyler [1,2], Ann Driessen [3], Dirk Callens [4], Laurence Roosens [4], Eveline Dirinck [5], An Verrijken [5], Luc Van Gaal [5] and Sven Francque [1,2,*]

1 Laboratory of Experimental Medicine and Pediatrics, Division of Gastroenterology and Hepatology, University of Antwerp, 2610 Antwerp, Belgium; eugenie.vanmieghem@gmail.com (E.V.M.); laura.depauw@student.uantwerpen.be (L.D.); thomas.vanwolleghem@uza.be (T.V.); luisa.vonghia@uza.be (L.V.); jonas.weyler@uza.be (J.W.)
2 Department of Gastroenterology and Hepatology, Antwerp University Hospital, 2650 Antwerp, Belgium
3 Department of Pathology, Antwerp University Hospital, 2650 Antwerp, Belgium; ann.driessen@uza.be
4 Department of Clinical Biology, Antwerp University Hospital, 2650 Antwerp, Belgium; dirk.callens@uza.be (D.C.); laurence.roosens@uza.be (L.R.)
5 Department of Endocrinology, Diabetology and Metabolism, Antwerp University Hospital, 2650 Antwerp, Belgium; eveline.dirinck@uza.be (E.D.); an.verrijken@uza.be (A.V.); luc.vangaal@uza.be (L.V.G.)
* Correspondence: wim.verlinden@uza.be (W.V.); sven.francque@uza.be (S.F.); Tel.: +32-3-760-2934 (W.V.); +32-3-821-4475 (S.F.)

Received: 28 October 2020; Accepted: 26 November 2020; Published: 27 November 2020

Abstract: The incidence of non-alcoholic fatty liver disease (NAFLD) is rising across the globe, with the presence of steatohepatitis leading to a more aggressive clinical course. Currently, the diagnosis of non-alcoholic steatohepatitis (NASH) is based on histology, though with the high prevalence of NAFLD, a non-invasive method is needed. The ^{13}C-aminopyrine breath test (ABT) evaluates the microsomal liver function and could be a potential candidate. We aimed to evaluate a potential change in liver function in NASH patients and to evaluate the diagnostic power of ABT to detect NASH. We performed a retrospective analysis on patients suspected of NAFLD who underwent a liver biopsy and ABT. 440 patients were included. ABT did not decrease in patients with isolated liver steatosis but decreased significantly in the presence of NASH without fibrosis and decreased even further with the presence of significant fibrosis. The predictive power of ABT as a single test for NASH was low but improved in combination with ALT and ultrasonographic steatosis. We conclude that microsomal liver function of patients with NASH is significantly decreased, even in the absence of fibrosis. The ABT is thus a valuable tool in assessing the presence of NASH; and could be used as a supplementary diagnostic tool in clinical practice.

Keywords: NASH; steatohepatitis; aminopyrine; microsomal; liver function; breath test

1. Introduction

Together with the obesity epidemic, incidences of non-alcoholic fatty liver disease (NAFLD) are rising across the globe. NAFLD is defined as an accumulation of fat in >5% of hepatocytes ocurring in the absence of significant alcohol consumption or any other cause of so-called "secondary" liver steatosis or disease. NAFLD includes two pathologically distinct conditions with different prognoses: isolated steatosis or non-alcoholic fatty liver (NAFL) and non-alcoholic steatohepatitis (NASH), which implies the presence of cell damage and inflammation. The latter covers a wide spectrum of disease severity, including fibrosis, cirrhosis and hepatocellular carcinoma [1].

The ^{13}C-aminopyrine breath test (ABT) has been widely used to evaluate microsomal hepatocellular function. Historically, it was the first breath test proposed for the assessment of patients with liver disease and is one of the most frequently utilized and most extensively validated tests for investigating microsomal liver function. The principle of the ABT is based on the selective metabolism of ^{13}C-aminopyrine in the liver by the cytochrome P450 mono-oxygenase system of the microsomes [2]. In these microsomes, ^{13}C-aminopyrine undergoes 2-step N-demethylation and the appearance of $^{13}CO_2$ in breath after administration means that the administered substance underwent microsomal liver oxidation [3,4]. Because N-demethylation of ^{13}C-aminopyrine has been shown to be the rate-limiting step, it has been assumed that the ABT reflects the activity of the cytochrome P450-dependent mono-oxygenase system and gives a global assessment of this system. It has been demonstrated that the N-demethylation of aminopyrine is catalyzed most efficiently by CYP2C19 and CYP2C8, followed by CYP2D6, 2C18, 1A2 and 2B6; and to a lesser extent by CYP2C9, 2A6, 1A1 and 3A4 [5,6]. Aminopyrine metabolism is mostly dependent on hepatic metabolic capacity (functional hepatic mass) rather than on portal blood flow [7]. The ABT has been shown to quantitively reflect the severity of cirrhosis, as assessed by other liver function tests [8], and the degree of fibrosis in chronic hepatitis [9–11].

Liver function assessment by breath tests based on several metabolic pathways has been studied in the context of NAFLD, mostly to non-invasively diagnose and stage the disease. These studies overall indicate a reduction of liver function in patients with NASH, though included only small groups of patients with significant fibrosis to cirrhosis in the NASH group, making it impossible to differentiate between the effect of NASH and the effect of fibrosis [4,12–15].

In this study, we aimed to evaluate a change in liver function measured by the ABT in relation to the presence of steatosis, steatohepatitis and fibrosis and the different degrees of severity hereof in a large, prospectively included cohort representing the whole spectrum of disease. Additionally, we aimed to evaluate the diagnostic power of the ABT to detect NASH and fibrosis.

2. Methodology

2.1. Study Group

We performed a single-center, retrospective study at the Antwerp University Hospital, a tertiary referral center on patient data consecutively collected between 2002 and 2018. Patients visiting the Obesity Clinic or the Hepatology Clinic due to overweight (BMI 25–29.9 kg/m^2), obesity (BMI ≥ 30 kg/m^2) or elevated liver enzymes with a suspicion of NAFLD (according to a pre-defined set of criteria) were included when both liver biopsy and ABT were performed. Each patient underwent a standard metabolic work-up combined with a liver-specific program (including ABT as a standard procedure), both approved by the Ethics Committee of the Antwerp University Hospital and requiring written informed consent of the patient (Reference 6/25/15, Belgian Registration Number B30020071389) [16].

2.2. Metabolic Work-Up

The metabolic work-up included a detailed questionnaire and a clinical examination with anthropometry. Height was measured to the nearest 0.5 cm and body weight was measured with a digital scale to the nearest 0.2 kg. BMI was calculated as weight in kilograms over height in meters squared. Waist circumference was measured at the mid-level between the lower rib margin and the iliac crest. A blood analysis included blood cell count, coagulation tests, electrolytes, kidney function tests, lipid profile (total and high density lipoprotein (HDL) cholesterols and triglycerides (TG)), liver tests (alanine aminotransferase (ALT), aspartate aminotransferase (AST), gamma glutamyl transpeptidase (GGT), alkaline phosphatase (ALP), total bilirubin and fractions), high-sensitive C-reactive protein (CRP), creatinine kinase, total protein, protein electrophoresis, glucose, insulin and thyroid function.

2.3. Hepatological Work-Up

The liver-specific program included additional blood analyses to exclude the classical aetiologies of liver disease (e.g., viral hepatitis and autoimmune disease): s-choline-esterase, carcino-embryonic antigen, α-foetoprotein, anti-nuclear factor, anti-neutrophil cytoplasm antigen antibodies, anti-smooth muscle antibodies, anti-mitochondrial antibodies, anti-liver–kidney microsome antibodies, serum copper and ceruloplasmin, α-1-antitrypsin, anti-hepatitis B core antibodies, hepatitis B surface antigen, anti-hepatitis C virus antibodies. Patients underwent a Doppler ultrasound of the abdomen with parameters of liver and spleen volume and liver vascularization and steatosis grading of the liver based on the Saverymuttu score (ultrasound steatosis, USS, scored 0–3) [17]. USS was scored as: isoechogenicity of the liver and the spleen: 0; slight increase in liver echogenicity, a slight exaggeration of liver and kidney echo discrepancy and relative preservation of echoes from the walls of the portal vein: 1; aforementioned abnormalities accompanied by loss of echoes from the walls of the portal veins, particularly from the peripheral branches, a greater posterior beam attenuation and a greater discrepancy between hepatic and renal echoes: 2; aforementioned abnormalities accompanied by a greater reduction in beam penetration, loss of echoes from most of the portal vein wall, including the main branches, and a large discrepancy between hepatic and renal echoes: 3. Patients also underwent a liver-spleen scintigraphy and an ABT.

2.4. Aminopyrine Breath Test

The ABT was carried out at home by the patients at rest after an overnight fasting. The ^{13}C-labelled aminopyrine was ingested orally together with water. Aminopyrine is absorbed rapidly and almost completely and breath samples were taken at 0, 30, 60, 90 and 120 min [18]. Peak excretion (ABTpeak) was determined and cumulative excretion (ABTcum) was calculated. Values are expressed as percentage of the administered dose per hour (%dose/h) or the calculated percentage of the administered dose over two hours (%dose/120 min). The analysis of the ABT was performed in the clinical laboratory of the Antwerp University Hospital and was executed by the Automated Breath ^{13}C Isotope Ratio Mass Spectrometer (Sercon, Crewe, UK). Normality values of the ABT are >5.4 %dose/h and >8.1 %dose/120 min for peak and cumulative excretion, respectively, based on the available literature and local experience [19].

2.5. Liver Biopsy

Liver biopsy was considered indicated in the presence of one or more of the following criteria: persistent abnormal liver tests (AST and/or ALT and/or GGT and/or ALP according to local lab upper limits of normal), ultrasound abnormality of the liver (enlarged liver, steatotic liver [17]), signs of liver disease on liver-spleen scintigraphy [20] and abnormal ABT [21]. A separate informed consent for liver biopsy was required. In patients who subsequently were referred to bariatric surgery, the liver biopsy was performed peri-operatively. The remaining patients were proposed for percutaneous or transjugular liver biopsy. The liver biopsy specimen was stored in formalin aldehyde. Haematoxylin–eosin stain, Sirius red (Fouchet) stain, periodic acid Schiff stain after diastase, reticulin stain (Gordon–Sweets), and Perl's iron stain were routinely performed on all biopsies and subsequently analysed by a team of experienced pathologists and hepatologists. Biopsies were re-assessed in batch by an experienced pathologist and this reading was used for further analysis. The diagnosis of NASH required the association of some degree of steatosis, some degree of ballooning, and some degree of lobular inflammation [1,22,23]. The different features were scored according to the NASH Clinical Research Network Scoring System [24]. Steatosis was graded as follows: less than 5% of liver parenchyma: 0; 5–33%: 1: 33–66%: 2; more than 66%: 3; Lobular inflammation was scored as: no foci: 0; less than two foci per x200 field: 1; 2–4 foci per x200 field: 2; more than four foci per x200 field: 3. Ballooning was scored as: none: 0; few ballooned cells: 1; many cells/prominent ballooning: 2. Fibrosis was staged: none: 0; perisinusoidal or periportal: 1; perisinusoidal and portal/periportal: 2; bridging

fibrosis: 3; cirrhosis: 4. The NAFLD Activity Score (NAS) was calculated as the unweighted sum of the scores for steatosis, ballooning, and lobular inflammation [24]. The length of the biopsy and the number of portal tracts were equally so reported by the pathologist. NASH was defined as the presence of steatosis (≥1), inflammation (≥1) and ballooning (≥1). Borderline NASH was defined as the presence of NASH and a NAS of 3-4. Definite NASH was defined as the presence of NASH and a NAS ≥ 5.

2.6. Patient Groups

Patients were excluded from further analysis if they had significant alcohol consumption (>20 g/day for women and >30 g/day for men using self-reported alcohol consumption levels) [25], or if another liver disease was diagnosed. Based on liver biopsy, the study population was divided into different subgroups: patients without signs of steatosis (S = 0) or liver fibrosis: noNAFLD; patients without significant fibrosis (F0–F1), with signs of steatosis (S ≥ 1), and either with the absence of NASH [NAFL (non-alcoholic fatty liver)] or with the presence of NASH (activity and ballooning ≥ 1) (NASH-noF); and patients with significant fibrosis (NAFLD-F).

2.7. Statistical Analysis

The data analyses were performed with SPSS version 25.0 software (IBM Corporation, Armonk, NY, USA). Descriptive statistics were produced for patient characteristics. The distribution of normality was evaluated by the Kolmogorov-Smirnov test and additional visual appraisal of the W-W probability plot. Significant differences in variables between the subgroups were ascertained using independent samples *t*-test for normally distributed continuous variables, the Mann–Whitney U tests for non-normally distributed continuous variables and the Chi-square test for categorical variables. Significant correlations were determined using the Spearman's rho test. Binary logistic regression analyses were carried out for peak excretion and cumulative excretion of the 13C-ABT. Other variables that were significantly correlated with NASH were included in multivariate logistic regression analyses. A backward elimination method was used to achieve a predictive model for both peak excretion and cumulative excretion separately. Area Under the Receiver Operating Curves (AUC) were generated using the ABT and the predictive models as test variables. AUC values were interpreted as follows: fail (50–60%), poor (60–70%), fair (70–80%), good (80–90%) or excellent (90–100%) [26,27]. Single cut-off values were chosen based on the highest sum of sensitivity and specificity (Youden index). Two-cut off model values were chosen based on 90% specificity and 90% sensitivity. AUROC curves of different tests within the same population were compared according to Delong (MedCalc version 14.12.0, MedCalc Software, Ostend, Belgium) [28]. $p < 0.05$ was considered statistically significant.

3. Results

3.1. Patient Characteristics

Four hundred and forty patients with a reliable liver biopsy and ABT were included. The total population had an average age of 46.1 years (SD 13.4), median BMI of 37.6 kg/m^2 (IQR 33.3; 41.7) and a gender distribution of 63.6%/36.4% female to male ratio. All patients (440) were classified according to the different patient groups: noNAFLD (71; 16.1%), NAFL (72; 16.2%), NASH-noF (176; 40.0%) and NAFLD-F (121; 27.5%).

3.2. NoNAFLD, NAFL, NASH-noF

Characteristics of the different subgroups are represented in Table 1. There was no statistical difference of the ABTpeak and ABTcum between noNAFLD and NAFL. The ABTpeak and the ABTcum of NASH-noF were, however, significantly lower compared to both the noNAFLD and the NAFL group (Figure 1).

In the NASH-noF group, there was a trend for a decreased ABTpeak and ABTcum between patients with borderline NASH and definite NASH, though these differences did not reach statistical

significance [9.20 (6.58; 11.45) vs. 7.65 (5.50; 10.48) %dose/h for ABTpeak ($p = 0.077$); and 12.90 (10.00; 16.55) vs. 10.95 (8.55; 15.13)%dose/120 min for ABTcum ($p = 0.085$), respectively].

In this population, significant positive correlations (Spearman's rho, $p < 0.05$) were found between ABTpeak and ALT (0.127), LDL cholesterol (0.124), serum albumin (0.182), and smoking (0.282) and significant negative correlations between ABTpeak and BMI (−0.199), waist (−0.157), platelet count (−0.161), steatosis grade (−0.164), lobular inflammation (−0.181), ballooning (−0.136), NAS score (−0.193) and USS (−0.136).

As for ABTcum, significant positive correlations were found with age (0.124), LDL cholesterol (0.132), albumin (0.185) and smoking (0.240) and significant negative correlations between ABTcum and BMI (−0.225), waist (−0.179), platelet count (−0.165), steatosis grade (−0.177), lobular inflammation (−0.195), ballooning (−0.158), NAS score (−0.214), fibrosis stage (−0.123) and USS (−0.145).

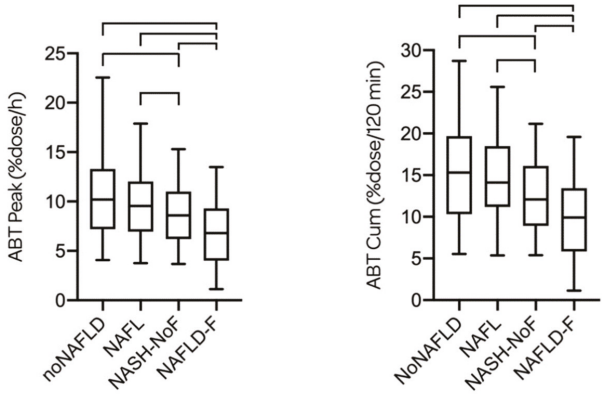

Figure 1. ABTpeak and ABTcum are given for the four subgroups. There was no statistical difference of the ABTpeak and ABTcum between noNAFLD [10.20 (7.20; 13.30) %dose/h and 15.30 (10.30; 19.70) %dose/120 min, respectively] and NAFL [9.55 (6.95; 12.03) %dose/h and 14.10 (11.20; 18.48) %dose/120 min, respectively]. The ABTpeak and the ABTcum of NASH-noF [8.60 (6.20; 11.00) %dose/h and 12.10 (8.90; 16.10) %dose/120 min, respectively] were significantly lower compared to both the noNAFLD and the NAFL group. The ABTpeak and the ABTcum of NAFLD-F [6.80 (4.00; 9.30) %dose/h and 9.90 (5.85; 13.45) %dose/120 min, respectively] were significantly lower compared to all three other subgroups.

The correlation between fibrosis stage and ABTcum in this group without significant fibrosis is most likely due to the confounding effect of NAS score, which was, as might be expected, lower in the NAFL and noNAFLD groups which consisted of less patients with fibrosis stage 1. When analysing this NASH-noF group, no difference of ABT could be observed between patients with fibrosis F0 or F1 [F0 8.4 (6.1–11.6) and F1 8.6 (6.3–10.2), $p = 0.423$; and F0 12.2 (8.9–16.5) and F1 12.1 (8.9–14.7), $p = 0.535$, for ABTpeak and ABTcum respectively]. In this group, there was no correlation between fibrosis stage and ABTpeak ($p = 0.803$) or ABTcum ($p = 0.833$).

3.3. Prediction of NASH in Non-Significant Fibrosis

In the combined groups of noNAFLD, NAFL and NASH-noF, a significant correlation ($p < 0.05$) could be found between the presence of NASH and age (0.155), waist (0.156), AST (0.227), ALT (0.268), ABTpeak (−0.174), ABTcum (−0.202) and USS (0.425). When separating ABTpeak and ABTcum, a remaining significant correlation could be found after logistic regression for ALT, USS and ABTpeak; and for ALT, USS and ABTcum. ALT and USS were significantly correlated with the NAS score ($p < 0.00001$, Spearman's rho 0.314 and 0.557, respectively). USS and ALT were significantly higher in the group of definite NASH compared to the group of borderline NASH.

Table 1. Patient characteristics.

Characteristic	NoNAFLD (*n* = 71)	NAFL (*n* = 72)	NASH-noF (*n* = 176)	NAFLD-F (*n* = 121)	*p* noNAFLD vs. NAFL	*p* noNAFLD vs. NASH-noF	*p* NAFL vs. NASH-noF
Age (yrs)	41.23 ± 12.19	45.35 ± 12.49	45.69 ± 12.83	50.03 ± 14.26	0.048 *	0.013 *	0.846
Gender (female)	60 (84.5%)	49 (68.1%)	111 (63.1%)	60 (49.6%)	0.021 *	0.001 *	0.456
Smoking (non-smoker)	52 (73.2%)	55 (76.4%)	139 (79.0%)	89 (73.4%)	0.659	0.259	0.554
BMI (kg/m^2)	36.80 (33.00; 40.30)	37.77 (32.61; 41.40)	37.70 (33.70; 41.80)	38.61 (32.97; 42.85)	0.474	0.187	0.724
Waist (cm)	111.0 ± 10.7	116.1 ± 15.9	116.9 ± 12.5	124.1 ± 14.6	0.023 *	<0.001 *	0.682
AST (U/L)	24.0 (21.0; 29.5)	26.0 (21.0; 29.8)	29.0 (24.0; 37.0)	37.0 (27.0; 52.0)	0.268	<0.001 *	0.007 *
ALT (U/L)	31.0 (24.0; 42.0)	35.0 (29.3; 46.0)	43.0 (32.0; 57.0)	48.0 (35.0; 75.0)	0.018 *	<0.00001 *	0.007 *
GGT (U/L)	30 (21; 49)	32 (26; 49)	36 (27; 49)	50 (33; 117)	0.13	0.026 *	0.47
PLT (10^9/L)	282 (252; 339)	268 (232; 323)	290 (246; 329)	249 (177; 302)	0.187	0.92	0.219
Tot chol (mg/dL)	201 (170; 226)	208 (176; 228)	203 (177; 227)	185 (160; 216)	0.805	0.717	0.905
HDL (mg/dL)	50 (42; 65)	47 (39; 56)	46 (39; 55)	41 (35; 51)	0.041 *	0.010 *	0.993
TG (mg/dL)	118 (84; 165)	135 (104; 204)	147 (105; 213)	148 (102; 208)	0.051	0.002 *	0.433
LDL (mg/dL)	118 (94; 142)	125 (98; 151)	120 (100; 146)	114 (82; 139)	0.632	0.672	0.911
Tot bili (mg/dL)	0.50 (0.40; 0.60)	0.50 (0.40; 0.70)	0.50 (0.40; 0.70)	0.60 (0.41; 0.80)	0.333	0.047 *	0.473
HbA1c (%)	5.50 (5.30; 5.70)	5.50 (5.30; 5.80)	5.60 (5.30; 5.90)	5.90 (5.50; 6.90)	0.048 *	0.011 *	0.661
Alb (g/dL)	4.37 ± 0.37	4.41 ± 0.37	4.46 ± 0.41	4.21 ± 0.72	0.539	0.097	0.333
INR	1.00 (1.00; 1.03)	1.01 (1.00; 1.04)	1.02 (1.00; 1.05)	1.04 (1.00; 1.12)	0.537	0.205	0.56
Steatosis							
0	71 (100%)	0	0	12 (9.9%)			
1	0	60 (83.3%)	67 (38.1%)	36 (29.8%)	<0.00001 *	<0.00001 *	<0.00001 *
2	0	11 (15.3%)	68 (38.6%)	37 (30.6%)			
3	0	1 (1.4%)	41 (23.3%)	36 (29.8%)			
Inflammation							
0	59 (83.1%)	53 (73.6%)	0	24 (19.8%)			
1	12 (16.9%	17 (23.6%)	115 (65.3%)	56 (46.3%)	0.204	<0.00001 *	<0.00001 *
2	0	2 (2.8%)	46 (26.1%)	26 (21.5%)			
3	0	0	15 (8.5%)	15 (12.4%)			
Ballooning							
0	60 (84.5%)	43 (59.7%)	0	16 (13.2%)	0.003 *	<0.00001 *	<0.00001 *
1	10 (14.1%)	22 (30.6%)	92 (52.3%)	48 (39.7%)			
2	1 (1.4%)	7 (9.7%)	84 (47.7%)	57 (47.1%)			

Table 1. *Cont.*

Characteristic	NoNAFLD (n = 71)	NAFL (n = 72)	NASH-noF (n = 176)	NAFLD-F (n = 121)	p noNAFLD vs. NAFL	p noNAFLD vs. NASH-noF	p NAFL vs. NASH-noF
NAS							
0	49 (69.0%)	0	0	6 (5.0%)			
1	19 (26.8%)	21 (29.2%)	0	5 (4.1%)			
2	2 (2.8%)	36 (50.0%)	0	9 (7.4%)	<0.00001 *	<0.00001 *	<0.00001 *
3	1 (1.4%)	13 (18.0%)	31 (17.6%)	18 (14.9%)			
4	0	2 (2.8%)	51 (29.0%)	20 (16.5%)			
5	0		43 (24.4%)	25 (20.7%)			
6	0		33 (18.8%)	20 (16.5%)			
7	0		15 (8.5%)	13 (10.7%)			
8	0		3 (1.7%)	5 (4.1%)			
USS							
0	25 (35.2%)	4 (5.6%)	6 (3.4%)	8 (6.6%)			
1	31 (43.7%)	28 (38.9%)	30 (17.0%)	25 (20.7%)			
2	11 (15.5%)	20 (27.8%)	52 (29.5%)	26 (21.5%)	<0.00001 *	<0.00001 *	0.001 *
3	4 (5.6%)	18 (25.0%)	80 (45.5%)	52 (43.0%)			
missing	0	2 (2.8%)	8 (4.5%)	10 (8.3%)			
ABTpeak	10.20 (7.20; 13.30)	9.55 (6.95; 12.03)	8.60 (6.20; 11.00)	6.80 (4.00; 9.30)	0.423	0.005 *	0.031 *
ABTcum	15.30 (10.30; 19.70)	14.10 (11.20; 18.48)	12.10 (8.90; 16.10)	9.90 (5.85; 13.45)	0.535	0.002 *	0.007 *

Patient characteristics of the subgroups: patients without NAFLD (noNAFLD), patients with non-alcoholic fatty liver (NAFL), patients with non-alcoholic steatohepatitis without significant fibrosis (NASH-noF) and patients with significant fibrosis (NAFLD-F). There was a significant difference between NAFLD-F and all three other subgroups for age, gender, waist circumference, AST, ALT, GGT, platelet count, total cholesterol, HDL, bilirubin, HbA1c, serum albumin, INR, steatosis, inflammation, ballooning, NAS, ABTpeak and ABTcum (full p values are given as Supplementary Table S1). LDL was significantly lower and TG higher in NAFLD-F compared to NASH-noF and noNAFLD, respectively. USS was significantly higher in NAFLD-F compared to noNAFLD and NAFL. Data are expressed as mean ± SD for normally distributed variables or as median (interquartile range) when distribution of the variable is skewed. p-value is calculated between different groups with * indicating statistical significance (<0.05). BMI, body mass index; AST, aspartate aminotransferase; ALT, alanine aminotransferase; GGT, gamma glutamyl transpeptidase; PLT, platelets; tot chol, total cholesterol; HDL, high density lipoprotein cholesterols; TG, triglycerides; LDL, low density lipoprotein cholesterols; tot bili, total bilirubin; HbA1c, haemoglobin A1c; Alb: albumin; INR, international normalized ratio; NAS, NAFLD activity score; USS, ultrasound steatosis score; ABTpeak, aminopyrine breath test peak value; ABTcum, aminopyrine breath test cumulative value.

Based on these data, two models were created to predict the presence of NASH:

PredABTpeak for NASH = −1.617+ (0.025 × ALT) + (0.909 x USS) + (−0.094 × ABTpeak)
PredABTcum for NASH = −1.457 + (0.025 × ALT) + (0.901 × USS) + (−0.075 × ABTcum)

AUROCs for the prediction of NASH and definite NASH for ABTpeak, ABTcum, ALT, USS as single tests and for the predictive models are represented in Table 2. The predictive models were significantly better ($p < 0.01$) than ABTpeak, ABTcum and ALT individually for the prediction of NASH and definite NASH, but not significantly better than USS ($p > 0.05$).

Table 2. AUROC to predict the presence of NASH and definite NASH.

Test	NASH	Definite NASH
ABTpeak	0.601 (0.539–0.663)	0.612 (0.544–0.681)
ABTcum	0.617 (0.555–0.679)	0.620 (0.553–0.687)
ALT	0.655 (0.595–0.715)	0.669 (0.604–0.734)
USS	0.744 (0.688–0.800)	0.772 (0.717–0.827)
PredABTpeak	0.785 (0.734–0.835)	0.814 (0.765–0.863)
PredABTcum	0.787 (0.737–0.837)	0.819 (0.770–0.867)

AUROC (represented with 95% confidence interval) to predict the presence of NASH and definite NASH for ABTpeak, ABTcum, ALT and US steatosis separately, and the predictive models PredABTpeak and PredABTcum combining ALT, USS and ABT.

Based on the predictive model of the ABTcum which showed a slightly higher AUROC than ABTpeak, we proposed cut-off values to determine the presence of NASH or definite NASH in Table 3. The predicted model was positively correlated to the presence of NASH. The higher the value, the higher the likelihood of NASH.

Table 3. Cut-off values to predict the presence of NASH and fibrosis.

	Cut-Off Value	Sens	Spec	PPV	NPV
NASH	0.2575	72.60%	71.60%	75.30%	68.70%
Def NASH	0.2575	87.60%	61.80%	38.10%	92.50%
Sign F	13.25	73.60%	51.40%	36.50%	83.70%
Adv F	10.1	63.50%	69.90%	30.00%	90.50%
Cirrhosis	5.05	51.50%	95.30%	52.80%	96.00%
NASH	>1.1210			82.90%	
No NASH	<−0.6185			80.00%	
Def NASH	>1.1346			64.10%	
No def NASH	<0.0120			93.30%	
Sign F	<7.05			53.70%	
No sign F	>17.45			86.50%	
Adv F	<7.05			46.30%	
No adv F	>18.25			90.70%	
Cirrhosis	<6.55			30.50%	
No cirrhosis	>19.45			94.70%	

Cut-off values to predict the presence of NASH in patients without significant fibrosis; and to predict fibrosis in the whole population with sensitivity, specificity, positive predictive value and negative predictive value. One and two cut-off models were created for each parameter. Using 1 cut-off, the PPV for definite NASH was low (78/162, 38.1%), but of those misclassified as definite NASH, 52% had borderline NASH. Using 2 cut-offs, the PPV for definite NASH was better (41/64, 64.1%), and with 61% of those misclassified having borderline NASH. Using two cut-off values can lead to patients with an indeterminate value. This "indeterminate" classification was present in 54%, 36%, 65%, 68% and 74% of cases for NASH, definite NASH, significant fibrosis, advanced fibrosis and cirrhosis, respectively. Def, definite NASH; Sign F, significant fibrosis; Adv F, advanced fibrosis; Sens, sensitivity; Spec, specificity; PPV, positive predictive value; NPV, negative predictive value.

3.4. Significant Fibrosis

This group consisted of 121 patients with 38.8% F2, 33.9% F3 and 27.3% F4 (i.e., cirrhosis); 28.1% did not have NASH, borderline NASH was present in 19.8% and definite NASH in 52.1% of these cases. In patients with significant fibrosis, ABTpeak and ABTcum are no longer significantly correlated to the presence of NASH (rho −0.104, $p = 0.258$ and rho −0.072, $p = 0.435$, respectively) nor to the NAS score (rho −0.053, $p = 0.566$ and −0.020, $p = 0.825$, respectively). In this population, fibrosis stage has a stronger (inverse) correlation with ABTpeak (rho −0.366, $p < 0.0001$) and ABTcum (rho −0.347, $p = 0.0001$). Fibrosis stage is, however, inversely correlated to the NAS score (rho −0.203, $p = 0.025$).

3.5. All Patients

In our entire population, both ABTpeak and ABTcum were independently positively correlated with smoking and serum albumin concentration and negatively correlated with BMI, the presence of NASH and fibrosis stage. Fibrosis was positively correlated with NAS (rho 0.311, $p < 0.0001$) and the presence of NASH (rho 0.222, $p < 0.0001$).

ABTpeak and ABTcum decreased significantly between each fibrosis stage; 9.1 (6.50; 11.80) and 13.40 (9.40; 17.35) for F0–1; 7.80 (6.20; 9.90) and 11.50 (8.80; 14.10) for F2; 6.70 (4.20; 9.40) and 9.50 (6.15; 13.80) for F3; and 3.50 (1.75; 6.80) and 5.00 (2.55; 10.80) for F4, respectively. Differences of ABTpeak and ABTcum for each fibrosis stage are represented in Figure 2.

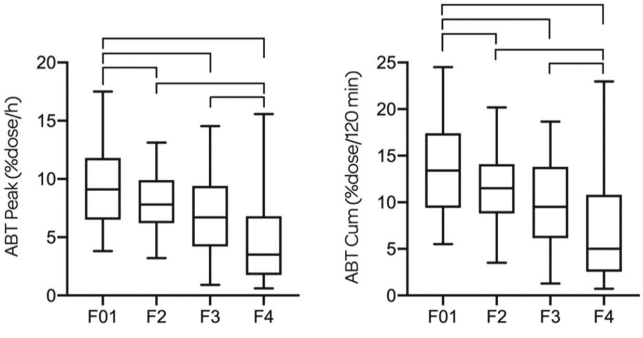

Figure 2. ABTpeak and ABTcum are given for every fibrosis stage in all patients. There is a significant difference of ABTpeak between F2–F4 ($p < 0.0001$) and F3–F4 ($p = 0.008$), but not between F2–F3 ($p = 0.133$). There is a significant difference of ABTcum between F2–F4 ($p < 0.0001$) and F3–F4 ($p = 0.013$), but not between F2–F3 ($p = 0.119$). The ABTpeak and ABTcum are both significantly higher for F0–1 compared to F2 ($p < 0.05$), F3 ($p < 0.001$) and F4 ($p < 0.0001$).

ABTpeak showed an AUROC of 0.612 (0.559–0.666), 0.674 (0.618–0.731), 0.718 (0.648–0.788) and 0.782 (0.682–0.882) for the prediction of NASH, significant fibrosis, advanced fibrosis and cirrhosis, respectively. ABTcum showed an AUROC of 0.616 (0.0566–0.673), 0.676 (0.619–0.732), 0.719 (0.650–0.788) and 0.769 (0.667–0.872) for the prediction of NASH, significant fibrosis, advanced fibrosis and cirrhosis, respectively.

Based on the ABTcum which showed a slightly higher AUROC than ABTpeak, we proposed cut-off values to determine the presence of significant fibrosis, advanced fibrosis or cirrhosis in Table 3.

4. Discussion

The ^{13}C-aminopyrine breath test has traditionally been used to estimate functional liver reserve in advanced liver disease. In this study, we demonstrate that non-alcoholic steatohepatitis, even in the absence of significant fibrosis, is associated with a significant impairment of hepatic microsomal function as measured by the ^{13}C-aminopyrine breath test. In the fibrotic NAFLD population, the effect

of fibrosis on ABT excretion was more important than the effect of inflammation. The ABT can be used as a tool in the prediction of the presence of NASH or fibrosis in the appropriate setting.

Fibrosis has been shown to be the strongest predictor of outcome in NAFLD, which does, however, not equal that it is as such the driver of disease progression [29]. Progression of NALF to bridging fibrosis concurs with transition to NASH and several longitudinal studies have recently confirmed the direct relationship between evolution in disease activity and hepatic inflammatory changes on one hand and the evolution in fibrosis on the other hand. NASH resolution was also shown to be the strongest predictor of fibrosis regression [30,31]. Similarly, SAF activity appeared to be strongly correlated with liver fibrosis stage, further supporting the concept of disease activity as the driving force of disease progression [32,33]. These observations demonstrate that NASH and fibrosis are closely linked.

Multiple serum biomarkers have been evaluated for the prediction of the presence and/or severity of NASH, though most biomarkers failed to demonstrate accuracy. Plasma cytokeratin 18 fragment levels are a marker of hepatocyte apoptosis and represent the most extensively evaluated biomarker of steatohepatitis, although the accuracy is modest. To date, non-invasive tests cannot reliably be used solely for the diagnosis of NASH [34,35]. More extensive research has been performed on non-invasive tools to asses liver fibrosis, though most scores for fibrosis are mainly developed and validated to exclude advanced fibrosis, and do not allow the reliable categorisation of individual liver fibrosis stages [34].

The ABT has mostly been studied in the setting of cirrhosis and end stage liver disease. Smaller studies have previously shown a significant decrease of liver function in NASH patients, measured by isotope breath tests, though these studies were confounded by a limited population size and the inclusion of patients with significant fibrosis to cirrhosis in the NASH groups [4,12–15].

In this study, we included a large population of patients at risk of NAFLD, by the presence of overweight or obesity, allowing us to investigate the effect of NASH in patients without significant fibrosis and thus isolating the steatohepatitis effect. We observed a significant decrease of microsomal liver function in patients with NASH compared to patients with NAFL and overweight patients without liver steatosis. Liver function was not different between the latter two groups indicating that isolated steatosis does not significantly decrease microsomal liver function. Within the NASH population there was a trend of a decreased ABT excretion between patients with borderline NASH and definite NASH, though these differences did not reach statistical significance. Overall, this indicates that steatohepatitis as such is associated with a significant decrease in microsomal hepatocyte function, which is relevant for our understanding of the pathophysiology of NASH.

Although extraction of aminopyrine seems to be independent of portal blood flow, a role for changes in the microcirculation that have shown to occur early in the development of NASH, even in the non-fibrotic stage, might indirectly play a role [36–39]. These changes are hypothesised to cause centrolobular hypoxia by aggravating the physiological portocentral oxygen gradient [40]. Hypoxia has been shown to impact on liver microsomal function, so these mechanisms could offer an additional explanation for the presence of microsomal dysfunction early in disease development.

People with overweight or obesity and other components of the metabolic syndrome are at risk of developing fatty liver which is characterized by the presence of large vacuoles of lipids within the cytosol. In addition to macrovacuolar steatosis, NASH implies the presence of cell damage and inflammation and is histologically characterized by microvesicular steatosis, portal and lobular inflammation, and the presence of hepatocyte injury in the form of ballooning and apoptosis. All these processes ultimately stimulate fibrogenesis. At least three major events are involved in the progression of fatty liver to NASH, including overproduction of ROS (reactive oxygen species) and RNS (reactive nitrogen species), lipotoxicity and increased release of proinflammatory and profibrogenic cytokines [41]. These changes impact the microsomal activity and are probably responsible for the decreased microsomal liver function that we observed. Studies with animals and human tissue have also shown an alteration of CYP 450 enzyme activity. CYP3A, a CYP which only plays a minimal role in the ABT, is downregulated,

presumably by obesity, elevated proinflammatory cytokines, noncytokine components and oxidative stress [42]. Some CYPs might not only be influenced by the presence of NASH, but could also play a causative role. It has been shown that CYP2E1 (which has no role in ABT) is overexpressed in non-alcoholic steatosis [43]. It is hypothesized that in the case of fat mobilisation as in diabetes mellitus, the hyperketonemia and other small organic molecules are both substrates and inducers of CYP2E1 that will lead to non-alcoholic fatty liver disease. This overexpressed CYP2E1 exhibits a high capacity to produce free radicals that are probably the cause of liver damage and lipid peroxidation in obese type 2 diabetes patients [44].

Since NASH seems to be the driving force for fibrosis development, its diagnosis is paramount, and the ABT could potentially help by discriminating isolated steatosis from NASH. The rising prevalence of NAFLD and the known disadvantages of liver biopsy (sampling error, cost, morbidity and mortality) illustrate the need for new non-invasive diagnostic techniques. Our current results suggest that ABT can indeed be helpful in the differentiation between patients with NASH and those with NAFL in patients without significant fibrosis. This test is non-invasive, innocuous, easy to administer and samples are transportable, which allows its use in primary and secondary care.

In our group without significant fibrosis, the ABT as a single test had rather poor predictive power, though when including ALT and USS into a predictive model, the predictive power strongly increased. A potential limitation of the use of this model in clinical practice could, however, be hampered by the absence of reliable tools to exclude significant fibrosis. Liver steatosis and ALT have both been related to the presence of NASH. Previous research has shown a correlation between the extent of steatosis (evaluated histologically or ultrasonographically) and the presence of NASH [45–47]. In line with our results, Ballestri et al. showed higher USS values in patients with NASH than in those with steatosis; and higher values in patients with definite NASH than in those with borderline NASH [48]. Although normal ALT does not exclude the presence of NASH, studies have shown that ALT levels are independently associated with NASH, even in patients with normal ALT, indicating that even a minor elevation in ALT level, albeit within normal limits, can reflect the presence of NASH-related liver damage [49].

Tribonias et al. found similar results with a substantial impairment of hepatic microsomal function as assessed by a simple non-invasive ABT in NASH patients including, however, patients with significant fibrosis in the NASH group [4]. Compared to our results, they found a higher AUROC [0.741 (0.576–0.905)] for ABTcum to diagnose the presence of NASH, though 25% of their NASH population was cirrhotic compared to 8% in our NASH population. More importantly, 31% of our patients with advanced fibrosis lost the combination of characteristics necessary for the diagnosis of NASH. This is in line with the general observation that with the progression of fibrosis, the characteristic triad of NASH and perisinusoidal fibrosis becomes less prominent or disappears [50].

In our study, we observed, apart from the effect of NASH on microsomal function, a decreasing ABT excretion with each fibrosis stage, which is in line with current literature. Previous reports support this observation and show that ABT results are associated with the severity of liver disease, and that they have a prognostic role in predicting death from liver failure in cirrhotic patients [21,51]. Moreover, we observed that from the moment significant fibrosis is present, the statistically significant influence of NASH on the ABT excretion can no longer be observed.

In our entire population, the predictive power of the cumulative ABT value was mostly higher than the peak ABT value, though not statistically significant. ABT proved to be a poor predictor of significant fibrosis as a single test with an AUROC of 0.676 for ABTcum. The power increased to a fair test to predict the presence of advanced fibrosis and cirrhosis with an AUROC of 0.719 and 0.769 for ABTcum, respectively.

Our findings clearly indicate that both steatohepatitis and fibrosis are associated with impairment of microsomal function. This implies that both these aspects should be taken into account when assessing the accuracy of the ABT as a non-invasive marker of disease. The mixing-up of both aspects may in part explain overall low accuracy and conflicting results in the literature.

ABT is not the only breath test used to investigate hepatic function. ^{13}C breath tests can explore either microsomal, cytosolic or mitochondrial hepatocellular subfunctions [2]. Previous research has shown that these other ^{13}C breath tests are also capable of distinguishing patients with various degrees of liver disease from normal subjects, as well as distinguishing patients with compensated cirrhosis from those with decompensated cirrhosis. Banasch et al. used a ^{13}C-methionine breath test to evaluate mitochondrial dysfunction. They showed in patients without significant fibrosis a difference of mitochondrial function between borderline and definite NASH, which was no longer present in patients with significant fibrosis [52]. In the borderline NASH group, however, 15% had significant fibrosis compared to 43% in the definite NASH group (and only 9% in the NAFL group). Correlation analyses confirmed the synergistic negative effect of NASH activity and fibrosis on individual breath test outcome. NASH activity and fibrosis were correlated as was observed in our study.

Miele et al. performed ^{13}C-octanoate breath tests (OBT) in patients with NAFLD and demonstrated the relationship between the presence of fibrosis and the impairment of liver function, expressed by lower OBT results than those of controls [53]. Park et al. showed that the ^{13}C-caffeine breath test, another test for microsomal function, reflected the extent of hepatic fibrosis in NALFD and was an independent predictor of significant fibrosis in these patients. They showed impaired liver function in NASH patients, but induced by the presence of significant fibrosis, as they found no correlation with steatosis or inflammation [14].

In our study, ABT results were found to have an inverse correlation with BMI, which is consistent with previous findings as increasing BMI has been repeatedly shown to be associated with worse liver histologic lesions in the NAFLD patients [4,54].

A weakness of our study is the fact that the majority of patients were obese, but the sample included relatively few diabetic patients. The generalizability of the findings to NAFLD patients with a different metabolic profile hence needs to be studied. Furthermore, there is the confounding effect of patient characteristics on the ABT and the cross-sectional nature of the study. Enzymatic functions explored by the ABT may be influenced by hormones, malnutrition, heart or renal failure, sex or xenobiotics such as medication or smoking [2]. No data concerning menstrual cycle or exogenous female sex hormones were obtained during our diagnostic work-up. Smoking induces CYP450 enzymes (primarily CYP1A2); hence a higher peak and cumulative excretion can be expected in smokers [55]. In our non-fibrotic population, smoking was independently correlated with ABT values, though smoking habits did not differ between our subpopulations. In the literature, older age and female gender are correlated with lower ABT values, which could not be observed in our population [56]. Genetic polymorphisms in CYPs are a major cause of the inter individual variation in drug metabolism. Several of the CYPs important for the aminopyrine metabolisation (such as CYP2C19, 2D6, 1A2, 2C9, 2A6) are known to be functionally polymorphic [44]. Rapid metabolisers will have higher ABT results compared to slow metabolisers. In this study, determination of CYP polymorphisms was not performed. Most likely it will not have influenced our findings due to the large subgroups. The strength of our study is first of all the large patient population, which allows us to compare groups independent from the impact of significant fibrosis and which decreases the confounding effect of ABT influencers in individual patients. Furthermore, a large proportion of the patients came in for a problem of overweight or obesity and underwent a liver assessment without a priori suspicion of liver disease. This implies that all patients underwent ABT, and not only those selected because of elevated liver tests or other indicators of liver disease, avoiding a lot of potential bias of which many biopsy-proven NAFLD cohort studies suffer. This methodological approach more closely resembles the context of use in which biomarkers for NAFLD will be used in the future and reinforces the validity of these results and their relevance for routine clinical practice.

To confirm our results, more studies should be performed in large patient groups without the confounding factor of significant or advanced fibrosis. Other compounds than aminopyrine can be used to assess the decreased microsomal function in NASH patients, such as caffeine, phenacetin or methacetin.

The observations in this study open new possibilities for the use of the ABT in NAFLD. The ABT can be incorporated in the diagnostic toolset for NASH (in our model, together with ALT and USS) or fibrosis assessment. A decreased microsomal liver function in patients with NASH might indicate a decreased metabolism of xenobiotics, which has a major impact considering the high global prevalence of NASH. Future studies of NASH medication should take this into account. The ABT could be used to monitor disease progression of inflammation in the absence of fibrosis. Furthermore, the ABT could be an additional tool the evaluate the potential improvement upon (new) therapeutic interventions.

5. Conclusions

The present study shows a decreased microsomal function in NASH patients without significant fibrosis compared to patients with simple steatosis, as assessed by ABT. Fibrosis, when present, has a stronger impact on ABT excretion compared to inflammation and decreases ABT excretion with each fibrosis stage. ABT might be a useful tool for the decision to conduct a liver biopsy in the NAFLD patients and potentially also for the prospective monitoring of disease progression or of the potential benefits after therapeutic interventions.

Supplementary Materials: The following are available online at http://www.mdpi.com/2227-9059/8/12/546/s1.

Author Contributions: Conceptualization, W.V., S.F., L.V.G.; methodology, W.V. and S.F.; validation, E.V.M., L.D., W.V. and S.F.; formal analysis, E.V.M., L.D., W.V.; investigation, E.V.M., L.D., T.V., L.V., A.D., D.C., L.R., E.D., A.V., J.W., W.V.; data curation, A.V.; writing—original draft preparation, W.V.; writing—review and editing, S.F.; visualization, W.V.; supervision, S.F. and L.V.G.; project administration, S.F. All authors have read and agreed to the published version of the manuscript.

Funding: This work is part of the project Hepatic and Adipose Tissue and Functions in the Metabolic Syndrome (HEPADIP), which is supported by the European Commission as an Integrated Project under the 6th Framework Program (contract LSHM-CT-2005-018734).

Conflicts of Interest: The authors declare no conflict of interest. The funders had no role in the design of the study; in the collection, analyses, or interpretation of data; in the writing of the manuscript, or in the decision to publish the results.

References

1. Marchesini, G.; Day, C.P.; Dufour, J.F.; Canbay, A.; Nobili, V.; Ratziu, V.; Tilg, H.; Roden, M.; Gastaldelli, A.; Yki-Jarvinen, H.; et al. EASL-EASD-EASO Clinical Practice Guidelines for the management of non-alcoholic fatty liver disease. *J. Hepatol.* **2016**, *64*, 1388–1402. [CrossRef] [PubMed]
2. Armuzzi, A.; Candelli, M.; Zocco, M.A.; Andreoli, A.; De Lorenzo, A.; Nista, E.C.; Miele, L.; Cremonini, F.; Cazzato, I.A.; Grieco, A.; et al. Review article: Breath testing for human liver function assessment. *Aliment. Pharmacol. Ther.* **2002**, *16*, 1977–1996. [CrossRef] [PubMed]
3. Afolabi, P.; Wright, M.; Wootton, S.A.; Jackson, A.A. Clinical utility of 13C-liver-function breath tests for assessment of hepatic function. *Dig. Dis. Sci.* **2013**, *58*, 33–41. [CrossRef] [PubMed]
4. Tribonias, G.; Margariti, E.; Tiniakos, D.; Pectasides, D.; Papatheodoridis, G.V. Liver function breath tests for differentiation of steatohepatitis from simple fatty liver in patients with nonalcoholic fatty liver disease. *J. Clin. Gastroenterol.* **2014**, *48*, 59–65. [CrossRef] [PubMed]
5. Niwa, T.; Sato, R.; Yabusaki, Y.; Ishibashi, F. Contribution of human hepatic cytochrome P450s and steroidogenic CYP17 to the N-demethylation of aminopyrine. *Xenobiotica* **1999**, *29*, 187–193. [CrossRef] [PubMed]
6. Niwa, T.; Imagawa, Y. Substrate specificity of human cytochrome P450 (CYP) 2C subfamily and effect of azole antifungal agents on CYP2C8. *J. Pharm. Pharm. Sci.* **2016**, *19*, 423–429. [CrossRef] [PubMed]
7. Brockmöller, J.; Ivar, R. Assessment of Liver Metabolic Function: Clinical Implications. *Clin. Pharmacokinet.* **1994**, *27*, 216–248. [CrossRef]
8. Bircher, J.; Küpfer, A.; Gikalov, I.; Preisig, R. Aminopyrine demethylation measured by breath analysis in cirrhosis. *Clin. Pharmacol. Ther.* **1976**, *20*, 484–492. [CrossRef]
9. Monroe, P.; Baker, A.; Schneider, J.; Krager, P.; Klein, P.; Schoeller, D. The aminopyrine breath test and serum bile acids reflect histologic severity in chronic hepatitis. *Hepatology* **1982**, *2*, 317–322. [CrossRef]

10. Giannini, E.; Fasoli, A.; Chiarbonello, B.; Malfatti, F.; Romagnoli, P.; Botta, F.; Testa, E.; Polegato, S.; Fumagalli, A.; Testa, R. 13C-aminopyrine breath test to evaluate severity of disease in patients with chronic hepatitis C virus infection. *Aliment. Pharmacol. Ther.* **2002**, *16*, 717–725. [CrossRef]
11. Herold, C.; Heinz, R.; Niedobitek, G.; Schneider, T.; Hahn, E.G.; Schuppan, D. Quantitative testing of liver function in relation to fibrosis in patients with chronic hepatitis B and C. *Liver* **2001**, *21*, 260–265. [CrossRef] [PubMed]
12. Fierbinteanu-Braticevici, C.; Plesca, D.A.; Tribus, L.; Panaitescu, E.; Braticevici, B. The role of 13C-methacetin breath test for the non-invasive evaluation of nonalcoholic fatty liver disease. *J. Gastrointest. Liver Dis.* **2013**, *22*, 149–156.
13. Portincasa, P.; Grattagliano, I.; Lauterburg, B.H.; Palmieri, V.O.; Palasciano, G.; Stellaard, F. Liver breath tests non-invasively predict higher stages of non-alcoholic steatohepatitis. *Clin. Sci.* **2006**, *111*, 135–143. [CrossRef] [PubMed]
14. Park, G.; Wiseman, E.; George, J.; Katelaris, P.; Seow, F.; Fung, C.; Ngu, M. Non-invasive estimation of liver fibrosis in non-alcoholic fatty liver disease using the 13 C-caffeine breath test. *J. Gastroenterol. Hepatol.* **2011**, *26*, 1411–1416. [PubMed]
15. Schmilovitz-Weiss, H.; Niv, Y.; Pappo, O.; Halpern, M.; Sulkes, J.; Braun, M.; Barak, N.; Rotman, Y.; Cohen, M.; Waked, A.; et al. The 13C-Caffeine Breath Test Detects Significant Fibrosis in Patients With Nonalcoholic Steatohepatitis. *J. Clin. Gastroenterol.* **2008**, *42*, 408–412. [CrossRef] [PubMed]
16. Francque, S.; Verrijken, A.; Caron, S.; Prawitt, J.; Paumelle, R.; Derudas, B.; Lefebvre, P.; Taskinen, M.; Van Hul, W.; Mertens, I.; et al. PPARα gene expression correlates with severity and histological treatment response in patients with non-alcoholic steatohepatitis. *J. Hepatol.* **2015**, *63*, 164–173. [CrossRef] [PubMed]
17. Saverymuttu, S.H.; Joseph, A.E.A.; Maxwell, J.D. Ultrasound scanning in the detection of hepatic fibrosis and steatosis. *Br. Med. J. (Clin. Res. Ed).* **1986**, *292*, 13–15. [CrossRef]
18. Volz, M.; Kellner, H. Kinetics and metabolism of pyrazolones (propyphenazone, aminopyrine and dipyrone). *Br. J. Clin. Pharmacol.* **1980**, *10*, 299S–308S. [CrossRef]
19. Giannini, E.G.; Fasoli, A.; Borro, P.; Botta, F.; Malfatti, F.; Fumagalli, A.; Testa, E.; Polegato, S.; Cotellessa, T.; Milazzo, S.; et al. 13C-galactose breath test and 13C-aminopyrine breath test for the study of liver function in chronic liver disease. *Clin. Gastroenterol. Hepatol.* **2005**, *3*, 279–285. [CrossRef]
20. Taylor, K.J.W.; Sullivan, D.; Simeone, J.; Rosenfield, A.T. Scintigraphy, ultrasound and CT scanning of the liver. *Yale J. Biol. Med.* **1977**, *50*, 437–455. [CrossRef]
21. Merkel, C.; Bolognesi, M.; Bellon, S.; Bianco, S.; Honisch, B.; Lampe, H.; Angeli, P.; Gatta, A. Aminopyrine breath test in the prognostic evaluation of patients with cirrhosis. *Gut* **1992**, *33*, 836–842. [CrossRef] [PubMed]
22. Brunt, E.M.; Kleiner, D.E.; Wilson, L.A.; Belt, P.; Neuschwander-Tetri, B.A. NASH Clinical Research Network The NAS and the histopathologic diagnosis in NAFLD: Distinct clinicopathologic meanings. *Hepatology* **2011**, *53*, 810–820. [CrossRef] [PubMed]
23. Chalasani, N.; Younossi, Z.; Lavine, J.E.; Charlton, M.; Cusi, K.; Rinella, M.; Harrison, S.A.; Brunt, E.M.; Sanyal, A.J. The diagnosis and management of nonalcoholic fatty liver disease: Practice guidance from the American Association for the Study of Liver Diseases. *Hepatology* **2018**, *67*, 328–357. [CrossRef] [PubMed]
24. Kleiner, D.E.; Brunt, E.M.; Van Natta, M.; Behling, C.; Contos, M.J.; Cummings, O.W.; Ferrell, L.D.; Liu, Y.C.; Torbenson, M.S.; Unalp-Arida, A.; et al. Design and validation of a histological scoring system for nonalcoholic fatty liver disease. *Hepatology* **2005**, *41*, 1313–1321. [CrossRef] [PubMed]
25. Ratziu, V.; Bellentani, S.; Cortez-Pinto, H.; Day, C.; Marchesini, G. A position statement on NAFLD/NASH based on the EASL 2009 special conference. *J. Hepatol.* **2010**, *53*, 372–384. [CrossRef] [PubMed]
26. Tape, T.G. Interpreting Diagnostic Tests: The Area under an ROC Curve. University of Nebraska Medical Center. Available online: http://gim.unmc.edu/dxtests/ROC3.htm (accessed on 18 November 2020).
27. Mandrekar, J.N. Receiver operating characteristic curve in diagnostic test assessment. *J. Thorac. Oncol.* **2010**, *5*, 1315–1316. [CrossRef] [PubMed]
28. DeLong, E.; DM, D.; Clarke-Pearson, D. Comparing the areas under two or more correlated receiver operating characteristic curves: A nonparametric approach. *Biometrics* **1988**, *44*, 837–845. [CrossRef]
29. Dulai, P.S.; Singh, S.; Patel, J.; Soni, M.; Prokop, L.; Younossi, Z.; Sebastiani, G.; Ekstedt, M.; Hagstrom, H.; Nasr, P.; et al. Increased risk of mortality by fibrosis stage in non-alcoholic fatty liver disease: Systematic review and meta-analysis. *Hepatology* **2017**, *65*, 1557–1565. [CrossRef]

30. Kleiner, D.E.; Brunt, E.M.; Wilson, L.A.; Behling, C.; Guy, C.; Contos, M.; Cummings, O.; Yeh, M.; Gill, R.; Chalasani, N.; et al. Association of histologic disease activity with progression of nonalcoholic fatty liver disease. *JAMA Netw. Open* **2019**, *2*, e1912565. [CrossRef]
31. Bunney, P.E.; Zink, A.N.; Holm, A.A.; Billington, C.J.; Kotz, C.M. Orexin activation counteracts decreases in nonexercise activity thermogenesis (NEAT) caused by high-fat diet. *Physiol. Behav.* **2017**, *176*, 139–148. [CrossRef]
32. Nascimbeni, F.; Bedossa, P.; Fedchuk, L.; Pais, R.; Charlotte, F.; Lebray, P.; Poynard, T.; Ratziu, V.; LIDO (Liver Injury in Diabetes and Obesity) Study Group. Clinical validation of the FLIP algorithm and the SAF score in patients with non-alcoholic fatty liver disease. *J. Hepatol.* **2020**, *72*, 828–838. [CrossRef] [PubMed]
33. Bedossa, P. Utility and appropriateness of the fatty liver inhibition of progression (FLIP) algorithm and steatosis, activity, and fibrosis (SAF) score in the evaluation of biopsies of nonalcoholic fatty liver disease. *Hepatology* **2014**, *60*, 565–575. [CrossRef] [PubMed]
34. Francque, S.; Lanthier, N.; Verbeke, L.; Reynaert, H.; van Steenkiste, C.; Vonghia, L.; Kwanten, W.; Weyler, J.; Trépo, E.; Cassiman, D.; et al. The Belgian Association for Study of the Liver guidance document on the management of adult and paediatric non-alcoholic fatty liver disease. *Acta Gastroenterol. Belgica* **2018**, *81*, 55–81.
35. Wai-Sun Wong, V.; Adams, L.; de Lédinghen, V.; Lai-Hung Wong, G.; Sookoian, S. Noninvasive biomarkers in NAFLD and NASH—Current progress and future promise. *Nat. Rev. Gastroenterol. Hepatol.* **2018**, *15*, 461–478. [CrossRef]
36. Hori, Y.; Shimizu, Y.; Aiba, T. Altered hepatic drug-metabolizing activity in rats suffering from hypoxemia with experimentally induced acute lung impairment. *Xenobiotica* **2018**, *48*, 576–583. [CrossRef]
37. Francque, S.; Laleman, W.; Verbeke, L.; Van Steenkiste, C.; Casteleyn, C.; Kwanten, W.; Van Dyck, C.; D'Hondt, M.; Ramon, A.; Vermeulen, W.; et al. Increased intrahepatic resistance in severe steatosis: Endothelial dysfunction, vasoconstrictor overproduction and altered microvascular architecture. *Lab. Investig.* **2012**, *92*, 1428–1439. [CrossRef]
38. Francque, S.; Verrijken, A.; Mertens, I.; Hubens, G.; Van Marck, E.; Pelckmans, P.; Van Gaal, L.; Michielsen, P. Noncirrhotic human nonalcoholic fatty liver disease induces portal hypertension in relation to the histological degree of steatosis. *Eur. J. Gastroenterol. Hepatol.* **2010**, *22*, 1449–1457. [CrossRef]
39. van der Graaff, D.; Kwanten, W.J.; Couturier, F.J.; Govaerts, J.S.; Verlinden, W.; Brosius, I.; D'Hondt, M.; Driessen, A.; De Winter, B.Y.; De Man, J.G.; et al. Severe steatosis induces portal hypertension by systemic arterial hyporeactivity and hepatic vasoconstrictor hyperreactivity in rats. *Lab. Investig.* **2018**, *98*, 1263–1275. [CrossRef]
40. van der Graaff, D.; Kwanten, W.J.; Francque, S.M. The potential role of vascular alterations and subsequent impaired liver blood flow and hepatic hypoxia in the pathophysiology of non-alcoholic steatohepatitis. *Med. Hypotheses* **2019**, *122*, 188–197. [CrossRef]
41. Begriche, K.; Massart, J.; Robin, M.A.; Bonnet, F.; Fromenty, B. Mitochondrial adaptations and dysfunctions in nonalcoholic fatty liver disease. *Hepatology* **2013**, *58*, 1497–1507. [CrossRef]
42. Cobbina, E.; Akhlaghi, F. Non-alcoholic fatty liver disease (NAFLD)–pathogenesis, classification, and effect on drug metabolizing enzymes and transporters. *Drug Metab. Rev.* **2017**, *49*, 197–211. [CrossRef] [PubMed]
43. Niemelä, O.; Parkkila, S.; Juvonen, R.O.; Viitala, K.; Gelboin, H.V.; Pasanen, M. Cytochromes P450 2A6, 2E1, and 3A and production of protein-aldehyde adducts in the liver of patients with alcoholic and non-alcoholic liver diseases. *J. Hepatol.* **2000**, *33*, 893–901. [CrossRef]
44. Elfaki, I.; Mir, R.; Almutairi, F.M.; Abu Duhier, F.M. Cytochrome P450: Polymorphisms and roles in cancer, diabetes and atherosclerosis. *Asian Pac. J. Cancer Prev.* **2018**, *19*, 2057–2070. [CrossRef] [PubMed]
45. Zardi, E.M.; De Sio, I.; Ghittoni, G.; Sadun, B.; Palmentieri, B.; Roselli, P.; Persico, M.; Caturelli, E. Which clinical and sonographic parameters may be useful to discriminate NASH from steatosis? *J. Clin. Gastroenterol.* **2011**, *45*, 59–63. [CrossRef]
46. Chalasani, N.; Wilson, L.; Kleiner, D.E.; Cummings, O.W.; Brunt, E.M.; Ünalp, A. Relationship of steatosis grade and zonal location to histological features of steatohepatitis in adult patients with non-alcoholic fatty liver disease. *J. Hepatol.* **2008**, *48*, 829–834. [CrossRef]
47. Liang, R.J.; Wang, H.H.; Lee, W.J.; Liew, P.L.; Lin, J.T.; Wu, M.S. Diagnostic value of ultrasonographic examination for nonalcoholic steatohepatitis in morbidly obese patients undergoing laparoscopic bariatric surgery. *Obes. Surg.* **2007**, *17*, 45–56. [CrossRef]

48. Ballestri, S.; Lonardo, A.; Romagnoli, D.; Carulli, L.; Losi, L.; Day, C.P.; Loria, P. Ultrasonographic fatty liver indicator, a novel score which rules out NASH and is correlated with metabolic parameters in NAFLD. *Liver Int.* **2012**, *32*, 1242–1252. [CrossRef]
49. Fracanzani, A.L.; Valenti, L.; Bugianesi, E.; Andreoletti, M.; Colli, A.; Vanni, E.; Bertelli, C.; Fatta, E.; Bignamini, D.; Marchesini, G.; et al. Risk of severe liver disease in nonalcoholic fatty liver disease with normal aminotransferase levels: A role for insulin resistance and diabetes. *Hepatology* **2008**, *48*, 792–798. [CrossRef]
50. Ahmed, M. Non-alcoholic fatty liver disease in 2015. *World J. Hepatol.* **2015**, *7*, 1450–1459. [CrossRef]
51. Herold, C.; Ganslmayer, M.; Ocker, M.; Zopf, S.; Gailer, B.; Hahn, E.; Schuppan, D. Inducibility of microsomal liver function may differentiate cirrhotic patients with maintained compared with severely compromised liver reserve. *J. Gastroenterol. Hepatol.* **2003**, *18*, 445_449. [CrossRef]
52. Banasch, M.; Ellrichmann, M.; Tannapfel, A.; Schmidt, W.E.; Goetze, O. The non-invasive 13C-methionine breath test detects hepatic mitochondrial dysfunction as a marker of disease activity in non-alcoholic steatohepatitis. *Eur. J. Med. Res.* **2011**, *16*, 258–264. [CrossRef] [PubMed]
53. Miele, L.; Greco, A.; Armuzzi, A.; Candelli, M.; Forgione, A.; Gasbarrini, A.; Gasbarrini, G. Hepatic mitochondrial beta-oxidation in patients with nonalcoholic steatohepatitis assessed bij 13C-octanoate breath test. *Am. J. Gastroenterol.* **2003**, *98*, 2335–2336. [CrossRef] [PubMed]
54. Dixon, J.B.; Bhathal, P.S.; O'Brien, P.E. Nonalcoholic fatty liver disease: Predictors of nonalcoholic steatohepatitis and liver fibrosis in the severely obese. *Gastroenterology* **2001**, *121*, 91–100. [CrossRef] [PubMed]
55. Hukkanen, J.; Jacob, P.; Peng, M.; Dempsey, D.; Benowitz, N.L. Effect of nicotine on cytochrome P450 1A2 activity. *Br. J. Clin. Pharmacol.* **2011**, *72*, 836–838. [CrossRef]
56. Caubet, M.S.; Laplante, A.; Caillé, J.; L, B.J. 13C aminopyrine and 13C caffeine breath test: Influence of gender, cigarette smoking and oral contraceptives intake. *Isot. Environ. Health Stud.* **2002**, *38*, 71–77. [CrossRef]

biomedicines

MDPI

Review

Extracellular Vesicles as Drivers of Non-Alcoholic Fatty Liver Disease: Small Particles with Big Impact

David Højland Ipsen and Pernille Tveden-Nyborg *

Department of Veterinary and Animal Sciences, Section of Experimental Animal Model, University of Copenhagen, Ridebanevej 9, 1870 Frederiksberg, Denmark; dhi@sund.ku.dk
* Correspondence: ptn@sund.ku.dk; Tel.: +45-35-33-31-67

Abstract: Nonalcoholic fatty liver disease (NAFLD) is becoming the leading chronic liver disease, negatively affecting the lives of millions of patients worldwide. The complex pathogenesis involves crosstalk between multiple cellular networks, but how the intricate communication between these cells drives disease progression remains to be further elucidated. Furthermore, the disease is not limited to the liver and includes the reprogramming of distant cell populations in different organs. Extracellular vesicles (EVs) have gained increased attention as mediators of cellular communication. EVs carry specific cargos that can act as disease-specific signals both locally and systemically. Focusing on NAFLD advancing to steatohepatitis (NASH), this review provides an update on current experimental and clinical findings of the potential role of EVs in hepatic inflammation and fibrosis, the main contributors to progressive NASH. Particular attention is placed on the characteristics of EV cargos and potential specificity to disease stages, with putative value as disease markers and treatment targets for future investigations.

Keywords: nonalcoholic fatty liver disease; nonalcoholic steatohepatitis; extracellular vesicles

Citation: Ipsen, D.H.; Tveden-Nyborg, P. Extracellular Vesicles as Drivers of Non-Alcoholic Fatty Liver Disease: Small Particles with Big Impact. *Biomedicines* **2021**, *9*, 93. https://doi.org/10.3390/biomedicines9010093

Received: 21 December 2020
Accepted: 16 January 2021
Published: 19 January 2021

1. Introduction

Nonalcoholic fatty liver disease (NAFLD) affects 25% of the world's population and encompasses a spectrum of hepatic conditions ranging from hepatic steatosis (termed NAFL) to inflammation (NASH), which can progress to fibrosis and ultimately cirrhosis [1]. Perplexingly, while considered a progressing disease, only up to 30% of NAFLD patients develop NASH, and it remains unclear what factors cause some patients to progress while others do not [1]. Hepatic lipid levels are increased in the early disease stages and are linked to the pathogenesis of the disease. Lipids such as free fatty acids, free cholesterol, diacylglycerols, ceramides, and phospholipids accumulate in hepatocytes with cell-damaging effects through lipotoxicity [2]. These lipotoxic hepatocytes are then capable of triggering and sustaining an inflammatory signaling cascade, proposedly through the release of extracellular vesicles (EVs) [2]. EVs are a small heterogeneous collection of particles released by cells and are characterized into three broad categories based on their size and biogenesis (Figure 1). Exosomes originate from the endosome and are the smallest EVs (30–150 nm in diameter). Microvesicles are larger (100–1000 nm in diameter) and are formed by the outward budding of the plasma membrane. Lastly, apoptotic bodies (50–5000 nm in diameter and usually in the large end of the scale) are released by dying cells [3,4]. However, differences in the techniques used to isolate EVs can make it hard to discriminate specific subpopulations, and consequently this review will not focus on specific subpopulations and collectively refer to all as EVs [5].

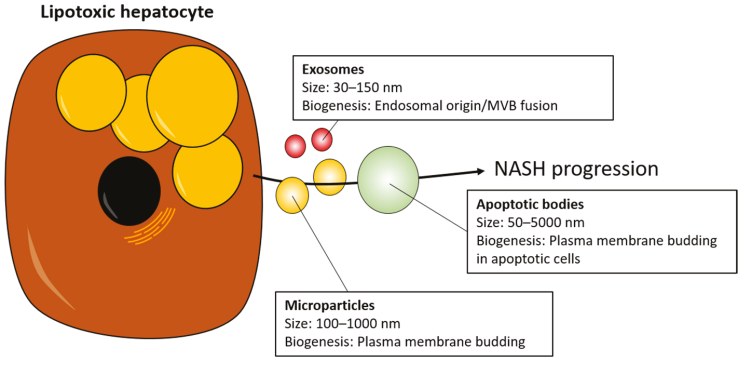

Figure 1. Lipotoxic hepatocytes release extracellular vesicles (EVs). Lipotoxic hepatocytes release EVs of various sizes and origins that can be subdivided into exosomes, microparticles, and apoptotic bodies. Exosome biogenesis is initiated by the inward budding of the endosomal membrane resulting in the formation of MVBs. These MVBs can then fuse with the plasma membrane, which releases the exosomes into the extracellular space. Both microparticles and apoptotic bodies result from the direct outward budding of the plasma membrane, with the latter from apoptotic cells [6]. MVB: multivesicular bodies. NASH: nonalcoholic steatohepatitis. Large, yellow circles: Intracellular lipid vesicles in hepatocyte; Black circle: Hepatocyte nucleus.

EVs facilitate cell-to-cell communication by delivering a specific cargo to recipient cells. The EV cargo is dynamic, and its content of nucleic acids, proteins, and lipids depends on the cell of origin and the status of that cell [5]. By delivering their cargos, EVs can promote or inhibit specific signaling pathways in the recipient cell and alter its phenotype, thereby playing an important role in disease development including NAFLD and progression to NASH. Whereas healthy hepatocytes produce EVs needed for cell survival and proliferation, stressed lipotoxic hepatocytes enhance the release of EVs that are able to promote disease progression by facilitating inflammation and fibrogenesis [7]. In this way, EVs contribute to hepatic inflammation via the recruitment of circulating immune cells and to hepatic fibrosis through the activation of hepatic stellate cells (HSCs), hereby promoting NASH progression [2]. The dynamic and varied cargos of EVs also suggest that they may act in different ways at different disease stages [6]. However, the role of EVs in cellular communication is intricate, and our understanding of EV function in NAFLD is rapidly changing. This review summarizes recent findings of EVs involvement in two of the major events in NAFLD progression: inflammation and fibrosis. We focus on the specific cargo mediating these effects in order to highlight potential therapeutic targets and potential disease biomarkers.

2. NASH Pathogenesis in Brief

The progression from a stage of bland steatosis to hepatic inflammation hallmarks the development of NASH. Lipotoxicity results in endoplasmic reticulum stress, lysosomal dysfunction, inflammasome activation, and cell death that collectively promotes the inflammation and infiltration of circulating immune cells [2]. The immunogenic environment of NASH is extremely complex and comprised of several cell types including monocytes, macrophages, neutrophils, natural killer cells, natural killer T cells, and T cells, infiltrating the liver and releasing a plethora of proinflammatory and -fibrogenic signaling molecules that promote disease progression and enhance the recruitment of additional immune cells in a self-sustaining feedforward loop [8]. Ultimately, chronic inflammation and injury signals activates HSCs which otherwise lie quiescent in the liver [9]. Activated HSCs are the primary cell type responsible for hepatic fibrosis and are characterized by increased proliferation and migration in addition to enhanced the production and deposition of extracellular matrices [9,10]. At the same time, they interact with infiltrating and

resident immune cells as well as other hepatic cells to maintain a proinflammatory and -fibrogenic milieu [10]. Liver injury, including NAFLD, also results in the capillarization of liver sinusoidal endothelial cells (LSECs) with the ensuing loss of both fenestration and LSEC differentiation [11]. Concomitantly, LSECs become unable to suppress HSC activation, which further promotes fibrosis [12]. Ultimately, the development of hepatic fibrosis hallmarks a more serious stage of the disease associated with a substantial increase in mortality [13].

NAFLD is not restricted to the liver. Intercellular and interorgan communication is central to disease development and progression and to the association with several serious co-morbidities in humans such as type 2 diabetes, cardiovascular disease, and adipose tissue dysfunction [14–16]. Although, the liver seems to actively contribute to a reprogramming of distant cell populations and the promotion of disease development in other organ systems, the precise nature of the crosstalk between the affected organs is not fully understood [17]. A more in-depth knowledge of the cellular communications network involved in NAFLD progression not only constitutes an important research objective, but may also constitute an attractive therapeutic option, e.g., by manipulating specific networks, blocking progression and/or promoting the resolution of disease.

3. EVs as Mediators of NASH Progression

3.1. EVs Promote Inflammation

The chemotaxis, adhesion, and infiltration of circulating immune cells with subsequent establishment of a proinflammatory phenotype are crucial features in NASH, which is maintained by both tissue resident Kupffer cells (especially in early disease stages) and bone marrow-derived macrophages [17,18]. NAFLD research has consequently targeted the determination of factors that leads to the activation and recruitment of these immune cells, of which EVs are gaining increased attention [18]. The injection of circulating EVs isolated from high-fat-fed mice with NAFLD into chow-fed mice led to the hepatic accumulation of immature myeloid cells and increased levels of alanine and aspartate aminotransferase, linking EV signaling to alterations in hepatic health [19]. In contrast, EVs isolated from the chow-fed control mice did not elicit a similar response, implicating a proinflammatory role of EVs following the ingestion of an unhealthy diet [19]. This could be important in NASH, as patients are reported to ingest unhealthy diets high in fat and sugar, similar to diets used to induce hepatic steatosis in animal models [20]. Supporting a key role in inflammation, EVs are linked to immune cell chemotaxis. In vitro, lipotoxic hepatocytes increased EV production and released EVs containing C-X-C motif chemokine ligand 10 (CXCL10) through a mixed linage kinase 3 (MLK-3)-dependent mechanism [21]. These EVs increased the migration of bone marrow-derived macrophages in vitro, which could subsequently be blocked by CXCL10-neutralizing antisera. In vivo, CXCL10 knockout decreased hepatic macrophage infiltration in a murine model of diet-induced NAFLD [21]. Interestingly, the migratory induction by CXCL10 was more potent when packaged into EVs compared to the free chemokine, highlighting a role of EV signaling in the pathogenesis of NALFD [21] (Figure 2). Substantiating the clinical relevance of these findings, increased circulating levels of CXCL10 have been reported in NASH patients compared to in both patients with only steatosis and healthy controls [22]. Additionally, both MLK-3 and CXCL10 expressions were increased in the livers of NASH patients [21,22].

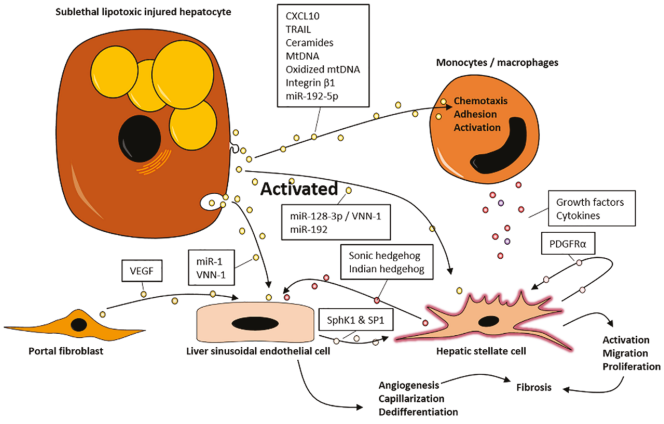

Figure 2. EVs as mediators of disease progression in NASH. EVs released by lipotoxic hepatocytes contain CXCL10, TRAIL, ceramides, mtDNA, oxidized mtDNA, integrin β1, and miR-192-5p that induce monocyte/macrophage chemotaxsis and promote a proinflammatory phenotype. Subsequently, activated immune cells release a plethora of cytokines and growth factors that activate hepatic stellates cells, thereby promoting fibrosis. Hepatic stellate cells may also be directly activated by miR-128-3p in VNN-1-expressing EVs and by EVs containing miR-192. Fibrosis is further facilitated by hepatocyte EVs carrying miR-1 and VNN-1 to liver sinusoidal endothelial cells resulting in angiogenesis, which is an important step in fibrosis. Likewise, portal fibroblasts may induce angiogenesis by releasing EVs containing VEGF. The hepatic stellate cells also actively contribute to disease progression via EV release, which reprogram recipient liver sinusoidal endothelial cells causing changes in their gene expression profile towards capillarization. Furthermore, liver sinusoidal endothelial cells may also promote hepatic stellate cell activation through EVs containing SphK1 and S1P, while the stellate cells themselves may initiate a self-sustaining signaling mechanism by releasing PDGFRα-enriched EVs. CXCL10: C-X-C motif chemokine ligand 10; mtDNA: mitochondrial DNA; PDGFRα: platelet-derived growth factor receptor α. S1P: sphingosine-1-phosphate. SphK1: sphingosine kinase 1. TRAIL: tumor necrosis factor-related apoptosis-inducing ligand. VEGF: vascular endothelial growth factor. VNN1: vanin 1.

EVs may also contain bioactive lipid species (Figure 2). Lipotoxicity in cultured hepatocytes-induced stress in the endoplasmatic reticulum (ER) was mediated by inositol requiring enzyme 1α (IRE1α) and caused release of EVs enriched in C16:0 ceramide [23]. When added to murine bone marrow-derived macrophages in vitro, the ceramide metabolite sphingosine-1-phosphate (S1P) promoted macrophage migration, which could be blocked by sphingosine kinase (SphK) that catalyzes the formation of S1P inhibitors and S1P receptor inhibitors, supporting a link between lipotoxicity and macrophage recruitment in NAFLD [23]. The inhibition of S1P signaling reduced hepatic inflammation and fibrosis in a mouse model of NASH, further supporting the role of cytotoxic lipids in promoting the disease [24]. In humans, the ceramide content in EVs was reported to be higher in patients with steatosis or NASH compared to in obese controls, and ceramide concentrations were nominally higher in NASH patients compared to in patients with only steatosis [23]. IRE1α activation also increased ceramide synthesis, resulting in augmented EV production and increased hepatic macrophage accumulation in mice with NAFLD [25]. Moreover, the intravenous injection of these EVs enhanced hepatic macrophage accumulation in otherwise healthy mice [25]. Collectively, this suggests a mechanistic link between EVs released via IRE1α activation and subsequent ceramide synthesis and the hepatic infiltration of macrophages in NAFLD/NASH [25].

The progressing oxidative stress and lipid overload in NASH eventually lead to mitochondrial dysfunction and potential oxidative damage to the mitochondrial DNA [26,27].

EVs from obese patients with liver injury (elevated alanine aminotransferase) contained increased levels of oxidized mitochondrial DNA compared to from lean controls [28]. These EVs and the isolated mitochondrial DNA could activate toll-like receptor 9, which belongs to a family of receptors that are widely implicated in NASH [18,28]. Total or lysosome-expressing cell-specific knockout of toll-like receptor 9 (e.g., in Kupffer cells and infiltrating macrophages) protects against NASH, suggesting an additional connection between EVs and the progression of inflammation [28]. Following chemotaxis, the adhesion of arriving immune cells to LSECs constitutes a critical step in NASH-related liver inflammation, in which immune cells must pass through the fenestrated capillary wall to enter the hepatic parenchyma. EVs derived from in vitro cultured lipotoxic hepatocytes contained integrin β1, which has been shown to contribute to cell adhesion [29]. These lipotoxic hepatocyte-derived EVs appeared to enhance the adhesion of primary mouse monocytes to liver endothelial sinusoidal cells, hereby promoting the monocyte infiltration of the liver parenchyma [29]. Corroborating these findings, anti-integrin β1 treatment attenuated hepatic inflammation by decreasing monocyte trafficking to the liver in mice with diet-induced NASH [29].

In addition, EVs contribute to hepatic inflammation by inducing a proinflammatory phenotype in recipient cells (Figure 2). Accordingly, ER stress in cultured lipotoxic hepatocytes prompted the production of EVs through the ligand-independent activation of death receptor 5 (DR5) and rho-associated, coiled-coil-containing protein kinase 1 (ROCK1) pathways [30,31]. These EVs contained more than 2000 proteins including tumor necrosis factor-related apoptosis-inducing ligand (TRAIL), which in turn was able to activate DR5 possibly promoting further EV production [31]. The activation of DR5 on macrophages by TRAIL-containing EVs in vitro stimulated the NF-κB pathway to induce a proinflammatory phenotype characterized by the increased production of IL6 and IL1β [31]. Likewise, EVs isolated from NASH patients induced similar effects on macrophages in vitro [31]. These findings support the link between hepatocyte lipotoxicity and macrophage-mediated inflammation and suggest the inhibition of ROCK1-facilitated EV release as a therapeutic target in NASH [31].

In addition to lipids, cytokines, and oxidized molecules, EVs also transport a diverse range of noncoding cargos including miRNAs, which can alter gene transcription in recipient cells. In both patients and animal models of NASH, EVs contained increased amounts of miR-192-5p compared to in healthy controls and expressed markers (ASGPR1 and CYP2E1) consistent with a hepatocyte origin [32]. In vitro, EVs released by lipotoxic hepatocytes were taken up by macrophages and delivered miR-192-5p [32]. Subsequently, miR-192-5p promoted macrophage activation by signaling through Rictor (rapamycin-insensitive companion of mammalian target of rapamycin) to reduce the phosphorylation of Akt and FoxO1, ultimately resulting in the transcription of proinflammatory genes (*iNOS*, *IL6*, and *TNFa*) [32]. EVs released from lipotoxic hepatocytes were taken up by other hepatocytes and macrophages, leading to NLRP3 inflammasome activation and IL1β secretion in vitro [33]. Thus, lipotoxicity also sustains hepatic inflammation by facilitating the production of EVs that can reprogram hepatocytes and macrophages. As mentioned, the oxidative stress and oxidization of mitochondrial DNA play a role in the recruitment of inflammatory cells to the liver, but may also contribute directly to the activation of macrophages. Accordingly, the treatment of primary hepatocytes with H_2O_2 enhanced the production of EVs enriched with mitochondrial DNA that in turn induced the expression of inflammatory genes (*Tnfa*, *Il1b*, and *Il6*) in macrophages in vitro [34]. Notably, the activation of IL22 signaling altered EV cargos by decreasing the amount of mitochondrial DNA in vitro and in vivo suggesting that increased IL22 may be protective for NASH progression and potentially valuable as a therapeutic target [34]. In support, a phase 2a open-label study found that IL22 therapy (n = 18) was effective against alcoholic steatohepatitis [35]. Collectively, these results support a clear relationship between hepatocyte lipotoxicity and the subsequent development of hepatic inflammation. Importantly, a range of these studies have reported induced lipotoxicity without overt cell death, which is similar to

the pathogenesis in vivo [21,23,31]. Thus, they underline a direct link between sublethal injury/stress induced by cytotoxic lipids in hepatocytes and the proinflammatory response as necessary for disease progression towards NASH.

3.2. EVs Promote Fibrosis

The risk of all-cause mortality and liver-related events increases with fibrosis progression (i.e., fibrosis stage) in patients with NAFLD [13]. Consequently, the development of fibrosis and the underlying mechanisms constitute a critical therapeutic target and endpoint in NAFLD research, with HSCs assumed as a pivotal role. Similar to inflammation, the links between lipid-laden hepatocytes and HSC activation remains poorly understood. EVs isolated from the plasma of high fat-fed NAFLD mice activated HSCs in vitro and increased mRNA levels of fibrosis-related genes *Col1a1*, *Col3a1*, *Mmp2*, and *Timp1* [36]. However, the EV cargo, which mediated this effect, was not characterized [36].

HSC activation is associated with decreased peroxisome proliferator-activated receptor γ (PPARγ) expression, while PPARγ agonists can reduce liver fibrosis in NASH patients [37]. miR-128-3p regulates PPARγ, and the expression of this miRNA was increased in the livers of both high fat- and choline-deficient amino acid-defined animal models of NAFLD [38]. Interestingly, lipotoxic hepatocytes released EVs containing increased levels of miR-128-3p, and these EVs suppressed PPARγ expression and promoted HSCs migration, proliferation, and activity in vitro [38]. The uptake of EVs was, partly, dependent on vanin-1 expression on the EV surface, with vanin-1-neutralizing antibodies leading to a decreased HSC activation in vitro and exemplifying the therapeutic potential of targeting EVs in the treatment of NASH [38] (Figure 2). The microarray analysis of EVs released by cultured lipotoxic hepatocytes identified 314 differentially regulated miRNAs compared to healthy hepatocytes [39]. In vitro, EVs from these lipotoxic hepatocytes increased the expression of the fibrogenic genes *ACTA2* (αSMA), *TGFB*, and *COL1A1* in HSCs, and this effect was, at least partially, mediated by miR-192 [39]. IL17 has been implicated in liver fibrosis, but the initial cellular origin and underlying signaling pathways are not yet fully elucidated, although EVs are likely to play a role [40]. Accordingly, EVs from CCl_4-treated hepatocytes promoted CCL20 and IL17A production in HSCs by signaling through toll-like receptor 3 in vitro. In response to CCL20/IL17A, IL17A production was substantially enhanced in γδ T cells [40].

Angiogenesis is mediated by LSECs and correlates positively with the degree of liver fibrosis in patients with NASH [41,42]. Located in the space of Disse, LSECs are anatomically situated close to HSCs and may play a role in their activation, although it is currently unclear how this takes place. Human umbilical vascular endothelial cells exposed to EVs released from lipotoxic hepatocytes increased migration and tube formation in vitro [43]. Similarly, derived EVs also promoted angiogenesis in vivo in mice [43]. In contrast, EVs isolated from mice fed a high fat and high carbohydrate diet did not induce angiogenesis in vitro [43]. However, mice in the latter study developed less severe NASH, indicating that proangiogenic EVs are only produced at later disease stages, at least in mice. Nevertheless, the angiogenic effects of the EVs were found to be dependent on EV internalization mediated by vanin-1 [43] (Figure 2). In conjunction with the role of vanin-1-positive EVs in HSC activation, these results support that vanin-1-positive EVs may be explored as therapeutic targets in NASH [38,43]. Clonally-derived rat HSCs activated by platelet-derived growth factor (PDGF)-BB in vitro produced EVs containing both sonic and indian hedgehog and induced gene expression changes associated with capillarization and nitric oxide in primary LSECs, thereby potentially contributing to the vascular changes associated with liver fibrosis [44]. Cytotoxic lipids transported by EVs also affect fibrogenesis. Similarly, circulating EVs containing increased levels of SphK1 and SP1 were found in mice with CCl_4-induced liver fibrosis [45]. EVs from SphK1-overexpressing LESCs contained increased levels of SphK1 and SP1 and induced HSC migration in vitro [45]. This accentuates that EVs can function as mediators of lipotoxicity and that they are able to transfer harmful lipid species to recipient cell populations, leading to changes in expression patterns and phenotypes

supporting EVs as central in the LSEC–HSC communication network. In healthy primary hepatocytes, EVs deliver SphK2, which increases S1P synthesis in recipient hepatocytes and promotes proliferation and liver regeneration following ischemia/reperfusion injury or partial hepatectomy [46]. This further supports the EVs role as dynamic vehicles of signal transfer between cell populations in the liver and implies SphK-/S1P signaling to be context-dependent [46].

The communication between vasculature and myofibroblasts (such as HSCs) is not unidirectional as a portal myofibroblasts signal to endothelial cells and promotes angiogenesis via EVs containing vascular endothelial growth factor A both in vivo and in vitro [47]. Furthermore, the expression of the portal myofibroblast marker *COL15A1* was increased in liver samples from patients with NASH and advanced fibrosis (bridging/cirrhosis), but not in patients with mild–moderate fibrosis or bland steatosis compared to in healthy controls [47]. *COL15A1* expression correlated with the endothelial marker von Willebrand factor, suggesting a link between fibrosis and angiogenesis [47]. Thus, EV-mediated angiogenesis may be an important contributor to the fibrogenesis from the portal areas in NASH (Figure 2). Still, fibrosis initially has a centrivenular origin in adult NASH, and the vast majority of myofibroblasts are derived from HSCs in NAFLD. HSCs rather than portal myofibroblats may, therefore, be a more relevant target for future antifibrotic treatments in NASH [9,48]. HSCs are not only affected by EVs released by other cells, but also release EVs that serve in a paracrine manner to activate additional HSCs and promote fibrosis. In vitro, EVs released by activated HSCs contained 337 different proteins associated with extracellular spaces or matrices and collagens, whereas quiescent HSCs produced EVs containing only 46 proteins that mainly associated with histones and keratins [49]. EVs extracted from activated HSCs enhanced the expression of fibrogenic genes (connective tissue growth factor (*Ctgf/Ccn2*), *Col1a1*, and *Acta2* (αSMA) in quiescent HSCs in vitro. Conversely, EVs from quiescent HSCs decrease fibrogenic gene expression in activated HSCs [49]. Cultured quiescent HSCs have also been shown to produce twist-related protein 1-containg EVs in turn promoting miR-214 expression [50]. These EVs inhibited the expression of CTGF in recipient HSCs, thereby ablating fibrogenic signaling [50]. Conversely, miR-214 and twist-related protein 1 levels were much lower in EVs isolated from activated HSCs in vitro, which could make these EVs less effective for suppressing fibrogenic signaling [50]. Moreover, levels of miR-214 and miR-199a-5p were increased in EVs from quiescent HSCs compared to from activated HSCs in vitro [51,52]. EVs released by quiescent HSCs and subsequently internalized by activated HSCs decrease the expression of markers of activation/fibrogenesis (CTGF/CCN2, COL1A1, and ACTA2 (αSMA)) in vitro [51,52]. Hence, EV-transported miRs seems to be important factors in the regulation of the HSC phenotype and hepatic fibrosis.

PDGF induces HSC proliferation and migration by binding to PDGF receptors [53]. PDGF plays a central role in NASH and is secreted by several cell types implicated in disease development and progression, including Kupffer cells, monocyte-derived macrophages, and biliary epithelial cells [53]. PDGF receptor α was enriched in circulating EVs isolated from cirrhotic patients with alcoholic-related liver disease, and in vitro cultured HSCs treated with PDGF-BB release PDGFRα-enriched EVs in a Src homology 2 domain tyrosine phosphatase 2 (SHP2)-dependent manner [54]. These EVs promoted migration of cultured HSCs and enhanced liver fibrosis when administrated to CCl_4-treated or bile duct-ligated mice [54]. Subsequent inhibition of SHP2 ameliorated fibrosis [54]. Mechanistically, SHP2 induced mTOR signaling, in turn inhibiting HSC autophagy and promoting the release of profibrogenic EVs [54]. This highlights an important role of autophagy in HSC-mediated liver fibrosis [55]. Together, these results illustrate a role of HSCs in the paracrine signaling associated with hepatic fibrosis and suggest that the activation of HSCs leads to qualitative and quantitative changes in their EV cargos, which can alter other HSCs and drive fibrosis progression. Conversely, an altered EV cargo may reduce HSC activation and inhibit profibrotic signaling.

4. EVs May Promote NASH via Organ Crosstalk

The detrimental effects of NASH are interlinked with other organ systems between which considerable crosstalk occurs. Accordingly, NASH is not only associated with increased risk of liver-related mortality, but also with cardiovascular death, type 2 diabetes mellitus, and chronic kidney disease [56]. However, the interplay between the liver and other organs in NAFL and NASH remains poorly understood. Recent reports suggest the liver as central in altering expression patterns in distant organs in response to lipid overload [57]. In mice, high-fat feeding leads to an accumulation of lipids in the liver prior to the accumulation in adipose tissue [57]. The increase in intrahepatic lipids leads to a geranylgeranyl diphosphate synthase (Ggpps)-dependent secretion of hepatocyte-derived EVs that enhanced lipid accumulation in preadipocytes in vitro [57]. This effect was mediated, at least in part, by the miRNA let-7e-5p, which enhanced adipocyte lipogenesis while decreasing fatty acid oxidation and increasing lipid accumulation. Furthermore, the adipose tissue fat mass decreased significantly in high fat-fed mice with liver-specific *Ggpps* knockout [57]. This seminal study emphasizes a role of the liver–adipose tissue axis and organ-to-organ signaling during NAFLD as well as a crucial role of hepatocyte-derived EVs in promoting metabolic adaptation in adipose tissue. Furthermore, EVs released by human subcutaneous and omental adipose tissue ex vivo inhibited insulin-mediated Akt phosphorylation in hepatocytes in vitro, suggesting the existence of a bidirectional communication between adipose cells and hepatocytes [58]. Cultured lipotoxic hepatocytes released EVs containing more than 500 differentially regulated miRNAs with a marked upregulation of miR-1. Subsequent in vitro and in vivo studies found that these EVs facilitate the crosstalk between the liver and vascular endothelium in NAFLD [59]. The EVs from lipotoxic hepatocytes delivered miR-1 to endothelial cells leading to endothelial inflammation and atherosclerosis, and the inhibition of miR-1 decreased the inflammation and the size of atherosclerotic lesion in high fat-fed *ApoE*$^{-/-}$ mice, directly linking NAFLD-induced lipotoxicity to cardiovascular disease through the composition of EV cargos [59].

5. EVs as Biomarkers in Patients with NASH

At present, the diagnosis of NASH relies almost exclusively on histopathological features assessed in liver biopsies. The procedure is costly, invasive and prone to sample variability, thereby constituting a major limiting factor in NASH research [60]. Although other diagnostic tools such as imaging techniques and serum markers are available and show promise, they are not unequivocally associated with disease progression, and there is a clear and urgent need to develop additional noninvasive procedures for accurate NASH diagnosis and longitudinal monitoring of disease development [61,62]. Since EVs are released to the circulation, they may well constitute an attractive option for a noninvasive diagnostic marker (Table 1).

Table 1. Cargos of circulating EVs as biomarkers in patients diagnosed with NAFLD.

Study Design & NAFLD Diagnosis	Cellular Source	EV Cargo
Cirrhotic NASH (*n* = 25, F4), pre-cirrhotic NASH (*n* = 25, F3) and healthy control (*n* = 25). Biopsy [63]	Total circulating and hepatocyte (ASGPR1- or SLC27A5-positive)	Proteomic signature of circulating EVs differentiates advanced NASH (F3 + F4) from healthy controls (AUROC = 0.77) and precirrhotic from cirrhotic NASH (AUROC = 0.80)
NAFLD (*n* = 67) vs. HCV patients (*n* = 42) or healthy controls (*n* = 44). Biopsy [64]	iNKT (Vα24/Vα11 positiv) or macrophages/monocytes (CD14^{+})	Number of iKT EVs to differentiate NAFLD from controls (AUROC= 0.92) and HCV (AUROC = 0.97) Number of CD14^{+} EVs differentiate NAFLD from controls (AUROC = 0.83) and HCV (AUROC > 0.99)

Table 1. *Cont.*

Study Design & NAFLD Diagnosis	Cellular Source	EV Cargo
Advanced NAFLD, fibrosis 3 and 4 (n = 9) vs. early NAFLD, fibrosis 0–2 (n = 17). Biopsy [65]	Leukocytes ($CD14^+$ or $CD16^+$) Endothelial cells (either $CD105^+$ $CD31^+$ $CD41/CD42^-$, $CD105^+$ $CD31^-$ $CD41/CD42^-$, or $CD105^-$ $CD31^+$ $CD41/CD42^-$)	↓ Number of leucocyte and endothelial cell EVs in advanced NAFLD
NASH with mild (F1–2) fibrosis (n = 17) vs. steatosis (n = 8). Biopsy [29]	Not examined	↑ Integrin β1 in NASH
NASH F0–1 fibrosis (n = 16) vs. bland steatosis (n = 16) or obese controls (n = 11). Biopsy for some [23]	Not examined	↑ C16:0 ceramides and S1P in bland steatosis and NASH. Nominally increased in NASH vs. bland steatosis
Obese/high ALT (n = 9) vs. obese/normal ALT (n = 19) or lean/normal ALT (n = 19). Elevated ALT [28]	Hepatocyte (ARG1 positive, CD41 negative)	↑ mtDNA in obese with high ALT
NASH (n = 47), steatosis (n = 30) and health controls (n = 19). Biopsy [66]	Not examined	↑ miRNA-122, -192 and -375 in NASH vs. steatosis or healthy controls miRNA-122 could to a degree identify NASH (AUROC = 0.71) and fibrosis (AUROC = 0.61)
Advanced NAFLD (n = 3) vs. early NALFD (n = 3). Biopsy [39] †	Not examined	↑ miRNA-122 and -192 in advanced NAFLD
NASH (n = 31) vs. healthy controls (n = 37). Biopsy [32]	Hepatocyte (ASPPR1 and CYP2E1 positive)	↑ miR-192-5p in NASH
NASH (n = 12), hepatitis B (n = 4) and controls (n = 24). Biopsy [67]	Not examined	miRNA panel (miR-1225-5p, -1275, -368, -762, 320c, -451, -1974, -630, -1207-5p, -720, -1246, and -486-5p) distinguish NASH from HBV and controls with accuracies of 87.5% and 88.9%, respectively
NAFLD/NASH (n = 34) vs. healthy controls (n = 19). Biopsy [68]	Not examined	↑ miRNA-16, -34a, and -122 in NAFLD/NASH miRNA-16 (AUROC = 0.96) and miRNA-122 (AUROC = 0.93) differentiates NAFLD from healthy controls

† Early NALFD = grade 1 steatosis, grades 0–1 fibrosis. Advanced NAFLD = grade 2 steatosis, grades 2–3 fibrosis [39]. ALT: alanine aminotransferase; AUROC: Area under the receiver operating characteristics curve EVs: extracellular vesciles; iNKT: invariant natural killer T cells; NAFLD: nonalcoholic fatty liver disease; NASH: nonalcoholic steatohepatitis. Up and down arrows: Increased and decreased markers, respectively.

Compared to in healthy controls (n = 25), the number of circulating EVs was increased in NASH patients with cirrhosis (n = 25, F4) and also nominally increased in precirrhotic (n = 25, F3) NASH patients [63]. Hepatocyte-specific EVs (ASGPR1- or SLC27A5-positive) accounted for 20% of the circulating EVs and ASPGR1-positive EVs correlated with fibrosis stage, NAFLD fibrosis score, and the enhanced liver fibrosis (ELF) score (designed to diagnose severe fibrosis (grades 3 and 4)). In addition, the total number of hepatocyte EVs could identify clinically relevant portal hypertension in cirrhotic patients (AUROC = 0.79). Finally, the authors identified proteomic signatures in EVs that enabled a differentiation between advanced NASH (pooled F3 and F4) and healthy controls (AUROC = 0.77) and between precirrhotic and cirrhotic NASH (AUROC = 0.80) [63]. This supports that the protein cargo of circulating EVs may be specifically related to the disease stage and may therefore be used to diagnose and stage patients with NASH. Kornek et al. analyzed circulating EVs for six different cell surface markers belonging to major immune cell populations involved in liver inflammation and fibrosis [64]. The number of circulating EVs from invariant natural killer cells and $CD14^+$ monocytes/macrophages differentiated patients

with NAFLD (n = 67) from patients with hepatitis C (n = 42) and healthy controls (n = 44) and may represent a novel diagnostic tool for not only separating NAFLD patients from healthy individuals, but also differentiating between various chronic liver diseases [64]. In patients with NAFLD and advanced fibrosis (n = 9, grades 3 and 4), the numbers of circulating leucocyte and endothelial cell EVs were decreased compared to in NAFLD with no/mild fibrosis (n = 17, grades 0–2) [65]. Furthermore, adding either $CD14^+$ or $CD16^+$ EVs to the ELF score improved its diagnostic potential [65]. In plasma from patients with alcohol/hepatitis C virus-related cirrhosis (n = 91) compared to in healthy controls (n = 30), EVs from leuko-endothelial ($CD31^+/CD41^-$), lymphocyte ($CD4^+$), and erythrocyte ($CD235a^+$) were increased, and EV-bound cytokeratin-18 correlated positively with liver disease activity (Child-Pugh score and Model for End-Stage Liver Disease (MELD) score) [69]. Likewise, circulating cytokeratin-18 levels (not EV-associated) were also found to be increased in patients with NASH (n = 41) compared to in patients without NASH (n = 54) and could be applied diagnostically (AUROC = 0.86) [70]. Constituting another potential biomarker, EV-associated integrin β1 expression was shown to promote disease progression by facilitating monocyte recruitment, and these EVs were also increased in patients with NASH and mild (F1–2) fibrosis compared to in patients with steatosis [29].

In accordance with the central role of lipids in NAFLD, C16 ceramide and S1P concentrations were increased in EVs isolated from patients with steatosis and even further in patients with NASH and none/mild (F0–1) fibrosis compared to in obese controls [23]. Mitochondrial DNA was also increased in EVs from obese patients with elevated alanine aminotransferase levels compared to from lean controls [28]. However, aminotransferase levels poorly predict NAFLD/NASH, and additional studies are needed to investigate the potential of EVs expressing mitochondrial DNA as markers in patients with biopsy-confirmed disease. EV-associated miRNA levels may also be useful in identifying patients with NASH. A small study reported higher levels of miRNA-122 and -129 in advanced (n = 3) compared to in early (n = 3) NAFLD [39]. EVs from patients with NAFLD/NASH (n = 34) contained higher levels of miRNA-16, -34a, and -122 compared to from healthy controls (n = 19), and EV miRNA-16 and -122 could differentiate between NASH and controls (AUROC = 0.96 and 0.93, respectively) [68]. Likewise, miRNA-122, -192, and -375 were enriched in EVs from patients with NASH (n = 47) compared to from those with steatosis (n = 30) or healthy controls (n = 19), and EV miRNA-122 could, to some degree, predict NASH (AUROC = 0.71) and fibrosis (AUROC = 0.61) [66]. EV miR-192-5p levels were higher in NASH patients (n = 31) compared to in healthy controls (n = 37) and could be investigated further as a NASH biomarker [32]. The microarray analysis of "exosome rich fractionated RNA" from patients with NASH (n = 12), hepatitis B (n = 4), and controls (n = 24) identified a panel of 12 miRNAs, which could differentiate NASH from both controls and hepatitis B patients [67].

6. Conclusions

EVs released into the local hepatic environment and to the systemic circulation may directly contribute to the development and progression of NASH. Central to the production of these EVs are lipotoxic hepatocytes, and the EVs released by these cells provide a tangible link between the initial lipid accumulation in NAFLD and the subsequent development of hepatic inflammation and fibrosis. Why some cells succumb to the detrimental effects of lipotoxicity and the initiate production of EVs is a target for future investigations. Likewise, the susceptibility of recipient cells of uptake of lipotoxic EVs may also constitute an important checkpoint in disease progression. However, the role of EVs as signal carriers appears central in facilitating disease progression and reprogramming of cell populations in NAFLD/NASH.

Author Contributions: Conceptualization, D.H.I. and P.T.-N.; writing of the original draft preparation, D.H.I.; writing of review and editing, D.H.I. and P.T.-N. All authors have read and agreed to the published version of the manuscript.

Funding: This research received no external funding.

Institutional Review Board Statement: Not applicable.

Informed Consent Statement: Not applicable.

Data Availability Statement: No new data were created or analyzed in this study. Data sharing is not applicable to this article.

Conflicts of Interest: The authors declare no conflict of interest.

References

1. Younossi, Z.M.; Koenig, A.B.; Abdelatif, D.; Fazel, Y.; Henry, L.; Wymer, M. Global epidemiology of nonalcoholic fatty liver disease-Meta-analytic assessment of prevalence, incidence, and outcomes. *Hepatology* **2016**, *64*, 73–84. [CrossRef] [PubMed]
2. Ibrahim, S.H.; Hirsova, P.; Gores, G.J. Non-alcoholic steatohepatitis pathogenesis: Sublethal hepatocyte injury as a driver of liver inflammation. *Gut* **2018**, *67*, 963–972. [CrossRef] [PubMed]
3. Doyle, L.M.; Wang, M.Z. Overview of Extracellular Vesicles, Their Origin, Composition, Purpose, and Methods for Exosome Isolation and Analysis. *Cells* **2019**, *8*, 727. [CrossRef] [PubMed]
4. Dorairaj, V.; Sulaiman, S.A.; Abu, N.; Murad, N.A.A. Extracellular Vesicles in the Development of the Non-Alcoholic Fatty Liver Disease: An Update. *Biomolecules* **2020**, *10*, 1494. [CrossRef] [PubMed]
5. Szabo, G.; Momen-Heravi, F. Extracellular vesicles in liver disease and potential as biomarkers and therapeutic targets. *Nat. Rev. Gastroenterol. Hepatol.* **2017**, *14*, 455–466. [CrossRef] [PubMed]
6. Huang-Doran, I.; Zhang, C.-Y.; Vidal-Puig, A. Extracellular Vesicles: Novel Mediators of Cell Communication in Metabolic Disease. *Trends Endocrinol. Metab.* **2017**, *28*, 3–18. [CrossRef]
7. Hernández, A.; Arab, J.P.; Reyes, D.; Lapitz, A.; Moshage, H.; Banales, J.M.; Arrese, M. Extracellular Vesicles in NAFLD/ALD: From Pathobiology to Therapy. *Cells* **2020**, *9*, 817. [CrossRef]
8. Narayanan, S.; Surette, F.A.; Hahn, Y.S. The Immune Landscape in Nonalcoholic Steatohepatitis. *Immune Netw.* **2016**, *16*, 147–158. [CrossRef]
9. Mederacke, I.; Hsu, C.C.; Troeger, J.S.; Huebener, P.; Mu, X.; Dapito, D.H.; Pradere, J.-P.; Schwabe, R.F. Fate tracing reveals hepatic stellate cells as dominant contributors to liver fibrosis independent of its aetiology. *Nat. Commun.* **2013**, *4*, 2823. [CrossRef]
10. Schuppan, D.; Surabattula, R.; Wang, X.Y. Determinants of fibrosis progression and regression in NASH. *J. Hepatol.* **2018**, *68*, 238–250. [CrossRef]
11. Miyao, M.; Kotani, H.; Ishida, T.; Kawai, C.; Manabe, S.; Abiru, H.; Tamaki, K. Pivotal role of liver sinusoidal endothelial cells in NAFLD/NASH progression. *Lab. Investig.* **2015**, *95*, 1130–1144. [CrossRef] [PubMed]
12. Deleve, L.D.; Wang, X.; Guo, Y. Sinusoidal endothelial cells prevent rat stellate cell activation and promote reversion to quiescence. *Hepatology* **2008**, *48*, 920–930. [CrossRef] [PubMed]
13. Taylor, R.S.; Taylor, R.J.; Bayliss, S.; Hagström, H.; Nasr, P.; Schattenberg, J.M.; Ishigami, M.; Toyoda, H.; Wong, V.W.; Peleg, N.; et al. Association between Fibrosis Stage and Outcomes of Patients With Nonalcoholic Fatty Liver Disease: A Systematic Review and Meta-Analysis. *Gastroenterology* **2020**, *158*, 1611–1625.e2. [CrossRef] [PubMed]
14. Ballestri, S.; Zona, S.; Targher, G.; Romagnoli, D.; Baldelli, E.; Nascimbeni, F.; Roverato, A.; Guaraldi, G.; Lonardo, A. Nonalcoholic fatty liver disease is associated with an almost twofold increased risk of incident type 2 diabetes and metabolic syndrome. Evidence from a systematic review and meta-analysis. *J. Gastroenterol. Hepatol.* **2016**, *31*, 936–944. [CrossRef] [PubMed]
15. Labenz, C.; Huber, Y.; Michel, M.; Nagel, M.; Galle, P.R.; Kostev, K.; Schattenberg, J.M. Impact of NAFLD on the Incidence of Cardiovascular Diseases in a Primary Care Population in Germany. *Dig. Dis. Sci.* **2020**, *65*, 2112–2119. [CrossRef]
16. Ghorpade, D.S.; Ozcan, L.; Zheng, Z.; Nicoloro, S.M.; Shen, Y.; Chen, E.; Blüher, M.; Czech, M.P.; Tabas, I. Hepatocyte-secreted DPP4 in obesity promotes adipose inflammation and insulin resistance. *Nature* **2018**, *555*, 673–677. [CrossRef]
17. Gehrke, N.; Schattenberg, J.M. Metabolic Inflammation-A Role for Hepatic Inflammatory Pathways as Drivers of Comorbidities in Nonalcoholic Fatty Liver Disease? *Gastroenterology* **2020**, *158*, 1929–1947.e6. [CrossRef]
18. Parthasarathy, G.; Revelo, X.; Malhi, H. Pathogenesis of Nonalcoholic Steatohepatitis: An Overview. *Hepatol. Commun.* **2020**, *4*, 478–492. [CrossRef]
19. Deng, Z.-B.; Liu, Y.; Liu, C.; Xiang, X.; Wang, J.; Cheng, Z.; Shah, S.V.; Zhang, S.; Zhang, L.; Zhuang, X.; et al. Immature myeloid cells induced by a high-fat diet contribute to liver inflammation. *Hepatology* **2009**, *50*, 1412–1420. [CrossRef]
20. Younossi, Z.; Anstee, Q.M.; Marietti, M.; Hardy, T.; Henry, L.; Eslam, M.; George, J.; Bugianesi, E. Global burden of NAFLD and NASH: Trends, predictions, risk factors and prevention. *Nat. Rev. Gastroenterol. Hepatol.* **2018**, *15*, 11–20. [CrossRef]
21. Ibrahim, S.H.; Hirsova, P.; Tomita, K.; Bronk, S.F.; Werneburg, N.W.; Harrison, S.A.; Goodfellow, V.S.; Malhi, H.; Gores, G.J. Mixed lineage kinase 3 mediates release of C-X-C motif ligand 10-bearing chemotactic extracellular vesicles from lipotoxic hepatocytes. *Hepatology* **2016**, *63*, 731–744. [CrossRef] [PubMed]
22. Zhang, X.; Shen, J.; Man, K.; Chu, E.S.; Yau, T.O.; Sung, J.C.; Go, M.Y.; Deng, J.; Lu, L.; Wong, V.W.; et al. CXCL10 plays a key role as an inflammatory mediator and a non-invasive biomarker of non-alcoholic steatohepatitis. *J. Hepatol.* **2014**, *61*, 1365–1375. [CrossRef] [PubMed]

23. Kakazu, E.; Mauer, A.S.; Yin, M.; Malhi, H. Hepatocytes release ceramide-enriched pro-inflammatory extracellular vesicles in an IRE1alpha-dependent manner. *J. Lipid Res.* **2016**, *57*, 233–245. [CrossRef] [PubMed]
24. Mauer, A.S.; Hirsova, P.; Maiers, J.L.; Shah, V.H.; Malhi, H. Inhibition of sphingosine 1-phosphate signaling ameliorates murine nonalcoholic steatohepatitis. *Am. J. Physiol. Gastrointest. Liver Physiol.* **2017**, *312*, G300–G313. [CrossRef]
25. Dasgupta, D.; Nakao, Y.; Mauer, A.S.; Thompson, J.M.; Sehrawat, T.S.; Liao, C.-Y.; Krishnan, A.; Lucien, F.; Guo, Q.; Liu, M.; et al. IRE1A Stimulates Hepatocyte-derived Extracellular Vesicles That Promote Inflammation in Mice with Steatohepatitis. *Gastroenterology* **2020**, *159*, 1487–1503.e17. [CrossRef] [PubMed]
26. Ipsen, D.H.; Lykkesfeldt, J.; Tveden-Nyborg, P. Molecular mechanisms of hepatic lipid accumulation in non-alcoholic fatty liver disease. *Cell. Mol. Life Sci.* **2018**, *75*, 3313–3327. [CrossRef]
27. Léveillé, M.; Estall, J.L. Mitochondrial Dysfunction in the Transition from NASH to HCC. *Metabolites* **2019**, *9*, 233. [CrossRef]
28. Garcia-Martinez, I.; Santoro, N.; Chen, Y.; Hoque, R.; Ouyang, X.; Caprio, S.; Shlomchik, M.J.; Coffman, R.L.; Candia, A.; Mehal, W.Z. Hepatocyte mitochondrial DNA drives nonalcoholic steatohepatitis by activation of TLR9. *J. Clin. Investig.* **2016**, *126*, 859–864. [CrossRef]
29. Guo, Q.; Furuta, K.; Lucien, F.; Sanchez, L.H.G.; Hirsova, P.; Krishnan, A.; Kabashima, A.; Pavelko, K.D.; Madden, B.; Alhuwaish, H.; et al. Integrin beta1-enriched extracellular vesicles mediate monocyte adhesion and promote liver inflammation in murine NASH. *J. Hepatol.* **2019**, *71*, 1193–1205. [CrossRef]
30. Cazanave, S.C.; Mott, J.L.; Bronk, S.F.; Werneburg, N.W.; Fingas, C.D.; Meng, X.W.; Finnberg, N.; El-Deiry, W.S.; Kaufmann, S.H.; Gores, G.J. Death receptor 5 signaling promotes hepatocyte lipoapoptosis. *J. Biol. Chem.* **2011**, *286*, 39336–39348. [CrossRef]
31. Hirsova, P.; Ibrahim, S.H.; Krishnan, A.; Verma, V.K.; Bronk, S.F.; Werneburg, N.W.; Charlton, M.R.; Shah, V.H.; Malhi, H.; Gores, G.J. Lipid-Induced Signaling Causes Release of Inflammatory Extracellular Vesicles From Hepatocytes. *Gastroenterology* **2016**, *150*, 956–967. [CrossRef] [PubMed]
32. Liu, X.; Pan, Q.; Cao, H.; Xin, F.; Zhao, Z.; Yang, R.; Zeng, J.; Zhou, H.; Fan, J.-G. Lipotoxic Hepatocyte-Derived Exosomal MicroRNA 192-5p Activates Macrophages Through Rictor/Akt/Forkhead Box Transcription Factor O1 Signaling in Nonalcoholic Fatty Liver Disease. *Hepatology* **2020**, *72*, 454–469. [CrossRef] [PubMed]
33. Cannito, S.; Morello, E.; Bocca, C.; Foglia, B.; Benetti, E.; Novo, E.; Chiazza, F.; Rogazzo, M.; Fantozzi, R.; Povero, D.; et al. Microvesicles released from fat-laden cells promote activation of hepatocellular NLRP3 inflammasome: A pro-inflammatory link between lipotoxicity and non-alcoholic steatohepatitis. *PLoS ONE* **2017**, *12*, e0172575. [CrossRef] [PubMed]
34. Hwang, S.; He, Y.; Xiang, X.; Seo, W.; Kim, S.; Ma, J.; Ren, T.; Park, S.H.; Zhou, Z.; Feng, D.; et al. Interleukin-22 Ameliorates Neutrophil-Driven Nonalcoholic Steatohepatitis Through Multiple Targets. *Hepatology* **2020**, *72*, 412–429. [CrossRef]
35. Arab, J.P.; Sehrawat, T.S.; Simonetto, D.A.; Verma, V.K.; Feng, D.; Tang, T.; Dreyer, K.; Yan, X.; Daley, W.L.; Sanyal, A.; et al. An Open-Label, Dose-Escalation Study to Assess the Safety and Efficacy of IL-22 Agonist F-652 in Patients With Alcohol-associated Hepatitis. *Hepatology* **2019**, *72*, 441–453. [CrossRef]
36. McCommis, K.S.; Hodges, W.T.; Brunt, E.M.; Nalbantoglu, I.; McDonald, W.G.; Holley, C.L.; Fujiwara, H.; Schaffer, J.E.; Colca, J.R.; Finck, B.N. Targeting the mitochondrial pyruvate carrier attenuates fibrosis in a mouse model of nonalcoholic steatohepatitis. *Hepatology* **2017**, *65*, 1543–1556. [CrossRef]
37. Skat-Rordam, J.; Ipsen, D.H.; Lykkesfeldt, J.; Tveden-Nyborg, P. A role of peroxisome proliferator-activated receptor gamma in non-alcoholic fatty liver disease. *Basic Clin. Pharmacol. Toxicol.* **2019**, *124*, 528–537. [CrossRef]
38. Povero, D.; Panera, N.; Eguchi, A.; Johnson, C.D.; Papouchado, B.G.; Horcel, L.d.; Pinatel, E.M.; Alisi, A.; Nobili, V.; Feldstein, A.E. Lipid-induced hepatocyte-derived extracellular vesicles regulate hepatic stellate cell via microRNAs targeting PPAR-gamma. *Cell. Mol. Gastroenterol. Hepatol.* **2015**, *1*, 646–663e4. [CrossRef]
39. Lee, Y.-S.; Kim, S.Y.; Ko, E.; Lee, J.-H.; Yi, H.-S.; Yoo, Y.J.; Je, J.; Suh, S.J.; Jung, Y.K.; Kim, J.H.; et al. Exosomes derived from palmitic acid-treated hepatocytes induce fibrotic activation of hepatic stellate cells. *Sci. Rep.* **2017**, *7*, 1–10. [CrossRef]
40. Seo, W.; Eun, H.S.; Kim, S.Y.; Yi, H.; Lee, Y.; Park, S.; Jang, M.; Jo, E.; Kim, S.C.; Han, Y.; et al. Exosome-mediated activation of toll-like receptor 3 in stellate cells stimulates interleukin-17 production by gammadelta T cells in liver fibrosis. *Hepatology* **2016**, *64*, 616–631. [CrossRef]
41. Kitade, M.; Yoshiji, H.; Noguchi, R.; Ikenaka, Y.; Kaji, K.; Shirai, Y.; Yamazaki, M.; Uemura, M.; Yamao, J.; Fujimoto, M.; et al. Crosstalk between angiogenesis, cytokeratin-18, and insulin resistance in the progression of non-alcoholic steatohepatitis. *World J. Gastroenterol.* **2009**, *15*, 5193–5199. [CrossRef] [PubMed]
42. Hammoutene, A.; Rautou, P.-E. Role of liver sinusoidal endothelial cells in non-alcoholic fatty liver disease. *J. Hepatol.* **2019**, *70*, 1278–1291. [CrossRef] [PubMed]
43. Povero, D.; Eguchi, A.; Niesman, I.R.; Andronikou, N.; Jeu, X.D.M.D.; Mulya, A.; Berk, M.; Lazic, M.; Thapaliya, S.; Parola, M.; et al. Lipid-induced toxicity stimulates hepatocytes to release angiogenic microparticles that require Vanin-1 for uptake by endothelial cells. *Sci. Signal.* **2013**, *6*, ra88. [CrossRef] [PubMed]
44. Witek, R.P.; Yang, L.; Liu, R.; Jung, Y.; Omenetti, A.; Syn, W.; Choi, S.S.; Cheong, Y.; Fearing, C.M.; Agboola, K.M.; et al. Liver cell-derived microparticles activate hedgehog signaling and alter gene expression in hepatic endothelial cells. *Gastroenterology* **2009**, *136*, 320–330.e2. [CrossRef]
45. Wang, R.; Ding, Q.; Yaqoob, U.; De Assuncao, T.M.; Verma, V.K.; Hirsova, P.; Cao, S.; Mukhopadhyay, D.; Huebert, R.C.; Shah, V.H. Exosome Adherence and Internalization by Hepatic Stellate Cells Triggers Sphingosine 1-Phosphate-dependent Migration. *J. Biol. Chem.* **2015**, *290*, 30684–30696. [CrossRef]

46. Nojima, H.; Freeman, C.M.; Schuster, R.M.; Japtok, L.; Kleuser, B.; Edwards, M.J.; Gulbins, E.; Lentsch, A.B. Hepatocyte exosomes mediate liver repair and regeneration via sphingosine-1-phosphate. *J. Hepatol.* **2016**, *64*, 60–68. [CrossRef]
47. Lemoinne, S.; Cadoret, A.; Rautou, P.; El Mourabit, H.; Ratziu, V.; Corpechot, C.; Rey, C.; Bosselut, N.; Barbu, V.; Wendum, D.; et al. Portal myofibroblasts promote vascular remodeling underlying cirrhosis formation through the release of microparticles. *Hepatology* **2015**, *61*, 1041–1055. [CrossRef]
48. Bedossa, P. Histological Assessment of NAFLD. *Dig. Dis. Sci.* **2016**, *61*, 1348–1355. [CrossRef]
49. Li, X.; Chen, R.; Kemper, S.; Brigstock, D.R. Dynamic Changes in Function and Proteomic Composition of Extracellular Vesicles from Hepatic Stellate Cells during Cellular Activation. *Cells* **2020**, *9*, 290. [CrossRef]
50. Chen, L.; Chen, R.; Kemper, S.; Charrier, A.; Brigstock, D.R. Suppression of fibrogenic signaling in hepatic stellate cells by Twist1-dependent microRNA-214 expression: Role of exosomes in horizontal transfer of Twist1. *Am. J. Physiol. Gastrointest. Liver Physiol.* **2015**, *309*, G491–G499. [CrossRef]
51. Chen, L.; Charrier, A.; Zhou, Y.; Chen, R.; Yu, B.; Agarwal, K.; Tsukamoto, H.; Lee, L.J.; Paulaitis, M.E.; Brigstock, D.R. Epigenetic regulation of connective tissue growth factor by MicroRNA-214 delivery in exosomes from mouse or human hepatic stellate cells. *Hepatology* **2014**, *59*, 1118–1129. [CrossRef] [PubMed]
52. Chen, L.; Chen, R.; Velazquez, V.M.; Brigstock, D.R. Fibrogenic Signaling Is Suppressed in Hepatic Stellate Cells through Targeting of Connective Tissue Growth Factor (CCN2) by Cellular or Exosomal MicroRNA-199a-5p. *Am. J. Pathol.* **2016**, *186*, 2921–2933. [CrossRef] [PubMed]
53. Tsuchida, T.; Friedman, S.L. Mechanisms of hepatic stellate cell activation. *Nat. Rev. Gastroenterol. Hepatol.* **2017**, *14*, 397–411. [CrossRef]
54. Kostallari, E.; Hirsova, P.; Prasnicka, A.; Verma, V.K.; Yaqoob, U.; Wongjarupong, N.; Roberts, L.R.; Shah, V.H. Hepatic stellate cell-derived platelet-derived growth factor receptor-alpha-enriched extracellular vesicles promote liver fibrosis in mice through SHP2. *Hepatology* **2018**, *68*, 333–348. [CrossRef] [PubMed]
55. Gao, J.; Wei, B.; De Assuncao, T.M.; Liu, Z.; Hu, X.; Ibrahim, S.H.; Cooper, S.A.; Cao, S.; Shah, V.H.; Kostallari, E. Hepatic stellate cell autophagy inhibits extracellular vesicle release to attenuate liver fibrosis. *J. Hepatol.* **2020**, *73*, 1144–1154. [CrossRef] [PubMed]
56. Adams, L.A.; Anstee, Q.M.; Tilg, H.; Targher, G. Non-alcoholic fatty liver disease and its relationship with cardiovascular disease and other extrahepatic diseases. *Gut* **2017**, *66*, 1138–1153. [CrossRef] [PubMed]
57. Zhao, Y.; Zhao, M.-F.; Jiang, S.; Wu, J.; Liu, J.; Yuan, X.-W.; Shen, D.; Zhang, J.-Z.; Zhou, N.; He, J.; et al. Liver governs adipose remodelling via extracellular vesicles in response to lipid overload. *Nat. Commun.* **2020**, *11*, 1–17. [CrossRef]
58. Kranendonk, M.E.; Visseren, F.L.; Van Herwaarden, J.A.; Hoen, E.N.N.; De Jager, W.; Wauben, M.H.; Kalkhoven, E. Effect of extracellular vesicles of human adipose tissue on insulin signaling in liver and muscle cells. *Obesity* **2014**, *22*, 2216–2223. [CrossRef] [PubMed]
59. Jiang, F.; Chen, Q.; Wang, W.; Ling, Y.; Yan, Y.; Xia, P. Hepatocyte-derived extracellular vesicles promote endothelial inflammation and atherogenesis via microRNA-1. *J. Hepatol.* **2020**, *72*, 156–166. [CrossRef]
60. Spengler, E.K.; Loomba, R. Recommendations for Diagnosis, Referral for Liver Biopsy, and Treatment of Nonalcoholic Fatty Liver Disease and Nonalcoholic Steatohepatitis. *Mayo Clin. Proc.* **2015**, *90*, 1233–1246. [CrossRef]
61. Mayo, R.; Crespo, J.; Martínez-Arranz, I.; Banales, J.M.; Arias, M.; Mincholé, I.; De La Fuente, R.A.; Jimenez-Agüero, R.; Alonso, C.; De Luis, D.A.; et al. Metabolomic-based noninvasive serum test to diagnose nonalcoholic steatohepatitis: Results from discovery and validation cohorts. *Hepatol. Commun.* **2018**, *2*, 807–820. [CrossRef] [PubMed]
62. Yang, M.; Xu, D.; Liu, Y.; Guo, X.; Li, W.; Guo, C.; Zhang, H.; Gao, Y.; Mao, Y.; Zhao, J. Combined Serum Biomarkers in Non-Invasive Diagnosis of Non-Alcoholic Steatohepatitis. *PLoS ONE* **2015**, *10*, e0131664. [CrossRef] [PubMed]
63. Povero, D.; Yamashita, H.; Ren, W.; Subramanian, M.G.; Myers, R.P.; Eguchi, A.; Simonetto, D.A.; Goodman, Z.D.; Harrison, S.A.; Sanyal, A.J.; et al. Characterization and Proteome of Circulating Extracellular Vesicles as Potential Biomarkers for NASH. *Hepatol. Commun.* **2020**, *4*, 1263–1278. [CrossRef] [PubMed]
64. Kornek, M.; Lynch, M.; Mehta, S.H.; Lai, M.; Exley, M.; Afdhal, N.H.; Schuppan, D. Circulating microparticles as disease-specific biomarkers of severity of inflammation in patients with hepatitis C or nonalcoholic steatohepatitis. *Gastroenterology* **2012**, *143*, 448–458. [CrossRef] [PubMed]
65. Welsh, J.A.; Scorletti, E.; Clough, G.F.; Englyst, N.A.; Byrne, C.D. Leukocyte extracellular vesicle concentration is inversely associated with liver fibrosis severity in NAFLD. *J. Leukoc. Biol.* **2018**, *104*, 631–639. [CrossRef]
66. Pirola, C.J.; Fernandez Gianotti, T.; Castano, G.O.; Mallardi, P.; San Martino, J.; Mora Gonzalez Lopez Ledesma, M.; Flichman, D.M.; Mirshahi, F.; Sanyal, A.J.; Sookoian, S.C. Circulating microRNA signature in non-alcoholic fatty liver disease: From serum non-coding RNAs to liver histology and disease pathogenesis. *Gut* **2015**, *64*, 8001–8002. [CrossRef]
67. Murakami, Y.; Toyoda, H.; Tanahashi, T.; Tanaka, J.; Kumada, T.; Yoshioka, Y.; Kosaka, N.; Ochiya, T.; Taguchi, Y.-H. Comprehensive miRNA expression analysis in peripheral blood can diagnose liver disease. *PLoS ONE* **2012**, *7*, e48366. [CrossRef]
68. Cermelli, S.; Ruggieri, A.; Marrero, J.A.; Ioannou, G.N.; Beretta, L. Circulating microRNAs in patients with chronic hepatitis C and non-alcoholic fatty liver disease. *PLoS ONE* **2011**, *6*, e23937. [CrossRef]
69. Rautou, P.; Bresson, J.; Sainte-Marie, Y.; Vion, A.; Paradis, V.; Renard, J.; Devue, C.; Heymes, C.; Letteron, P.; Elkrief, L.; et al. Abnormal plasma microparticles impair vasoconstrictor responses in patients with cirrhosis. *Gastroenterology* **2012**, *143*, 166–176.e6. [CrossRef]
70. Tamimi, T.I.A.-R.; Elgouhari, H.M.; Alkhouri, N.; Yerian, L.M.; Berk, M.P.; Lopez, R.; Schauer, P.R.; Zein, N.N.; Feldstein, A.E. An apoptosis panel for nonalcoholic steatohepatitis diagnosis. *J. Hepatol.* **2011**, *54*, 1224–1229. [CrossRef]

biomedicines

MDPI

Review

Role of Leptin in Non-Alcoholic Fatty Liver Disease

Carlos Jiménez-Cortegana [1,†], Alba García-Galey [1,†], Malika Tami [1], Pilar del Pino [2], Isabel Carmona [2], Soledad López [1], Gonzalo Alba [1] and Víctor Sánchez-Margalet [1,*]

[1] Department of Medical Biochemistry and Molecular Biology, School of Medicine, Virgen Macarena University Hospital, University of Seville, 41073 Seville, Spain; cjcortegana@us.es (C.J.-C.); albaggaley97@gmail.com (A.G.-G.); mali_k@hotmail.es (M.T.); slopez9@us.es (S.L.); galbaj@us.es (G.A.)

[2] Unit of Digestive Diseases, Virgen Macarena University Hospital, 41073 Seville, Spain; pilardelpino4@gmail.com (P.d.P.); icarmonasoria@gmail.com (I.C.)

* Correspondence: margalet@us.es

† Both authors should be considered as first authors.

Abstract: Non-alcoholic fatty liver disease (NAFLD), which affects about a quarter of the global population, poses a substantial health and economic burden in all countries, yet there is no approved pharmacotherapy to treat this entity, nor well-established strategies for its diagnosis. Its prevalence has been rapidly driven by increased physical inactivity, in addition to excessive calorie intake compared to energy expenditure, affecting both adults and children. The increase in the number of cases, together with the higher morbimortality that this disease entails with respect to the general population, makes NAFLD a serious public health problem. Closely related to the development of this disease, there is a hormone derived from adipocytes, leptin, which is involved in energy homeostasis and lipid metabolism. Numerous studies have verified the relationship between persistent hyperleptinemia and the development of steatosis, fibrinogenesis and liver carcinogenesis. Therefore, further studies of the role of leptin in the NAFLD spectrum could represent an advance in the management of this set of diseases.

Keywords: fatty liver; steatohepatitis; obesity; metabolic syndrome; leptin

Citation: Jiménez-Cortegana, C.; García-Galey, A.; Tami, M.; del Pino, P.; Carmona, I.; López, S.; Alba, G.; Sánchez-Margalet, V. Role of Leptin in Non-Alcoholic Fatty Liver Disease. *Biomedicines* **2021**, *9*, 762. https://doi.org/10.3390/biomedicines9070762

Academic Editor: Ronit Shiri-Sverdlov

Received: 24 May 2021
Accepted: 17 June 2021
Published: 30 June 2021

Publisher's Note: MDPI stays neutral with regard to jurisdictional claims in published maps and institutional affiliations.

1. Introduction

Leptin is a 16 kDa adipocyte-derived hormone described for the first time by Zhang et al. (1994) as the product of the *obese (Ob) gene* [1], although its existence was predicted some decades before in leptin-deficient (ob/ob) and leptin receptor-deficient (db/db) mice [2,3]. Leptin primary amino acid *sequences* show differences in vertebrates, while secondary and tertiary structures are similar [4] and alike to the long-chain helical cytokine family, which includes interleukin (IL) 6, IL-11 (interleukin 11), G-CSF (granulocyte-colony stimulating factor) or oncostatin M, among many others [5].

Leptin is characterized by having pleiotropic effects due to the great variety of leptin receptors (known as Ob-R or LEPR), thus being able to affect many biological processes at different levels. The six existing spliced Ob-R forms are called Ob-Ra, Ob-Rb, Ob-Rc, Ob-Rd, Ob-Re and Ob-Rf, and belong to the class I cytokine superfamily [6,7] but differ from each other in the lengths of their cytoplasmic regions [8]. The most important leptin receptor is the long isoform Ob-Rb since it can fully transduce activation signals into the cell [9], including signaling pathways such as Janus kinase (JAK) 2/signal transducer and activator of transcription (STAT) 3, insulin receptor substrate (IRS)/phosphatidylinositol-3 kinase (PI3K), or Src homology 2 domain-containing phosphatase 2 (SHP2)/mitogen-activated protein kinase (MAPK) [10].

This adipokine, leptin, is mostly recognized for playing a key role in the central control of both energy metabolism [11] and obesity [12], but also has important regulatory functions in different physiological systems and diseases, such as reproduction [13], bone physiology [14], autoimmunity [15], and cancer [16], among many others [17]. Moreover,

in the last few decades, data from experimental models and both observational and interventional studies have shown that leptin plays a role in non-alcoholic fatty liver disease (NAFLD) [18], a clinicopathologic entity which develops in the absence of excessive alcohol consumption (typically defined as <20 g per day in women and <30 g per day in men) and comprises a spectrum of diseases, that include steatosis, non-alcoholic steatohepatitis (NASH), hepatic fibrosis, cirrhosis, and hepatocellular carcinoma (HCC) [19].

Today, several problems are associated with NAFLD. This entity is the leading cause of liver disease worldwide and its prevalence is increasing [20], affecting both adults and children [21]. Most patients are asymptomatic for a long time, making it difficult to identify and manage NAFLD and its progression and, in most cases, the disease is detected in advanced stages [22,23]. In addition, there is no authorized effective pharmacological treatments to improve patient outcomes [24]. Therefore, the need to increase research efforts on effective diagnostic and prognosis is essential, suggesting leptin is a powerful tool in the disease. For all those reasons, the purpose of this article is to review the existing literature to better understand the role of leptin in the NAFLD spectrum and to take this hormone into account as a possible clinical non-invasive biomarker or target of treatment for this disease.

2. Non-Alcoholic Fatty Liver Disease (NAFLD): Characteristics and Signaling Pathways of Leptin Receptor

NAFLD is a clinicopathologic entity comprising a broad spectrum of liver diseases ranging from simple steatosis to NASH, a more aggressive form of NAFLD and associated with varying degrees of hepatic fibrosis, cirrhosis, and HCC [25]. NAFLD has been rapidly driven by daily life, including actions such as sedentarism or excessive caloric intake compared to energy expenditure, affecting about 25% of the world population [19,20,26]. This pathological condition is detected in approximately 90% of obese (body mass index, BMI $\geq$ 30 kg/m^2) and 25% of lean patients (BMI 20.0–24.9 kg/m^2) and can be affected by other factors (e.g., age, sex, and race) [27]. The highest rates of NAFLD are in South America (31%) and the Middle East (32%), followed by Asia (27%), the United States (24%), Europe (23%), and Africa (14%) [28]. This makes NAFLD in the leading cause of liver disease worldwide and will probably become the most common indication for liver transplantation and the most frequent etiology of HCC in the following decades [21,27].

NAFLD is also considered the hepatic component of the metabolic syndrome, whose prevalence is increasing worldwide at the same time as obesity and type 2 diabetes-mellitus (T2DM) [29,30]. In fact, the Latin American Association for the Study of the Liver (ALEH) recommended the renaming of NAFLD to "Metabolic Dysfunction Associated Fatty Liver Disease (MAFLD)", and the adoption of positive criteria to diagnose the disease, independently of alcohol intake or other liver diseases. By contrast, the American Association for the Study of Liver Diseases (AASLD) required that there is no significant alcohol consumption or coexisting etiologies of chronic liver disease [23,31,32].

The pathogenesis of NAFLD entail a complex interplay between environmental factors, obesity, changes in the microbiota and predisposing genetic variants that result in altered lipid homeostasis and hepatocyte triglyceride accumulation [19]. In turn, NAFLD is mainly related to metabolic syndrome and adipokines, which not only contribute to pathogenesis, but are also involved in the progression to NASH and cirrhosis [30,33]. In this sense, the physiological role of leptin in the liver was known before this adipokine was discovered, as both db/db and ob/ob mice were shown to present alterations in the liver function, including steatosis [34,35]. Table 1 summarizes research articles related to human NAFLD throughout this review.

Table 1. Overview about reviewed research articles in human non-alcoholic fatty liver disease (NAFLD) spectrum.

Author (Year)	Country	No Patients	Conclusions
Jacobs et al. (2011) [29]	Netherlands	434	Insulin resistance (IR) mediated between 75–80% of the association of the metabolic syndrome with alanine aminotransferase, as well as suggesting that IR, adipose tissue inflammation and endothelial dysfunction may contribute to NAFLD progression.
Hossain et al. (2015) [36]	Bangladesh	110	IR was independently associated with serum leptin levels irrespective of adiposity and glycemic status in male prediabetic subjects. In addition, serum leptin was increased in the female patients, accompanied by pancreatic beta cell dysfunction and IR. However, their relationship with NAFLD was not affected by the degree of adiposity.
Cernea et al. (2018) [37]	Romania	159	Hepatic steatosis was positively correlated with serum leptin and leptin resistance, and negatively with serum Ob-R. Leptin/Ob-R, and leptin resistance did not made a significant contribution to hepatic fibrosis.
Angulo et al. (2004) [38]	U.S.A.	88	There was no association between serum leptin and hepatic fibrosis. However, there was a correlation between leptin with more advanced NAFLD-related liver fibrosis.
Chitturi et al. (2002) [39]	Australia	36 patients and 47 controls	Hyperleptinemia in NASH was correlated with some factors (e.g., age and extent of hepatic steatosis), but not with inflammation or fibrotic severity.
Ataseven et al. (2006) [40]	Turkey	45 patients (23 cirrhosis + 22 HCC) and 25 controls	In cirrhosis and HCC patients there was a decrease of serum leptin levels due to, at least partly, the presence of nutritional and metabolic abnormalities, including malnutrition, and high ghrelin levels.
Naveau et al. (2006) [41]	France	209	Serum leptin was independently correlated with steatosis and may play an important role in severity of fibrosis.
Ockenga et al. (2007) [42]	Germany	40 liver cirrhosis + 31 controls	Patients had bound leptin and soluble leptin receptor levels significantly increased compared with controls, without changes in free leptin.
Ertle et al. (2011) [43]	Germany	162	NAFLD/NASH posed a risk factor for HCC, even in the absence of cirrhosis.

Leptin Receptor Signaling and NAFLD

Leptin acts by binding to its receptors. Specifically, Ob-Rb isoform is the main leptin receptor as it provokes signaling cascades [31]. After the binding between leptin and Ob-Rb in hepatic cells, intracellular signaling is initiated and JAK2 phosphorylation and activation is allowed. Thus, three tyrosine residues (Tyr985, Tyr1077 and Tyr1138) located in the intracellular domain of Ob-Rb are phosphorylated by JAK2. Tyr985 induces SHP2 signaling pathway and the activation of MAPK, Tyr1077 mediates the activation of STAT5, and Tyr1138 activates both STAT5 and STAT3 [30,44–48]. Subsequently, STAT3 leads to increased gene expression of suppressors of cytokine signaling (SOCS)-3, which acts as a negative feedback inhibiting both leptin and insulin signaling. SOCS-3 overexpression causes resistance to those hormones. Therefore, SOCS-3 downregulation could be a potential approach to prevent and/or treat hepatic diseases [46,49,50]. JAK2 activity is also modulated by phosphorylation of both IRS1 and IRS2, and activation of PI3K, which is essential for leptin to exert its effect on food intake. Likewise, adenosine monophosphate-activated protein

kinase (AMPK) activity is stimulated by leptin in peripheral tissues promoting catabolic pathways such as fatty acid oxidation or glucose transport and inhibited in the brain to regulate food intake through a series of hypothalamic neuropeptides [49]. Phosphatidyl inositol 3-Kinase/PI3K/Akt/mammalian target of rapamycin (mTOR) is also activated, improving insulin sensitivity in the liver by suppressing hepatic glucose production [51]. Figure 1 outlines leptin signaling pathways and their implications in the NAFLD spectrum.

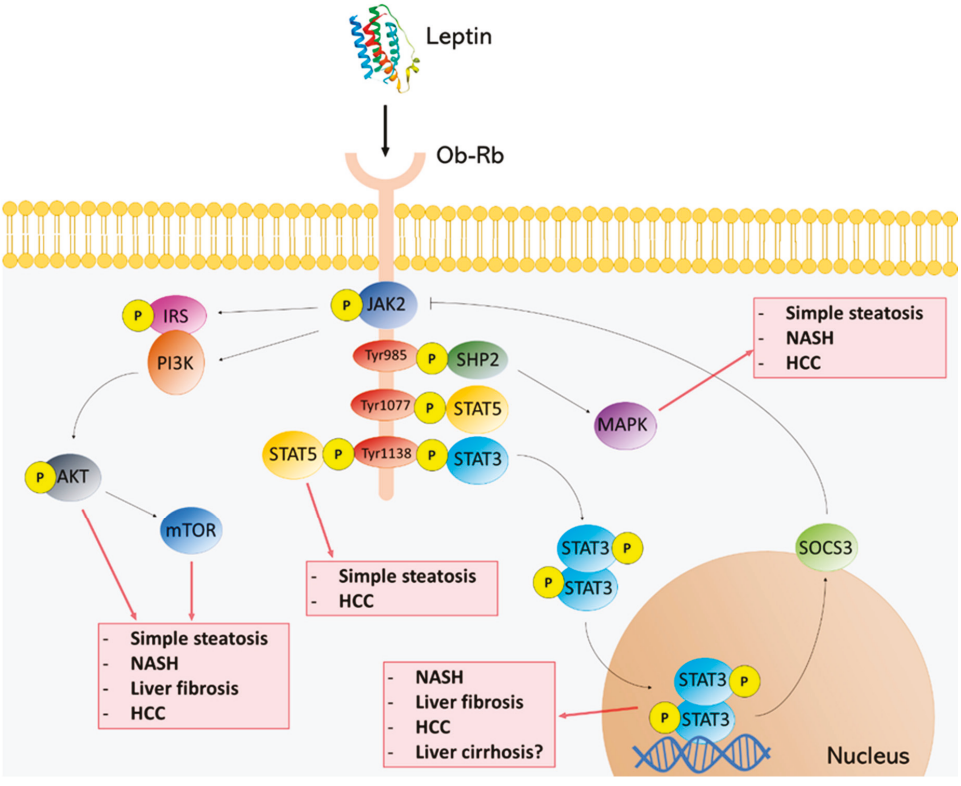

Figure 1. Leptin signaling pathways in the NAFLD spectrum. Leptin/Ob-Rb interaction activates different pathways via JAK2 phosphorylation. The consequent signaling cascade can exert a disruptive role through the activation and phosphorylation of some component implied in this signaling network, such as signal transducer and activator of transcription (STAT)3, STAT5, mitogen-activated protein kinase (MAPK) or AKT/mammalian target of rapamycin (mTOR) pathways, thus favoring some malignancies of the NAFLD spectrum.

Leptin and other inflammatory adipokines such as IL-6 or TNF-α (Tumor nechrosis factor) promote insulin resistance, which has been extensively described in the pathophysiology of NAFLD during the last few decades [52–54], as it provokes the inhibition of lipid oxidation together with increased synthesis of fatty acids and triglycerides [19,36,37]. Specifically, leptin could antagonize some insulin functions by modifying the sensitivity of adipocytes to the inhibitory action that insulin exerts on lipid accumulation, decreasing the binding capacity of insulin receptors in the liver, and inhibiting insulin secretion in pancreatic islets [36–38]. Hyperleptinemia damages pancreatic β-cells and inhibits JAK2/PI3K signaling in obese patients with T2DM and NAFLD. This signaling pathway is known as the "leptin-insulin pathway" and under normal conditions is activated to regulate glucose metabolism. In addition, hyperleptinemia increases the expression of sterol regulatory element-binding protein 1 (SREBP-1) in the liver, causing lipogenesis [55]. In addition,

Sahin-Efe et al. (2018) demonstrated that leptin levels were increased in patients with T2DM, thus being a risk predictor for the development of this disease [56].

Moreover, some pathologies can cause NAFLD. This is the case of congenital or acquired lipodystrophy, which is characterized by the total or partial absence of subcutaneous adipose tissue and promotes ectopic accumulation of fat in other locations, including the liver, which leads to severe insulin resistance and the development of NAFLD [57,58]. Patients with lipodystrophy are treated with leptin recombinant treatments, such as metreleptin, approved by the United States Food and Drug Administration (FDA) and the Japanese Pharmaceuticals and Medical Devices Agency, since it improves many associated metabolic disorders such as insulin sensitivity, glucose tolerance, hypertriglyceridemia or NAFLD [59–61]. At the same time, work is being done on the development of leptin analogues, leptin receptor agonists or drugs that act on downstream leptin pathways [62].

3. Leptin in the NAFLD Spectrum

NAFLD comprises a set of liver diseases, some of them irreversible. NAFLD development is divided into three main steps: simple steatosis, NASH, and liver cirrhosis. However, NAFLD can eventually trigger in HCC. Simple steatosis is caused by factors such as high-fat and/or high sugar diet, obesity, T2DM, and other metabolic diseases, while NASH can be developed by inflammation and hepatocyte apoptosis. If liver fibrosis is provoked in this step, cirrhosis (and possibly HCC) will be also developed [63]. In the following sections we are going to review the role of leptin in the pathogenesis of NAFLD, which is summarized in Figure 2.

3.1. Leptin and Hepatic Steatosis

Hepatic steatosis has different degrees of severity related to liver damage in NAFLD: from simple steatosis to NASH, which is the most important disease in the NAFLD spectrum, since its prevalence is estimated to be approximately 1.5–6.5% in the general population, and considerably increasing this percentage in obese individuals [20]. Although most patients present isolated steatosis, about one third develop NASH, which confers a higher risk of progression to more advanced stages of NAFLD. In this step, inflammation develops when triglycerides levels exceed hepatic physiological adaptive mechanisms that leads to the process of lipotoxicity by which reactive oxygen species (ROS), endoplasmic reticulum stress and hepatocellular injury are produced. In turn, liver cell injury activates the immune and apoptotic pathways, leading to cell death. This event is also one of the main drivers for the development of fibrosis and cirrhosis over time [64].

Hepatic steatosis can be caused by both aberrant lipid and glucose metabolism. One of leptin functions is to limit the storage of triglycerides in adipocytes and non-adipose tissues including the liver, thereby preventing lipotoxicity. Under normoleptinemia conditions, leptin exerts an anti-steatotic effect and improves insulin sensitivity by suppressing hepatic glucose production and lipogenesis [50,65]. This explains the improvement or prevention of hepatic steatosis development in ob/ob mice, linked to leptin administration [66]. Similarly, the anti-steatosis action of leptin has been observed in non-obese mice with uncontrolled type 1 diabetes mellitus (T1DM), in which such treatment induces a significant reduction of lipogenic and cholesterogenic transcription factors and decreases the lipids located in plasma and different tissues [67]. In this regard, one anti-steatotic mechanism carried out by leptin is to regulate components of the lipid synthesis in the liver, such as the transcription factor carbohydrate responsive element binding protein (ChREBP) [68].

Leptin has also been suggested to have a synergistic effect when used together with insulin, probably inhibiting the production of very low-density lipoproteins (VLDL) [10,67,69]. According to this, leptin has been shown to improve insulin resistance and hepatic steatosis in lypodystrophic mice [70]. Hackl et al. (2019) showed that brain leptin protects from ectopic lipid accumulation and could be a therapeutic strategy to improve obesity-related steatosis [71]. Moreover, this disease has been shown to alleviate upregulating leptin levels

by using metformin [72] and through leptin signaling pathways by using a modification of Samjunghwan, an herbal formula used in traditional Korean medicine [73].

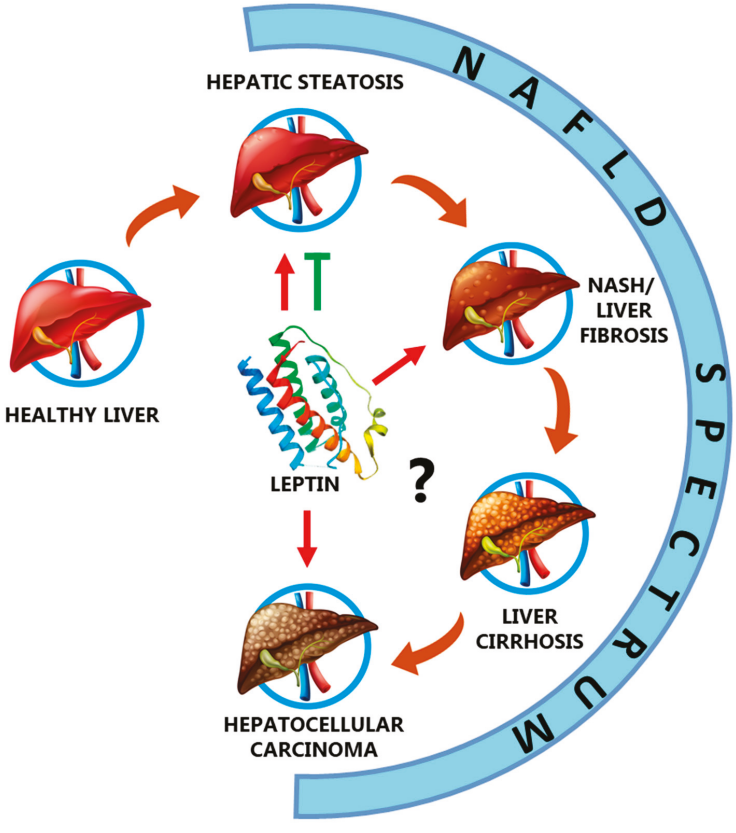

Figure 2. Role of leptin in the NAFLD spectrum. Leptin has been demonstrated to have antisteatotic effects, although this hormone could also contribute to worsening of hepatic steatosis under certain circumstances such as hyperleptinemia. In addition, leptin is involved in the pathogenesis of NAFLD by promoting NASH and liver fibrosis. However, the role of leptin in NAFLD-related cirrhosis and NAFLD-related hepatocellular carcinoma is unknown, but there is much evidence to confirm the protumoral role of this adipokine in liver malignancies Table 1.

By contrast, high leptin levels have also been associated with hepatic steatosis and NAFLD pathogenesis since a high percentage of NAFLD patients have been observed to suffer obesity, which is closely related with hyperleptinemia [47,50,74]. The failure of elevated leptin levels to correct hepatic steatosis lies in the generation of a state of resistance to this hormone. Several mechanisms, including phosphorylation of Tyr985 in Ob-Rb and increased expression of SOCS-3, attenuate leptin signaling and promote a cellular resistance to leptin in obesity, which predominantly take place in the arcuate nucleus [75]. The severity of hepatic steatosis correlates with leptin levels, especially in patients with high BMI. In the case of lean patients with NAFLD, there are a number of genetic factors that seem to contribute to the development of steatosis rather than leptinemia, and these are hypobetalipoproteinemia and some metabolic disorders such as cystic fibrosis or celiac disease [76]. In addition, leptin has been reflected to have a pathogenic role in hepatic insulin resistance and/or a failure of the antisteatotic actions [39]. Cernea et al. (2018) observed an increased prevalence of NAFLD steatosis in T2DM patients [37]. Along the same lines,

Pavlidis et al. (2011) showed that steatosis grade at baseline was significantly greater as leptin concentrations increased in chronic hepatitis C patients [77] and Eshraghian et al. (2020) demonstrated for the first time that alterations in adiponectin, leptin and insulin resistance were correlated with hepatic steatosis in liver transplant recipients [78].

3.2. Leptin, Non-Alcoholic Steatohepatitis (NASH), and Fibrosis

In NAFLD, most patients have simple steatosis, but those with NASH can advance to the next step of the disease, which is fibrosis. The mechanisms of progression from simple steatosis to NASH are not entirely clear, but some factors are known to be involved in the process [79], including an inflammation caused by the incomplete oxidation of hepatic accumulated lipids, which generates toxic metabolites and produces apoptosis of hepatocytes, thus activating inflammatory cells [80]. If inflammation becomes chronic, then fibrosis will be developed [81]. Related to this, leptin could promote NAFLD by playing its well-known role in the inflammatory process [17].

Advanced fibrosis implies an increased risk for developing other NAFLD-related complications, such as cirrhosis and HCC. For that reason, an early diagnosis of patients with advanced fibrosis is crucial [82]. In this sense, leptin has been shown to be a contributing factor in fibrogenesis [60]. Rotundo et al. (2018) showed that leptin levels were simultaneously increased with the degree of liver fibrosis, especially in patients with a high BMI, while their lean counterparts had lower rates of fibrosis and inflammation [76]. Some studies have reported that Ob-R on Kupffer cells (KC) and sinusoidal endothelial cells increases the expression of matrix remodeling enzymes, which induce the fibrosis cascade in hepatic stellate cells (HSC). Specifically, in KC leptin upregulates the expression of TGF- β, which is likely to contribute to HSC activation via paracrine signaling [18,76,83].

Activated HSC also contribute to increase inflammation and liver fibrosis by releasing TGF-β1, angiopoietin-1, VEGF (vascular endothelial growth factor), and collagen-I. In addition, HSC appear to produce leptin, and have also been proposed to express Ob-Rb, which establishes a vicious cycle by stimulating proliferation and preventing apoptosis of HSC and thus affecting hepatic inflammation and fibrosis [18]. KC can be activated by leptin via peroxynitrite-mediated oxidative stress [84], which promotes $CD8^+CD57^+$ T cells, found in NASH progression [85]. Also, prolonged hyperleptinemia may result in HSC, KC, and sinusoidal cell activation, that could trigger both the proinflammatory and profibrogenic cascade [50].

3.3. Leptin and Liver Cirrhosis

According to several studies with small sample sizes, progression from NASH to liver cirrhosis can occur in up to 25% of patients. This high disease burden has led to an increase in the number of NASH-related transplants, possibly becoming in the leading cause of liver transplantation worldwide in coming decades, displacing the hepatitis C virus [86]. Up to now, leptin concentration in patients with NAFLD-related cirrhosis has not been studied. However, leptin is known to induce VEGF on HSC, contributing to the irreversibility of cirrhosis and, potentially, to NASH progression [87].

There are references in other types of liver cirrhosis about leptin, in which this hormone has been demonstrated to be in both high [88] and low [40] levels. Even leptin has also been found to be uncorrelated with the existence of cirrhosis in alcoholic liver disease [41]. Interestingly, Ockenga et al. (2007) analyzed in vivo hepatic substrate and leptin metabolism in 40 patients with liver cirrhosis and 31 healthy controls, showing that patients had bound leptin and soluble leptin receptor levels significantly increased when compared with controls, without changes in free leptin, suggesting a different role for those components in both metabolic and inflammatory processes in cirrhotic patients [42].

3.4. Leptin and Hepatocellular Carcinoma

Obesity and T2DM are cancer promoters and, in coexistence with NAFLD, the aggressive potential can be underestimated. HCC is the neoplasm most closely related to obesity

in men. In this regard, HCC incidence increased by 3% per year in the last decade, unlike other malignancies also associated with obesity, such as breast or colon cancer, whose incidences remained stable or decreased. In part, this fact may be explained by the increase in the prevalence of NASH [89]. NAFLD patients have been shown to develop HCC in both early and late stages of the disease, being more common in the latter, providing evidence for a potential association between NAFLD and HCC [90]. The mechanisms of HCC development in a cirrhotic liver include destruction of hepatocytes due to chronic injury, and their subsequent regeneration and compensatory cyclic proliferation. NAFLD patients usually present insulin resistance which, together with hepatic steatosis and chronic low-grade inflammation, favors the creation of an ideal environment for tumor development and growth [91].

In HCC there are some established risk factors, including chronic hepatitis B, chronic hepatitis C, alcohol consumption, and NAFLD, all of them potentially linked to leptin [92]. As with NAFLD-related cirrhosis, there no clinical studies that analyze the role of leptin in NAFLD-related HCC. However, the procarcinogenic role of leptin in HCC patients seems clear. Additionally, high leptin levels alone are also considered to increase the risk of HCC [93]. In fact, in vitro studies suggest that this hormone is increased during the proliferation, migration, and invasiveness of HCC cells through activation of PI3K/AKT signaling pathways, mainly in obese patients [44] and have been demonstrated to take part in the angiogenesis process [94], as well as both JAK2/STAT and ERK pathways [95]. In line with this, a lack of leptin action has been shown to reduce the angiogenic process in experimental steatohepatitis [96]. Leptin also upregulates the expression of VEGF by oxygen-independent activation of hypoxia-inducible factor 1alpha (HF1α) in HSC [97]. Moreover, the analysis of circulating leptin levels has been found to be increased in both cirrhotic and non-cirrhotic patients regardless of the previous pathology [98], including NASH [43]. In this regard, more studies have also reported the role of leptin and Ob-R as a critical regulator in HCC development and progression [94,99,100].

However, Elinav et al. (2006) suggested a beneficial role of leptin in HCC murine models since this hormone decreased tumor size and improved survival [101]. In the same year, similar conclusions were drawn by analyzing both leptin and Ob-Rb in HCC patients [102,103]. Despite this, there is sufficient evidence to suggest the critical role of leptin in liver carcinogenesis, that may also be potentially fostered by NAFLD progression.

4. Concluding Remarks

NAFLD is a worldwide health problem due to its increasing prevalence, so the research on its diagnosis, follow-up, and subsequent treatment has become essential. Moreover, NAFLD requires a multidisciplinary approach given its high risk of cardiovascular morbidity and mortality. In this sense, there is an urgent need for non-invasive diagnostic methods to replace liver biopsy, so that early diagnosis and treatment monitoring is possible in a large part of the population. Leptin, due to its direct relationship with body fat levels and insulin resistance, has been shown to be an independent predictor of the presence or development of NAFLD. This adipokine has been shown to have antisteatotic effects, although it has also been associated with hepatic steatosis and may promote more advanced stages of NAFLD that include NASH and liver fibrosis. The role of leptin in both NAFLD-related cirrhosis and HCC has never been studied. Its functions in other liver cirrhosis remains controversial. However, there is much evidence to establish the protumoral role of this hormone in HCC derived from other liver diseases.

Treatment with leptin has proven to be effective in patients with congenital leptin deficiency; however, its use in the rest of the affected subjects remains controversial, which highlights the importance of continuing the line of research on the development of leptin analogues that conserve the antisteatotic effect and lack proinflammatory and profibrogenic action, as well as leptin sensitizers, or their synergistic effect when associated with different drugs. While further observational studies and large clinical trials with long-term follow-up are needed to fully evaluate the efficiency of the use of this adipokine, leptin could be

used as an interesting biomarker in the diagnosis and follow-up of NAFLD, including the combination of leptin level measurement together with metabolic analyses, lipid profile, and glucose levels.

Author Contributions: Conceptualization (V.S.-M., I.C.), Resources (C.J.-C., A.G.-G., M.T., P.d.P.), analysis and writing (C.J.-C., A.G.-G., M.T., P.d.P., S.L., G.A., I.C., V.S.-M., Funding acquisition (I.C., V.S.-M.). All authors have read and agreed to the published version of the manuscript.

Funding: Sociedad Andaluza de Patología Digestiva.

Institutional Review Board Statement: Not applicable.

Informed Consent Statement: Not applicable.

Data Availability Statement: Not applicable.

Conflicts of Interest: The authors declare no conflict of interest.

References

1. Zhang, Y.; Proenca, R.; Maffei, M. Positional cloning of the mouse obese gene and its human homologue. *Nature* **1994**, *372*, 425–432. [CrossRef] [PubMed]
2. Ingalls, A.M.; Dickie, M.M.; Snell, G.D. Obese, a new mutation in the house mouse. *J. Hered.* **1950**, *41*, 317–318. [CrossRef] [PubMed]
3. Hummel, K.P.; Dickie, M.M.; Coleman, D.L. Diabetes, a new mutation in the mouse. *Science* **1966**, *153*, 1127–1128. [CrossRef]
4. Denver, R.J.; Bonett, R.M.; Boorse, G.C. Evolution of leptin structure and function. *Neuroendocrinology* **2011**, *94*, 21–38. [CrossRef]
5. Zhang, F.; Basinski, M.B.; Beals, J.M.; Briggs, S.L.; Churgay, L.M.; Clawson, D.K.; DiMarchi, R.D.; Furman, T.C.; Hale, J.E.; Hsiung, H.M.; et al. Crystal structure of the obese protein leptin-E100. *Nature* **1997**, *387*, 206–209. [CrossRef]
6. Tartaglia, L.A.; Dembski, M.; Weng, X.; Deng, N.; Culpepper, J.; Devos, R.; Richards, G.J.; Campfield, L.A.; Clark, F.T.; Deeds, J.; et al. Identification and expression cloning of a leptin receptor OB-R. *Cell* **1995**, *83*, 1263–1271. [CrossRef]
7. Tartaglia, L.A. The leptin receptor. *J. Biol. Chem.* **1997**, *272*, 6093–6096. [CrossRef]
8. Myers, M.G., Jr. Leptin receptor signaling and the regulation of mammalian physiology. *Recent Prog. Horm. Res.* **2004**, *59*, 287–304. [CrossRef]
9. Gorska, E.; Popko, K.; Stelmaszczyk-Emmel, A.; Ciepiela, O.; Kucharska, A.; Wasik, M. Leptin receptors. *Eur. J. Med. Res.* **2010**, *15* (Suppl. 2), 50–54. [CrossRef]
10. Park, H.-Y.; Ahima, R.S. Leptin signaling. *F1000Prime Rep.* **2014**, *6*, 73. [CrossRef]
11. Deck, C.A.; Honeycutt, J.L.; Cheung, E.; Reynolds, H.M.; Borski, R.J. Assessing the Functional Role of Leptin in Energy Homeostasis and the Stress Response in Vertebrates. *Front. Endocrinol.* **2017**, *8*, 63. [CrossRef]
12. Montserrat-de la Paz, S.; Pérez-Pérez, A.; Vilariño-García, T.; Jiménez-Cortegana, C.; Muriana, F.J.G.; Millán-Linares, M.C.; Sánchez-Margalet, V. Nutritional modulation of leptin expression and leptin action in obesity and obesity-associated complications. *J. Nutr. Biochem.* **2021**, *89*, 108561. [CrossRef]
13. Pérez-Pérez, A.; Toro, A.; Vilariño-García, T.; Maymó, J.; Guadix, P.; Dueñas, J.L.; Fernández-Sánchez, M.; Varone, C.; Sánchez-Margalet, V. Leptin action in normal and pathological pregnancies. *J. Cell. Mol. Med.* **2018**, *22*, 716–727. [CrossRef] [PubMed]
14. Reid, I.R.; Baldock, P.A.; Cornish, J. Effect of leptin on the skeleton. *Endocr. Rev.* **2018**, *39*, 938–959. [CrossRef]
15. Navarini, L.; Margiotta, D.P.E.; Vadacca, M.; Afeltra, A. Leptin in autoimmune mechanisms of systemic rheumatic diseases. *Cancer Lett.* **2018**, *423*, 139–146. [CrossRef]
16. Sánchez-Jiménez, F.; Pérez-Pérez, A.; De la Cruz-Merino, L.; Sánchez-Margalet, V. Obesity and Breast cancer: Role of leptin. *Front. Oncol.* **2019**, *9*, 596. [CrossRef] [PubMed]
17. Pérez-Pérez, A.; Sánchez-Jiménez, F.; Vilariño-García, T.; Sánchez-Margalet, V. Role of leptin in inflammation and vice versa. *Int. J. Mol. Sci.* **2020**, *21*, 5887. [CrossRef] [PubMed]
18. Polyzos, S.A.; Kountouras, J.; Mantzoros, C.S. Leptin in nonalcoholic fatty liver disease: A narrative review. *Metabolism* **2015**, *64*, 60–78. [CrossRef]
19. Arab, J.P.; Arrese, M.; Trauner, M. Recent Insights into the Pathogenesis of Nonalcoholic Fatty Liver Disease. *Annu. Rev. Pathol. Mech. Dis.* **2018**, *13*, 321–350. [CrossRef]
20. Younossi, Z.M.; Koenig, A.B.; Abdelatif, D.; Fazel, Y.; Henry, L.; Wymer, M. Global epidemiology of nonalcoholic fatty liver disease—Meta-analytic assessment of prevalence, incidence, and outcomes. *Hepatology* **2016**, *64*, 73–84. [CrossRef]
21. Diehl, A.M.; Day, C. Cause, Pathogenesis, and Treatment of Nonalcoholic Steatohepatitis. *N. Engl. J. Med.* **2017**, *377*, 2063–2072. [CrossRef]
22. Di Sessa, A.; Cirillo, G.; Guarino, S.; Marzuillo, P.; Miraglia-del Giudice, E. Pediatric non-alcoholic fatty liver disease: Current perspectives on diagnosis and management. *Pediatric Health Med. Ther.* **2019**, *10*, 89–97. [CrossRef]

23. Shiha, G.; Korenjak, M.; Eskridge, W.; Casanovas, T.; Velez-Moller, P.; Högström, S.; Richardson, B.; Munoz, C.; Siguroardóttir, S.; Coulibaly, A.; et al. Redefining fatty liver disease: An international patient perspective. *Lancet Gastroenterol. Hepatol.* **2020**, *6*, 73–79. [CrossRef]
24. Lanuza, F.; Sapunar, J.; Hofmann, E. Management of non-alcoholic fatty liver disease. *Rev. Med. Chil.* **2018**, *146*, 894–901. [CrossRef] [PubMed]
25. Brunt, E.M.; Wong, V.W.-S.; Nobili, V.; Day, C.P.; Sookoian, S.; Maher, J.J.; Bugianesi, E.; Sirlin, C.B.; Neuschwander-Tetri, B.A.; Rinella, M.E. Non-alcoholic fatty liver disease. *Nat. Rev. Dis. Primers* **2015**, *1*, 15080. [CrossRef] [PubMed]
26. Flier, J.S. Obesity Wars: Molecular Progress Confronts an Expanding Epidemic. *Cell* **2004**, *116*, 337–350. [CrossRef]
27. Younossi, Z.; Anstee, Q.M.; Marietti, M.; Hardy, T.; Henry, L.; Eslam, M.; George, J.; Bugianesi, E. Global burden of NAFLD and NASH: Trends, predictions, risk factors and prevention. *Nat. Rev. Gastroenterol. Hepatol.* **2018**, *15*, 11–20. [CrossRef]
28. Estes, C.; Anstee, Q.M.; Arias-Loste, M.T.; Bantel, H.; Bellentani, S.; Caballeria, J.; Colombo, M.; Craxi, A.; Crespo, J.; Day, C.P.; et al. Modeling NAFLD disease burden in China, France, Germany, Italy, Japan, Spain, United Kingdom, and United States for the period 2016–2030. *J. Hepatol.* **2018**, *69*, 896–904. [CrossRef]
29. Jacobs, M.; Van Greevenbroek, M.M.J.; Van der Kallen, C.J.H.; Ferreira, I.; Feskens, E.J.M.; Jansen, E.H.J.M.; Schalkwijk, C.G.; Stehouwer, C. The association between the metabolic syndrome and alanine amino transferase is mediated by insulin resistance via related metabolic intermediates (the Cohort on Diabetes and Atherosclerosis Maastricht [CODAM] study). *Metabolism* **2011**, *60*, 969–975. [CrossRef]
30. Polyzos, S.A.; Aronis, K.N.; Kountouras, J.; Raptis, D.D.; Vasiloglou, M.F.; Mantzoros, C.S. Circulating leptin in non-alcoholic fatty liver disease: A systematic review and meta-analysis. *Diabetologia* **2016**, *59*, 30–43. [CrossRef]
31. Mendez-Sanchez, N.; Arrese, M.; Gadano, A.; Oliveira, C.P.; Fassio, E.; Arab, J.P.; Chávez-Tapia, N.C.; Dirchwolf, M.; Torre, A.; Ridruejo, E.; et al. The Latin American Association for the Study of the Liver (ALEH) position statement on the redefinition of fatty liver disease. *Lancet Gastroenterol. Hepatol.* **2021**, *6*, 65–72. [CrossRef]
32. The Lancet Gastroenterology & Hepatology. Redefining non-alcoholic fatty liver disease: What's in a name? *Lancet Gastroenterol. Hepatol.* **2020**, *5*, 419. [CrossRef]
33. Polyzos, S.A.; Kountouras, J.; Zavos, C. Nonalcoholic fatty liver disease: The pathogenetic roles of insulin resistance and adipocytokines. *Curr. Mol. Med.* **2009**, *9*, 299–314. [CrossRef] [PubMed]
34. Bray, G.A. Obesity, a disorder of nutrient partitioning: The MONA LISA hypothesis. *J. Nutr.* **1991**, *121*, 1146–11462. [CrossRef] [PubMed]
35. Martínez-Una, M.; López-Mancheno, Y.; Diéguez, C.; Fernández-Rojo, M.A.; Novelle, M.G. Unraveling the Role of Leptin in Liver Function and Its Relationship with Liver Diseases. *Int. J. Mol. Sci.* **2020**, *21*, 9368. [CrossRef]
36. Hossain, I.A.; Akter, S.; Rahman, M.K.; Ali, L. Gender specific association of serum leptin and insulinemic indices with nonalcoholic fatty liver disease in prediabetic subjects. *PLoS ONE* **2015**, *10*, 1–12. [CrossRef]
37. Cernea, S.; Roiban, A.L.; Both, E.; Huţanu, A. Serum leptin and leptin resistance correlations with NAFLD in patients with type 2 diabetes. *Diabetes Metab. Res. Rev.* **2018**, *34*, 1–11. [CrossRef]
38. Angulo, P.; Alba, L.M.; Petrovic, L.M.; Adams, L.A.; Lindor, K.D.; Jensen, M.D. Leptin, insulin resistance, and liver fibrosis in human nonalcoholic fatty liver disease. *J. Hepatol.* **2004**, *41*, 943–949. [CrossRef]
39. Chitturri, S.; Farrell, G.; Frost, L.; Kriketos, A.; Lin, R.; Fung, C.; Liddle, C.; Samarasinghe, D.; George, J. Serum leptin in NASH correlates with hepatic steatosis but not fibrosis: A manifestation of lipotoxicity? *Hepatology* **2002**, *36*, 403–409. [CrossRef]
40. Ataseven, H.; Bahcecioglu, I.H.; Kuzu, N.; Yalniz, M.; Celebi, S.; Erensoy, A.; Ustundag, B. The levels of ghrelin, leptin, TNF-alpha, and IL-6 in liver cirrhosis and hepatocellular carcinoma due to HBV and HDV infection. *Mediat. Inflamm.* **2006**, *2006*, 78380. [CrossRef]
41. Naveau, S.; Perlemuter, G.; Chaillet, M.; Raynard, B.; Balian, A.; Beuzen, F.; Portier, A.; Galanaud, P.; Emilie, D.; Chaput, J.-C. Serum leptin in patients with alcoholic liver disease. *Alcohol. Clin. Exp. Res.* **2006**, *30*, 1422–1428. [CrossRef] [PubMed]
42. Ockenga, J.; Tietge, U.J.F.; Böker, K.H.W.; Manns, M.P.; Brabant, G.; Bahr, M.J. Distinct roles of free leptin, bound leptin and soluble leptin receptor during the metabolic-inflammatory response in patients with liver cirrhosis. *Aliment. Pharmacol. Ther.* **2007**, *25*, 1301–1309. [CrossRef] [PubMed]
43. Ertle, J.; Dechene, A.; Sowa, J.P.; Penndorf, V.; Herzer, K.; Kaiser, G.; Schlaak, J.F.; Gerken, G.; Syn, W.-K.; Canbay, A. Non-alcoholic fatty liver disease progresses to hepatocellular carcinoma in the absence of apparent cirrhosis. *Int. J. Cancer* **2011**, *128*, 2436–2443. [CrossRef]
44. Robertson, S.A.; Leinninger, G.M.; Myers, M.G., Jr. Molecular and neural mediators of leptin action. *Physiol. Behav.* **2008**, *94*, 637–642. [CrossRef]
45. Wauman, J.; Zabeau, L.; Tavernier, J. The leptin receptor complex: Heavier than expected? *Front. Endocrinol.* **2017**, *8*, 30. [CrossRef]
46. Park, H.K.; Ahima, R.S. Physiology of leptin: Energy homeostasis, neuroendocrine function and metabolism. *Metabolism* **2015**, *64*, 24–34. [CrossRef]
47. Adolph, T.E.; Grander, C.; Grabherr, F.; Tilg, H. Adipokines and non-alcoholic fatty liver disease: Multiple interactions. *Int. J. Mol. Sci.* **2017**, *18*, 1649. [CrossRef]

48. Myers, M.G.; Cowley, M.A.; Münzberg, H. Mechanisms of leptin action and leptin resistance. *Annu. Rev. Physiol.* **2008**, *70*, 537–556. [CrossRef]
49. Münzberg, H.; Morrison, C.D. Structure, production and signaling of leptin. *Metabolism* **2015**, *64*, 13–23. [CrossRef] [PubMed]
50. Polyzos, S.A.; Kountouras, J.; Zavos, C.; Deretzi, G. The potential adverse role of leptin resistance in nonalcoholic fatty liver disease: A hypothesis based on critical review of the literature. *J. Clin. Gastroenterol.* **2011**, *45*, 50–54. [CrossRef] [PubMed]
51. German, J.; Kim, F.; Schwartz, G.J.; Havel, P.J.; Rhodes, C.J.; Schwartz, M.W.; Morton, G.J. Hypothalamic leptin signaling regulates hepatic insulin sensitivity via a neurocircuit involving the vagus nerve. *Endocrinology* **2009**, *150*, 4502–4511. [CrossRef]
52. Utzschneider, K.M.; Kahn, S.E. Review: The role of insulin resistance in nonalcoholic fatty liver disease. *J. Clin. Endocrinol. Metab.* **2006**, *91*, 4753–4761. [CrossRef] [PubMed]
53. Bugianesi, E.; Moscatiello, S.; Ciaravella, M.F.; Marchesini, G. Insulin resistance in nonalcoholic fatty liver disease. *Curr. Pharm. Des.* **2010**, *16*, 1941–1951. [CrossRef]
54. Khan, R.S.; Bril, F.; Cusi, K.; Newsome, P.N. Modulation of Insulin Resistance in Nonalcoholic Fatty Liver Disease. *Hepatology* **2019**, *70*, 711–724. [CrossRef] [PubMed]
55. Wu, L.; Chen, G.; Liu, W.; Yang, X.; Gao, J.; Huang, L.; Guan, H.; Li, Z.; Zheng, Z.; Li, M.; et al. Intramuscular injection of exogenous leptin induces adiposity, glucose intolerance and fatty liver by repressing the JAK2-STAT3/PI3K pathway in a rat model. *Gen. Comp. Endocrinol.* **2017**, *252*, 88–96. [CrossRef] [PubMed]
56. Sahin-Efe, A.; Upadhyay, J.; Ko, B.J.; Dincer, F.; Park, K.H.; Migdal, A.; Vokonas, P.; Mantzoros, C. Irisin and leptin concentrations in relation to obesity, and developing type 2 diabetes: A cross sectional and a prospective case-control study nested in the Normative Aging Study. *Metabolism* **2018**, *79*, 24–32. [CrossRef] [PubMed]
57. Polyzos, S.A.; Kountouras, J.; Zavos, C.; Stergiopoulos, C. Adipocytokines in insulin resistance and non-alcoholic fatty liver disease: The two sides of the same coin. *Med. Hypotheses.* **2010**, *74*, 1089–1090. [CrossRef]
58. Polyzos, S.A.; Perakakis, N.; Mantzoros, C.S. Fatty liver in lipodystrophy: A review with a focus on therapeutic perspectives of adiponectin and/or leptin replacement. *Metabolism* **2019**, *96*, 66–82. [CrossRef]
59. Chan, J.L.; Lutz, K.; Cochran, E.; Huang, W.; Peters, Y.; Weyer, C.; Gorden, P. Clinical effects of long-term metreleptin treatment in patients with lipodystrophy. *Endocr. Pract.* **2011**, *17*, 922–932. [CrossRef]
60. Polyzos, S.A.; Mantzoros, C.S. Leptin in Health and Disease: Facts and Expectations at its Twentieth Anniversary. *Metabolism* **2015**, *64*, 5–12. [CrossRef]
61. Boutari, C.; Mantzoros, C.S. Adiponectin and leptin in the diagnosis and therapy of NAFLD. *Metabolism* **2020**, *103*, 154028. [CrossRef]
62. DePaoli, A.M. Leptin in common obesity and associated disorders of metabolism. *J. Endocrinol.* **2014**, *223*, T71–T81. [CrossRef] [PubMed]
63. Wang, J.; He, W.; Tsai, P.-J.; Chen, P.-H.; Ye, M.; Guo, J.; Su, Z. Mutual interaction between endoplasmic reticulum and mitochondria in nonalcoholic fatty liver disease. *Lipids Health Dis.* **2020**, *19*, 72. [CrossRef]
64. Hirsova, P.; Gores, G.J. Death Receptor-Mediated Cell Death and Proinflammatory Signaling in Nonalcoholic Steatohepatitis. *Cell. Mol. Gastroenterol. Hepatol.* **2015**, *1*, 17–27. [CrossRef]
65. Moon, H.-S.; Dalamaga, M.; Kim, S.-Y.; Polyzos, S.A.; Hamnvik, O.-P.; Magkos, F.; Paruthi, J.; Mantzoros, C.S. Leptin's role in lipodystrophic and nonlipodystrophic insulin-resistant and diabetic individuals. *Endocr. Rev.* **2013**, *34*, 377–412. [CrossRef]
66. Asilmaz, E.; Cohen, P.; Miyazaki, M.; Dobrzyn, P.; Ueki, K.; Fayzikhodjaeva, G.; Soukas, A.A.; Kahn, C.R.; Ntambi, J.M.; Socci, N.D.; et al. Site and mechanism of leptin action in a rodent form of congenital lipodystrophy. *J. Clin. Investig.* **2004**, *113*, 414–424. [CrossRef]
67. Wang, M.-Y.; Chen, L.; Clark, G.O.; Lee, Y.; Stevens, R.D.; Ilkayeva, O.R.; Wenner, B.R.; Bain, J.R.; Charron, M.J.; Newgard, C.B.; et al. Leptin therapy in insulin-deficient type I diabetes. *Proc. Natl. Acad. Sci. USA* **2010**, *107*, 4813–4819. [CrossRef]
68. Denechaud, P.-D.; Dentin, R.; Girard, J.; Postic, C. Role of ChREBP in hepatic steatosis and insulin resistance. *FEBS Lett.* **2008**, *582*, 68–73. [CrossRef]
69. Huang, W.; Metlakunta, A.; Dedousis, N.; Ortmeyer, H.K.; Stefanovic-Racic, M.; O'Doherty, R.M. Leptin augments the acute suppressive effects of insulin on hepatic very low-density lipoprotein production in rats. *Endocrinology* **2009**, *150*, 2169–2174. [CrossRef]
70. Cortés, V.A.; Cautivo, K.M.; Rong, S.; Garg, A.; Horton, J.D.; Agarwal, A.K. Leptin ameliorates insulin resistance and hepatic steatosis in Agpat2-/- lipodystrophic mice independent of hepatocyte leptin receptors. *J. Lipid Res.* **2014**, *55*, 276–288. [CrossRef]
71. Hackl, M.T.; Fürnsinn, C.; Schuh, C.M.; Krssak, M.; Carli, F.; Guerra, S.; Freudenthaler, A.; Baumgartner-Parzer, S.; Helbich, T.H.; Luger, A.; et al. Brain leptin reduces liver lipids by increasing hepatic triglyceride secretion and lowering lipogenesis. *Nat. Commun.* **2019**, *10*, 2717. [CrossRef] [PubMed]
72. Tang, X.; Li, J.; Xiang, W.; Cui, Y.; Xie, B.; Wang, X.; Xu, Z.; Gan, L. Metformin increases hepatic leptin receptor and decreases steatosis in mice. *J. Endocrinol.* **2016**, *230*, 227–237. [CrossRef]
73. Lim, D.-W.; Bose, S.; Wang, J.-H.; Choi, H.S.; Kim, Y.-M.; Chin, Y.-M.; Jeon, S.-H.; Kim, J.-F.; Kim, H. Modified SJH alleviates FFAs-induced hepatic steatosis through leptin signaling pathways. *Sci. Rep.* **2017**, *7*, 45425. [CrossRef]

74. Vernon, G.; Baranova, A.; Younossi, Z.M. Systematic review: The epidemiology and natural history of non-alcoholic fatty liver disease and non-alcoholic steatohepatitis in adults. *Aliment. Pharmacol. Ther.* **2011**, *34*, 274–285. [CrossRef]
75. Samuel, V.T.; Shulman, G.I. Mechanisms for insulin resistance: Common threads and missing links. *Cell* **2012**, *148*, 852–871. [CrossRef]
76. Rotundo, L.; Persaud, A.; Feurdean, M.; Ahlawat, S.; Kim, H.S. The Association of leptin with severity of non-alcoholic fatty liver disease: A population-based study. *Clin. Mol. Hepatol.* **2018**, *24*, 392–401. [CrossRef]
77. Pavlidis, C.; Panoutsopoulos, G.I.; Tiniakos, D.; Koutsounas, S.; Vlachogiannakos, J.; Zouboulis-Vafiadis, I. Serum leptin and ghrelin in chronic hepatitis C patients with steatosis. *World J. Gastroenterol.* **2011**, *17*, 5097–5104. [CrossRef] [PubMed]
78. Eshraghian, A.; Nikeghbalian, S.; Shamsaeefar, A.; Kazemi, K.; Fattahi, M.R.; Malek-Hosseini, S.A. Hepatic steatosis and liver fat contents in liver transplant recipients are associated with serum adipokines and insulin resistance. *Sci. Rep.* **2020**, *10*, 12701. [CrossRef] [PubMed]
79. Tilg, H.; Adolph, T.E.; Moschen, A.R. Multiple Parallel Hits Hypothesis in Nonalcoholic Fatty Liver Disease: Revisited After a Decade. *Hepatology* **2021**, *73*, 833–842. [CrossRef]
80. Hirsova, P.; Ibrahim, S.H.; Gores, G.J.; Malhi, H. Lipotoxic lethal and sublethal stress signaling in hepatocytes: Relevance to NASH pathogenesis. *J. Lipid. Res.* **2016**, *57*, 1758–1770. [CrossRef] [PubMed]
81. Schuppan, D.; Surabattula, R.; Wang, X.Y. Determinants of fibrosis progression and regression in NASH. *J. Hepatol.* **2018**, *68*, 238–250. [CrossRef]
82. Stal, P. Liver fibrosis in non-alcoholic fatty liver disease-diagnostic challenge with prognostic significance. *World J. Gastroenterol.* **2015**, *21*, 11077–11087. [CrossRef]
83. Koyama, Y.; Brenner, D.A. Liver inflammation and fibrosis. *J. Clin. Investig.* **2017**, *127*, 55–64. [CrossRef]
84. Chatterjee, S.; Ganini, D.; Tokar, E.J.; Kumar, A.; Das, S.; Corbett, J.; Kaddiska, M.B.; Waalkes, M.P.; Diehl, A.M.; Mason, R.P. Leptin is key to peroxynitrite-mediated oxidative stress and Kupffer cell activation in experimental non-alcoholic steatohepatitis. *J. Hepatol.* **2013**, *58*, 778–784. [CrossRef]
85. Seth, R.K.; Das, S.; Kumar, A.; Chanda, A.; Kadiiska, M.B.; Michelotti, G.; Manautou, J.; Diehl, A.M.; Chatterjee, S. CYP2E1-dependent and leptin-mediated hepatic CD57 expression on CD8+ T cells aid progression of environment-linked nonalcoholic steatohepatitis. *Toxicol. Appl. Pharmacol.* **2014**, *274*, 42–54. [CrossRef] [PubMed]
86. Mundi, M.S.; Velapati, S.; Patel, J.; Kellogg, T.A.; Abu-Dayyeh, B.K.; Hurt, R.T. Evolution of NAFLD and Its Management. *Nutr. Clin. Pract.* **2020**, *35*, 72–84. [CrossRef]
87. Procaccini, C.; Galgani, M.; De Rosa, V.; Carbone, F.; La Rocca, C.; Ranucci, G.; Iorio, R.; Matarese, G. Leptin: The prototypic adipocytokine and its role in NAFLD. *Curr. Pharm. Des.* **2010**, *16*, 1902–1912. [CrossRef]
88. Otte, C.; Otte, J.-M.; Strodthoff, D.; Bornstein, S.R.; Fölsch, U.R.; Mönig, H.; Kloehn, S. Expression of leptin and leptin receptor during the development of liver fibrosis and cirrhosis. *Exp. Clin. Endocrinol. Diabetes* **2004**, *112*, 10–17. [CrossRef]
89. Sanyal, A.J. Past, present and future perspectives in nonalcoholic fatty liver disease. *Nat. Rev. Gastroenterol. Hepatol.* **2019**, *16*, 377–386. [CrossRef]
90. Duan, X.F.; Tang, P.; Li, Q.; Yu, Z.T. Obesity, adipokines and hepatocellular carcinoma. *Int. J. Cancer* **2013**, *133*, 1776–1783. [CrossRef]
91. Vanni, E.; Bugianesi, E. Obesity and liver cancer. *Clin. Liver Dis.* **2014**, *18*, 191–203. [CrossRef]
92. Wang, S.-N.; Lee, K.-T.; Ker, C.-G. Leptin in hepatocellular carcinoma. *World J. Gastroenterol.* **2010**, *16*, 5801–5809. [CrossRef]
93. Zhang, L.; Yuan, Q.; Li, M.; Chai, D.; Deng, W.; Wang, W. The association of leptin and adiponectin with hepatocellular carcinoma risk and prognosis: A combination of traditional, survival, and dose-response meta-analysis. *BMC Cancer* **2020**, *20*, 1167. [CrossRef]
94. Ribatti, D.; Belloni, A.S.; Nico, B.; Di Comite, M.; Crivellato, E.; Vacca, A. Leptin-leptin receptor are involved in angiogenesis in human hepatocellular carcinoma. *Peptides* **2008**, *29*, 1596–1602. [CrossRef]
95. Saxena, N.K.; Titus, M.A.; Ding, X.; Floyd, J.; Srinivasan, S.; Sitaraman, S.V.; Anania, F.A. Leptin as a novel profibrogenic cytokine in hepatic stellate cells: Mitogenesis and inhibition of apoptosis mediated by extracellular regulated kinase (Erk) and Akt phosphorylation. *FASEB J.* **2004**, *18*, 1612–1614. [CrossRef]
96. Kitade, M.; Yoshiji, H.; Kojima, H.; Ikenaka, Y.; Noguchi, R.; Kaji, K.; Yoshii, J.; Yanase, K.; Namisaki, T.; Asada, K.; et al. Leptin-mediated neovascularization is a prerequisite for progression of nonalcoholic steatohepatitis in rats. *Hepatology* **2006**, *44*, 983–991. [CrossRef]
97. Aleffi, S.; Petrai, I.; Bertolani, C.; Parola, M.; Colombatto, S.; Novo, E.; Vizzutti, F.; Anania, F.A.; Milani, S.; Rombouts, K.; et al. Upregulation of proinflammatory and proangiogenic cytokines by leptin in human hepatic stellate cells. *Hepatology* **2005**, *42*, 1339–1348. [CrossRef] [PubMed]
98. Sadik, N.A.; Ahmed, A.; Ahmed, S. The significance of serum levels of adiponectin, leptin, and hyaluronic acid in hepatocellular carcinoma of cirrhotic and noncirrhotic patients. *Hum. Exp. Toxicol.* **2012**, *31*, 311–321. [CrossRef] [PubMed]
99. Mittenbühler, M.J.; Sprenger, H.-G.; Gruber, S.; Wunderlich, C.M.; Kern, L.; Brüning, J.C.; Wunderich, F.T. Hepatic leptin receptor expression can partially compensate for IL-6Rα deficiency in DEN-induced hepatocellular carcinoma. *Mol. Metab.* **2018**, *17*, 122–133. [CrossRef] [PubMed]

100. Huang, H.; Zhan, J.; Ling, F.; Huang, Y.; Yang, M.; Zhang, Y.; Wei, Y.; Zhang, Q.; Wang, H.; Song, L.; et al. Leptin Receptor (LEPR) promotes proliferation, migration, and invasion and inhibits apoptosis in hepatocellular carcinoma by regulating ANXA7. *Cancer Cell Int.* **2021**, *21*, 4. [CrossRef] [PubMed]
101. Elinav, E.; Abd-Elnabi, A.; Pappo, O.; Bernstein, I.; Klein, A.; Engelhardt, D.; Rabbani, E.; Ilan, Y. Supression of hepatocellular carcinoma growth in mice via leptin is associated with inhibition of tumor cell growth and natural killer cell activation. *J. Hepatol.* **2006**, *44*, 529–536. [CrossRef] [PubMed]
102. Wang, S.N.; Yeh, Y.T.; Yang, S.F.; Chai, C.Y.; Lee, K.T. Potential role of leptin expression in hepatocellular carcinoma. *J. Clin. Pathol.* **2006**, *59*, 930–934. [CrossRef] [PubMed]
103. Wang, S.N.; Chuang, S.C.; Yeh, Y.T.; Yang, S.F.; Chai, C.Y.; Chen, W.T.; Kuo, K.K.; Chen, J.S.; Lee, K.T. Potential prognostic value of leptin receptor in hepatocellular carcinoma. *J. Clin. Pathol.* **2006**, *59*, 1267–1271. [CrossRef] [PubMed]

biomedicines

MDPI

Review

Depression and Cognitive Impairment—Extrahepatic Manifestations of NAFLD and NASH

Martina Colognesi †, Daniela Gabbia † and Sara De Martin *

Department of Pharmaceutical and Pharmacological Sciences, University of Padova, L.go Meneghetti 2, 35131 Padova, Italy; martina.colognesi@studenti.unipd.it (M.C.); daniela.gabbia@unipd.it (D.G.)

* Correspondence: sara.demartin@unipd.it; Tel.: +39-0498275077

† M.C. and D.G. share first co-authorship.

Received: 29 June 2020; Accepted: 18 July 2020; Published: 21 July 2020

Abstract: Non-alcoholic fatty liver disease (NAFLD) and its complication non-alcoholic steatohepatitis (NASH) are important causes of liver disease worldwide. Recently, a significant association between these hepatic diseases and different central nervous system (CNS) disorders has been observed in an increasing number of patients. NAFLD-related CNS dysfunctions include cognitive impairment, hippocampal-dependent memory impairment, and mood imbalances (in particular, depression and anxiety). This review aims at summarizing the main correlations observed between NAFLD development and these CNS dysfunctions, focusing on the studies investigating the mechanism(s) involved in this association. Growing evidences point at cerebrovascular alteration, neuroinflammation, and brain insulin resistance as NAFLD/NASH-related CNS manifestations. Since the pharmacological options available for the management of these conditions are still limited, further studies are needed to unravel the mechanism(s) of NAFLD/NASH and their central manifestations and identify effective pharmacological targets.

Keywords: non-alcoholic fatty liver disease; NAFLD; steatohepatitis; NASH; cognitive impairment; memory dysfunction; Alzheimer's disease; neurodegeneration

1. Introduction

Non-alcoholic fatty liver disease (NAFLD) is considered the hepatic manifestation of metabolic syndrome and is associated with progressive hepatocellular lipid accumulation, mostly of triglycerides, up to more than 10% of liver weight [1]. This disease comprises a wide range of liver disorders, from simple non-alcoholic fatty liver (NAFL) to non-alcoholic steatohepatitis (NASH) and, if not treated, can lead to threatening complications such as cirrhosis and hepatocellular carcinoma [2]. Generally, NAFLD is considered a benign and reversible condition, although one-third of NAFLD patients eventually progress to NASH, which is characterized by inflammation and hepatocellular injury [3]. While the causes involved in the establishment of NAFLD have been largely investigated, the main factors controlling the progression of NAFLD toward NASH remain pretty much unknown and are currently intensively studied. Many experimental evidences suggested that lipotoxicity, proinflammatory mediators, and oxidative stress may have a central role in this process [3], which can occur in the presence or absence of a high amount of dietary fat ingestion [1]. Moreover, the consumption of imbalanced diets (e.g., excessive fat and sugar intake), as well as the alteration of gut microbiome are involved in NAFLD development and progression [4–6]. In particular, high fat and high sugar diets, besides promoting the deposition of fat in the liver, could modify microbiome composition and affect gut barrier integrity, facilitating bacterial translocation and inflammation. Inflammation and oxidative stress have also shown to play a pivotal role in extrahepatic diseases, including many different central nervous system (CNS) diseases such as, for instance, Alzheimer's disease (AD). Accordingly, extensive

evidences obtained in the last years have revealed that NAFLD may represent a risk factor for CNS impairment [7].

Several observations suggest that a correlation may exist between metabolic liver diseases, such as NAFLD and NASH, and CNS disorders, starting from the increased risk of developing AD, mild cognitive impairment (MCI), and dementia in patients with dyslipidemic disorders, and an association with neurodegeneration and cognitive deficits has been observed in patients with metabolic syndrome-related diseases such as type 2 diabetes mellitus (T2DM) and obesity [3].

In this review, we want to point the attention to depression and mild and severe cognitive impairment, which are becoming a serious health threat, and in recent years have been associated to NAFLD and NASH.

2. Cognitive Dysfunction and Brain Abnormalities

2.1. Depression

Depression is one of the most common CNS diseases involved in adult premature death and it is characterized by specific cognitive and somatic abnormalities over time. The common symptoms of patients with depressive disorders are mood imbalances or anhedonia [8], which are also associated with social dysfunction and cognitive and functional impairment [9].

Since depression is known to be associated with chronic liver disease (CLD) [10,11], and considering that nearly 30% of patients with NAFLD show major depressive disorder (MDD) with a prevalence higher than the general population [12], it is plausible to hypothesize that a correlation exists between NAFLD and depression. However, controversial results have been obtained by the different studies that tried to validate this hypothesis (Table 1). While dated population-based studies reported that NAFLD is absolutely not correlated to depressive disorders [10], other studies conducted in the same period or more recently reported the existence of a possible association between depression and NAFLD [12,13]. In particular, the study of Youssef and collaborators provided robust evidence of the correlation between depressive symptoms and hepatocyte ballooning, one of the main hallmarks of NAFLD progression, even after the adjustment for potential confounding factors such as age, sex, ethnicity, body mass index (BMI), diabetes mellitus, systemic hypertension, smoking, alcohol consumption, and anxiety symptoms. Indeed, a multivariate data analysis showed more severe hepatocyte ballooning in patients with mood disorders, validating the hypothesis of a NAFLD role in depressive symptoms [13]. Accordingly, Tomeno and collaborators suggested a correlation between the severity of steatosis and MDD comorbidity in NAFLD patients. These findings were confirmed by higher levels of serum markers of liver dysfunction such as aspartate aminotransferase (ALT), alanine aminotransferase (AST), γ-glutamyl transpeptidase (GGT), and high-sensitivity C-reactive protein (hs-CRP) in NAFLD patients affected by MDD [12]. Although the results of these pioneering studies need to be confirmed by other investigations, they pointed the attention on the relationship between NAFLD severity and MDD.

For a better understanding of the liver disease influence on depressive disorders, preclinical evaluations were performed in animal models of NASH to verify the presence of behavioral mood changes in these models. The forced swimming test was used in one of these studies to assess depressive-like behavior, like despair and anhedonia, in rats. Rats with NASH showed a lack of struggle to escape, in contrast with their normal attitude. This result demonstrated that NASH rats were affected by a sense of hopelessness, which is normally associated with depression [14].

Table 1. Principal clinical studies reporting an association between depressive disorders and NAFLD.

Study	Settings and Study Design	Subjects	Methods	Results and Conclusions
Lee et al. (2013) [10]	Cross-sectional national survey, population-based	10231 NHANES participants in the 18th year or older	PHQ-9 survey to screen depression associated with hematologic and biochemical tests and viral hepatitis	Depression and chronic hepatitis C are independently associated, but not metabolic syndrome
Tomeno et al. (2015) [12]	Population-based	258 participants	Blood test monitoring and lifestyle counseling for 48 weeks, with assessment of insulin resistance through HOMA-IR	32 NAFLD patients were comorbid with MDD and showed higher biochemical parameters (ALT, AST, GGT, ferritin, hs-CRP, and cholinesterase) than NAFLD patients without MDD. Only NAFLD patients without MDD improved their conditions with treatment.
Youssef et al. (2013) [13]	Cross-sectional analyses, population-based	567 participants aged 20 and older	HADS questionnaire to assess severity of depression and anxiety	Severe depressive symptoms were associated with increased hepatocyte ballooning
Elwing et al. (2006) [11]	Case-control comparison	36 patients undergoing cholecystectomy and 36 matched control subjects	Structured interview to assess psychiatric illnesses	Lifetime MDD has significantly increased rates in NASH subjects, in accordance with PHQ-9.
Filipović et al. (2018) [15]	Population-based	40 NAFLD positive participants aged from 34 to 57, and 36 controls aged from 39 to 53	3D T1-weighted MR images to measure gray and white matter volume and brain lateral ventricles, Serbian version of the MoCA test to assess cognitive functioning and Hamilton's depression rating scale to evaluate depression level	Cognitive status declined in NAFLD patients, according to the MoCA index. These patients had reduced gray and white matter volumes and higher risk of depression.

NHANES: National Health and Nutrition Examination Survey; PHQ-9: Patient Health Questionnaire; HOMA-IR: Homeostasis Model for the Assessment of Insulin Resistance; HADS: Hospital Anxiety & Depression Scale; MoCA: Montreal Cognitive Assessment.

Depression and anxiety have been associated not only with NAFLD, but they have also shown to be strictly involved in pathological features typical of NAFLD progression to NASH, such as insulin resistance and inflammation. The study of Elwing and collaborators tried to evaluate the correlation between these mood disorders and liver histological features. Their findings provide evidence that depression is directly associated with hepatic inflammatory markers, suggesting its active role in NASH progression [11]. One recent study investigated the possible changes of brain tissue volumes in NAFLD patients. They found a significant reduction of white and gray brain volumes and an increased volume of lateral ventricles, with respect to healthy patients. This ulterior remark suggests a higher risk of depression in NAFLD-diagnosed patients [15].

2.2. Cognitive Impairment

Mild cognitive impairment (MCI) is defined as an impairment in cognition more severe than that generally associated with normal memory and cognitive changes merely due to aging (clinically considered as "age-related cognitive decline"). However, this condition is less problematic than dementia or other cognitive deficits which significantly impair daily functions [16]. Among the different cognitive features which could be impaired, we will focus on memory, social functioning, visuospatial function, and executive functioning.

As far as metabolic syndrome and its components are concerned, including liver manifestations as NAFLD/NASH, many recent population-based studies have suggested their involvement in cognitive impairment, from mild ones up to dementia [17]. Although there are studies providing evidences that metabolic syndrome [18,19] and NASH [3,14] are associated with cognitive deficits, whether NAFLD may lead to cognitive impairment remains controversial (Table 2).

One of the first studies suggesting the presence of functional and cognitive impairment in NAFLD patients was a study by Elliott and collaborators [20]. The main conclusion they achieved was that NAFLD patients had a significantly worse cognitive function with respect to controls, supporting the idea that NAFLD may influence cognitive features.

A lead study in this field has been performed by Seo and collaborators and confirmed the hypothesis of the independent association between NAFLD and cognitive impairment after the analysis of the data obtained from the Third National Health and Nutrition Examination Survey (NHANES III). The authors considered patients with cognitive impairment, excluding possible confounding factors (e.g., BMI, waist circumference, diabetes mellitus, hypertension, hypercholesterolemia, history of acute myocardial infarction, heart failure, and stroke) and considering factors known to affect cognition, such as cardiovascular disease. They observed an increase of liver enzymes, surrogate marker of NAFLD presence and progression to NASH, even without histological signs of advanced liver dysfunction [21].

It is well known that screening tools like the Montreal Cognitive Assessment (MoCA) are quite useful and more sensitive than others for diagnosing forms of cognitive decline in old adults and patients with MCI [22]. Celikbilek and collaborators utilized for the first time the Turkish version of the MoCA test to investigate whether patients with NAFLD show more probability to manifest cognitive impairment than healthy subjects. The results showed a correlation between liver dysfunction and cognitive impairment, in particular, in the visuospatial and executive function domains, both associated with the prefrontal cortex (PFC) [23].

Recent studies tried to assess which brain region(s) may be affected by NAFLD and reported that these patients were characterized by lower levels of metabolic activity in some brain areas, e.g., PFC, hippocampus, and amygdala, due to low levels of dopamine in the PFC and cerebellum and of noradrenaline in the striatum [14]. Taken together, these observations validate the hypothesis of NAFLD implication in cognitive impairment.

Table 2. Principal clinical studies reported on cognitive impairment, MCI, and NAFLD patients.

Study	Settings and Study Design	Subjects	Methods	Results and Conclusions
Elliott et al. (2013) [20]	Cohort study	224 NAFLD participants and 100 controls	PHAQ and CFQ were used to evaluate functional and physical ability and cognitive abilities.	NAFLD patients showed significantly worse functional abilities, and they had more difficulties in specific daily activities than controls.
Seo et al. (2016) [21]	Cross-sectional population-based analysis	4472 participants aged from 20 to 59	Assessment of liver enzyme activity and cognitive evaluation using SRTT, SDLT, and SDST	NAFLD patients showed lower performance on the SDLT, and NAFLD resulted independently associated with lower cognitive performance.
Celikbilek et al. (2018) [23]	Prospective cross-sectional population-based analysis	70 participants and 73 age- and sex-matched controls aged from 18 to 70	Turkish version of the MoCA test to evaluate cognitive functions	Deficits were observed in each cognitive domain, mainly in the visuospatial and executive functioning. NAFLD patients reported significantly lower MoCA test scores.
An et al. (2019) [24]	Cross-sectional population-based analysis	23 NAFLD participants and 21 matched controls	BDI was used to assess depressive symptoms, and RBANS was used to characterize neurocognitive deficits.	BDI mean score indicated a moderate depression in NAFLD patients, and women reported significant association with visuospatial memory deficit.
Weinstein et al. (2019) [25]	Cross-sectional population-based analysis	1287 participants	Trail-making test to measure executive functioning. Similarity test was used to assess abstract reasoning skills, and the Hooper visual organization test was used to measure visual perception.	NAFLD and cognitive performances were not associated; however, poorer performances on the trail-making and similarities tests were linked to increased risk of advanced fibrosis in NAFLD participants.

PHAQ: Patient-Reported Outcomes Measurement Information System, Health Assessment Questionnaire; CFQ: Cognitive Failures Questionnaire; SRTT: Simple Reaction Time Test; SDLT: Serial Digit Learning Test; SDST: Symbol-Digit Substitution Test; BDI: Beck Depression Inventory; RBANS: Repeatable Battery for Assessment of Neuropsychological Status.

Another study investigated the possible correlation between cognitive status and NAFLD using the MoCA test, finding a lower MoCA score and a reduction in white and gray brain volumes in NAFLD patients [15]. In combination with the reduced gray and white volumes, these authors found an increase of lateral ventricles volumes, justifying the constant total brain volume in presence of different cognitive situations between the tested group. The main conclusion achieved by this study is that patients with NAFLD have a risk four times higher of manifesting lower cognitive abilities and depleted cognitive performance and deficit, and also confirmed the higher concentration of AST in NAFLD patients with cognitive deficit [15]. The correlation between higher levels of AST and ALT and poorer cognitive function, especially in visuospatial memory, was also supported by a recent population-based study conducted by An and collaborators [24].

Besides these results, there are also studies that found no correlation between NAFLD per se and cognitive impairment, as found in a cross-sectional study by Weinstein et al. [25], who associated poorer cognitive function (mainly in the executive areas) with an increased risk of advanced liver fibrosis but not NAFLD. These results suggest that the association between NAFLD and cognition may be influenced by the specific cognitive brain domains studied and also by the type of liver dysfunction.

Finally, to which extent sleep apnea and chronic intermittent hypoxia, which are known to result in cognitive impairment [26] and also to be associated with the metabolic syndrome and NAFLD/NASH [27], contributes to the cognitive impairment found in NAFLD still remains to be elucidated.

2.3. Neurodegenerative Diseases: Alzheimer's Disease

Alzheimer's disease is a neurodegenerative disorder which may derive from MCI progression [22] and it is characterized by the progressive atrophy of cortical and medial temporal structures, CNS areas involved in memory and learning deficits [28]. It belongs to a series of neurodegenerative disease provoking pathophysiological brain changes via accumulation of misfolded proteins, in particular, peptide variants of amyloid-β (Aβ). Progressive protein deposition causes amyloid and senile plaques formation with synaptic dysfunction, dendritic spines loss, and neuronal death [7].

The AD etiology remains unclear, but there are many possible mechanisms, other than aging, proposed to explain its development. Recently, a number of studies provided evidence of a strict correlation between metabolic syndrome-associated diseases, such as diabetes mellitus and NAFLD, and neurodegenerative disorders, like AD [29]. Indeed, de la Monte and collaborators introduced the concept that AD could be considered a neurodegenerative disorder mediated by insulin resistance, since similar abnormalities were found in both pathologies [28]. NAFLD is known to be associated with a dysregulated lipid metabolism and increased cellular oxidative stress, and these same characteristics are present in AD, underlining their possible interconnection. Furthermore, epidemiological data suggested that dyslipidemic and insulin-dependent diseases play a key role as cofactors of AD pathogenesis [3].

The hypothesis of a correlation between AD and NAFLD is very recent, and most studies are performed in animal models and not in human patients. One aspect implicated in the development of metabolic syndrome, NAFLD, and potentially AD is the consumption of a high fat diet (HFD). A number of experimental studies used this type of diet in animal models to verify whether an association exists between AD and metabolic syndrome related diseases [30]. One of the first studies conducted in mice chronically fed with HFD showed a time-dependent decline in brain weight with respect to controls. Subtle histopathological abnormalities like neuronal loss foci and cellular apoptosis were also found in brain tissue, pointing to a correlation between HFD-induced NAFLD and mild neuropathological brain lesions [31]. Kim and collaborators evaluated the possible impact of NAFLD in AD pathogenesis, using an AD transgenic mouse model. Their findings suggested an acceleration in neurodegeneration and in Aβ plaque formation after HFD-induced acute inflammation and NAFLD development [30]. The fact that HFD and fructose-rich diets may quicken AD cognitive decline has also been confirmed in recent experimental studies [32–34].

A population-based study was carried out to assess whether different biological markers, together with neuropsychological evaluations, could provide a robust method to measure MCI and early AD progression (Table 3). The authors of this study considered different covariates in their evaluations, such as age, sex, BMI, years of education, and APOE ε4 status, and the results they obtained suggested that ALT and AST to ALT ratio, whose levels increased in NAFLD patients, were directly associated with poor cognition and greater Aβ deposition in brain areas [35].

Currently, there is a great interest in confirming the existence of a correlation between NAFLD and AD, probably because these diseases are widespread worldwide, and an effective pharmacological treatment is still missing for both of them. New approaches are in the phase of optimization, as suggested by Karbalaei and collaborators, who used a systems biology method to investigate the genes involved in both NAFLD and AD pathophysiological pathways, providing another evidence of their reciprocal interconnection [36].

Table 3. Principal clinical study reported on the Alzheimer's disease and NAFLD connection.

Study	Settings and Study Design	Subjects	Methods	Results and Conclusions
Nho et al. (2019) [35]	Cohort study	1581 participants aged around 70	Evaluation of cerebrospinal fluid biomarkers and brain atrophy (magnetic resonance), and scores for executive functioning and memory	Increased ALT and AST to ALT ratio in AD patients were linked to poor cognition.

3. Molecular and Pathophysiological Pathways Connecting NAFLD/NASH to Cognitive Impairment

The pathogenesis of NAFLD and NASH is a quite complex process involving multiple pathways and risk factors, first of all being diet imbalances. The progressive lipid deposition in the liver leads to the alteration of lipid metabolism/lipid peroxidation, insulin resistance, oxidative stress, and inflammatory damage. This promotes a state of peripheral insulin resistance and low-grade systemic inflammation. For this reason, an increasing amount of evidence suggests that NAFLD and NASH not only affect liver function, but also induce multiple extrahepatic manifestations that also involve the central nervous system, e.g., depression, cognitive impairment, AD, and dementia. Moreover, emerging evidence has demonstrated the link between microbiome composition and gut impairment, and the development of both liver diseases and cognitive dysfunctions [37,38]. It could be hypothesized that the same detrimental stimuli that lead to NAFLD and NASH in the liver could induce cognitive impairment or AD-type neurodegeneration in the brain.

Many signaling pathways are demonstrated to be altered in both NAFLD/NASH and CNS dysfunction (depression, cognitive impairment, dementia, and AD), suggesting that these diseases share, at least in part, the same pathogenetic mechanisms. Some studies reported conflicting results and whether there is a causal relation between liver damage and the development of cognitive dysfunction or if steatosis triggers for other subsequent deleterious pathogenetic mechanisms remains to be fully understood [23,39].

The main pathways involved in the NALFD/NASH-related brain dysfunction are summarized in Figure 1. Three are the main pathological aspects accounted to link NAFLD/NASH to cognitive impairment, i.e., cerebrovascular alteration, neuroinflammation, and brain insulin resistance. Accordingly, the study of Karbalaei et al. suggested three putative groups of genes involved in both AD and NAFLD related to carbohydrate metabolism, long fatty acid metabolism, and interleukin signaling pathways [36].

One of the first brain area affected by early stage chronic liver diseases is the cerebellum; then, brain injury could progress to the hippocampus or prefrontal cortex (PFC), brain areas crucial for cognition, memory, learning, and mood regulation [40–43].

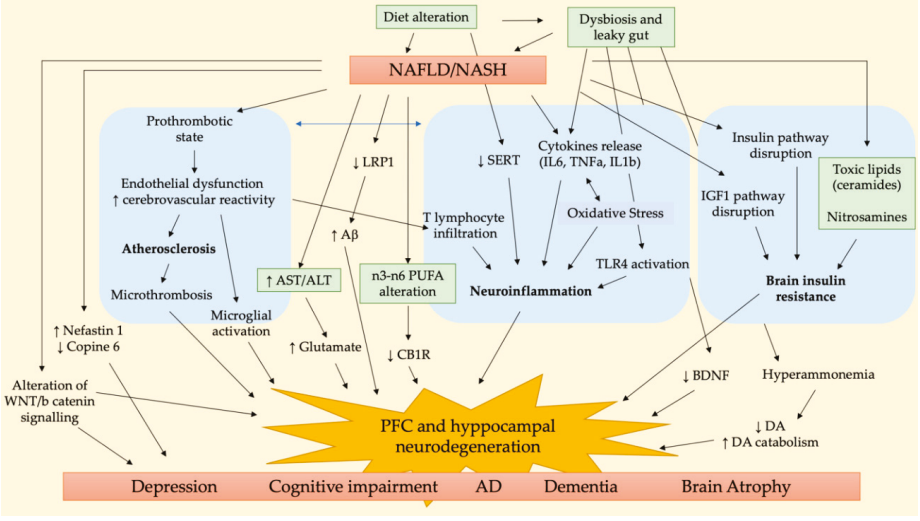

Figure 1. Main pathophysiological pathways involved in NAFLD/NASH and cognitive impairment.

The histological analysis of NASH patients' cerebella revealed the presence of parenchymal microthrombi, neurodegeneration in the Purkinje layer, and glial alteration in the molecular layer, in addition to the activation of microglia and astrocytes of white matter. Some of these features are also observed in some neurodegenerative and vascular diseases, e.g., AD, vascular dementia, and atherosclerosis [44].

Petta and collaborators observed in NAFLD patients the presence of cerebral lesions in PFC white matter, whose prevalence increases as liver function worsens, e.g., in NASH and advanced fibrosis, probably due to the proinflammatory and proatherogenic state typical of these advanced stages of liver diseases [45]. This is coherent with the fact that liver steatosis is characterized by a proinflammatory state that promotes atherosclerosis, endothelial dysfunction, platelet, and microglia activation in the brain. These alterations induce micro- and macrovascular damage, which is responsible for clinical and subclinical cerebrovascular dysfunctions [39]. The activation of inflammatory pathways characteristic of NAFLD and NASH induces the production and release of some inflammatory, prothrombotic, and oxidative stress mediators, e.g., the cytokines IL6, TNFα, and IL1β. Moreover, the increased production of reactive oxygen species could sustain the inflammatory cascade, further increasing IL6 release, neuroinflammation, and neurodegeneration [30]. It has been demonstrated that the peripheral inflammation observed in NASH patients may lead to endothelial damage and formation of microthrombi in the brain parenchyma, leading to neuroinflammation. It has been hypothesized that this phenomenon can be due to infiltrating CD4+ T lymphocytes that have been observed in the cerebellar meninges of these patients [44]. In addition, Ghareeb and collaborators observed an alteration in neurotransmitter activities induced by NAFLD, in addition to oxidative stress and metabolic dysfunction, and suggested that this may represent a risk factor for cognitive dysfunction and neurodegeneration [46]. In detail, they observed an increased activity of acetylcholine esterase (AChE) and monoamine oxidase (MAO) in NAFLD liver and brain tissues with respect to controls, accompanied to an increase of ATPase activity, and the inflammatory markers IL6 and TNF-α in the brain.

The Western diet (WD), a diet rich in fat and sugar, is considered one of the main risk factors for NAFLD/NASH, and its implication in the context of neuropsychiatric disorders and cognitive decline is a raising evidence. In the brain, it has been observed that WD is able to increase the

activity of the endocannabinoid (eCB) system in the limbic areas controlling emotions, due to the increase of phospholipidic n-6/n-3 PUFA ratio in neuronal membranes and of n-6 PUFAs in the cytoplasm of hippocampal neurons. Cytoplasmatic n-6 PUFAs could be transformed into eCBs, lipid mediators binding to CB1 receptors (CB1R), reducing GABA release from interneurons located in CA1 area and altering theta oscillations. As a consequence of these alterations, WD could lead to an increase vulnerability to neuropsychiatric disorders and cognitive decline [47]. Moreover, an excessive consumption of fructose, a monosaccharide mainly used as sweetening agent in soft drinks, in addition to systemic metabolic alterations, was able to induce oxidative stress, thereby causing lipid peroxidation and protein nitrosylation in the hippocampus and reducing the expression of synaptic proteins, leading to impaired synaptic function, thus affecting learning and memory in a long-lived animal model [48]. Accordingly, many reports investigating the association between obesity and cognitive impairment have reported that the consumption of high-fat and high-sugar diet is able to increase oxidative stress, inflammation, and AChE activity, leading to cerebrovascular changes and neuronal loss in the hippocampus, disrupt myelination and axonal transmission, and decrease of dopamine (DA) and serotonin (5-HT) in the hippocampus, two of the key neurotransmitters involved in learning and memory processes [33,34,49,50].

Several pieces of evidence have demonstrated that unhealthy diets, e.g., the Western diet or high fructose intake, could greatly influence gut microbiome composition by decreasing anti-inflammatory autochthonous bacteria and increasing proinflammatory pathological ones. This affects intestinal permeability ("leaky gut") and leads to an increase of LPS/endotoxin entry into portal and systemic circulation [38]. This process could worsen liver steatosis and induce NASH progression by causing a widespread pro-inflammatory status. CNS function can also be impaired by these events through the gut–brain axis [51–53]. These studies further suggest the key role of the consumption of unbalanced diets and gut dysbiosis in the development of NAFLD/NASH, cognitive impairment, and AD.

An interesting review on the influence of liver dysfunction on AD progression suggested that chronic liver diseases may worsen amyloid burden due to an imbalance in peripheral amyloid-β (Aβ) clearance, leading to higher Aβ circulating levels. This can be due to a low hepatic expression of low-density lipoprotein receptor-related protein 1 (LRP-1), necessary for Aβ clearance, consequent to liver dysfunction and chronic inflammation. Furthermore, these features were proposed to negatively affect blood–brain barrier (BBB) integrity, thus contributing to a vicious cycle in Aβ clearance [7].

An impaired Wnt/β-catenin signaling pathway was reported to be involved in the pathogenesis of depression and AD [54,55]; thus, the dysregulated expression of proteins of this pathway observed in NAFLD rats could also be responsible for related cognitive impairment [56].

Another study demonstrated that the behavioral and cognitive impairments observed in rats with NAFLD could be linked to an imbalance of nesfatin-1 and copine 6 in the hippocampus and PFC [56]. Nesfatin-1 is able to regulate appetite, glucose, and energy metabolism, but also plays a role in mood and cognitive function [57,58]; thus, its increased plasma levels in NAFLD could be responsible for the observed cognitive dysfunction. Copine 6, a calcium sensor, plays an important role in brain-derived neurotrophic factor (BDNF)-dependent changes in dendritic spines, regulating neurotransmission, and promoting synaptic plasticity, learning and memory [59,60]. A decrease of copine 6 expression was related to depression-like behavior and immune activation and was also observed in NAFLD rats [56,61]. Another hypothesized mechanism leading to an increased risk of dementia and cognitive dysfunction in NAFLD/NASH subjects is related to chronic hyperglycemia and brain insulin resistance. It has been proposed that peripheral insulin resistance could trigger cognitive function through a liver–brain axis of neurodegeneration due to an excessive peripheral production of neurotoxic lipids, e.g., ceramides and nitrosamines, that pass across the blood–brain barrier (BBB) and affect neuronal activity, particularly in the hippocampus and PFC [3]. In the CNS, insulin orchestrates a network of pro-growth and pro-survival signals by activating intracellular pathways, e.g., insulin and insulin-like growth factor type 1 (IGF-1) signaling, thus promoting mitogenesis, cell survival, energy metabolism, and motility. Studies using different experimental models have demonstrated that NASH could

increase the hepatic production of ceramides, nitrosamines, and related molecules, causing insulin resistance, oxidative stress, and brain injury. Liver-derived cytotoxic lipids enter the circulation, activate proinflammatory cytokine-mediated injury, and disrupt endothelial cell-to-cell junctions, thus increasing BBB permeability and penetrating in the CNS. Moreover, myelin degradation further increases endogenous ceramide production, exacerbating brain insulin resistance, neuroinflammation, oxidative stress, and neurotransmitter paucity, thus leading to neurocognitive deficits [3,31,62].

Recent evidences have demonstrated a close correlation between the alteration of gut microbiota (dysbiosis) and NASH development due to the increased intestinal permeability to lipopolysaccharide (LPS) that activates Toll-like receptor 4 (TLR4) of hepatic Kupffer cells (KCs) and hepatic stellate cells (HSCs), triggering the pro-inflammatory cytokine cascade that induces and maintains NASH. In the brain, the LPS-activated inflammatory cascade induces a decrease in BDNF expression, reduces the number of viable cells in the pyramidal layer, and promotes neurodegeneration and atrophy of hippocampal neurons, thus affecting CNS function and causing degenerative dementia and cognitive impairment [63].

A recent study of Higarza and collaborators demonstrated that a high-fat, high-cholesterol diet induces not only NASH but also dysbiosis, decreasing microbial short chain fatty acid (SCFA) production and increasing ammonia. Since hyperammonemia has been correlated to neuroinflammation and cognitive impairment, these authors suggested that diet-induced dysbiosis disrupts brain metabolism and function, factors contributing to the behavioral deficits observed in NASH. Additionally, they observed an increased DA catabolism in this NASH model, causing a drop of DA levels in the PFC and an increase of DOPA/DA ratio in the cerebellum. This suggests that insulin resistance could lead to dopaminergic dysfunction and a reduction of mitochondrial oxidative activity [14].

4. Pharmacological Strategies to Improve NAFLD/NASH-Related Cognitive Impairment

Although the increasing prevalence of NAFLD/NASH has made the need of effective treating options a priority, no therapy for NAFLD patients has been yet approved, and weight loss and increased physical activity remain the two gold standard interventions [64]. Several pharmacological agents have been studied and/or are in the pipeline for their effect on metabolic targets, the anti-inflammatory pathway, or fibrogenesis. Four agents (a PPARα/δ agonist, a FXR agonist, a CCR2/CCR5 antagonist, and an ASK1 inhibitor) are undergoing phase III clinical trials to be evaluated for their ability to reduce insulin resistance and the proinflammatory cascades responsible for NASH progression [65]. In this context, the development of a pharmacological option active also on the brain manifestations of NAFLD/NASH is a great challenge for scientists. Some interventions have been proposed in the last few years; nevertheless, their real usefulness as clinical pharmacological treatments needs to be further demonstrated.

Since insulin resistance is a distinctive feature of both steatohepatitis and AD, some studies have proposed the use of insulin-sensitizing agents, such as PPAR agonists, that are able to activate insulin-responsive genes and their signaling pathways to treat liver and brain insulin resistance-mediated diseases [66]. Early treatment with PPAR agonists has shown to effectively prevent brain atrophy, neurodegeneration, and its associated learning and memory impairment, preserving neurons expressing the insulin receptor and IGF receptor and maintaining cholinergic homeostasis and myelin expression [67,68]. Their antioxidant activity in the CNS was also reported to further sustain their therapeutic use in the content of oxidative stress-related diseases such as NAFLD, NASH, and AD.

Other studies demonstrated that in early stage AD patients, an improvement or stabilization of their cognitive impairment was obtained with intranasal insulin administration, leading to increased brain insulin levels [69–72].

Some studies have reported that chromium picolinate is able to improve insulin sensitivity by reducing glucose and insulin levels in overweight or obese subjects, and to increase HDL cholesterol and decrease LDL levels, thus controlling metabolic syndrome risk factors [73,74]. Moreover, this agent

could improve cognitive function in elderly people, reducing semantic interference on learning, recall, and memory [75,76]. These positive effects on the insulin signaling pathway, both at the systemic and central level, suggest the use of chromium picolinate as a dietary supplement in NAFLD-related cognitive impairment and AD, even though clinical studies need to be performed to support this hypothesis.

The use of dietary supplements is widely exploited to support the dietary interventions in patients with metabolic syndrome, obesity, and NAFLD. A recent study on resveratrol, a polyphenol naturally present in grapes, blueberries, raspberries, and mulberries, has reported the improvement of both liver metabolic dysfunction and behavioral and cognitive impairments in a rat model of NAFLD [77]. Resveratrol administration to NAFLD rats is able to ameliorate the imbalanced expression of copine 6, p-catenin, and p-GSK3β in the hippocampus and PFC, restoring normal protein levels and improving the altered Wnt/β-catenin signaling pathway. This study further supports previous evidences on the effect of resveratrol in reducing Aβ plaque formation associated with AD [78].

Another study investigating the effect of *Curcuma* derivatives demonstrated their ability in improving high-fat and high-sugar diet-induced obesity, oxidative stress, memory impairment, and neurodegeneration. These effects have been attributed to the antioxidant properties and anticholinesterase activity of curcuminoids and terpenoids present in the tested extract. Furthermore, they increased serotonin and dopamine levels, exerting neuroprotection of hippocampal neurons [79].

Since several pieces of evidence suggested that liver steatosis may negatively affect cognitive performance in AD subjects, n3-PUFA supplementation can be considered as an option to improve NAFLD-related brain dysfunction, since these fatty acids are able to improve liver n3/n6 PUFA imbalance and modulate many neuronal functions, protecting them from oxidative stress and inhibiting signaling pathways responsible for tau phosphorylation in AD and dementia patients [80].

As stated before, the gut–brain axis and dysbiosis could play a role in the cognitive impairment of NAFLD and NASH patients. Starting from the observation that probiotics have demonstrated to improve NASH by decreasing LPS-induced pro-inflammatory cytokines, such as IL6 and TNF-α [81], a study of Mohammed et al. investigated the effect of *Lactobacillus plantarum* (*LP EMCC-1039*) administration on cognitive performance and liver function in dysbiosis-induced NASH in rats. *LP EMCC-1039* supplementation was correlated to an improvement of cognitive function in these animals due to the modulation of TLR4/BDNF signaling pathway, and an increase of viable cells and of the thickness of the pyramidal layer was observed [63].

5. Conclusions

In conclusion, increasing evidences suggest that a correlation exists between NAFLD/NASH and CNS diseases or dysfunctions such as depression, MCI, AD, and dementia. Growing evidences point at cerebrovascular alteration, neuroinflammation, and brain insulin resistance as NAFLD/NASH-related CNS manifestations. Unfortunately, the pharmacological options available for the management of these conditions are still limited, both in number and in efficacy. Further experimental and clinical studies are needed to gain new insights about the mechanism(s) of NAFLD/NASH and their central manifestations and identify effective pharmacological targets, after the comprehension of the complex mechanisms involved in the NAFLD/NASH, including the regulation of the gut–brain axis by diet and microbiome composition.

Author Contributions: Writing—original draft preparation, M.C., D.G.; writing—review and editing, S.D.M. All authors have read and agreed to the published version of the manuscript.

Funding: This research received no external funding. D.G. post-doctoral fellowship was supported by the University of Padova (DEMA_SID19_01).

Conflicts of Interest: The authors declare no conflict of interest.

References

1. Engin, A. Non-Alcoholic Fatty Liver Disease. In *Obesity and Lipotoxicity*; Engin, A.B., Engin, A., Eds.; Advances in Experimental Medicine and Biology; Springer International Publishing: Cham, Switzerland, 2017; Volume 960, pp. 443–467, ISBN 978-3-319-48380-1.
2. Ekstedt, M.; Nasr, P.; Kechagias, S. Natural History of NAFLD/NASH. *Curr. Hepatol. Rep.* **2017**, *16*, 391–397. [CrossRef] [PubMed]
3. De la Monte, S.M.; Longato, L.; Tong, M.; Wands, J.R. Insulin resistance and neurodegeneration: Roles of obesity, type 2 diabetes mellitus and non-alcoholic steatohepatitis. *Curr. Opin. Investig. Drugs* **2009**, *10*, 1049–1060. [PubMed]
4. Elshaghabee, F.M.F.; Rokana, N.; Panwar, H.; Heller, K.J.; Schrezenmeir, J. Probiotics for dietary management of non-alcoholic fatty liver disease. *Environ. Chem. Lett.* **2019**, *17*, 1553–1563. [CrossRef]
5. Gabbia, D.; Roverso, M.; Guido, M.; Sacchi, D.; Scaffidi, M.; Carrara, M.; Orso, G.; Russo, F.P.; Floreani, A.; Bogialli, S.; et al. Western Diet-Induced Metabolic Alterations Affect Circulating Markers of Liver Function before the Development of Steatosis. *Nutrients* **2019**, *11*, 1602. [CrossRef]
6. Gabbia, D.; Saponaro, M.; Sarcognato, S.; Guido, M.; Ferri, N.; Carrara, M.; De Martin, S. Fucus vesiculosus and Ascophyllum nodosum Ameliorate Liver Function by Reducing Diet-Induced Steatosis in Rats. *Mar. Drugs* **2020**, *18*, 62. [CrossRef]
7. Estrada, L.D.; Ahumada, P.; Cabrera, D.; Arab, J.P. Liver Dysfunction as a Novel Player in Alzheimer's Progression: Looking Outside the Brain. *Front. Aging Neurosci.* **2019**, *11*, 174. [CrossRef]
8. Kaltenboeck, A.; Harmer, C. The neuroscience of depressive disorders: A brief review of the past and some considerations about the future. *Brain Neurosci. Adv.* **2018**, *2*. [CrossRef]
9. Gonda, X.; Pompili, M.; Serafini, G.; Carvalho, A.F.; Rihmer, Z.; Dome, P. The role of cognitive dysfunction in the symptoms and remission from depression. *Ann. Gen. Psychiatry* **2015**, *14*, 27. [CrossRef]
10. Lee, K.; Otgonsuren, M.; Younoszai, Z.; Mir, H.M.; Younossi, Z.M. Association of Chronic Liver Disease with Depression: A Population-Based Study. *Psychosomatics* **2013**, *54*, 52–59. [CrossRef]
11. Elwing, J.E.; Lustman, P.J.; Wang, H.L.; Clouse, R.E. Depression, Anxiety, and Nonalcoholic Steatohepatitis. *Psychosom. Med.* **2006**, *68*, 563–569. [CrossRef]
12. Tomeno, W.; Kawashima, K.; Yoneda, M.; Saito, S.; Ogawa, Y.; Honda, Y.; Kessoku, T.; Imajo, K.; Mawatari, H.; Fujita, K.; et al. Non-alcoholic fatty liver disease comorbid with major depressive disorder: The pathological features and poor therapeutic efficacy: Fatty liver comorbid with depression. *J. Gastroenterol. Hepatol.* **2015**, *30*, 1009–1014. [CrossRef]
13. Youssef, N.A.; Abdelmalek, M.F.; Binks, M.; Guy, C.D.; Omenetti, A.; Smith, A.D.; Diehl, A.M.E.; Suzuki, A. Associations of depression, anxiety and antidepressants with histological severity of nonalcoholic fatty liver disease. *Liver Int.* **2013**, *33*, 1062–1070. [CrossRef]
14. Higarza, S.G.; Arboleya, S.; Gueimonde, M.; Gómez-Lázaro, E.; Arias, J.L.; Arias, N. Neurobehavioral dysfunction in non-alcoholic steatohepatitis is associated with hyperammonemia, gut dysbiosis, and metabolic and functional brain regional deficits. *PLoS ONE* **2019**, *14*, e0223019. [CrossRef]
15. Filipović, B.; Marković, O.; Đurić, V.; Filipović, B. Cognitive Changes and Brain Volume Reduction in Patients with Nonalcoholic Fatty Liver Disease. *Can. J. Gastroenterol. Hepatol.* **2018**, *2018*, 9638797. [CrossRef] [PubMed]
16. Sanford, A.M. Mild Cognitive Impairment. *Clin. Geriatr. Med.* **2017**, *33*, 325–337. [CrossRef]
17. Celikbilek, A.; Celikbilek, M. Cognitive impairment in patients with nonalcoholic fatty liver disease with liver fibrosis. *Liver Int.* **2020**, *40*, 1239. [CrossRef] [PubMed]
18. Panza, F.; Frisardi, V.; Seripa, D.; P Imbimbo, B.; Sancarlo, D.; D'Onofrio, G.; Addante, F.; Paris, F.; Pilotto, A.; Solfrizzi, V. Metabolic Syndrome, Mild Cognitive Impairment and Dementia. *CAR* **2011**, *8*, 492–509. [CrossRef]
19. Levin, B.E.; Llabre, M.M.; Dong, C.; Elkind, M.S.V.; Stern, Y.; Rundek, T.; Sacco, R.L.; Wright, C.B. Modeling Metabolic Syndrome and Its Association with Cognition: The Northern Manhattan Study. *J. Int. Neuropsychol. Soc.* **2014**, *20*, 951–960. [CrossRef]
20. Elliott, C.; Frith, J.; Day, C.P.; Jones, D.E.J.; Newton, J.L. Functional Impairment in Alcoholic Liver Disease and Non-alcoholic Fatty Liver Disease Is Significant and Persists over 3 Years of Follow-Up. *Dig. Dis. Sci.* **2013**, *58*, 2383–2391. [CrossRef] [PubMed]

21. Seo, S.W.; Gottesman, R.F.; Clark, J.M.; Hernaez, R.; Chang, Y.; Kim, C.; Ha, K.H.; Guallar, E.; Lazo, M. Nonalcoholic fatty liver disease is associated with cognitive function in adults. *Neurology* **2016**, *86*, 1136–1142. [CrossRef]
22. Jongsiriyanyong, S.; Limpawattana, P. Mild Cognitive Impairment in Clinical Practice: A Review Article. *Am. J. Alzheimers Dis. Other Demen.* **2018**, *33*, 500–507. [CrossRef] [PubMed]
23. Celikbilek, A.; Celikbilek, M.; Bozkurt, G. Cognitive assessment of patients with nonalcoholic fatty liver disease. *Eur. J. Gastroenterol. Hepatol.* **2018**, *30*, 944–950. [CrossRef] [PubMed]
24. An, K.; Starkweather, A.; Sturgill, J.; Salyer, J.; Sterling, R.K. Association of CTRP13 With Liver Enzymes and Cognitive Symptoms in Nonalcoholic Fatty Liver Disease. *Nurs. Res.* **2019**, *68*, 29–38. [CrossRef] [PubMed]
25. Weinstein, G.; Davis-Plourde, K.; Himali, J.J.; Zelber-Sagi, S.; Beiser, A.S.; Seshadri, S. Non-alcoholic fatty liver disease, liver fibrosis score and cognitive function in middle-aged adults: The Framingham Study. *Liver Int.* **2019**, *39*, 1713–1721. [CrossRef] [PubMed]
26. Vanek, J.; Prasko, J.; Genzor, S.; Ociskova, M.; Kantor, K.; Holubova, M.; Slepecky, M.; Nesnidal, V.; Kolek, A.; Sova, M. Obstructive sleep apnea, depression and cognitive impairment. *Sleep Med.* **2020**, *72*, 50–58. [CrossRef]
27. Parikh, M.P.; Gupta, N.M.; McCullough, A.J. Obstructive Sleep Apnea and the Liver. *Clin. Liver Dis.* **2019**, *23*, 363–382. [CrossRef]
28. De la Monte, S.M. Insulin Resistance and Neurodegeneration: Progress Towards the Development of New Therapeutics for Alzheimer's Disease. *Drugs* **2017**, *77*, 47–65. [CrossRef]
29. De la Monte, S.M.; Tong, M. Brain metabolic dysfunction at the core of Alzheimer's disease. *Biochem. Pharm.* **2014**, *88*, 548–559. [CrossRef]
30. Kim, D.-G.; Krenz, A.; Toussaint, L.E.; Maurer, K.J.; Robinson, S.-A.; Yan, A.; Torres, L.; Bynoe, M.S. Non-alcoholic fatty liver disease induces signs of Alzheimer's disease (AD) in wild-type mice and accelerates pathological signs of AD in an AD model. *J. Neuroinflamm.* **2016**, *13*, 1. [CrossRef]
31. Lyn-Cook, L.E.; Lawton, M.; Tong, M.; Silbermann, E.; Longato, L.; Jiao, P.; Mark, P.; Wands, J.R.; Xu, H.; de la Monte, S.M. Hepatic ceramide may mediate brain insulin resistance and neurodegeneration in type 2 diabetes and non-alcoholic steatohepatitis. *J. Alzheimers Dis.* **2009**, *16*, 715–729. [CrossRef]
32. Pinçon, A.; De Montgolfier, O.; Akkoyunlu, N.; Daneault, C.; Pouliot, P.; Villeneuve, L.; Lesage, F.; Levy, B.I.; Thorin-Trescases, N.; Thorin, É.; et al. Non-Alcoholic Fatty Liver Disease, and the Underlying Altered Fatty Acid Metabolism, Reveals Brain Hypoperfusion and Contributes to the Cognitive Decline in APP/PS1 Mice. *Metabolites* **2019**, *9*, 104. [CrossRef] [PubMed]
33. Beilharz, J.E.; Maniam, J.; Morris, M.J. Diet-Induced Cognitive Deficits: The Role of Fat and Sugar, Potential Mechanisms and Nutritional Interventions. *Nutrients* **2015**, *7*, 6719–6738. [CrossRef]
34. Guimarães, C.A.; Biella, M.S.; Lopes, A.; Deroza, P.F.; Oliveira, M.B.; Macan, T.P.; Streck, E.L.; Ferreira, G.C.; Zugno, A.I.; Schuck, P.F. In vivo and in vitro effects of fructose on rat brain acetylcholinesterase activity: An ontogenetic study. *Acad. Bras. Cienc.* **2014**, *86*, 1919–1926. [CrossRef]
35. Nho, K.; Kueider-Paisley, A.; Ahmad, S.; MahmoudianDehkordi, S.; Arnold, M.; Risacher, S.L.; Louie, G.; Blach, C.; Baillie, R.; Han, X.; et al. Association of Altered Liver Enzymes With Alzheimer Disease Diagnosis, Cognition, Neuroimaging Measures, and Cerebrospinal Fluid Biomarkers. *JAMA Netw. Open* **2019**, *2*, e197978. [CrossRef]
36. Karbalaei, R.; Allahyari, M.; Rezaei-Tavirani, M.; Asadzadeh-Aghdaei, H.; Zali, M.R. Protein-protein interaction analysis of Alzheimer's disease and NAFLD based on systems biology methods unhide common ancestor pathways. *Gastroenterol. Hepatol. Bed. Bench.* **2018**, *11*, 27–33. [PubMed]
37. Hu, X.; Wang, T.; Jin, F. Alzheimer's disease and gut microbiota. *Sci. China Life Sci.* **2016**, *59*, 1006–1023. [CrossRef] [PubMed]
38. Fukui, H. Role of Gut Dysbiosis in Liver Diseases: What Have We Learned So Far? *Diseases* **2019**, *7*, 58. [CrossRef]
39. Lombardi, R.; Fargion, S.; Fracanzani, A.L. Brain involvement in non-alcoholic fatty liver disease (NAFLD): A systematic review. *Dig. Liver Dis.* **2019**, *51*, 1214–1222. [CrossRef]
40. Felipo, V.; Ordoño, J.F.; Urios, A.; El Mlili, N.; Giménez-Garzó, C.; Aguado, C.; González-Lopez, O.; Giner-Duran, R.; Serra, M.A.; Wassel, A.; et al. Patients with minimal hepatic encephalopathy show impaired mismatch negativity correlating with reduced performance in attention tests. *Hepatology* **2012**, *55*, 530–539. [CrossRef]

41. Felipo, V.; Urios, A.; Giménez-Garzó, C.; Cauli, O.; Andrés-Costa, M.-J.; González, O.; Serra, M.A.; Sánchez-González, J.; Aliaga, R.; Giner-Durán, R.; et al. Non invasive blood flow measurement in cerebellum detects minimal hepatic encephalopathy earlier than psychometric tests. *World J. Gastroenterol.* **2014**, *20*, 11815–11825. [CrossRef]
42. Butz, M.; Timmermann, L.; Braun, M.; Groiss, S.J.; Wojtecki, L.; Ostrowski, S.; Krause, H.; Pollok, B.; Gross, J.; Südmeyer, M.; et al. Motor impairment in liver cirrhosis without and with minimal hepatic encephalopathy. *Acta Neurol. Scand.* **2010**, *122*, 27–35. [CrossRef] [PubMed]
43. Giménez-Garzó, C.; Garcés, J.J.; Urios, A.; Mangas-Losada, A.; García-García, R.; González-López, O.; Giner-Durán, R.; Escudero-García, D.; Serra, M.A.; Soria, E.; et al. The PHES battery does not detect all cirrhotic patients with early neurological deficits, which are different in different patients. *PLoS ONE* **2017**, *12*, e0171211. [CrossRef] [PubMed]
44. Balzano, T.; Forteza, J.; Borreda, I.; Molina, P.; Giner, J.; Leone, P.; Urios, A.; Montoliu, C.; Felipo, V. Histological Features of Cerebellar Neuropathology in Patients With Alcoholic and Nonalcoholic Steatohepatitis. *J. Neuropathol. Exp. Neurol.* **2018**, *77*, 837–845. [CrossRef] [PubMed]
45. Petta, S.; Tuttolomondo, A.; Gagliardo, C.; Zafonte, R.; Brancatelli, G.; Cabibi, D.; Cammà, C.; Di Marco, V.; Galvano, L.; La Tona, G.; et al. The Presence of White Matter Lesions Is Associated With the Fibrosis Severity of Nonalcoholic Fatty Liver Disease. *Medicine (Baltimore)* **2016**, *95*, e3446. [CrossRef]
46. Ghareeb, D.A.; Hafez, H.S.; Hussien, H.M.; Kabapy, N.F. Non-alcoholic fatty liver induces insulin resistance and metabolic disorders with development of brain damage and dysfunction. *Metab. Brain Dis.* **2011**, *26*, 253. [CrossRef]
47. Dagnino-Subiabre, A. Stress and Western diets increase vulnerability to neuropsychiatric disorders: A common mechanism. *Nutr. Neurosci.* **2019**, 1–11. [CrossRef]
48. Rivera, D.S.; Lindsay, C.B.; Codocedo, J.F.; Carreño, L.E.; Cabrera, D.; Arrese, M.A.; Vio, C.P.; Bozinovic, F.; Inestrosa, N.C. Long-Term, Fructose-Induced Metabolic Syndrome-Like Condition Is Associated with Higher Metabolism, Reduced Synaptic Plasticity and Cognitive Impairment in Octodon degus. *Mol. Neurobiol.* **2018**, *55*, 9169–9187. [CrossRef]
49. Singh, D.P.; Kondepudi, K.K.; Bishnoi, M.; Chopra, K. Altered Monoamine Metabolism in High Fat Diet Induced Neuropsychiatric Changes in Rats. *J. Obes. Weight Loss Ther.* **2014**, *4*, 1–5. [CrossRef]
50. Castellani, G.; Contarini, G.; Mereu, M.; Albanesi, E.; Devroye, C.; D'Amore, C.; Ferretti, V.; De Martin, S.; Papaleo, F. Dopamine-mediated immunomodulation affects choroid plexus function. *Brain Behav. Immun.* **2019**, *81*, 138–150. [CrossRef]
51. Paik, Y.-H.; Schwabe, R.F.; Bataller, R.; Russo, M.P.; Jobin, C.; Brenner, D.A. Toll-Like receptor 4 mediates inflammatory signaling by bacterial lipopolysaccharide in human hepatic stellate cells. *Hepatology* **2003**, *37*, 1043–1055. [CrossRef]
52. Baothman, O.A.; Zamzami, M.A.; Taher, I.; Abubaker, J.; Abu-Farha, M. The role of Gut Microbiota in the development of obesity and Diabetes. *Lipids Health Dis.* **2016**, *15*, 108. [CrossRef] [PubMed]
53. Takeda, S.; Sato, N.; Morishita, R. Systemic inflammation, blood-brain barrier vulnerability and cognitive/non-cognitive symptoms in Alzheimer disease: Relevance to pathogenesis and therapy. *Front. Aging Neurosci.* **2014**, *6*, 171. [CrossRef] [PubMed]
54. Folke, J.; Pakkenberg, B.; Brudek, T. Impaired Wnt Signaling in the Prefrontal Cortex of Alzheimer's Disease. *Mol. Neurobiol.* **2019**, *56*, 873–891. [CrossRef] [PubMed]
55. Xu, L.-Z.; Xu, D.-F.; Han, Y.; Liu, L.-J.; Sun, C.-Y.; Deng, J.-H.; Zhang, R.-X.; Yuan, M.; Zhang, S.-Z.; Li, Z.-M.; et al. BDNF-GSK-3β-β-Catenin Pathway in the mPFC Is Involved in Antidepressant-Like Effects of Morinda officinalis Oligosaccharides in Rats. *Int. J. Neuropsychopharmacol.* **2017**, *20*, 83–93. [CrossRef]
56. Chen, Z.; Xu, Y.-Y.; Wu, R.; Han, Y.-X.; Yu, Y.; Ge, J.-F.; Chen, F.-H. Impaired learning and memory in rats induced by a high-fat diet: Involvement with the imbalance of nesfatin-1 abundance and copine 6 expression. *J. Neuroendocr.* **2017**, *29*. [CrossRef] [PubMed]
57. Ge, J.-F.; Xu, Y.-Y.; Qin, G.; Peng, Y.-N.; Zhang, C.-F.; Liu, X.-R.; Liang, L.-C.; Wang, Z.-Z.; Chen, F.-H. Depression-like Behavior Induced by Nesfatin-1 in Rats: Involvement of Increased Immune Activation and Imbalance of Synaptic Vesicle Proteins. *Front. Neurosci.* **2015**, *9*, 429. [CrossRef] [PubMed]
58. Ge, J.-F.; Xu, Y.-Y.; Qin, G.; Pan, X.-Y.; Cheng, J.-Q.; Chen, F.-H. Nesfatin-1, a potent anorexic agent, decreases exploration and induces anxiety-like behavior in rats without altering learning or memory. *Brain Res.* **2015**, *1629*, 171–181. [CrossRef]

59. Reinhard, J.R.; Kriz, A.; Galic, M.; Angliker, N.; Rajalu, M.; Vogt, K.E.; Ruegg, M.A. The calcium sensor Copine-6 regulates spine structural plasticity and learning and memory. *Nat. Commun.* **2016**, *7*, 11613. [CrossRef]
60. Burk, K.; Ramachandran, B.; Ahmed, S.; Hurtado-Zavala, J.I.; Awasthi, A.; Benito, E.; Faram, R.; Ahmad, H.; Swaminathan, A.; McIlhinney, J.; et al. Regulation of Dendritic Spine Morphology in Hippocampal Neurons by Copine-6. *Cereb. Cortex.* **2018**, *28*, 1087–1104. [CrossRef]
61. Han, Y.-X.; Tao, C.; Gao, X.-R.; Wang, L.; Jiang, F.-H.; Wang, C.; Fang, K.; Chen, X.-X.; Chen, Z.; Ge, J.-F. BDNF-Related Imbalance of Copine 6 and Synaptic Plasticity Markers Couples With Depression-Like Behavior and Immune Activation in CUMS Rats. *Front. Neurosci.* **2018**, *12*, 731. [CrossRef]
62. Tong, M.; Neusner, A.; Longato, L.; Lawton, M.; Wands, J.R. Nitrosamine Exposure Causes Insulin Resistance Diseases: Relevance to Type 2 Diabetes Mellitus, Non-Alcoholic Steatohepatitis, and Alzheimer's Disease. *J. Alzheimer's Dis.* **2010**, *37*, 827–844.
63. Mohammed, S.K.; Magdy, Y.M.; El-Waseef, D.A.; Nabih, E.S.; Hamouda, M.A.; El-Kharashi, O.A. Modulation of hippocampal TLR4/BDNF signal pathway using probiotics is a step closer towards treating cognitive impairment in NASH model. *Physiol. Behav.* **2020**, *214*, 112762. [CrossRef] [PubMed]
64. Younossi, Z.M. Non-alcoholic fatty liver disease—A global public health perspective. *J. Hepatol.* **2019**, *70*, 531–544. [CrossRef] [PubMed]
65. Alkhouri, N.; Scott, A. An update on the pharmacological treatment of nonalcoholic fatty liver disease: Beyond lifestyle modifications. *Clin. Liver Dis.* **2018**, *11*, 82–86. [CrossRef]
66. De la Monte, S.M. Brain Insulin Resistance and Deficiency as Therapeutic Targets in Alzheimer's Disease. *Curr. Alzheimer Res.* **2012**, *9*, 35–66. [CrossRef]
67. De la Monte, S.M.; Tong, M.; Lester-Coll, N.; Plater, J.; Wands, J.R. Therapeutic rescue of neurodegeneration in experimental type 3 diabetes: Relevance to Alzheimer's disease. *J. Alzheimer's Dis.* **2006**, *10*, 89–109. [CrossRef]
68. Landreth, G. Therapeutic use of agonists of the nuclear receptor PPARgamma in Alzheimer's disease. *Curr. Alzheimer Res.* **2007**, *4*, 159–164. [CrossRef]
69. Reger, M.A.; Watson, G.S.; Frey, W.H.; Baker, L.D.; Cholerton, B.; Keeling, M.L.; Belongia, D.A.; Fishel, M.A.; Plymate, S.R.; Schellenberg, G.D.; et al. Effects of intranasal insulin on cognition in memory-impaired older adults: Modulation by APOE genotype. *Neurobiol. Aging* **2006**, *27*, 451–458. [CrossRef]
70. Benedict, C.; Hallschmid, M.; Hatke, A.; Schultes, B.; Fehm, H.L.; Born, J.; Kern, W. Intranasal insulin improves memory in humans. *Psychoneuroendocrinology* **2004**, *29*, 1326–1334. [CrossRef]
71. Benedict, C.; Hallschmid, M.; Schmitz, K.; Schultes, B.; Ratter, F.; Fehm, H.L.; Born, J.; Kern, W. Intranasal insulin improves memory in humans: Superiority of insulin aspart. *Neuropsychopharmacology* **2007**, *32*, 239–243. [CrossRef]
72. Watson, G.S.; Cholerton, B.A.; Reger, M.A.; Baker, L.D.; Plymate, S.R.; Asthana, S.; Fishel, M.A.; Kulstad, J.J.; Green, P.S.; Cook, D.G.; et al. Preserved cognition in patients with early Alzheimer disease and amnestic mild cognitive impairment during treatment with rosiglitazone: A preliminary study. *Am. J. Geriatr. Psychiatry* **2005**, *13*, 950–958. [CrossRef] [PubMed]
73. De Martin, S.; Gabbia, D.; Carrara, M.; Ferri, N. The Brown Algae Fucus vesiculosus and Ascophyllum nodosum Reduce Metabolic Syndrome Risk Factors: A Clinical Study. *Nat. Prod. Commun.* **2018**, *13*, 1691–1694. [CrossRef]
74. Havel, P.J. A scientific review: The role of chromium in insulin resistance. *Diabetes Educ.* **2004**, *30* (Suppl. S3), 2–14.
75. Krikorian, R.; Eliassen, J.C.; Boespflug, E.L.; Nash, T.A.; Shidler, M.D. Improved cognitive-cerebral function in older adults with chromium supplementation. *Nutr. Neurosci.* **2010**, *13*, 116–122. [CrossRef]
76. Smorgon, C.; Mari, E.; Atti, A.R.; Dalla Nora, E.; Zamboni, P.F.; Calzoni, F.; Passaro, A.; Fellin, R. Trace elements and cognitive impairment: An elderly cohort study. *Arch. Gerontol. Geriatr.* **2004**, *38*, 393–402. [CrossRef]
77. Chen, X.-X.; Xu, Y.-Y.; Wu, R.; Chen, Z.; Fang, K.; Han, Y.-X.; Yu, Y.; Huang, L.-L.; Peng, L.; Ge, J.-F. Resveratrol Reduces Glucolipid Metabolic Dysfunction and Learning and Memory Impairment in a NAFLD Rat Model: Involvement in Regulating the Imbalance of Nesfatin-1 Abundance and Copine 6 Expression. *Front. Endocrinol.* **2019**, *10*, 434. [CrossRef]

78. Karuppagounder, S.S.; Pinto, J.T.; Xu, H.; Chen, H.-L.; Beal, M.F.; Gibson, G.E. Dietary supplementation with resveratrol reduces plaque pathology in a transgenic model of Alzheimer's disease. *Neurochem. Int.* **2009**, *54*, 111–118. [CrossRef]
79. Rao, L.S.N.; Kilari, E.K.; Kola, P.K. Protective effect of Curcuma amada acetone extract against high-fat and high-sugar diet-induced obesity and memory impairment. *Nutr. Neurosci.* **2019**, 1–14. [CrossRef]
80. Cole, G.M.; Ma, Q.-L.; Frautschy, S.A. Omega-3 fatty acids and dementia. *Prostaglandins Leukot. Essent. Fat. Acids* **2009**, *81*, 213–221. [CrossRef]
81. Medina, J.; Fernández-Salazar, L.I.; García-Buey, L.; Moreno-Otero, R. Approach to the pathogenesis and treatment of nonalcoholic steatohepatitis. *Diabetes Care* **2004**, *27*, 2057–2066. [CrossRef]

biomedicines

MDPI

Review

Insights into the Impact of Microbiota in the Treatment of NAFLD/NASH and Its Potential as a Biomarker for Prognosis and Diagnosis

Julio Plaza-Díaz [1,2,3], Patricio Solis-Urra [4], Jerónimo Aragón-Vela [5,*], Fernando Rodríguez-Rodríguez [6], Jorge Olivares-Arancibia [6,7] and Ana I. Álvarez-Mercado [2,3,8,*]

1 Children's Hospital of Eastern Ontario Research Institute, Ottawa, ON K1H 8L1, Canada; jrplaza@ugr.es
2 Department of Biochemistry and Molecular Biology II, School of Pharmacy, University of Granada, 18071 Granada, Spain
3 Instituto de Investigación Biosanitaria IBS.GRANADA, Complejo Hospitalario Universitario de Granada, 18014 Granada, Spain
4 Faculty of Education and Social Sciences, Universidad Andres Bello, Viña del Mar 2531015, Chile; patricio.solis.u@gmail.com
5 Department of Nutrition, Exercise, and Sport (NEXS), University of Copenhagen, DK-2200 Copenhagen, Denmark
6 IRyS Research Group, School of Physical Education, Pontificia Universidad Católica de Valparaíso, Valparaíso 2374631, Chile; fernando.rodriguez@pucv.cl (F.R.-R.); jorge.olivares.ar@gmail.com (J.O.-A.)
7 Grupo AFySE, Investigación en Actividad Física y Salud Escolar, Escuela de Pedagogía en Educación Física, Facultad de Educación, Universidad de las Américas, Santiago 8370035, Chile
8 Institute of Nutrition and Food Technology "José Mataix", Center of Biomedical Research, University of Granada, Avda. del Conocimiento s/n. Armilla, 18016 Granada, Spain
* Correspondence: jeroav@ugr.es (J.A.-V.); alvarezmercado@ugr.es (A.I.Á.-M.); Tel.: +34-958241000 (ext. 41599) (A.I.Á.-M.)

Citation: Plaza-Díaz, J.; Solis-Urra, P.; Aragón-Vela, J.; Rodríguez-Rodríguez, F.; Olivares-Arancibia, J.; Álvarez-Mercado, A.I. Insights into the Impact of Microbiota in the Treatment of NAFLD/NASH and Its Potential as a Biomarker for Prognosis and Diagnosis. *Biomedicines* **2021**, *9*, 145. https://doi.org/10.3390/biomedicines9020145

Academic Editors: Ronit Shiri-Sverdlov and Sabine Baumgartner
Received: 30 December 2020
Accepted: 31 January 2021
Published: 3 February 2021

Publisher's Note: MDPI stays neutral with regard to jurisdictional claims in published maps and institutional affiliations.

Abstract: Non-alcoholic fatty liver disease (NAFLD) is an increasing cause of chronic liver illness associated with obesity and metabolic disorders, such as hypertension, dyslipidemia, or type 2 diabetes mellitus. A more severe type of NAFLD, non-alcoholic steatohepatitis (NASH), is considered an ongoing global health threat and dramatically increases the risks of cirrhosis, liver failure, and hepatocellular carcinoma. Several reports have demonstrated that liver steatosis is associated with the elevation of certain clinical and biochemical markers but with low predictive potential. In addition, current imaging methods are inaccurate and inadequate for quantification of liver steatosis and do not distinguish clearly between the microvesicular and the macrovesicular types. On the other hand, an unhealthy status usually presents an altered gut microbiota, associated with the loss of its functions. Indeed, NAFLD pathophysiology has been linked to lower microbial diversity and a weakened intestinal barrier, exposing the host to bacterial components and stimulating pathways of immune defense and inflammation via toll-like receptor signaling. Moreover, this activation of inflammation in hepatocytes induces progression from simple steatosis to NASH. In the present review, we aim to: (a) summarize studies on both human and animals addressed to determine the impact of alterations in gut microbiota in NASH; (b) evaluate the potential role of such alterations as biomarkers for prognosis and diagnosis of this disorder; and (c) discuss the involvement of microbiota in the current treatment for NAFLD/NASH (i.e., bariatric surgery, physical exercise and lifestyle, diet, probiotics and prebiotics, and fecal microbiota transplantation).

Keywords: non-alcoholic steatohepatitis; intestinal permeability; microbiota; probiotics; physical exercise; fecal microbiota transplantation

1. Introduction

Non-alcoholic fatty liver disease (NAFLD), which is characterized by an increase in fat accumulation in the form of micro and macro vacuoles of lipids into hepatocytes (named

steatosis), is the most common liver disorder worldwide [1]. Steatosis is classified as mild (5–33%), moderate (34–66%), or severe (more than 66%) [2] depending on the fat number in vacuoles within the cytoplasm of hepatocytes. Additionally, other histopathological features should be taken into account in the presence of steatosis including inflammation, fibrosis, and ballooning degeneration [3]. Indeed, NAFLD comprises a large pathological spectrum ranging from simple steatosis to steatohepatitis with a variable degree of fibrosis and cirrhosis [4]. Importantly, liver steatosis is also a critical part of the evaluation of donors' livers because it is very frequent and may negatively impact recipient outcomes [3,5].

The worldwide prevalence of NAFLD varies widely from 20% to 30% [6] in western countries and increases with age [7]. This disease represents a major health problem because it is associated with the risk of progression to liver cirrhosis, liver cancer, and even increased cardiovascular and solid neoplasm risk [8]. Metabolic syndrome (MetS) is a cluster of metabolic abnormalities including glucose intolerance/insulin resistance, abdominal obesity, atherogenic dyslipidemia, increased blood pressure, a proinflammatory, and a prothrombotic state [9]. MetS provokes the alteration of the metabolic homeostasis of several organs including the liver [10]. The development of NAFLD is strongly associated with MetS given the fact that approximately 90% of the patients with NAFLD have more than one feature of MetS [9]. Glucose and triglycerides, both considered key components of MetS, are overproduced by the fatty liver [11]. In addition, insulin resistance is implied in failure in the formation and utilization of free fatty acids, which ultimately induces steatosis [12]. The liver is therefore a key player of metabolic abnormalities associated with MetS [11]. Unfortunately, obesity and type 2 diabetes (T2DM) are frequently observed in the general population. Evidence suggests that insulin resistance is the major factor associated with steatosis and potentially steatohepatitis, which may precede the development of T2DM. In fact, subjects suffering from NAFLD typically meet the diagnostic criteria for MetS [13]. However, not all patients with these conditions have NAFLD and not all patients with NAFLD suffer from one of these conditions [14]. In this regard, approximately 10% to 25% of people suffering NAFLD can progress to non-alcoholic steatohepatitis (NASH) [7], a more serious form of NAFLD which notably raises the possibilities of progression to cirrhosis and hepatocellular carcinoma (HCC). Besides, it is estimated that 10–15% of patients with NASH will develop HCC [15]. Bearing in mind the aforementioned, NAFLD in general and particularly NASH are ongoing global problems for public health systems. Nevertheless, the exact reason why some patients only develop steatosis and others progress to develop steatohepatitis and fibrosis is not completely understood [14]. It is probably the result of multiple metabolic abnormalities in the setting of a genetic predisposition, being the initial step of the accumulation of fat in the hepatocytes. When chronic NAFLD appears, lobular inflammation and hepatocellular damage can occur, leading to NASH. Moreover, NASH can be described as a necro-inflammatory complication of persistent hepatic steatosis [4]. In recent years, it has been mentioned and described that NAFLD might result from multiple hits with parallel consequences, such as gut and adipose tissue-derived factors [16]. The "first hit" is characterized by insulin resistance, leading to the accumulation of fat in hepatocytes, augmented lipid peroxidation and absolute free fatty acid uptake in the liver, free fatty acid synthesis from cytosolic substrates, the formation of triglycerides, and decreased apolipoprotein B-100 synthesis [17]. The "second hit" occurs through oxidative stress, which describes the progression to liver fibrosis. Reactive oxygen species can stimulate hepatocellular injury through the inhibition and inactivation of mitochondrial respiratory chain enzymes, membrane sodium channels, and glyceraldehyde-3-phosphate dehydrogenase. Reactive oxygen species promote lipid peroxidation, Fas Ligand induction, and cytokine production, adding fibrosis and hepatocellular injury [17]. Tumor necrosis factor-alpha (TNF-α) is up-regulated in NASH, which stimulates other pro-inflammatory cytokines such as interleukin (IL)-6, transforming growth factor beta (TGF-β), and platelet-derived growth factor, as well as augments insulin resistance [18]. On the other hand, a second and most recent theory is the "Multiple-hit" theory, which suggests that inflammation occurs before steatosis in environmentally and

genetically predisposed individuals [19]. The "multiple hit" hypothesis contemplates multiple factors operating in genetically predisposed subjects to provoke NAFLD; such factors comprise insulin resistance, nutritional factors, hormones secreted from the adipose tissue, genetic and epigenetic factors, and gut microbiota [20].

Other alterations in gut microbiota (i.e., overnutrition, genetic factors or inadequate lifestyle patterns) [21] have also been reported to promote the development of NAFLD/NASH by mediating inflammation, insulin resistance, bile acids, and choline metabolism [22]. Increased intestinal permeability may be associated with inflammatory changes in NASH due to the strong link between the two processes [23]. The activation of inflammation due to both dysbiosis and alterations in intestinal permeability via toll-like receptor (TLR) signaling in hepatocytes induces progression from simple steatosis to NASH [24]. Furthermore, endotoxin levels were observed to be higher in NAFLD patients with severe fibrosis than in those with mild fibrosis, revealing that the mechanism of fibrotic progression via the endotoxin in NAFLD may be closely associated with gut permeability. Additionally, in patients with NASH, a higher prevalence of small intestinal bacterial overgrowth [25] has been associated with higher levels of TNF-α [26] related to increased expression of TLR-4 on CD14-positive monocytes and higher plasma IL-8 levels [27]. However, neither the pathophysiology of NAFLD/NASH nor the gut microbiota alterations in these patients have been totally characterized, although modulation of the gut microbiota should be a sustainable strategy to manage NAFLD/NASH and comorbidities. Accordingly, strategies such as weight loss via diet and routine modifications are positive commendations to ameliorate liver damage [28]. On the other hand, physical exercise is an additional tool with potential benefits to microbiota composition, gut barrier integrity, and the metabolic profile, including a reduction in the adiposity profile and improvement of inflammation and immune parameters [28].

Concerning diagnosis, liver biopsies remain the gold standard for histological evaluation despite their limitations, invasiveness, and economic cost [29]. More accurate, cheaper, and non-invasive methods are needed for determining the extent of steatosis and its potential in progressing to a more severe status.

The present review summarizes human and animal studies aimed to determine the impact of the gut microbiota alterations in NASH and their suitability as biomarkers for prognosis and diagnosis. Finally, we discuss the implication of microbiota in the current treatments for NAFLD/NASH.

2. Diagnosis and Monitoring of NAFLD/NASH

NASH is the active form of NAFLD, with hepatic necroinflammation and faster fibrosis progression. The increasing number of patients that develop NASH-related end-stage liver disease makes it mandatory to establish NAFLD and NASH biomarkers for prognostication and selection of patients for treatment and monitoring [30]. Therefore, it is of critical importance to take into account histological characteristics such as the degree of steatosis, necroinflammation, and fibrosis to evaluate NAFLD patients [30].

Nowadays, liver biopsies remain the gold standard for histological evaluation, although both invasive and non-invasive methods are currently used to detect and track NAFLD and NASH [30]. Liver biopsies are used by clinicians to measure how much ballooning, inflammation, and scarring have occurred in the liver using different scoring scales and algorithms to classify the stages of NAFLD [31]. Nonetheless, this technique presents limitations such as the potential of sampling errors, interpretation of the histopathology, and unsuitability for continuous monitoring and invasiveness [30]. To note, non-invasive imaging techniques have improved over time and may be used to help determine the progression of steatosis, fibrosis, and liver stiffness [31]. Examples of well-established techniques are conventional ultrasonography (the most commonly used to identify fatty liver), computed tomography, or magnetic resonance imaging as well as newer imaging technologies, such as ultrasound elastography, quantitative ultrasound techniques, magnetic resonance elastography, and magnetic resonance-based fat quantitation techniques [32]. On

the other hand, standard liver function tests (e.g., elevated liver-associated enzymes such as aspartate aminotransferase and alanine aminotransferase) have shown low sensitivity and specificity as steatosis markers, graft rejection, liver injury, and a poor correlation with the severity of histopathological findings [33]. Researchers have also addressed developing several types of biomarkers including hormones, pro-inflammatory cytokines and proteins, adipokines, and carrier proteins [34]. For instance, plasma cytokeratin 18 fragment levels are related to hepatocyte apoptosis, representing the most extensively evaluated biomarker of steatohepatitis, although the accuracy is modest. In addition, several gene polymorphisms (such as *PNPLA3* and *TM6SF2*) have been shown to correlate with NAFLD and its severity [30].

In this regard, PNPLA3 is the first locus to be reproducibly and strongly related to susceptibility to steatosis and fibrosis/cirrhosis in liver diseases [35]. Indeed, the PNPLA3 polymorphism, rs738409[G] coding for I148M, induces a decrease in enzymatic activity in the hydrolysis of emulsified triglycerides in hepatocytes [36]. The PNPLA3 protein is a lipase that acts in triglycerides in hepatocytes and in hepatic stellate cells (in retinyl esters). PNPLA3 polymorphism, rs738409[G], provokes the loss of its function and triglyceride accumulation in hepatocytes [35]. By contrast, the present lack of high-throughput studies focused on proteomics or metabolomics to establish novel and reliable diagnostic biomarkers for NAFLD hampers epidemiologic studies [7].

In summary, current biomarkers for detecting, classifying, and tracking different features of NAFLD and NASH (namely, steatosis, necroinflammation, or fibrosis) present limitations due to their lack of accuracy, reproducibility, responsiveness, feasibility or economic cost. This shows the need for more effective, less invasive, and more affordable methods for determining the extent of steatosis and its potential in progressing to a more severe status. Thus, all these challenges have increased the interest in developing novel methods for the diagnosis (biomarkers, gut microbiota, among others) and prediction of the different stages of NAFLD/NASH.

3. Microbiota and Non-Alcoholic Steatohepatitis

The microbiome involves all of the genetic information inside the microbiota defined as "the full collection of microbes, i.e., bacteria, fungi, virus, etc., that naturally exists within a particular biological niche such as an organism, soil or a body of water, among others" [28,37]. Indeed, the word "microbiome" is also referred to as the metagenome of the microbiota [38]. The mutual communication between the microbiota and the liver is performed through the portal vein, which transports gut-derived products to the liver, and the feedback of bile and antibodies from the liver to the intestine [28,37].

The mucus barrier composition is determined by the microbiota as indicated through studies on germ-free mice that when colonized with the microbiota acquire similar mucus from donors [39]. This probably is due to the capability of goblet cells to sense the presence of bacterial products and to produce Muc2 after triggering the NLRP (Nucleotide-binding oligomerization domain, leucine-rich repeat and pyrin-domain containing proteins)-6-inflammasome pathway [40]. Besides, studies performed in animals have shown alterations in TLR signaling related to the leaky gut syndrome by the action of bacterial lipopolysaccharide (LPS). In humans, modifications in the profile of the gut microbiota associated with alterations in intestinal permeability have also been related to liver disease [28]. In consequence, metabolites produced by the microbiota, the immune system, and the liver show a strategic function in the pathogenesis of alcoholic liver disease and NAFLD/NASH [37]. Gut barrier impairment (which induces intestinal permeability) is the dynamic variable that enables portal influx of pathogen-associated molecular patterns (PAMPs), e.g., LPS, and microbiome-derived metabolites to the liver, activating a pro-inflammatory cascade that exacerbates hepatic inflammation [41].

Metagenomic analyses reveal that NASH and cirrhosis are related to changes in the gut microbiota composition [42,43]. In particular, it has been shown that *Eubacterium*

rectale and *Bacteroides vulgates* enhancement is associated with NAFLD, probably through damaging metabolic intermediaries in the altered microbiome of the host [44].

Patients with NASH showed augmented intestinal permeability and decreased intestinal bacterial overgrowth that are correlated with the severity of steatosis [45]. Likewise, mice deficient in junctional adhesion molecule A (Jam-A), an essential constituent of tight junctions that regulate the paracellular route of solutes avoiding molecules such as LPS cross the epithelium [46], are also more susceptible to NASH development [47]. Some authors have reported that just below the epithelium there is another cellular barrier-dominated gut vascular barrier that senses the entry to the liver and portal circulation [48,49]. Enteric pathogens such as *Salmonella typhimurium* have proven tactics to evade this gut vascular barrier via delaying the WNT/b-catenin signaling pathway [50]. In this regard, preventing the gut vascular barrier disruption with obeticholic acid treatment might prevent the development of NASH [50]. In addition, a recent study in a heterodimeric integrin receptor has shown that by blocking this integrin receptor known as $\alpha_4\beta_7$, the recruitment of $CD4^+$ T cells to the intestine and liver not only reduces hepatic inflammation and fibrosis but also protects the metabolic imbalances related to NASH [51].

Under healthy conditions, the gut microbiota composition is mostly stable, showing dissimilarities mainly at the species level. However, studies in humans revealed that the microbiota differs in patients with NASH. Accordingly, *Enterobacteria* and *Proteobacteria* present increased abundance relative, whereas anti-inflammatory bacterial strains such as *Faecalibacterium prausnitzii* are diminished [52]. In addition, important variables are related to the gut microbiota in the characterization of NASH, such as the serum bile acid profile and the hepatic gene expression pattern that support an increased bile acid production in NASH patients [53].

A better understanding of the patient microbiota interactions and the response to different actions/managements will be essential for the enhancement of NASH therapies and the elaboration of novel approaches targeting the alterations in microbiota associated with NASH.

4. Research Studies on Gut Microbiota and Non-Alcoholic Steatohepatitis

The global burden of NASH is high, affecting one in four adults and presenting a substantial geographic variation in prevalence [54]. Liver-detailed mortality of NASH patients was estimated to be 15.44/1000 person-years. Moreover, the impact of NASH as a cause of liver-related mortality may increase several-fold as the age at onset of disease decreases not just to childhood but to the in-utero state [55]. Indeed, this may potentially increase the duration and progression of liver disease. Another important factor is genetic susceptibility which means and unquestionable causal issue, e.g., despite the much lower daily caloric intake in Central and South America than in North America and western Europe, the prevalence of NASH is higher in these regions probably due to the association of this population with an increased prevalence of the rs738409 G allele of the *PNPLA3* gene [56].

4.1. Animal Studies

Animal studies have mostly been performed in rodents, revealing a potential causal role of gut microbiota in NAFLD. Several studies performed in animal models evaluating the implication of several genes in microbiota alteration and NASH pathogenesis have been recently reported. For instance, hepatic MyD88 regulates the production of bioactive lipid compounds that are implicated in glucose, inflammation, and lipid metabolism. The deletion of MyD88 in mice fed with a normal diet provoked changes in the gene expression, plasma, and liver metabolome. Moreover, gut microbes similar to those reported have been observed in diet-induced obesity and diabetic subjects [57].

On the other hand, it is well known that Sirtuin 3 (SIRT3) shows a defensive function against NAFLD by refining hepatic mitochondrial dysfunction [58,59]. SIRT3 knockout mice fed with a chow diet or high-fat diet were used to evaluate the relationship between gut microbiota and SIRT3 in NAFLD development. Results from this study showed that

SIRT3 deletion accelerated gut microbial dysbiosis after a high-fat diet with augmented levels of *Desulfovibrio* and *Oscillibacter* and reduced *Alloprevotella* abundance. In addition, these mice had augmented LPS levels and dysfunction of cannabinoid receptor 1 and 2 expressions in both the colon and the liver, which were significantly linked to the variations observed in gut microbiota [58].

The disruption of the gene F11r encoding Jam-A has showed deficiencies in intestinal epithelial permeability in mice fed with a normal diet or a diet high in saturated fat, fructose, and cholesterol. Mice with F11r gene knockout developed NASH features and increased levels of inflammatory microbial taxa related to Firmicutes and *Proteobacteria* compared with wild type mice [47].

To note, contemporary studies have proposed a key function for the inflammasome/caspase-1 in NASH development. Knockout mice (caspases 1/11 and Nlrp3) were evaluated with a standard fat diet or a high-fat diet. Caspases 1/11 knockout mice were predisposed to hepatic steatosis irrespective of the type of diet received. The lack of caspases 1/11 was also linked to higher hepatic triacylglycerol levels. Additionally, increased levels of *Proteobacteria* and a higher Firmicutes/Bacteroidetes ratio were found in the gut of caspases 1/11 knockout mice nourished with a high-fat diet [60]. To evaluate the implication of Nlrp3 in the development of NAFLD, Nlrp3 knockout mice were fed with a Western-lifestyle diet with fructose in drinking water or a chow diet. Knock-out Nlrp3 mice showed increased peroxisome proliferator-activated receptor-γ2 expression and triglyceride contents, greater adipose tissue inflammation and histological liver damage, as well as dysbiotic microbiota with bacterial translocation, related to an increase in TLR4 and TLR9 hepatic expression. After antibiotic treatment, the abundance of Gram-negative species and translocation of bacteria were reduced, and adverse effects were repaired both in the liver and adipose tissue [61]. Higher TLR4, TLR9, MyD88, Casp1, and NLPR3 expression levels were also found in animals that received a high-fat and choline-deficient diet. Concerning the composition of gut microbiota, the number of operational taxonomic units and the Bray-Curtis dissimilarity index were significantly different compared with the control group [62].

A recent study [63] reported that bile acids modulated through microbial modulation were critical to normalize obesity-induced metabolic disorders in hamsters. In addition, these authors found that the elimination of the gut microbiota increased hepatic bile acid synthesis and inhibited the microbial dihydroxylation and deconjugation in the gut [63]. Mice fed with either a low-fat diet with casein or a high fat-diet with casein, fish, or mutton protein were analyzed. The different types of protein in the high-fat diet significantly impacted the gut microbiota composition, with changes in *Prevotellaceae* UCG-003, *Ruminococcaceae* UCG-005, *Desulfovibrio*, the *Lachnospiraceae* NK4A136 group, *Lactobacillus*, and *Akkermansia*, intestinal inflammatory gene expression, serum endotoxin level, and changes in nine metabolites associated with hepatic MetS [64]. The hepatocyte-specific loss of the bacterial wall sensor nucleotide-binding oligomerization domain-containing (NOD) 2 transformed the gut microbiota composition, augmenting *Clostridiales* and diminishing *Erysipelotrichaceae*, among other taxa, verifying that NOD2 protects diet-induced NAFLD in mice [65]. Rats fed a high-fat and choline-deficient diet (a well-established nutritional model of NASH) showed a significantly higher delta Lee index, abdominal adipose tissue, and abdominal circumference, as well as other biochemical parameters compared to control standard diet animals. In this line, the methionine–choline-deficient diet induced steatohepatitis and a decrease in the gut microbiota diversity although these changes in gut microbiota differ from those observed in human subjects with NASH [66]. Using a different nutritional model, a high-fat high-cholesterol diet stimulated fatty liver, steatohepatitis, fibrosis, and NAFLD–HCC development, while a high-fat low-cholesterol diet induced only hepatic steatosis in mice. Microbiota composition was also altered in this model, showing an increase in *Mucispirillum*, *Desulfovibrio*, *Anaerotruncus*, and *Desulfovibrionaceae* and low levels of *Bifidobacterium* and *Bacteroides* in the high-fat high-cholesterol diet-fed

group. In addition, dietary cholesterol induced changes in gut bacterial metabolites with augmented levels of taurocholic acid and decreased 3-indole propionic acid [67].

The recognized translational model for NAFLD/NASH, i.e., Leiden mice [68,69], was used by Gart et al. to test several energy-dense diets. Animals were fed with chow, butterfat–fructose, lard fat–sucrose, or a diet with lard fat–sucrose and fructose water. General variations in microbiota were detected in all groups as well as modifications in plasma short-chain fatty acids (SCFAs) [70].

On the other hand, proton pump inhibitors have been shown to stimulate the progression of alcoholic liver disease, NAFLD, and NASH in mice by growing *Enterococcus* spp. and *Enterococcus faecalis* [71].

Germ-free mice received microbiota from four donors subjected to different diets, i.e., (1) control diet, (2) high-fat diet-responders, (3) high-fat diet non-responders, and (4) a quercetin-supplemented high-fat diet to investigate changes in NAFLD development. The high-fat diet non-responders and quercetin-supplemented high-fat diet groups had higher levels of *Desulfovibrio* and *Oscillospira*, diminished levels of *Bacteroides* and *Oribacterium*, higher stimulation of hepatic bile acid transporters, and suppression of hepatic lipogenic and bile acid synthesis genes. The authors suggested a hepatoprotective effect in the high-fat diet non-responders and of the quercetin-supplemented high-fat diet [72].

Initial infant gut colonization through microbes plays an important role in immunity and metabolic function [73]. Germ-free mice were colonized with stool microbes from 2-week-old human infants born to obese or normal-weight mothers. The stool from infants had higher hepatic gene expression for endoplasmic reticulum stress and innate immunity together with periportal inflammation histological signs, similar to pediatric cases of NAFLD. These results postulate useful data supporting the role of maternal obesity-associated infant dysbiosis in children with obesity and NAFLD [73].

Bearing in mind all the aforementioned, studies in animals seem to be a good tool to explore the implication of microbiota in NAFLD/NASH even when many limitations to extrapolating information to humans have to be considered. Overall, animal models are very helpful to shed light on the effect of alterations in the gut microbiota in hepatic disease, especially when NAFLD patients present different severities, heterogeneous lesions, and variable demographic characteristics (e.g., age, sex, or ethnicity). Additionally, the complexity of human behavior, diet, physical activity, environment, psychological stress, or genetics affects the gut microbiota, which may lead to discrepancies and controversial results.

Although animal models of NAFLD/NASH do not always show all the histological alterations compared with humans (e.g., hepatocyte ballooning) and the microbiota are not strictly the same between species, the effect of an unbalanced microbiota on hepatic disease or the possibly of providing proof of concept may be more reasonable through appraisal of experimental models. Moreover, animal studies have advantages such as reduced biological variation or easy housing and monitoring or control of the diet/environment—all factors with a great impact on the microbiota profile.

4.2. Human Studies (Adults and Children)

It has been described that the relationship between *Bacteroides* and a Western-type diet has a pro-inflammatory effect related to the pathogenesis of NASH [44]. In addition, it is known that patients with NAFLD show a different bacterial community with lower biodiversity compared with healthy individuals [74]. Non-virulent endotoxin-producing strains of pathogenic species overgrowing in the gut of patients with obesity can act as contributory agents for the initiation of NAFLD. The most important molecular mechanism is mediated through the TLR4 receptor; this receptor can modulate the different steps in NAFLD evolution and related metabolic disorders [75]. Concerning the NASHmicrobiota association, *Bacteroides* abundance was significantly increased in NASH patients, whereas *Prevotella* was reduced. *Ruminococcus* was higher in patients with fibrosis, and the *Bacteroides* relative abundance was independently related to NASH. Alterations in metabolic pathways were associated with carbohydrate, lipid, and amino acid metabolism [76].

Metagenomic analyses of diagnosed patients with NAFLD, NASH, and obesity compared with control individuals revealed an increase in Actinobacteria and reduced Bacteroidetes in NAFLD patients. In NASH patients, low *Oscillospira* levels were related to high *Dorea* and *Ruminococcus* and high 2-butanone and 4-methyl-2-pentanone levels [42]. In the same line, another study reported decreased Bacteroidetes and *Ruminococcaceae* as well as increased *Lactobacillaceae* and *Veillonellaceae* and *Dorea* abundances in NAFLD patients [77]. In addition, in patients with advanced fibrosis, serum and fecal bile acid quantities increased, with serum glycocholic acid fecal deoxycholic acid levels associated with *Bacteroidaceae* and *Lachnospiraceae* [78]. In concordance with these results, *Ruminococcaceae* and *Veillonellaceae* were the central microbiota related to fibrosis severity in non-obese subjects, and bile acids and propionate were elevated in non-obese patients with significant fibrosis [79]. In the same line, a prospective cross-sectional study was conducted to characterize the differences between non-obese adults with and without NAFLD in fecal microbiota. It revealed that NAFLD patients presented additional Bacteroidetes and fewer Firmicutes that produced SCFAs, and 7α-dehydroxylating bacteria decreased. By contrast Gram-negative bacteria were predominant in NAFLD patients [80].

In children with NAFLD, alanine aminotransferase activity and concentrations of some inflammation and insulin resistance markers were significantly higher in plasma as well as other variables related to the bacterial response. By contrast, soluble CD14 serum, D-lactate plasma levels, and small intestinal bacterial overgrowth did not vary [81]. In a study performed in one hundred and twenty-five children and adolescents who were overweight and obese aged 10–18 years and 120 children and adolescents matched for age, those with obesity and who were overweight presented intestinal dysbiosis (37.6%), and 62.4% were small intestinal bacterial overgrowth negative. Children with combined obesity or who were overweight and with a positive small intestinal bacterial overgrowth showed indications of impaired liver function (i.e., high levels of aminotransferases, aspartate aminotransferases, alanine aminotransferase) as well as hypertension and MetS [82]. Low alpha diversity has also been related to a high hepatic fat fraction in adolescents. The most important taxa associated with these changes were *Bilophila* and *Paraprevotella* [83].Table 1 summarizes the principal information from gut microbiota and non-alcoholic steatohepatitis studies.

Table 1. Main information from gut microbiota and non-alcoholic steatohepatitis studies.

Reference	Animal Model/Study Population	Main Changes/Microbiota Alterations
Chen et al., 2019 [58]	Knockout of SIRT3 HFD in mice	Impairment of dysbiosis after a HFD with ↑*Desulfovibrio*, *Oscillibacter* and ↓*Alloprevotella* abundances, ↑ LPS levels and dysfunction, ↑cannabinoid receptor 1 and 2 expressions in the colon and liver
Rahman et al., 2016 [47]	Knockout of the F11 receptor gene in mice	Developed NASH features, ↑levels of inflammatory microbial taxa related to Firmicutes and *Proteobacteria*
de Sant'Ana et al., 2019 [60]	Knockout mice (caspases 1/11 and Nlrp3 HFD)	↑*Proteobacteria* and Firmicutes/Bacteroidetes ratio were found in the gut of caspases 1/11 knock-out mice
Pierantonelli et al., 2017 [61]	Nlrp3 knock-out mice	After antibiotic treatment, the abundance of Gram-negative species and translocation of bacteria were reduced, and adverse effects were repaired both in the liver and adipose tissue
Sun et al., 2019 [63]	Hamsters	Microbial modulation of bile acids was modulated, which was key in ameliorating obesity-induced metabolic disorders

Table 1. *Cont.*

Reference	Animal Model/Study Population	Main Changes/Microbiota Alterations
Ahmad et al., 2020 [64]	Mice C57BL/6J HFD	HFD induced changes in *Prevotellaceae* UCG-003, *Ruminococcaceae* UCG-005, *Desulfovibrio*, the *Lachnospiraceae* NK4A136 group, *Lactobacillus*, and *Akkermansia*
Cavallari et al., 2020 [65]	Mice (NOD2 knockout)	↑*Clostridiales* and ↓*Erysipelotrichaceae*, NOD2 protection of NAFLD features
Schneider et al., 2019 [66]	Rats with NASH induced by a methionine–choline deficient diet	↓gut microbiota diversity (different from that observed in human NASH subjects)
Zhang et al., 2020 [67]	Mice, C57BL/6 male, high-fat high-cholesterol diet	↑*Mucispirillum*, *Desulfovibrio*, *Anaerotruncus*, and *Desulfovibrionaceae* and ↓*Bifidobacterium* and *Bacteroides*
Gart et al., 2018 [70]	Leiden mice	General variations in microbiota modifications in plasma and short-chain fatty acids
Llorente et al., 2017 [71]	Sublytic *Atp4a*$^{Sl/Sl}$ mice, Proton pump inhibitors	↑progression of liver disease, ↑ *Enterococcus* spp., ↑*Enterococcus faecalis*
Petrov et al., 2019 [72]	Germ-free mice, High-fat diet non-responder, Quercetin-supplemented HFD	↑*Desulfovibrio* and *Oscillospira*, ↓*Bacteroides* and *Oribacterium*, ↑stimulation of hepatic bile acid transporters ↓hepatic lipogenic and bile acid synthesis genes
Boursier et al., 2016 [76]	Humans, NASH patients, NASH patients+ fibrosis	↑*Bacteroides* abundance ↓*Prevotella*,↑*Ruminococcus*
Del Chierico et al., 2017 [42]	Humans with NASH	↓*Oscillospira* levels related to ↑*Dorea* and *Ruminococcus* and high 2-butanone and 4-methyl-2-pentanone levels
Adams et al., 2020 [78]	Human patients with advanced fibrosis	↑serum and fecal bile acid quantities Serum glycocholic acid fecal deoxycholic acid levels were associated with *Bacteroidaceae* and *Lachnospiraceae*
Lee et al., 2020 [79]	Fibrosis in non-obese human subjects	Fibrosis severity associated with *Ruminococcaceae* and *Veillonellaceae*, ↑bile acids and propionate were elevated in non-obese patients with significant fibrosis
Belei et al., 2017 [82]	Children with combined obesity or who were overweight and had positive small intestinal bacterial overgrowth	Impaired liver function, Hypertension, Metabolic syndrome
Stanislawski et al., 2018 [83]	Adolescents	↓alpha diversity related to a high hepatic fat fraction in adolescents. Altered *Bilophila* and *Paraprevotella* levels

Abbreviations: HFD, high-fat diet; LPS, lipopolysaccharide; NAFLD, non-alcoholic fatty liver disease; NASH, non-alcoholic steatohepatitis; Nlrp3, NLR family pyrin domain containing 3; NOD2, nucleotide-binding oligomerization domain containing protein 2; SIRT3, NAD-dependent deacetylase sirtuin-3; ↑means increment; ↓means reduction.

5. Strategies to Treat Non-Alcoholic Steatohepatitis and the Implication for the Microbiota

NASH is one of the most recurrent causes of cirrhosis. Since the number of approved drugs and their effectivity are limited, it is fundamental to look for beneficial methods that can lead to the prevention or reversal of the progression of NASH [84,85]. In addition, the modulation of gut microbiota brings added benefits by itself or in combination with other interventions (i.e., diet, exercise, bariatric surgery, probiotics administration, etc.). This is a field of growing interest for the scientific community widely approached in the last

years by the authors. In the present section, we remark on some studies and results in this regard.

5.1. Bariatric Surgery

Bariatric surgery is effective in obesity care and causes prolonged weight loss with potential decreases in hepatic fat, inflammation, and fibrosis [86,87]. A systematic review and meta-analysis [88] in 2008 considered the effects on histology after bariatric surgery in NAFLD patients. The authors concluded that fibrosis, steatohepatitis, and steatosis features were enhanced in most patients succeeding weight loss after bariatric surgery. Most studies described favorable effects on steatosis, and more than half of the studies revealed significant enhancements in histological inflammation. Recently, a systematic review and meta-analysis included forty-three studies divided into behavioral weight loss programs, pharmacotherapy, and bariatric surgery studies with 2809 participants. The authors concluded there is a dose-response association with liver inflammation, ballooning, and NAFLD or NASH resolution; however, there were incomplete data of a dose-response association with NAFLD activity score or fibrosis [89].

Evidence shows that the gut microbiota is a key mediator of the metabolic beneficial effects and weight loss observed after bariatric surgery. In this line, significant changes in the microbiota and related genes have been reported after this procedure [90–92]. For instance, a study performed on obese patients reported increased gut microbial diversity and alterations in the relative abundances of 31 species after being submitted to bariatric surgery [93]. Suggested mechanisms for the reported changes in microbiota are (1) food choices and preferences, reduction of food consumption, and nutrient malabsorption or diet therapy after surgery; (2) Changes in bile acids that alter the 7α-dehydroxylation capacity of the intestinal microbiota and impair the synthesis of the secondary bile acids; (3) changes in hormones related to both energy metabolism and microbiota such as leptin and ghrelin; (4) pH changes along the stomach induced by bariatric surgery. In this sense, a high pH can strongly affect microbiota (e.g., Bacteroidetes decrease due to pH changes after bariatric surgery, while Firmicutes and Actinobacteria increase) [94].

5.2. Physical Exercise as a Potential Treatment for NAFLD/NASH

Given the lack of pharmacologically approved treatment, physical activity and exercise is one of the most promising modifiable lifestyle components related to NAFLD/NASH development [95–97]. Indeed, physical inactivity is related to the progression of the disease [98,99], being one of the main problems for these subjects. Previous studies suggest that physical exercise benefits the prevention of several metabolic risk factors related to NAFLD, such as insulin resistance, dyslipidemia, and hypertension, reducing intrahepatic lipids [100]. In this line, the most extensive and simple outcome related to the benefits of exercise is weight loss, with the potential to attenuate or reverse the course of disease [100,101]. Despite this, physical exercise provides benefits to the management of NALFD even in the absence of weight loss, suggesting other mechanisms by which the exercise confers benefits against NAFLD/NASH [100,102]. In terms of metabolism, physical exercise generates a proliferation of angiogenic factors and proliferation of endothelial cells which induce an increase in capillarization, which favors the consumption of fatty acids, reducing their entry into the liver [103]. This type of disease is commonly associated with obese and diabetic people; therefore, it is of vital importance to lose weight, given that there is evidence that excess liver fat (independent of NASH) is associated with increased cardiometabolic risk [104]. Although there is no precise training program, it is known that physical exercise is capable of modulating hepatic steatosis, improving insulin sensitivity or affecting body composition of patients with NAFLD/NASH [105], even without dietary intervention [100].

Microbiota Role in the Relationship of Physical Exercise with NAFLD/NASH

Physical exercise has been demonstrated to impact the composition and functional capacity of microbiota with potential health benefits [106–109]. Thus, it appears that the benefits of physical exercise could have a common link through the intestinal microbiota. The taxonomic changes in the microbiome through physical exercise have been analyzed in depth [106]. Although the field remains to be further investigated, a recent study pointed out these changes in the intestinal microbiota caused by exercise could be beneficial for NAFLD patients [96]. Thus, the principal evidence is provided by studies on obesity or diabetic patients, suggesting a close relationship with NAFLD/NASH patients. Indeed, it was reported that such alterations in the intestinal microbiota were associated with improved circulating insulin, LDL cholesterol, liver mass, and liver triglycerides [110]. In rodent models, a high-fat diet induced gut microbiota dysbiosis and reduced the relative abundance of *Parabacteroides*, *Flavobacterium*, and *Alkaliphilus* [96]. Moreover, the practice of physical exercise corrected the imbalanced microbiota composition, reaching similar values to the control, which could be associated with a protective effect against early obesity and NAFLD [96]. In addition, physical exercise programs did show increased relative abundances of *Verrucomicrobia* and decreased *Proteobacteria* in overweight women [111], as well as a decrease in the Firmicutes/Bacteroidetes ratio in T2DM patients [112].

In addition, the concomitant effect of exercise on the gut in NAFLD/NASH patients would be related to the close relationship between the gut and liver. The microbiome and metabolites of the gut can directly reach the liver, being modulated by the gut barrier permeability, which is profoundly affected in these patients, as we discussed in our previous study [28]. The effects of physical exercise on endotoxemia and metabolites related to the gut are also potential mechanisms related to improvements in NAFLD/NASH [112,113]. For example, physical exercise increased the abundance of SCFAs, butyrate, and other SCFAs [109]. Furthermore, exercise exerts an effect on other gut-derived metabolites related to hepatic metabolism such as bile acid, choline, and ethanol [113]. On the other hand, exercise restores these genetic capacities to the level of control mice, possibly contributing to improved metabolic alterations, including NAFLD [114]. This improvement is mainly related to a decrease in the expression of genes involved in lipid metabolism, such as SREBP-1c, FAT/Cd36, and C/EBPa [96]. Interestingly, a recent study compared the effect of exercise vs. caloric restriction in obesity-prone HFD-fed rats, showing that only physical exercise increased insulin sensitivity and achieved greater LDL reduction, mainly due to exercise-induced microbiome modifications [110]. Indeed, these changes could be due to a reduced abundance of the *Bacteroidales S24-7* and *Rikenellaceae* families, which positively correlated with liver triglycerides [110]. However, the direct influence of physical exercise on changes in the microbiome has not been studied extensively in NAFLD/NASH patients. A recent study extensively discussed the effect of physical exercise on the microbiome in NAFLD/NASH [113]. Nonetheless it has not been defined what type of training generates a greater effect, possibly due to the fact that moderately intense physical activity may quickly lead to a reduction in intrahepatic lipid contents [115].

In summary, physical exercise has been shown to improve hepatic steatosis in NAFLD and should be included as part of the clinical care of all patients, with several metabolic mechanisms proposed. In addition, despite physical exercise being one of the proposed mechanisms, the effect of the specific role of exercise on microbiota in NAFLD/NASH must be clarified. However, it seems that total exercise duration and amount might be important for ameliorating liver steatosis [116]. Thus, the principal recommendation is achieving the recent physical activity recommendation, which consists of 150–300 min of moderate–intensive physical activity per week, with the inclusion of both aerobic and muscle-strengthening activities. In addition, individuals should start with small amounts of physical activity, and some physical activity is better than none, especially for those not currently meeting these recommendations; further, reducing sedentary behaviors are recommend [113,117,118].

5.3. Diet Calorie-Restricted and the Mediterranean Diet

Modification of host-microbiota interactions with personalized nutrition is a new therapeutic opportunity for both disease control and prevention. The function and composition of the intestinal microbiota are formed from infancy when the individual is colonized by bacteria from the parents and the immediate environment, a route that strongly impacts the microbiota composition in adulthood [119,120]. On the other hand, it is well known that high-fat, high-sugar, hypercaloric diets raise the hepatic steatosis risk [121]. Weight loss accomplished through caloric restriction decreases hepatic inflammation and fibrosis and reduces NASH [122]. Studies have shown that a weight loss of 7–10% ends in improvements in the nonalcoholic fatty liver disease activity score, and a weight loss of $\geq$10% produces a resolution of 90% for NASH, 45% fibrosis regression, and a 100% steatosis resolution [122]. Diet calorie-restriction is the most essential element in NASH nutritional interventions [123]. The Mediterranean diet was recommended for NAFLD patients by the recent European Association for the Study of the Liver; the European Association for the Study of Diabetes; and the European Association for the Study of Obesity Clinical Practice Guidelines [124] since this diet may contribute to partially restore a healthy gut microbiota [125,126].

5.4. Probiotic Supplementation

There is an interaction between the intestinal microbiota, related metabolites, and inflammation factors which control the progression and development of NAFLD. In consequence, modulation of the gut microbiota by probiotics appears to be a safe and sustainable strategy for the treatment of NASH. Probiotic supplementation significantly diminished inflammatory biomarkers such as TNF-α and C-reactive protein in NAFLD patients [127]. A systematic review conducted to evaluate the microbiome targeted in NAFLD patients included twenty-one randomized clinical trials; nine evaluated probiotics, and 12 evaluated synbiotics. Probiotic and synbiotic treatments were related to a significant decrease in alanine aminotransferase activity and liver stiffness measurement through elastography as well as augmented odds of progress in hepatic steatosis [128].

In NASH patients, oligofructose increased *Bifidobacterium*, which was inversely associated with obesity and plasma LPS [129]. The intake of a probiotic cocktail produced changes in the microbiota profile (specifically altering the abundance of pathogenic *Enterobacteria*) and feces' structure, findings that were associated with the improvement of liver inflammation [130]. Accordingly, *Lactobacillus reuteri* and metronidazole either alone or in combination with metformin were administered to rats with NASH showing beneficial effects on the lipid profile, oxidative stress, liver function, autophagic, and inflammatory biomarkers compared with animals treated only with metformin. In addition, gut microbiota changes were observed in the abundances of Firmicutes and Bacteroidetes and propionate, butyrate, and acetate ratios with the amendment of insulin resistance [131].

5.5. Fecal Microbiota Transplantation

Fecal microbiota transplantation (FMT) has been prevalent in recent years. FMT is the transplantation of useful bacteria from feces of healthy donors into the gastrointestinal tract of patients to repair the equilibrium of intestinal microbiota [132,133]. The procedure includes the compilation of filtered stools collected from either a healthy donor or from the recipient himself (autologous FMT) at a specific time before the initiation of disease and associated dysbiosis and its connection to the intestinal tract of a patient suffering from a certain medical condition [134]. FMT is efficient and successful treatment in *Clostridium difficile* infection (CDI) in humans [135,136]. In 2010, the United States Infectious Diseases Society of America and Society for Healthcare Epidemiology of America suggested FMT as a treatment plan for CDI in their clinical guidelines [137]. A recent study in patients with NAFLD has shown that FMT did not improve insulin resistance or hepatic proton density fat fraction, but FMT was able to reduce small intestinal permeability in patients [138]. Besides, there are several studies registered on FMT and liver disease on the clinicaltrials.

gov webpage; regarding NASH and FMT, there are five studies with complete registration data, three of them with not recruiting status yet from Spain, the United States and India, and the other two with an unknown status from the United States and India.

6. Future Perspectives

Nowadays, NAFLD/NASH has risen to pandemic proportions mainly due to our sedentary lifestyle and Westernized diets with an increasing number of patients developing NASH-related end-stage liver disease. Although NAFLD has become a common disease, its exact cause has not been elucidated, and it is almost certainly not the same in every patient; even the mechanism whereby some patients progress to NASH is still unclear. All this is hampered by the fact that current methods of diagnosis present several limitations and are invasive (e.g., liver biopsy), expensive, inaccurate, or inadequate (e.g., techniques based on image acquisition), or have a low predictive potential (e.g., biochemical markers). In consequence, there is an urgent need for a better understanding of the underlying pathophysiology and diagnosis procedure of NASH. New approaches must consider other NAFLD/NASH-related parameters whose levels and/or alterations would account for the diagnosis, prognostication, and selection of patients for treatment and monitoring.

In recent years, several authors have evaluated whether patients suffering from liver disease present a distinctive microbiota profile. The results extracted from the text undoubtedly highlight differences in the microbiota profile of patients compared with healthy individuals that have been associated with both severity and progression of the hepatic disease. Nevertheless, the current knowledge is still limited and sometimes the sample size is relatively small. To our knowledge, to date, all the authors reported the differences/changes found as "potential biomarkers" and there are no microbiota-related biomarkers currently used in clinical practice. In consequence, more research is needed to validate and establish trustworthy and more precise microbiota-related biomarkers. In our view, results need to show higher reproducibility, eliminating discrepancies in patient cohorts, animal models, comparison groups, or health baseline status.

Nevertheless, and despite the broad heterogeneity of basic and clinical research on NASH and its systemic complications performed (e.g., bariatric surgery, physical exercise and lifestyle, diet, probiotics or fecal microbiota transplantation), the studies all highlight the crucial role of gut microbiota to maintain the homeostasis of the organism and the implication of the gut–liver axis in the pathogenesis of liver diseases NAFLD, NASH, and HCC and acute liver failure. Moreover, specific microbiota profiles linked to these disorders have been suggested. Microbiota also shift hepatic metabolism through the regulation of hepatic gene expression (Figure 1). Thus, alterations in gut microbiota are emerging as an important tool for determining the occurrence and progression of NAFLD/NASH. Moreover, it is mandatory to take advantage of the current advances in metagenomics techniques. The new knowledge together with proteomics and metabolomics results would be immensely helpful to establish cheaper, novel, and reliable diagnostic biomarkers.

To conclude, the current restrictions in pharmacological treatments for NAFLD/NASH, the limitations of current biomarkers for diagnosis and progression, together with the advancement in the knowledge of NAFLD/NASH microbiota show the need to open a new window the scientific community must explore. New approaches in this sense might provide possible answers in both basic and clinical research to basic questions about prognosis, diagnosis, and monitoring of this huge economic and global health burden.

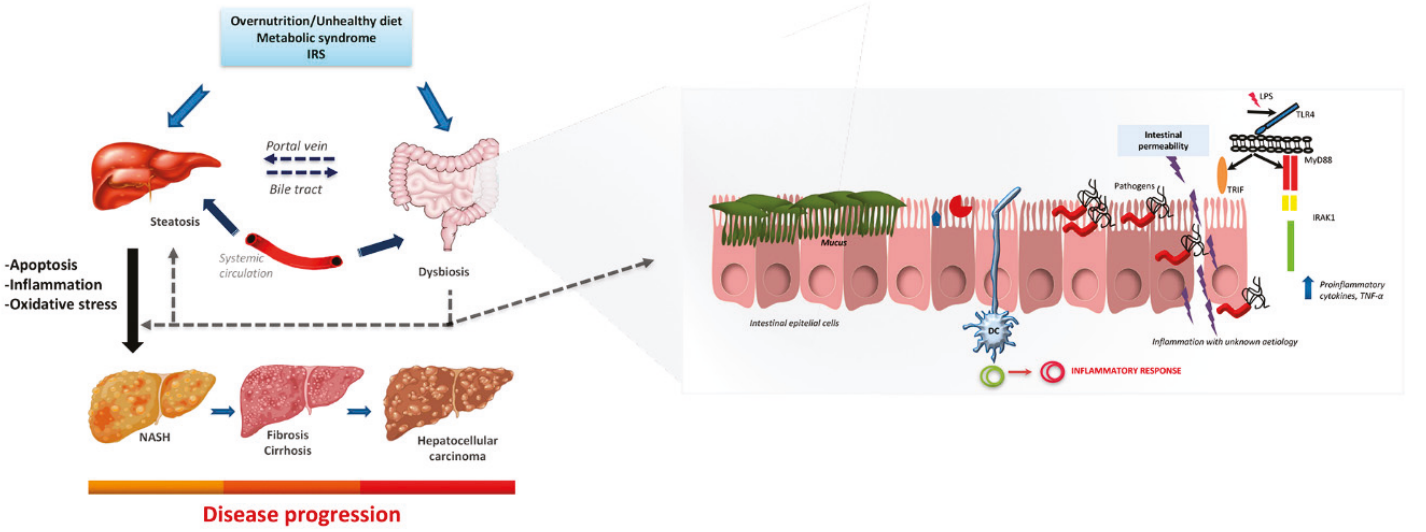

Figure 1. Impact of gut microbiota in hepatic disease. Schematic representation of the main factors involved in the development of NAFLD and the influence of gut microbiota and intestinal permeability through the gut-liver axis. Abbreviations: DC, dendritic cells; IRAK-4; Interleukin 1 Receptor Associated Kinase 4; IRS, insulin resistance syndrome; LPS, lipopolysaccharide; MyD88, Myeloid differentiation primary response 8; NAFLD, Non-alcoholic fatty liver disease; NASH, Nonalcoholic steatohepatitis; TLR4, toll-like receptor; TNF-α, Tumor Necrosis Factor alpha; TRIF, TIR-domain-containing adapter-inducing interferon-β.

Author Contributions: J.P.-D., P.S.-U., J.A.-V., F.R.-R., J.O.-A. and A.I.Á.-M. participated in the bibliographic search, discussion, and writing of the manuscript. J.P.-D. and A.I.Á.-M. designed the work. A.I.Á.-M. revised the manuscript. All authors have read and agreed with the published version of the manuscript. We thank Celia Cortez for revising and editing the English text.

Funding: This research received no external funding.

Acknowledgments: Julio Plaza-Diaz is part of the "UGR Plan Propio de Investigación 2016" and the "Excellence actions: Unit of Excellence on Exercise and Health (UCEES), University of Granada". Patricio Solis-Urra was supported by a grant from the National Agency for Research and Development (ANID) BECAS Chile/72180543. Julio Plaza-Diaz is supported by a grant awarded to postdoctoral researchers at foreign universities and research centers from the "Fundación Ramón Areces", Madrid, Spain. Jerónimo Aragón-Vela was funded by a Postdoctoral fellowship from the 'Fundación Alfonso Martín Escudero' (Spain). We are grateful to Belén Vázquez-González for her assistance with the illustration service.

Conflicts of Interest: The authors declare no conflict of interest.

References

1. Brunt, E.M.; Wong, V.W.; Nobili, V.; Day, C.P.; Sookoian, S.; Maher, J.J.; Bugianesi, E.; Sirlin, C.B.; Neuschwander-Tetri, B.A.; Rinella, M.E. Nonalcoholic fatty liver disease. *Nat. Rev. Dis. Primers* **2015**, *1*, 15080. [CrossRef] [PubMed]
2. Nassir, F.; Rector, R.S.; Hammoud, G.M.; Ibdah, J.A. Pathogenesis and Prevention of Hepatic Steatosis. *Gastroenterol. Hepatol. (N. Y.)* **2015**, *11*, 167–175.
3. McCormack, L.; Dutkowski, P.; El-Badry, A.M.; Clavien, P.A. Liver transplantation using fatty livers: Always feasible? *J. Hepatol.* **2011**, *54*, 1055–1062. [CrossRef] [PubMed]
4. Benedict, M.; Zhang, X. Non-alcoholic fatty liver disease: An expanded review. *World J. Hepatol.* **2017**, *9*, 715–732. [CrossRef] [PubMed]
5. Alvarez-Mercado, A.I.; Gulfo, J.; Romero Gomez, M.; Jimenez-Castro, M.B.; Gracia-Sancho, J.; Peralta, C. Use of Steatotic Grafts in Liver Transplantation: Current Status. *Liver Transpl.* **2019**, *25*, 771–786. [CrossRef]
6. Lopez-Velazquez, J.A.; Silva-Vidal, K.V.; Ponciano-Rodriguez, G.; Chavez-Tapia, N.C.; Arrese, M.; Uribe, M.; Mendez-Sanchez, N. The prevalence of nonalcoholic fatty liver disease in the Americas. *Ann. Hepatol.* **2014**, *13*, 166–178. [CrossRef]
7. Sherif, Z.A.; Saeed, A.; Ghavimi, S.; Nouraie, S.M.; Laiyemo, A.O.; Brim, H.; Ashktorab, H. Global Epidemiology of Nonalcoholic Fatty Liver Disease and Perspectives on US Minority Populations. *Dig. Dis. Sci.* **2016**, *61*, 1214–1225. [CrossRef]
8. Romero-Gomez, M.; Zelber-Sagi, S.; Trenell, M. Treatment of NAFLD with diet, physical activity and exercise. *J. Hepatol.* **2017**, *67*, 829–846. [CrossRef]
9. Almeda-Valdés, P.; Cuevas-Ramos, D.; Aguilar-Salinas, C.A. Metabolic syndrome and non-alcoholic fatty liver disease. *Ann. Hepatol.* **2009**, *8*, 18–24. [CrossRef]
10. Heindel, J.J.; Blumberg, B.; Cave, M.; Machtinger, R.; Mantovani, A.; Mendez, M.A.; Nadal, A.; Palanza, P.; Panzica, G.; Sargis, R.; et al. Metabolism disrupting chemicals and metabolic disorders. *Reprod. Toxicol.* **2017**, *68*, 3–33. [CrossRef]
11. Yki-Jarvinen, H. Non-alcoholic fatty liver disease as a cause and a consequence of metabolic syndrome. *Lancet Diabetes Endocrinol.* **2014**, *2*, 901–910. [CrossRef]
12. Donadon, V.; Balbi, M.; Perciaccante, A.; Casarin, P.; Zanette, G. Insulin resistance and hyperinsulinemia in patients with chronic liver disease and *Hepatocellular carcinoma*. *Clin. Med. Endocrinol. Diabetes* **2009**, *2*, CMED. S3116. [CrossRef]
13. Karim, M.F.; Al-Mahtab, M.; Rahman, S.; Debnath, C.R. Non-alcoholic Fatty Liver Disease (NAFLD)—A Review. *Mymensingh Med. J.* **2015**, *24*, 873–880. [PubMed]
14. Review, T.; LaBrecque, D.R.; Abbas, Z.; Anania, F.; Ferenci, P.; Khan, A.G.; Goh, K.L.; Hamid, S.S.; Isakov, V.; Lizarzabal, M.; et al. World Gastroenterology Organisation global guidelines: Nonalcoholic fatty liver disease and nonalcoholic steatohepatitis. *J. Clin. Gastroenterol.* **2014**, *48*, 467–473. [CrossRef]
15. Lee, J.; Hong, S.W.; Rhee, E.J.; Lee, W.Y. GLP-1 Receptor Agonist and Non-Alcoholic Fatty Liver Disease. *Diabetes Metab. J.* **2012**, *36*, 262–267. [CrossRef]
16. Tilg, H.; Moschen, A.R. Evolution of inflammation in nonalcoholic fatty liver disease: The multiple parallel hits hypothesis. *Hepatology* **2010**, *52*, 1836–1846. [CrossRef]
17. Giorgio, V.; Prono, F.; Graziano, F.; Nobili, V. Pediatric non alcoholic fatty liver disease: Old and new concepts on development, progression, metabolic insight and potential treatment targets. *BMC Pediatr.* **2013**, *13*, 40. [CrossRef]
18. Mendes, F.D.; Lindor, K.D. Recent advances in the treatment of non-alcoholic fatty liver disease. *Expert Opin. Investig. Drugs* **2005**, *14*, 29–35. [CrossRef]
19. Kim, K.H.; Lee, M.S. Pathogenesis of Nonalcoholic Steatohepatitis and Hormone-Based Therapeutic Approaches. *Front. Endocrinol. (Lausanne)* **2018**, *9*, 485. [CrossRef]
20. Buzzetti, E.; Pinzani, M.; Tsochatzis, E.A. The multiple-hit pathogenesis of non-alcoholic fatty liver disease (NAFLD). *Metabolism* **2016**, *65*, 1038–1048. [CrossRef]

21. Soto-Angona, O.; Anmella, G.; Valdes-Florido, M.J.; De Uribe-Viloria, N.; Carvalho, A.F.; Penninx, B.; Berk, M. Non-alcoholic fatty liver disease (NAFLD) as a neglected metabolic companion of psychiatric disorders: Common pathways and future approaches. *BMC Med.* **2020**, *18*, 261. [CrossRef] [PubMed]
22. Ma, J.; Zhou, Q.; Li, H. Gut Microbiota and Nonalcoholic Fatty Liver Disease: Insights on Mechanisms and Therapy. *Nutrients* **2017**, *9*, 1124. [CrossRef] [PubMed]
23. Luther, J.; Garber, J.J.; Khalili, H.; Dave, M.; Bale, S.S.; Jindal, R.; Motola, D.L.; Luther, S.; Bohr, S.; Jeoung, S.W.; et al. Hepatic Injury in Nonalcoholic Steatohepatitis Contributes to Altered Intestinal Permeability. *Cell. Mol. Gastroenterol. Hepatol.* **2015**, *1*, 222–232. [CrossRef] [PubMed]
24. Joshi-Barve, S.; Kirpich, I.; Cave, M.C.; Marsano, L.S.; McClain, C.J. Alcoholic, Nonalcoholic, and Toxicant-Associated Steatohepatitis: Mechanistic Similarities and Differences. *Cell. Mol. Gastroenterol. Hepatol.* **2015**, *1*, 356–367. [CrossRef]
25. Dukowicz, A.C.; Lacy, B.E.; Levine, G.M. Small intestinal bacterial overgrowth: A comprehensive review. *Gastroenterol. Hepatol. (N. Y.)* **2007**, *3*, 112–122.
26. Bibbo, S.; Ianiro, G.; Dore, M.P.; Simonelli, C.; Newton, E.E.; Cammarota, G. Gut Microbiota as a Driver of Inflammation in Nonalcoholic Fatty Liver Disease. *Mediators Inflamm.* **2018**, *2018*, 9321643. [CrossRef]
27. Grabherr, F.; Grander, C.; Effenberger, M.; Adolph, T.E.; Tilg, H. Gut Dysfunction and Non-alcoholic Fatty Liver Disease. *Front. Endocrinol. (Lausanne)* **2019**, *10*, 611. [CrossRef]
28. Plaza-Diaz, J.; Solis-Urra, P.; Rodriguez-Rodriguez, F.; Olivares-Arancibia, J.; Navarro-Oliveros, M.; Abadia-Molina, F.; Alvarez-Mercado, A.I. The Gut Barrier, Intestinal Microbiota, and Liver Disease: Molecular Mechanisms and Strategies to Manage. *Int. J. Mol. Sci.* **2020**, *21*, 8351. [CrossRef]
29. Hadizadeh, F.; Faghihimani, E.; Adibi, P. Nonalcoholic fatty liver disease: Diagnostic biomarkers. *World J. Gastrointest. Pathophysiol.* **2017**, *8*, 11–26. [CrossRef]
30. Wong, V.W.; Adams, L.A.; de Ledinghen, V.; Wong, G.L.; Sookoian, S. Noninvasive biomarkers in NAFLD and NASH-current progress and future promise. *Nat. Rev. Gastroenterol. Hepatol.* **2018**, *15*, 461–478. [CrossRef]
31. Townsend, S.A.; Newsome, P.N. Non-alcoholic fatty liver disease in 2016. *Br. Med. Bull.* **2016**, *119*, 143–156. [CrossRef] [PubMed]
32. Li, Q.; Dhyani, M.; Grajo, J.R.; Sirlin, C.; Samir, A.E. Current status of imaging in nonalcoholic fatty liver disease. *World J. Hepatol.* **2018**, *10*, 530. [CrossRef] [PubMed]
33. Angelico, M. Donor liver steatosis and graft selection for liver transplantation: A short review. *Eur. Rev. Med. Pharmacol. Sci.* **2005**, *9*, 295–297. [PubMed]
34. Ye, J.Z.; Li, Y.T.; Wu, W.R.; Shi, D.; Fang, D.Q.; Yang, L.Y.; Bian, X.Y.; Wu, J.J.; Wang, Q.; Jiang, X.W.; et al. Dynamic alterations in the gut microbiota and metabolome during the development of methionine-choline-deficient diet-induced nonalcoholic steatohepatitis. *World J. Gastroenterol.* **2018**, *24*, 2468–2481. [CrossRef] [PubMed]
35. Trepo, E.; Romeo, S.; Zucman-Rossi, J.; Nahon, P. PNPLA3 gene in liver diseases. *J. Hepatol.* **2016**, *65*, 399–412. [CrossRef] [PubMed]
36. Shen, J.; Wong, G.L.; Chan, H.L.; Chan, R.S.; Chan, H.Y.; Chu, W.C.; Cheung, B.H.; Yeung, D.K.; Li, L.S.; Sea, M.M.; et al. PNPLA3 gene polymorphism and response to lifestyle modification in patients with nonalcoholic fatty liver disease. *J. Gastroenterol. Hepatol.* **2015**, *30*, 139–146. [CrossRef]
37. Albillos, A.; de Gottardi, A.; Rescigno, M. The gut-liver axis in liver disease: Pathophysiological basis for therapy. *J. Hepatol.* **2020**, *72*, 558–577. [CrossRef] [PubMed]
38. Tenorio-Jiménez, C.; Martínez-Ramírez, M.J.; Castillo-Codes, D.; Arraiza-Irigoyen, C.; Tercero-Lozano, M.; Camacho, J.; Chueca, N.; García, F.; Olza, J.; Plaza-Díaz, J. Lactobacillus reuteri V3401 reduces inflammatory biomarkers and modifies the gastrointestinal microbiome in adults with metabolic syndrome: The PROSIR study. *Nutrients* **2019**, *11*, 1761. [CrossRef]
39. Jakobsson, H.E.; Rodriguez-Pineiro, A.M.; Schutte, A.; Ermund, A.; Boysen, P.; Bemark, M.; Sommer, F.; Backhed, F.; Hansson, G.C.; Johansson, M.E. The composition of the gut microbiota shapes the colon mucus barrier. *EMBO Rep.* **2015**, *16*, 164–177. [CrossRef]
40. Birchenough, G.M.; Nystrom, E.E.; Johansson, M.E.; Hansson, G.C. A sentinel goblet cell guards the colonic crypt by triggering Nlrp6-dependent Muc2 secretion. *Science* **2016**, *352*, 1535–1542. [CrossRef]
41. Tilg, H.; Moschen, A.R.; Szabo, G. Interleukin-1 and inflammasomes in alcoholic liver disease/acute alcoholic hepatitis and nonalcoholic fatty liver disease/nonalcoholic steatohepatitis. *Hepatology* **2016**, *64*, 955–965. [CrossRef] [PubMed]
42. Del Chierico, F.; Nobili, V.; Vernocchi, P.; Russo, A.; De Stefanis, C.; Gnani, D.; Furlanello, C.; Zandona, A.; Paci, P.; Capuani, G.; et al. Gut microbiota profiling of pediatric nonalcoholic fatty liver disease and obese patients unveiled by an integrated meta-omics-based approach. *Hepatology* **2017**, *65*, 451–464. [CrossRef] [PubMed]
43. Leung, C.; Rivera, L.; Furness, J.B.; Angus, P.W. The role of the gut microbiota in NAFLD. *Nat. Rev. Gastroenterol. Hepatol.* **2016**, *13*, 412–425. [CrossRef] [PubMed]
44. Boursier, J.; Diehl, A.M. Nonalcoholic Fatty Liver Disease and the Gut Microbiome. *Clin. Liver Dis.* **2016**, *20*, 263–275. [CrossRef] [PubMed]
45. Miele, L.; Valenza, V.; La Torre, G.; Montalto, M.; Cammarota, G.; Ricci, R.; Masciana, R.; Forgione, A.; Gabrieli, M.L.; Perotti, G.; et al. Increased intestinal permeability and tight junction alterations in nonalcoholic fatty liver disease. *Hepatology* **2009**, *49*, 1877–1887. [CrossRef] [PubMed]

46. Buckley, A.; Turner, J.R. Cell Biology of Tight Junction Barrier Regulation and Mucosal Disease. *Cold Spring Harb. Perspect. Biol.* **2018**, *10*. [CrossRef]
47. Rahman, K.; Desai, C.; Iyer, S.S.; Thorn, N.E.; Kumar, P.; Liu, Y.; Smith, T.; Neish, A.S.; Li, H.; Tan, S.; et al. Loss of Junctional Adhesion Molecule A Promotes Severe Steatohepatitis in Mice on a Diet High in Saturated Fat, Fructose, and Cholesterol. *Gastroenterology* **2016**, *151*, 733–746. [CrossRef] [PubMed]
48. Spadoni, I.; Zagato, E.; Bertocchi, A.; Paolinelli, R.; Hot, E.; Di Sabatino, A.; Caprioli, F.; Bottiglieri, L.; Oldani, A.; Viale, G.; et al. A gut-vascular barrier controls the systemic dissemination of bacteria. *Science* **2015**, *350*, 830–834. [CrossRef]
49. Spadoni, I.; Fornasa, G.; Rescigno, M. Organ-specific protection mediated by cooperation between vascular and epithelial barriers. *Nat. Rev. Immunol.* **2017**, *17*, 761–773. [CrossRef]
50. Mouries, J.; Brescia, P.; Silvestri, A.; Spadoni, I.; Sorribas, M.; Wiest, R.; Mileti, E.; Galbiati, M.; Invernizzi, P.; Adorini, L.; et al. Microbiota-driven gut vascular barrier disruption is a prerequisite for non-alcoholic steatohepatitis development. *J. Hepatol.* **2019**, *71*, 1216–1228. [CrossRef]
51. Rai, R.P.; Liu, Y.; Iyer, S.S.; Liu, S.; Gupta, B.; Desai, C.; Kumar, P.; Smith, T.; Singhi, A.D.; Nusrat, A.; et al. Blocking integrin alpha4beta7-mediated CD4 T cell recruitment to the intestine and liver protects mice from western diet-induced non-alcoholic steatohepatitis. *J. Hepatol.* **2020**, *73*, 1013–1022. [CrossRef] [PubMed]
52. Gerbes, A.; Zoulim, F.; Tilg, H.; Dufour, J.F.; Bruix, J.; Paradis, V.; Salem, R.; Peck-Radosavljevic, M.; Galle, P.R.; Greten, T.F.; et al. Gut roundtable meeting paper: Selected recent advances in hepatocellular carcinoma. *Gut* **2018**, *67*, 380–388. [CrossRef] [PubMed]
53. Jiao, N.; Baker, S.S.; Chapa-Rodriguez, A.; Liu, W.; Nugent, C.A.; Tsompana, M.; Mastrandrea, L.; Buck, M.J.; Baker, R.D.; Genco, R.J.; et al. Suppressed hepatic bile acid signalling despite elevated production of primary and secondary bile acids in NAFLD. *Gut* **2018**, *67*, 1881–1891. [CrossRef] [PubMed]
54. Rinella, M.; Charlton, M. The globalization of nonalcoholic fatty liver disease: Prevalence and impact on world health. *Hepatology* **2016**, *64*, 19–22. [CrossRef]
55. Bruce, K.D.; Cagampang, F.R.; Argenton, M.; Zhang, J.; Ethirajan, P.L.; Burdge, G.C.; Bateman, A.C.; Clough, G.F.; Poston, L.; Hanson, M.A.; et al. Maternal high-fat feeding primes steatohepatitis in adult mice offspring, involving mitochondrial dysfunction and altered lipogenesis gene expression. *Hepatology* **2009**, *50*, 1796–1808. [CrossRef]
56. Romeo, S.; Kozlitina, J.; Xing, C.; Pertsemlidis, A.; Cox, D.; Pennacchio, L.A.; Boerwinkle, E.; Cohen, J.C.; Hobbs, H.H. Genetic variation in PNPLA3 confers susceptibility to nonalcoholic fatty liver disease. *Nat. Genet.* **2008**, *40*, 1461–1465. [CrossRef]
57. Duparc, T.; Plovier, H.; Marrachelli, V.G.; Van Hul, M.; Essaghir, A.; Stahlman, M.; Matamoros, S.; Geurts, L.; Pardo-Tendero, M.M.; Druart, C.; et al. Hepatocyte MyD88 affects bile acids, gut microbiota and metabolome contributing to regulate glucose and lipid metabolism. *Gut* **2017**, *66*, 620–632. [CrossRef]
58. Chen, M.; Hui, S.; Lang, H.; Zhou, M.; Zhang, Y.; Kang, C.; Zeng, X.; Zhang, Q.; Yi, L.; Mi, M. SIRT3 Deficiency Promotes High-Fat Diet-Induced Nonalcoholic Fatty Liver Disease in Correlation with Impaired Intestinal Permeability through Gut Microbial Dysbiosis. *Mol. Nutr. Food Res.* **2019**, *63*, e1800612. [CrossRef]
59. Zeng, X.; Yang, J.; Hu, O.; Huang, J.; Ran, L.; Chen, M.; Zhang, Y.; Zhou, X.; Zhu, J.; Zhang, Q.; et al. Dihydromyricetin Ameliorates Nonalcoholic Fatty Liver Disease by Improving Mitochondrial Respiratory Capacity and Redox Homeostasis Through Modulation of SIRT3 Signaling. *Antioxid. Redox Signal.* **2019**, *30*, 163–183. [CrossRef]
60. De Sant'Ana, L.P.; Ribeiro, D.J.S.; Martins, A.M.A.; Dos Santos, F.N.; Correa, R.; Almeida, R.D.N.; Eberlin, M.N.; Maurice, C.F.; Magalhaes, K.G. Absence of the Caspases 1/11 Modulates Liver Global Lipid Profile and Gut Microbiota in High-Fat-Diet-Induced Obese Mice. *Front. Immunol.* **2019**, *10*, 2926. [CrossRef]
61. Pierantonelli, I.; Rychlicki, C.; Agostinelli, L.; Giordano, D.M.; Gaggini, M.; Fraumene, C.; Saponaro, C.; Manghina, V.; Sartini, L.; Mingarelli, E.; et al. Lack of NLRP3-inflammasome leads to gut-liver axis derangement, gut dysbiosis and a worsened phenotype in a mouse model of NAFLD. *Sci. Rep.* **2017**, *7*, 12200. [CrossRef] [PubMed]
62. Longo, L.; Ferrari, J.T.; Rampelotto, P.H.; Dellavia, G.H.; Pasqualotto, A.; Oliveira, C.P.; Cerski, C.T.S.; da Silveira, T.R.; Uribe-Cruz, C.; Álvares-da-Silva, M.R. Gut Dysbiosis and Increased Intestinal Permeability Drive microRNAs, NLRP-3 Inflammasome and Liver Fibrosis in a Nutritional Model of Non-Alcoholic Steatohepatitis in Adult Male Sprague Dawley Rats. *Clin. Exp. Gastroenterol.* **2020**, *13*, 351–368. [CrossRef] [PubMed]
63. Sun, L.; Pang, Y.; Wang, X.; Wu, Q.; Liu, H.; Liu, B.; Liu, G.; Ye, M.; Kong, W.; Jiang, C. Ablation of gut microbiota alleviates obesity-induced hepatic steatosis and glucose intolerance by modulating bile acid metabolism in hamsters. *Acta Pharm. Sin. B* **2019**, *9*, 702–710. [CrossRef] [PubMed]
64. Ahmad, M.I.; Ijaz, M.U.; Hussain, M.; Haq, I.U.; Zhao, D.; Li, C. High-Fat Proteins Drive Dynamic Changes in Gut Microbiota, Hepatic Metabolome, and Endotoxemia-TLR-4-NFkappaB-Mediated Inflammation in Mice. *J. Agric. Food Chem.* **2020**, *68*, 11710–11725. [CrossRef]
65. Cavallari, J.F.; Pokrajac, N.T.; Zlitni, S.; Foley, K.P.; Henriksbo, B.D.; Schertzer, J.D. NOD2 in hepatocytes engages a liver-gut axis to protect against steatosis, fibrosis, and gut dysbiosis during fatty liver disease in mice. *Am. J. Physiol. Endocrinol. Metab.* **2020**, *319*, E305–E314. [CrossRef]
66. Schneider, K.M.; Mohs, A.; Kilic, K.; Candels, L.S.; Elfers, C.; Bennek, E.; Schneider, L.B.; Heymann, F.; Gassler, N.; Penders, J.; et al. Intestinal Microbiota Protects against MCD Diet-Induced Steatohepatitis. *Int. J. Mol. Sci.* **2019**, *20*, 308. [CrossRef]

67. Zhang, X.; Coker, O.O.; Chu, E.S.; Fu, K.; Lau, H.C.H.; Wang, Y.X.; Chan, A.W.H.; Wei, H.; Yang, X.; Sung, J.J.Y.; et al. Dietary cholesterol drives fatty liver-associated liver cancer by modulating gut microbiota and metabolites. *Gut* **2020**. [CrossRef]
68. Liang, W.; Menke, A.L.; Driessen, A.; Koek, G.H.; Lindeman, J.H.; Stoop, R.; Havekes, L.M.; Kleemann, R.; van den Hoek, A.M. Establishment of a general NAFLD scoring system for rodent models and comparison to human liver pathology. *PLoS ONE* **2014**, *9*, e115922. [CrossRef]
69. Morrison, M.C.; Kleemann, R.; van Koppen, A.; Hanemaaijer, R.; Verschuren, L. Key Inflammatory Processes in Human NASH Are Reflected in Ldlr(-/-).Leiden Mice: A Translational Gene Profiling Study. *Front. Physiol.* **2018**, *9*, 132. [CrossRef]
70. Gart, E.; Souto Lima, E.; Schuren, F.; de Ruiter, C.G.F.; Attema, J.; Verschuren, L.; Keijer, J.; Salic, K.; Morrison, M.C.; Kleemann, R. Diet-Independent Correlations between Bacteria and Dysfunction of Gut, Adipose Tissue, and Liver: A Comprehensive Microbiota Analysis in Feces and Mucosa of the Ileum and Colon in Obese Mice with NAFLD. *Int. J. Mol. Sci.* **2018**, *20*, 1. [CrossRef]
71. Llorente, C.; Jepsen, P.; Inamine, T.; Wang, L.; Bluemel, S.; Wang, H.J.; Loomba, R.; Bajaj, J.S.; Schubert, M.L.; Sikaroodi, M.; et al. Gastric acid suppression promotes alcoholic liver disease by inducing overgrowth of intestinal Enterococcus. *Nat. Commun.* **2017**, *8*, 837. [CrossRef] [PubMed]
72. Petrov, P.D.; Garcia-Mediavilla, M.V.; Guzman, C.; Porras, D.; Nistal, E.; Martinez-Florez, S.; Castell, J.V.; Gonzalez-Gallego, J.; Sanchez-Campos, S.; Jover, R. A Network Involving Gut Microbiota, Circulating Bile Acids, and Hepatic Metabolism Genes That Protects Against Non-Alcoholic Fatty Liver Disease. *Mol. Nutr. Food Res.* **2019**, *63*, e1900487. [CrossRef] [PubMed]
73. Soderborg, T.K.; Clark, S.E.; Mulligan, C.E.; Janssen, R.C.; Babcock, L.; Ir, D.; Young, B.; Krebs, N.; Lemas, D.J.; Johnson, L.K.; et al. The gut microbiota in infants of obese mothers increases inflammation and susceptibility to NAFLD. *Nat. Commun.* **2018**, *9*, 4462. [CrossRef]
74. Yun, Y.; Kim, H.N.; Lee, E.J.; Ryu, S.; Chang, Y.; Shin, H.; Kim, H.L.; Kim, T.H.; Yoo, K.; Kim, H.Y. Fecal and blood microbiota profiles and presence of nonalcoholic fatty liver disease in obese versus lean subjects. *PLoS ONE* **2019**, *14*, e0213692. [CrossRef] [PubMed]
75. Fei, N.; Bruneau, A.; Zhang, X.; Wang, R.; Wang, J.; Rabot, S.; Gerard, P.; Zhao, L. Endotoxin Producers Overgrowing in Human Gut Microbiota as the Causative Agents for Nonalcoholic Fatty Liver Disease. *mBio* **2020**, *11*. [CrossRef] [PubMed]
76. Boursier, J.; Mueller, O.; Barret, M.; Machado, M.; Fizanne, L.; Araujo-Perez, F.; Guy, C.D.; Seed, P.C.; Rawls, J.F.; David, L.A.; et al. The severity of nonalcoholic fatty liver disease is associated with gut dysbiosis and shift in the metabolic function of the gut microbiota. *Hepatology* **2016**, *63*, 764–775. [CrossRef]
77. Demir, M.; Lang, S.; Martin, A.; Farowski, F.; Wisplinghoff, H.; Vehreschild, M.; Krawczyk, M.; Nowag, A.; Scholz, C.J.; Kretzschmar, A.; et al. Phenotyping non-alcoholic fatty liver disease by the gut microbiota: Ready for prime time? *J. Gastroenterol. Hepatol* **2020**, *35*, 1969–1977. [CrossRef]
78. Adams, L.A.; Wang, Z.; Liddle, C.; Melton, P.E.; Ariff, A.; Chandraratna, H.; Tan, J.; Ching, H.; Coulter, S.; de Boer, B.; et al. Bile acids associate with specific gut microbiota, low-level alcohol consumption and liver fibrosis in patients with non-alcoholic fatty liver disease. *Liver Int.* **2020**, *40*, 1356–1365. [CrossRef]
79. Lee, G.; You, H.J.; Bajaj, J.S.; Joo, S.K.; Yu, J.; Park, S.; Kang, H.; Park, J.H.; Kim, J.H.; Lee, D.H.; et al. Distinct signatures of gut microbiome and metabolites associated with significant fibrosis in non-obese NAFLD. *Nat. Commun.* **2020**, *11*, 4982. [CrossRef]
80. Wang, B.; Jiang, X.; Cao, M.; Ge, J.; Bao, Q.; Tang, L.; Chen, Y.; Li, L. Altered Fecal Microbiota Correlates with Liver Biochemistry in Nonobese Patients with Non-alcoholic Fatty Liver Disease. *Sci. Rep.* **2016**, *6*, 32002. [CrossRef]
81. Nier, A.; Engstler, A.J.; Maier, I.B.; Bergheim, I. Markers of intestinal permeability are already altered in early stages of non-alcoholic fatty liver disease: Studies in children. *PLoS ONE* **2017**, *12*, e0183282. [CrossRef] [PubMed]
82. Belei, O.; Olariu, L.; Dobrescu, A.; Marcovici, T.; Marginean, O. The relationship between non-alcoholic fatty liver disease and small intestinal bacterial overgrowth among overweight and obese children and adolescents. *J. Pediatr. Endocrinol. Metab.* **2017**, *30*, 1161–1168. [CrossRef] [PubMed]
83. Stanislawski, M.A.; Lozupone, C.A.; Wagner, B.D.; Eggesbo, M.; Sontag, M.K.; Nusbacher, N.M.; Martinez, M.; Dabelea, D. Gut microbiota in adolescents and the association with fatty liver: The EPOCH study. *Pediatr. Res.* **2018**, *84*, 219–227. [CrossRef] [PubMed]
84. Charlton, M.R.; Burns, J.M.; Pedersen, R.A.; Watt, K.D.; Heimbach, J.K.; Dierkhising, R.A. Frequency and outcomes of liver transplantation for nonalcoholic steatohepatitis in the United States. *Gastroenterology* **2011**, *141*, 1249–1253. [CrossRef]
85. Shaker, M.; Tabbaa, A.; Albeldawi, M.; Alkhouri, N. Liver transplantation for nonalcoholic fatty liver disease: New challenges and new opportunities. *World J. Gastroenterol.* **2014**, *20*, 5320–5330. [CrossRef]
86. Madsbad, S.; Dirksen, C.; Holst, J.J. Mechanisms of changes in glucose metabolism and bodyweight after bariatric surgery. *Lancet Diabetes Endocrinol.* **2014**, *2*, 152–164. [CrossRef]
87. Lassailly, G.; Caiazzo, R.; Buob, D.; Pigeyre, M.; Verkindt, H.; Labreuche, J.; Raverdy, V.; Leteurtre, E.; Dharancy, S.; Louvet, A.; et al. Bariatric Surgery Reduces Features of Nonalcoholic Steatohepatitis in Morbidly Obese Patients. *Gastroenterology* **2015**, *149*, 379–388. [CrossRef]
88. Mummadi, R.R.; Kasturi, K.S.; Chennareddygari, S.; Sood, G.K. Effect of bariatric surgery on nonalcoholic fatty liver disease: Systematic review and meta-analysis. *Clin. Gastroenterol. Hepatol.* **2008**, *6*, 1396–1402. [CrossRef]

89. Koutoukidis, D.A.; Koshiaris, C.; Henry, J.A.; Noreik, M.; Morris, E.; Manoharan, I.; Tudor, K.; Bodenham, E.; Dunnigan, A.; Jebb, S.A.; et al. The effect of the magnitude of weight loss on non-alcoholic fatty liver disease: A systematic review and meta-analysis. *Metabolism* **2020**, *115*, 154455. [CrossRef]
90. Magouliotis, D.E.; Tasiopoulou, V.S.; Sioka, E.; Chatedaki, C.; Zacharoulis, D. Impact of Bariatric Surgery on Metabolic and Gut Microbiota Profile: A Systematic Review and Meta-analysis. *Obes. Surg.* **2017**, *27*, 1345–1357. [CrossRef]
91. Nicoletti, C.F.; Cortes-Oliveira, C.; Pinhel, M.A.S.; Nonino, C.B. Bariatric Surgery and Precision Nutrition. *Nutrients* **2017**, *9*, 974. [CrossRef] [PubMed]
92. Anhe, F.F.; Varin, T.V.; Schertzer, J.D.; Marette, A. The Gut Microbiota as a Mediator of Metabolic Benefits after Bariatric Surgery. *Can. J. Diabetes* **2017**, *41*, 439–447. [CrossRef] [PubMed]
93. Palleja, A.; Kashani, A.; Allin, K.H.; Nielsen, T.; Zhang, C.; Li, Y.; Brach, T.; Liang, S.; Feng, Q.; Jorgensen, N.B.; et al. Roux-en-Y gastric bypass surgery of morbidly obese patients induces swift and persistent changes of the individual gut microbiota. *Genome Med.* **2016**, *8*, 67. [CrossRef] [PubMed]
94. Ulker, I.; Yildiran, H. The effects of bariatric surgery on gut microbiota in patients with obesity: A review of the literature. *Biosci. Microbiota Food Health* **2019**, *38*, 3–9. [CrossRef] [PubMed]
95. Rodriguez, B.; Torres, D.M.; Harrison, S.A. Physical activity: An essential component of lifestyle modification in NAFLD. *Nat. Rev. Gastroenterol. Hepatol.* **2012**, *9*, 726–731. [CrossRef]
96. Carbajo-Pescador, S.; Porras, D.; Garcia-Mediavilla, M.V.; Martinez-Florez, S.; Juarez-Fernandez, M.; Cuevas, M.J.; Mauriz, J.L.; Gonzalez-Gallego, J.; Nistal, E.; Sanchez-Campos, S. Beneficial effects of exercise on gut microbiota functionality and barrier integrity, and gut-liver crosstalk in an in vivo model of early obesity and non-alcoholic fatty liver disease. *Dis. Model Mech.* **2019**, *12*. [CrossRef]
97. Stefani, L.; Galanti, G. Physical Exercise Prescription in Metabolic Chronic Disease. *Adv. Exp. Med. Biol.* **2017**, *1005*, 123–141. [CrossRef]
98. Macavei, B.; Baban, A.; Dumitrascu, D.L. Psychological factors associated with NAFLD/NASH: A systematic review. *Eur. Rev. Med. Pharmacol. Sci.* **2016**, *20*, 5081–5097.
99. Stine, J.G.; Schreibman, I.; Navabi, S.; Kang, M.; Dahmus, J.; Soriano, C.; Rivas, G.; Hummer, B.; Beyer, M.; Tressler, H.; et al. Nonalcoholic steatohepatitis Fitness Intervention in Thrombosis (NASHFit): Study protocol for a randomized controlled trial of a supervised aerobic exercise program to reduce elevated clotting risk in patients with NASH. *Contemp. Clin. Trials. Commun.* **2020**, *18*, 100560. [CrossRef]
100. Baker, C.J.; Martinez-Huenchullan, S.F.; D'Souza, M.; Xu, Y.; Li, M.; Bi, Y.; Johnson, N.A.; Twigg, S.M. Effect of exercise on hepatic steatosis: Are benefits seen without dietary intervention? A systematic review and meta-analysis. *J. Diabetes* **2021**, *13*, 63–77. [CrossRef]
101. Dixon, J.B.; Bhathal, P.S.; Hughes, N.R.; O'Brien, P.E. Nonalcoholic fatty liver disease: Improvement in liver histological analysis with weight loss. *Hepatology* **2004**, *39*, 1647–1654. [CrossRef] [PubMed]
102. Huber, Y.; Pfirrmann, D.; Gebhardt, I.; Labenz, C.; Gehrke, N.; Straub, B.K.; Ruckes, C.; Bantel, H.; Belda, E.; Clement, K.; et al. Improvement of non-invasive markers of NAFLD from an individualised, web-based exercise program. *Aliment. Pharmacol. Ther.* **2019**, *50*, 930–939. [CrossRef] [PubMed]
103. Hoier, B.; Rufener, N.; Bojsen-Moller, J.; Bangsbo, J.; Hellsten, Y. The effect of passive movement training on angiogenic factors and capillary growth in human skeletal muscle. *J. Physiol.* **2010**, *588*, 3833–3845. [CrossRef] [PubMed]
104. Arulanandan, A.; Ang, B.; Bettencourt, R.; Hooker, J.; Behling, C.; Lin, G.Y.; Valasek, M.A.; Ix, J.H.; Schnabl, B.; Sirlin, C.B.; et al. Association Between Quantity of Liver Fat and Cardiovascular Risk in Patients With Nonalcoholic Fatty Liver Disease Independent of Nonalcoholic Steatohepatitis. *Clin. Gastroenterol. Hepatol.* **2015**, *13*, 1513–1520 e1511. [CrossRef] [PubMed]
105. Hashida, R.; Kawaguchi, T.; Bekki, M.; Omoto, M.; Matsuse, H.; Nago, T.; Takano, Y.; Ueno, T.; Koga, H.; George, J.; et al. Aerobic vs. resistance exercise in non-alcoholic fatty liver disease: A systematic review. *J. Hepatol.* **2017**, *66*, 142–152. [CrossRef] [PubMed]
106. Ortiz-Alvarez, L.; Xu, H.; Martinez-Tellez, B. Influence of Exercise on the Human Gut Microbiota of Healthy Adults: A Systematic Review. *Clin. Transl. Gastroenterol.* **2020**, *11*, e00126. [CrossRef] [PubMed]
107. Monda, V.; Villano, I.; Messina, A.; Valenzano, A.; Esposito, T.; Moscatelli, F.; Viggiano, A.; Cibelli, G.; Chieffi, S.; Monda, M.; et al. Exercise Modifies the Gut Microbiota with Positive Health Effects. *Oxid. Med. Cell. Longev.* **2017**, *2017*, 3831972. [CrossRef] [PubMed]
108. Liu, Y.; Wang, Y.; Ni, Y.; Cheung, C.K.Y.; Lam, K.S.L.; Wang, Y.; Xia, Z.; Ye, D.; Guo, J.; Tse, M.A.; et al. Gut Microbiome Fermentation Determines the Efficacy of Exercise for Diabetes Prevention. *Cell Metab.* **2020**, *31*, 77–91.e5. [CrossRef]
109. Mailing, L.J.; Allen, J.M.; Buford, T.W.; Fields, C.J.; Woods, J.A. Exercise and the Gut Microbiome: A Review of the Evidence, Potential Mechanisms, and Implications for Human Health. *Exerc. Sport Sci. Rev.* **2019**, *47*, 75–85. [CrossRef]
110. Welly, R.J.; Liu, T.W.; Zidon, T.M.; Rowles, J.L., 3rd; Park, Y.M.; Smith, T.N.; Swanson, K.S.; Padilla, J.; Vieira-Potter, V.J. Comparison of Diet versus Exercise on Metabolic Function and Gut Microbiota in Obese Rats. *Med. Sci. Sports Exerc.* **2016**, *48*, 1688–1698. [CrossRef]
111. Munukka, E.; Ahtiainen, J.P.; Puigbo, P.; Jalkanen, S.; Pahkala, K.; Keskitalo, A.; Kujala, U.M.; Pietila, S.; Hollmen, M.; Elo, L.; et al. Six-Week Endurance Exercise Alters Gut Metagenome That Is not Reflected in Systemic Metabolism in Over-weight Women. *Front. Microbiol.* **2018**, *9*, 2323. [CrossRef] [PubMed]

112. Motiani, K.K.; Collado, M.C.; Eskelinen, J.J.; Virtanen, K.A.; Loyttyniemi, E.; Salminen, S.; Nuutila, P.; Kalliokoski, K.K.; Hannukainen, J.C. Exercise Training Modulates Gut Microbiota Profile and Improves Endotoxemia. *Med. Sci. Sports Exerc.* **2020**, *52*, 94–104. [CrossRef] [PubMed]
113. Houttu, V.; Boulund, U.; Grefhorst, A.; Soeters, M.R.; Pinto-Sietsma, S.J.; Nieuwdorp, M.; Holleboom, A.G. The role of the gut microbiome and exercise in non-alcoholic fatty liver disease. *Ther. Adv. Gastroenterol.* **2020**, *13*, 1756284820941745. [CrossRef] [PubMed]
114. Denou, E.; Marcinko, K.; Surette, M.G.; Steinberg, G.R.; Schertzer, J.D. High-intensity exercise training increases the diversity and metabolic capacity of the mouse distal gut microbiota during diet-induced obesity. *Am. J. Physiol. Endocrinol. Metab.* **2016**, *310*, E982–E993. [CrossRef] [PubMed]
115. Orci, L.A.; Gariani, K.; Oldani, G.; Delaune, V.; Morel, P.; Toso, C. Exercise-based Interventions for Nonalcoholic Fatty Liver Disease: A Meta-analysis and Meta-regression. *Clin. Gastroenterol. Hepatol.* **2016**, *14*, 1398–1411. [CrossRef] [PubMed]
116. Keating, S.E.; Hackett, D.A.; Parker, H.M.; O'Connor, H.T.; Gerofi, J.A.; Sainsbury, A.; Baker, M.K.; Chuter, V.H.; Caterson, I.D.; George, J.; et al. Effect of aerobic exercise training dose on liver fat and visceral adiposity. *J. Hepatol.* **2015**, *63*, 174–182. [CrossRef]
117. Bull, F.C.; Al-Ansari, S.S.; Biddle, S.; Borodulin, K.; Buman, M.P.; Cardon, G.; Carty, C.; Chaput, J.P.; Chastin, S.; Chou, R.; et al. World Health Organization 2020 guidelines on physical activity and sedentary behaviour. *Br. J. Sports Med.* **2020**, *54*, 1451–1462. [CrossRef]
118. European Association for the Study of the, L.; European Association for the Study of, D.; European Association for the Study of, O. EASL-EASD-EASO Clinical Practice Guidelines for the management of non-alcoholic fatty liver disease. *Diabetologia* **2016**, *59*, 1121–1140. [CrossRef]
119. Gomez de Aguero, M.; Ganal-Vonarburg, S.C.; Fuhrer, T.; Rupp, S.; Uchimura, Y.; Li, H.; Steinert, A.; Heikenwalder, M.; Hapfelmeier, S.; Sauer, U.; et al. The maternal microbiota drives early postnatal innate immune development. *Science* **2016**, *351*, 1296–1302. [CrossRef]
120. Koenig, J.E.; Spor, A.; Scalfone, N.; Fricker, A.D.; Stombaugh, J.; Knight, R.; Angenent, L.T.; Ley, R.E. Succession of microbial consortia in the developing infant gut microbiome. *Proc. Natl. Acad. Sci. USA* **2011**, *108* (Suppl. S1), 4578–4585. [CrossRef]
121. Koopman, K.E.; Caan, M.W.; Nederveen, A.J.; Pels, A.; Ackermans, M.T.; Fliers, E.; la Fleur, S.E.; Serlie, M.J. Hypercaloric diets with increased meal frequency, but not meal size, increase intrahepatic triglycerides: A randomized controlled trial. *Hepatology* **2014**, *60*, 545–553. [CrossRef] [PubMed]
122. Vilar-Gomez, E.; Martinez-Perez, Y.; Calzadilla-Bertot, L.; Torres-Gonzalez, A.; Gra-Oramas, B.; Gonzalez-Fabian, L.; Friedman, S.L.; Diago, M.; Romero-Gomez, M. Weight Loss Through Lifestyle Modification Significantly Reduces Features of Nonalcoholic Steatohepatitis. *Gastroenterology* **2015**, *149*, 367–378.e5. [CrossRef] [PubMed]
123. Boden, G. High- or low-carbohydrate diets: Which is better for weight loss, insulin resistance, and fatty livers? *Gastroenterology* **2009**, *136*, 1490–1492. [CrossRef] [PubMed]
124. European Association for the Study of the, L.; European Association for the Study of, D.; European Association for the Study of, O. EASL-EASD-EASO Clinical Practice Guidelines for the management of non-alcoholic fatty liver disease. *J. Hepatol.* **2016**, *64*, 1388–1402. [CrossRef]
125. Haro, C.; Garcia-Carpintero, S.; Alcala-Diaz, J.F.; Gomez-Delgado, F.; Delgado-Lista, J.; Perez-Martinez, P.; Rangel Zuniga, O.A.; Quintana-Navarro, G.M.; Landa, B.B.; Clemente, J.C.; et al. The gut microbial community in metabolic syndrome patients is modified by diet. *J. Nutr. Biochem.* **2016**, *27*, 27–31. [CrossRef]
126. Haro, C.; Garcia-Carpintero, S.; Rangel-Zuniga, O.A.; Alcala-Diaz, J.F.; Landa, B.B.; Clemente, J.C.; Perez-Martinez, P.; Lopez-Miranda, J.; Perez-Jimenez, F.; Camargo, A. Consumption of Two Healthy Dietary Patterns Restored Microbiota Dysbiosis in Obese Patients with Metabolic Dysfunction. *Mol. Nutr. Food Res.* **2017**, *61*, 1700300. [CrossRef]
127. Pan, X.; Wen, S.W.; Kaminga, A.C.; Liu, A. Gut metabolites and inflammation factors in non-alcoholic fatty liver disease: A systematic review and meta-analysis. *Sci. Rep.* **2020**, *10*, 8848. [CrossRef]
128. Sharpton, S.R.; Maraj, B.; Harding-Theobald, E.; Vittinghoff, E.; Terrault, N.A. Gut microbiome-targeted therapies in nonalcoholic fatty liver disease: A systematic review, meta-analysis, and meta-regression. *Am. J. Clin. Nutr.* **2019**, *110*, 139–149. [CrossRef]
129. Bomhof, M.R.; Parnell, J.A.; Ramay, H.R.; Crotty, P.; Rioux, K.P.; Probert, C.S.; Jayakumar, S.; Raman, M.; Reimer, R.A. Histological improvement of non-alcoholic steatohepatitis with a prebiotic: A pilot clinical trial. *Eur. J. Nutr.* **2019**, *58*, 1735–1745. [CrossRef]
130. Manzhalii, E.; Virchenko, O.; Falalyeyeva, T.; Beregova, T.; Stremmel, W. Treatment efficacy of a probiotic preparation for non-alcoholic steatohepatitis: A pilot trial. *J. Dig. Dis.* **2017**, *18*, 698–703. [CrossRef]
131. Ahmed, L.A.; Salem, M.B.; Seif El-Din, S.H.; El-Lakkany, N.M.; Ahmed, H.O.; Nasr, S.M.; Hammam, O.A.; Botros, S.S.; Saleh, S. Gut microbiota modulation as a promising therapy with metformin in rats with non-alcoholic steatohepatitis: Role of LPS/TLR4 and autophagy pathways. *Eur. J. Pharmacol.* **2020**, *887*, 173461. [CrossRef] [PubMed]
132. Zeng, W.; Shen, J.; Bo, T.; Peng, L.; Xu, H.; Nasser, M.I.; Zhuang, Q.; Zhao, M. Cutting Edge: Probiotics and Fecal Microbiota Transplantation in Immunomodulation. *J. Immunol. Res.* **2019**, *2019*, 1603758. [CrossRef] [PubMed]
133. Sanchez-Rodriguez, E.; Egea-Zorrilla, A.; Plaza-Diaz, J.; Aragon-Vela, J.; Munoz-Quezada, S.; Tercedor-Sanchez, L.; Abadia-Molina, F. The Gut Microbiota and Its Implication in the Development of Atherosclerosis and Related Cardiovascular Diseases. *Nutrients* **2020**, *12*, 605. [CrossRef]
134. Leshem, A.; Horesh, N.; Elinav, E. Fecal Microbial Transplantation and Its Potential Application in Cardiometabolic Syndrome. *Front. Immunol.* **2019**, *10*, 1341. [CrossRef] [PubMed]

135. Brandt, L.J.; Aroniadis, O.C.; Mellow, M.; Kanatzar, A.; Kelly, C.; Park, T.; Stollman, N.; Rohlke, F.; Surawicz, C. Long-term follow-up of colonoscopic fecal microbiota transplant for recurrent Clostridium difficile infection. *Am. J. Gastroenterol.* **2012**, *107*, 1079–1087. [CrossRef]
136. van Nood, E.; Vrieze, A.; Nieuwdorp, M.; Fuentes, S.; Zoetendal, E.G.; de Vos, W.M.; Visser, C.E.; Kuijper, E.J.; Bartelsman, J.F.; Tijssen, J.G.; et al. Duodenal infusion of donor feces for recurrent Clostridium difficile. *N. Engl. J. Med.* **2013**, *368*, 407–415. [CrossRef]
137. Cohen, S.H.; Gerding, D.N.; Johnson, S.; Kelly, C.P.; Loo, V.G.; McDonald, L.C.; Pepin, J.; Wilcox, M.H. Society for Healthcare Epidemiology of America; Infectious Diseases Society of America. Clinical practice guidelines for Clostridium difficile infection in adults: 2010 update by the society for healthcare epidemiology of America (SHEA) and the infectious diseases society of America (IDSA). *Infect Control Hosp. Epidemiol.* **2010**, *31*, 431–455. [CrossRef]
138. Craven, L.; Rahman, A.; Nair Parvathy, S.; Beaton, M.; Silverman, J.; Qumosani, K.; Hramiak, I.; Hegele, R.; Joy, T.; Meddings, J.; et al. Allogenic Fecal Microbiota Transplantation in Patients With Nonalcoholic Fatty Liver Disease Improves Abnormal Small Intestinal Permeability: A Randomized Control Trial. *Am. J. Gastroenterol.* **2020**, *115*, 1055–1065. [CrossRef]

biomedicines

MDPI

Review

Magnesium, Little Known But Possibly Relevant: A Link between NASH and Related Comorbidities

Jorge Simón [1,2,*], Teresa Cardoso Delgado [1], Luis Alfonso Martinez-Cruz [1] and Maria Luz Martínez-Chantar [1,2,*,†]

[1] Liver Disease Laboratory, Center for Cooperative Research in Biosciences (CIC bioGUNE), Basque Research and Technology Alliance (BRTA), Bizkaia Technology Park, Building 801A, 48160 Derio, Bizkaia, Spain; tcardoso@cicbiogune.es (T.C.D.); amartinez@cicbiogune.es (L.A.M.-C.)

[2] Centro de Investigación Biomédica en Red de Enfermedades Hepáticas y Digestivas (CIBERehd), 48160 Derio, Bizkaia, Spain

* Correspondence: jsimon@cicbiogune.es (J.S.); mlmartinez@cicbiogune.es (M.L.M.-C.); Tel.: +34-944-061318 (J.S. & M.L.M.-C.); Fax: +34-944-061301 (J.S. & M.L.M.-C.)

† Senior authorship: mlmartinez@cicbiogune.es.

Abstract: Non-alcoholic steatohepatitis (NASH) is characterized by an abnormal hepatic lipid accumulation accompanied by a necro-inflammatory process and a fibrotic response. It comprises from 10% to 30% of cases of patients with non-alcoholic liver disease, which is a global health problem affecting around a quarter of the worldwide population. Nevertheless, the development of NASH is often surrounded by a pathological context with other comorbidities, such as cardiovascular diseases, obesity, insulin resistance or type 2 diabetes mellitus. Dietary imbalances are increasingly recognized as the root cause of these NASH-related comorbidities. In this context, a growing concern exists about whether magnesium consumption in the general population is sufficient. Hypomagnesemia is a hallmark of the aforementioned NASH comorbidities, and deficiencies in magnesium are also widely related to the triggering of complications that aggravate NASH or derived pathologies. Moreover, the supplementation of this cation has proved to reduce mortality from hepatic complications. In the present review, the role of magnesium in NASH and related comorbidities has been characterized, unraveling the relevance of maintaining the homeostasis of this cation for the correct functioning of the organism.

Keywords: non-alcoholic steatohepatitis (NASH); magnesium (Mg^{2+}); obesity; insulin resistance (IR); type 2 diabetes mellitus (T2DM); hypertension; cardiovascular diseases (CVD)

Citation: Simón, J.; Delgado, T.C.; Martinez-Cruz, L.A.; Martínez-Chantar, M.L. Magnesium, Little Known But Possibly Relevant: A Link between NASH and Related Comorbidities. *Biomedicines* **2021**, *9*, 125. https://doi.org/10.3390/biomedicines9020125

Academic Editors: Ronit Shiri-Sverdlov and Sabine Baumgartner

Received: 10 January 2021
Accepted: 23 January 2021
Published: 27 January 2021

1. Introduction

1.1. Non-Alcoholic Steatohepatitis: An Overview

Non-alcoholic steatohepatitis, or NASH, is a term used to define a pathophysiological stage of the liver characterized by an abnormal lipid accumulation (steatosis), inflammation, hepatocellular damage and fibrosis development [1]. NASH is included in the group of conditions that define the spectrum of non-alcoholic fatty liver disease (NAFLD), together with non-alcoholic fatty liver (NAFL or steatosis) and cirrhosis [2]. NAFLD has an estimated prevalence of 25% in the worldwide population, whereas NASH is estimated to affect 3–12% of the global population [3]. The highest rates of NAFLD are reported in South America and the Middle East, followed by Asia, USA and Europe, and they are expected to increase within the next years due to current lifestyle and dietary habits [3,4]. Remarkably, the development of NAFLD/NASH has been widely characterized as a risk factor for the development of hepatocellular carcinoma (HCC), contributing to 10–12% of cases in Western populations, and 1–6% of cases in Asian populations [5,6]. HCC is the second leading cause of cancer-related death and the fifth most common type of cancer worldwide [7]. Furthermore, both NASH and NAFLD patients usually present an elevated risk not only of liver-related morbidity and mortality, but also other metabolic comorbidi-

ties, such as insulin resistance (IR) and type 2 diabetes mellitus (T2DM), hypertension and cardiovascular diseases (CVD) or obesity [3].

The liver plays a key role in the metabolism of all biomolecules, but perturbations in lipid balance lead to the development of steatosis. In NAFLD, the genetic background or nutritional imbalances lead to a downregulation of the pathways involved in hepatic lipid clearance: (i) very-low-density lipoprotein (VLDL) secretion and (ii) fatty acid oxidation (FAO) or an upregulation in those that promote hepatic lipid content as (iii) de novo lipogenesis (DNL) and (iv) fatty acid (FA) uptake [8]. Although steatosis is usually considered a "brand" condition, chronic abnormal lipid deposition together with other hepatic insults or even other events beyond the liver, that include, for example, gut dysbiosis and adipose tissue inflammation, contribute to the development of NASH. In this context, the most common lipid-derived complications comprise of the excessive development of reactive oxygen species (ROS) and oxidative stress, the appearance of endoplasmic reticulum stress (ERS), mitochondrial dysfunction with subsequent decreased FAO capacity, and the production of lipotoxic species, which are of relevance [2,9]. These hits promote the development of liver fibrosis, characterized by an excessive extracellular matrix (ECM) deposition because of a chronic damage and a wound healing response [10]. In such an environment, hepatocytes suffer from an inflammatory and apoptotic signaling that leads to their death [11], activating Kupffer cells (KCs) to promote the release of inflammatory cytokines [12] and hepatic stellate cells (HSCs) to secrete ECM components [13].

1.2. Nutritional Imbalances in Non-Alcoholic Steatohepatitis: A Potential Role of Magnesium

Unhealthy nutritional habits and dietary imbalances are beginning to be recognized as the root cause of many diseases. Particularly, it was previously mentioned that NASH has metabolic perturbations that are the most common cause of development [14]. High-fat and high-sugar diets, such as the Western diet, lead to an increased fatty acid uptake by the liver and adipose tissue while promoting hepatic DNL [15]. Although an excessive calorie intake leads to the spread of overweight and obesity worldwide, currently affecting 38% of the worldwide population and expected to increase in the coming years [16], unhealthy dietary habits are also often accompanied by some imbalances in certain nutrients. In particular, deficiencies in dietary micronutrients have been identified.

Magnesium, or Mg^{2+} in its free form, is a micronutrient widely distributed in the food supply, both in plant and animal foods. Most green vegetables, legumes, peas, beans and nuts are rich in magnesium, as are some shellfish and spices. The daily recommended intake (DRI) for elemental magnesium is age-dependent, and lower for women (e.g., 19–30 years: 310 mg; 31 years and older: 320 mg) than men (e.g., 19–30 years: 400 mg; 31 years and older: 420 mg). Magnesium DRI increases for pregnant women and lactation periods. The cation is absorbed in the duodenum and ileum by both active and passive processes, and this process is affected by different nutrients, such as fiber content [17]. Under healthy conditions, the kidney plays a central role in magnesium homeostasis. In the last few years, a growing concern has emerged about the defective magnesium consumption in the general population, as, according to the National Health and Nutrition Examination Survey (NHANES), 79% of US adults do not meet the DRI of the cation [18].

Mg^{2+} is the most predominant divalent cation in the cell, with concentrations ranging from 5–20 mM, and extracellular Mg^{2+} accounts for only 1% of the total content in the organism [19,20]. Magnesium plays a role as cofactor in more than 300 enzymatic reactions, especially in those involving adenosine-triphosphate (ATP) or guanosine triphosphate (GTP), where the cation forms ATP-Mg or GTP-Mg stable complexes required for many biological processes such as glucose stabilization, lipogenesis, protein synthesis, nucleic acids synthesis, coenzymes activity or methylation, among others [19]. The maintenance of magnesium homeostasis is crucial for the correct development of the organism, whereas perturbations have been related to the triggering of an inflammatory response, mitochondrial dysfunction and the decrease of the antioxidant capacity [21]. These alterations in such biological processes have been reported to occur in comorbidities associated with

NASH such as obesity, hypertension, CVD and/or the development of IR or T2DM. Indeed, perturbations in Mg^{2+} homeostasis have been reported, not only in liver pathologies but also in concomitant systemic complications [22–24].

In the present review we aim to highlight the relevance of Mg^{2+} homeostasis and the development of systemic complications accompanying NASH.

2. Magnesium and Systemic Complications during Non-Alcoholic Steatohepatitis

2.1. Magnesium in Non-Alcoholic Fatty Liver Disease and Cancer

The spread of unhealthy lifestyle habits, together with inadequate nutritional behavior, are making NAFLD and the pathologies comprised in its spectrum the leading cause of chronic liver disease worldwide. Although, to date, the role of Mg^{2+} in the development of NASH has not been explored in depth, a clinical study showed a protective effect of Mg^{2+} intake in patients with liver diseases. Remarkably, an increased intake of 100 mg (25–33% increase of the daily recommended intake) showed a 49% reduction of liver-derived mortality [25], suggesting a possible role of the cation depletion in the development of liver diseases. Related to cirrhosis, the most severe stage of the pathologies that comprise the spectrum of NAFLD, decreased hepatic magnesium levels have been reported to promote collagen deposition in the liver, a hallmark of liver fibrosis [26,27]. The role of the cation is of relevance in the mitochondria from hepatocytes, where low intramitochondrial magnesium content has been described in cirrhosis with the subsequent decreased ATP production and increased hepatocellular damage [28]. The role of protein kinase Cε (PKCε) and its relationship with Mg^{2+} has also been characterized, as hypomagnesemia leads to a deficient PKCε translocation and subsequent fibrinogen and collagen deposition [29]. There is an existing link between low intrahepatic magnesium levels and an increased inflammatory response, as under low hepatic Mg^{2+} content, an over-activation of leukocytes and macrophages has been characterized, together with the recruitment of more inflammatory cells to the liver [30]. Moreover, the supplementation of this cation has been proposed as anti-cirrhotic therapy, because in vivo studies have demonstrated its protective effect [31].

As aforementioned, the development of NASH and other pathologies ranging in NAFLD may increase the risk of developing HCC. Related to this, the biological functions of the cation have been characterized, as Mg^{2+} plays a key role in DNA synthesis. Therefore, hypomagnesemia leads to dysfunctions in DNA damage repair mechanisms, modulation of cell cycle progression, cell proliferation and differentiation, and apoptosis with the subsequent tumor growth promotion and metastasis of the tumor [32,33]. Although molecular mechanisms that link hypomagnesemia and tumor development have not been elucidated yet, an in vitro study suggests a possible relationship between magnesium levels and a dysregulation of mitogen-activated protein kinase (MAPK)/extracellular signal-related kinase (ERK) signaling [34].

Finally, a continuous magnesium loss has been related to alcohol consumption [35], leading to the aggravation of alcoholic liver disease [26]. Related to this, Mg^{2+}-deficient livers show an increased KC activation through the toll-like receptor type 4 (TLR4), promoting ROS generation [36] and pro-inflammatory cytokine release [37]. Remarkably, Mg^{2+} supplementation in patients with alcoholic steatohepatitis prevents the progression of the disease, reducing the transaminases levels in serum and decreasing liver-related morbidity [38].

In summary, even though several studies suggest the relationship between hypomagnesemia and the development of liver diseases (Figure 1), to date there is no evidence that characterizes the relationship between the cation and NASH, so it could be a research topic of interest.

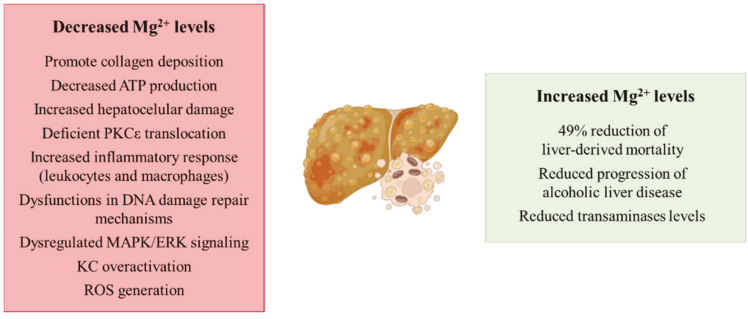

Figure 1. Schematic representation of the contribution of decreased and increased magnesium levels to the development of liver diseases. Abbreviations: PKCε: protein kinase Cε; MAPK: mitogen-activated protein kinase; ERK: extracellular signal-related kinase; KC: Kupffer cell; ROS: reactive oxygen species.

2.2. Magnesium in Overweight and Obesity

Overweight and obesity are complex and multifactorial diseases that affect over 1/3 of the world population. Similar to the epidemiology of NASH and NAFLD, these conditions are expected to even increase to a 38% prevalence of overweight and a 20% prevalence of obesity by 2030 [39]. Obesity is defined by an excessive body weight, in consequence of an excessive adiposity or body fatness. Healthy individuals show a body mass index (BMI) comprised between 18.5 and 24.99, whereas the BMI of overweight patients is between 25 and 29.99. Regarding the obese population, they can be classified into three subgroups: class I (BMI from 30 to 34.99), class II (BMI from 35 to 39.99) and class III (BMI higher than 40) [39]. Obesity greatly increases the risk of developing other chronic diseases such as those mentioned in the present manuscript: liver diseases (NASH/NAFLD), IR, T2DM, hypertension and CVD. Indeed, the development of NASH and overweight/obesity seem to follow a parallel direction. The risk of developing metabolic-derived liver complications has been reported to be two-fold higher in obese patients when compared with healthy non-obese patients [40].

Related to the possible role that Mg^{2+} perturbations may have in the development of alterations in obesity, hypomagnesemia has been identified in serum from obese patients [41]. Remarkably, a higher consumption of the cation is associated with a lower BMI, waist circumference and serum glucose levels in patients [42]. Related to the effect of the supplementation of the magnesium cation, it has been reported to improve the metabolic profile of normal-weight metabolically obese individuals in several parameters such as blood pressure (BP), fasting glucose and serum triglyceride levels [43]. Other studies have associated low magnesium concentrations with chronic inflammatory stress related to obese subjects, where hypomagnesemia enhances tumor necrosis factor (TNF) and interleukin-6 (IL-6) expression that might even contribute to the aggravation of other pathologies such as hepatic ones [44]. Additionally, Mg^{2+} consumption prevents the induction of obesity in in vivo models, suggesting a pivotal role of the cation in maintaining energy homeostasis [45]. However, other studies highlight the relevance of accompanying magnesium supplementation with a protein-sparing modified low-calorie diet in order to avoid the loss of the cation from the organism, as the supplementation alone cannot obtain this goal [46]. Nevertheless, the supplementation of the cation has been deeply characterized to improve the metabolic profile of obese individuals by decreasing the amount of low-density lipoprotein (LDL) and increasing high-density lipoprotein (HDL) levels [47].

Finally, other studies have focused on the impact of magnesium modulation in the adipocyte. It has been known for a long time that the adipocyte is not only a simple storage depot for body energy, but in fact an endocrine organ playing a very relevant role in obesity [48]. Interestingly, magnesium supplementation has been shown to result in

a shift by increasing the frequency distribution of large adipocytes whereas magnesium deficiency did not modify adipocyte size but increased their number in in vivo models of obesity [49]. This is far more relevant considering that the age-related changes in adipose tissue lipid storage may lead to the proliferation of adipocytes in order to sustain lipid accumulation, making more difficult the loss of adipose tissue in elder patients [49]. In fact, the adipose tissue expansion by adipocyte proliferation has been characterized to be feasible for promoting obesity development [50] and magnesium levels appear to modulate this adipocyte proliferation.

Overall, hypomagnesemia can contribute to the development of obesity, whereas supplementation with the Mg^{2+} cation appears to prevent and reduce obesity prevalence by targeting inflammation and adipocyte proliferation (Figure 2).

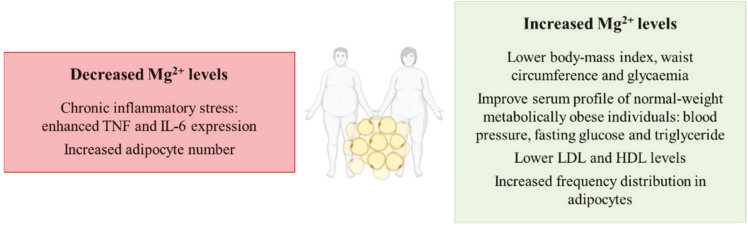

Figure 2. Schematic representation of the contribution of decreased and increased magnesium levels to the development of overweight or obesity. Abbreviations: TNF: tumor necrosis factor; IL-6: interleukin-6; LDL: low-density lipoprotein; HDL: high-density lipoprotein.

2.3. Magnesium in Insulin Resistance and Type 2 Diabetes Mellitus

Insulin Resistance (IR) and type 2 Diabetes mellitus (T2DM) constitute together with obesity the main worldwide global epidemics, termed "diabesity". Whereas the prevalence rates of IR syndrome have been reported to be 3–16%, with a higher incidence in white populations, the global prevalence of T2DM has been estimated to be 6.3% of the world's population, being higher in elder patients [51]. IR is primarily an acquired condition related to an excessive body fat, being characterized by a deficient response to insulin leading to the reduction of glucose incorporation in the liver, adipose tissue and muscle. Therefore, glucose levels in serum increase and the pancreas synthesizes more insulin in order to overcome this perturbation. IR precedes the development of T2DM by 10–15 years of chronicity, in the case of a persistent hyperglycemia and an impaired insulin secretion [52]. The elevated levels of endogenous insulin are associated with IR and results in weight gain, which exacerbates IR in turn, fueling a vicious cycle that persists, with pancreatic β-cells that cannot meet the insulin demand. Furthermore, the deficient glucose incorporation by the three aforementioned tissues (adipose tissue, liver and muscle) has an impact in promoting hepatic gluconeogenesis through the impaired insulin secretion [52]. Likewise, this promotes DNL, contributing to steatosis development and blunting hepatic homeostasis.

Hypomagnesemia in both IR and T2DM patients has been described, as they often show not only a reduced intake of the cation but they also present an augmented urinary loss [22,53]. As mentioned earlier, urinary excretion of magnesium by the kidneys is very pertinent, and both hyperglycemia and hyperinsulinemia in T2DM increase urinary excretion and decrease tubular Mg^{2+} reabsorption [54]. T2DM patients in particular have also been characterized to present alterations in the status of the cation, especially in poorly controlled glycemic patients [55]. For instance, it has been estimated that around 50% of T2DM patients suffer from hypomagnesemia [56]. Related to this, more elevated glycated hemoglobin levels, as a marker of chronic T2DM development, are frequently observed in those elder patients that are more prone to suffer from hypomagnesemia [23]. The development of hepatic nephropathy as a T2DM-derived complication is also promoted under hypomagnesemia conditions [57]. Related to the molecular mechanisms that connect

magnesium and the development of IR/T2DM, the cation plays a role as a co-factor in the phosphatidylinositol-3-kinase/protein kinase B (PI3K/AKT) pathway by which insulin exerts its role in peripheral tissues [58]. The transition from a transient IR stage to T2DM development might imply hypomagnesemia as a potential mediator, as Mg^{2+} deficiencies have been reported to alter the pancreatic insulin recreation by disrupting the normal activity of β-cells [59]. In β-cells, the insulin secretion is mainly controlled by the GLUT2/glucokinase (GK) tandem that acts as a glucose sensor and Mg^{2+} directly affects the GK activity [56]. Thus, hypomagnesemia impacts the ATP-sensitive K^+ (KATP) channels that depolarize the β-cell membrane for the insulin release, leading to an uncontrolled insulin secretion [59]. Furthermore, hypomagnesemia may also reduce insulin sensitivity by promoting oxidative stress and/or inflammation as free radicals are often increased in T2DM [60] and pro-inflammatory cytokines such as IL-6 decrease the expression of GLUT4 and the activity of the PI3K pathway responsible in insulin-mediated signaling [61]. Remarkably, the effect of Mg^{2+} perturbations over insulin resistance development has been reported to be reversible, so that the recovery of normal levels of the cation could solve the pathology [62]. In this context, Mg^{2+} supplementation shows a significant improvement in plasma glucose, lipoprotein and triglycerides profile and BP in diabetic patients [63].

Therefore, as summarized in Figure 3, a depletion of magnesium, favored by the reduced intake as well as its continuous excretion by the urinary system together with a decreased reabsorption, may contribute to IR and T2DM development. On the contrary, the supplementation of the cation has been shown to exert a protective effect both on IR and T2DM.

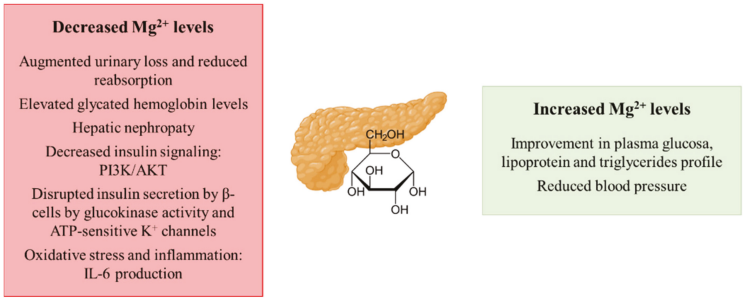

Figure 3. Schematic representation of the contribution of decreased and increased magnesium levels to the development of insulin resistance and type 2 diabetes mellitus. Abbreviations: PI3K: phosphatidylinositol-3-kinase; AKT: protein kinase B.

2.4. Magnesium in Hypertension and Cardiovascular Diseases (CVD)

Hypertension is a growing health concern that over a decade ago was already estimated to affect around 31.1% of the global population (1.39 billion patients) [64]. This condition is characterized by an elevated BP and can be caused by many risk factors, such as high sodium intake, low potassium intake, obesity, alcoholic consumption, physical inactivity and an unhealthy diet [64]. Hypertension can be classified into stage 1 and stage 2 hypertension if systolic pressure is between 130–140, or higher than 140, respectively. Interestingly, elevated glucose levels caused either by IR or T2DM are also a risk factor of developing this condition [65]. Apart from being a major public health problem, hypertension is a major risk factor for the development of CVDs as it promotes left ventricular hypertrophy [66]. CVDs are by far the leading cause of death in the world, with 17.9 million deaths in 2015, which is expected to be at 22.2 million deaths by 2030 [67]. Concerning the different alterations that comprise the spectrum of CVDs, the most relevant are coronary artery disease, cerebrovascular disease, peripheral artery disease and aortic atherosclerosis [68]. Similar to hypertension, unhealthy lifestyle habits such as smoking, alcohol consumption and dietary

imbalances highly increase the risk of developing CVDs [69]. Moreover, cardiovascular mortality is the most important cause of metabolic syndrome-related deaths.

Regarding the involvement of magnesium perturbations in the development of hypertension and cardiovascular diseases, there are several works than point out a relationship between the two conditions. Similar to the other conditions previously mentioned, the supplementation of the cation reduces BP in case of IR, pre-T2DM and other non-communicable chronic diseases [70]. Remarkably, a higher effect is observed in those patients with the most elevated BP [71]. Additionally, Mg^{2+} deficiencies are related to a reduction in endothelial functionality, a risk factor for atherosclerosis [24,72], while the supplementation regulates vascular tone and calcification, preventing atherogenesis and thrombosis development [73]. The cation is essential for many physiological, biochemical and cellular processes that regulate cardiovascular function, modulating vascular smooth muscle tone and the endothelial function [24]. Investigators also have characterized that Mg^{2+} plays a role in the proliferation and migration of endothelial and vascular muscle cells, the modulation of neuronal excitation and intracardiac conduction, as well as the myocardial contraction [73]. During cardiac potential, Mg^{2+} plays a role in the depolarization–repolarization processes, in that Mg^{2+} depletion alters electrocardiogram activity [74]. Low serum levels of the cation are related to increased atherosclerosis, coronary artery disease, arrhythmias and heart failure [73]. Correlated to this, lower intracellular levels of Mg^{2+} in skeletal muscle are related to aortic distensibility [75] and the appearance of arrhythmias [76]. The cation has been also reported to be essential for maintaining cell membrane potential, mitochondrial integrity from cardiomyocytes and to play a role in anti-oxidative pathways. [77]. Patients with T2DM that show perturbations in Mg^{2+} levels show alterations in echocardiographic indices and increased heart volume [78]. Similar to other studies in obese, IR or T2DM patients, the supplementation of Mg^{2+} in patients with CVD has also been reported to exert a protective role [77]. Houston and colleagues characterized that Mg^{2+} acts as a calcium channel blocker, increasing the production of nitric oxide (NO), improving endothelial dysfunction and inducing vasodilatation [79]. Additionally, scientific evidence highlights the relationship between Mg^{2+} deficiencies and an elevated risk of stroke [24]. Regarding the mechanisms that contribute to the aforementioned processes related to hypomagnesemia, the development of oxidative and inflammatory stress is of relevance [22], together with the contribution of the lipid profile and the increased susceptibility of lipoproteins to peroxidation [80]

Overall, magnesium appears to play a role in the development of CVDs as deficiencies in the cation are related to atherogenesis and perturbations in skeletal muscle functionality (Figure 4).

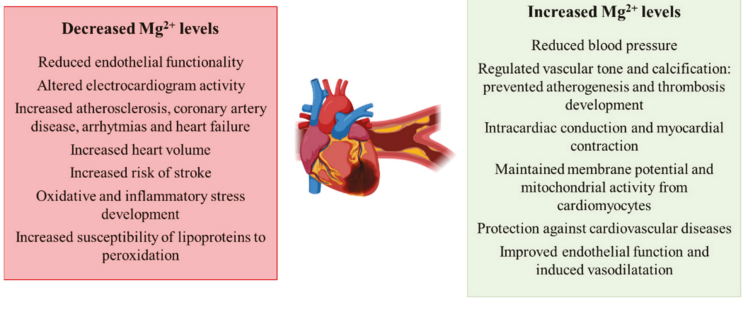

Figure 4. Schematic representation of the contribution of decreased and increased magnesium levels to the development of hypertension and cardiovascular diseases.

3. Discussion

Between the systemic complications that normally accompany NASH development, obesity, IR and TD2M, hypertension and CVDs are the most common and relevant [3].

Indeed, it is evident that a relationship exists among all of them, as the development of one pathology is often accompanied by another. The development of NASH is frequently the consequence of a chronic overweight or obese state, whereas the metabolic disorders' consequence of obesity lead to dysregulations that disturb glucose homeostasis, leading to IR or T2DM. In the meantime, elevated glucose levels in serum are also another cause of hypertension, where dysregulations in lipid metabolism lead to atherogenesis and promote the development of CVDs. In such an environment, the existence of an oxidative and inflammatory stress condition contributes to the development or aggravation of all aforementioned pathologies. Related to this, the role of Mg^{2+} deficiencies has been widely characterized.

Although NASH and related pathologies have their own specific complications, studies about the role of magnesium point in the same direction. Low magnesium concentrations have been related to many liver pathologies as cirrhosis, liver cancer or alcoholic liver disease. Moreover, hypomagnesemia is related to the development of a higher BMI—characteristic of obesity development—a higher risk of developing T2DM, and the development of atherogenesis and alterations in the cardiac muscle that lead to CVDs. Indeed, in the case of the pancreas, the cation has been characterized to play a role in insulin secretion by β-cells so that the loss of Mg^{2+} could contribute to the transition from IR to T2DM [59] and, in the meantime, decrease the insulin response from peripheral tissues [61]. Cardiomyocytes and endothelial cells in the cardiovascular system also require the cation for their correct functioning [77,79]. Another common feature of the cation in all of the conditions is the fact that the supplementation of the subjects, either in vivo or in clinical samples, prevents the development of such conditions. It must be mentioned that the role of the cation in NASH development has not been totally elucidated to date. However, the supplementation of the cation reduces the risk of liver-related death [25] so a positive effect is expected. Similarly, such supplementation also exerts a protective role over obesity, IR or T2DM and CVD development. Herein, the aforementioned role of Mg^{2+} in the prevention of oxidative and inflammatory stress could be a common mechanism. Moreover, considering the impact of mitochondrial dysfunction in the NASH-related comorbidities, other potential underlying mechanisms include the role of magnesium in the regulation of mitochondrial function. Finally, as the Mg^{2+} content can influence Ca^{2+} levels, and, for example, it has been shown that T2DM may cause endothelial dysfunction by remodeling the intracellular Ca^{2+} toolkit [81], this mechanism should be taken into account when investigating the protective roles of Mg^{2+} in IR, T2DM, CVD, and other NASH-related comorbidities.

On the one hand, considering the preventive role of the supplementation of Mg^{2+}, the encouragement of the global population by health authorities to increase their nutritional intake of Mg^{2+} may reduce the prevalence of the pathologies mentioned in the present work. This can be achieved either by supplementation or by promoting the consumption of magnesium-rich food, such as green vegetables, nuts, seeds and unprocessed cereals [82]. Considering the information from NHANES that reveals that 79% of the adult population does not fulfill the DRI of 300–400 mg/day, this is a key point that preventive actions should focus on [18]. The potential effectivity of magnesium supplementation may be a research topic of interest towards the development of therapies. Thus, it would be interesting to evaluate its properties in either preclinical or clinical studies.

On the other hand, the physicochemical properties of the cation make essential the activity of Mg^{2+} transporters that allow its flux across cell membranes participating in the processes of intake, excretion and reabsorption [83]. In this aspect, although several transporters such as the cyclin M family (CNNM), magnesium transporter 1 (MagT1), MRS2 or the solute carrier family 41 (SLC41) have been characterized [84–86], their potential role in the development of NASH and related comorbidities remains largely unknown. CNNMs have been associated with a number of genetic diseases affecting ion flux and cancer development via their association with phosphatases of regenerating liver (PRL) [87], whereas deficiencies in MagT1 have been linked to immunodeficiencies [88]. Otherwise,

mutations in MRS2 have been linked to demyelination [89] and SLC41 are related to abnormal locomotor functioning [90]. Related to the role of perturbations of Mg^{2+} homeostasis in the development of several diseases in which immune responses or essential biological processes are altered, the role of these proteins might be a research topic of interest for therapy development against NASH or related morbidities.

Funding: This work was supported by grants from the Ministerio de Ciencia y Innovación, Gobierno España: SAF2017-87301-R and RTI2018-096759-A-100 integrado en el Plan Estatal de Investigación Científica y Técnica y Innovación, cofinanciado con Fondos FEDER (to M.L.M.-C. and T.C.D., respectively); La Caixa Foundation Program (to M.L.M.-C), Fundacion BBVA UMBRELLA project (to M.L.M.-C), Programa Retos RTC2019-007125-1 (to M.L.M.-C., J.S.), Proyectos Investigacion en Salud DTS20/00138 (to M.L.M.-C., J.S.)Asociación Española contra el Cáncer (T.C.D.) and grants from the Spanish Ministry of Economy and Competitiveness BFU2016-77408-R and (MINECO/FEDER, UE) MICINN CONSOLIDER-INGENIO 2010 Program [grant number CSD2008-00005], ERA-Net E-Rare EJP RD Joint Transnational Call for Rare Diseases FIGHT-CNNM2 (EJPRD19-040) and from Instituto Carlos III, Spain (REF G95229142) to L.A.M-C. Ciberehd_ISCIII_MINECO is funded by the Instituto de Salud Carlos III. We thank MINECO for the Severo Ochoa Excellence Accreditation to CIC bioGUNE (SEV-2016-0644).

Institutional Review Board Statement: Not Applicable.

Informed Consent Statement: Not Applicable.

Data Availability Statement: Not Applicable.

Conflicts of Interest: The authors declare no conflict of interest.

References

1. Marra, F.; Lotersztajn, S. Pathophysiology of NASH: Perspectives for a targeted treatment. *Curr. Pharm. Des.* **2013**, *19*, 5250–5269. [CrossRef]
2. Simon, J.; Ouro, A.; Ala-Ibanibo, L.; Presa, N.; Delgado, T.C.; Martínez-Chantar, M.L. Sphingolipids in non-alcoholic fatty liver disease and hepatocellular carcinoma: Ceramide turnover. *Int. J. Mol. Sci.* **2020**, *21*, 40. [CrossRef] [PubMed]
3. Younossi, Z.; Anstee, Q.M.; Marietti, M.; Hardy, T.; Henry, L.; Eslam, M.; George, J.; Bugianesi, E. Global burden of NAFLD and NASH: Trends, predictions, risk factors and prevention. *Nat. Rev. Gastroenterol. Hepatol.* **2018**, *15*, 11–20. [CrossRef] [PubMed]
4. Mishra, A.; Younossi, Z.M. Epidemiology and Natural History of Non-alcoholic Fatty Liver Disease. *J. Clin. Exp. Hepatol.* **2012**, *2*, 135–144. [CrossRef]
5. Bertot, L.C.; Adams, L.A. Trends in hepatocellular carcinoma due to non-alcoholic fatty liver disease. *Expert Rev. Gastroenterol. Hepatol.* **2019**, *13*, 179–187. [CrossRef]
6. Wong, S.-W.; Ting, Y.-W.; Chan, W.-K. Epidemiology of non-alcoholic fatty liver disease-related hepatocellular carcinoma and its implications. *JGH Open Open Access J. Gastroenterol. Hepatol.* **2018**, *2*, 235–241. [CrossRef] [PubMed]
7. Mittal, S.; El-Serag, H.B. Epidemiology of hepatocellular carcinoma: Consider the population. *J. Clin. Gastroenterol.* **2013**, *47*, S2–S6. [CrossRef]
8. Simon, J.; Nuñez-García, M.; Fernández-Tussy, P.; Barbier-Torres, L.; Fernández-Ramos, D.; Gómez-Santos, B.; Buqué, X.; Lopitz-Otsoa, F.; Goikoetxea-Usandizaga, N.; Serrano-Macia, M.; et al. Targeting Hepatic Glutaminase 1 Ameliorates Non-alcoholic Steatohepatitis by Restoring Very-Low-Density Lipoprotein Triglyceride Assembly. *Cell Metab.* **2020**, *31*, 605–622. [CrossRef]
9. Fernando, D.H.; Forbes, J.M.; Angus, P.W.; Herath, C.B. Development and Progression of Non-Alcoholic Fatty Liver Disease: The Role of Advanced Glycation End Products. *Int. J. Mol. Sci.* **2019**, *20*, 5037. [CrossRef]
10. Friedman, S.L. Reversibility of hepatic fibrosis and cirrhosis—Is it all hype? *Nat. Clin. Pract. Gastroenterol. Hepatol.* **2007**, *4*, 236–237. [CrossRef]
11. Canbay, A.; Friedman, S.; Gores, G.J. Apoptosis: The Nexus of Liver Injury and Fibrosis. *Hepatology* **2004**, *39*, 273–278. [CrossRef]
12. Canbay, A.; Feldstein, A.E.; Higuchi, H.; Werneburg, N.; Grambihler, A.; Bronk, S.F.; Gores, G.J. Kupffer Cell Engulfment of Apoptotic Bodies Stimulates Death Ligand and Cytokine Expression. *Hepatology* **2003**, *38*, 1188–1198. [CrossRef] [PubMed]
13. Mederacke, I.; Hsu, C.C.; Troeger, J.S.; Huebener, P.; Mu, X.; Dapito, D.H.; Pradere, J.; Schwabe, R.F. Fate-tracing reveals hepatic stellate cells as dominant contributors to liver fibrosis independent of its etiology. *Nat. Commun.* **2013**, *4*, 2823. [CrossRef] [PubMed]
14. Hallsworth, K.; Adams, L.A. Lifestyle modification in NAFLD/NASH: Facts and figures. *JHEP Rep. Innov. Hepatol.* **2019**, *1*, 468–479. [CrossRef] [PubMed]
15. Paglialunga, S.; Dehn, C.A. Clinical assessment of hepatic de novo lipogenesis in non-alcoholic fatty liver disease. *Lipids Health Dis.* **2016**, *15*, 159. [CrossRef]
16. Chooi, Y.C.; Ding, C.; Magkos, F. The epidemiology of obesity. *Metabolism* **2019**, *92*, 6–10. [CrossRef]

17. Greger, J.L.; Baligar, P.; Abernathy, R.P.; Bennett, O.A.; Peterson, T. Calcium, magnesium, phosphorus, copper, and manganese balance in adolescent females. *Am. J. Clin. Nutr.* **1978**, *31*, 117–121. [CrossRef]
18. Ervin, R.B.; Wang, C.-Y.; Wright, J.D.; Kennedy-Stephenson, J. Dietary intake of selected minerals for the United States population: 1999–2000. *Adv. Data* **2004**, 1–5.
19. Aikawa, J.K. *Magnesium: Its Biologic Significance*; CRC Series on Cations of Biological Significance; CRC Press: Boca Raton, FL, USA, 1981; Volume 1, ISBN 084935871X.
20. Swaminathan, R. Magnesium metabolism and its disorders. *Clin. Biochem. Rev.* **2003**, *24*, 47–66.
21. Liu, M.; Dudley, S.C., Jr. Magnesium, Oxidative Stress, Inflammation, and Cardiovascular Disease. *Antioxidants* **2020**, *9*, 907.
22. Barbagallo, M.; Dominguez, L.J.; Galioto, A.; Ferlisi, A.; Cani, C.; Malfa, L.; Pineo, A.; Busardo', A.; Paolisso, G. Role of magnesium in insulin action, diabetes and cardio-metabolic syndrome X. *Mol. Asp. Med.* **2003**, *24*, 39–52. [CrossRef]
23. Barbagallo, M.; Di Bella, G.; Brucato, V.; D'Angelo, D.; Damiani, P.; Monteverde, A.; Belvedere, M.; Dominguez, L.J. Serum ionized magnesium in diabetic older persons. *Metabolism* **2014**, *63*, 502–509. [CrossRef] [PubMed]
24. Rosique-Esteban, N.; Guasch-Ferré, M.; Hernández-Alonso, P.; Salas-Salvadó, J. Dietary Magnesium and Cardiovascular Disease: A Review with Emphasis in Epidemiological Studies. *Nutrients* **2018**, *10*, 168. [CrossRef] [PubMed]
25. Wu, L.; Zhu, X.; Fan, L.; Kabagambe, E.K.; Song, Y.; Tao, M.; Zhong, X.; Hou, L.; Shrubsole, M.J.; Liu, J.; et al. Magnesium intake and mortality due to liver diseases: Results from the Third National Health and Nutrition Examination Survey Cohort. *Sci. Rep.* **2017**, *7*, 17913. [CrossRef]
26. Liu, M.; Yang, H.; Mao, Y. Magnesium and liver disease. *Ann. Transl. Med.* **2019**, *7*, 578. [CrossRef]
27. Rayssiguier, Y.; Chevalier, F.; Bonnet, M.; Kopp, J.; Durlach, J. Influence of magnesium deficiency on liver collagen after carbon tetrachloride or ethanol administration to rats. *J. Nutr.* **1985**, *115*, 1656–1662. [CrossRef]
28. Panov, A.; Scarpa, A. Mg^{2+} control of respiration in isolated rat liver mitochondria. *Biochemistry* **1996**, *35*, 12849–12856. [CrossRef]
29. Konno, Y.; Ohno, S.; Akita, Y.; Kawasaki, H.; Suzuki, K. Enzymatic properties of a novel phorbol ester receptor/protein kinase, nPKC. *J. Biochem.* **1989**, *106*, 673–678. [CrossRef]
30. Malpuech-Brugère, C.; Nowacki, W.; Daveau, M.; Gueux, E.; Linard, C.; Rock, E.; Lebreton, J.; Mazur, A.; Rayssiguier, Y. Inflammatory response following acute magnesium deficiency in the rat. *Biochim. Biophys. Acta* **2000**, *1501*, 91–98. [CrossRef]
31. Paik, Y.H.; Yoon, Y.J.; Lee, H.C.; Jung, M.K.; Kang, S.H.; Chung, S.I.; Kim, J.K.; Cho, J.Y.; Lee, K.S.; Han, K.H. Antifibrotic effects of magnesium lithospermate B on hepatic stellate cells and thioacetamide-induced cirrhotic rats. *Exp. Mol. Med.* **2011**, *43*, 341–349. [CrossRef]
32. Frick, D.N.; Banik, S.; Rypma, R.S. Role of divalent metal cations in ATP hydrolysis catalyzed by the hepatitis C virus NS3 helicase: Magnesium provides a bridge for ATP to fuel unwinding. *J. Mol. Biol.* **2007**, *365*, 1017–1032. [CrossRef] [PubMed]
33. Blaszczyk, U.; Duda-Chodak, A. Magnesium: Its role in nutrition and carcinogenesis. *Rocz. Panstw. Zakl. Hig.* **2013**, *64*, 165–171. [PubMed]
34. Liu, Y.; Li, X.; Zou, Q.; Liu, L.; Zhu, X.; Jia, Q.; Wang, L.; Yan, R. Inhibitory effect of magnesium cantharidate on human hepatoma SMMC-7721 cell proliferation by blocking MAPK signaling pathway. *Chin. J. Cell. Mol. Immunol.* **2017**, *33*, 347–351.
35. Adachi, M.; Brenner, D.A. Clinical syndromes of alcoholic liver disease. *Dig. Dis.* **2005**, *23*, 255–263. [CrossRef] [PubMed]
36. Adachi, M.; Ishii, H. Role of mitochondria in alcoholic liver injury. *Free Radic. Biol. Med.* **2002**, *32*, 487–491. [CrossRef]
37. Weiskirchen, R.; Tacke, F. Cellular and molecular functions of hepatic stellate cells in inflammatory responses and liver immunology. *Hepatobiliary Surg. Nutr.* **2014**, *3*, 344–363.
38. Poikolainen, K.; Alho, H. Magnesium treatment in alcoholics: A randomized clinical trial. *Subst. Abus. Treat. Prev. Policy* **2008**, *3*, 1. [CrossRef]
39. Hruby, A.; Hu, F.B. The Epidemiology of Obesity: A Big Picture. *Pharmacoeconomics* **2015**, *33*, 673–689. [CrossRef]
40. Portillo-Sanchez, P.; Bril, F.; Maximos, M.; Lomonaco, R.; Biernacki, D.; Orsak, B.; Subbarayan, S.; Webb, A.; Hecht, J.; Cusi, K. High Prevalence of Nonalcoholic Fatty Liver Disease in Patients With Type 2 Diabetes Mellitus and Normal Plasma Aminotransferase Levels. *J. Clin. Endocrinol. Metab.* **2015**, *100*, 2231–2238. [CrossRef]
41. Shamnani, G.; Rukadikar, C.; Gupta, V.; Singh, S.; Tiwari, S.; Bhartiy, S.; Sharma, P. Serum magnesium in relation with obesity. *Natl. J. Physiol. Pharm. Pharmacol.* **2018**, *8*, 1. [CrossRef]
42. Castellanos-Gutiérrez, A.; Sánchez-Pimienta, T.G.; Carriquiry, A.; da Costa, T.H.M.; Ariza, A.C. Higher dietary magnesium intake is associated with lower body mass index, waist circumference and serum glucose in Mexican adults. *Nutr. J.* **2018**, *17*, 114. [CrossRef] [PubMed]
43. Rodríguez-Moran, M.; Guerrero-Romero, F. Oral magnesium supplementation improves the metabolic profile of metabolically obese, normal-weight individuals: A randomized double-blind placebo-controlled trial. *Arch. Med. Res.* **2014**, *45*, 388–393. [CrossRef] [PubMed]
44. Nielsen, F.H. Magnesium, inflammation, and obesity in chronic disease. *Nutr. Rev.* **2010**, *68*, 333–340. [CrossRef] [PubMed]
45. Kurstjens, S.; van Diepen, J.A.; Overmars-Bos, C.; Alkema, W.; Bindels, R.J.M.; Ashcroft, F.M.; Tack, C.J.J.; Hoenderop, J.G.J.; de Baaij, J.H.F. Magnesium deficiency prevents high-fat-diet-induced obesity in mice. *Diabetologia* **2018**, *61*, 2030–2042. [CrossRef]
46. de Leeuw, I.H.; van Gaal, L.; Vanroelen, W. Magnesium and obesity: Effects of treatment on magnesium and other parameters. *Magnesium* **1987**, *6*, 40–47. [PubMed]

47. Simental-Mendía, L.E.; Simental-Mendía, M.; Sahebkar, A.; Rodríguez-Morán, M.; Guerrero-Romero, F. Effect of magnesium supplementation on lipid profile: A systematic review and meta-analysis of randomized controlled trials. *Eur. J. Clin. Pharmacol.* **2017**, *73*, 525–536. [CrossRef]
48. Mohamed-Ali, V.; Pinkney, J.H.; Coppack, S.W. Adipose tissue as an endocrine and paracrine organ. *Int. J. Obes.* **1998**, *22*, 1145–1158. [CrossRef]
49. Devaux, S.; Adrian, M.; Laurant, P.; Berthelot, A.; Quignard-Boulangé, A. Dietary magnesium intake alters age-related changes in rat adipose tissue cellularity. *Magnes. Res.* **2016**, *29*, 175–183. [CrossRef]
50. Antonopoulos, A.S.; Tousoulis, D. The molecular mechanisms of obesity paradox. *Cardiovasc. Res.* **2017**, *113*, 1074–1086. [CrossRef]
51. Khan, M.A.B.; Hashim, M.J.; King, J.K.; Govender, R.D.; Mustafa, H.; Al Kaabi, J. Epidemiology of Type 2 Diabetes—Global Burden of Disease and Forecasted Trends. *J. Epidemiol. Glob. Health* **2020**, *10*, 107–111. [CrossRef]
52. Zheng, Y.; Ley, S.H.; Hu, F.B. Global aetiology and epidemiology of type 2 diabetes mellitus and its complications. *Nat. Rev. Endocrinol.* **2018**, *14*, 88–98. [CrossRef] [PubMed]
53. Walti, M.K.; Zimmermann, M.B.; Walczyk, T.; Spinas, G.A.; Hurrell, R.F. Measurement of magnesium absorption and retention in type 2 diabetic patients with the use of stable isotopes. *Am. J. Clin. Nutr.* **2003**, *78*, 448–453. [CrossRef] [PubMed]
54. McNair, P.; Christensen, M.S.; Christiansen, C.; Madsbad, S.; Transbøl, I. Renal hypomagnesaemia in human diabetes mellitus: Its relation to glucose homeostasis. *Eur. J. Clin. Investig.* **1982**, *12*, 81–85. [CrossRef] [PubMed]
55. Mather, H.M.; Levin, G.E. Magnesium status in diabetes. *Lancet* **1979**, *1*, 924. [CrossRef]
56. Gommers, L.M.M.; Hoenderop, J.G.J.; Bindels, R.J.M.; de Baaij, J.H.F. Hypomagnesemia in Type 2 Diabetes: A Vicious Circle? *Diabetes* **2016**, *65*, 3–13. [CrossRef] [PubMed]
57. Tin, A.; Grams, M.E.; Maruthur, N.M.; Astor, B.C.; Couper, D.; Mosley, T.H.; Selvin, E.; Coresh, J.; Kao, W.H.L. Results from the Atherosclerosis Risk in Communities study suggest that low serum magnesium is associated with incident kidney disease. *Kidney Int.* **2015**, *87*, 820–827. [CrossRef]
58. Gutierrez-Rodelo, C.; Roura-Guiberna, A.; Olivares-Reyes, J.A. Molecular Mechanisms of Insulin Resistance: An Update. *Gac. Med. Mex.* **2017**, *153*, 214–228.
59. Kostov, K. Effects of Magnesium Deficiency on Mechanisms of Insulin Resistance in Type 2 Diabetes: Focusing on the Processes of Insulin Secretion and Signaling. *Int. J. Mol. Sci.* **2019**, *20*, 1351. [CrossRef]
60. Barbagallo, M.; Dominguez, L.J. Magnesium and aging. *Curr. Pharm. Des.* **2010**, *16*, 832–839. [CrossRef]
61. Chen, L.; Chen, R.; Wang, H.; Liang, F. Mechanisms Linking Inflammation to Insulin Resistance. *Int. J. Endocrinol.* **2015**, *2015*, 508409. [CrossRef]
62. Kandeel, F.R.; Balon, E.; Scott, S.; Nadler, J.L. Magnesium deficiency and glucose metabolism in rat adipocytes. *Metabolism* **1996**, *45*, 838–843. [CrossRef]
63. Verma, H.; Garg, R. Effect of magnesium supplementation on type 2 diabetes associated cardiovascular risk factors: A systematic review and meta-analysis. *J. Hum. Nutr. Diet. Off. J. Br. Diet. Assoc.* **2017**, *30*, 621–633. [CrossRef]
64. Mills, K.T.; Stefanescu, A.; He, J. The global epidemiology of hypertension. *Nat. Rev. Nephrol.* **2020**, *16*, 223–237. [CrossRef] [PubMed]
65. Saklayen, M.G. The Global Epidemic of the Metabolic Syndrome. *Curr. Hypertens. Rep.* **2018**, *20*, 12. [CrossRef] [PubMed]
66. Singh, S.; Shankar, R.; Singh, G.P. Prevalence and Associated Risk Factors of Hypertension: A Cross-Sectional Study in Urban Varanasi. *Int. J. Hypertens.* **2017**, *2017*, 5491838. [CrossRef]
67. Ruan, Y.; Guo, Y.; Zheng, Y.; Huang, Z.; Sun, S.; Kowal, P.; Shi, Y.; Wu, F. Cardiovascular disease (CVD) and associated risk factors among older adults in six low-and middle-income countries: Results from SAGE Wave 1. *BMC Public Health* **2018**, *18*, 778. [CrossRef]
68. Benjamin, E.J.; Virani, S.S.; Callaway, C.W.; Chamberlain, A.M.; Chang, A.R.; Cheng, S.; Chiuve, S.E.; Cushman, M.; Delling, F.N.; Deo, R.; et al. Heart Disease and Stroke Statistics-2018 Update: A Report From the American Heart Association. *Circulation* **2018**, *137*, e67–e492. [CrossRef]
69. Hinton, W.; McGovern, A.; Coyle, R.; Han, T.S.; Sharma, P.; Correa, A.; Ferreira, F.; de Lusignan, S. Incidence and prevalence of cardiovascular disease in English primary care: A cross-sectional and follow-up study of the Royal College of General Practitioners (RCGP) Research and Surveillance Centre (RSC). *BMJ Open* **2018**, *8*, e020282. [CrossRef]
70. Dibaba, D.T.; Xun, P.; Song, Y.; Rosanoff, A.; Shechter, M.; He, K. The effect of magnesium supplementation on blood pressure in individuals with insulin resistance, prediabetes, or noncommunicable chronic diseases: A meta-analysis of randomized controlled trials. *Am. J. Clin. Nutr.* **2017**, *106*, 921–929. [CrossRef]
71. Kawano, Y.; Matsuoka, H.; Takishita, S.; Omae, T. Effects of magnesium supplementation in hypertensive patients: Assessment by office, home, and ambulatory blood pressures. *Hypertension* **1998**, *32*, 260–265. [CrossRef]
72. Nguyen, H.; Odelola, O.A.; Rangaswami, J.; Amanullah, A. A review of nutritional factors in hypertension management. *Int. J. Hypertens.* **2013**, *2013*, 698940. [CrossRef] [PubMed]
73. Tangvoraphonkchai, K.; Davenport, A. Magnesium and Cardiovascular Disease. *Adv. Chronic Kidney Dis.* **2018**, *25*, 251–260. [CrossRef] [PubMed]
74. Efstratiadis, G.; Sarigianni, M.; Gougourelas, I. Hypomagnesemia and cardiovascular system. *Hippokratia* **2006**, *10*, 147–152. [PubMed]

75. Resnick, L.M.; Militianu, D.; Cunnings, A.J.; Pipe, J.G.; Evelhoch, J.L.; Soulen, R.L. Direct magnetic resonance determination of aortic distensibility in essential hypertension: Relation to age, abdominal visceral fat, and in situ intracellular free magnesium. *Hypertension* **1997**, *30*, 654–659. [CrossRef] [PubMed]
76. Del Gobbo, L.C.; Song, Y.; Poirier, P.; Dewailly, E.; Elin, R.J.; Egeland, G.M. Low serum magnesium concentrations are associated with a high prevalence of premature ventricular complexes in obese adults with type 2 diabetes. *Cardiovasc. Diabetol.* **2012**, *11*, 23. [CrossRef] [PubMed]
77. DiNicolantonio, J.J.; Liu, J.; O'Keefe, J.H. Magnesium for the prevention and treatment of cardiovascular disease. *Open Heart* **2018**, *5*, e000775. [CrossRef]
78. Barbagallo, M.; Gupta, R.K.; Resnick, L.M. Cellular ions in NIDDM: Relation of calcium to hyperglycemia and cardiac mass. *Diabetes Care* **1996**, *19*, 1393–1398. [CrossRef]
79. Houston, M. The role of magnesium in hypertension and cardiovascular disease. *J. Clin. Hypertens.* **2011**, *13*, 843–847. [CrossRef]
80. Rayssiguier, Y.; Gueux, E.; Bussière, L.; Durlach, J.; Mazur, A. Dietary magnesium affects susceptibility of lipoproteins and tissues to peroxidation in rats. *J. Am. Coll. Nutr.* **1993**, *12*, 133–137. [CrossRef]
81. Berra-Romani, R.; Guzmán-Silva, A.; Vargaz-Guadarrama, A.; Flores-Alonso, J.C.; Alonso-Romero, J.; Treviño, S.; Sánchez-Gómez, J.; Coyotl-Santiago, N.; García-Carrasco, M.; Moccia, F. Type 2 Diabetes Alters Intracellular Ca(2+) Handling in Native Endothelium of Excised Rat Aorta. *Int. J. Mol. Sci.* **2019**, *21*, 250. [CrossRef]
82. Gröber, U.; Schmidt, J.; Kisters, K. Magnesium in Prevention and Therapy. *Nutrients* **2015**, *7*, 8199–8226. [CrossRef] [PubMed]
83. Jahnen-Dechent, W.; Ketteler, M. Magnesium basics. *Clin. Kidney J.* **2012**, *5*, i3–i14. [CrossRef] [PubMed]
84. Kolisek, M.; Zsurka, G.; Samaj, J.; Weghuber, J.; Schweyen, R.J.; Schweigel, M. Mrs2p is an essential component of the major electrophoretic Mg2+ influx system in mitochondria. *EMBO J.* **2003**, *22*, 1235–1244. [CrossRef]
85. Goytain, A.; Quamme, G.A. Identification and characterization of a novel mammalian Mg^{2+} transporter with channel-like properties. *BMC Genom.* **2005**, *6*, 48. [CrossRef] [PubMed]
86. Schlingmann, K.P.; Waldegger, S.; Konrad, M.; Chubanov, V.; Gudermann, T. TRPM6 and TRPM7-Gatekeepers of human magnesium metabolism. *Biochim. Biophys. Acta Mol. Basis Dis.* **2007**, *1772*, 813–821. [CrossRef]
87. Chen, Y.S.; Kozlov, G.; Fakih, R.; Funato, Y.; Miki, H.; Gehring, K. The cyclic nucleotide-binding homology domain of the integral membrane protein CNNM mediates dimerization and is required for Mg(2+) efflux activity. *J. Biol. Chem.* **2018**, *293*, 19998–20007. [CrossRef] [PubMed]
88. Matsuda-Lennikov, M.; Biancalana, M.; Zou, J.; Ravell, J.C.; Zheng, L.; Kanellopoulou, C.; Jiang, P.; Notarangelo, G.; Jing, H.; Masutani, E.; et al. Magnesium transporter 1 (MAGT1) deficiency causes selective defects in N-linked glycosylation and expression of immune-response genes. *J. Biol. Chem.* **2019**, *294*, 13638–13656. [CrossRef]
89. Kuramoto, T.; Kuwamura, M.; Tokuda, S.; Izawa, T.; Nakane, Y.; Kitada, K.; Akao, M.; Guénet, J.-L.; Serikawa, T. A mutation in the gene encoding mitochondrial Mg^{2}+ channel MRS2 results in demyelination in the rat. *PLoS Genet.* **2011**, *7*, e1001262. [CrossRef]
90. Fleig, A.; Schweigel-Röntgen, M.; Kolisek, M. Solute carrier family SLC41: What do we really know about it? *Wiley Interdiscip. Rev. Membr. Transp. Signal.* **2013**, *2*, 227–239. [CrossRef]

biomedicines

MDPI

Article

Dulaglutide Alone and in Combination with Empagliflozin Attenuate Inflammatory Pathways and Microbiome Dysbiosis in a Non-Diabetic Mouse Model of NASH

Katharina Luise Hupa-Breier [1,*], Janine Dywicki [1], Björn Hartleben [2], Freya Wellhöner [1], Benjamin Heidrich [1], Richard Taubert [1], Young-Seon Elisabeth Mederacke [1], Maren Lieber [1], Konstantinos Iordanidis [1], Michael P. Manns [1], Heiner Wedemeyer [1], Matthias Hardtke-Wolenski [1,3] and Elmar Jaeckel [1]

[1] Department of Gastroenterology, Hepatology and Endocrinology, Hannover Medical School, 30625 Hannover, Germany; janine.dywicki@gmx.de (J.D.); Wellhoener.Freya@mh-hannover.de (F.W.); heidrich.benjamin@mh-hannover.de (B.H.); taubert.richard@mh-hannover.de (R.T.); Mederacke.Young-Seon@mh-hannover.de (Y.S.M.); Lieber.Maren@mh-hannover.de (M.L.); Jordanidis.Konstantinos@mh-hannover.de (K.I.); Manns.Michael@mh-hannover.de (M.P.M.); Wedemeyer.heiner@mh-hannover.de (H.W.); matthias.hardtke-wolenski@uk-essen.de (M.H.-W.); Jaeckel.Elmar@mh-hannover.de (E.J.)

[2] Department of Pathology, Hannover Medical School, 30625 Hannover, Germany; hartleben.Bjoern@mh-hannover.de

[3] Department of Gastroenterology and Hepatology, Essen University Hospital, University Duisburg-Essen, 45147 Essen, Germany

* Correspondence: hupa.katharina@mh-hannover.de; Tel.: +49-(0)-511-532-6992

Citation: Hupa-Breier, K.L.; Dywicki, J.; Hartleben, B.; Wellhöner, F.; Heidrich, B.; Taubert, R.; Mederacke, Y.S.; Lieber, M.; Iordanidis, K.; Manns, M.P.; et al. Dulaglutide Alone and in Combination with Empagliflozin Attenuate Inflammatory Pathways and Microbiome Dysbiosis in a Non-Diabetic Mouse Model of NASH. *Biomedicines* **2021**, *9*, 353. https://doi.org/10.3390/biomedicines9040353

Academic Editor: Ronit Shiri-Sverdlov

Received: 8 February 2021
Accepted: 25 March 2021
Published: 30 March 2021

Publisher's Note: MDPI stays neutral with regard to jurisdictional claims in published maps and institutional affiliations.

Abstract: Dysregulation of glucose homeostasis plays a major role in the pathogenesis of non-alcoholic steatohepatitis (NASH) as it activates proinflammatory and profibrotic processes. Beneficial effects of antiglycemic treatments such as GLP-1 agonist or SGLT-2 inhibitor on NASH in patients with diabetes have already been investigated. However, their effect on NASH in a non-diabetic setting remains unclear. With this aim, we investigated the effect of long-acting GLP1-agonist dulaglutide and SGLT-2 inhibitor empagliflozin and their combination in a non-diabetic mouse model of NASH. C57BL/6 mice received a high-fat-high-fructose (HFHC) diet with a surplus of cholesterol for 16 weeks. After 12 weeks of diet, mice were treated with either dulaglutide, empagliflozin or their combination. Dulaglutide alone and in combination with empagliflozin led to significant weight loss, improved glucose homeostasis and diminished anti-inflammatory and anti-fibrotic pathways. Combination of dulaglutide and empagliflozin further decreased MoMFLy6C^{High} and CD4^{+}Foxp3^{+} T cells. No beneficial effects for treatment with empagliflozin alone could be shown. While no effect of dulaglutide or its combination with empaglifozin on hepatic steatosis was evident, these data demonstrate distinct anti-inflammatory effects of dulaglutide and their combination with empagliflozin in a non-diabetic background, which could have important implications for further treatment of NASH.

Keywords: liver disease; non-alcoholic steatohepatitis; GLP-1 agonist; SGLT-2 inhibitor; type 2 diabetes; innate immune system; adaptive immune system; metabolic syndrome

1. Introduction

Non-alcoholic fatty liver disease (NAFLD) is one of the most common liver diseases worldwide, which affects nearly 25% of the global adult population, and the incidence is even further increasing [1]. NAFLD includes non-alcoholic fatty liver (NAFL) as well as the more severe form, non-alcoholic steatohepatitis (NASH). A hallmark of both pathological states is the accumulation of fat in more than 5% of hepatocytes. In addition to steatosis, NASH includes also hepatocyte injury and inflammation, which can lead to end-stage liver cirrhosis and its associated complications [2]. Furthermore, NASH is a significant risk

factor for the development of hepatocellular carcinoma [3]. However, a majority of the patients are dying due to cardiovascular events, which might be explained in part by the specific pathogenesis of NASH [4].

The main risk factors for NASH are central obesity, dyslipidemia, insulin resistance and type 2 diabetes mellitus (T2DM). Therefore, it was recently proposed to change the nomenclature into "metabolic associated fatty liver disease" (MAFLD) [5].

Therapeutic options in patients with NASH are still rare, but urgently needed. Currently, loss of weight and physical activity are the only established therapeutic strategies [6]. As glucose homeostasis is an important driver in the pathogenesis of NASH, antiglycemic treatments such as GLP-1 agonists have already been successfully tested for treatment of NASH in diabetic patients. GLP-1 agonists stimulate glucose-dependent insulin secretion and suppress hepatic glucagon production. They further delay gastric emptying and decrease the appetite, therefore leading to weight loss [7]. Inhibitors of the sodium-glucose cotransporter 2 (SGLT-2) such as empagliflozin are the latest novel class of anti-diabetic drugs. By inhibition of the renal SGLT-2 transporter, they prevent glucose reabsorption and therefore improve the blood glucose level and reduce glucotoxicity [8]. Some studies could already show some short-term beneficial effects of the early SGLT-2- inhibitors in patients with diabetes and NASH [9]. The combination of both GLP-1 agonist and SGLT-2-inhibitor already showed remarkable improvements of the metabolic condition in the treatment of T2DM [8] and therefore seems to be a promising therapy concept for NASH and diabetes. However, there is insufficient evidence for both anti-diabetic agents and its combination regarding the effectiveness of NASH in a non-diabetic background and their distinct pathomechanism [10]. Therefore, further studies are urgently needed. To this end, we tested the new long-acting GLP-1 agonist dulaglutide and the SGLT-2 inhibitor empagliflozin alone or in combination in a mouse model of NASH.

2. Materials and Methods

2.1. In Vivo Animal Model

Animal care and all animal experiments were executed according to protocols approved by the animal welfare commission of the Hannover Medical School, local ethics Animal Review Board (Niedersaechsisches Landesamt für Verbraucherschutz und Lebensmittelsicherheit/LAVES, Oldenburg, Germany (protocol 13/1152, 12.06.2013 and protocol 17/2456, 27.06.2017) and in accordance with the ARRIVE guidelines.

We used 6–8-week-old C57BL/6HanJ Ztm mice. Animals were fed a high-fat-high-carbohydrate (HFHC) diet with a surplus of cholesterol (Ssniff EF R/M D12330 mod.*/surwit + 1% Cholesterol; Diet#: E15771-34, S3542-E005; Ssniff, Soest, Germany) with 45 g/L 55% Fructose/45% Sucrose (Sigma, Darmstadt, Germany) in the drinking water for 16 weeks. After 12 weeks of the diet, pharmacological treatment was started with either dulaglutide (10 nmol/kg, Eli Lilly, Bad Homburg, Germany) [11], empagliflozin (10 mg/kg, Boehringer Ingelheim, Ingelheim am Rhein, Germany)) [12], a combination of dulaglutide and empagliflozin or vehicle. Further details regarding the in vivo animal model are provided in the Supplementary Data.

2.2. Serum Analysis

After 16 weeks of HFHC diet, an intraperitoneal glucose-tolerance test (IPGTT) was performed. Further details are provided in the Supplementary Data. For serum analysis, blood samples were collected via a retro orbital withdrawal. Aspartate aminotransferase (AST) and alanine transaminase (ALT) were determined by photometric enzyme activity assays by the Olympus AU400 Chemistry Analyzer (OLY-AU400, Hamburg, Germany) using 40–50 µL of murine serum as described before [13].

2.3. Liver Triglycerides

Frozen liver was minced into pieces and homogenized in standard diluent (Cayman Chemical, Ann Arbour, Michigan, USA) with 20 µg/mL Leupeptin (Serva Electrophoresis

GmbH, Heidelberg, Germany) via a rod-homogenizer for 10–15 s. Homogenates were centrifuged at 4 °C for 10 min at 10,000× *g*. Supernatant was aliquoted for triglyceride and protein quantification. Colorimetric detection and quantitation of total protein was performed using the Pierce™ BCA Protein Assay Kit (Thermo Fisher Scientific Waltham, Waltham, MA, USA). Triglyceride in supernatant was detected via the Cobas® 8000 modular analyzer (HITACHI/Roche, Basel, Schweiz).

2.4. Histology

Murine liver was fixed in formalin and embedded in paraffin. Paraffin-embedded sections (2 µm) were stained with haematoxylin and eosin (H&E) for assessment of liver histology, with periodic-acid Schiff reaction (PAS) for assessment of glycogen accumulation and with silver for evaluation of fibrosis. Afterwards, they were graded with the NAFLD-activity score (NAS). In short, sections were graded for lobular inflammation, hepatocyte ballooning and steatosis [14]. Grading was done by a blinded pathologist, who is experienced in the scoring of human NASH. Histological images were acquisited with the ZEISS Imager.M1. -microscope (ZEISS, Oberkochen, Germany), ZEISS Plan.Apochromat (20 er/08 + 10/0,45) objective (ZEISS, Oberkochen, Germany) and ZEISS Axiocam 506 mono camera (ZEISS, Oberkochen, Germany). ZEISS ZEN v2.3. blue edition (2011) software (ZEISS, Oberkochen, Germany) was used for acquisition as well as for further image processing.

2.5. Flow Cytometry

Livers and spleens were perfused with PBS and dissected from mice. Organs were then minced using a nylon cell strainer (70 µm, BD Falcon, Franklin Lakes, NJ, USA) and washed with phosphate-buffered saline supplemented with 2% fetal calf serum. Afterwards, spleens were lysed in red blood cell lysis buffer (Sigma-Aldrich, Munich, Germany). Intrahepatic leucocytes and monocytes were isolated by using 40/70%- percoll density gradients (Percoll, GE Healthcare, Chicago, IL, USA). Subsequently, cells were stained with fluorochrome-conjugated antibodies for multicolor fluorescence-activated cell sorting (FACS) analysis. Detailed information about the antibodies used are provided in the Supplementary Data. All acquisitions were done with a LSRII SORP interfaced to DIVA software (BD Biosciences, San Jose, CA, USA).

2.6. Real-Time PCR

For real-time PCR, the TaqMan Gene Expression Assay was used. Please see the Supplementary Data for a detailed list of assays. For amplification, the PreAmp master Mix (Fluidigm, PN 1005580, South San Francisco, CA, USA) was used. Amplification was performed according to the manufacturer's guidelines. For PCR, the 48.48 Dynamic Array TM IFC, Assay loading reagent (Fluidigm, PN 85000736), GE Sample Loading Reagent (Fluidigm, PN 85000735, 85000746) and the Master Mix (TaqMan Gene Expression Master Mix, Applied Bioscience, PN 4369016, Thermofisher, Waltham, MA, USA) were used. RT-PCR was performed according to the manufacturer's guidelines.

2.7. Stool Analysis

Fresh stool was collected from every animal after 16 weeks of HFHC diet. For stool collection, mice were set into a clean plastic cage and fresh stool was collected and immediately put on dry ice. Afterwards, stool was stored at −80 °C until further preparation. DNA preparation and bioinformatic analyses were performed according to the methods described before [15]. Further details are listed in the Supplementary Data [16–19].

2.8. Statistics

Statistical analysis was performed with GraphPad Prism v5.0. The unpaired Student 2-tailed *t*-test with Welsh-correction was applied for comparisons of differences between the means of two groups. Non-parametric Mann–Whitney test was applied for comparing

the NAS-Score. The trapezoidal rule was used to determine the area under the curve (AUC). *p*-values <0.05 were considered as significant. All results are presented as mean with standard error of the mean (SEM). Graphs were created using the GraphPad Prism v5.0 program and Power Point v2010.

For analysis of the RT-PCR, the Fluidigm Real-Time PCR Analysis Software V.3.0.2 was used. Data were normalized by the mean values of the housekeeping genes glyceraldehyde-3-phosphate dehydrogenase (Gapdh) and actin β (actb) from the genes of interest. Heat map and principal component analysis (PCA) of the –delta Ct values were performed via the using Qlucore Omics Explorer v3.3 (Qlucore, Lund, Sweden). For analysis *p*-values were set to $\leq$0.049 for two group comparisons (*t*-test) and for multigroup comparisons (F-test) (ANOVA) ($p < 0.05$ and $q < 0.2$). *, difference significant with $p < 0.05$. **, difference significant with $p < 0.01$ ***, difference highly significant with $p < 0.001$. A *p*-value > 0.05 was considered to be not significant (ns).

3. Results

3.1. Dulaglutide Corrected Obesity and Reduced Adipose Tissue

Weight loss is the most important treatment option for NASH so far and therefore an important aim of potential therapeutical treatments. After 16 weeks of HFHC diet and 4 weeks of treatment (Figure 1a), we analyzed the body weight and body composition of the mice. Here, both treatment with dulaglutide as well as its combination with empagliflozin led to significant weight loss during the time of treatment and significantly reduced the total bodyweight at the end of treatment compared to saline control and treatment with empagliflozin alone (Figure 1b). In line with this finding, dulaglutide significantly reduced the amount of white adipose tissue (WAT), brown adipose tissue (BAT) and visceral adipose tissue (VAT) compared to saline control (Figure 1c). Also, the combined treatment significantly reduced WAT and VAT, but had no additional effect compared to dulaglutide (Figure 1c). Treatment with empagliflozin had no influence on the bodyweight or subset of adipose tissue. Therefore, both dulaglutide and combined treatment are effective for weight loss and reduction of adipose tissue.

3.2. Combination of Dulaglutide and Empagliflozin Markly Improved Glycemic Control. Dulaglutide Improved Hyperglycemia and Diminished AST-Elevation

Although there were no differences in the basal fasting glucose levels, dulaglutide accelerated glucose reduction after injection, so that these mice reached basal fasting glucose levels at the end of the test compared to saline vehicle-treated mice (Figure 2a). Also, the AUC glucose was significantly reduced (Figure 2b). The combined treatment of dulaglutide and empagliflozin further improved glycemic control via reduced basal fasting glucose levels as well as over the course of glucose test compared to either dulaglutide or empagliflozin alone (Figure 2a). Interestingly, empagliflozin had no effect on hyperglycemia. Therefore, these data show that dulaglutide and combination of dulaglutide and empagliflozin improve the metabolic function even in a non-diabetic setting.

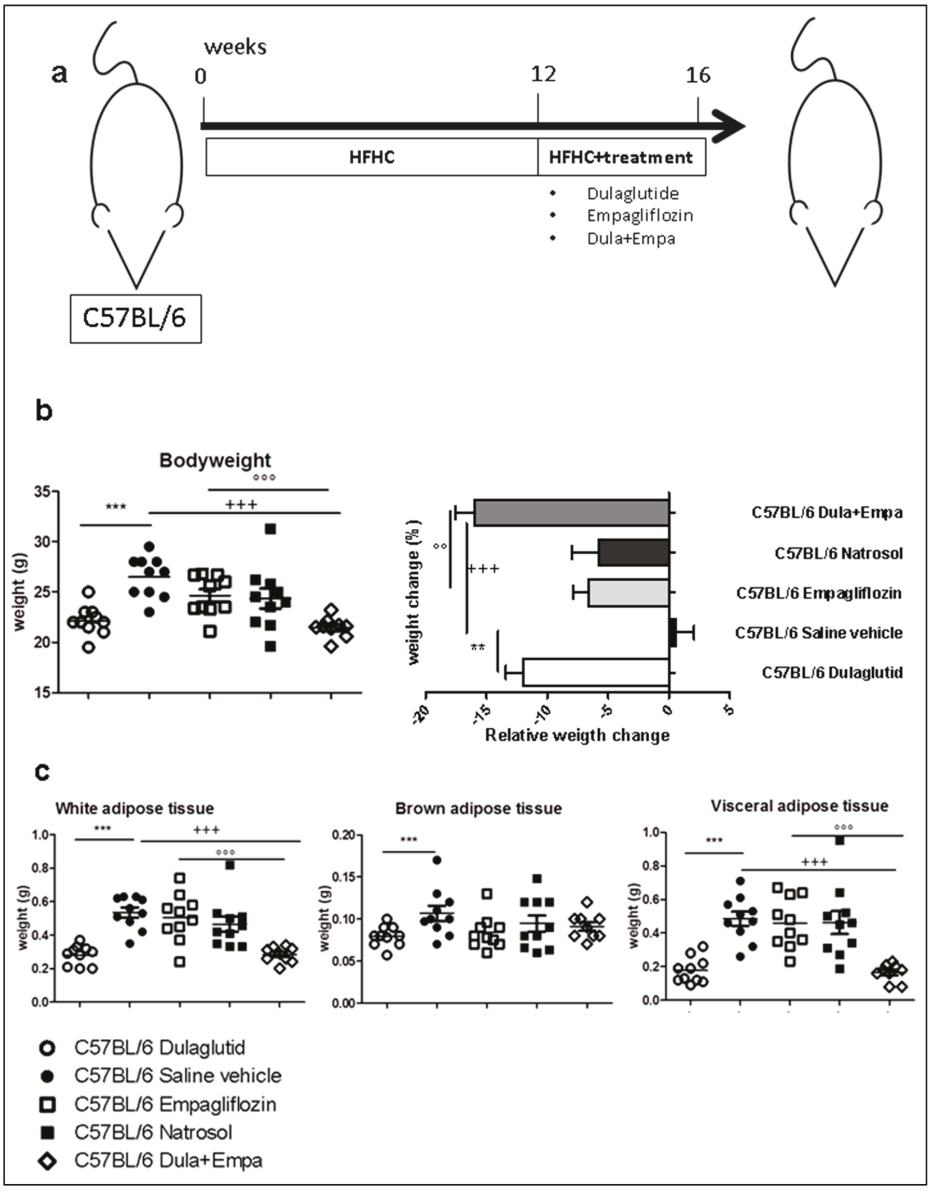

Figure 1. Body composition (**a**) C57BL/6 mice received a high-fat-high-fructose (HFHF) diet for a total of 16 weeks, additional pharmacological therapy administered for the last 4 weeks (week 13–16). (**b**) Body weight and relative weight change after 16 weeks of HFHC diet. (**c**) Body fat composition was analyzed by weight determination of white adipose tissue (WAT), brown adipose tissue (BAT) and visceral adipose tissue (VAT) after sacrification. Data are presented as mean ± SEM. C57BL/6 Dulaglutide: $n = 10$, C57BL/6 Saline vehicle: $n = 10$, C57BL/6 Empagliflozin: $n = 10$, C57BL/6 Natrosol: $n = 10$; C57BL/6 Dula + Empa: $n = 9$. Unpaired *t*-test with Welsh-correction was used for comparison between two groups. * $p < 0.05$; ** $p < 0.01$; *** $p < 0.001$ was used for comparison of Dulaglutide vs. Saline vehicle; + $p < 0.05$; ++ $p < 0.01$; +++ $p < 0.001$ was used for comparison of Dula + Empa vs. Saline vehicle, ° $p < 0.05$; °° $p < 0.01$; °°° $p < 0.001$ was used for the comparison of Dula + Empa vs. Empagliflozin.

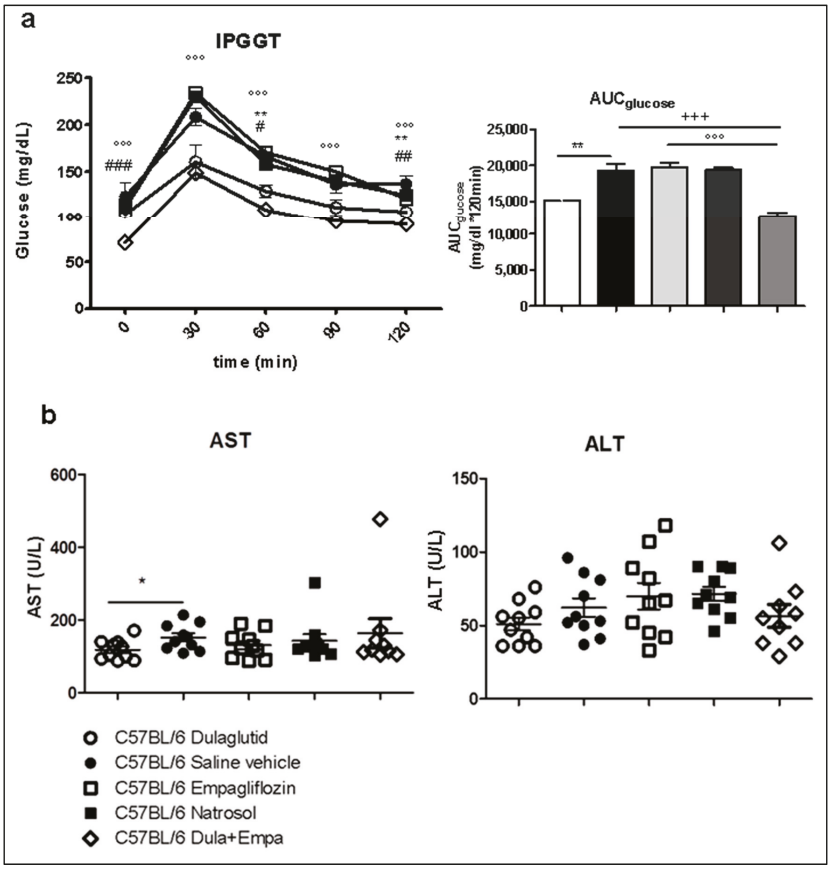

Figure 2. Metabolic parameters and transaminases (**a**) Intraperitoneal (i.p) glucose tolerance test. The trapezoidal rule was used to determine the area under the curve for glucose (AUC glucose). (**b**) Biochemical analyses of alanine (ALT) and aspartate (AST) transaminases in blood serum. Data are presented as mean ± SEM. Unpaired *t*-test with Welsh-correction was used for comparison between two groups. C57BL/6 Dulaglutide: $n = 10$, C57BL/6 Saline vehicle: $n = 10$, C57BL/6 Empagliflozin: $n = 10$, C57BL/6 Natrosol: $n = 10$; C57BL/6 Dula + Empa: $n = 9$; * $p < 0.05$; ** $p < 0.01$; *** $p < 0.001$ was used for comparison of Dulaglutide vs. Saline vehicle + $p < 0.05$; ++ $p < 0.01$; +++ $p < 0.001$ was used for comparison of Dula + Empa vs. Saline vehicle ° $p < 0.05$; °° $p < 0.01$; °°° $p < 0.001$ was used for the comparison of Dula + Empa vs. Empagliflozin # $p < 0.05$, ## $p < 0.01$, ### $p < 0.001$ was used for comparison of Dulaglutide vs. Dula + Empa.

We further analyzed the treatment effect on transaminases levels as a marker for hepatocyte damage. Here, treatment with dulaglutide alone significantly reduced the aspartate-aminotransferase (AST). Neither the treatment with empagliflozin nor the combined treatment influenced AST levels. No significant changes in the alanine-aminotransferase (ALT) levels were detected (Figure 2B).

3.3. No Histological Apparent Treatment Effects after Development of Moderate NASH

After 16 weeks of HFHC diet, the histological development of NASH was analyzed by an experienced pathologist. Paraffin-embedded liver sections were stained with haematoxylin and eosin (H&E) for assessment of liver histology, periodic-acid Schiff reaction (PAS) for assessment of glycogen accumulation and silver staining for evaluation of fibrosis (Figure S1A). All animals developed moderate steatosis, mild inflammation and mild ballooning, which defines NASH with a median NAS Score 3–4 (Figure S1B). No significant

changes have been detected after any of the treatments according to the total NAS-score. All animals developed mild periportal fibrosis with a median score of 0–1 (Table S1), but no significant treatment effect was seen. Furthermore, we measured the intrahepatic triglyceride content. Surprisingly, the liver triglyceride content was not affected by any treatment (Figure S1C).

3.4. Combination of Dulaglutide and Empagliflozine Attenuates Activation of Innate and Adaptive Immune System

As both the adaptive and innate immune system play an important role in the pathogenesis of NASH, we analyzed the intrahepatic subsets of immune cells using flow-cytometry. Although no significant changes regarding the adaptive immune system were seen for each single treatment (Figure 3a and Figure S2), the combined treatment decreased the number of $Foxp3^+$ regulatory T (Treg) cells compared to single treatment with empagliflozin as well as control mice (Figure 3a). There was no difference in the expression of CD62L (L-Selectin) on $CD4^+$ and $CD8^+$ cells, which is an adhesion molecule of the selectin family, which mediates lymphocyte homing and might induce proinflammatory processes [20] (Figure S2a). Furthermore, no difference in the subsets of $Ki67^+$ cells have been detected (Figure S2a).

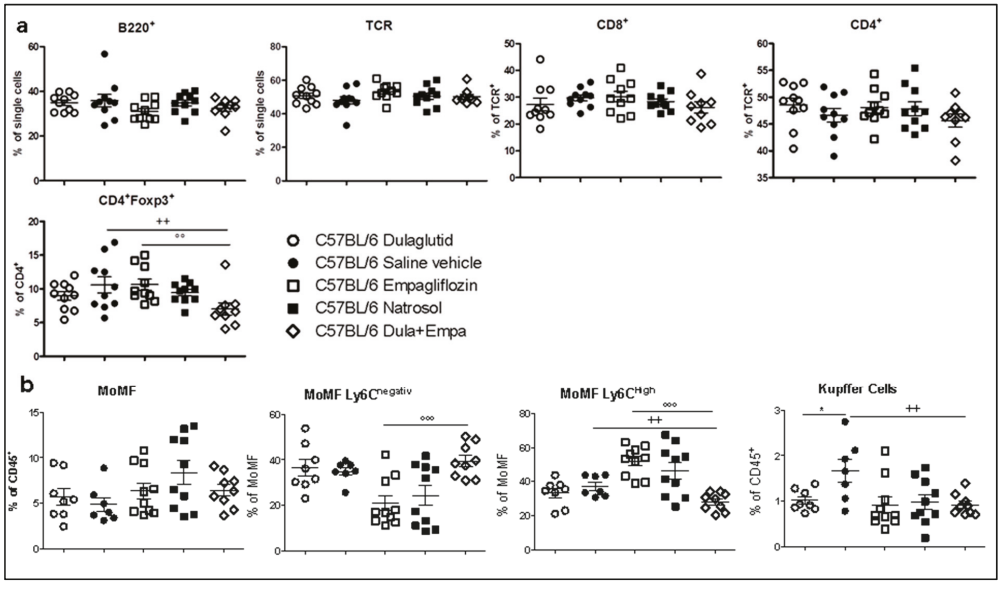

Figure 3. Flow cytometry analyses of the innate and adaptive immune system (**a**) Flow cytometry analyses of the adaptive immune system focusing on the intrahepatic subsets of $CD4^+$ T cells and $CD8^+$ T cells (**b**) Analyses of s of intrahepatic liver macrophages. Data are presented as mean ± SEM. Unpaired *t*-test with Welsh-correction was used for comparison between treatment and control group. C57BL/6 Dulaglutide: $n = 10$, C57BL/6 Saline vehicle: $n = 10$, C57BL/6 Empagliflozin: $n = 10$, C57BL/6 Natrosol: $n = 10$; C57BL/6 Dula + Empa: $n = 9$. * $p < 0.05$; ** $p < 0.01$; *** $p < 0.001$ was used for comparison of Dulaglutide vs. saline vehicle. + $p < 0.05$; ++ $p < 0.01$; +++ $p < 0.001$ was used for comparison of Dula + Empa vs. Saline vehicle. ° $p < 0.05$; °° $p < 0.01$; °°° $p < 0.001$ was used for the comparison of Dula + Empa vs. Empagliflozin.

In the subset of the cytokine production of intrahepatic lymphocytes, we could see a significant reduction in $CD8^+IL17^+$ cells as wells as a trend ($p = 0.09$) towards reduced $CD4^+IFNgamma^+$ after combined treatment compared to empagliflozin (Figure S2b). Interestingly, empagliflozin also decreased the amount of $CD8^+TNFalpha^+$. The lower Treg numbers might be further indicating lower intrahepatic IL-2 availability.

Macrophages are important drivers of chronic inflammation in the liver and contribute to the progression from simple steatosis to steatohepatitis. Polarization of monocyte-derived macrophages (MoMF) into the pro-inflammatory macrophages (MoMFLy6C^{high}) is influenced by various stimuli such as fatty acids or signals from the gut–liver axis [21]. Therefore, it is important that the combined treatment with dulaglutide and empagliflozin significantly diminished the amount of proinflammatory MoMFLy6C^{high} compared to empagliflozin and control group. Conversely, the amount of MoMFLy6C^{neg} cells were significantly increased after combined treatment (Figure 3b). Kupffer cells are involved in both activation of pro-inflammatory macrophages as well as integration of signals from the gut-liver axis and lipid metabolism. Both dulaglutide as well as the combined treatment significantly reduced the amount of Kupffer cells compared to saline vehicle (Figure 3b), which is associated with diminished inflammation. In summary, combined pharmacological treatment significantly attenuated the pro-inflammatory reaction of the innate and adaptive immune system and is even more effective than any of the single treatments.

3.5. Dulaglutide and Combined Treatment Diminished Pro-Inflammatory Pathways and Attenuated Pro-Fibrotic Pathways, whereas Empagliflozin Enhanced Pro-Inflammatory and Pro-Fibrotic Pathways

To determine the genetic effects of drug treatment on the pathogenesis of lipid metabolism, inflammation and development of fibrosis, we analyzed 22 genes, which represent key transcripts in the pathways of inflammation, fibrosis and fatty acid metabolism. Genes that were expressed significantly different upon PCA analysis were plotted in a heat map (Figure S3) as well as in diagrams to visualize changes in the pathways of inflammation, inflammasome, lipid metabolism and fibrosis (Figure 4a–d). Although dulaglutide did not induce histological changes, we could demonstrate anti-inflammatory and anti-fibrotic effects on a molecular level as it significantly decreased the expression of the pro-inflammatory markers CCL2, CD11c, TNF and IL-1 beta as well as the expression of the pro-fibrotic marker TIMP-1 compared to Saline vehicle (Figure 4a–d). Surprisingly, treatment with empagliflozin revealed pro-inflammatory and pro-fibrotic effects due to increased expression of the pro-inflammatory markers NLRP-3, CCL2, TLR-9 and TLR-4, CD11c, CD36 and enhancement of FABP-4 and collagen (Figure 4a–d) compared to vehicle.

Comparing the combined treatment with empagliflozin-mono, expression of pro-inflammatory markers CCL-2, CD11c, TGIF-2 as well as pro-fibrotic markers TIMP-1 and collagen was significantly decreased, suggesting a dominant effect of the dulaglutide treatment (Figure 4a–d). The expression of SREBF-1 increased after treatment with dulaglutide and empagliflozin. Although no changes between the dulaglutide group and combined treatment group could be detected, the combined treatment also significantly diminished the expression of pro-inflammatory as well as pro-fibrotic markers.

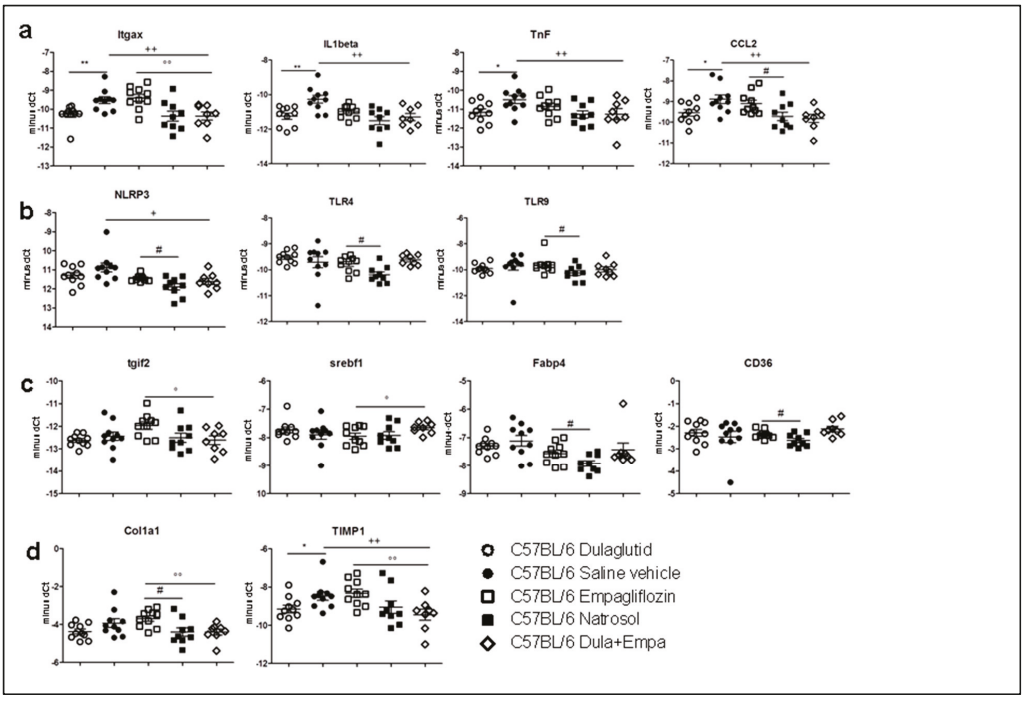

Figure 4. Gene expression. Normalized gene expression representing pathways of inflammation, inflammasome, fibrosis and lipid metabolism. Genes that were expressed significantly differently upon PCA were exemplarily chosen to visualize changes in the pathways of (**a**) inflammation, (**b**) inflammasome, (**c**) lipid metabolism and (**d**) fibrosis. Unpaired *t*-test with Welsh-correction was used for comparison between treatment and control group. One-way ANOVA with Tukey's multicomparison test was used for differences between treatment groups. C57BL/6 Dulaglutide: $n = 10$, C57BL/6 Saline vehicle: $n = 10$, C57BL/6 Empagliflozin: $n = 10$, C57BL/6 Natrosol: $n = 10$; C57BL/6 Dula + Empa: $n = 9$. * $p < 0.05$; ** $p < 0.01$; *** $p < 0.001$ was used for comparison of Dulaglutide vs. Saline vehicle. # $p < 0.05$; ## $p < 0.01$; ### $p < 0.001$ was used for comparison of Empagliflozin vs. Natrosol. + $p < 0.05$; ++ $p < 0.01$; +++ $p < 0.001$ was used for comparison of Dula + Empa vs. Saline vehicle. ° $p < 0.05$; °° $p < 0.01$; °°° $p < 0.001$ was used for the comparison of Dula + Empa vs. Empagliflozin.

3.6. Microbiome Diversity Is Enhanced by Dulaglutide and Combination of Dulaglutide and Empagliflozine

Besides lipid and glucose metabolism, the gut–liver axis also contributes to the progression of NASH. In particular, microbiome dysbiosis causes flux of microbial endotoxins to the liver, which then further promotes pro-inflammatory and pro-fibrotic processes [22]. Therefore, we analyzed the changes in the microbiome after treatment. In total, we analyzed 18,656 reads per sample and could classify six different phyla and 47 different genera. Only 0.02% of reads could not be assigned at phylum level.

Alpha diversity on genus level was significantly augmented after dulaglutide treatment compared to the saline control group in both Shannon- and Simpson-diversity index (Figure 5a). Also, combined treatment enhanced microbiome dysbiosis compared to saline vehicle. On phylum level, significant differences in beta diversity could be observed when comparing dulaglutide treatment with the saline vehicle (Figure 5b). Interestingly, an increase of *Bacteriodetes* and a concomitant lower abundance of *Firmicutis* were seen, which are both related to lower insulin resistance and obesity in humans and mice. Additionally, the increase of *Bacteriodetes* and concomitant reduction of *Firmicutis* was also seen after empagliflozin treatment and combined treatment.

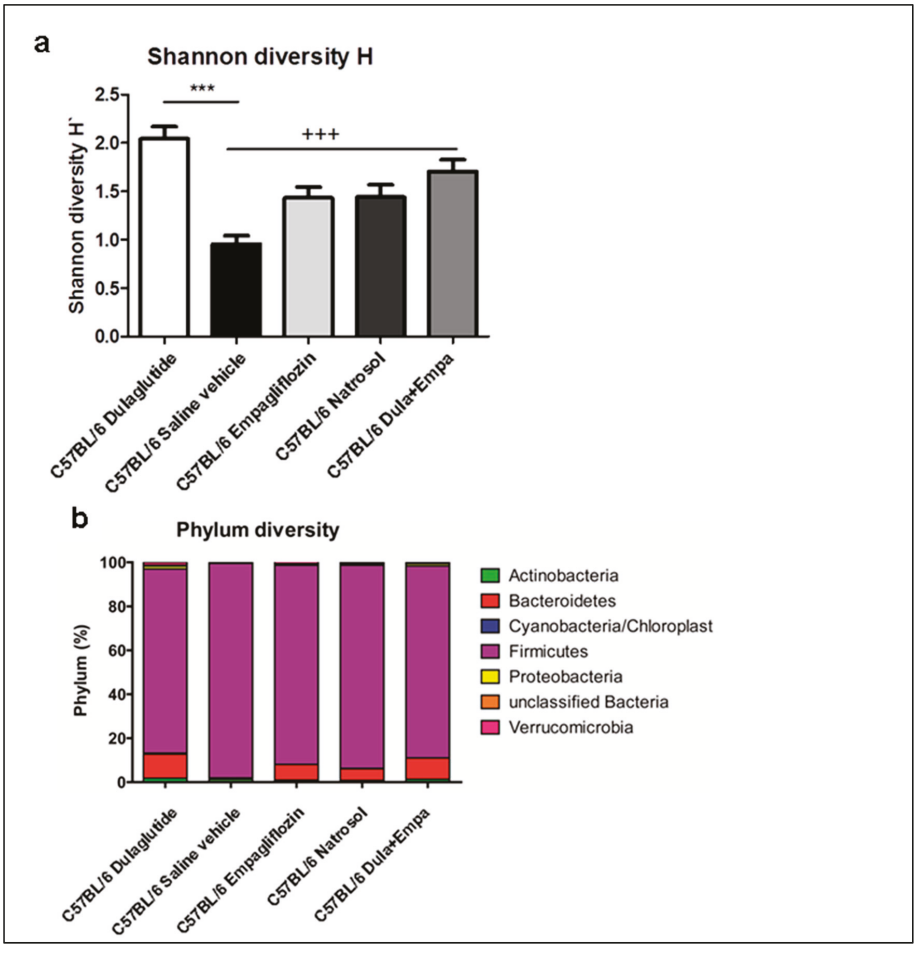

Figure 5. Microbiome diversity (**a**) Analysis of the genus diversity of intestinal microbiota using the Shannon H score. Data are presented as mean ± SEM. Unpaired *t*-test with Welsh-correction was used for comparison between treatment and control group. (**b**) Detailed composition of the phylum diversity. C57BL/6 Dulaglutide: $n = 10$, C57BL/6 Saline vehicle: $n = 10$, C57BL/6 Empagliflozin: $n = 10$, C57BL/6 Natrosol: $n = 10$; C57BL/6 Dula + Empa: $n = 9$. * $p < 0.05$; ** $p < 0.01$; *** $p < 0.001$ was used for comparison of Dulaglutide vs. Saline vehicle. + $p < 0.05$; ++ $p < 0.01$; +++ $p < 0.001$ was used for comparison of Dula + Empa vs. Saline vehicle.

Analyses of microbiome similarities were performed on genus level. Here, we could show significant differences between the dulaglutide-group and the control group. Determination of the relative abundance of different genera, treatment with dulaglutide as well as treatment with empagliflozin and combined treatment were associated with significant differences in the relative abundance of different genera (Table S2). However, there are more differences between combined treatments with empagliflozin than with dulaglutide, which underlines the dominant effect of dulaglutide.

To summarize, we could show significant improvement of microbiome dysbiosis after dulaglutide treatment and its combination with empagliflozin, which correlates with diminished activation of pro-inflammatory and pro-fibrotic pathways in our previous analyses.

4. Discussion

To our knowledge, this is the first study investigating the effects of the new, long-acting GLP-1 agonist dulaglutide and the SGLT-2 inhibitor empagliflozin alone and in combination in a dietary mice model for non-alcoholic steatohepatitis.

Dulaglutide corrects obesity and improves glycemic control even in a non-diabetic mouse model and therefore improves important risk factors for the pathogenesis of NASH. The combination therapy with GLP-1 agonist and SGLT-2 inhibitor is meant to be a promising treatment as their effects are supplementary.

A few studies have already examined this combination and have shown beneficial effects on glycemic control and body weight in humans [23]. In our study, we could confirm beneficial effects of combined treatment on glycemic control compared to monotherapy with GLP-1. However, the effect of the combination on the HbA1c- reduction in the mentioned study was less than the additive effect of SGLT-2 inhibition alone plus GLP-1-agonist alone.

Furthermore, our data clearly demonstrated anti-inflammatory effects of both dulaglutide and the combination of dulaglutide and empagliflozin. A previous study also demonstrated strong anti-inflammatory effect of GLP-1 agonist as an important pathway to improve NASH. Furthermore, they postulated that this effect might be partly independent from body weight reduction and glycemic improvement [24].

In our study, the anti-inflammatory effects are mediated by various pathways. Kupffer cells, the resident macrophages of the liver, play a critical role in the onset of NASH, as their activation results in the release of various inflammatory mediators, such as chemokine (C-C motif) ligand (CCL2) and TNF alpha [25]. CCL-2 mediates the recruitment of MoMF. These MoMFs can be further divided into proinflammatory monocytes (MoMF Ly6C^{high}) and anti-inflammatory monocytes (MoMF Ly6C^{low}). In NASH, proinflammatory MoMF strongly promote chronic inflammation and therefore play a critical role in pathogenesis of NASH. In line with the decrease of Kupffer cells, we observed a decrease of CCL2-gene expression in the liver as a marker for decreased inflammation. In addition, the expressions of TNF alpha and IL1beta were significantly decreased after dulaglutide treatment. Previously it was shown that GLP-1 agonist liraglutide modulated the Kupffer cell M2-polarization and inhibits inflammasome activation, which might contribute to the anti-inflammatory effect of dulaglutide [26]. Additionally, another study investigating liraglutide in NASH showed improvement of ER stress, which might also contribute to the anti-inflammatory action of GLP-1 agonists [27].

Importantly, we could show an even stronger attenuation of pro-inflammatory activation of innate and adaptive immune system marked by decreased Treg population as well as decreased pro-inflammatory macrophages (MoMF Ly6C^{high}) and Kupffer cells in a combined treatment group. Although our data did not show any significant effect of empagliflozin on innate immunity, a previous study in a diabetic mouse model showed improvement of inflammation and insulin resistance by reduction of pro-inflammatory macrophages [28]. Therefore, the combination of dulaglutide and empagliflozin has additive effects on pro-inflammatory process.

Previous animal and human studies already suggested that the gut microbiome plays an important role in the pathogenesis of NASH as the flux of microbial endotoxins to the liver further promotes pro-inflammatory and pro-fibrotic processes [29]. Most importantly, reduced microbial diversity and an increase of bacteria belonging to the *Firmicutes* phylum as well as decreased of *Bacteriodetes* seem to be associated with NASH [30]. Therefore, the increased *Firmicutes:Bacteriodetes* ratio, which is mostly pronounced in the saline vehicle group of our study, might be associated with NAFLD development. In the current study, *Firmicutes* are the very dominant phylum and are even more dominant compared to other studies [30], with a very low overall abundance of *Bacteriodetes*. In particular, lack of *Bacteriodetes* in the saline group is surprising. As other studies demonstrated microbiome dysbiosis after high-salt diet [31], the application of saline might also influence the microbiome and explain this finding. Most important, we could show a significant improvement

of microbiome diversity after dulaglutide treatment and in particular with an increased relative abundance of *Bacteriodetes,* but also after combined treatment. Previous studies showed a correlation between weight loss and increase of abundance of *Bacteriodetes* as well as an association between improvement of metabolic situation and increase of *Bacteriodetes* after GLP-1 treatment [32]. Furthermore, the significant increase of *Akkermansia* spp. after dulaglutide treatment might be in correlation to improvement of the metabolic situation as *Akkermansia* spp., which is a mucin-degrading short fatty acid-producing species, is decreased in obesity and showed negative correlation to markers of gut permeability and inflammation [29]. However, the gut microbiome in mice might also be influenced by different environmental factors such as diet [33], which should be considered in terms of interpretation. In summary, the improvement of microbiome dysbiosis after dulaglutide and combined treatment consorts the improvement of metabolic dysfunction and strengthens their anti-inflammatory effects. Furthermore, the combination showed even stronger anti-fibrotic effects by downregulation of Col1a1 and TIMP-1. Although we could demonstrate significant attenuation of anti-inflammatory and anti-fibrotic pathways, no improvements on the intrahepatic steatosis and the histological outcome of NASH were detected for any of the treatments. Regarding the intrahepatic steatosis, previous data suggest that GLP-1 agonists improve hepatic steatosis by reduction of de novo lipogenesis and improving insulin signaling pathways [34]. However, we could not show any significant effect of dulaglutide on hepatic steatosis nor in pathways of lipogenesis. In line with our findings, quantitative hepatic steatosis in mice model of NASH using MCD diet was also unaffected by GLP-1 treatment [35], although GLP-1 treatment attenuated hepatic inflammation. However, it has to be mentioned that MCD diet induces NASH by different pathways compared to HFHC diet used in our model [36] and might not be suitable to represent the common features of the metabolic syndrome. On the other hand, another study investigating GLP-1 agonist in diabetic mice models showed significant improvement of intrahepatic steatosis, but only mild histological improvement of inflammation [37]. Furthermore, improvement of hepatic steatosis seems to be associated with the amount of weight loss.

As insulin resistance promotes dysregulation of peripheral lipolysis and de novo lipogenesis, which then leads to accumulation of free fatty acids in the liver [2], the effects of GLP-1 agonists on hepatic steatosis might be less prominent when hyperinsulinemia and hyperglycemia are not present and seem not to be directly correlated with their anti-inflammatory properties. Furthermore, the degree of effectiveness of GLP-1 agonists seems to be according to the manifestation of diabetes and obesity, which is important to take into account when comparing different mouse models.

A shortcoming of the study might be the moderate histological manifestation of NASH in this mice model. It is well known from other forms of hepatitis, e.g., autoimmune hepatitis, that histological changes follow biochemical improvements, but months later. Therefore, a prolonged duration of diet as well as a prolonged duration of treatment might be required to determine the histological effects.

The pathogenesis of NASH is a complex interaction between environmental factors and genetic determinants. On the one hand, this complex interplay could not be completely represented by a single animal model [36]. However, on the other hand animal models are extremely helpful to analyze distinct pathways without interference as such analyses are not possible in the human setting. Therefore, our animal model could reflect distinct pathways in the pathogenesis of NASH in a non-diabetic setting.

Beyond weight loss and improvement of insulin resistance, the positive effects of GLP-1 agonists also seem to be multifactorial-mediated with additional pleiotropic effects, especially on improvement of cardiovascular disease. As our mouse model replicates only moderate features of the metabolic syndrome in a non-diabetic setting, some pleotropic effects of GLP-1 agonist might not be present in our model.

Previous meta-analysis of human studies investigating the impact of GLP-1 agonist in NASH showed promising results with improvement of hepatic steatosis, histological reso-

lution of NASH and decrease of transaminases [38,39]. However, it should be mentioned that the majority of the patients were diabetic.

Previous studies with a lesser amount of diabetic patients [40,41] could show improvement of metabolic parameters and resolution of NASH, but could not show histological improvement of fibrosis, which is in line with our findings. Therefore, the beneficial effects of GLP-1 agonist might be more pronounced in patients with diabetes. Furthermore, as GLP-1 agonists mainly improve the underlying harmful metabolic dysfunction first, the entire long-term improvement of NASH and fibrosis might require even more prolonged treatment and follow-up period.

We could not detect any effect of empagliflozin treatment, neither on the metabolic situation nor on the histological outcome of NASH. Instead, empagliflozin significantly increased expression of pro-inflammatory and pro-fibrotic genes. These data are partly unexpected, as previous data from human and animal studies with SGLT-2 inhibitors showed improvement of NASH [42]. To rule out technical issues, the pharmacological effect of empagliflozin was proven by increased glucosuria after empagliflozin treatment (Figure S4). The absent effect on body weight can partly be explained by the mild total weight gain in both oral gavage treatment groups, so that the daily oral gavage might also decrease the overall food intake. So far, empagliflozin has been only tested for NASH in a streptozotocin-induced NASH-mouse model [12], where it showed improvement of hepatic steatosis and fibrosis. Compared to our mouse model, the streptozotocin-induced mouse model provides a severe diabetic phenotype, but without any other features of the metabolic syndrome. A recently published study in patients without diabetes also revealed no significant reduction of hepatic steatosis after empagliflozin treatment compared to the control group [43]. In contrast to other anti-diabetic agents, SGLT- inhibitors are independent of beta-cell function as they inhibit the sodium-glucose cotransporter 2 (SGLT-2) in the proximal tubulus of the kidney [8,44]. In human studies, the glucose-lowering effect of empagliflozin is more potent in patients with higher HbA1c-values [45]. In line with our findings, recent clinical trials of SGLT-2 inhibitors in non-diabetic patients with chronic kidney disease or heart failure have also demonstrated divergent results regarding the metabolic effects in non-diabetic patients [46,47] meaning that the metabolic effects in non-diabetic patients are not as strong as in diabetic patients [48], although they had similar preserved cardiorenal protection. Overall, the effect and indication of SGLT-2-inhibitors for non-diabetic patients in regard to NASH should be critically reviewed and therefore, further studies are needed. So far, the combination of GLP-1 agonist and SGLT-2- inhibitors has been successfully tested in patient with type 2 diabetes [49–51], where combination therapy further improved hyperglycemia and obesity. This is mainly explained by their synergistic mechanism of action. While GLP-1 agonists stimulate insulin secretion and suppress glucagon production, SGLT-2-inhibitors improve hyperglycemia by enhanced glucosuria [8].

Nevertheless, the additive effect was less pronounced in using lower dosing and more pronounced in severe diabetic situations in these studies. Therefore, the lack of treatment effects by empagliflozin might explain the limited effect of combined treatment compared to dulaglutide-mono treatment with only slightly additional effects on the one hand. On the other hand, one study could show that the SGLT-2-inhibitors induced increase of endogenous glucose production could not be suppressed by combination with GLP-1 agonist [52], which might attenuate the additional benefits, in particular in a non-diabetic situation.

Furthermore, in the studies mentioned above, no additional effects on lipid level were detected. As dyslipidemia is an important risk factor for development of steatohepatitis, in particular in the absence of diabetes, this might also contribute to the marginal benefit on NASH.

Further limitation of the study might be the lack of an equal control group for the combined treatment. However, comparing both control groups for the individual treatments,

we could not see any significant differences. Therefore, we might expect a similar outcome after a combined treatment with saline and Natrosol compared to single treatment.

In conclusion, our results did demonstrate no beneficial effects of empagliflozin on the development of NASH in a non-diabetic setting. Furthermore, these data suggest that GLP-1 agonists and SGLT-2 inhibitors are less effective for the prevention of hepatic steatosis in a non-diabetic background compared to previous studies. Nevertheless, the study demonstrates important anti-inflammatory effects of dulaglutide and the combination of dulaglutide and empagliflozine by modulating pro-inflammatory immune response and microbiome dysbiosis. As development of hepatic fibrosis is strongly triggered by inflammation, this might have important implications for the treatment of NASH, e.g., in combination with anti-steatotic treatment. Therefore, further studies are needed to investigate the long-term impact of both agents on NASH and hepatic fibrosis in a non-diabetic background.

Supplementary Materials: The following are available online at https://www.mdpi.com/article/10.3390/biomedicines9040353/s1; Supplementary Materials and Methods; Figure S1: Histological outcome of NAFLD after HFHC diet; Figure S2: Innate and adaptive immune system; Figure S3: Heat map.; Figure S4: Glucosuria after empagliflozin treatment; Table S1: Histological Scoring for NASH; Table S2: Analyzing the relative abundance of different genera.

Author Contributions: Conceptualization: K.L.H.-B., M.H.-W., E.J.; methodology: E.J., M.H.-W., B.H. (Benjamin Heidrich); validation: K.L.H.-B., F.W.; formal analysis: K.L.H.-B., R.T., F.W., B.H. (Benjamin Heidrich); investigation, K.L.H.-B., J.D., M.L., K.I., B.H. (Björn Hartleben); resources: E.J., M.P.M., H.W.; writing—original draft preparation: K.L.H.-B.; writing—review and editing: E.J., Y.S.M., M.P.M., H.W., J.D., R.T., F.W., B.H. (Benjamin Heidrich), B.H. (Björn Hartleben), M.H.-W.; visualization: K.L.H.-B.; supervision: M.H.-W., E.J., H.W.; project administration: E.J., M.H.-W.; funding acquisition: K.L.H.-B., E.J. All authors have read and agreed to the published version of the manuscript.

Funding: The authors were supported by grants from the Deutsche Forschungsgemeinschaft (SFB 738, SFB TR127). Additionally, the work of K.L.H.-B. was supported by PRACTIS—Clinician Scientist Program of Hannover Medical School, funded by the German Research Foundation (DFG, ME 3696/3-1, RAW). We acknowledge support by the German Research Foundation (DFG) and the Open Access Publication Fund of Hannover Medical School (MHH). The funders had no influence on study design, data collection and analysis, decision to publish or preparation of the manuscript.

Institutional Review Board Statement: All animal experiments were executed according to protocols approved by the animal welfare commission of the Hannover Medical School and local ethics Animal Review Board (Niedersaechsisches Landesamt für Verbraucherschutz und Lebensmittelsicherheit/LAVES, Oldenburg, Germany) covered by study number 13/1152 and 17/2456.

Informed Consent Statement: Not applicable.

Data Availability Statement: The data presented in this study are available on request from the corresponding author.

Acknowledgments: We thank Martin Hapke for assistance in animal handling and sample acquisition. We thank Peter Schürmann for technical support. We thank Edgar Dawkins for language editing of the manuscript.

Conflicts of Interest: E.J. has received honoraria and travel support from Lilly GmbH (Bad Homburg, Germany) and Boehringer Ingelheim (Ingelheim am Rhein, Germany). M.P.M received honoraria, travel support and grants from Gilead (Foster City, CA, USA) and Falk Pharma (Freiburg, Germany). He acts as principal investigator and consultant for Novartis (Basel, Switzerland), Aram Chol (Galmed Pharmaceuticals, Tel Avivi, Israel), Gilead, Intercept (London, UK), Falk Pharma and Genfit (Loos, France). H.W received lecture fees from Falk Pharma, Gore (Newark, DE, USA), Merz (Frankfurt am Main, Germany) and Norgine (Amsterdam, Netherlands) and acts as a Principal Investigator for Falk Pharma. He received grants from Merz and Norgine. These activities do not relate to the current manuscript which was done without any support from the abovementioned companies. K.L.H.-B., J.D., B.H. (Björn Hartleben), B.H. (Benjamin Heidrich), F.W., R.T., Y.-S.E.M., M.L., K.I. and M.H.-W declare no conflicts of interest.

References

1. Younossi, Z.M.; Henry, L.; Bush, H.; Mishra, A. Clinical and Economic Burden of Nonalcoholic Fatty Liver Disease and Nonalcoholic Steatohepatitis. *Clin. Liver Dis.* **2018**, *22*, 1–10. [CrossRef]
2. Buzzetti, E.; Pinzani, M.; Tsochatzis, E.A. The multiple-hit pathogenesis of non-alcoholic fatty liver disease (NAFLD). *Metabolism* **2016**, *65*, 1038–1048. [CrossRef] [PubMed]
3. Jiang, C.-M.; Pu, C.-W.; Hou, Y.-H.; Chen, Z.; Alanazy, M.; Hebbard, L. Non alcoholic steatohepatitis a precursor for hepatocellular carcinoma development. *World J. Gastroenterol.* **2014**, *20*, 16464–16473. [CrossRef] [PubMed]
4. Patel, S.S.; Siddiqui, M.S. The Interplay Between Nonalcoholic Fatty Liver Disease and Atherosclerotic Heart Disease. *Hepatology* **2019**, *69*, 1372–1374. [CrossRef]
5. Eslam, M.; Sanyal, A.J.; George, J.; Neuschwander-Tetri, B.; Tiribelli, C.; Kleiner, D.E.; Brunt, E.; Bugianesi, E.; Yki-Järvinen, H.; Grønbæk, H.; et al. MAFLD: A Consensus-Driven Proposed Nomenclature for Metabolic Associated Fatty Liver Disease. *Gastroenterology* **2020**, *158*, 1999–2014.e1. [CrossRef]
6. Roeb, E.; Steffen, H.M.; Bantel, H.; Baumann, U.; Canbay, A.; Demir, M.; Drebber, U.; Geier, A.; Hampe, J.; Hellerbrand, C.; et al. S2k Guideline non-alcoholic fatty liver disease. *Z. Gastroenterol.* **2015**, *53*, 668–723.
7. Bifari, F.; Manfrini, R.; Cas, M.D.; Berra, C.; Siano, M.; Zuin, M.; Paroni, R.; Folli, F. Multiple target tissue effects of GLP-1 analogues on non-alcoholic fatty liver disease (NAFLD) and non-alcoholic steatohepatitis (NASH). *Pharmacol. Res.* **2018**, *137*, 219–229. [CrossRef] [PubMed]
8. DeFronzo, R.A. Combination therapy with GLP-1 receptor agonist and SGLT2 inhibitor. *Diabetes Obes. Metab.* **2017**, *19*, 1353–1362. [CrossRef]
9. Seko, Y.; Nishikawa, T.; Umemura, A.; Yamaguchi, K.; Moriguchi, M.; Yasui, K.; Kimura, M.; Iijima, H.; Hashimoto, T.; Sumida, Y.; et al. Efficacy and safety of canagliflozin in type 2 diabetes mellitus patients with biopsy-proven nonalcoholic steatohepatitis classified as stage 1–3 fibrosis. *Diabetes Metab. Syndr. Obes. Targets Ther.* **2018**, *11*, 835–843. [CrossRef] [PubMed]
10. Sumida, Y.; Yoneda, M. Current and future pharmacological therapies for NAFLD/NASH. *J. Gastroenterol.* **2018**, *53*, 362–376. [CrossRef]
11. Byrd, R.A.; Sorden, S.D.; Ryan, T.; Pienkowski, T.; LaRock, R.; Quander, R.; Wijsman, J.A.; Smith, H.W.; Blackbourne, J.L.; Rosol, T.J.; et al. Chronic Toxicity and Carcinogenicity Studies of the Long-Acting GLP-1 Receptor Agonist Dulaglutide in Rodents. *Endocrinology* **2015**, *156*, 2417–2428. [CrossRef]
12. Jojima, T.; Tomotsune, T.; Iijima, T.; Akimoto, K.; Suzuki, K.; Aso, Y. Empagliflozin (an SGLT2 inhibitor), alone or in combination with linagliptin (a DPP-4 inhibitor), prevents steatohepatitis in a novel mouse model of non-alcoholic steatohepatitis and diabetes. *Diabetol. Metab. Syndr.* **2016**, *8*, 1–11. [CrossRef]
13. Hardtke-Wolenski, M.; Fischer, K.; Noyan, F.; Schlue, J.; Falk, C.S.; Stahlhut, M.; Woller, N.; Kuehnel, F.; Taubert, R.; Manns, M.P.; et al. Genetic predisposition and environmental danger signals initiate chronic autoimmune hepatitis driven by CD4+T cells. *Hepatology* **2013**, *58*, 718–728. [CrossRef] [PubMed]
14. Kleiner, D.E.; Makhlouf, H.R. Histology of Nonalcoholic Fatty Liver Disease and Nonalcoholic Steatohepatitis in Adults and Children. *Clin. Liver Dis.* **2016**, *20*, 293–312. [CrossRef]
15. Heidrich, B.; Vital, M.; Plumeier, I.; Döscher, N.; Kahl, S.; Kirschner, J.; Ziegert, S.; Solbach, P.; Lenzen, H.; Potthoff, A.; et al. Intestinal microbiota in patients with chronic hepatitis C with and without cirrhosis compared with healthy controls. *Liver Int.* **2018**, *38*, 50–58. [CrossRef]
16. Camarinha-Silva, A.; Jáuregui, R.; Chaves-Moreno, D.; Oxley, A.P.; Schaumburg, F.; Becker, K.; Wos-Oxley, M.L.; Pieper, D.H. Comparing the anterior nare bacterial community of two discrete human populations using Illumina amplicon sequencing. *Environ. Microbiol.* **2014**, *16*, 2939–2952. [CrossRef] [PubMed]
17. Chomczynski, P. A reagent for the single-step simultaneous isolation of RNA, DNA and proteins from cell and tissue samples. *Biotechniques* **1993**, *15*, 532.
18. Cole, J.R.; Wang, Q.; Fish, J.A.; Chai, B.; McGarrell, D.M.; Sun, Y.; Brown, C.T.; Porras-Alfaro, A.; Kuske, C.R.; Tiedje, J.M. Ribosomal Database Project: Data and tools for high throughput rRNA analysis. *Nucleic Acids Res.* **2014**, *42*, D633–D642. [CrossRef]
19. Wang, Q.; Garrity, G.M.; Tiedje, J.M.; Cole, J.R. Naive Bayesian classifier for rapid assignment of rRNA sequences into the new bacterial taxonomy. *Appl. Environ. Microbiol.* **2007**, *73*, 5261–5267. [CrossRef] [PubMed]
20. Drescher, H.K.; Schippers, A.; Rosenhain, S.; Gremse, F.; Bongiovanni, L.; De Bruin, A.; Eswaran, S.; Gallage, S.U.; Pfister, D.; Szydlowska, M.; et al. L-Selectin/CD62L Is a Key Driver of Non-Alcoholic Steatohepatitis in Mice and Men. *Cells* **2020**, *9*, 1106. [CrossRef] [PubMed]
21. Lefere, S.; Tacke, F. Macrophages in obesity and non-alcoholic fatty liver disease: Crosstalk with metabolism. *JHEP Rep.* **2019**, *1*, 30–43. [CrossRef]
22. Jadhav, K.; Cohen, T.S. Can You Trust Your Gut? Implicating a Disrupted Intestinal Microbiome in the Progression of NAFLD/NASH. *Front. Endocrinol.* **2020**, *11*, 592157. [CrossRef] [PubMed]
23. Frías, J.P.; Hardy, E.; Ahmed, A.; Öhman, P.; Jabbour, S.; Wang, H.; Guja, C. Effects of exenatide once weekly plus dapagliflozin, exenatide once weekly alone, or dapagliflozin alone added to metformin monotherapy in subgroups of patients with type 2 diabetes in the DURATION-8 randomized controlled trial. *Diabetes Obes. Metab.* **2018**, *20*, 1520–1525. [CrossRef] [PubMed]

24. Rakipovski, G.; Rolin, B.; Nøhr, J.; Klewe, I.; Frederiksen, K.S.; Augustin, R.; Hecksher-Sørensen, J.; Ingvorsen, C.; Polex-Wolf, J.; Knudsen, L.B. The GLP-1 Analogs Liraglutide and Semaglutide Reduce Atherosclerosis in ApoE(-/-) and LDLr(-/-) Mice by a Mechanism That Includes Inflammatory Pathways. *JACC Basic Transl. Sci.* **2018**, *3*, 844–857. [CrossRef] [PubMed]
25. Tacke, F. Targeting hepatic macrophages to treat liver diseases. *J. Hepatol.* **2017**, *66*, 1300–1312. [CrossRef] [PubMed]
26. Li, Z.; Feng, P.-P.; Zhao, Z.-B.; Zhu, W.; Gong, J.P.; Du, H.-M. Liraglutide protects against inflammatory stress in non-alcoholic fatty liver by modulating Kupffer cells M2 polarization via cAMP-PKA-STAT3 signaling pathway. *Biochem. Biophys. Res. Commun.* **2019**, *510*, 20–26. [CrossRef]
27. Fang, T.; Huang, S.; Chen, Y.; Chen, Z.; Chen, J.; Hu, W. Glucagon Like Peptide-1 Receptor Agonists Alters Pancreatic and Hepatic Histology and Regulation of Endoplasmic Reticulum Stress in High-fat Diet Mouse Model. *Exp. Clin. Endocrinol. Diabetes* **2020**. [CrossRef]
28. Xu, L.; Nagata, N.; Chen, G.; Nagashimada, M.; Zhuge, F.; Ni, Y.; Sakai, Y.; Kaneko, S.; Ota, T. Empagliflozin reverses obesity and insulin resistance through fat browning and alternative macrophage activation in mice fed a high-fat diet. *BMJ Open Diabetes Res. Care* **2019**, *7*, e000783. [CrossRef]
29. Ghetti, F.D.F.; Oliveira, D.G.; De Oliveira, J.M.; Ferreira, L.E.V.V.D.C.; Cesar, D.E.; Moreira, A.P.B. Influence of gut microbiota on the development and progression of nonalcoholic steatohepatitis. *Eur. J. Nutr.* **2018**, *57*, 861–876. [CrossRef] [PubMed]
30. Xie, G.; Wang, X.; Liu, P.; Wei, R.; Chen, W.; Rajani, C.; Hernandez, B.Y.; Alegado, R.; Dong, B.; Li, D.; et al. Distinctly altered gut microbiota in the progression of liver disease. *Oncotarget* **2016**, *7*, 19355–19366. [CrossRef]
31. Wang, C.; Huang, Z.; Yu, K.; Ding, R.; Ye, K.; Dai, C.; Xu, X.; Zhou, G.; Li, C. High-Salt Diet Has a Certain Impact on Protein Digestion and Gut Microbiota: A Sequencing and Proteome Combined Study. *Front. Microbiol.* **2017**, *8*, 1838. [CrossRef] [PubMed]
32. Castaner, O.; Goday, A.; Park, Y.-M.; Lee, S.-H.; Magkos, F.; Toh Ee Shiow, S.-A.; Schröder, H. The Gut Microbiome Profile in Obesity: A Systematic Review. *Int. J. Endocrinol.* **2018**, *2018*, 4095789. [CrossRef] [PubMed]
33. Gómez-Zorita, S.; Aguirre, L.; Milton-Laskibar, I.; Fernández-Quintela, A.; Trepiana, J.; Kajarabille, N.; Mosqueda-Solís, A.; González, M.; Portillo, M.P. Relationship between Changes in Microbiota and Liver Steatosis Induced by High-Fat Feeding—A Review of Rodent Models. *Nutrition* **2019**, *11*, 2156. [CrossRef] [PubMed]
34. Svegliati-Baroni, G.; Saccomanno, S.; Rychlicki, C.; Agostinelli, L.; De Minicis, S.; Candelaresi, C.; Faraci, G.; Pacetti, D.; Vivarelli, M.; Nicolini, D.; et al. Glucagon-like peptide-1 receptor activation stimulates hepatic lipid oxidation and restores hepatic signalling alteration induced by a high-fat diet in nonalcoholic steatohepatitis. *Liver Int.* **2011**, *31*, 1285–1297. [CrossRef] [PubMed]
35. Somm, E.; Montandon, S.A.; Loizides-Mangold, U.; Gaïa, N.; Lazarevic, V.; De Vito, C.; Perroud, E.; Bochaton-Piallat, M.-L.; Dibner, C.; Schrenzel, J.; et al. The GLP-1R agonist liraglutide limits hepatic lipotoxicity and inflammatory response in mice fed a methionine-choline deficient diet. *Transl. Res.* **2021**, *227*, 75–88. [CrossRef]
36. Farrell, G.; Schattenberg, J.M.; Leclercq, I.; Yeh, M.M.; Goldin, R.; Teoh, N.; Schuppan, D. Mouse Models of Nonalcoholic Steatohepatitis: Toward Optimization of Their Relevance to Human Nonalcoholic Steatohepatitis. *Hepatology* **2019**, *69*, 2241–2257. [CrossRef] [PubMed]
37. Jouihan, H.; Will, S.; Guionaud, S.; Boland, M.L.; Oldham, S.; Ravn, P.; Celeste, A.; Trevaskis, J.L. Superior reductions in hepatic steatosis and fibrosis with co-administration of a glucagon-like peptide-1 receptor agonist and obeticholic acid in mice. *Mol. Metab.* **2017**, *6*, 1360–1370. [CrossRef]
38. Dong, Y.; Lv, Q.; Li, S.; Wu, Y.; Li, L.; Li, J.; Zhang, F.; Sun, X.; Tong, N. Efficacy and safety of glucagon-like peptide-1 receptor agonists in non-alcoholic fatty liver disease: A systematic review and meta-analysis. *Clin. Res. Hepatol. Gastroenterol.* **2017**, *41*, 284–295. [CrossRef] [PubMed]
39. Mantovani, A.; Petracca, G.; Beatrice, G.; Csermely, A.; Lonardo, A.; Targher, G. Glucagon-Like Peptide-1 Receptor Agonists for Treatment of Nonalcoholic Fatty Liver Disease and Nonalcoholic Steatohepatitis: An Updated Meta-Analysis of Randomized Controlled Trials. *Metabolism* **2021**, *11*, 73. [CrossRef]
40. Newsome, P.N.; Buchholtz, K.; Cusi, K.; Linder, M.; Okanoue, T.; Ratziu, V.; Sanyal, A.J.; Sejling, A.-S.; Harrison, S.A. A Placebo-Controlled Trial of Subcutaneous Semaglutide in Nonalcoholic Steatohepatitis. *N. Engl. J. Med.* **2021**, *384*, 1113–1124. [CrossRef] [PubMed]
41. Armstrong, M.J.; Gaunt, P.; Aithal, G.P.; Barton, D.; Hull, D.; Parker, R.; Hazlehurst, J.M.; Guo, K.; Abouda, G.; Aldersley, M.A.; et al. Liraglutide safety and efficacy in patients with non-alcoholic steatohepatitis (LEAN): A multicentre, double-blind, randomised, placebo-controlled phase 2 study. *Lancet* **2016**, *387*, 679–690. [CrossRef]
42. Honda, Y.; Imajo, K.; Kato, T.; Kessoku, T.; Ogawa, Y.; Tomeno, W.; Kato, S.; Mawatari, H.; Fujita, K.; Yoneda, M.; et al. The Selective SGLT2 Inhibitor Ipragliflozin Has a Therapeutic Effect on Nonalcoholic Steatohepatitis in Mice. *PLoS ONE* **2016**, *11*, e0146337. [CrossRef]
43. Taheri, H.; Malek, M.; Ismail-Beigi, F.; Zamani, F.; Sohrabi, M.; Babaei, M.R.; Khamseh, M.E. Effect of Empagliflozin on Liver Steatosis and Fibrosis in Patients With Non-Alcoholic Fatty Liver Disease Without Diabetes: A Randomized, Double-Blind, Placebo-Controlled Trial. *Adv. Ther.* **2020**, *37*, 4697–4708. [CrossRef]
44. DeFronzo, R.A.; Norton, L.; Abdul-Ghani, R.A.D.L.N.M. Renal, metabolic and cardiovascular considerations of SGLT2 inhibition. *Nat. Rev. Nephrol.* **2017**, *13*, 11–26. [CrossRef] [PubMed]

45. Ridderstråle, M.; Andersen, K.R.; Zeller, C.; Kim, G.; Woerle, H.J.; Broedl, U.C. Comparison of empagliflozin and glimepiride as add-on to metformin in patients with type 2 diabetes: A 104-week randomised, active-controlled, double-blind, phase 3 trial. *Lancet Diabetes Endocrinol.* **2014**, *2*, 691–700. [CrossRef]
46. Cherney, D.Z.I.; Dekkers, C.C.J.; Barbour, S.J.; Cattran, D.; Gafor, A.H.A.; Greasley, P.J.; Laverman, G.D.; Lim, S.K.; Di Tanna, G.L.; Reich, H.N.; et al. Effects of the SGLT2 inhibitor dapagliflozin on proteinuria in non-diabetic patients with chronic kidney disease (DIAMOND): A randomised, double-blind, crossover trial. *Lancet Diabetes Endocrinol.* **2020**, *8*, 582–593. [CrossRef]
47. Papazafiropoulou, A.K.; Melidonis, A.; Antonopoulos, S. Effects of glucagon-like peptide-1 receptor agonists and sodium-glucose cotransporter 2 inhibitors on cardiorenal and metabolic outcomes in people without diabetes. *Curr. Pharm. Des.* **2020**. [CrossRef]
48. Petrie, M.C.; Verma, S.; Docherty, K.F.; Inzucchi, S.E.; Anand, I.; Belohlávek, J.; Böhm, M.; Chiang, C.-E.; Chopra, V.K.; De Boer, R.A.; et al. Effect of Dapagliflozin on Worsening Heart Failure and Cardiovascular Death in Patients With Heart Failure With and Without Diabetes. *JAMA* **2020**, *323*, 1353–1368. [CrossRef]
49. Frías, J.P.; Guja, C.; Hardy, E.; Ahmed, A.; Dong, F.; Öhman, P.; Jabbour, S.A. Exenatide once weekly plus dapagliflozin once daily versus exenatide or dapagliflozin alone in patients with type 2 diabetes inadequately controlled with metformin monotherapy (DURATION-8): A 28 week, multicentre, double-blind, phase 3, randomised controlled trial. *Lancet Diabetes Endocrinol.* **2016**, *4*, 1004–1016. [CrossRef] [PubMed]
50. Ishihara, H.; Yamaguchi, S.; Nakao, I.; Sakatani, T. Ipragliflozin Add-on Therapy to a GLP-1 Receptor Agonist in Japanese Patients with Type 2 Diabetes (AGATE): A 52-Week Open-Label Study. *Diabetes Ther.* **2018**, *9*, 1549–1567. [CrossRef]
51. Ludvik, B.; Frías, J.P.; Tinahones, F.J.; Wainstein, J.; Jiang, H.; Robertson, K.E.; García-Pérez, L.-E.; Woodward, D.B.; Milicevic, Z. Dulaglutide as add-on therapy to SGLT2 inhibitors in patients with inadequately controlled type 2 diabetes (AWARD-10): A 24-week, randomised, double-blind, placebo-controlled trial. *Lancet Diabetes Endocrinol.* **2018**, *6*, 370–381. [CrossRef]
52. Martinez, R.; Al-Jobori, H.; Ali, A.M.; Adams, J.; Abdul-Ghani, M.; Triplitt, C.; DeFronzo, R.A.; Cersosimo, E. Endogenous Glucose Production and Hormonal Changes in Response to Canagliflozin and Liraglutide Combination Therapy. *Diabetes* **2018**, *67*, 1182–1189. [CrossRef] [PubMed]

biomedicines

MDPI

Article

Mitochondrial Transfer by Human Mesenchymal Stromal Cells Ameliorates Hepatocyte Lipid Load in a Mouse Model of NASH

Mei-Ju Hsu [1,†], Isabel Karkossa [2,†], Ingo Schäfer [3], Madlen Christ [1], Hagen Kühne [1], Kristin Schubert [2], Ulrike E. Rolle-Kampczyk [2], Stefan Kalkhof [2,4,5], Sandra Nickel [1], Peter Seibel [3], Martin von Bergen [2,6] and Bruno Christ [1,*]

1 Applied Molecular Hepatology Laboratory, Department of Visceral, Transplant, Thoracic and Vascular Surgery, University of Leipzig Medical Center, 04103 Leipzig, Germany; hsumeiju@gmail.com (M.-J.H.); madlen.christ@medizin.uni-leipzig.de (M.C.); hagen.kuehne@freenet.de (H.K.); sandra.brueckner@medizin.uni-leipzig.de (S.N.)
2 Department of Molecular Systems Biology, Helmholtz Centre for Environmental Research (UFZ), 04318 Leipzig, Germany; isabel.karkossa@ufz.de (I.K.); kristin.schubert@ufz.de (K.S.); ulrike.rolle-kampczyk@ufz.de (U.E.R.-K.); stefan.kalkhof@hs-coburg.de (S.K.); martin.vonbergen@ufz.de (M.v.B.)
3 Molecular Cell Therapy, Center for Biotechnology and Biomedicine, Leipzig University, 04103 Leipzig, Germany; ingo.schaefer@bbz.uni-leipzig.de (I.S.); peter.seibel@bbz.uni-leipzig.de (P.S.)
4 Institute for Bioanalysis, University of Applied Sciences Coburg, 96450 Coburg, Germany
5 Department of Therapy Validation, Fraunhofer Institute for Cell Therapy and Immunology, 04103 Leipzig, Germany
6 Institute of Biochemistry, Leipzig University, 04103 Leipzig, Germany
* Correspondence: bruno.christ@medizin.uni-leipzig.de; Tel.: +49-341-97-13552
† These authors contributed equally to this work.

Received: 14 August 2020; Accepted: 10 September 2020; Published: 14 September 2020

Abstract: Mesenchymal stromal cell (MSC) transplantation ameliorated hepatic lipid load; tissue inflammation; and fibrosis in rodent animal models of non-alcoholic steatohepatitis (NASH) by as yet largely unknown mechanism(s). In a mouse model of NASH; we transplanted bone marrow-derived MSCs into the livers; which were analyzed one week thereafter. Combined metabolomic and proteomic data were applied to weighted gene correlation network analysis (WGCNA) and subsequent identification of key drivers. Livers were analyzed histologically and biochemically. The mechanisms of MSC action on hepatocyte lipid accumulation were studied in co-cultures of hepatocytes and MSCs by quantitative image analysis and immunocytochemistry. WGCNA and key driver analysis revealed that NASH caused the impairment of central carbon; amino acid; and lipid metabolism associated with mitochondrial and peroxisomal dysfunction; which was reversed by MSC treatment. MSC improved hepatic lipid metabolism and tissue homeostasis. In co-cultures of hepatocytes and MSCs; the decrease of lipid load was associated with the transfer of mitochondria from the MSCs to the hepatocytes via tunneling nanotubes (TNTs). Hence; MSCs may ameliorate lipid load and tissue perturbance by the donation of mitochondria to the hepatocytes. Thereby; they may provide oxidative capacity for lipid breakdown and thus promote recovery from NASH-induced metabolic impairment and tissue injury.

Keywords: non-alcoholic steatohepatitis (NASH); tunneling nanotubes (TNTs); primary hepatocytes; organelle transfer; mesenchymal stromal cells

1. Introduction

Obesity is a prevalent health problem worldwide, which has been attributed mainly to Western-style diets in combination with reduced physical activity. It is often associated with metabolic co-morbidities, such as diabetes type 2 and non-alcoholic fatty liver diseases (NAFLD), the latter of which has a global prevalence of 24% and is currently the leading cause of chronic liver disease in Europe and in the USA [1]. NAFLD may progress from simple steatosis to chronically inflammatory diseases like non-alcoholic steatohepatitis (NASH), cirrhosis, and hepatocellular carcinoma (HCC) [2,3]. On the cellular level, hepatocyte mitochondrial, peroxisomal and microsomal oxidation of fatty acids, and basal lipophagy [4] are involved in the utilization of hepatic lipids. However, impairment of lipid metabolism may cause an imbalance of utilization and storage, eventually contributing to hepatocyte lipid overload. Lipotoxicity induces endoplasmic reticulum (ER) stress, leading to calcium release from the ER, thus raising cytosolic calcium levels, which in turn interferes with protective autophagy and inhibits the breakdown of lipids, thus aggravating cellular lipid overload [5]. In addition, mitochondrial dysfunction is contributing to the pathogenesis of NAFLD by favoring hepatic lipid storage, and by promoting the production of reactive oxygen species (ROS) as well as lipid peroxidation [6–8]. Besides mitochondrial β-oxidation, peroxisomes are involved in long-chain fatty acid β-oxidation and microsomes in ω-oxidation of fatty acids. Like mitochondrial impairment, dysfunction of peroxisomal and microsomal fatty acid metabolism contributes to the pathogenesis of NASH by favoring lipid storage and production of ROS, respectively [9,10].

Pharmacological therapy may address NASH-associated co-morbidities like diabetes [11], yet, liver transplantation in NASH patients has been shown to reduce the risk of progression into HCC [12,13]. Indeed, NASH features the second most common indication for liver transplantation in the USA [1,14]. However, the invasiveness of organ transplantation, lifelong immune suppression, the shortage of donor livers, and eventually the high costs altogether fostered the search for alternative therapy approaches [15,16]. Mesenchymal stromal cells (MSCs) have been demonstrated to ameliorate NASH in rodent animal models [17–19]. Transplantation of hepatocyte-like cells derived from human bone marrow mesenchymal stromal cells (MSCs) alleviated lipid load, ameliorated hepatic inflammation as well as fibrosis, and enhanced proliferation of host hepatocytes in an experimental model of NASH in the immunodeficient mouse [20]. In line, transplantation of MSCs decreased fibrosis and activation of hepatic stellate cells in mouse and rat liver cirrhosis triggered by carbon tetrachloride (CCl_4) [21,22]. MSC restored ammonia and purine metabolism in a mouse model of acute liver failure [23], improved acute liver injury caused by acetaminophen [24], and enhanced liver regeneration in mice and rats after extended hepatectomy [25,26]. Clinically, the application of MSC ameliorated inborn errors of liver metabolism, such as ornithine carbamoyltransferase deficiency [27], decreased the severe bleeding complications in a hemophilia A patient [28], and improved liver function in cirrhotic patients [29–31]. However, some studies revealed only transient or even negligible effects of MSC treatment of liver diseases [32,33]. Thus, the identification of the mechanisms involved in MSC action is crucial to improve the therapeutic potential of MSCs.

Here, we showed in a mouse model of NASH and in co-cultures of fat-laden hepatocytes and MSCs that MSCs shifted pathological lipid storage to utilization likely by the transfer of MSC-derived functional mitochondria to the hepatocytes.

2. Experimental Section

2.1. Experimental Design

Xenotransplantation of human bone marrow-derived mesenchymal stromal cells was performed in immunodeficient Pfp/Rag2$^{-/-}$ mice (C57BL6, B6.129S6-Rag2(tm1Fwa)Prf1(tm1Clrk)N12. Taconic; Ejby, Denmark). At the age of 12 weeks, male mice were either fed a NASH−inducing methionine-choline-deficient diet (MP Biomedicals, Eschwege, Germany), or kept on a standard rodent chow. After five weeks of feeding, all mice underwent 1/3 partial hepatectomy and received 1.5×10^6 human MSCs

(differentiated into the hepatocytic lineage) via splenic injection as described before [34]. PBS served as the vehicle control. The four resulting groups represented +NASH+MSC, +NASH-MSC, -NASH+MSC, and -NASH-MSC. The procedures for the isolation and hepatocytic differentiation of MSCs from human bone marrow have been described in detail previously [35], and were approved by the Institutional Ethics Review Board Leipzig (Ethik-Kommission an der Medizinischen Fakultät der Universität Leipzig; file no. 282/11-lk; 1 December 2016). After surgery, respective feeding regimes were continued for another week until mice were sacrificed, and livers harvested. Mice were housed under controlled conditions at a 12-h light/dark cycle, at an ambient temperature of 22 ± 2 °C, and humidity of 50%–60%. All experimental procedures involving animals were approved by the federal authorities of Saxony (Saxon State Directorate Chemnitz; file no. TVV_54_16; 2 May 2017) and followed the guidelines of the animal welfare act.

2.2. Proteome and Metabolome Analyses

2.2.1. Liver Metabolite and Protein Extraction and Preparation for Protein Quantification by Stable Isotope Labeling of Mammals (SILAM)

Frozen liver tissue samples (100–200 mg) were homogenized with a ball mill in 500 µL of lysis buffer A (40 mM Tris base, 7 M urea, 4% CHAPS, 100 mM dithiothreitol (DTT), 0.5% (*v*/*v*) biolyte). Benzonase was added and the homogenates were incubated at room temperature for 20 min and afterwards centrifuged at 12.000× *g* for 20 min at 30 °C. The resulting supernatant was collected, and the pellet was again extracted using 500 µL of lysis buffer B (40 mM Tris base, 5 M urea, 2 M thiourea, 4% CHAPS, 100 mM DTT, 0.5% (*v*/*v*) biolyte). After centrifugation, the supernatants of the first and the second extraction were combined. Then, 50 µL of the combined supernatants were desalted to 50 mM ammonium bicarbonate by centrifugal filtration using filtration units (molecular weight cutoff of 10 kDa, Vivacon 500, Sartorius Group, Göttingen, Germany). The permeate was applied for metabolomics analyses. The protein concentrations in the retentate were determined using a detergent-compatible colorimetric protein assay (660 nm Protein Assay, Thermo Scientific–Pierce, Dreieich, Germany). Analogously, a protein extract of a liver of a $^{13}C_6$-lysine-labeled black6 mouse ($^{13}C_6$-lysine, 97%, Cambridge Isotope Laboratories, Inc., Tewksbury, MA, USA) was prepared as an isotope-labeled standard.

2.2.2. In-Gel Tryptic Digestion and Liquid Chromatography-Tandem Mass Spectrometry (GeLC-MS/MS)

Protein mixtures were mixed with 0.5 M Tris-HCl buffer (pH 6.8) containing 40% (*v*/*v*) SDS, 20% (*v*/*v*) glycerol, 2% (*v*/*v*) bromophenol-blue, and 10% (*v*/*v*) 2-mercaptoethanol. After heating for 5 min at 95 °C, a 1-D-SDS-PAGE was carried out using Laemmli's protocol. Proteins were stained with Coomassie Brillant Blue G-250 and each lane was cut into 10 pieces of equal size. Gel pieces were washed twice in 200 µL of ACN/50 mM ABC (ammonium bicarbonate, Fluka (Thermo Fisher Scientific, Dreieich, Germany), 1:1, (*v*/*v*)) for 10 min at room temperature (RT). Reduction and alkylation of disulfide bonds were performed by adding 10 mM dithiothreitol/10 mM ABC (Thermo Fisher Scientific, Dreieich, Germany) for 30 min at RT followed by incubation in 100 mM iodacetamide/10 mM ABC (Sigma-Aldrich, Taufkirchen, Germany) for 30 min at RT in the dark. After another washing step in 10 mM ABC for 10 min at RT, proteins were digested by incubating each gel slice with 300 ng of trypsin (Promega, Mannheim, Germany) in 50 mM ABC at 37 °C overnight. Proteolysis was quenched by 10% formic acid and proteolytic peptides were extracted. Samples were dried by vacuum centrifugation and resuspended in 20 µL of 0.1% formic acid. Extracted peptides were analyzed by online reversed-phase nanoscale liquid chromatography tandem mass spectrometry on a NanoAcquity UPLC system (Waters Corporation, Milford, MA, USA) connected to an LTQ-Orbitrap XL ETD (Thermo Fisher Scientific, Waltham, MA, USA) and equipped with a chip-based nano ESI source (TriVersaNanoMate, Advion, Ithaca, NY, USA) as described previously [36]. Protein identification and relative quantification were performed using Proteome Discoverer (version 1.4, Thermo Scientific,

Bremen, Germany). Oxidation (methionine) and acetylation (protein N-termini) were used as variable modifications, while carbamidomethylation (cysteine) was set as a fixed modification. A database search was carried out by the search engine MASCOT against the UniProt mouse reference proteome (www.uniprot.org, 05-2014). Relative protein quantification was performed based on the measured ratios (treated mouse vs. isotopically labeled mouse standard) of all lysine-containing peptides. Fold changes (FCs) between different groups were calculated in reference to the internal control.

2.2.3. Metabolome

Targeted metabolomics was conducted using the AbsoluteIDQ p150 kit (BIOCRATES Life Sciences AG, Innsbruck, Austria) as described before [26]. In brief, metabolites were extracted from the livers as descripted above, and prepared according to the manufacturer's protocol [37]. Multiple reaction monitoring was carried out on an Agilent 1100 series binary HPLC system (Agilent Technologies, Waldbronn, Germany) coupled to a 4000 QTRAP (AB Sciex, Darmstadt, Germany) via a TurboIon spray source. The data evaluation for the quantification of metabolite concentrations was performed with the MetIQ software package.

2.3. Combined Analysis and Visualization of Proteome and Metabolome Data

2.3.1. Weighted Gene Correlation Network Analysis (WGCNA)

FCs of proteins and metabolites were analyzed in R-3.5.0 with the use of several packages [38–46]. Hierarchical clustering was conducted with Euclidean distance measure. To unravel changes for single proteins and metabolites, the data were filtered for analytes that were quantified at least in duplicate for the particular comparison, and the Student's *t*-test was performed for analytes that were identified at least in triplicate (Supplementary Material file 1, FCs and *p*-values proteomics, FCs and *p*-values metabolomics). For WGCNA, the average log2-transformed FCs of proteins and metabolites that were quantified at least in duplicate over all data sets (406 proteins and 148 metabolites) were scaled to integer values between 0 and 100 (Supplementary Material file 1, WGCNA data). The networks were constructed across all the measured samples with the R package WGCNA [47] as described before [48]. The used trait matrix, containing the different comparisons, may be found in the Supplementary Material file 1, WGCNA trait matrix. The soft power threshold for WGCNA was set to 18 to arrive at the network adjacency. The Topology Overlap Matrix (TOM) was created using a cut height of 0.15 and a minimum module size of 25. The analysis identified 11 modules of co-expressed analytes, identified with different colors. A summary of the analytes that were assigned to each module can be found in the Supplementary Material file 1, WGCNA module contents. Finally, for each of the obtained modules, significantly enriched KEGG (Kyoto Encyclopedia of Genes and Genomes) pathways were determined using R-3.5.0 [49–51] without defining a *p*-value threshold. For this purpose, the mouse database was used as background [52]. Lists of all enriched pathways for each module can be found in the Supplementary Material file 1, WGCNA KEGG results.

2.3.2. Identification of Key Drivers

Identification of trait-specific key drivers was performed based on the WGCNA results as described before [48]. Therefore, module- and trait-specific gene significances and module memberships were calculated for each analyte. Key drivers were assumed to be analytes with absolute gene significance ≥0.75 and absolute module membership ≥0.75 (Supplementary Material file 1, WGCNA key drivers). Gene names (Supplementary Material file 1, FCs and *p*-values proteomics) and KEGG pathways (Supplementary Material file 1, KEGG pathway mapping) were assigned to proteins using the DAVID Bioinformatics Resources 6.8 [53]. Thus, key drivers for the observed effects were identified. From the whole proteome, proteins that are related to mmu03320: PPAR signaling pathway, mmu04975: Fat digestion and absorption, mmu04610: Complement and coagulation cascades, mmu00190: Oxidative phosphorylation, mmu00480: Glutathione metabolism, mmu04932:

Non-alcoholic fatty liver disease (NAFLD), mmu04146: Peroxisome, mmu00061: Fatty acid biosynthesis, mmu00062: Fatty acid elongation, mmu01212: Fatty acid metabolism, and mmu00071: Fatty acid degradation were extracted for deeper insights into effects (Supplementary Material file 2, Figure S1).

2.4. Immunohistochemistry

A comprehensive list of antibodies used throughout this study is given in Supplementary Material file 2, Table S1. Mouse livers were fixed in 4% paraformaldehyde overnight and embedded in paraffin. Slices of 1 µm were dewaxed and rehydrated by standard procedures. Heat-mediated epitope retrieval was done in either citrate buffer (pH 6.0) or Tris-EDTA buffer (pH 9.0) for 30 min. Endogenous peroxidases were blocked with 3% hydrogen peroxide/methanol for 20 min followed by a 60-min blocking step in 5% BSA/0.5% Tween20, and additionally a 15-min avidin and 15-min biotin block (SP-2001, Avidin-Biotin Blocking Kit, Vectorlabs, Eching, Germany). Primary antibodies against Cyp2e1 (1:200, ab28146, abcam, Cambridge, UK) and 4-HNE (1:500, HNE11-S, Alpha Diagnostic International, San Antonio, TX, USA) were applied overnight at 4 °C, subsequently coupled to biotin-labelled secondary goat anti-rabbit antibody (1:200, 111-065-003, Dianova, Hamburg, Germany), and visualized by the Vectastain Elite ABC Kit (PK-6100, Vectorlabs, Eching, Germany) followed by DAB chromogen (Thermo Fisher Scientific, Dreieich, Germany) incubation. Hematoxylin was used as a nuclei counterstain. For immunofluorescence, slices were blocked in 5% goat serum/PBS (ccpro, Oberdorla, Germany) for 20 min and in 5% BSA/0.5% Tween20 for 60 min. Sections were subsequently incubated with primary antibodies against CD36 (1:100, NB400-144, Novusbio, Wiesbaden-Nordenstadt, Germany), E-cadherin (1:200, BD 610182, eBioscience, Heidelberg, Germany), and β-catenin (1:500, BD 610154, eBioscience, Heidelberg, Germany) overnight at 4 °C. Corresponding secondary antibodies, i.e., goat anti-rabbit AlexaFlour 568 (1:200, A11036, Life Technologies, Ober-Olm, Germany) to CD36, goat-anti-mouse Cy3 (1: 300, 115-165-003, Dianova, Hamburg, Germany) to E-cadherin, and goat anti-mouse AlexaFlour 488 (1:300, 115-545-003, Dianova, Hamburg, Germany) to β-catenin, were applied for 1 h at room temperature followed by nuclear staining with DAPI (1:1000, Carl Roth GmbH + Co. KG, Karlsruhe, Germany) for 5 min, respectively. Slides were mounted with 50% glycerol solution and lacquer, and images taken using the Zeiss Axio Observer.Z1 microscope. For the co-stain of human mitochondria in mouse hepatocytes, antigen retrieval using dewaxed slices was performed by heating for 30 min in citrate buffer (14,746, SignalStain unmasking solution, Cell Signaling Technology, Frankfurt/Main, Germany) and subsequent cooling on ice for 30 min. After two washings in PBS, slices were blocked for 80 min using 5% goat serum and 0.3% TritonX-100 in PBS. Primary antibodies against mouse cyclophilin A (1:100, 2175, Cell Signaling Technology, Frankfurt/Main, Germany) and anti-human mitochondria (1:200, MAB 1273, Millipore, Darmstadt, Germany) were added overnight at 4 °C, and slices washed 3 times with PBS thereafter. The first secondary antibody (1:200 goat anti-mouse Cy3; 115-165-003, Dianova, Hamburg, Germany) was added for 60 min at room temperature and slices were washed 2 times for 10 min each with PBS. The second secondary antibody (1:500 goat anti-rabbit AlexaFluor 488, 4412, Cell Signaling Technology, Frankfurt/Main, Germany) was added for 60 min at room temperature. After 3 washings for 5 min each with PBS, nuclei were stained with DAPI and slides finally mounted with 50% glycerol solution and lacquer. Images were taken using the Zeiss Axio Observer.Z1 microscope equipped with ApoTome.2 at 40× magnification.

2.5. Western Blotting

In total, 30–40 mg of liver tissue were lysed in RIPA buffer (50 mM Tris, 150 mM NaCl, 0.1% SDS, 1% Triton X-100, 1 mM EDTA+EGTA, 0.5% Na-deoxycholate, pH 7.5) supplemented with protease inhibitors (Roche, Mannheim, Germany). Crude lysates were centrifuged at 13,000 rpm for 15 min and the clear supernatant was collected. The protein concentration was determined by the bicinchoninic acid assay. Then, 50 µg of protein were subjected to standard SDS gel electrophoresis and blotted onto PVDF membranes. Non-specific binding was blocked with 5% skim milk (vinculin), or 5% BSA (PPARα, CD36) in Tris-buffered saline Tween-20 (TBS-T) for two hours. The primary and secondary antibodies

used were as follows: anti-PPARα (1:1000, MAI-822 Thermo Fischer Scientific, Dreieich, Germany), anti-CD36 (1:1000, NB400-144, Novusbio, Wiesbaden-Nordenstadt, Germany), anti-Vinculin (1:3000, 05-386, Merck, Darmstadt, Germany), anti-rabbit-HRP (1:7500, BD 554021, eBioscience, Heidelberg, Germany), and anti-mouse-HRP (1:7500, BD 554002, eBioscience, Heidelberg, Germany). Blots were developed using the enhanced chemiluminescence Prime reagent kit (GE Healthcare, Buckinghamshire, UK). Vinculin was used for the normalization and calculation of the relative abundances.

2.6. Quantification of Liver Triglyceride Content

In total, 100 mg of liver tissue were homogenized in 1 mL of 5% Igepal (I3021, Sigma-Aldrich, Taufkirchen, Germany) using a pestle and mortar. Samples were heated for 4 min at 95 °C in a thermomixer, cooled at room temperature, heated again, and then centrifuged using a microcentrifuge at maximal speed. Supernatants were collected and diluted 1:10 with distilled water. Then, 25 µL of the samples were pre-warmed at 37 °C for 1–5 min and subjected to the Triglyceride Assay Kit-Quantification (ab65336, Abcam, Berlin, Germany), essentially as described by the supplier.

2.7. Isolation of Primary Mouse Hepatocytes and Co-Culture with Hepatocytic Differentiated MSCs

Primary hepatocytes (HCs) were isolated from male Pfp/Rag2$^{-/-}$ mouse livers by the two-step liver perfusion with collagenase (NB4G, Serva Electrophoresis GmbH, Heidelberg, Germany) as described [54]. HCs and hepatocytic differentiated MSCs at the cell number ratios as indicated were initially seeded onto collagen-coated dishes at a total cell density of 40,000 cells/cm^2 and grown for 3 h in minimal essential medium (MEM) (Merck, Darmstadt, Germany) containing 2% fetal calf serum (FCS) (Gibco, Darmstadt, Germany) to allow for attachment. The medium was replaced by either standard hepatocyte growth medium (HGM, [55]) supplemented with EGF and HGF (20 ng/mL each) serving as the control, or two different steatosis-inducing media: methionine-choline-deficient (MCD, c.c.pro Oberdorla, Germany) or HGM supplemented with 0.5 mM palmitic acid (C16:0). To identify potential paracrine effects mediated by the MSCs, conditioned media were collected from MSCs, hepatocytes, and co-cultures of both after 2 days of culture, centrifuged at 270× *g* to remove cell debris, and subsequently used to treat hepatocytes under control (HGM) and treatment conditions (MCD or C16:0) for an additional 1 and 2 days. Phase contrast pictures were captured with a Primovert inverted microscope with the Zen software (Zeiss, Jena, Germany).

2.8. Cell Labeling with Fluorescent Vital Dyes

To highlight MSCs in co-culture with hepatocytes using a fluorescence microscope, MSCs in suspension were pre-labeled prior to seeding with either 5-(and 6)-carboxyfluorescein diacetate succinimidyl ester (CFSE; Ex/Em: 494/521) or CellTrace Yellow (Ex/Em: 546/579) at a final concentration of 5 µM by shaking in the dark at 37 °C for 30 min. Cells were subsequently washed with PBS containing 20% of FCS, followed by two washes with 5% FCS [56]. Fluorescent dyes as mentioned above were from Thermo Fisher Scientific, Dreieich, Germany. To label mitochondria, MSCs in suspension were stained with 500 nM of MitoTracker Deep Red (Ex/Em: 644/665) or 150 nM of MitoTracker Red CMXRos (Ex/Em: 579/599) in PBS at 37 °C for 45 min with gentle shaking, followed by 3 washes with PBS. MitoTracker dyes were kindly provided by Prof. Dr. Lea Ann Dailey and Dr. Lysann Tietze, Institute of Pharmacy, University of Halle-Wittenberg, Halle, Germany. Labeled cells in suspension were kept in the dark on ice prior to further use.

2.9. Fluorescence Staining after Cell Fixation

Cells grown on coverslips were fixed with 3.7% formaldehyde at room temperature for 15 min, followed by 3 washings with PBS. Neutral triglycerides and lipids were labeled with Oil red O (ORO) as previously described [57]. For immunostaining, fixed cells were permeabilized with 0.1% Triton X-100 for 5 min at RT, followed by blocking with PBS containing 5% BSA for 1 h and additional blocking with 5% normal goat serum for 1 h. Cells were further stained with the mouse anti-human mitochondria

antibody (1:400, MAB1273, Millipore, Darmstadt, Germany), or the rabbit anti-apoptosis-inducing factor (AIF) antibody (1:400, Rabbit mAb 5318, Cell Signaling Technology, Frankfurt/Main, Germany, kindly provided by Prof. Dr. Gabriela Aust, Department of Visceral, Transplant, Thoracic and Vascular Surgery, University of Leipzig Medical Center, Leipzig, Germany) in 1% BSA overnight at 4 °C. The following day, cells were incubated with goat anti-mouse antibodies conjugated with Cy3 (115-165-003, Dianova, Hamburg, Germany) or goat anti-rabbit antibodies conjugated with Alexa Fluor 488 (A11008, Thermo Fisher Scientific, Dreieich, Germany). To visualize cell morphology and discriminate between MSCs and hepatocytes, cells were stained with 0.1% CytoPainter Phalloidin-iFlour405 (ab176752, Abcam, Berlin, Germany) in 1% BSA in PBS for 1.5 h at RT to label F-actin. Where indicated, nuclei were counterstained with 1 μg/mL of 4,6-diamidino-2-phenylindole (DAPI).

2.10. Image Capture and Analysis

Images were taken using the Zeiss Axio Observer.Z1 inverted microscope at 20× magnification, or with ApoTome.2 at 40×. Lipid content was quantified by image analysis using the ImageJ software (ImageJ 1.42, National Institutes of Health, Bethesda, MD, USA). Results were normalized as the percentage amount of stain/100 HCs out of 6-10 microscopic visual fields per group. Results from 4 independent experiments are expressed as mean ± standard deviation (SD). Pictures of time-lapse live cell imaging were captured at an interval of 15 min using a laser scanning confocal microscope (Leica Microsystems, Wetzlar, Germany) at a magnification of 20×. One-μm-thick sections were acquired with a total z volume of 25 μm, and the maximum intensity projections are presented (cf. Figure 5B,C, and Supplementary Material file 2, Figure S6A–C).

2.11. Morphological Subtyping of Mitochondria

The cells were stained with 150 nM of MitoTracker Red CMXRos as described under 'Cell labeling with fluorescent vital dyes', followed by fixation. Pictures were captured using the Zeiss Axio Observer.Z1 inverted microscope equipped with ApoTome.2 with a 40× objective. Intact cells were cropped using Adobe Photoshop CS6 (v. 13.0, München, Germany). On average, the mitochondrial morphology of 18.31 hepatocytes and 12.58 MSC per group was analyzed by the automatic subtyping and quantification software MicroP, as developed and described by Peng et al. [58].

2.12. RNA Isolation, cDNA Synthesis and PCR

RNA was isolated using the QIAzol Lysis Reagent (Qiagen, Hilden, Germany). The cDNA was synthesized using the Maxima H Minus First Strand cDNA Synthesis Kit (Thermo Fischer Scientific, Dreieich, Germany). PCR was carried out using the PCR Master Mix (2×) (Thermo Fischer Scientific, Dreieich, Germany) and appropriate primer pairs as listed in Supplementary Material file 2, Table S2. PCR products were separated in Tris/borate/EDTA (TBE) agarose gels and quantified with ImageJ. Beta-2-microglobulin (B2M) was used for normalization.

2.13. Statistical Analysis

Results are shown as means ± standard deviation (SD) from 3–7 livers in each group run in analytical duplicates unless otherwise indicated. Statistical comparisons, if not otherwise indicated, were made using either the paired *t*-test or two-way ANOVA. Differences between groups were considered significant at a p value of ≤ 0.05.

3. Results

We and others have shown that the transplantation of mesenchymal stromal cells into mice suffering from NASH attenuated the lipid load, reduced inflammation, and resolved fibrosis [18,34,59,60]. Yet, the mechanism behind remained mainly elusive. Here, we aimed by omics approaches in combination with network analyses to identify pathways and key players in NASH, which were affected by MSC

treatment. Potential mechanisms of MSC action as deduced from the WGNCA were investigated in co-cultures of hepatocytes and MSCs.

3.1. WGCNA Suggests a Shift from Lipid Storage to Utilization by MSCs

Based on the protein and metabolite intensities, which were obtained by applying untargeted proteomics and targeted metabolomics to mouse livers, ratios were calculated for the following comparisons to get insights into the mechanisms of the MSC treatment: +NASH-MSC vs. -NASH-MSC, +NASH+MSC vs. -NASH-MSC, -NASH+MSC vs. -NASH-MSC, +NASH+MSC vs. +NASH-MSC, +NASH-MSC vs. -NASH+MSC, and +NASH+MSC vs. -NASH+MSC. Those values were used for further analyses.

By WGCNA, co-expressed proteins and metabolites were summarized into modules, followed by correlation of the obtained module eigengenes (modules first principal component) with traits. In total, 11 modules were identified and the results of the correlation with selected traits are shown in Figure 1A, while the complete module–trait correlation can be found in Supplementary Material file 2, Figure S2. For each of the obtained modules, significantly enriched pathways were determined using KEGG (Kyoto Encyclopedia of Genes and Genomes, Supplementary Material file 1, WGCNA KEGG results). Anti-correlations for NASH and MSCs are observable for the magenta, turquoise, black, and blue module, showing significant (p-value ≤ 0.05) enrichment of KEGG pathways related to amino acid biosynthesis and central carbon metabolism (Supplementary Material file 2, Figure S2). Additionally, in the case of +NASH-MSC vs. -NASH-MSC and +NASH+MSC vs. +NASH-MSC, the described anti-correlation was observable but for the red, brown, green, green-yellow, yellow, and purple module that also showed significant enrichment of pathways connected to amino acid metabolism and central carbon metabolism, and in addition also to fatty acid degradation and metabolism as well as peroxisome proliferator-activated receptor (PPAR) signaling. The PPAR signaling showed the highest enrichment in the brown module, which positively correlated with +NASH-MSC vs. -NSH-MSC and negatively with +NASH+MSC vs. +NASH-MSC. This indicates that proteins that are assigned to this pathway in KEGG tended to show increased abundances upon NASH and decreased abundances upon MSC treatment. Interestingly, the comparison of +NASH+MSC vs. -NASH-MSC did not lead to high correlations, neither in the brown module containing PPAR signaling pathway-related proteins, nor in most of the other modules, indicating that the MSCs were successfully used to treat NASH, resulting in expression profiles similar to what was observable in the control group (Figure 1A).

Furthermore, a key driver analysis was conducted for the traits NASH and +NASH+MSC vs. +NASH-MSC based on the WGCNA results (Supplementary Material file 1, WGCNA key drivers). This analysis allowed the identification of analytes that were highly connected to the particular modules and traits, suggesting their critical role as mediators for the observed effects (Supplementary Material file 2, Figure S3). KEGG pathways were assigned to all, within this study, identified proteins (Supplementary Material file 1, KEGG pathway mapping) to identify the functions of the selected key drivers. Thereby, we focused on the following KEGG pathways: Non-alcoholic fatty liver disease (NAFLD), PPAR signaling pathway, fat digestion and absorption, complement and coagulation cascades, oxidative phosphorylation, glutathione metabolism, peroxisome, fatty acid biosynthesis, fatty acid elongation, fatty acid metabolism, and fatty acid degradation (Supplementary Material file 2, Figure S1). Figure 1B shows Log2(FCs) and p-values for a selection of the obtained key drivers. Apparently, metabolites gave information about NASH effects and more importantly also about effects upon MSC treatment. This was also true for the identified key driver proteins that furthermore gave insights into affected pathways. Proteins that were identified to be key drivers were mainly related to cellular stress (e.g., Sod2, Gstm2, Mgst1, Gstp1), as indicated by their contribution to the KEGG pathways glutathione metabolism and peroxisome. Furthermore, lipid metabolism was affected (e.g., Apob, Fasn), with an assignment of key drivers to fat digestion and absorption as well as fatty acid biosynthesis and metabolism. Interestingly, several of the identified key drivers showed opposite Log2(FCs) for +NASH+MSC vs. +NASH-MSC compared to the other investigated ratios, indicating

that the MSC treatment of NASH compensated the NASH effects. In summary, the WGCNA showed an anti-correlation of NASH effects and effects upon MSC treatment as well as only minor effects for the MSC-treated NASH as compared to the control group. This indicated that MSCs reversed NASH effects, which was also confirmed by the expression profiles of the identified key drivers.

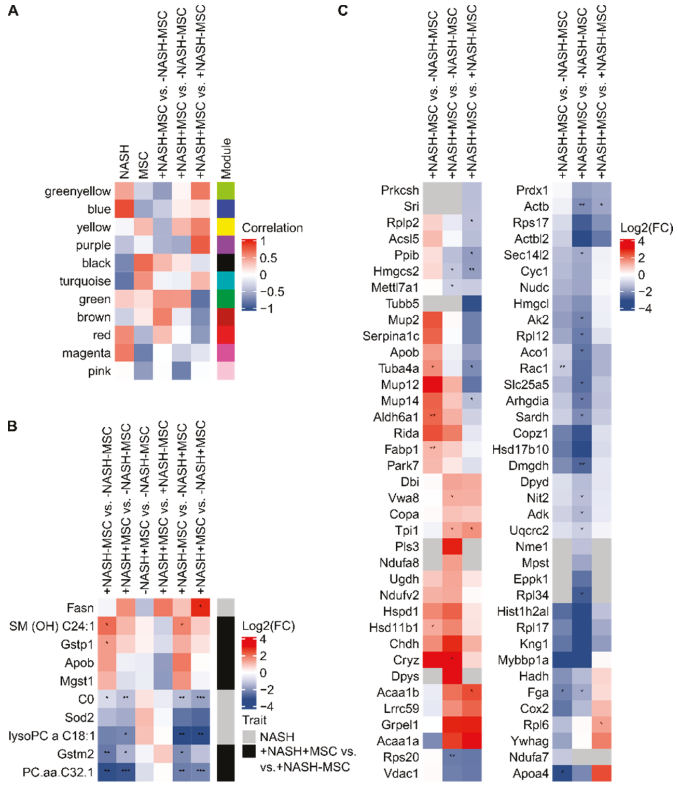

Figure 1. Integrative analysis of proteome and metabolome. (**A**) Correlations of WGCNA-created modules with relevant traits. Based on this, key drivers for the traits NASH and +NASH+MSC vs. +NASH-MSC were identified; (**B**) Log2(FCs) and *p*-values for selected key drivers; (**C**) Log2(FCs) and *p*-values are presented for selected candidates, which showed differences, albeit not significant throughout, between +NASH-MSC and +NASH+MSC. Significances are indicated with asterisks (*p*-value ≤ 0.05: *, *p*-value ≤ 0.01: **, *p*-value ≤ 0.001: ***). Euclidean clustering was applied to all heatmaps shown.

The hepatic acute-phase reaction is the defense response of the liver to injury, trauma, or inflammation [61]. It is associated with an increase of the expression of 'positive' acute-phase proteins (APP) on the expense of the 'negative' APPs [61]. The proteome analysis showed that the APPs Serpina1c (alpha-1-antitrypsin), which can be assigned to complement and coagulation cascades in KEGG, and several Mup (major urinary proteins) were significantly increased in +NASH-MSC livers as compared to control livers (Figure 1C). This increase was ameliorated in NASH livers receiving MSCs to levels comparable to the control group. Moreover, analysis of differentially expressed proteins revealed that compared to healthy (-NASH-MSC) control livers, +NASH-MSC livers showed a marked decrease in the expression of mitochondrial proteins Ndufa7 (NADH dehydrogenase 1 alpha subunit 7, KEGG: Oxidative phosphorylation, NAFLD), Cox2 (cytochrome c oxidase subunit 2, KEGG: Oxidative phosphorylation, NAFLD), and Hadh (hydroxyacyl-CoA dehydrogenase, KEGG: Fatty acid

elongation, degradation, and metabolism). Ndufa7 and Cox2, as parts of complexes I and IV of the respiratory chain, and Hadh, as a key factor in the metabolism of short-chain fatty acids, are directly involved in mitochondrial β-oxidation and energy production. In addition, cytosolic proteins Acsl5 (long-chain fatty acid-CoA (Coenzyme A) ligase 5, KEGG: Fatty acid biosynthesis, degradation, and metabolism, PPAR signaling pathway, peroxisome) and Fabp1 (liver-specific fatty acid-binding protein 1, KEGG: PPAR signaling pathway, fat digestion and absorption) were increased in +NASH-MSC livers, indicating the stimulation of fatty acid activation towards triglyceride synthesis. Furthermore, the peroxisomal Acaa1a (acetyl-coenzyme A acyltransferase 1, KEGG: Fatty acid degradation and metabolism, PPAR signaling pathway) showed decreased abundances in NASH livers, which might be associated with the reduction of peroxisomal lipid oxidation. In addition, the fat digestion and absorption-related proteins Apoa4 (apolipoprotein A4) and Apob (apolipoprotein B100) showed the opposite behavior in +NASH-MSC livers compared to MSC-treated NASH livers, with Apoa4 being decreased in NASH livers compared to controls, whilst Apob was increased. This indicates an impairment of lipoprotein secretion (Figure 1C). Taken together, in the NASH livers, lipid metabolism seemed to be shifted from utilization to storage. As a hallmark of NASH, liver lipid deposition is increased due to the excess provision of fatty acids from the adipose tissue in conjunction with the impairment of hepatocyte mitochondrial β-oxidation, involving a decrease in respiratory chain activity [62], and impairment of the secretion of triglycerides via very low density lipoproteins (VLDL). The latter has been shown to be hampered due to decreased expression of the microsomal triglyceride transfer protein (MTTP), a chaperone involved in VLDL assembly [63]. The proteomic changes as described above and the decrease in serum and increase in liver triglycerides, respectively, as shown in our previous study in this NASH model [34], may suggest that the impairment of fatty acid oxidation and triglyceride secretion contributed, at least in part, to hepatosteatosis and inflammation in livers of the MCD diet-fed mice and amelioration by MSC treatment. Since mitochondrial impairment might be a major cause of lipid accumulation, we anticipated that MSC treatment might improve mitochondrial function.

Since MSCs, besides others, reversed the NASH-induced decrease of Acaa1a, and PPAR signaling was among the significantly enriched pathways in the modules that showed an anti-correlation between +NASH-MSC vs. -NASH-MSC and +NASH+MSC vs. +NASH-MSC, we speculated that this pathway could play a role in the attenuation of pathological lipid storage in NASH livers. Thus, we analyzed the expression of the peroxisome proliferator-activated receptor alpha (PPARα), the key regulator of peroxisomes and liver lipid metabolism [64]. Semi-quantitative Western blot analysis revealed that PPARα was suppressed to low levels in +NASH-MSC livers. Upon MSC transplantation, PPARα was re-expressed, albeit to a significantly lower extent than in controls (-NASH-MSC), corroborating that peroxisomal lipid metabolism may potentially contribute to MSC-mediated lipid clearance (Figure 2A). In addition to the uptake by Fatp1, fatty acids are transported into hepatocytes by the fatty acid translocase CD36. Semi-quantitative Western blot analysis of CD36 revealed that expression was upregulated in +NASH-MSC as compared to -NASH-MSC livers, which was not impacted by MSC treatment (Figure 2A). As verified by fluorescence immunohistochemistry, it seemed that predominant peripheral, presumably membranous localization of CD36 in +NASH-MSC livers changed to predominant cytoplasmic localization in +NASH+MSC-livers (Figure 2B). Since translocase activity of CD36 is associated with membrane localization [65], the cytoplasmic shift by MSC treatment might indicate the attenuation of fatty acid uptake.

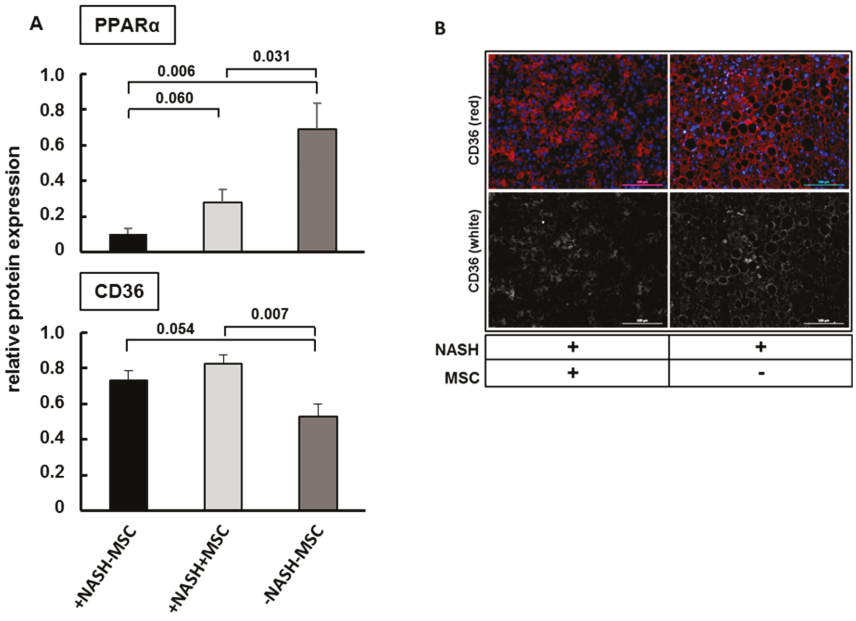

Figure 2. Expression of CD36 and PPARα in MCD-treated mice with and without MSC application. (**A**) Upregulation of CD36 expression and downregulation of PPARα in NASH livers and partial reversal by MSCs as shown by semiquantitative Western blot analysis of liver cytosolic extracts from 6 different animals in each group. Vinculin was used for normalization. Values represent means ± SEM and significant differences as indicated by the *p*-values over the horizontal lines were identified by applying the Student's *t*-test for unpaired values; (**B**) fluorescent immunohistochemical detection of CD36 in representative liver slices of +NASH-MSC livers and after treatment with MSC (+NASH+MSC). Scale bar 100 μm.

In summary, we reason that MSC alleviated the lipid burden in NASH livers by the improvement of lipid utilization by mitochondria in conjunction with the mutual balance of fatty acid import and lipid export.

3.2. Improvement of Tissue Homeostasis by MSCs

NASH is associated with an increased expression of Cyp2e1, a cytochrome P450 family member involved in the metabolism of polyunsaturated fatty acids [66]. The enzyme produces reactive oxygen species, leading to lipid peroxidation and formation of the byproduct 4-hydroxynonenal (4-HNE) [67]. To evaluate, whether oxidative stress was increased in NASH livers, we analyzed 4-hydroxynonenal (4-HNE) and Cyp2e1 by immunohistochemistry. In control livers, Cyp2e1 was zonally expressed in pericentral hepatocytes both untreated (-NASH-MSC) and treated with MSCs (-NASH+MSC), which was paralleled by weak zonal detection of 4-HNE. In NASH livers, both Cyp2e1 and 4-HNE were increased particularly in perivenous regions displaying a high fat content. Treatment with MSCs lowered both again to levels comparable to controls (Figure 3A), suggesting that MSCs ameliorated oxidative stress associated with enhanced lipid oxidation in NASH livers.

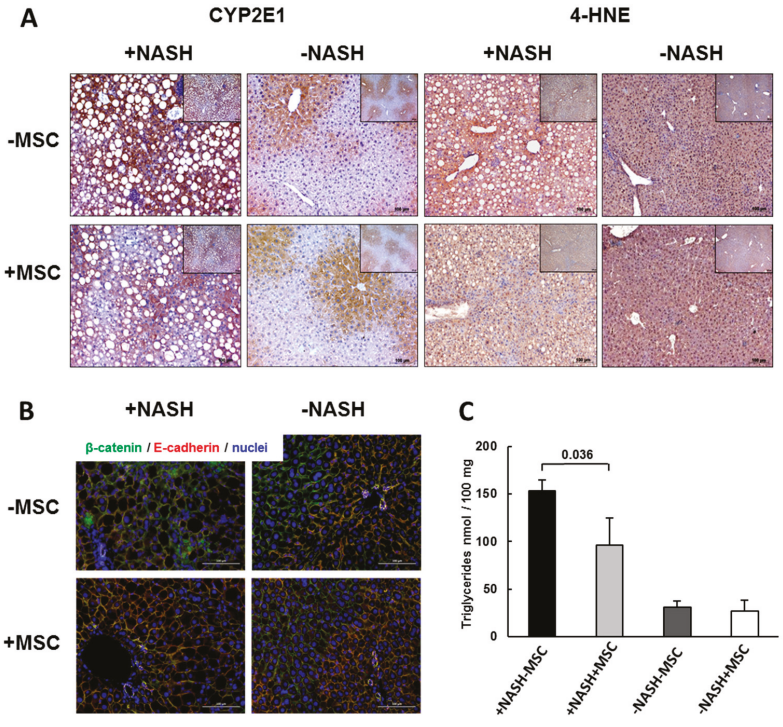

Figure 3. Liver tissue deterioration in MCD-treated mice and reversal by MSCs. (**A**) Immunohistochemical detection of Cyp2e1 and 4-HNE reveals an increase in perivenous localization in NASH livers, and restoration of zonation to nearly normal by MSC treatment. Pictures are representative for 3 different animals out of each group. White "holes" represent lipid droplets in NASH livers (original magnification 10×). The insets show lower magnifications for an overview impression (original magnification 5×). (**B**) luorescent immunohistochemical detection of adherens junction proteins β-catenin (green fluorescence) and E-cadherin (red, yellow in the overlay) indicates periportal zonation of E-cadherin, which is lost in NASH livers and restored by treatment with MSCs. Pictures are representative for 3 different animals out of each group. Scale bar 100 µm. (**C**) Hepatic triglycerides in control (-NASH) and in MCD diet-fed (+NASH) mice either treated without (-MSC) or with (+MSC) human bone marrow-derived MSCs. Values are means ± SD from 5 animals in each group. The horizontal line indicates the significant difference between the +NASH-MSC and the +NASH+MSC group at $p = 0.036$. In addition to Johnson transformation, an ANOVA was performed $p = 0.0001$, post-hoc Dunett T $p = 0.024$.

Liver function is strongly dependent on the polar orientation of hepatocytes along the sinusoids, i.e., facing the bile canaliculi with their apical and the sinusoids with their basolateral side. Chronic liver damage induces hepatocyte epithelial-mesenchymal transitions (EMTs) with a loss of hepatocyte polarity and eventually functionality [68]. The periportal expression of E-cadherin (E-cad), indicative for the epithelial organization of the hepatic parenchyma, was abrogated in NASH mouse livers as shown before [69]. Here, we confirmed this finding by immunohistochemical detection of E-cad and β-catenin (β-cat) co-localizing in the cell membrane at adherens junctions. In -NASH-MSC livers, both proteins were co-localized in periportal hepatocytes, indicating intact adherens junctions and hepatocyte polarity. In +NASH-MSC livers, however, periportal enrichment of E-cad was abrogated. Treatment with MSCs restored cell–cell contacts, and periportal expression of E-cad re-appeared co-localizing with β-catenin, comparable to -NASH-MSC control livers (Figure 3B). Consistent with

the improvement of tissue homeostasis, MSC treatment lowered hepatic triglycerides significantly by about 40% (Figure 3C).

Taken together, MSCs thus supported restoration of tissue homeostasis by the alleviation of NASH-associated pathomechanisms like lipid load, oxidative stress, acute damage response, and EMT, corroborating results shown previously [34]. Since the WGNCA and key driver analysis suggested that the metabolic overload might be due to mitochondrial impairment, these data might corroborate the hypothesis that the MSCs might restore mitochondrial function.

3.3. MSCs Decreased Hepatocyte Lipid Load In Vitro

In order to study MSCs' effects on fat-laden hepatocytes (HCs) in more detail, we established an in vitro model of hepatocyte steatosis by growing primary mouse HCs in steatosis-inducing medium, i.e., methionine-choline-deficient medium (MCD) or hepatocyte growth medium (HGM) supplemented with palmitic acid (C16:0). HGM served as a control. The mouse hepatocyte cultures in HGM and MCD medium were initially characterized in terms of the functional maintenance of hepatocyte-specific metabolism. No differences of urea synthesis were observed between the culture of cells in HGM or MCD medium. As expected [70,71], the synthesis rate decreased after one day of culture and then remained stable until 5 days of culture. The expression of selected lipid metabolism genes did not show obvious differences between culture in HGM or MCD medium. Changes over time were similar under all conditions tested. The expression of albumin was equal at each point in time, and under both culture conditions, indicating that the MCD medium did not affect hepatocyte-specific functions (Supplementary Material file 2, Figure S4A,B). Lipid content was quantified after 3 days of culture by image analysis of lipids after staining with Oilred O (ORO) (Figure 4A). Compared with the HGM group, MCD and C16:0 triggered a significant increase in the accumulation of lipids by 1.71- and 2.28-fold, respectively (Figure 4B). To gain further insight into the mechanisms involved in the amelioration of lipid load in livers of NASH mice by MSC treatment, HCs were co-cultured with MSCs at ratios of HCs to MSCs of 1:0, 10:1, 5:1, 1:1, or 0:1, and grown in HGM (Figure 4C), MCD (Figure 4D), or C16:0 (Figure 4E) for an additional 3 days. To note, the morphology of nuclei featured differences between HCs and MSCs, with the former displaying round-shaped and mostly binuclear with intensive DAPI staining and prominent nucleoli, and the latter presenting with oval-shaped nuclei and weaker DAPI staining. This clear distinction allowed us to readily discriminate between HCs and MSCs using fluorescence microscopy. Furthermore, the ORO staining in MSCs was undetectable under all treatment conditions (Figure 4C–E(e)), indicating that the MSCs did not accumulate lipids. When HCs were co-cultured at decreasing HC to MSC ratios, a decrease in ORO staining was observed (Figure 4C–E(a–d)). Co-culture of HCs and MSCs at a ratio of 1:1 significantly decreased the lipid load in HC from 12.56% ± 2.7 to 6.51% ± 2.39 when cultured in HGM, from 24.46 % ± 8.75 to 7.62% ± 4.18 in MCD medium, and from 28.67% ± 6.66 to 17.00% ± 2.65 in C16:0 (Figure 4F), suggesting that the MSCs supported lipid degradation in the hepatocytes. The expression of the mRNAs of Acaa1a, Acaa1b, and PPARα was higher in co-cultures in MCD medium as compared to hepatocytes alone (Supplementary Material file 2, Figure S4C), indicating that the MSCs also improved functional features in the mouse hepatocytes. This corroborated data in vivo showing a correction of lipid metabolism by MSC treatment.

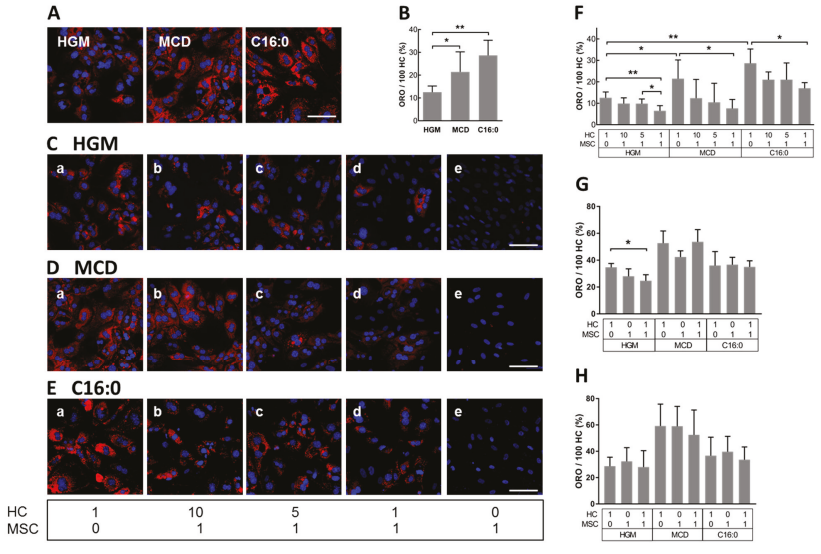

Figure 4. Induction of lipid droplet formation in cultured hepatocytes (HCs) by steatosis-inducing medium and reversal by MSCs in co-culture. Primary HCs were either cultured in HGM medium or treated with steatosis-inducing MCD medium or HGM supplemented with 0.5 mM palmitic acid (C16:0) for 3 days. (**A**) Visualization of hepatocyte lipids with Oil red O (red) and (**B**) quantification. HCs cultured (**a**) alone or together with MSCs at ratios of HCs to MSCs of (**b**) 10:1, (**c**) 5:1, (**d**) 1:1, or (**e**) 0:1 were grown for 3 days either in (**C**) HGM, or in (**D**) MCD, or in (**E**) HGM supplemented with C16:0. (**C–E**) lipid stain and (**F**) quantification. Nuclei were counterstained with DAPI (blue). Conditioned media were collected from either HC (1:0) or MSC (0:1) mono-cultures, or co-culture (ratio 1:1) and transferred to HCs grown for an additional (**G**) 1 or (**H**) 2 days in either HGM, MCD medium, or HGM supplemented with C16:0. The lipid stain with Oil red O was quantified by image analysis and the results from 3 independent cell cultures were normalized as the percentage amount of stain/100 hepatocytes and expressed as mean ± SD. Statistical comparisons were made using unpaired *t*-tests, and differences between groups were considered significant if the *p*-value was ≤0.05. *: $p \leq 0.05$; **: $p \leq 0.01$. Scale bar 100 µm. MSCs: human bone marrow-derived mesenchymal stromal cells; HCs: mouse primary hepatocytes; HGM: hepatocyte growth medium; MCD: methionine-choline-deficient medium.

MSCs may exert their effects via paracrine mechanisms involving soluble factors [72,73], or via extracellular vesicles [74]. Therefore, conditioned media (HGM, MCD, or C16:0) were collected separately from HCs, MSCs, and co-cultures of both after 48 h of culture. The media were subsequently added to HCs grown for 2 days in corresponding media and hepatocyte lipid load was determined after another 1 (Figure 4G) or 2 days (Figure 4H) by image analysis of ORO-stained lipid droplets.

A significant decrease in lipid accumulation in HCs was observed only when HCs were grown in HGM and treated with conditioned medium from co-cultures for one additional day (Figure 4G). The effect was no longer observed the day after (Figure 4H). No other condition revealed a lipid-reducing effect of the conditioned media, implicating that the lipolytic effect of MSCs in HCs was largely not mediated by soluble factors derived from MSCs, suggesting that direct cell-to-cell communication was required.

3.4. MSCs Communicated with Hepatocytes via Tunneling Nanotubes in a Microtubule-Dependent Manner

Irrespective of the growth in different media, MSCs communicated directly with hepatocytes in co-cultures via long filopodium-like tubes originating from the MSCs and touching the HCs or other MSCs (Figure 5A). These tubes were enriched in F-actin (cf. Figure 6A), one of the indispensable

features of tunneling nanotubes (TNTs), thus potentially classifying them as TNTs. Using a live cell analysis system, we observed that the formation of TNTs was achieved by cell–cell contact between the MSCs and the targeted cell, followed by subsequent moving of the MSCs apart and leaving a tubular structure behind (Supplementary Material file 2, Figure S5). TNTs are known to exchange molecular and corpuscular messages between cells, and mitochondria are common cargos of TNTs [75–77]. To understand the direction of communication between HCs and MSCs, the MSCs were pre-labeled with MitoTracker Deep Red FM and CellTrace™ Yellow prior to co-culture. The pre-labeling procedure was toxic to the HCs. Therefore, pre-labeled MSCs were co-cultured with HCs and the whole culture was stained with CellTrace™ CFSE the next day to serve as a counterstain (Figure 5B,C). The results unraveled a bi-directional cargo exchange between HCs and MSCs. The net speed of cargo transportation from HCs to MSCs (Figure 5B) and from MSCs to HCs (Figure 5C) was 627 and 1656 nm/min, respectively.

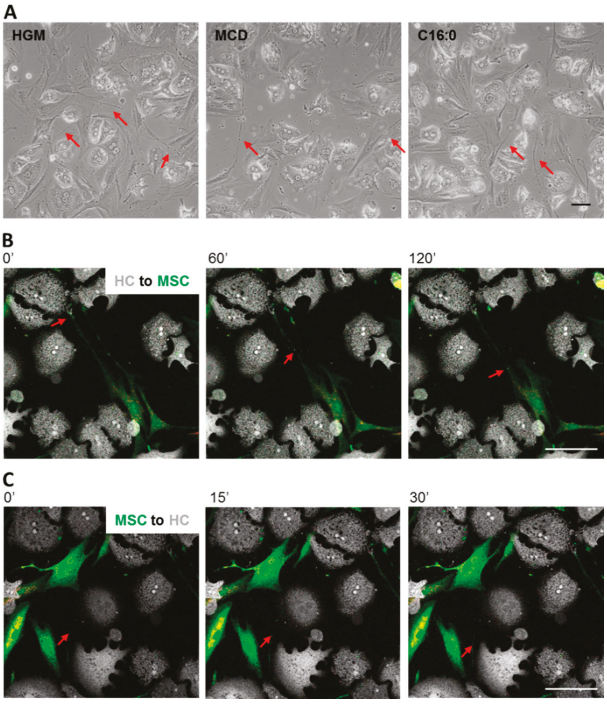

Figure 5. TNT-mediated cargo exchange between HCs and MSCs. (**A**) On day 1 of co-culture, the TNT structures (red arrows) derived from MSCs were readily detectable by phase contrast microscopy in cultures grown under all tested conditions. Scale bar 100 µm. Corresponding movies may be opened in Supplementary Material file 3; (**B**) The delivery of cargos from HCs to MSCs and (**C**) from MSCs to HCs was monitored by co-culture of HCs and MSCs pre-labeled with CellTrace™ Yellow and MitoTracker™ Deep Red FM (pseudo-colored green and red, respectively). The whole culture was stained with CellTrace™ CFSE (pseudo-colored white) and the pictures were captured using time-lapse confocal imaging. When the first picture was taken, this time point was designated as time 0, to which the other time points refer. The direction of movement of cargos in the TNTs is indicated by the red arrows. Scale bar 100 µm. Higher magnification images are available in Supplementary Material file 2, Figure S6A–C. Corresponding movies may be opened in Supplementary Material file 4.

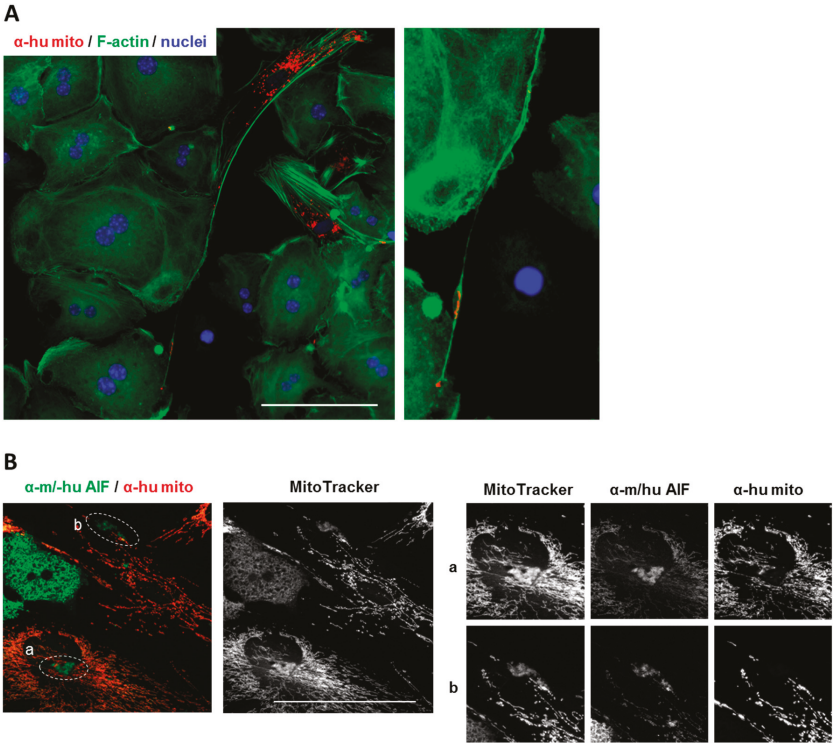

Figure 6. TNTs between HCs and MSCs are used to transport mitochondria. (**A**) Human MSC-derived mitochondria, stained in red with the anti-human-specific antibody against human mitochondria, are delivered to co-cultured mouse hepatocytes (mostly bi-nucleated). F-actin was stained with Phalloidin-iFluor 488 (green), nuclei with DAPI. Scale bar; 100 μm. Right panel: Computational enlargement of an area as shown on the left panel; (**B**) Mouse and human mitochondrial apoptosis-inducing factor (AIF) (green) and human mitochondria (red) were detected by fluorescent immunocytochemistry using species-specific antibodies, and cells were further stained with MitoTracker™ Deep Red FM (white). (**a**) and (**b**) show higher magnification pictures (computational enlargements) of circled areas shown in the panels on the left. Scale bar 100 μm.

To note, though the MSCs were pre-labeled with MitoTracker to visualize the potential movement of mitochondria in TNTs, the observability was limited by the magnification and the photostability of the fluorophore. Therefore, we confirmed the involvement of human mitochondria in TNT transportation by using the anti-human mitochondria antibody, clearly indicating the transport of MSC-derived human mitochondria into the mouse hepatocytes via TNTs (Figure 6A; Supplementary Material file 2, Figure S7A). In addition, our preliminary data also show that human peroxisomes were delivered towards HCs via the TNTs (Supplementary Material file 2, Figure S7B).

The anti-AIF (anti-apoptosis-inducing factor) monoclonal antibody detects the mitochondrial antigen AIF of both mouse and human origin. AIF does not necessarily locate in the mitochondria; it is also released to the cytoplasm in response to mitochondrial membrane permeabilization [78]. In the co-culture of human MSCs and mouse hepatocytes, AIF staining was mainly enriched in HCs. Yet, also in the MSCs, AIF was detectable in patches and a weaker staining in the MSC mitochondrial network (Figure 6B). The origin and nature of the AIF in the MSCs was further confirmed by using the anti-human mitochondria antibody and MitoTracker. The patchy AIF in the MSCs co-localized with MitoTracker but was negative for anti-human mitochondria staining (Figure 6B(a,b)), suggesting

that these structures were derivatives of mitochondria of mouse origin. At present, we cannot say that mouse mitochondria in the MSCs were delivered via the TNTs, but the results corroborate the assumption of a bi-directional exchange between HCs and MSCs. The functional meaning, however, remains elusive and needs further investigations.

To further confirm the character of the TNTs and unravel potential functional consequences, we examined the expression of relevant molecular motors or proteins by RT-PCR using human-specific primers in association with the two most studied cytoskeleton proteins related to TNT delivery, tubulin (representing microtubule-based transport) and actin (representing actin-based transport). Compared with MSC mono-cultures, the mRNA expression of human microtubule-associated proteins, namely Ras homolog family member T1 (Rhot1, also known as mitochondrial Rho GTPase 1; MIRO1) and kinesin family member 5B (KIF5B), were upregulated in co-cultures (Figure 7A). However, neither inducers of actin-based TNTs, RAS like proto-oncogene A (RALA) and TNFα-induced protein 2 (TNFAIP2), were altered. The results implied that in the co-culture with mouse hepatocytes, human MSCs may facilitate the expression of the microtubule-related but not actin-related gene expression to foster human MSC-derived TNT-dependent cargo transport.

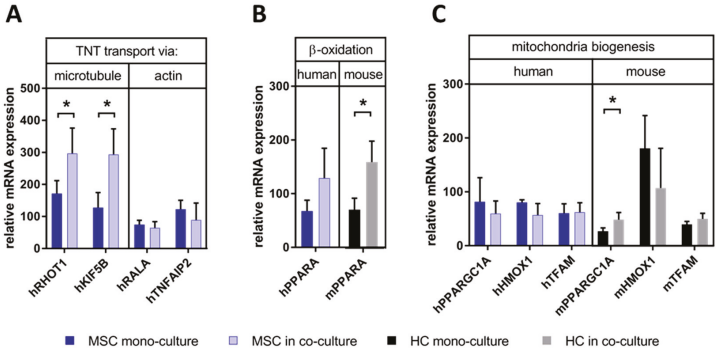

Figure 7. Expression of factors involved in (**A**) microtubule- and actin-based tubular transport, (**B**) hepatocyte lipid utilization, and (**C**) mitochondria biogenesis. Expression levels were analyzed by RT-PCR using species-specific primer pairs (blue/light blue columns for the use of human (h) primers, black/grey columns for the use of mouse (m) primers) and mRNA levels normalized with beta-2-microglobulin. Results are expressed as mean ± SD. Statistical comparisons from 3-5 independent cell cultures were made using the 2-way ANOVA test after log transformation, and differences between groups were considered significant if the p value was ≤0.05 (*). h: human; m: mouse; RHOT: Ras Homolog Family Member T1, also known as mitochondrial Rho GTPase 1 (MIRO1); KIF5B: kinesin family member 5B; RALA: RAS like proto-oncogene A; TNFAIP2: TNFα-induced protein 2; PPARGC1A: PPARα coactivator 1α, also known as PGC1α; HMOX1: heme oxygenase-1; TFAM: mitochondrial transcription factor A; PPARA: peroxisome proliferator-activated receptor α.

3.5. MSCs May Have Enhanced Lipid Utilization in HCs by Eliciting Oxidative Capacity

We hypothesized that the transportation of organelles from MSCs to HCs may promote lipid utilization in HCs in two ways: 1) By the activation of the key regulators of lipid utilization, like, e.g., peroxisome proliferator-activated receptor α (PPARA), and/or 2) by increasing the lipid-oxidizing capacity in HCs by the increase in the amount of MSC-derived mitochondria. To discriminate between human and mouse effects, we used species-specific primer pairs in RT-PCR experiments. The expression of mouse PPARA, but not human PPARA, was significantly higher in co-culture than in HC mono-culture (Figure 7B), corroborating the gene array results as shown above (Supplementary Material file 2, Figure S4C) and further suggesting that MSCs may elicit the utilization of lipids and fatty acids in HCs. Next, we analyzed the expression of markers involved in mitochondria biogenesis like PGC1α, mitochondrial transcription factor A (TFAM), and heme oxygenase-1 (HMOX1)

by species-specific RT-PCR to discriminate between mouse and human effects. Only the expression of mouse PGC1α (PPARGC1A; PPARγ coactivator 1 α), a regulator of mitochondria biogenesis, was significantly enhanced in co-cultures with MSCs as compared with HCs alone (Figure 7C). Albeit not significantly, there was a trend of higher expression of mTFAM, while mHMOX1 was even decreased if affected at all. No human markers of mitochondria biogenesis were changed in co- vs. mono-cultures (Figure 7C). Therefore, also taking the results as shown in Figure 8A,B into account, it may be suggested that the MSCs might promote mitochondria biogenesis in the mouse hepatocytes. This, however, needs further confirmation.

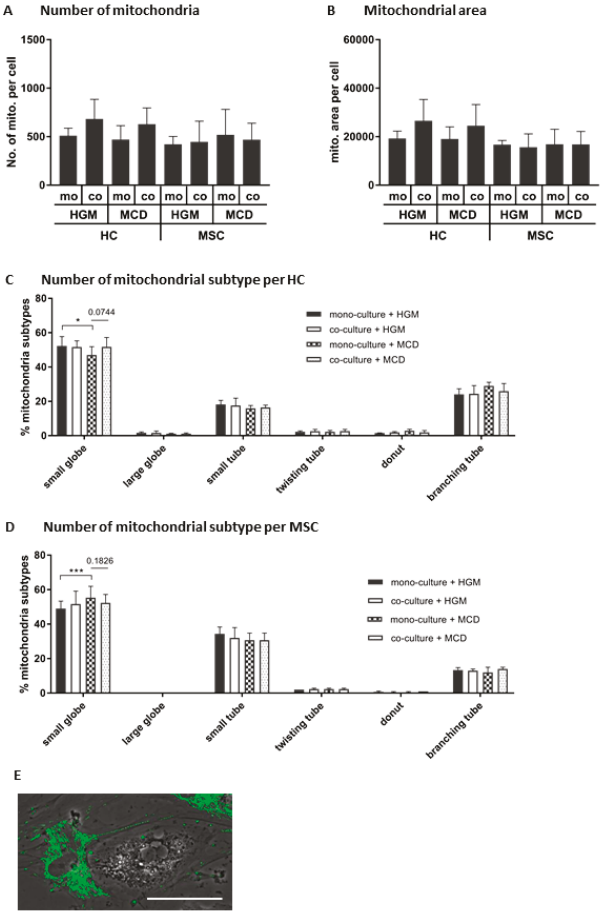

Figure 8. Profiling of cell-type-specific mitochondria in co-cultures of mouse hepatocytes and human MSCs. On day 1 of co-culture, fluorescence images of cells stained with MitoTracker Red CMXRos were analyzed for the (**A**) number and (**B**) area of mitochondria and percentages of mitochondria subtypes (**C**) in HCs and (**D**) in MSCs using the software MicroP. The statistical comparisons from 4 independent cell cultures were made using the 2-way ANOVA test. Results are expressed as mean ± SD. Statistical comparisons were made using unpaired *t*-tests, and differences between groups were considered significant for the *p*-values *: $p \leq 0.05$; ***: $p \leq 0.001$. (**E**) The globular morphology of MSC mitochondria was confirmed (cf. also Supplementary Material file 2, Figure S7) in MSCs co-cultured with HCs in HGM or MCD medium. The mitochondria were stained (pseudo-colored in green) and the picture was merged with the light microscopy image. Scale bar 50 μm. mo: mono-culture; co: co-culture.

Neither the number (Figure 8A) nor the area (Figure 8B) of mitochondria in MSCs and HCs were altered by any treatment. Yet, albeit not significant, there was a trend of higher mitochondria numbers in HCs when co-cultured with MSCs, both in HGM and in MCD medium, suggesting that MSCs might increase the number of mitochondria in HCs, in line with data shown in Figure 7C. The percentage of one of the mitochondrial subtypes, small globules, was significantly decreased in HCs when cultured in MCD medium, which was reversed in part in co-cultures with MSCs (Figure 8C). When cultured in MCD medium, the percentage of small globules was significantly increased in MSCs, suggesting that this condition might increase specific subtypes of mitochondria in MSCs (Figure 8D). Taking into consideration the mitochondrial globular shape as shown in Figure 6A in co-cultures of HCs and MSCs, it was very obvious that preferentially small dotted (small globules) MSC-derived mitochondria were detectable in TNT bridging to HCs (Figure 8E).

Taken together, these results show that MSCs may deliver mitochondria (and bona fide peroxisomes) to HCs, which might support lipid breakdown both by providing oxidative capacity and by support of the hepatocytes' own capacity of lipid utilization potentially by the support of mitochondria biogenesis. However, the mutual interactions between recipient and donor mitochondria and the impact on the recipient lipid metabolism remains to be further elucidated.

3.6. Human BM-MSCs Delivered Mitochondria to Mouse Hepatocytes In Vivo

In order to show that human mitochondria from transplanted MSCs were delivered to mouse hepatocytes after hepatic transplantation in vivo, liver slices were co-stained with an anti-mouse-specific cyclophilin and the anti-human-specific mitochondria antibody. Image analysis using the Zeiss Axio Observer.Z1 microscope equipped with ApoTome.2 showed that human mitochondria were only detectable in livers, which received human MSC transplants (Figure 9A). Signals co-localized with cyclophilin (Figure 9B), clearly indicating that donor human MSC-derived mitochondria were delivered to the host mouse hepatocytes. At this point in time, these results would be in line with the hypothesis that the delivery could involve TNTs as demonstrated in vitro (cf. Figure 6A).

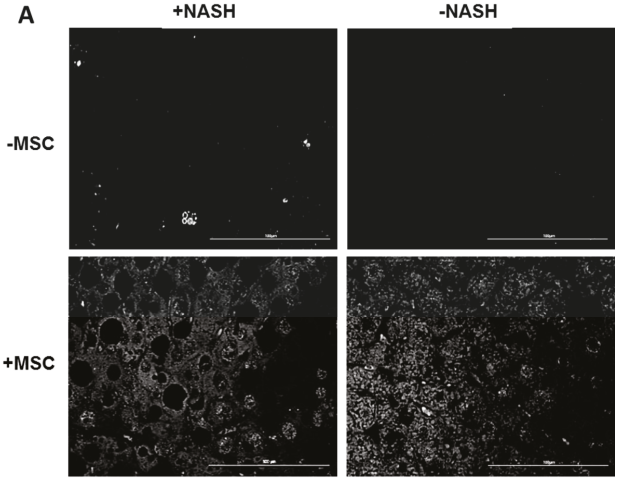

Figure 9. *Cont.*

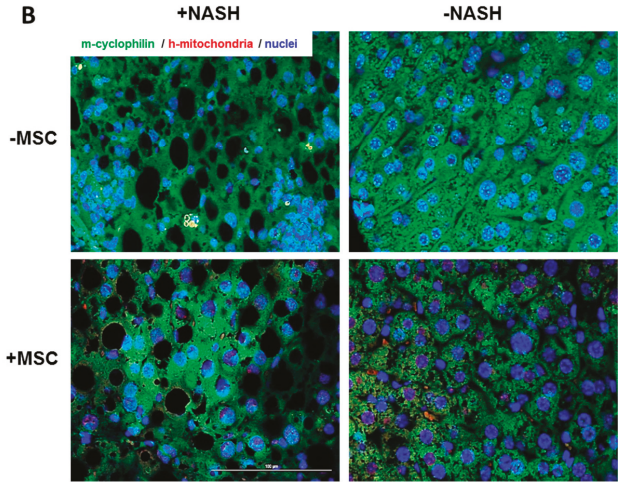

Figure 9. Human MSC-derived mitochondria in mouse hepatocytes of animals receiving MSC transplants. Here, 2-µm slices of mouse livers either fed the control (-NASH) or the MCD diet (+NASH) and treated without (-MSC) or with (+MSC) human bone marrow-derived MSC were co-stained with the anti-mouse cyclophilin or the anti-human mitochondria antibody and images captured using the Zeiss Axio Observer.Z1 microscope equipped with ApoTome.2 with a 40× objective. (**A**) Black and white images of pictures shown in (B) indicate human mitochondria (lower panels) in livers, which were transplanted with human MSCs. Non-transplanted livers (upper panels) were void of signals; (**B**) Immuno-fluorescent co-stain of mouse cyclophilin (green channel), and human mitochondria (red channel) indicating human mitochondria in mouse hepatocytes; nuclei were stained with DAPI (blue).

4. Discussion

4.1. Pathobiochemical Consequences of Changes in Metabolic Protein Expression and Correction by MSCs

Based on the proteomics and metabolomics data, the WGCNA predicted a MCD diet-induced deregulation of central carbon and amino acid metabolism likely associated with mitochondrial dysfunction, which were reversed by MSC treatment, rendering most of the affected metabolic pathways not significantly different from controls.

NASH is characterized by the accumulation of triglycerides in hepatocytes, a predominant sign of metabolic impairment. In the MCD model of NASH, it has been shown that VLDL secretion is inhibited due to the attenuated expression of the chaperone microsomal triglyceride transfer protein (MTP), which is essential for the proper folding of apolipoprotein B (ApoB) [79]. Here, we showed that ApoB was slightly increased, likely due to the accumulation of the non-functional protein, while the expression of ApoA4, involved in VLDL secretion [80], was downregulated. The increased expression of hepatocyte fatty acid transporters Fatp1 and CD36 fostered fatty acid uptake and together with the perturbance of lipid (lipoprotein) secretion likely caused an imbalance of lipid metabolism favoring storage over secretion. In addition to the attenuation of triglyceride secretion, the utilization of fatty acids by mitochondrial β-oxidation seemed to be impaired by the downregulation of proteins of the respiratory chain as obvious from the key driver analysis. Further, at the individual level of expressed genes, Acaa1a and b, involved in peroxisomal fatty acid oxidation, were downregulated, indicating an additional impairment of peroxisomal lipid utilization. In total, these findings are consistent with NASH-induced changes in central carbon and amino acid metabolism (as side reactions associated with glycolysis and the tricarboxylic acid cycle [81]) promoting lipid storage due to failure of lipid utilization and secretion as commonly observed in rodent NASH models and in humans [82–84].

Taken together, the pathobiochemical changes in the mouse liver upon MCD diet feeding are in line with major features of NASH as described [85,86]. In the study presented here, MSCs ameliorated the hepatic lipid load consistent with the improvement of NASH-induced metabolic changes as unraveled by WGCNA. To our knowledge, this is the first study to show the impact of MSCs on key metabolic pathways involved in the pathogenesis of NASH. However, the molecular and/or cellular mechanism(s) engaged remain open. Since it is conceivable that the MSCs did not impact on each individual biochemical pathway separately, or even by different mechanisms, it may be assumed that the MSCs primarily attenuated the hepatocyte lipid load by a unique mechanism, and consecutively improved overall metabolic homeostasis.

4.2. Histopathological Consequences of Hepatocyte Lipid Load and Improvement by MSCs

The accumulation of lipids in hepatocytes is associated with an overproduction of reactive oxygen species (ROS) that progressively exceeds the cellular detoxification capabilities. Microsomal Cyp2e1 is a major site of fatty acid metabolism, which has been found to be elevated in fatty liver diseases in humans and rodents [66]. Cyp2e1 plays a critical part in the pathogenesis of NASH by the production of ROS, which foster protein and lipid peroxidation associated with cellular stress and damage [67]. This is in line with our findings of increased Cyp2e1 and elevated 4-HNE as a byproduct of lipid peroxidation in the NASH livers. As identified by the key driver analysis in the NASH livers, the upregulation of proteins involved in protection from oxidative stress like Mgst1 and Gstp1 [87] may be interpreted as an adaptive response to increased oxidative stress, while downregulation of proteins like Sod2 involved in mitochondrial superoxide detoxification may even aggravate oxidative stress and mitochondrial impairment [88].

Alpha-1-antitrypsin and major urinary proteins increased in the NASH livers, indicative for the onset of the acute-phase reaction, the hepatic defense response to injury and inflammation. Likewise, the expression and localization of the cell adhesion proteins E-cadherin and β-catenin changed in the NASH as compared to control livers, indicative for the perturbation of the epithelial organization of the hepatic parenchyma. Epithelial-mesenchymal transitions in the liver have been attributed to be essential in regeneration of the liver after injury [89]. Hence, tissue deterioration in the NASH livers may indicate regeneration due to hepatocellular death.

MSC ameliorated oxidative stress, inflammation, and tissue damage, corroborating our previous results showing regression of fibrosis and cell death as well as attenuation of inflammatory pathways [20], consistent with findings demonstrating resolution of inflammation, fibrosis, and lipid load in rodent models of NASH [90,91]. The mechanisms behind, however, remain elusive. Again, it is unlikely that the MSCs impacted on single individual pathways involved in the perturbation of tissue homeostasis by different modes of action. Therefore, we hypothesize that the overall improvement of tissue homeostasis secondarily followed the attenuation of the hepatocyte lipid load. This implies that metabolic improvement preceded the restoration of tissue architecture, which was likely to be achieved by the regenerative capacity of the liver itself.

4.3. Mitochondrial Transfer by MSCs May Attenuate Hepatocyte Lipid Load

Previous reports including mouse datasets into WGCNA approaches identified mitochondrial dysfunction as a key event in the pathogenesis of NASH [92], consistent with our data that aberrant expression of mitochondrial proteins may drive mitochondrial dysfunction. Indeed, in consequence of insulin resistance, the increased flux of free fatty acids from the adipose tissue to the liver has long been suggested as a major cause of the metabolic overload and eventually dysfunction of mitochondria in the pathogenesis of NASH [7,8,93]. Based on these facts, we hypothesized that the improvement of mitochondrial function in the host liver by transplanted MSCs may play a central role in the amelioration of lipid load in the NASH livers. In the in vitro experiments, we observed a physical long-distance connection between MSCs and hepatocytes. These protrusions contained filamentous actin and carried whole organelles, features that have been specifically attributed to

phenomena called tunneling nanotubes (TNTs) [94,95]. TNTs are thin membranous structures mediating direct intercellular communication between non-adjacent cells. They have been shown to transport subcellular components, e.g., mitochondria and lysosomes as well as plasma membrane components, mRNA, electrical signals, and calcium ions [96]. Our in vitro data present evidence for a transfer of mitochondria from MSCs to the hepatocytes via TNTs. Since the steatosis-inducing media used here is known to cause mitochondrial dysfunction associated with excess lipid storage, ROS generation, and cytotoxicity [97,98], the donation of functional mitochondria by the MSCs might contribute to the attenuation of lipid load in the hepatocytes. Hence, we suggest that the transferred mitochondria may compensate for a lack of oxidative phosphorylation capacity and thereby improve lipid utilization, which is in line with the lipid-lowering effect of MSCs as shown both in vitro and in vivo. Our work does not provide direct evidence that the delivery of mitochondria is involved in the reduction of triglycerides in hepatocytes. We used inhibitors of the respiratory chain and microtubule assembly in order to demonstrate correction of hepatocyte metabolism by MSC-derived donor mitochondria. Yet, most of the inhibitors were toxic to the hepatocytes, thus not allowing to discriminate between toxicity and specific effects on targets to be inhibited. It may not be excluded that part of the hepatocyte lipid resources may be metabolized by the MSC transplants. This would require the transfer of lipids to the MSCs, which we neither observed in vitro nor in vivo. Additionally, MSCs may have stimulated lipid breakdown in the host hepatocytes to release free fatty acids, which then could be metabolized by the MSCs. This would require some paracrine mechanisms, which, however, we may exclude, because MSC-derived conditioned medium was not effective. In addition, MSCs did not accumulate lipids in vitro, indicating that their lipid metabolism might be different from the hepatocytes. Indeed, in their niche, MSC energy metabolism may primarily rely on anaerobic glycolysis rather than oxidative phosphorylation [99]. Our results are consistent with data shown in a high-fat diet-fed mouse model, in which MSC transplants improved mitochondrial morphology and metabolic performance in the host liver [100]. This may describe a general mechanism of MSC action, since stem cell-derived donor mitochondria increased oxidative phosphorylation and ATP generation, and reduced ROS production in host cells like, e.g., myeloma cells [101], macrophages [102], cardiomyocytes [103], and airway epithelial cells [104]. Thus, the concept of MSC-derived mitochondrial transfer to improve recipient cell oxidative metabolism is now well established [105]. However, in our model of NASH, mechanistic questions remain open: How are diseased mitochondria cleared from the hepatocytes (e.g., by mitophagy)? Which are the mechanisms protecting the donated healthy mitochondria? How is the pool of donor mitochondria replenished in donating MSC? These questions are topics of our current work.

In our mouse model, we saw that MSC transplants entered the liver parenchyma primarily at the periportal area of the liver sinusoid, resulting in zonal enrichment of the MSCs [20]. For this animal model, we calculated that a 1% repopulation of the hepatic parenchyma by transplanted MSCs may be achieved, i.e., 6.6×10^5 transplanted cells in the host liver [106]. Assuming that a cell on average may contain 1500 mitochondria [107], this cell number corresponds to 9.9×10^8 donor mitochondria. A mouse liver contains 66×10^6 hepatocytes [108] corresponding to 9.9×10^{10} mitochondria. In conclusion, 1% on average of all mitochondria in a mouse hepatocyte ought to be of human MSC donor origin. This is in the same order of magnitude as shown in a co-culture model of human bone marrow-derived MSCs and myeloma cells, which improved cellular respiration in the range of 10–50% depending on the cell line under investigation [101]. If we assume in a simple approximation that this increase would solely contribute to lipid degradation and oxidation, this would account for the decrease in hepatocyte lipid content as shown here in vivo and in vitro of roughly 40%.

5. Conclusions

Metabolically, the diet-induced NASH was characterized by an impairment of the central carbon metabolism likely due to mitochondrial and peroxisomal dysfunction. The enhancement of membrane transporters of fatty acids may have increased fatty acid uptake. In association with the impairment of utilization and lipoprotein secretion, the enhancement of triglyceride synthesis and storage may follow. MSCs, transplanted into a mouse host liver, ameliorated lipid storage and associated perturbance of tissue homeostasis likely by the donation of healthy mitochondria to the hepatocytes via TNTs, thus providing oxidative capacity for lipid breakdown and eventually restoration of tissue homeostasis.

Supplementary Materials: The following are available online at http://www.mdpi.com/2227-9059/8/9/350/s1, Supplementary Material file 1: data sets for WGCNA; Supplementary Material file 2: Tables S1 and S2, Figures S1–S7; Supplementary Material file 3: Video S1; Supplementary Material file 4: Videos S2 and S3.

Author Contributions: Conceptualization, M.-J.H., I.K., S.K., M.v.B., P.S. and B.C.; methodology, M.-J.H., I.K., I.S., M.C., H.K., K.S., U.E.R.-K., S.K. and S.N.; software, I.S., I.K., K.S. and U.E.R.-K.; validation, H.K., M.C., S.K. and S.N.; formal analysis, M.-J.H., I.K., M.C., I.S., H.K., S.K. and S.N.; investigation, M.-J.H., I.K., S.K., I.S., M.C., H.K., S.K. and S.N.; resources, M.C., K.S., U.E.R.-K., P.S., M.v.B. and B.C.; data curation, M.-J.H., I.K., M.C. and B.C.; writing—original draft preparation, M.-J.H., I.K., H.K. and B.C.; writing—review and editing, M.-J.H., I.K., M.C., S.K., S.N., P.S., M.v.B. and B.C.; visualization, M.-J.H., I.K., M.C., H.K., S.K., S.N. and B.C.; supervision, K.S., U.E.R.-K., P.S., M.v.B. and B.C.; project administration, M.v.B. and B.C.; funding acquisition, M.-J.H. and B.C. All authors have read and agreed to the published version of the manuscript.

Funding: This research was funded by the Deutsche Forschungsgemeinschaft, grant number CH109/22-2 (BC) and by the Ministry of Science and Technology, Taiwan Postdoctoral Research Abroad Program, grant number 105-2917-I-564-071 (M.-J.H.). Martin von Bergen is grateful for funding by the DFG CRC 1382 Gut-Liver Axis-Functional Circuits and Therapeutic Targets.

Acknowledgments: The authors are deeply thankful for the valuable contributions to this study made by Sandra Winkler and Sven Baumann. The authors greatly appreciate the technical support by Jacqueline Kobelt. We acknowledge support from Leipzig University for Open Access Publishing.

Conflicts of Interest: The authors declare no conflict of interest. The funders had no role in the design of the study; in the collection, analyses, or interpretation of data; in the writing of the manuscript, or in the decision to publish the results.

References

1. Younossi, Z.; Anstee, Q.M.; Marietti, M.; Hardy, T.; Henry, L.; Eslam, M.; George, J.; Bugianesi, E. Global burden of nafld and nash: Trends, predictions, risk factors and prevention. *Nat. Rev. Gastroenterol. Hepatol.* **2018**, *15*, 11–20. [CrossRef]
2. Tilg, H.; Moschen, A.R. Mechanisms behind the link between obesity and gastrointestinal cancers. *Best Pract. Res. Clin. Gastroenterol.* **2014**, *28*, 599–610. [CrossRef] [PubMed]
3. Calle, E.E.; Rodriguez, C.; Walker-Thurmond, K.; Thun, M.J. Overweight, obesity, and mortality from cancer in a prospectively studied cohort of U.S. Adults. *N. Engl. J. Med.* **2003**, *348*, 1625–1638. [CrossRef] [PubMed]
4. Singh, R.; Kaushik, S.; Wang, Y.; Xiang, Y.; Novak, I.; Komatsu, M.; Tanaka, K.; Cuervo, A.M.; Czaja, M.J. Autophagy regulates lipid metabolism. *Nature* **2009**, *458*, 1131–1135. [CrossRef]
5. Park, H.W.; Park, H.; Semple, I.A.; Jang, I.; Ro, S.H.; Kim, M.; Cazares, V.A.; Stuenkel, E.L.; Kim, J.J.; Kim, J.S.; et al. Pharmacological correction of obesity-induced autophagy arrest using calcium channel blockers. *Nat. Commun.* **2014**, *5*, 4834. [CrossRef] [PubMed]
6. Nassir, F.; Ibdah, J.A. Role of mitochondria in nonalcoholic fatty liver disease. *Int. J. Mol. Sci.* **2014**, *15*, 8713–8742. [CrossRef]
7. Pessayre, D.; Fromenty, B. Nash: A mitochondrial disease. *J. Hepatol.* **2005**, *42*, 928–940. [CrossRef] [PubMed]
8. Begriche, K.; Igoudjil, A.; Pessayre, D.; Fromenty, B. Mitochondrial dysfunction in nash: Causes, consequences and possible means to prevent it. *Mitochondrion* **2006**, *6*, 1–28. [CrossRef] [PubMed]
9. Hall, D.; Poussin, C.; Velagapudi, V.R.; Empsen, C.; Joffraud, M.; Beckmann, J.S.; Geerts, A.E.; Ravussin, Y.; Ibberson, M.; Oresic, M.; et al. Peroxisomal and microsomal lipid pathways associated with resistance to hepatic steatosis and reduced pro-inflammatory state. *J. Biol. Chem.* **2010**, *285*, 31011–31023. [CrossRef]
10. Wu, Z.; Yang, F.; Jiang, S.; Sun, X.; Xu, J. Induction of liver steatosis in bap31-deficient mice burdened with tunicamycin-induced endoplasmic reticulum stress. *Int. J. Mol. Sci.* **2018**, *19*, 2291. [CrossRef]

11. Sumida, Y.; Yoneda, M. Current and future pharmacological therapies for nafld/nash. *J. Gastroenterol.* **2018**, *53*, 362–376. [CrossRef] [PubMed]
12. Lewin, S.M.; Mehta, N.; Kelley, R.K.; Roberts, J.P.; Yao, F.Y.; Brandman, D. Liver transplantation recipients with nonalcoholic steatohepatitis have lower risk hepatocellular carcinoma. *Liver Transplant. Off. Publ. Am. Assoc. Study Liver Dis. Int. Liver Transplant. Soc.* **2017**, *23*, 1015–1022. [CrossRef]
13. Cholankeril, G.; Wong, R.J.; Hu, M.; Perumpail, R.B.; Yoo, E.R.; Puri, P.; Younossi, Z.M.; Harrison, S.A.; Ahmed, A. Liver transplantation for nonalcoholic steatohepatitis in the us: Temporal trends and outcomes. *Dig. Dis. Sci.* **2017**, *62*, 2915–2922. [CrossRef] [PubMed]
14. Noureddin, M.; Vipani, A.; Bresee, C.; Todo, T.; Kim, I.K.; Alkhouri, N.; Setiawan, V.W.; Tran, T.; Ayoub, W.S.; Lu, S.C.; et al. Nash leading cause of liver transplant in women: Updated analysis of indications for liver transplant and ethnic and gender variances. *Am. J. Gastroenterol.* **2018**, *113*, 1649–1659. [CrossRef] [PubMed]
15. Alfaifi, M.; Eom, Y.W.; Newsome, P.N.; Baik, S.K. Mesenchymal stromal cell therapy for liver diseases. *J. Hepatol.* **2018**, *68*, 1272–1285. [CrossRef]
16. Christ, B.; Bruckner, S.; Winkler, S. The therapeutic promise of mesenchymal stem cells for liver restoration. *Trends Mol. Med.* **2015**, *21*, 673–686. [CrossRef]
17. Rinella, M.E.; Elias, M.S.; Smolak, R.R.; Fu, T.; Borensztajn, J.; Green, R.M. Mechanisms of hepatic steatosis in mice fed a lipogenic methionine choline-deficient diet. *J. Lipid Res.* **2008**, *49*, 1068–1076. [CrossRef]
18. Pelz, S.; Stock, P.; Bruckner, S.; Christ, B. A methionine-choline-deficient diet elicits nash in the immunodeficient mouse featuring a model for hepatic cell transplantation. *Exp. Cell Res.* **2012**, *318*, 276–287. [CrossRef]
19. Wang, H.; Wang, D.; Yang, L.; Wang, Y.; Jia, J.; Na, D.; Chen, H.; Luo, Y.; Liu, C. Compact bone-derived mesenchymal stem cells attenuate nonalcoholic steatohepatitis in a mouse model by modulation of cd4 cells differentiation. *Int. Immunopharmacol.* **2017**, *42*, 67–73. [CrossRef]
20. Winkler, S.; Christ, B. Treatment of nash with human mesenchymal stem cells in the immunodeficient mouse. *Methods Mol. Biol.* **2014**, *1213*, 51–56.
21. Tanimoto, H.; Terai, S.; Taro, T.; Murata, Y.; Fujisawa, K.; Yamamoto, N.; Sakaida, I. Improvement of liver fibrosis by infusion of cultured cells derived from human bone marrow. *Cell Tissue Res.* **2013**, *354*, 717–728. [CrossRef] [PubMed]
22. Bruckner, S.; Zipprich, A.; Hempel, M.; Thonig, A.; Schwill, F.; Roderfeld, M.; Roeb, E.; Christ, B. Improvement of portal venous pressure in cirrhotic rat livers by systemic treatment with adipose tissue-derived mesenchymal stromal cells. *Cytotherapy* **2017**, *19*, 1462–1473. [CrossRef] [PubMed]
23. Banas, A.; Teratani, T.; Yamamoto, Y.; Tokuhara, M.; Takeshita, F.; Osaki, M.; Kato, T.; Okochi, H.; Ochiya, T. Rapid hepatic fate specification of adipose-derived stem cells and their therapeutic potential for liver failure. *J. Gastroenterol. Hepatol.* **2009**, *24*, 70–77. [CrossRef]
24. Stock, P.; Bruckner, S.; Winkler, S.; Dollinger, M.M.; Christ, B. Human bone marrow mesenchymal stem cell-derived hepatocytes improve the mouse liver after acute acetaminophen intoxication by preventing progress of injury. *Int. J. Mol. Sci.* **2014**, *15*, 7004–7028. [CrossRef] [PubMed]
25. Herrero, A.; Prigent, J.; Lombard, C.; Rosseels, V.; Daujat-Chavanieu, M.; Breckpot, K.; Najimi, M.; Deblandre, G.; Sokal, E.M. Adult-derived human liver stem/progenitor cells infused 3 days postsurgery improve liver regeneration in a mouse model of extended hepatectomy. *Cell Transplant.* **2017**, *26*, 351–364. [CrossRef]
26. Tautenhahn, H.M.; Bruckner, S.; Baumann, S.; Winkler, S.; Otto, W.; von Bergen, M.; Bartels, M.; Christ, B. Attenuation of postoperative acute liver failure by mesenchymal stem cell treatment due to metabolic implications. *Ann. Surg.* **2016**, *263*, 546–556. [CrossRef]
27. Sokal, E.M.; Stephenne, X.; Ottolenghi, C.; Jazouli, N.; Clapuyt, P.; Lacaille, F.; Najimi, M.; de Lonlay, P.; Smets, F. Liver engraftment and repopulation by in vitro expanded adult derived human liver stem cells in a child with ornithine carbamoyltransferase deficiency. *Jimd Rep.* **2014**, *13*, 65–72.
28. Sokal, E.M.; Lombard, C.A.; Roelants, V.; Najimi, M.; Varma, S.; Sargiacomo, C.; Ravau, J.; Mazza, G.; Jamar, F.; Versavau, J.; et al. Biodistribution of liver-derived mesenchymal stem cells after peripheral injection in a hemophilia a patient. *Transplantation* **2017**, *101*, 1845–1851. [CrossRef]

29. Kharaziha, P.; Hellstrom, P.M.; Noorinayer, B.; Farzaneh, F.; Aghajani, K.; Jafari, F.; Telkabadi, M.; Atashi, A.; Honardoost, M.; Zali, M.R.; et al. Improvement of liver function in liver cirrhosis patients after autologous mesenchymal stem cell injection: A phase i-ii clinical trial. *Eur. J. Gastroenterol. Hepatol.* **2009**, *21*, 1199–1205. [CrossRef]
30. Jang, Y.O.; Kim, Y.J.; Baik, S.K.; Kim, M.Y.; Eom, Y.W.; Cho, M.Y.; Park, H.J.; Park, S.Y.; Kim, B.R.; Kim, J.W.; et al. Histological improvement following administration of autologous bone marrow-derived mesenchymal stem cells for alcoholic cirrhosis: A pilot study. *Liver Int. Off. J. Int. Assoc. Study Liver* **2014**, *34*, 33–41. [CrossRef]
31. Suk, K.T.; Yoon, J.H.; Kim, M.Y.; Kim, C.W.; Kim, J.K.; Park, H.; Hwang, S.G.; Kim, D.J.; Lee, B.S.; Lee, S.H.; et al. Transplantation with autologous bone marrow-derived mesenchymal stem cells for alcoholic cirrhosis: Phase 2 trial. *Hepatology* **2016**, *64*, 2185–2197. [CrossRef] [PubMed]
32. Kanazawa, Y.; Verma, I.M. Little evidence of bone marrow-derived hepatocytes in the replacement of injured liver. *Proc. Natl. Acad. Sci. USA* **2003**, *100* (Suppl. 1), 11850–11853. [CrossRef] [PubMed]
33. Higashiyama, R.; Moro, T.; Nakao, S.; Mikami, K.; Fukumitsu, H.; Ueda, Y.; Ikeda, K.; Adachi, E.; Bou-Gharios, G.; Okazaki, I.; et al. Negligible contribution of bone marrow-derived cells to collagen production during hepatic fibrogenesis in mice. *Gastroenterology* **2009**, *137*, 1459–1466.e1451. [CrossRef] [PubMed]
34. Winkler, S.; Borkham-Kamphorst, E.; Stock, P.; Bruckner, S.; Dollinger, M.; Weiskirchen, R.; Christ, B. Human mesenchymal stem cells towards non-alcoholic steatohepatitis in an immunodeficient mouse model. *Exp. Cell Res.* **2014**, *326*, 230–239. [CrossRef] [PubMed]
35. Stock, P.; Bruckner, S.; Ebensing, S.; Hempel, M.; Dollinger, M.M.; Christ, B. The generation of hepatocytes from mesenchymal stem cells and engraftment into murine liver. *Nat. Protoc.* **2010**, *5*, 617–627. [CrossRef] [PubMed]
36. Müller, S.A.; Kohajda, T.; Findeiss, S.; Stadler, P.F.; Washietl, S.; Kellis, M.; von Bergen, M.; Kalkhof, S. Optimization of parameters for coverage of low molecular weight proteins. *Anal. Bioanal. Chem.* **2010**, *398*, 2867–2881. [CrossRef] [PubMed]
37. Römisch-Margl, W.; Prehn, C.; Bogumil, R.; Röhring, C.; Suhre, K.; Adamski, J. Procedure for tissue sample preparation and metabolite extraction for high-throughput targeted metabolomics. *Metabolomics* **2012**, *8*, 133–142. [CrossRef]
38. Wickham, H.; Bryan, J. Readxl: Read Excel Files. Available online: https://CRAN.R-project.org/package=readxl (accessed on 10 September 2020).
39. Spiess, A.N. Qpcr: Modelling and Analysis of Real-Time pcr Data. R Package v. 1.4-1. Available online: https://CRAN.R-project.org/package=qpcR (accessed on 10 September 2020).
40. Wickham, H.; Henry, L. Tidyr: EASILY tidy Data with "Spread ()" and "Gather ()" Functions. R Package Version 0.8. 0. Available online: https://CRAN.R-project.org/package=tidyr (accessed on 10 September 2020).
41. Wickham, H. The split-apply-combine strategy for data analysis. *J. Stat. Softw.* **2011**, *40*, 1–29. [CrossRef]
42. Mahto, A. Splitstackshape: Stack and Reshape Datasets after Splitting Concatenated Values. Available online: https://CRAN.R-project.org/package=splitstackshape (accessed on 10 September 2020).
43. Love, M.I.; Huber, W.; Anders, S. Moderated estimation of fold change and dispersion for rna-seq data with deseq2. *Genome Biol.* **2014**, *15*, 550. [CrossRef]
44. Gu, Z.; Eils, R.; Schlesner, M. Complex heatmaps reveal patterns and correlations in multidimensional genomic data. *Bioinformatics* **2016**, *32*, 2847–2849. [CrossRef]
45. Sakai, R. Dendsort: Modular Leaf Ordering Methods for Dendrogram Nodes. R Package Version 0.3. 3. *F1000 Res.* **2015**, *3*, 177. [CrossRef] [PubMed]
46. Xiao, N. Ggsci: Scientific Journal and Sci-fi Themed Color Palettes For'ggplot2'. R Package Version 2. 2018. Available online: https://CRAN.R-project.org/package=ggsci (accessed on 10 September 2020).
47. Langfelder, P.; Horvath, S. Wgcna: An r package for weighted correlation network analysis. *BMC Bioinform.* **2008**, *9*, 559. [CrossRef] [PubMed]
48. Karkossa, I.; Bannuscher, A.; Hellack, B.; Bahl, A.; Buhs, S.; Nollau, P.; Luch, A.; Schubert, K.; von Bergen, M.; Haase, A. An in-depth multi-omics analysis in rle-6tn rat alveolar epithelial cells allows for nanomaterial categorization. *Part Fibre Toxicol* **2019**, *16*, 38. [CrossRef] [PubMed]
49. Yu, G.; Wang, L.G.; Han, Y.; He, Q.Y. Clusterprofiler: An r package for comparing biological themes among gene clusters. *Omics A J. Integr. Biol.* **2012**, *16*, 284–287. [CrossRef] [PubMed]

50. Durinck, S.; Spellman, P.T.; Birney, E.; Huber, W. Mapping identifiers for the integration of genomic datasets with the r/bioconductor package biomart. *Nat. Protoc.* **2009**, *4*, 1184–1191. [CrossRef]
51. Durinck, S.; Moreau, Y.; Kasprzyk, A.; Davis, S.; De Moor, B.; Brazma, A.; Huber, W. Biomart and bioconductor: A powerful link between biological databases and microarray data analysis. *Bioinformatics* **2005**, *21*, 3439–3440. [CrossRef]
52. Carlson, M. Org.Mm.Eg.Db: Genome Wide Annotation for Mouse. 2018. Available online: https://bioconductor.org/packages/release/data/annotation/html/org.Mm.eg.db.html (accessed on 10 September 2020). [CrossRef]
53. Huang, D.W.; Sherman, B.T.; Lempicki, R.A. Systematic and integrative analysis of large gene lists using david bioinformatics resources. *Nat. Protoc.* **2009**, *4*, 44–57. [CrossRef]
54. Winkler, S.; Hempel, M.; Bruckner, S.; Mallek, F.; Weise, A.; Liehr, T.; Tautenhahn, H.M.; Bartels, M.; Christ, B. Mouse white adipose tissue-derived mesenchymal stem cells gain pericentral and periportal hepatocyte features after differentiation in vitro, which are preserved in vivo after hepatic transplantation. *Acta Physiol.* **2015**, *215*, 89–104. [CrossRef]
55. Block, G.D.; Locker, J.; Bowen, W.C.; Petersen, B.E.; Katyal, S.; Strom, S.C.; Riley, T.; Howard, T.A.; Michalopoulos, G.K. Population expansion, clonal growth, and specific differentiation patterns in primary cultures of hepatocytes induced by hgf/sf, egf and tgf alpha in a chemically defined (hgm) medium. *J. Cell Biol.* **1996**, *132*, 1133–1149. [CrossRef]
56. Quah, B.J.; Warren, H.S.; Parish, C.R. Monitoring lymphocyte proliferation in vitro and in vivo with the intracellular fluorescent dye carboxyfluorescein diacetate succinimidyl ester. *Nat. Protoc.* **2007**, *2*, 2049–2056. [CrossRef]
57. Winkler, S.; Hempel, M.; Hsu, M.J.; Gericke, M.; Kuhne, H.; Bruckner, S.; Erler, S.; Burkhardt, R.; Christ, B. Immune-deficient pfp/rag2(-/-) mice featured higher adipose tissue mass and liver lipid accumulation with growing age than wildtype c57bl/6n mice. *Cells* **2019**, *8*, 775. [CrossRef] [PubMed]
58. Peng, J.Y.; Lin, C.C.; Chen, Y.J.; Kao, L.S.; Liu, Y.C.; Chou, C.C.; Huang, Y.H.; Chang, F.R.; Wu, Y.C.; Tsai, Y.S.; et al. Automatic morphological subtyping reveals new roles of caspases in mitochondrial dynamics. *PLoS Comput. Biol.* **2011**, *7*, e1002212. [CrossRef] [PubMed]
59. Lee, C.W.; Hsiao, W.T.; Lee, O.K. Mesenchymal stromal cell-based therapies reduce obesity and metabolic syndromes induced by a high-fat diet. *Transl. Res. J. Lab. Clin. Med.* **2017**, *182*, 61–74.e68. [CrossRef] [PubMed]
60. Seki, A.; Sakai, Y.; Komura, T.; Nasti, A.; Yoshida, K.; Higashimoto, M.; Honda, M.; Usui, S.; Takamura, M.; Takamura, T.; et al. Adipose tissue-derived stem cells as a regenerative therapy for a mouse steatohepatitis-induced cirrhosis model. *Hepatology* **2013**, *58*, 1133–1142. [CrossRef]
61. Ramadori, G.; Christ, B. Cytokines and the hepatic acute-phase response. *Semin. Liver Dis.* **1999**, *19*, 141–155. [CrossRef] [PubMed]
62. Lee, J.; Park, J.S.; Roh, Y.S. Molecular insights into the role of mitochondria in non-alcoholic fatty liver disease. *Arch. Pharmacal Res.* **2019**, *42*, 935–946. [CrossRef]
63. Musso, G.; Gambino, R.; Cassader, M. Recent insights into hepatic lipid metabolism in non-alcoholic fatty liver disease (nafld). *Prog. Lipid Res.* **2009**, *48*, 1–26. [CrossRef] [PubMed]
64. Pawlak, M.; Lefebvre, P.; Staels, B. Molecular mechanism of pparalpha action and its impact on lipid metabolism, inflammation and fibrosis in non-alcoholic fatty liver disease. *J. Hepatol.* **2015**, *62*, 720–733. [CrossRef]
65. Bonen, A.; Campbell, S.E.; Benton, C.R.; Chabowski, A.; Coort, S.L.; Han, X.X.; Koonen, D.P.; Glatz, J.F.; Luiken, J.J. Regulation of fatty acid transport by fatty acid translocase/cd36. *Proc. Nutr. Soc.* **2004**, *63*, 245–249. [CrossRef]
66. Aubert, J.; Begriche, K.; Knockaert, L.; Robin, M.A.; Fromenty, B. Increased expression of cytochrome p450 2e1 in nonalcoholic fatty liver disease: Mechanisms and pathophysiological role. *Clin. Res. Hepatol. Gastroenterol.* **2011**, *35*, 630–637. [CrossRef]
67. Leung, T.M.; Nieto, N. Cyp2e1 and oxidant stress in alcoholic and non-alcoholic fatty liver disease. *J. Hepatol.* **2013**, *58*, 395–398. [CrossRef] [PubMed]
68. Xie, G.; Diehl, A.M. Evidence for and against epithelial-to-mesenchymal transition in the liver. *Am. J. Physiol. Gastrointest. Liver Physiol.* **2013**, *305*, G881–G890. [CrossRef]

69. Hempel, M.; Schmitz, A.; Winkler, S.; Kucukoglu, O.; Bruckner, S.; Niessen, C.; Christ, B. Pathological implications of cadherin zonation in mouse liver. *Cell. Mol. Life Sci. Cmls* **2015**, *72*, 2599–2612. [CrossRef] [PubMed]
70. Aurich, H.; Koenig, S.; Schneider, C.; Walldorf, J.; Krause, P.; Fleig, W.E.; Christ, B. Functional characterization of serum-free cultured rat hepatocytes for downstream transplantation applications. *Cell Transplant.* **2005**, *14*, 497–506. [CrossRef] [PubMed]
71. Schneider, C.; Aurich, H.; Wenkel, R.; Christ, B. Propagation and functional characterization of serum-free cultured porcine hepatocytes for downstream applications. *Cell Tissue Res.* **2006**, *323*, 433–442. [CrossRef]
72. Winkler, S.; Hempel, M.; Bruckner, S.; Tautenhahn, H.M.; Kaufmann, R.; Christ, B. Identification of pathways in liver repair potentially targeted by secretory proteins from human mesenchymal stem cells. *Int. J. Mol. Sci.* **2016**, *17*, 1099. [CrossRef]
73. van Poll, D.; Parekkadan, B.; Cho, C.H.; Berthiaume, F.; Nahmias, Y.; Tilles, A.W.; Yarmush, M.L. Mesenchymal stem cell-derived molecules directly modulate hepatocellular death and regeneration in vitro and in vivo. *Hepatology* **2008**, *47*, 1634–1643. [CrossRef]
74. Varderidou-Minasian, S.; Lorenowicz, M.J. Mesenchymal stromal/stem cell-derived extracellular vesicles in tissue repair: Challenges and opportunities. *Theranostics* **2020**, *10*, 5979–5997. [CrossRef]
75. Shen, J.; Zhang, J.H.; Xiao, H.; Wu, J.M.; He, K.M.; Lv, Z.Z.; Li, Z.J.; Xu, M.; Zhang, Y.Y. Mitochondria are transported along microtubules in membrane nanotubes to rescue distressed cardiomyocytes from apoptosis. *Cell Death Dis.* **2018**, *9*, 81. [CrossRef]
76. Vignais, M.L.; Caicedo, A.; Brondello, J.M.; Jorgensen, C. Cell connections by tunneling nanotubes: Effects of mitochondrial trafficking on target cell metabolism, homeostasis, and response to therapy. *Stem Cells Int.* **2017**, *2017*, 6917941. [CrossRef]
77. Lu, J.; Zheng, X.; Li, F.; Yu, Y.; Chen, Z.; Liu, Z.; Wang, Z.; Xu, H.; Yang, W. Tunneling nanotubes promote intercellular mitochondria transfer followed by increased invasiveness in bladder cancer cells. *Oncotarget* **2017**, *8*, 15539–15552. [CrossRef] [PubMed]
78. Ravagnan, L.; Roumier, T.; Kroemer, G. Mitochondria, the killer organelles and their weapons. *J. Cell. Physiol.* **2002**, *192*, 131–137. [CrossRef] [PubMed]
79. Sparks, J.D.; Sparks, C.E. Overindulgence and metabolic syndrome: Is foxo1 a missing link? *J. Clin. Investig.* **2008**, *118*, 2012–2015. [CrossRef] [PubMed]
80. Hoover-Plow, J.; Huang, M. Lipoprotein(a) metabolism: Potential sites for therapeutic targets. *Metab. Clin. Exp.* **2013**, *62*, 479–491. [CrossRef] [PubMed]
81. Mazat, J.P.; Ransac, S. The fate of glutamine in human metabolism. The interplay with glucose in proliferating cells. *Metabolites* **2019**, *9*, 81. [CrossRef]
82. Cazanave, S.; Podtelezhnikov, A.; Jensen, K.; Seneshaw, M.; Kumar, D.P.; Min, H.K.; Santhekadur, P.K.; Banini, B.; Mauro, A.G.; Oseini, A.M.; et al. The transcriptomic signature of disease development and progression of nonalcoholic fatty liver disease. *Sci. Rep.* **2017**, *7*, 17193. [CrossRef]
83. Teufel, A.; Itzel, T.; Erhart, W.; Brosch, M.; Wang, X.Y.; Kim, Y.O.; von Schonfels, W.; Herrmann, A.; Bruckner, S.; Stickel, F.; et al. Comparison of gene expression patterns between mouse models of nonalcoholic fatty liver disease and liver tissues from patients. *Gastroenterology* **2016**, *151*, 513–525.e510. [CrossRef]
84. Bessone, F.; Razori, M.V.; Roma, M.G. Molecular pathways of nonalcoholic fatty liver disease development and progression. *Cell. Mol. Life Sci. Cmls* **2019**, *76*, 99–128. [CrossRef]
85. Lambert, J.E.; Ramos-Roman, M.A.; Browning, J.D.; Parks, E.J. Increased de novo lipogenesis is a distinct characteristic of individuals with nonalcoholic fatty liver disease. *Gastroenterology* **2014**, *146*, 726–735. [CrossRef]
86. Hyotylainen, T.; Jerby, L.; Petaja, E.M.; Mattila, I.; Jantti, S.; Auvinen, P.; Gastaldelli, A.; Yki-Jarvinen, H.; Ruppin, E.; Oresic, M. Genome-scale study reveals reduced metabolic adaptability in patients with non-alcoholic fatty liver disease. *Nat. Commun.* **2016**, *7*, 8994. [CrossRef]
87. Hardwick, R.N.; Fisher, C.D.; Canet, M.J.; Lake, A.D.; Cherrington, N.J. Diversity in antioxidant response enzymes in progressive stages of human nonalcoholic fatty liver disease. *Drug Metab. Dispos. Biol. Fate Chem.* **2010**, *38*, 2293–2301. [CrossRef] [PubMed]
88. Velarde, M.C.; Flynn, J.M.; Day, N.U.; Melov, S.; Campisi, J. Mitochondrial oxidative stress caused by sod2 deficiency promotes cellular senescence and aging phenotypes in the skin. *Aging* **2012**, *4*, 3–12. [CrossRef] [PubMed]

89. Oh, S.H.; Swiderska-Syn, M.; Jewell, M.L.; Premont, R.T.; Diehl, A.M. Liver regeneration requires yap1-tgfbeta-dependent epithelial-mesenchymal transition in hepatocytes. *J. Hepatol.* **2018**, *69*, 359–367. [CrossRef]
90. Ezquer, M.; Ezquer, F.; Ricca, M.; Allers, C.; Conget, P. Intravenous administration of multipotent stromal cells prevents the onset of non-alcoholic steatohepatitis in obese mice with metabolic syndrome. *J. Hepatol.* **2011**, *55*, 1112–1120. [CrossRef]
91. Watanabe, T.; Tsuchiya, A.; Takeuchi, S.; Nojiri, S.; Yoshida, T.; Ogawa, M.; Itoh, M.; Takamura, M.; Suganami, T.; Ogawa, Y.; et al. Development of a non-alcoholic steatohepatitis model with rapid accumulation of fibrosis, and its treatment using mesenchymal stem cells and their small extracellular vesicles. *Regen. Ther.* **2020**, *14*, 252–261. [CrossRef]
92. Chella Krishnan, K.; Kurt, Z.; Barrere-Cain, R.; Sabir, S.; Das, A.; Floyd, R.; Vergnes, L.; Zhao, Y.; Che, N.; Charugundla, S.; et al. Integration of multi-omics data from mouse diversity panel highlights mitochondrial dysfunction in non-alcoholic fatty liver disease. *Cell Syst.* **2018**, *6*, 103–115.e107. [CrossRef] [PubMed]
93. Sobaniec-Lotowska, M.E.; Lebensztejn, D.M. Ultrastructure of hepatocyte mitochondria in nonalcoholic steatohepatitis in pediatric patients: Usefulness of electron microscopy in the diagnosis of the disease. *Am. J. Gastroenterol.* **2003**, *98*, 1664–1665. [CrossRef] [PubMed]
94. Kimura, S.; Hase, K.; Ohno, H. The molecular basis of induction and formation of tunneling nanotubes. *Cell Tissue Res.* **2013**, *352*, 67–76. [CrossRef]
95. Rustom, A.; Saffrich, R.; Markovic, I.; Walther, P.; Gerdes, H.H. Nanotubular highways for intercellular organelle transport. *Science* **2004**, *303*, 1007–1010. [CrossRef]
96. Jash, E.; Prasad, P.; Kumar, N.; Sharma, T.; Goldman, A.; Sehrawat, S. Perspective on nanochannels as cellular mediators in different disease conditions. *Cell Commun. Signal. Ccs* **2018**, *16*, 76. [CrossRef]
97. Moravcova, A.; Cervinkova, Z.; Kucera, O.; Mezera, V.; Rychtrmoc, D.; Lotkova, H. The effect of oleic and palmitic acid on induction of steatosis and cytotoxicity on rat hepatocytes in primary culture. *Physiol. Res.* **2015**, *64*, S627–S636. [CrossRef] [PubMed]
98. Caballero, F.; Fernandez, A.; Matias, N.; Martinez, L.; Fucho, R.; Elena, M.; Caballeria, J.; Morales, A.; Fernandez-Checa, J.C.; Garcia-Ruiz, C. Specific contribution of methionine and choline in nutritional nonalcoholic steatohepatitis: Impact on mitochondrial s-adenosyl-l-methionine and glutathione. *J. Biol. Chem.* **2010**, *285*, 18528–18536. [CrossRef] [PubMed]
99. Alijani, N.; Johari, B.; Moradi, M.; Kadivar, M. A review on transcriptional regulation responses to hypoxia in mesenchymal stem cells. *Cell Biol. Int.* **2020**, *44*, 14–26. [CrossRef] [PubMed]
100. Newell, C.; Sabouny, R.; Hittel, D.S.; Shutt, T.E.; Khan, A.; Klein, M.S.; Shearer, J. Mesenchymal stem cells shift mitochondrial dynamics and enhance oxidative phosphorylation in recipient cells. *Front. Physiol.* **2018**, *9*, 1572. [CrossRef]
101. Marlein, C.R.; Piddock, R.E.; Mistry, J.J.; Zaitseva, L.; Hellmich, C.; Horton, R.H.; Zhou, Z.; Auger, M.J.; Bowles, K.M.; Rushworth, S.A. Cd38-driven mitochondrial trafficking promotes bioenergetic plasticity in multiple myeloma. *Cancer Res.* **2019**, *79*, 2285–2297. [CrossRef]
102. Jackson, M.V.; Morrison, T.J.; Doherty, D.F.; McAuley, D.F.; Matthay, M.A.; Kissenpfennig, A.; O'Kane, C.M.; Krasnodembskaya, A.D. Mitochondrial transfer via tunneling nanotubes is an important mechanism by which mesenchymal stem cells enhance macrophage phagocytosis in the in vitro and in vivo models of ards. *Stem Cells* **2016**, *34*, 2210–2223. [CrossRef]
103. Zhang, Y.; Yu, Z.; Jiang, D.; Liang, X.; Liao, S.; Zhang, Z.; Yue, W.; Li, X.; Chiu, S.M.; Chai, Y.H.; et al. Ipsc-mscs with high intrinsic miro1 and sensitivity to tnf-alpha yield efficacious mitochondrial transfer to rescue anthracycline-induced cardiomyopathy. *Stem Cell Rep.* **2016**, *7*, 749–763. [CrossRef]
104. Ahmad, T.; Mukherjee, S.; Pattnaik, B.; Kumar, M.; Singh, S.; Kumar, M.; Rehman, R.; Tiwari, B.K.; Jha, K.A.; Barhanpurkar, A.P.; et al. Miro1 regulates intercellular mitochondrial transport & enhances mesenchymal stem cell rescue efficacy. *EMBO J.* **2014**, *33*, 994–1010.
105. Han, D.; Zheng, X.; Wang, X.; Jin, T.; Cui, L.; Chen, Z. Mesenchymal stem/stromal cell-mediated mitochondrial transfer and the therapeutic potential in treatment of neurological diseases. *Stem Cells Int.* **2020**, *2020*, 8838046. [CrossRef]
106. Christ, B.; Dollinger, M.M. The generation of hepatocytes from mesenchymal stem cells and engraftment into the liver. *Curr. Opin. Organ Transplant.* **2011**, *16*, 69–75. [CrossRef]

107. Neumann, E. Kraftwerke unserer Zellen. *Top Life Aktuell* **2010**, *1005*. Available online: http://www.toplife.at/gesundheit/artikel172.html (accessed on 30 June 2020).
108. Kraft, E.; Stickl, H. Comparative measurement of the growth of rat liver by means of square grid and leitz' integration table on histological slices. *Virchows Archiv Fur Pathol. Anat. und Physiol. und fur Klin. Med.* **1954**, *324*, 650–661. [CrossRef] [PubMed]

MDPI
St. Alban-Anlage 66
4052 Basel
Switzerland
Tel. +41 61 683 77 34
Fax +41 61 302 89 18
www.mdpi.com

Biomedicines Editorial Office
E-mail: biomedicines@mdpi.com
www.mdpi.com/journal/biomedicines

MDPI
St. Alban-Anlage 66
4052 Basel
Switzerland

Tel: +41 61 683 77 34
Fax: +41 61 302 89 18

www.mdpi.com

ISBN 978-3-0365-2979-0